

Synthetic Applications of Molybdenum and Tungsten Dearomatization Agents

Justin Henry Wilde
Plainville, Connecticut

B.S., University of Connecticut, 2012

A Dissertation presented to the Graduate Faculty
of the University of Virginia in Candidacy for the Degree of
Doctor of Philosophy

Department of Chemistry

University of Virginia
May 2020

Copyright Information

Chapters 2, 3, and 6 are published works which are copyright by the American Chemical Society. These works are reproduced herein in accordance with Section II.1 of the American Chemical Society Journal Publishing Agreement. Chapters 4 and 5 are drafts of future manuscripts and may subsequently be published in whole or part.

Chapter 2: Wilde, J. H.; Myers, J. T.; Dickie, D. A.; Harman, W. D. “Molybdenum-Promoted Dearomatization of Pyridines” *Organometallics* 2020.

DOI: 10.1021/acs.organomet.0c00047

Chapter 3: Wilde, J. H.; Smith, J. A.; Dickie, D. A.; Harman, W. D. “Molybdenum-Promoted Synthesis of Isoquinuclidines with Bridgehead CF₃ Groups” *J. Am. Chem. Soc.* 2019, 141, 47, 18890-18899. DOI: 10.1021/jacs.9b10781

Chapter 6: Myers, J. T.;[#] Wilde, J. H.;[#] Sabat, M.; Dickie, D. A.; Harman, W. D. “Michael-Michael-Ring-Closure Reactions for a Dihapto-Coordinated Naphthalene Complex of Molybdenum” *Organometallics* 2020. DOI: 10.1021/acs.organomet.0c00110

[#] joint first authorship

Acknowledgements

Scientific writing is characterized by formality and detachment. A perfect scientist should be an impartial observer. In reality, of course, research is often intertwined with one's personal life. These acknowledgements provide a 'peek behind the curtain' at the relationships that guided my research.

Prior to coming to UVa, I had always lived in Connecticut. Moving to Virginia was admittedly a challenging transition. I didn't know anyone here, and I came with only the bare essentials (a bed not being one of those, necessitating snoozing in a sleeping bag for a few months). I didn't know what to expect from grad school, and suffice it to say, my first impressions were not what I had envisioned. I began to think it just wasn't for me. However, it was through the help of many that I overcame these difficulties and grew both professionally and personally.

Perhaps no individual was as influential as my advisor, Dr. W. Dean Harman. Dean has an uncommon combination of scientific rigor and 'soft skills' that make him an ideal mentor. Through his personal understanding and seemingly boundless knowledge of chemistry, I learned more in these years than I ever imagined possible. When my optimism towards research wavered, Dean provided the encouragement that rekindled my enthusiasm. I am confident in my scientific skills and understanding in large part because of Dean, and for this I am so grateful.

I would also like to thank the numerous Harman Lab members, who have played a substantial role in my time here. Jeff, Bri, and Phil for their 'tough love' training, Ben for his sympathetic ear, Steven for his tireless inventory and nitrogen tank management, and Katy for her motivating organic chemistry rivalry (and I haven't forgotten those

tickets to ‘A Concert for Charlottesville’, thanks!). Jacob, my fellow cohort, has always been there to discuss anything, whether new chemistry or just lab frustrations. Spencer has brought a welcome sense of energy to the lab, and our younger lab members, Jonathan and Justin W. P., are expanding our chemistry in exciting ways. The newest members, Megan and Mary, are sure to do great things, as well (once the Covid-19 situation is over and the lab reopens)!

My family has also been extremely important to me during my time in grad school. No one was as willing to listen to my griping as my mom. My dad helped me move down, furnished my apartment, and even came to visit, which provided a nice change of pace. My brother Matthew, grandma Marie, and aunt Sharon provided much-needed moral, and financial, support. If it weren’t for them, I might still be using that sleeping bag and driving my stall-prone 1996 Buick! I’d also like to thank my soon-to-be wife, Jillian. Though we met years earlier at UConn, we reconnected during my second year in Virginia. Every day I am thankful for her love (and her willingness to drive from Maryland every other weekend).

There are many others I haven’t named who have provided assistance. Please know that the absence of mention is due only to lack of space, not appreciation. In closing, I’d like to acknowledge committee members, Dr. Gunnoe, Dr. Pu, Dr. Pires, and Dr. Neumann. Thank you for taking the time to evaluate my research.

Abstract

Chapter 1: A brief survey of pyridine chemistry is provided. Nucleophilic and electrophilic substitutions are reviewed, followed by an overview of dearomatization methods. An emphasis is placed on the prior art of organometallic-promoted dearomatization, comparing the chemistry of various pyridine metal complexes.

Chapter 2: A second-row transition metal complex $\{\text{MoTp}(\text{NO})(\text{DMAP})\}$ is shown to form dihapto-coordinate complexes with a range of substituted pyridines bearing both electron-withdrawing and electron-donating substituents. Subsequent reactivity of the pyridine ligand is demonstrated by protonation and nucleophilic addition reactions.

Chapter 3: The preparation of the complex $\text{MoTp}(\text{NO})(\text{DMAP})(4,5\text{-}\eta^2\text{-(2-trifluoromethyl)pyridine})$ (DMAP = 4-(dimethylamino)pyridine; Tp = tris(pyrazolyl)borate) is described. The CF_3 substituent is found to preclude $\kappa\text{-N}$ coordination, allowing for direct coordination without protection of the nitrogen. The dihapto-coordinate complex can be isolated as a single diastereomer, methylated, and reacted with a range of nucleophiles. Oxidative decomplexation affords the free dihydropyridines in good yield (75–90%). As a demonstration of synthetic utility, a series of novel bridgehead CF_3 -substituted isoquinuclidines was prepared from these decomplexed dihydropyridines.

Chapter 4: Dihapto-coordinate 1,2-dihydropyridine complexes of the metal complex $\{\text{WTP}(\text{NO})(\text{PMe}_3)\}$ are derived from pyridine-borane. These complexes are demonstrated to undergo protonation at C6 followed by regioselective amination at C5 with a variety of primary and secondary amines. The addition takes place stereoselectively *anti* to the metal center, producing exclusively *cis*-disubstituted

products. The resulting tetrahydropyridines can be successfully liberated by oxidation, providing a route to molecules of potential medicinal interest.

Chapter 5: The synthesis of methylphenidate analogs from pyridine is described. The dihapto-coordinated metal complex $\text{WTP}(\text{NO})(\text{PMe}_3)(3,4\text{-}\eta^2\text{-pyridine})$ can be functionalized on nitrogen and subsequently reacted with a Reformatsky enolate to yield a dihydropyridine methylphenidate precursor. An ensuing stereo- and regio- selective tandem electrophilic, nucleophilic addition allows incorporation of diverse functionality. The elaborated molecule can be liberated by treatment with an oxidant, demonstrating the synthetic utility of this chemistry.

Chapter 6: The complex $\text{MoTp}(\text{NO})(\text{DMAP})(\eta^2\text{-naphthalene})$ is demonstrated to undergo Michael–Michael ring-closure (MIMIRC) reactions promoted by trimethylsilyl triflate. The resulting hexahydrophenanthrenes are formed stereoselectively, with isolation of a single dominant isomer. Combining the MIMIRC sequence with an oxidative decomplexation step, the final tricyclics can be synthesized from the naphthalene complex with overall yields between 19 and 50% (for four steps). This reaction sequence is shown to be capable of producing a steroidal core directly from naphthalene, providing access to a biologically relevant carbon framework.

Table of Contents

Abstract	i
Copyright Information	ii
Acknowledgements	iii
Table of Contents	vii
List of Figures	ix
List of Schemes	xii
List of Tables	xv
List of Abbreviations	xvi
Chapter 1: A Survey of Pyridine Chemistry	1
Properties of Pyridine	2
Substitution Reactions of Pyridine	3
Dearomatization of Pyridine	6
Organometallic Dearomatization	8
Further Development of Mo and W Dearomatization	15
References	17
Chapter 2: Molybdenum-Promoted Dearomatization of Pyridines	22
Introduction	23
Results	25
Discussion	39
Conclusion	41
Experimental Section	42
Single crystal X-ray Diffraction Experimental Details	60
References	65
Chapter 3: Molybdenum-Promoted Synthesis of Isoquinuclidines with Bridgehead CF₃ Groups	70
Introduction	71
Results and Discussion	73
Conclusion	83
Experimental Section	84
Single crystal X-ray Diffraction Experimental Details	107
References	112

Chapter 4: Tungsten-Promoted Synthesis of Amino-tetrahydropyridines	116
Introduction	117
Results and Discussion	117
Conclusion	126
Experimental Section	127
References	140
Chapter 5: Synthesis of Methylphenidate Analogs via Tungsten Dearomatization	143
Introduction	144
Results and Discussion	145
Conclusion	156
Experimental Section	157
Single crystal X-ray Diffraction Experimental Details	169
References	171
Chapter 6: Michael-Michael-Ring-Closure Reactions for a Dihapto-Coordinated Naphthalene Complex of Molybdenum	173
Introduction	174
Results	175
Discussion	186
Conclusion	189
Experimental Section	189
Single crystal X-ray Diffraction Experimental Details	199
References	201
Chapter 7: Concluding Remarks	205
References	209
Appendix	211

List of Figures

Chapter 1:

Figure 1.1: Common drugs containing a pyridine moiety

Figure 1.2: Resonance structures of pyridine and resulting polarization

Figure 1.3: Direct alkylation and arylation of pyridine via a dihydropyridine intermediate

Figure 1.4: Two mechanisms of nucleophilic substitution with displacement of a leaving group

Figure 1.5: Direct metallation of pyridine with and without the presence of an *ortho*-directing group

Figure 1.6: Synthesis of metallated pyridines via metal-halogen exchange

Figure 1.7: Diastereoselective addition to 4-Methoxy-3-(triisopropylsilyl)pyridine to generate a versatile alkaloid precursor

Figure 1.8: Synthesis of a 6-azabicyclo[3.1.0]hex-3-en-2-ol via photoreaction

Figure 1.9: Organic transformations of a hexahapto-coordinated pyridine ligand

Figure 1.10: Hydride-induced C-N bond cleavage of an η^2 -(N,C) pyridine complex

Figure 1.11: Synthesis of an η^2 -lutidine osmium(II) complex and its subsequent reactivity

Figure 1.12: Organic molecules produced from derivatization of the tungsten(0) η^2 -N-acetylpyridinium complex

Figure 1.13: Tungsten-promoted dearomatization of electron-rich pyridines

Figure 1.14: Azabicyclo[3.2.1]octene synthesis from a molybdenum 2-oxopyridinyl complex

Figure 1.15: Enantiocontrolled synthesis of substituted piperidines using a molybdenum π -complex

Chapter 2:

Figure 2.1: η^2 -Molybdenum pyridine complexes in equilibrium coordination diastereomer ratio (cdr) and assignment of stereochemistry via NOE interactions

Figure 2.2: ORTEP diagram (50% ellipsoids) of the solid-state structure MoTp(NO)(DMAP)(3,4- η^2 -(2-CF₃)pyridine), showing significant dearomatization

Figure 2.3: ORTEP diagram (50% ellipsoids) of the solid state structure determination of Mo(η^2 -Tp)(DMAP)(NO)(κ^2 -bipy)

Figure 2.4: ORTEP diagrams of methoxy (20) and piperidine (21) additions to pyridinium complex 10

Figure 2.5: ORTEP of ring-opened-complex 22B

Figure 2.6: Comparison of molybdenum ring-opening to the Zincke-König reaction and a related tungsten reaction

Chapter 3:

Figure 3.1: The proposed stabilization of a dihapto-coordinated molybdenum-pyridine complex by a CF₃ group and the enabled stereoselective synthesis of novel isoquinuclidines

Figure 3.2: ORTEP diagram (50% probability) of a single diastereomer of the methylated TFP complex 3 and its Grignard addition product

Figure 3.3: A comparison of several methods used to generate 6-(trifluoromethyl)-1,2-dihydropyridines

Figure 3.4: ORTEP diagram (50% probability) of isoquinuclidine compounds

Figure 3.5: Dihydropyridine product mixture under Mo-free reaction conditions

Chapter 4:

Figure 4.1: The range of amine organics produced by tungsten-mediated amination of pyridine (yield over 2 steps)

Chapter 5:

Figure 5.1: Enantiomers and diastereomers of methylphenidate

Figure 5.2: ORTEP diagram (50% ellipsoids) of the solid-state structure of compound **79A**, revealing the *erythro* stereochemistry

Figure 5.3: ORTEP diagram (50% ellipsoids) of the solid-state structure of compound **87A**, elucidating the stereochemistry

Chapter 6:

Figure 6.1: Synthesis, numbering scheme (major isomer; dr = 8:1), and ORTEP diagram of compound **92** (50% ellipsoidal probability)

Figure 6.2: ORTEP diagram of compound **93** (50% ellipsoidal probability)

Figure 6.3: Side-products from the MIMIRC reaction

Figure 6.4: ORTEP diagram of **98** (50% ellipsoidal probability)

Figure 6.5: ORTEP diagram of **100** (50% ellipsoidal probability)

Figure 6.6: Examples of natural and unnatural steroid cores. Blue: *trans*-B/C and *trans*-C/D ring fusions (common); pink: *cis*-B/C ring fusion; green: *cis*-C/D ring fusion

List of Schemes

Chapter 2:

Scheme 2.1: Synthesis of tetrahydropyridines from pyridine via metal-promoted dearomatization

Scheme 2.2: Nitrogen and carbon protonation of pyridine complexes

Scheme 2.3: Intramolecular face-flip isomerization for η^2 -pyridinium complexes

Scheme 2.4: Synthesis of a single coordination diastereomer via Solid-state Induced Control of Kinetically Unstable Isomer (SICKUS) method

Scheme 2.5: Nucleophilic additions to the methylpyridinium complex

Scheme 2.6: Ring-opening of a dihydropyridine complex

Scheme 2.7: Preparation of the 1-methyldihydropyridine complex 25 and its nitrogen-directed protonation to make an η^2 -1,4-dihydropyridinium complex (26).

Scheme 2.8: Oxidative liberation of dihydropyridines and subsequent cycloaddition to generate novel isoquinuclidines

Chapter 3:

Scheme 3.1: Synthesis of TFP complex, the NOE correlations that differentiate the two diastereomers, and the selective conversion to a single diastereomer of the methylated pyridinium complex

Scheme 3.2: The addition of various nucleophiles to the methylated pyridine complex

Scheme 3.3: Decomplexation of DHP and its elaboration to isoquinuclidines

Scheme 3.4: Enantioenriched preparation of isoquinuclidine from α -pinene precursor

Chapter 4:

Scheme 4.1: Synthesis of dihydropyridine complexes [W] = WTp(NO)(PMe₃)

Scheme 4.2: Synthesis of allyl complex via protonation. [W] = WTp(NO)(PMe₃)

Scheme 4.3: Reversible addition of an amine to a tungsten allyl complex and irreversible elimination upon warming

Scheme 4.4: Synthesis of aminotetrahydropyridine products

Scheme 4.5: Variation of second electrophile to produce an acylsulfonamide

Chapter 5:

Scheme 5.1: Previous work and proposed Reformatsky-like reaction

Scheme 5.2: Metal-mediated synthesis of methylphenidate core

Scheme 5.3: Protonation and nucleophilic additions to a methylphenidate dihydropyridine derivative

Scheme 5.4: Oxidative decomplexation of functionalized methylphenidate organics

Scheme 5.5: Synthesis of various N-protected pyridinium complexes. Only major coordination diastereomer is shown.

Scheme 5.6: Comparison of methyl α -bromophenylacetate addition to tosyl- and acetylpyridinium complexes

Scheme 5.7: Functionalization of a tosylmethylphenidate complex, followed by oxidative decomplexation of the resulting tetrahydropyridine

Chapter 6:

Scheme 6.1: The proposed acid-promoted Michael-Michael-Ring-Closure (MIMIRC) sequence with an η^2 -coordinated naphthalene

Scheme 6.2: Proposed mechanism of a Michael-Michael-Ring-Closure with EVK

Scheme 6.3: [A+B] Michael-Michael ring closure reactions (products are formed as racemic mixtures)

Chapter 7:

Scheme 7.1: Proposed synthesis of nitrogenous bi- and tricyclic ring systems

List of Tables

Chapter 2:

Table 2.1: Cyclic voltammetry and IR data for neutral molybdenum pyridine complexes

Table 2.2: Crystal data for compounds **4a**, **28**, **6**, **7**, **17** and **19**.

Table 2.3: Crystal data for compounds **20**, **21**, **22b**, **25** and **26**

Chapter 3:

Table 3.1: Dihydropyridine product ratio under various Mo-free reaction conditions

Table 3.2: Crystal data for compounds **10**, **15**, **18**, and **16**

Table 3.3: Crystal data for compounds **11**, **12**, **13**, **14**

Table 3.4: Crystal data for compounds **39**, **R-39**, **40**, **41**

Table 3.5: Crystal data for compounds **35A**, **36A·HCl** and **37A·HCl**

Chapter 5:

Table 5.1: Crystal Data for **79A** and **87A**

Chapter 6:

Table 6.1: Coupling constants for **100** where H13 is cis to H14 and H12

Table 6.2: Coupling constants for **100** where H13 is trans to H14 and H12

Table 6.3: Comparison of predicted and measured dihedral angles for **100**

Table 6.4: Crystal Data for the X-ray diffraction structures **92**, **93**, **98** and **100**

List of Abbreviations

Bipy	2,2'-Bipyridyl
Boc	<i>tert</i> -Butoxycarbonyl
CAN	Ceric ammonium nitrate
Cbz	Benzyloxycarbonyl
cdr	Coordination diastereomer ratio
Cp	Cyclopentadienyl (Cyclopentadienide Anion)
Cp*	Pentamethylcyclopentadienyl (Pentamethylcyclopentadienide Anion)
DDQ	2,3-Dichloro-5,6-dicyano-p-benzoquinone
DHP	Dihydropyridine
DIBAL	Diisobutylaluminum hydride
DMA	N,N-dimethylacetamide
DMAP	4-(Dimethylamino)pyridine
DME	1,2-Dimethoxyethane
DMF	N,N-Dimethylformamide
DPhAT	Diphenylammonium triflate
dr	Diastereomeric ratio
DTBP	2,6-Di- <i>tert</i> -butylpyridine
EA	Elemental analysis
er	Enantiomeric ratio
ESI	Electrospray ionization
EVK	Ethyl vinyl ketone

HATR	Horizontal attenuated total reflectance
HRMS	High-resolution mass spectrometry
IR	Infrared
KTp	Potassium hydridotris(pyrazolyl)borate
LDA	Lithium diisopropylamide
LiDMM	Lithium dimethylmalonate
MIMIRC	Michael-Michael-Ring Closure
MS	Mass spectrometry
MTDA	Methyl trimethylsilyl dimethylketene acetal
MVK	Methyl vinyl ketone
NHE	Normal hydrogen electrode
NMR	Nuclear magnetic resonance
NMM	N-methylmaleimide
NOE	Nuclear Overhauser effect
Nuc	Nucleophile
ORTEP	Oak Ridge Thermal Ellipsoid Program
OTf	Trifluoromethanesulfonate (Triflate) anion
PG	Protecting group
pyr	Pyridine
Pz	A pyrazole group in hydridotris(pyrazolyl)borate
SC-XRD	Single Crystal X-ray Diffraction
TBAH	Tetrabutylammonium hexafluorophosphate
TFA	Trifluoroacetic acid

TFAA	Trifluoroacetic anhydride
THF	Tetrahydrofuran
THP	Tetrahydropyridine
TLC	Thin layer chromatography
TMS	Trimethylsilyl
TP	Hydridotris(pyrazolyl)borate anion
Ts	p-Toluenesulfonyl (Tosyl)
Ts-ICN	p-Toluenesulfonyl isocyanate

Chapter 1: A Survey of Pyridine Chemistry

Properties of Pyridine

Aromatic molecules are abundant in nature due to their stability, and many of these compounds are available commercially at low cost. One such compound is pyridine, a six-membered heterocycle containing a benzene core with one -CH unit replaced by nitrogen. Initially obtained from the pyrolysis of bone, pyridine was later sourced from coal tar. More recently, pyridine and its derivatives have been synthesized in large quantities by reactions such as the Chichibabin pyridine synthesis.¹

Besides being useful as solvents and bases, pyridines are common in biologically-active substances. Niacin (vitamin B3) and the metabolically-indispensable nicotinamide adenine dinucleotide (NAD) both contain pyridine moieties.² Many drugs feature the pyridine core as well, including nicotine, isoniazid, omeprazole, and zopiclone.

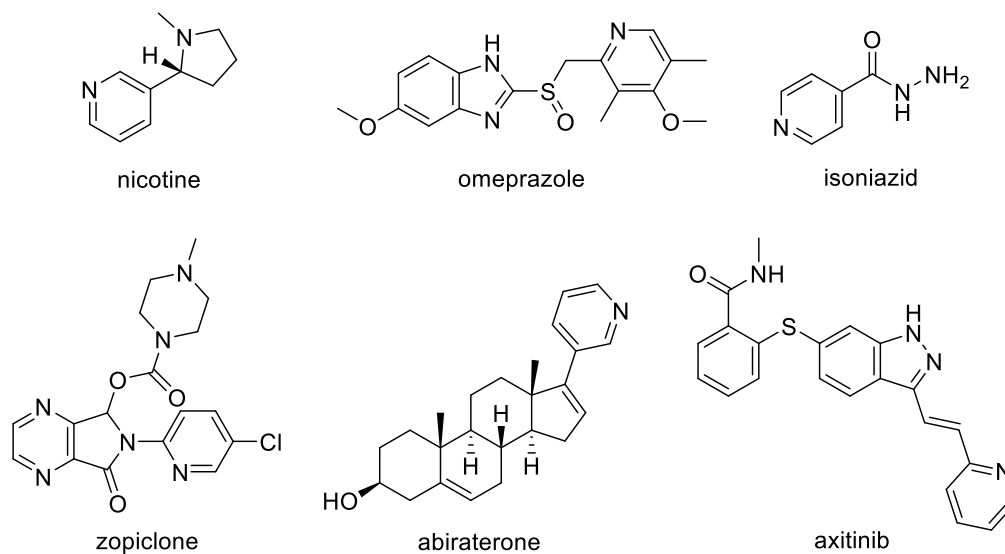


Figure 1.1: Common drugs containing a pyridine moiety

Saturated derivatives of pyridines, known as piperidines, are also abundant in compounds of medicinal interest. In fact, about 60% of all FDA-approved small molecule

drugs contain a nitrogen heterocycle, and the most abundant of these is piperidine (followed by pyridine).³ Piperidines are theoretically accessible from addition reactions to pyridine, but this approach is limited by the stability of the pyridine π system. The π system of pyridine contains $4n + 2$ electrons in a conjugated, planar, cyclic array, which imparts an aromatic stabilization energy of approximately 28 kcal/mol (compare with 36 kcal/mol for benzene).¹ Because of this large stabilization, pyridine generally participates in reactions that re-establish or do not disrupt the aromatic π system.

Substitution Reactions of Pyridine

The sp^2 lone pair on nitrogen is not involved in the aromatic system, and thus readily reacts with electrophiles. The pyridine nitrogen may be protonated, nitrated⁴, N-oxidized,⁵ sulfonated,⁶ halogenated,^{7,8} acylated⁹, and alkylated. Many of these derivatives are useful in organic synthesis. For example, pyridine-N-oxide is used as an oxidant, while N-acyl derivatives of 4-(dimethylamino)pyridine are catalysts in acylation reactions.¹⁰ Pyridinium poly(hydrogen fluoride) is a convenient fluorinating agent that avoids the use of gaseous HF.¹¹ Electrophilic substitution is possible at carbon but requires harsh conditions or highly activated pyridines due to preemptive addition to nitrogen, which generates electron-poor pyridinium cations.^{12,13} Nevertheless, nitration, sulfonation, bromination, chlorination, and acetoxymercuration have all been reported for unsubstituted pyridine.¹ All of these reactions occur at the β position, which is less positively polarized than either the α or γ positions (Figure 2).

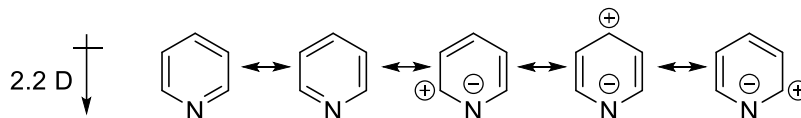


Figure 1.2: Resonance structures of pyridine and resulting polarization

More commonly, pyridine is reacted with nucleophiles to form an intermediate dihydropyridine. The dihydropyridine can then transfer a hydride to generate substituted products.¹⁴ The hydride transfer is often more difficult than the analogous proton transfer that occurs during electrophilic substitution, and an oxidizing agent is often required as a hydride acceptor.

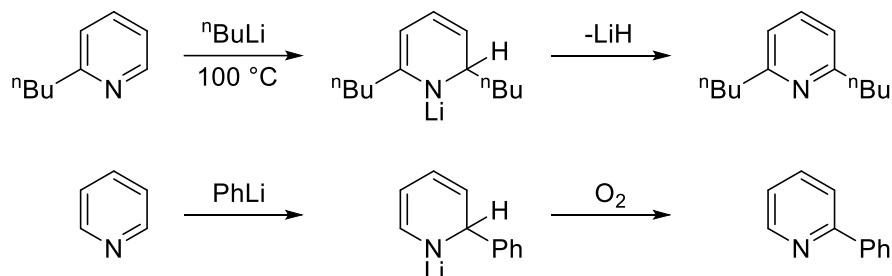


Figure 1.3: Direct alkylation and arylation of pyridine via a dihydropyridine intermediate

Elimination of a good leaving group is also possible. The substituent is generally a halogen, though examples are also known with nitro, alkoxy, sulfonyloxy, and methoxy substituents.¹ As both the electron-withdrawing effect and the leaving group ability are important, fluoropyridines are the most reactive of the halogenated pyridines.

Nucleophilic substitution usually takes place at either the α or γ position, since this allows the nitrogen to stabilize the resulting negative charge. When a leaving group occupies a β position, a Substitution Nucleophilic Elimination Addition reaction may occur via the

intermediacy of a 3,4-pyridyne. In this case, mixtures of β and γ substituted products may be formed.¹⁵

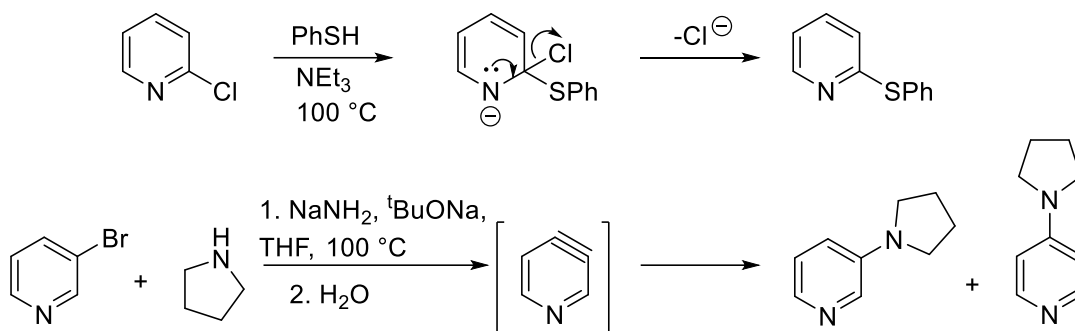


Figure 1.4: Two mechanisms of nucleophilic substitution with displacement of a leaving group

An alternative approach for the generation of substituted pyridines relies on metallation. Pyridine itself may be selectively metallated at the α position by a mixture of 2 molar equivalents *n*-BuLi and 1 molar equivalent dimethylaminoethanol (DMAE). The LiDMAE formed *in situ* directs an intramolecular delivery of *n*-BuLi, providing the observed regioselectivity.¹⁶ Alternatively, *ortho*-directing groups on pyridine allow for β or γ lithiation.¹⁷ These metallated derivatives can be reacted with a range of electrophiles to introduce diverse functionality.

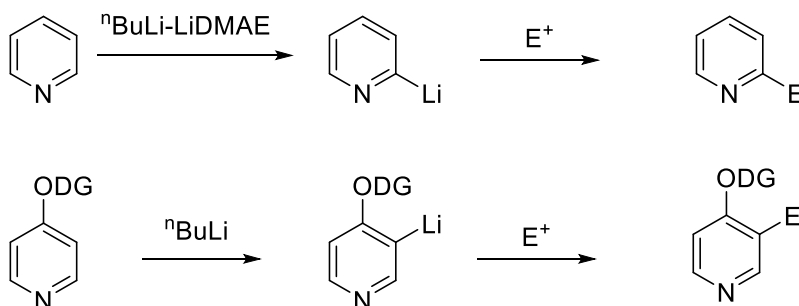


Figure 1.5: Direct metallation of pyridine with and without the presence of an *ortho*-directing group (ODG)

Metal-halogen exchange presents a complementary method for the formation of lithio-pyridines. Bromo-pyridines will react with *n*-BuLi, trimethylsilyllithium, and lithium dimethylaminomethoxide to yield the lithated derivative. Pyridyl Grignard reagents are also accessible from bromo- or iodo-pyridines and isopropylmagnesium chloride.¹⁸

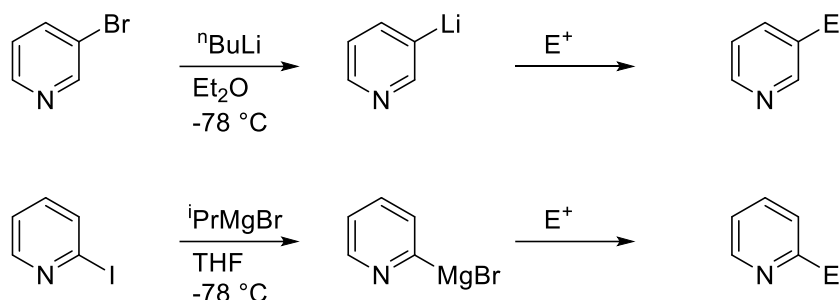


Figure 1.6: Synthesis of metallated pyridines via metal-halogen exchange

Dearomatization of Pyridine

In all of the reactions previously discussed, the end product is a functionalized pyridine. There are many reactions, however, that generate dearomatized compounds. As previously stated, many dihydropyridines are unstable, and are thought to be intermediates in certain substitution reactions. Nucleophilic addition to N-activated pyridines is far easier than for the parent compound, and the resulting dihydropyridines are far more stable than the N-lithio salts that would otherwise result. Although regioselectivity of addition can be problematic, suitable choice of the N-activating group and nucleophile can allow for highly regioselective reactions.¹⁹ As a general rule, hard nucleophiles tend to favor α addition, whereas softer nucleophiles often prefer addition to the γ position. The presence of ring substituents can also have a significant impact on regioselectivity. If the N-activating group is chiral, stereoselectivity may be achievable.

Comins has extensively investigated the stereo- and regioselective dearomatization of pyridines via the use of chiral acylating agents and has used the resulting compounds in the synthesis of numerous natural products.^{20,21}

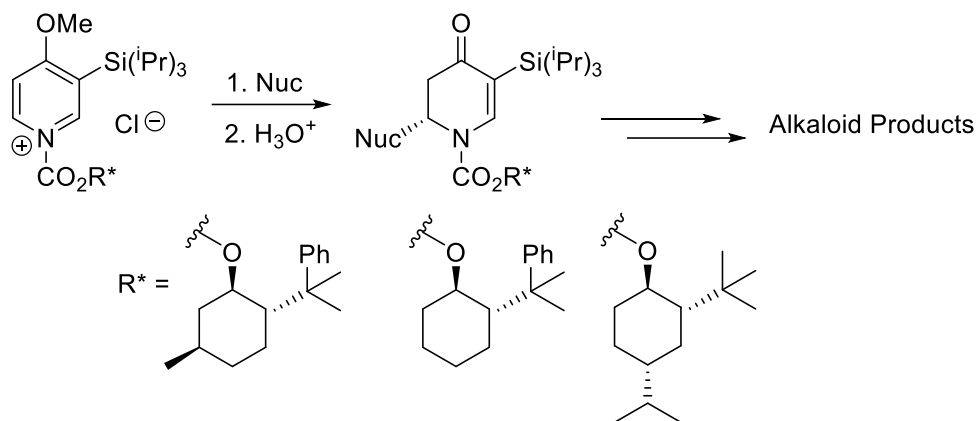


Figure 1.7: Diastereoselective addition to 4-Methoxy-3-(triisopropylsilyl)pyridine to generate a versatile alkaloid precursor

Reduction of pyridine or pyridinium salts presents another route to dearomatization. Even pyridine itself is reduced far more easily than benzene, for example by catalytic hydrogenation over palladium or nickel alloy.²² Chiral piperidines may be produced by diastereoselective hydrogenation of a chiral precursor or, alternatively, by enantioselective hydrogenation of a prochiral substrate with a chiral catalyst.^{23,24} The former approach was explored by Glorius, who reported a highly efficient diastereoselective Pd-catalyzed hydrogenation of N-(2-pyridyl)-oxazolidinones using chiral oxazolidinone auxiliaries.²⁵ Asymmetric reduction of N-benzyliminopyridinium ylides was achieved by Charette with an iridium phosphinooxazoline complex.²⁶ Although there are several examples of asymmetric pyridine hydrogenation based on chiral-modified heterogeneous catalysts, the *ee* is often

poor.^{27,28} Dissolving metal reductions analogous to the Birch reduction of benzene are also known for pyridine, e.g. reduction of alkylpyridines with Na/NH₃ in the presence of ethanol provides 1,4-dihydropyridines.²⁹

Cycloadditions may also effect dearomatization. Simple pyridines are not observed to participate in thermal electrocyclic reactions, unlike pyridones (which are already somewhat dearomatized). Nevertheless, photochemical cycloadditions of pyridine have been observed, in addition to other photochemical couplings and rearrangements. These reactions are typically quite limited in scope, though some synthetic utility has been realized. Pyridinium salts, for example, may be used to generate 6-azabicyclo[3.1.0]hex-3-en-2-ols via photoreaction.³⁰

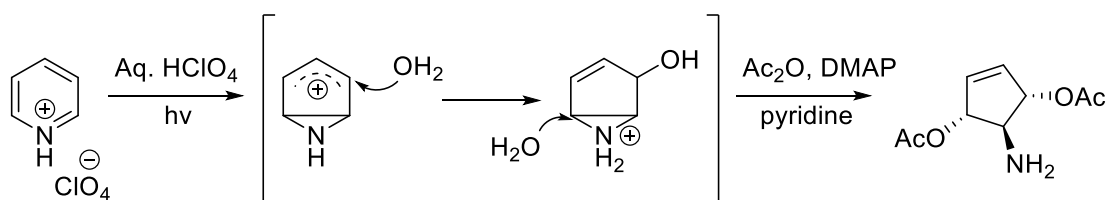


Figure 1.8: Synthesis of a 6-azabicyclo[3.1.0]hex-3-en-2-ol via photoreaction

Organometallic Dearomatization

Transition-metal-mediated dearomatization reactions are fairly well established for benzene and related arenes. Most commonly, these reactions rely upon electrophilic metal complexes, including (Arene)Cr(CO)₃, [(Arene)Mn(CO)₃]⁺, and (Arene)FeCp⁺.^{31,32} Such complexes feature η^6 coordination and are characterized by the strong electron-withdrawing effect of the metal, which activates the arene towards nucleophilic additions. Dihapto-coordinate dearomatization complements this more common methodology.

Bonding in these π -basic η^2 arene complexes is dominated by $d\pi$ to π^* back-bonding, which activates the arene to electrophilic addition.³³

The dearomatization of pyridine via its coordination to a metal is complicated by the typical thermodynamic preference for κN coordination. Although far less common, other coordination modes are known. Pyridine usually behaves as a spectator ligand in its κN complexes, but it is often far more reactive when coordinated η^2 or η^6 . The presence of various substituents can prohibit nitrogen coordination for steric or electronic reasons, allowing access to η^6 or η^2 pyridine complexes.^{34,35} Unsubstituted pyridine has also been coordinated η^6 , typically by specialized or circuitous routes.³⁶ For example, (η^6 -pyridine) $\text{Cr}(\text{CO})_3$ has been prepared by hexahapto coordination of 2,6-bis(trimethylsilyl)pyridine followed by removal of the TMS groups with fluoride. This complex may be deprotonated by LDA and subsequently reacted with MeI to generate the corresponding η^6 2-methylpyridine complex.³⁷ Nucleophiles (DIBAL, RLi) will also add to the α position of the pyridine ligand in (η^6 -pyridine) $\text{Cr}(\text{CO})_3$ to yield dihydropyridines.^{38,39} Ruthenium(II) and molybdenum(0) have also been demonstrated to form an η^6 -pyridine complexes, although without subsequent modification of the pyridine ligand.⁴⁰⁻⁴² These limited examples contrast with the substantial chemistry known for (η^6 -benzene) $\text{Cr}(\text{CO})_3$.

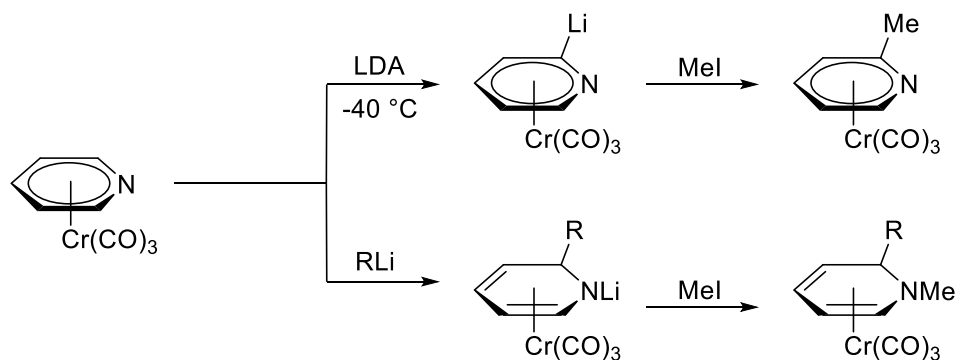


Figure 1.9: Organic transformations of a hexahapto-coordinated pyridine ligand

In most systems with η^2 pyridine coordination, the coordination takes place through nitrogen and an adjacent carbon, rather than two carbon atoms. One such complex is $[\eta^2(\text{N,C})\text{-}2,4,6\text{-NC}_5^t\text{Bu}_3\text{H}_2]\text{Ta}(\text{OAr})_2\text{Cl}$, which is capable of promoting C-N bond cleavage of the bound 2,4,6-tri-*tert*-butylpyridine via reaction with hydride, Grignard, and organolithium nucleophiles.⁴³ A similar tantalum complex with unsubstituted pyridine, $(\text{silox})_3\text{Ta}[(\eta^2\text{-}(\text{N,C})\text{-NC}_5\text{H}_5)]$, is also known,^{44,45} as are the second-row analogs with niobium.⁴⁶ Zirconium-catalyzed coupling of propene and 2-picoline was found to proceed through a $\eta^2(\text{N,C})$ complex, and analogous complexes are also known for yttrium, scandium, and lutetium.⁴⁷⁻⁴⁹

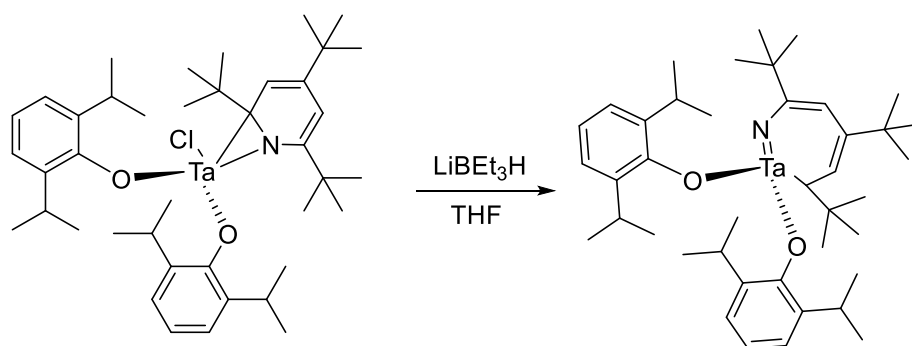


Figure 1.10: Hydride-induced C-N bond cleavage of an $\eta^2(\text{N,C})$ pyridine complex

The $\eta^2(\text{C,C})$ coordination mode of pyridines is rare, with essentially every example provided by the work of W. D. Harman. The osmium(II) system $\{(\text{NH}_3)_5\text{Os}\}^{2+}$ was shown to form an η^2 -coordinate complex with 2,6-lutidine, although this complex undergoes an intramolecular rearrangement to form a lutidinium ylide.⁵⁰ This osmium system was also found to be capable of binding N-protonated and N-methylated pyridiniums, though in all of these cases no modification of the pyridine was possible.⁵¹ The complex $\text{TpRe}(\text{CO})(\text{MeIm})(\eta^2\text{-2,6-lutidine})$ was also synthesized, but no subsequent reactions were carried out with this species.⁵²

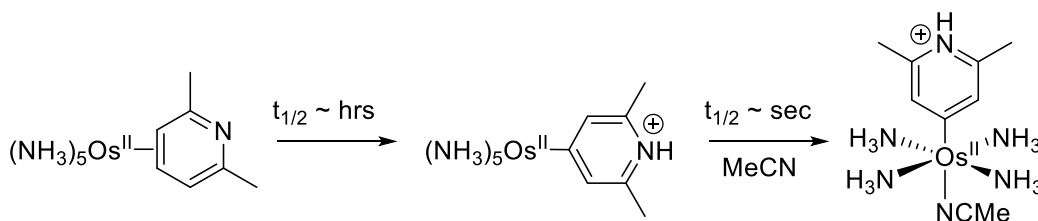


Figure 1.11: Synthesis of an η^2 -lutidine osmium(II) complex and its subsequent reactivity

Unlike with these previous two systems, significant organic utility was demonstrated for the third-generation dearomatization agent, $\{\text{TpW}(\text{NO})(\text{PMe}_3)\}$. This tungsten(0) system appears to have stronger backbonding than any of its predecessors. As a result, the coordinated arene is more activated towards electrophilic addition. A range of η^2 coordinated pyridines were synthesized with this system, generally bearing bulky or electron-donating substituents at the 2-position.⁵³ The parent pyridine complex, $\text{TpW}(\text{NO})(\text{PMe}_3)(3,4\text{-}\eta^2\text{-pyridine})$, was also synthesized via coordination of pyridine-borane and subsequent removal of the borane protecting group.⁵⁴ Although an η^2 to κN isomerization occurs in solution, addition of an N-acetyl group preempts isomerization

and stabilizes the dihapto-coordinate complex. This withdrawing group also activates the complex towards subsequent nucleophilic addition.⁵⁵ The resulting dihydropyridine complexes are amenable to a second tandem electrophilic-nucleophilic addition sequence, yielding highly functionalized tetrahydropyridines.^{56,57} [4+2] cyclocondensations of the dihydropyridine complexes are also possible;⁵⁸ in other cases, the dihydropyridine undergoes a ring-scission reaction to yield η^2 -cyanine and η^2 -merocyanine complexes.⁵⁹

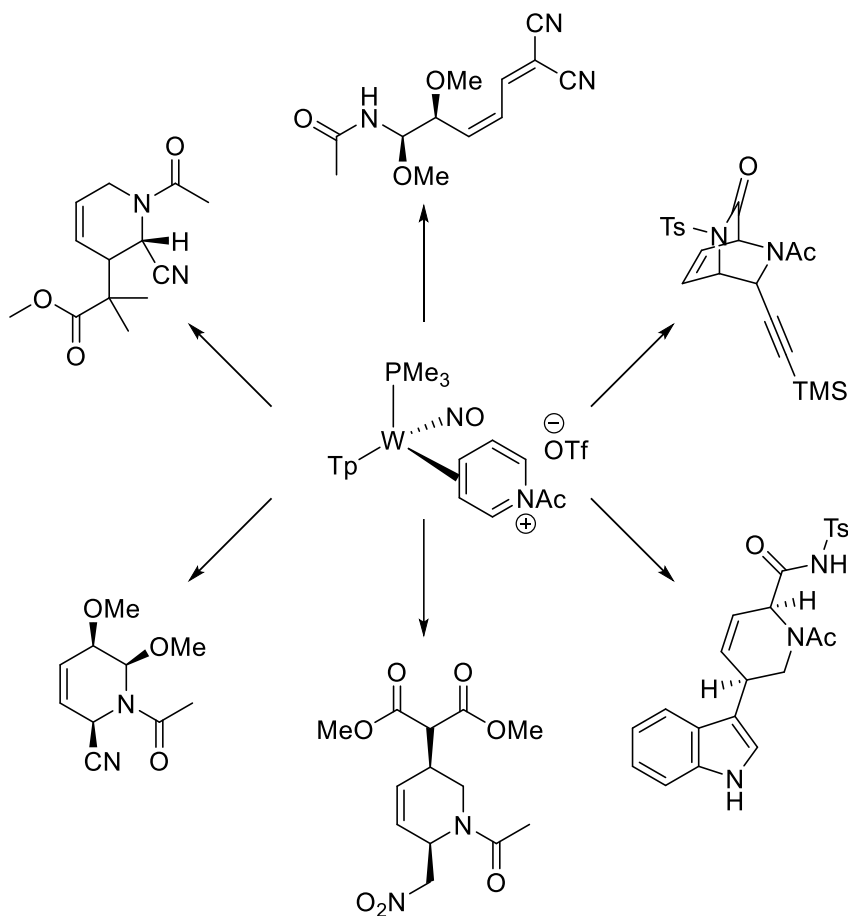


Figure 1.12: Organic molecules produced from derivatization of the tungsten(0) η^2 -N-acetylpiperidinium complex

More limited chemistry with substituted pyridines is also known:

TpW(NO)(PMe₃)(3,4- η^2 -2-(dimethylamino)pyridine) undergoes diprotonation and

subsequent addition of a weak nucleophile (thiophene, 2-methylfuran) to yield amidines.⁶⁰ $\text{TpW}(\text{NO})(\text{PMe}_3)(3,4\text{-}\eta^2\text{-2,6-dimethoxypyridine})$ also takes part in cycloadditions with various electron-poor alkenes and alkynes to provide isoquinuclidines, though isolation of some of the free organics was hindered by their tendency to undergo retro-cycloaddition and ring-opening reactions.⁵⁷ The analogous lutidine complex exhibited similar reactivity, and in this case isolation of the free organic was accomplished.⁶¹

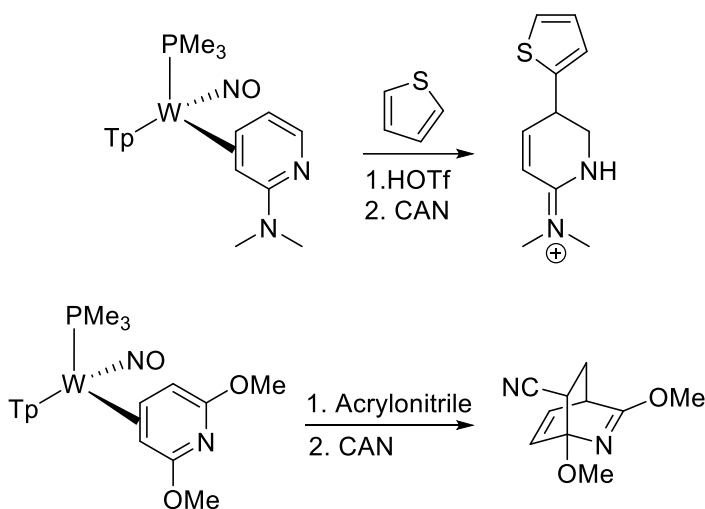


Figure 1.13: Tungsten-promoted dearomatization of electron-rich pyridines

Dihapto coordinate arene complexes of an analogous second row metal complex, $\{\text{TpMo}(\text{NO})(\text{L})\}$ ($\text{L} = 1\text{-methylimidazole, ammonia, or } 4\text{-(dimethylamino)pyridine}$), have also been synthesized, although no examples of a pyridine complex were published prior to the work described herein.^{62,63} Given the weaker backbonding and higher susceptibility to oxidation in this system, it was uncertain whether it would be useful for organic transformations of pyridine ligands. Although not directly derived from pyridine, useful organic chemistry has been demonstrated with molybdenum by Liebeskind, who has, for

example, used $\text{TpMo}(\text{CO})_2(2\text{-oxopyridinyl})$ to generate 2-substituted azabicyclo[3.2.1]octenes via a [5 + 2] cycloaddition reaction. These reactions are stereo- and regioselective, and capable of generating products of high enantiomeric purity.⁶⁴

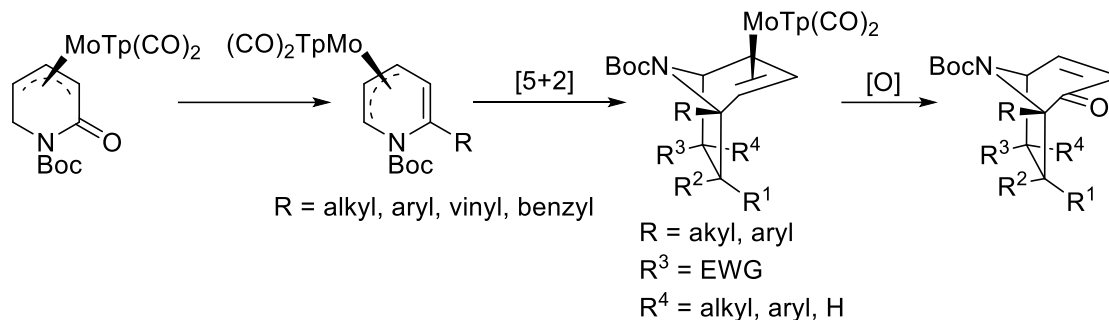


Figure 1.14: Azabicyclo[3.2.1]octene synthesis from a molybdenum 2-oxopyridinyl complex

Liebeskind has also used this organometallic enantiomeric scaffolding approach with (-)- $\text{Tp}(\text{CO})_2[(\eta^3\text{-}2,3,4)\text{-}(1\text{S},2\text{S})\text{-}1\text{-benzyl-oxycarbonyl-5-oxo-5,6-dihydro-2H-pyridin-2-yl)]\text{molybdenum}$ to synthesize 2,6-*cis*-3-*trans* and 2,3,6-*cis* trisubstituted dehydropiperidines,⁶⁵ and to prepare 2,6-disubstituted piperidines in an enantiocontrolled synthesis from *meso*- $\eta^3\text{-}(3,4,5)\text{-dihydropyridinylmolybdenum}$ complexes.⁶⁶

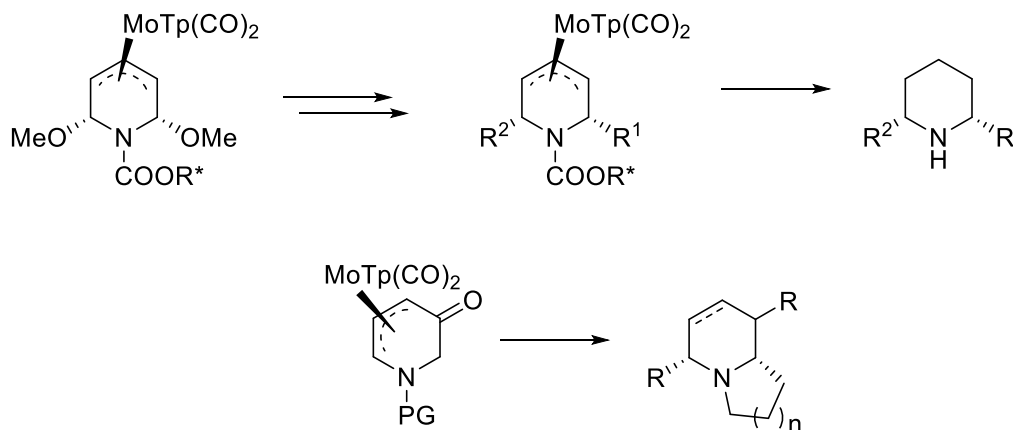


Figure 1.15: Enantiocontrolled synthesis of substituted piperidines via a Mo π -complex

Further Development of Molybdenum and Tungsten Promoted Dearomatization

This document details an effort to expand the range of organic products accessible from organometallic dearomatization. The overall goal of this project was to make dihapto-coordinate dearomatization more appealing to the wider synthetic chemistry community. Throughout, the advantages and limitations of molybdenum- and tungsten-promoted dearomatization were assessed.

It was hoped that the use of a second-row metal would result in synthetically useful changes in reactivity, forming products that were inaccessible with previous metal systems. Novel C,C- η^2 pyridine complexes of molybdenum were synthesized, and their organic transformations were explored. The reactivity of various pyridines bearing electron-withdrawing and electron-donating substituents is discussed in chapter 2. Chapter 3 specifically focuses on the products accessible from the molybdenum 2-(trifluoromethyl)pyridine complex.

We also wished to re-examine the older tungsten system with a new focus on preparing compounds of potential medicinal interest. As discussed in chapter 4, amine nucleophiles were investigated. Amines can be among the most challenging functionalities to incorporate by traditional organic methods, and unique problems were encountered with nucleophilic addition of amines. Furthermore, the synthesis of drug analogs was probed in an attempt to demonstrate the utility of organometallic dearomatization in the synthesis of chemical libraries. Chapter 5 details this aspect of the project, which was conducted with methylphenidate analogs.

Towards this broader goal of producing molecules of potential medicinal interest, a molybdenum η^2 -naphthalene complex was studied; this work is presented in chapter 6. The aim of this project was to develop methods to access complex carbocyclic frameworks, such as those found in steroids. As with the previous chapters, this section seeks to provide synthetic chemists with another tool to generate compounds occupying underrepresented chemical space.

References

- (1) Joule, J. A.; Mills, K. *Heterocyclic Chemistry*; John Wiley & Sons, 2010.
- (2) Foster, J. W.; Moat, A. G. *Microbiological Reviews* **1980**, *44*, 83.
- (3) Vitaku, E.; Smith, D. T.; Njardarson, J. T. *Journal of Medicinal Chemistry* **2014**, *57*, 10257.
- (4) Olah, G. A.; Narang, S. C.; Olah, J. A.; Pearson, R. L.; Cupas, C. A. *Journal of the American Chemical Society* **1980**, *102*, 3507.
- (5) Jain, S. L.; Sain, B. *Chemical Communications* **2002**, 1040.
- (6) Baumgarten, P. *Berichte der deutschen chemischen Gesellschaft (A and B Series)* **1930**, *63*, 1330.
- (7) Popov, A. I.; Rygg, R. H. *Journal of the American Chemical Society* **1957**, *79*, 4622.
- (8) Umemoto, T.; Tomita, K. *Tetrahedron Letters* **1986**, *27*, 3271.
- (9) King, J. A.; Bryant, G. L. *The Journal of Organic Chemistry* **1992**, *57*, 5136.
- (10) Scriven, E. F. V. *Chemical Society Reviews* **1983**, *12*, 129.
- (11) Olah, G. A.; Welch, J. T.; Vankar, Y. D.; Nojima, M.; Kerekes, I.; Olah, J. A. *The Journal of Organic Chemistry* **1979**, *44*, 3872.
- (12) Cañibano, V.; Rodríguez, J. F.; Santos, M.; Sanz-Tejedor, M. A.; Carreño, M. C.; González, G.; García-Ruano, J. L. *Synthesis* **2001**, *2001*, 2175.
- (13) Suzuki, H.; Iwaya, M.; Mori, T. *Tetrahedron Letters* **1997**, *38*, 5647.
- (14) Abramovitch, R. A.; Giam, C.-S. *Canadian Journal of Chemistry* **1964**, *42*, 1627.
- (15) Jamart-Gregoire, B.; Leger, C.; Caubere, P. *Tetrahedron Letters* **1990**, *31*, 7599.
- (16) Gros, P.; Fort, Y.; Caubère, P. *Journal of the Chemical Society, Perkin Transactions I* **1997**, 3597.

- (17) Rouquet, G.; Blakemore, D. C.; Ley, S. V. *Chemical Communications* **2014**, *50*, 8908.
- (18) Trécourt, F.; Breton, G.; Bonnet, V.; Mongin, F.; Marsais, F.; Quéguiner, G. *Tetrahedron* **2000**, *56*, 1349.
- (19) Bull, J. A.; Mousseau, J. J.; Pelletier, G.; Charette, A. B. *Chemical Reviews* **2012**, *112*, 2642.
- (20) L. Comins, D.; Zhang, Y.-m.; Zheng, X. *Chemical Communications* **1998**, 2509.
- (21) Comins, D. L.; Stolze, D. A.; Thakker, F.; McArdle, C. L. *Tetrahedron Letters* **1998**, *39*, 5693.
- (22) Lunn, G.; Sansone, E. B. *The Journal of Organic Chemistry* **1986**, *51*, 513.
- (23) Wang, D.-S.; Chen, Q.-A.; Lu, S.-M.; Zhou, Y.-G. *Chemical Reviews* **2012**, *112*, 2557.
- (24) Glorius, F. *Organic & Biomolecular Chemistry* **2005**, *3*, 4171.
- (25) Glorius, F.; Spielkamp, N.; Holle, S.; Goddard, R.; Lehmann, C. W. *Angewandte Chemie International Edition* **2004**, *43*, 2850.
- (26) Legault, C. Y.; Charette, A. B. *Journal of the American Chemical Society* **2005**, *127*, 8966.
- (27) Blaser, H. U.; Hönig, H.; Studer, M.; Wedemeyer-Exl, C. *Journal of Molecular Catalysis A: Chemical* **1999**, *139*, 253.
- (28) Raynor, S. A.; Thomas, J. M.; Raja, R.; Johnson, B. F. G.; Bell, R. G.; Mantle, M. D. *Chemical Communications* **2000**, 1925.
- (29) Birch, A. J.; Karakhanov, E. A. *Journal of the Chemical Society, Chemical Communications* **1975**, 480.

- (30) Kaplan, L.; Pavlik, J. W.; Wilzbach, K. E. *Journal of the American Chemical Society* **1972**, *94*, 3283.
- (31) Pape, A. R.; Kaliappan, K. P.; Kündig, E. P. *Chemical Reviews* **2000**, *100*, 2917.
- (32) Kundig, E. P. *Transition Metal Arene Complexes in Organic Synthesis and Catalysis*, 2004; Vol. 7.
- (33) Liebov, B. K.; Harman, W. D. *Chemical Reviews* **2017**, *117*, 13721.
- (34) Goti, A.; Semmelhack, M. F. *Journal of Organometallic Chemistry* **1994**, *470*, C4.
- (35) Davies, S. G.; Edwards, A. J.; Shipton, M. R. *Journal of the Chemical Society, Perkin Transactions 1* **1991**, 1009.
- (36) Elschenbroich, C.; Koch, J.; Kroker, J.; Wünsch, M.; Massa, W.; Baum, G.; Stork, G. *Chemische Berichte* **1988**, *121*, 1983.
- (37) Davies, S. G.; Shipton, M. R. *Journal of the Chemical Society, Perkin Transactions 1* **1991**, 501.
- (38) Davies, S. G.; Shipton, M. R. *Journal of the Chemical Society, Chemical Communications* **1989**, 995.
- (39) Davies, S. G.; Shipton, M. R. *Journal of the Chemical Society, Perkin Transactions 1* **1991**, 757.
- (40) Chaudret, B.; Jalon, F. A. *Journal of the Chemical Society, Chemical Communications* **1988**, 711.
- (41) Fish, R. H.; Fong, R. H.; Anh, T.; Baralt, E. *Organometallics* **1991**, *10*, 1209.
- (42) Zhu, G.; Pang, K.; Parkin, G. *Inorganica Chimica Acta* **2008**, *361*, 3221.

- (43) Gray, S. D.; Weller, K. J.; Bruck, M. A.; Briggs, P. M.; Wigley, D. E. *Journal of the American Chemical Society* **1995**, *117*, 10678.
- (44) Neithamer, D. R.; Parkanyi, L.; Mitchell, J. F.; Wolczanski, P. T. *Journal of the American Chemical Society* **1988**, *110*, 4421.
- (45) Covert, K. J.; Neithamer, D. R.; Zonneville, M. C.; LaPointe, R. E.; Schaller, C. P.; Wolczanski, P. T. *Inorganic Chemistry* **1991**, *30*, 2494.
- (46) Veige, A. S.; Kleckley, T. S.; Chamberlin, R. M.; Neithamer, D. R.; Lee, C. E.; Wolczanski, P. T.; Lobkovsky, E. B.; Glassey, W. V. *Journal of Organometallic Chemistry* **1999**, *591*, 194.
- (47) Jordan, R. F.; Taylor, D. F. *Journal of the American Chemical Society* **1989**, *111*, 778.
- (48) Den Haan, K. H.; Wielstra, Y.; Teuben, J. H. *Organometallics* **1987**, *6*, 2053.
- (49) Watson, P. L. *Journal of the Chemical Society, Chemical Communications* **1983**, 276.
- (50) Cordone, R.; Taube, H. *Journal of the American Chemical Society* **1987**, *109*, 8101.
- (51) Cordone, R.; Harman, W. D.; Taube, H. *Journal of the American Chemical Society* **1989**, *111*, 2896.
- (52) Meiere, S. H.; Brooks, B. C.; Gunnoe, T. B.; Carrig, E. H.; Sabat, M.; Harman, W. D. *Organometallics* **2001**, *20*, 3661.
- (53) Delafuente, D. A.; Kosturko, G. W.; Graham, P. M.; Harman, W. H.; Myers, W. H.; Surendranath, Y.; Klet, R. C.; Welch, K. D.; Trindle, C. O.; Sabat, M.; Harman, W. D. *J. Am. Chem. Soc.* **2007**, *129*, 406.

- (54) Harrison, D. P.; Welch, K. D.; Nichols-Nieler, A. C.; Sabat, M.; Myers, W. H.; Harman, W. D. *J. Am. Chem. Soc.* **2008**, *130*, 16844.
- (55) Harrison, D. P.; Zottig, V. E.; Kosturko, G. W.; Welch, K. D.; Sabat, M.; Myers, W. H.; Harman, W. D. *Organometallics* **2009**, *28*, 5682.
- (56) Harrison, D. P.; Sabat, M.; Myers, W. H.; Harman, W. D. *J. Am. Chem. Soc.* **2010**, *132*, 17282.
- (57) Kosturko, G. W.; Harrison, D. P.; Sabat, M.; Myers, W. H.; Harman, W. D. *Organometallics* **2009**, *28*, 387.
- (58) Harrison, D. P.; Iovan, D. A.; Myers, W. H.; Sabat, M.; Wang, S.; Zottig, V. E.; Harman, W. D. *J. Am. Chem. Soc.* **2011**, *133*, 18378.
- (59) Harrison, D. P.; Kosturko, G. W.; Ramdeen, V. M.; Nichols-Nieler, A. C.; Payne, S. J.; Sabat, M.; Myers, W. H.; Harman, W. D. *Organometallics* **2010**, *29*, 1909.
- (60) Pienkos, J. A.; Knisely, A. T.; MacLeod, B. L.; Myers, J. T.; Shivokevich, P. J.; Teran, V.; Sabat, M.; Myers, W. H.; Harman, W. D. *Organometallics* **2014**, *33*, 5464.
- (61) Graham, P. M.; Delafuente, D. A.; Liu, W.; Myers, W. H.; Sabat, M.; Harman, W. D. *Journal of the American Chemical Society* **2005**, *127*, 10568.
- (62) Mocella, C. J.; Delafuente, D. A.; Keane, J. M.; Warner, G. R.; Friedman, L. A.; Sabat, M.; Harman, W. D. *Organometallics* **2004**, *23*, 3772.
- (63) Myers, J. T.; Shivokevich, P. J.; Pienkos, J. A.; Sabat, M.; Myers, W. H.; Harman, W. D. *Organometallics* **2015**, *34*, 3648.
- (64) Garnier, E. C.; Liebeskind, L. S. *Journal of the American Chemical Society* **2008**, *130*, 7449.

(65) Wong, H.; Garnier-Amblard, E. C.; Liebeskind, L. S. *Journal of the American Chemical Society* **2011**, *133*, 7517.

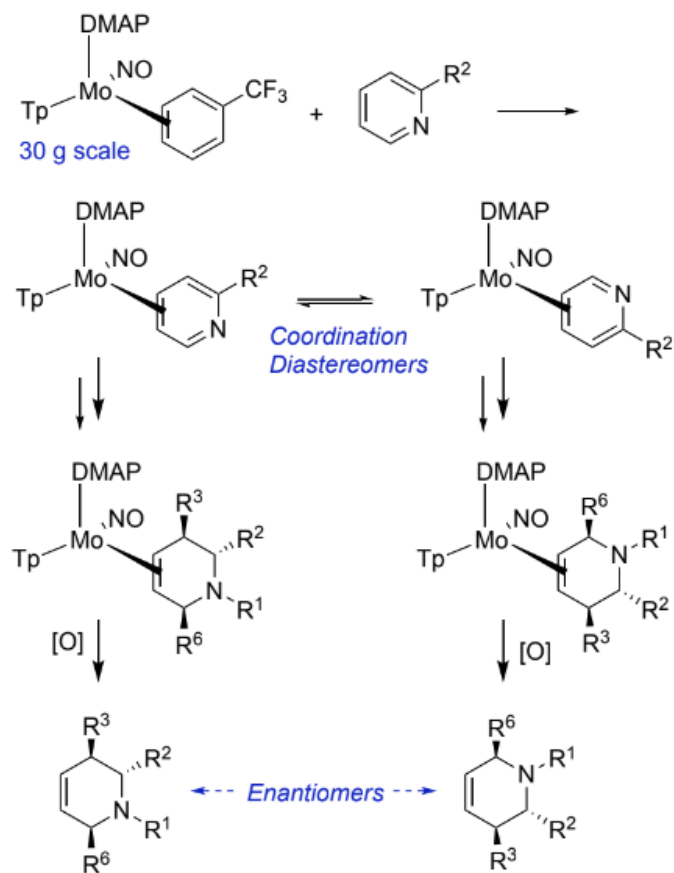
(66) Shu, C.; Liebeskind, L. S. *Journal of the American Chemical Society* **2003**, *125*, 2878.

Chapter 2: Molybdenum-Promoted Dearomatization of Pyridines

Introduction

The coordination of benzene by a transition metal across two carbons (η^2) profoundly affects the chemical reactivity of the aromatic ligand. Such action provides access to a wide range of novel organic transformations for the bound aromatic.¹⁻⁴ The present study originated from an interest to develop a similar synthetic methodology for η^2 -pyridine species. Nitrogen-bound pyridine complexes are ubiquitous in the literature, but other coordination modes are far less common.⁵⁻¹⁴ Especially unusual are dihapto-coordinate pyridine complexes, although several examples are known for heavy-metals.⁸⁻¹⁵ In particular, the tungsten complex $[\text{WTp}(\text{NO})(\text{PMe}_3)(\eta^2\text{-N-acetylpyridinium})]^+$ has been shown to undergo an extensive array of pyridine-based reactions leading to tetrahydropyridines. Limited chemistry with η^2 -pyridines bearing electron-donating substituents has also been reported.¹⁶⁻²²

Known second-row η^2 -pyridine complexes have tended to involve nitrogen (C,N - η^2).^{23,24} However, given the chemical similarities of the $\{\text{WTp}(\text{NO})(\text{PMe}_3)\}$ and $\{\text{MoTp}(\text{NO})(\text{DMAP})\}$ systems (DMAP = 4-(dimethylamino)pyridine; Tp = tris(pyrazolyl)borate),²⁵ we anticipated that C,C - η^2 bound pyridine complexes might be accessible for the latter system.



Scheme 2.1: Synthesis of tetrahydropyridines from pyridine via metal-promoted dearomatization

This publication details the syntheses and a preliminary survey of ligand-centered reactivity for pyridine complexes of the form $\text{MoTp}(\text{NO})(\text{DMAP})(\text{C},\text{C}\text{-}\eta^2\text{-pyridine})$. The ultimate goal of this study is to develop new synthetic routes from pyridines to functionalized tetrahydropyridines via a sequence of molybdenum-directed addition reactions (**Scheme 2.1**). However, given that $\text{MoTp}(\text{NO})(\text{DMAP})(\eta^2\text{-benzene})$ is substantially less stable ($t_{1/2} \sim 30$ sec in solution at 25 °C) than the analogous tungsten complex ($t_{1/2} \sim 1$ h),²⁵ it was uncertain whether such dihapto-coordinate molybdenum

pyridine complexes, with this or any other second-row metal, would be amenable to isolation and subsequent organic transformations.

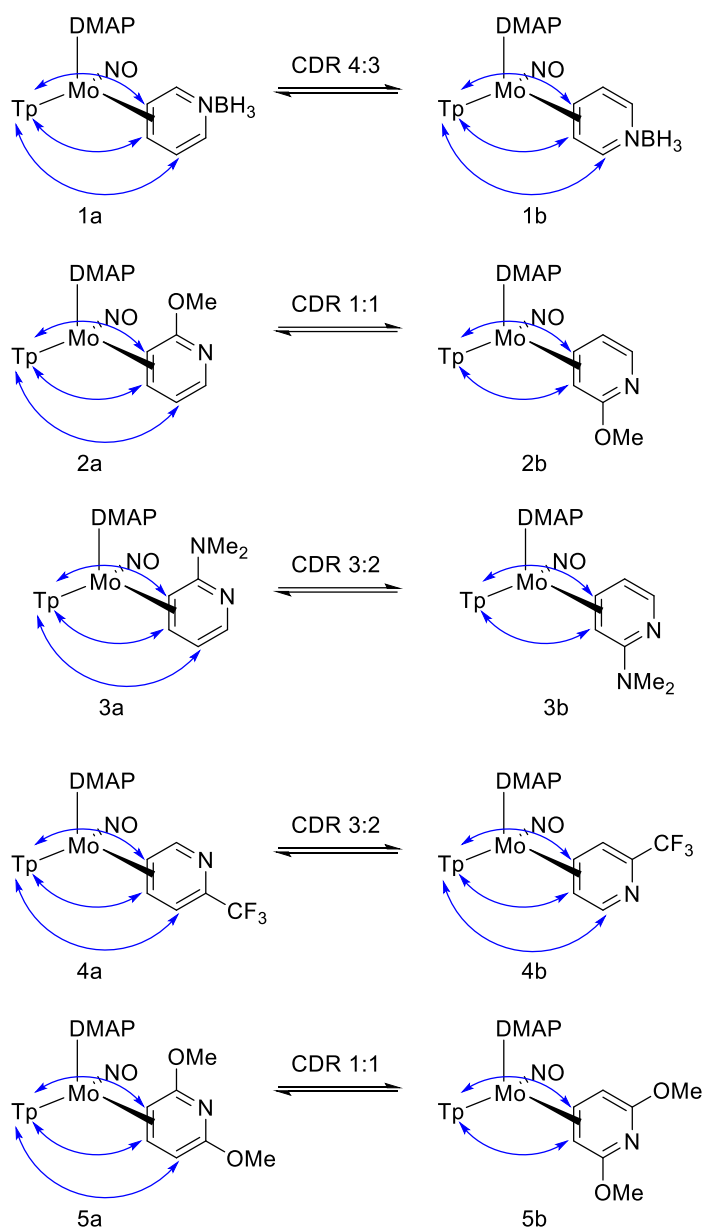
Results

Since nitrogen coordination could preempt the desired dihapto-coordination, various pyridines were tested as possible ligands for {MoTp(NO)(DMAP)} in which either the 2-position or nitrogen was substituted (**Figure 2.1**). Owing to the chemical incompatibility of sodium and pyridines, Mo(0) pyridine complexes cannot be formed cleanly via direct reduction of MoTp(NO)(DMAP)I in a pyridine solution. Instead, the precursor complex MoTp(NO)(DMAP)(η^2 -PhCF₃) was first prepared²⁵ (30 g scale) and then allowed to undergo ligand exchange in a THF solution of pyridine borane (**1a/b**), 2-methoxypyridine (**2a/2b**), 2-(dimethylamino)pyridine (**3a/3b**), 2-(trifluoromethyl)pyridine (**4a/4b**), and 2,6-dimethoxypyridine (**5a/5b**). Complexes **1-5** are all formed as a thermodynamic mixture of coordination diastereomers (Figure 1), differing by which face of the prochiral ligand is coordinated. All compounds were prepared cleanly with coordination diastereomer ratios (cdr) ranging from 1:1 to 3:2, with the exception of the pyridine-borane complex.²⁶ Coordination stereo- and regiochemistry was determined by 1D and 2D ¹H NMR techniques. The protons attached to the metal-bound carbons are significantly more shielded than those in the free ligand due to the influence of the metal. Protons H3 and H4 in complex **4a**, for example, have upfield signals at 3.68 ppm and 3.11 ppm, respectively. Furthermore, these protons have characteristic NOE correlations with a proton of the Tp pyrazole ring trans to the NO. A third NOE correlation is also sometimes present with the “allylic” pyridine proton, away from the DMAP ligand, and a pyrazole ring proton trans to the DMAP (complexes **1a-5a**;

1b, 4b). These NOSEY data, in conjunction with COSY correlations, allowed unambiguous assignment of relative stereochemistries for **1-5**.¹⁵

An ORTEP diagram is provided for the SC-XRD for complex **4a** (**Figure 2.2**), which confirms coordination across C4 and C5. The C4-C5 bond length has been increased to an average of 1.43 Å (cf. 1.40 (CC), 1.34 (CN) Å). Further, expanded C3-C4 (1.42) and C2-N (1.39) bonds and contracted C2-C3 (1.36) and N-C6 (1.30) bonds indicate significant dearomatization.

Cyclic voltammograms of complexes **1-5** revealed $E_{p,a}$ values in the range of +0.05 V to -0.41 V (**Table 2.1**). As anticipated, complexes with more electron-rich pyridine ligands (e.g., **2, 3, 5**) have lower $E_{p,a}$ values and are more readily oxidized. Conversely, the NO stretching frequencies are higher for the more electron-deficient pyridine complexes (e.g., **1, 4**), indicating these ligands are more π -acidic. In cases where comparative data are available, each of these $E_{p,a}$'s was found to be several hundred millivolts more negative than for the analogous tungsten complexes,^{16,27} which indicates that the molybdenum complexes are significantly more sensitive to oxidation. This observation is consistent with the trend noted previously with the related η^2 -PhCF₃ and η^2 -naphthalene complexes of these metals.^{15,25,28}



Key NOE Interactions

Figure 2.1: η^2 -Molybdenum pyridine complexes in equilibrium coordination diastereomer ratio (cdr) and assignment of stereochemistry via NOE interactions

Table 2.1: Cyclic voltammetry and IR data for neutral molybdenum pyridine complexes.

Compound	$E_{p,a}$ (V)	ν_{NO} (cm^{-1})
5	-0.38	1567
3	-0.45	1573
2	-0.27	1577
4	+0.08	1584
1	+0.05	1607
6	+0.53	1601
7	+0.44	1591
8	+0.83	1623

V, NHE @ 100 mV/s in CH_3CN .

Several other pyridines were also screened, including unsubstituted pyridine, 2-picoline, 3-picoline, 4-picoline, 2-ethylpyridine, and 2-isopropylpyridine, all of which coordinated through nitrogen, as evidenced by a chemically reversible couple around $E_{1/2} = -0.9$ V.²⁷ Of note, the reaction of bipy (2,2'-bipyridine) and $\text{MoTp}(\text{NO})(\text{DMAP})(\eta^2\text{-PhCF}_3)$ produces a complex (**28**) that differs significantly in appearance (deep magenta) from the other pyridine complexes (**1-5**, yellow-orange). Electrochemical data indicate a complex that is more reducing ($E_{p,a} = -0.42$ V, NHE), and ^1H NMR data fail to show any upfield ring-protons. These data suggest a complex in which both pyridine rings are bound κN , which would require one of the pyrazole rings of Tp to be displaced from the metal center. This structure was confirmed by SC-XRD (**28**; **Figure 2.3**).

Attempted exchanges of $\text{MoTp}(\text{NO})(\text{DMAP})(\eta^2\text{-PhCF}_3)$ with pyridinium triflate and methylpyridinium triflate were unsuccessful, leading only to oxidation. 2-chloropyridine, 2-fluoropyridine, and 2-hydroxypyridine also resulted in apparent oxidation of the molybdenum, as evidenced by lack of ^1H NMR signals, as well as cyclic voltammetric data inconsistent with either η^2 or κN coordination.

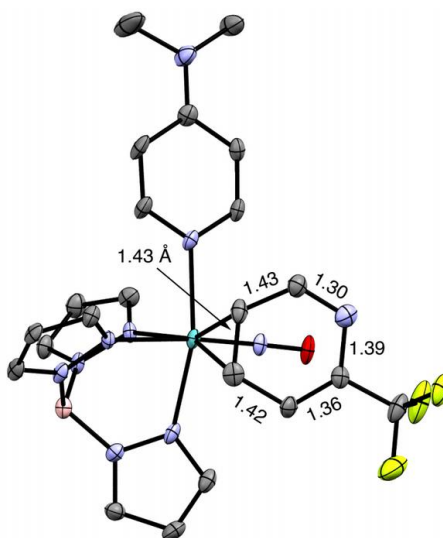


Figure 2.2: ORTEP diagram (50% ellipsoids) of the solid-state structure MoTp(NO)(DMAP)(3,4- η^2 -(2-CF₃)pyridine), showing significant dearomatization

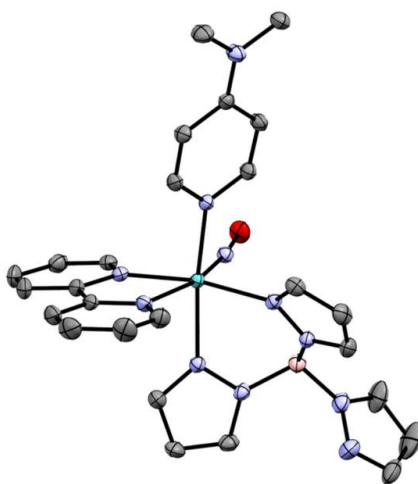
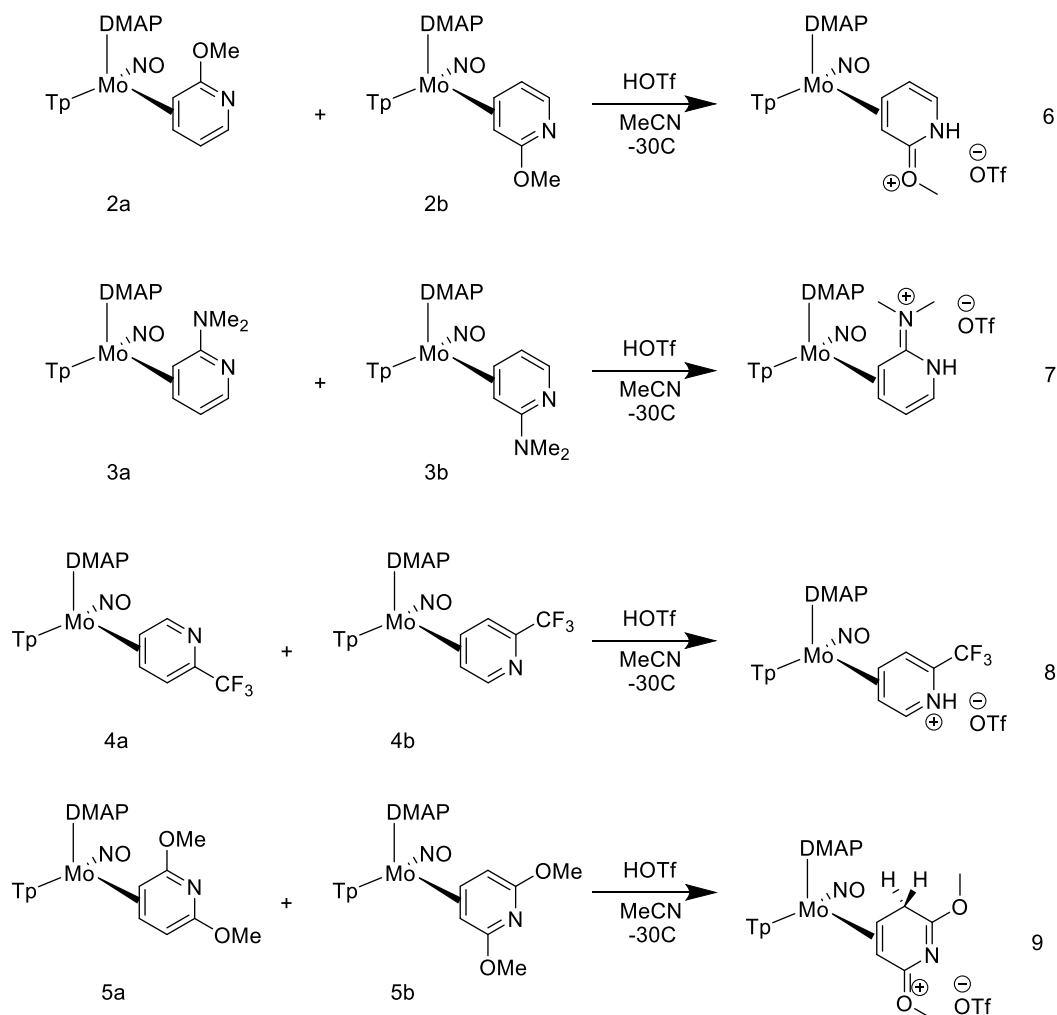


Figure 2.3: ORTEP diagram (50% ellipsoids) of the solid state structure determination of Mo(η^2 -Tp)(NO)(κ^2 -bipy) (**28**). Solvent molecules, H atoms, and non-coordinating bipy omitted for clarity.

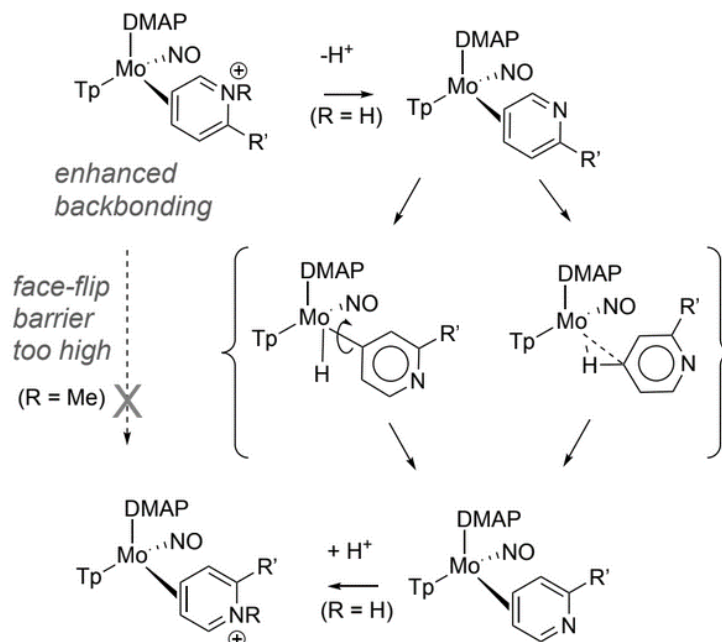
Initial investigations of the reactivity of the dihapto-coordinate pyridine complexes focused on protonation. These molybdenum complexes are highly susceptible to acid oxidation,²⁹ thus *strong* acid and low temperatures are required to ensure complete and irreversible protonation at nitrogen. Once protonated in this manner, the Mo(I)/Mo(0) reduction potential is shifted dramatically positive (*vide infra*), minimizing the chance of metal oxidation. Thus, the complexes of 2-methoxypyridine, 2-(dimethylamino)pyridine, 2-(trifluoromethyl)pyridine, and 2,6-dimethoxypyridine protonate at nitrogen using 0.25 M HOTf in MeCN at -30 °C, as shown in **Scheme 2.2** to yield **6**, **7**, **8** and **9**, respectively. Attempts to protonate at ambient temperature or with weaker acids resulted in immediate oxidation. Cyclic voltammetry of these N-protonated complexes revealed $E_{p,a}$ values shifted significantly positive (~ 800 mV) from those of the neutral precursors (see **Table 2.1**). In addition to protonation at nitrogen (**9N**), the 2,6-dimethoxypyridine complex was found to protonate at carbon to produce complex **9C**, analogous to the chemistry of the related tungsten system.²⁷ A set of diastereotopic methylene protons with a coupling constant of 22.5 Hz was evident in the ¹H NMR spectrum of **9C**. The ratio of carbon protonation to nitrogen protonation in the precipitated solid was 3:1. Significantly, all of the protonated complexes (**6-9**) could be isolated as single coordination diastereomers by equilibrating in MeCN overnight (25 °C), and recovered in modest yield (30-50%). We believe this must occur through the deprotonated form of the pyridinium complex (**Scheme 2.3**), where backbonding interactions are weaker, allowing either a sigma complex or oxidative addition intermediate to form through which intramolecular face-flipping can occur.³⁰ Subsequent

reactions of these protonated complexes with nucleophiles (e.g. NaCN, MeMgBr, lithium dimethylmalonate) returned only starting material or deprotonated product.



Scheme 2.2: Nitrogen and carbon protonation of pyridine complexes.

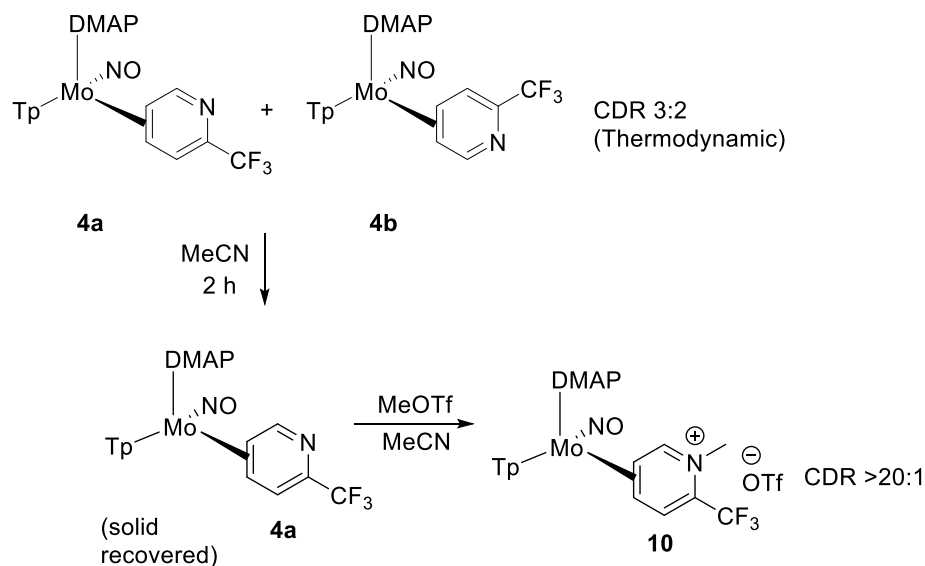
Complexes **2-4** could also be methylated using MeOTf in MeCN (complex **5** was oxidized under these conditions), but once in their methylated forms, interconversion of diastereomers was not thermally accessible, owing to the significantly enhanced backbonding interaction between the molybdenum and η^2 -pyridinium ligand (**Scheme 2.3**).^{16,30} Further, separation by chromatography or solubility differences was unsuccessful making these derivatives impractical for organic modifications.



Scheme 2.3: Intramolecular face-flip isomerization for η^2 -pyridinium complexes (6 – 8; $\text{R} = \text{H}$; $\text{R}' = \text{OMe}, \text{NMe}_2, \text{CF}_3$).

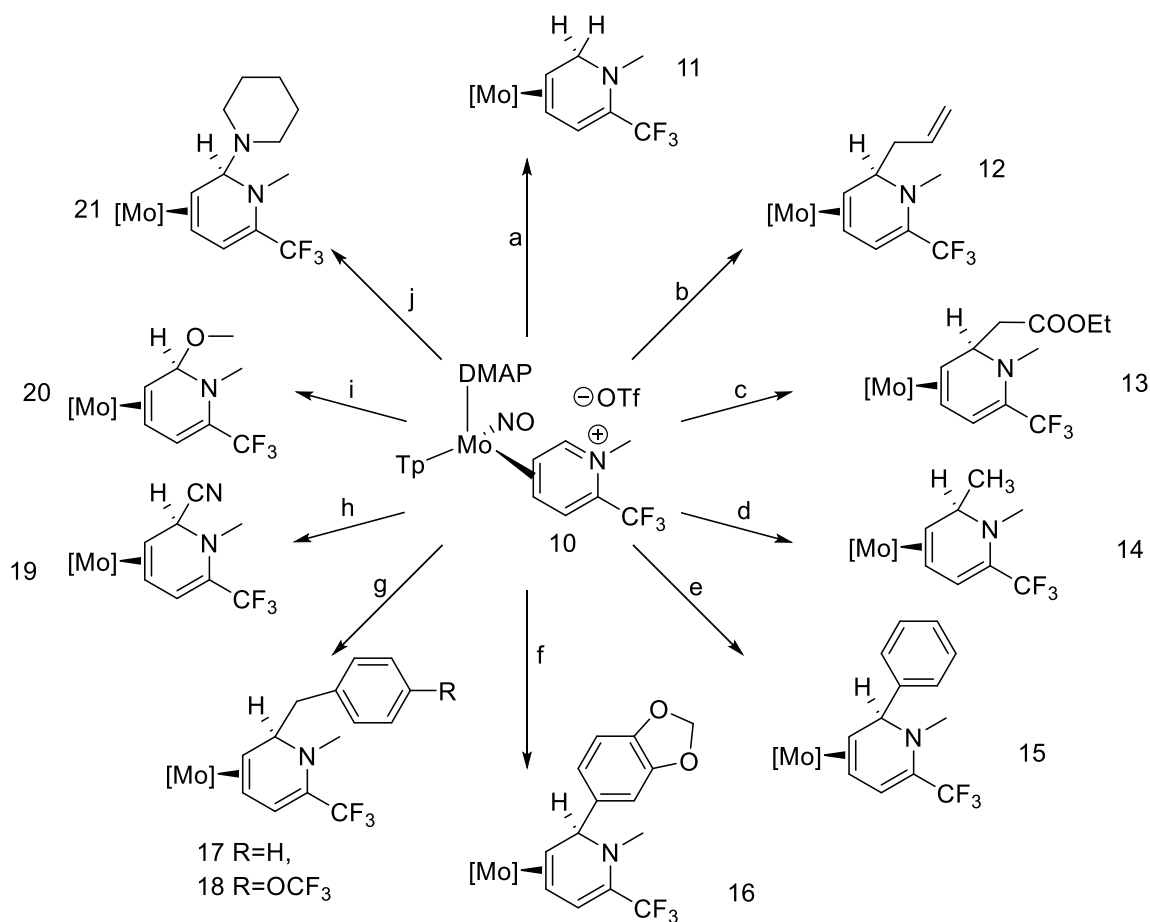
Fortuitously, it was discovered that stirring the *neutral* 2-(trifluoromethyl)pyridine complex **4** in MeCN for 2 h permits facile isolation of a single coordination diastereomer (**4a**) in 70% percent yield. In this case, the driving force for the isomerization is the lower solubility of **4a** compared to **4b** in acetonitrile. Once **4a** is isolated in solid form (SICKUS method),³¹ it is re-introduced into solution containing methyl triflate. Methylation occurs rapidly, pre-empting the reformation of the **4a/4b** equilibrium. The electron-withdrawing trifluoromethyl substituent also appeared to make the complex more resistant to oxidation than the analogues bearing electron-donating groups. Thus, this complex was selected as a model for more thorough exploration of organic reactivity (Scheme 4). Treatment of solid **4a** with MeOTf pre-dissolved in MeCN results in quantitative N-methylation to form complex **10**. Once methylated, isomerization is no

longer an issue on the timescale of organic reactions, with no change in the coordination diastereomer ratio observed by ^1H NMR after 24 h at 25°C in MeCN.



Scheme 2.4: Synthesis of a single coordination diastereomer via Solid-state Induced Control of Kinetically Unstable Isomer (SICKUS) method.³¹

Complex **10** was then subjected to a range of nucleophiles to effect the formation of dihydropyridine complexes (Scheme 5). The reactions were conducted at room temperature using hydride, organomagnesium, and organozinc reagents, among others. In every case, addition was found to take place stereoselectively *anti* to the metal at C2. The details of some of these organic reactions have been disclosed separately.³² Remarkably, these include are cases of amine and alkoxy additions to C2 of pyridine. ORTEP diagrams of the solid-state structures for **20** and **21** are provided in **Figure 2.4**, showing the addition *anti* to metal coordination.



Scheme 2.5: Nucleophilic additions to the methylpyridinium complex. **a:** KBH₄, MeOH (**11**); **b:** BrCH₂CHCH₂, Zn, THF (**12**); **c:** BrCH₂CO₂Et, Zn, THF (**13**); **d:** MeMgBr, THF (**14**); **e:** PhMgBr, THF (**15**); **f:** 3,4-(methylenedioxy)PhMgBr, THF (**16**); **g:** BnMgBr, THF (**17**, **18**); **h:** NaCN, MeCN (**19**); **i:** NBu₄OH, MeOH (**20**); **j:** piperidine (**21**).

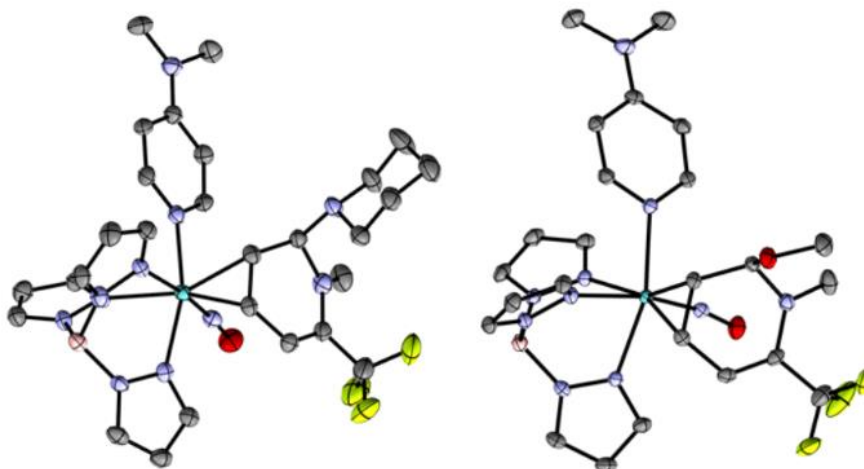
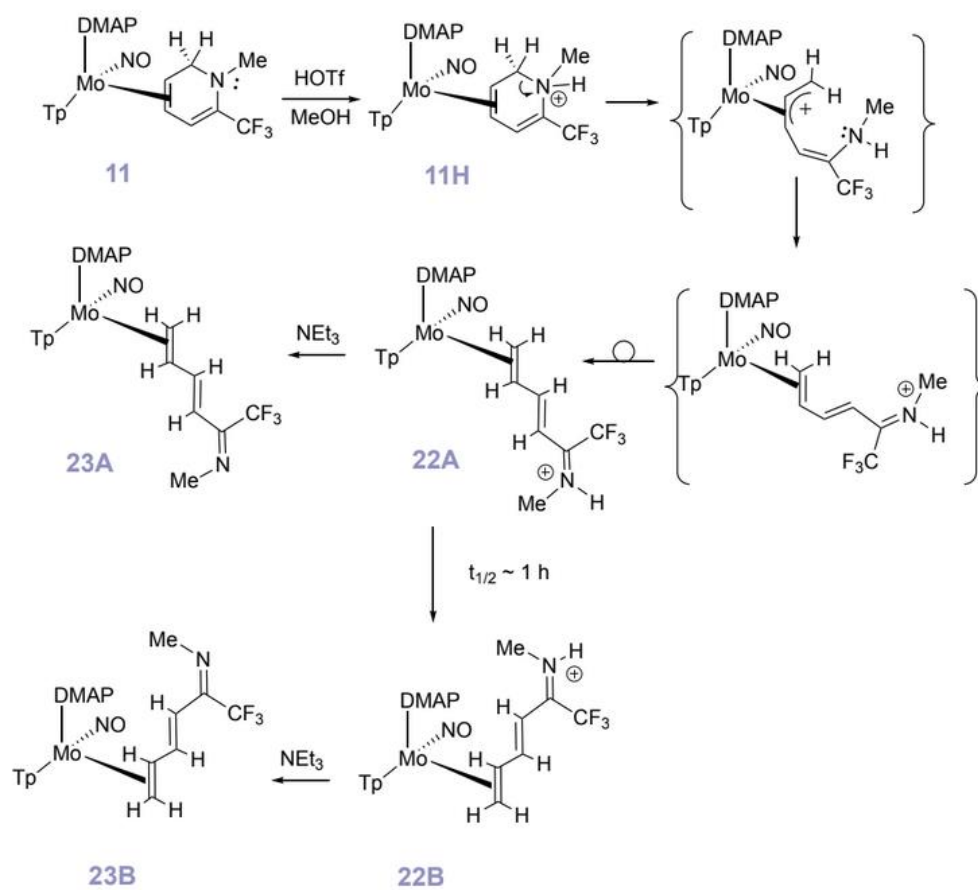


Figure 2.4: ORTEP diagrams of methoxy (**20**) and piperidine (**21**)

additions to pyridinium complex **10**. Hydrogen atoms are omitted for clarity, as is a non-coordinating piperidine molecule in **21**.

Subsequently, the hydride addition product **11** was carried on to further reactions in hopes of finding conditions to perform addition across the remaining uncoordinated double bond (**Scheme 2.1**). Treatment of the η^2 -dienamine **11** with 0.25 M HOTf in MeCN resulted in oxidation of the metal, even at $-40\text{ }^\circ\text{C}$. Attempted protonation with 0.25 M HOTf in MeOH gave an unexpected product, which was ultimately determined to be the ring-opened cation **22** (**Scheme 2.6**). Compound **22** can be deprotonated with NEt_3 to yield the neutral complex **23**. All attempts to convert **11** into a tetrahydropyridine product were ultimately preempted by either oxidation of the $\text{Mo}(0)$ or the ring-opening of **11** to form **22**.



Scheme 2.6: Ring-opening of a dihydropyridine complex (triflate anions omitted).

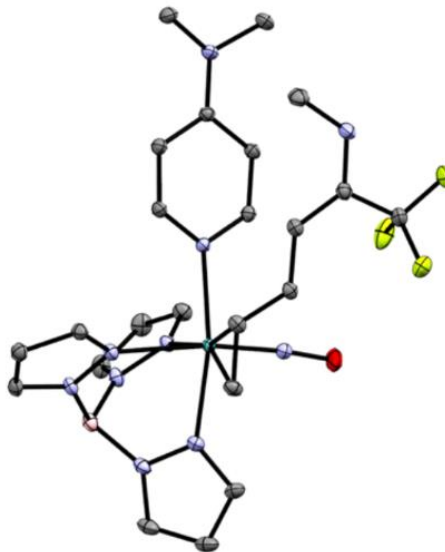
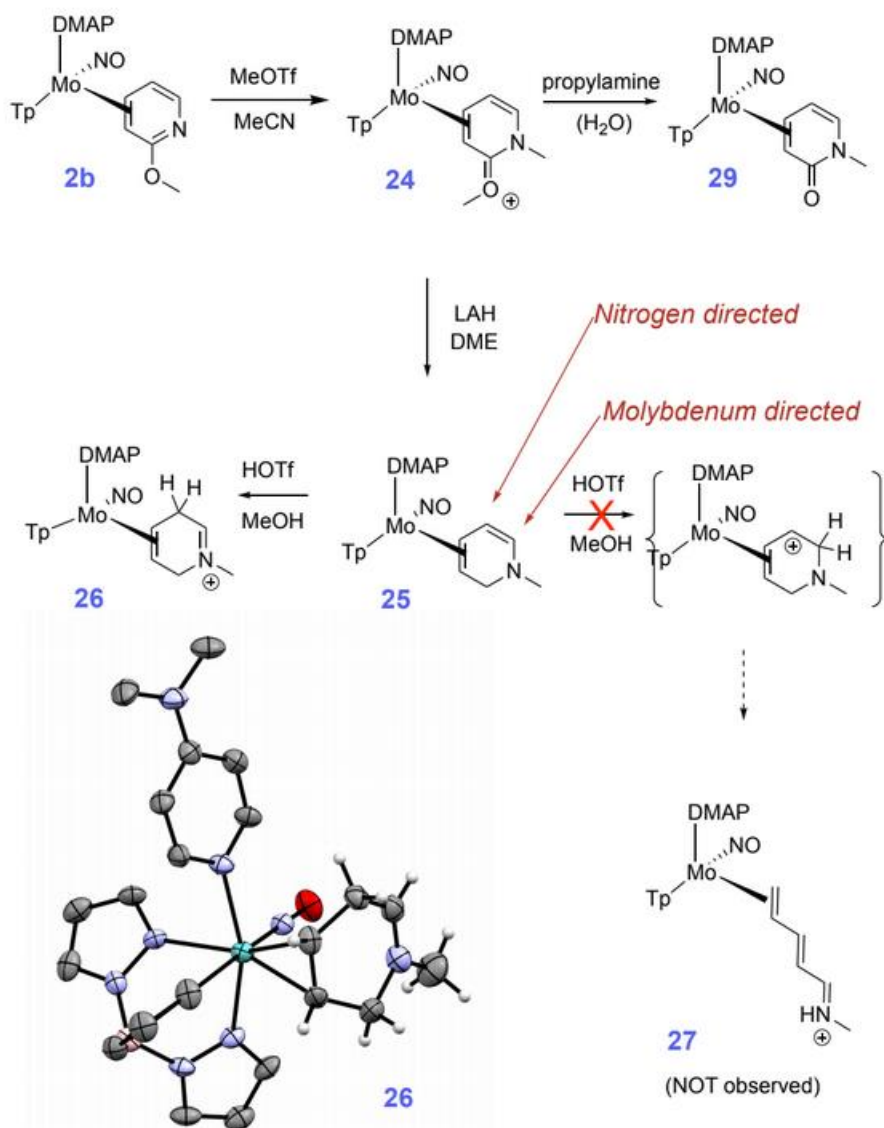


Figure 2.5: ORTEP of ring-opened-complex **22B**. The solvent, triflate anion, and H atoms have been omitted for clarity.

We questioned whether the CF_3 group played an important role in the ring-opening of the methylated dihydropyridinium ligand of **11H**. To get at this issue, the 2-methoxypyridine complex **2b** was first methylated to form the pyridinium salt **24**, then this complex was reduced with LAH in DME. Gratifyingly, reduction of the oxonium was immediately followed by elimination of methanol and a further reduction to the parent methyl dihydropyridine complex **25**. Parenthetically, **24** can also be hydrolyzed to the 1-methyl-2-pyridone complex **29**. Complex **25** was found to be extraordinarily susceptible to oxidation. Not only is the organic ligand in this species an unstabilized enamine, the π -donation from the metal is also a factor. In contrast to the nitrogen protonation observed for **11**, protonation of **25** is driven by the π -donation from the ring-nitrogen into the $\text{C5}=\text{C6}$ bond (i.e., an enamine; **Scheme 2.7**). This reaction provides a rare example of a dihapto-coordinated 1,4-dihydropyridinium complex **26**.

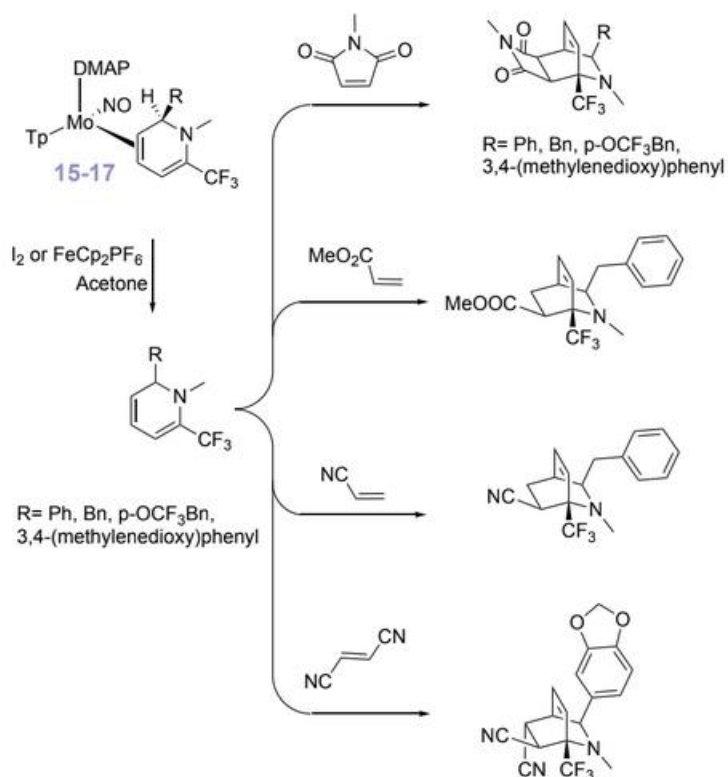


Scheme 2.7: Preparation of the 1-methyldihydropyridine complex **25** and its nitrogen-directed protonation to make an η^2 -1,4-dihydropyridinium complex (**26**).

ORTEP diagram rendered at 50% probability.

Finally, efforts were made to separate a dihydropyridine from the metal center. It was found that the free organics could be obtained in good yield (70-90%) via oxidative decomplexation by treating the dihydropyridine complexes with FeCp₂PF₆ or I₂ in acetone (**Scheme 2.8**). To demonstrate the utility of these molecules in organic synthesis,

several were allowed to undergo a Diels-Alder reaction with various dienophiles. The details for the syntheses of these molecules have been published previously.³³



Scheme 2.8: Oxidative liberation of dihydropyridines and subsequent cycloaddition to generate novel isoquinuclidines.

Discussion

In contrast to the tungsten analog, {TpW(NO)(PMe₃)}, the molybdenum core is less π -basic, resulting in substantial chemical differences. Molybdenum η^2 complexes undergo exchange and isomerization much more readily; for example, while TpW(NO)(PMe₃)(3,4- η^2 -pyridine) converts to its κ N isomer with a half-life of 78 min at 22 °C,²⁷ the corresponding molybdenum complex completely isomerizes within seconds at the same temperature, as determined by cyclic voltammetry. The E_{p,a} values for molybdenum η^2 -pyridine and arene complexes are consistently about 0.4 V more

negative than those of tungsten,^{16,27} signaling increased susceptibility to oxidation. Though such differences give rise to distinct challenges in the molybdenum system, there are several advantages as well. The oxidative decomplexation of the final organic products proceeds under milder conditions (O_2 or I_2),^{25,32} resulting in increased functional group tolerance (functional groups susceptible to oxidants) and higher yields. Processes that rely upon isomerization, such as conversion to a single coordination diastereomer, proceed more quickly, as exploited in the synthesis of the 2-(trifluoromethyl)pyridine complex (**4**).

Synthesizing complexes of η^2 -azatrienes such as **22** directly from the conjugated ligand would be difficult, given the many potential binding sites and stereochemistries. The pyridine ring-opening encountered is reminiscent of the Zincke-König reaction in which highly activated pyridinium salts react with secondary amines to produce, after hydrolysis, 5-amino-2,4-pentadienals.^{34,35} So called “Zincke aldehydes” have been widely used in organic synthesis and their literature has been reviewed.³⁶⁻³⁸ Whereas in the Zincke-König reaction, the amine plays a key role as a π -donor (**Figure 2.6**), in the case of the conversion of **11** to **22B**, the molybdenum itself plays this key role. Thus, an azatriene is formed, lacking the more traditional “push-pull” architecture. Wolczanski et al. have reported the ring scission of dihapto-coordinated pyridines forming a binuclear niobium complex,³⁹ and more recently, a report from our own group demonstrated the formation of η^2 -cyanine and η^2 -merocyanine complexes by treatment of $TpW(NO)(PMe_3)(\eta^2\text{-N-acetylpyridinium})$ with certain nucleophiles.¹⁹ Here it appears that both the O donor and the tungsten are needed to effect ring-cleavage. Returning to molybdenum, the trifluoromethyl substituent on pyridine appears to play a key role in the

ring-opening reaction as well. The parent methyl-dihydropyridine complex was prepared as a control and subjected to HOTf/MeOH, but in this case, without an EWG on either the nitrogen or adjacent ring-carbon, ring scission is not facilitated and only a 2,5-dihydropyridinium complex resulted (**26**). Unfortunately, when ring-opening does occur, it is irreversible and precludes further modification of the dihapto-coordinate ligand, as treatment with nucleophiles (MeMgBr, NaCN, NaBH₃CN) only results in deprotonation.

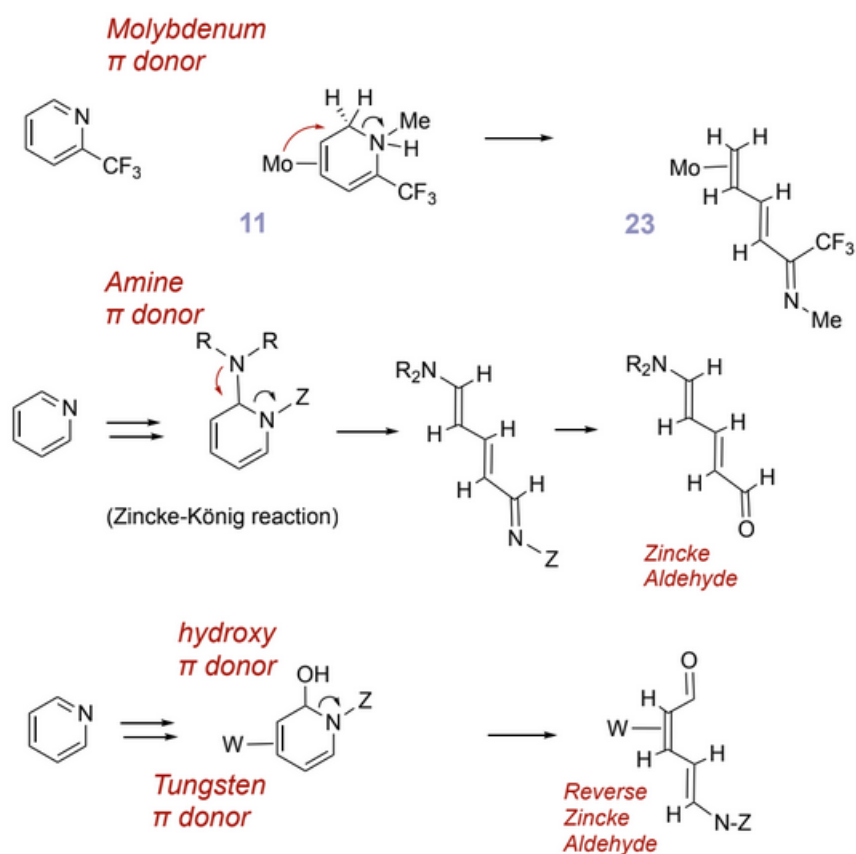


Figure 2.6: Comparison of molybdenum ring-opening to the Zincke-König reaction and a related tungsten reaction.

Conclusion

Molybdenum can successfully form a range of dihapto-coordinate pyridine complexes, which are stable enough to isolate and utilize for subsequent organic

reactions. Although the tetrahydropyridines initially sought were inaccessible with the system that was probed, molybdenum-promoted dearomatization was successful in selectively yielding functionalized 1,2-dihydropyridines, which are useful for an array of organic transformations, as exemplified by the synthesis of isoquinuclidines via Diels-Alder chemistry (*vide supra*). It has also been demonstrated that a single enantiomer of the 2-(trifluoromethyl)pyridine complex may be synthesized, ultimately resulting in enantiopure organic products. Thus, dihapto-coordinate molybdenum chemistry presents a novel way of preparing compounds with potential applications in medicinal chemistry.³²

Experimental Section

General Methods. NMR spectra were obtained on a 600 or 800 MHz spectrometer (22-25 °C). All chemical shifts are reported in ppm, and proton and carbon shifts are referenced to tetramethylsilane (TMS) utilizing residual ¹H or ¹³C signals of the deuterated solvents as an internal standard. Coupling constants (J) are reported in hertz (Hz). Infrared spectra (IR) were recorded as a glaze on a spectrometer fitted with a horizontal attenuated total reflectance (HATR) accessory or on a diamond anvil ATR assembly. Electrochemical experiments were performed under a nitrogen atmosphere. Cyclic voltammetry data were taken at ambient temperature (22-25 °C) at 100 mV/s in a standard three-electrode cell with a glassy carbon working electrode, N,N-dimethylacetamide (DMA) or acetonitrile (MeCN) solvent, and tetrabutylammonium hexafluorophosphate (TBAH) electrolyte (approximately 0.5 M). All potentials are reported versus NHE (normal hydrogen electrode) using cobaltocenium hexafluorophosphate ($E_{1/2} = -0.78$ V), ferrocene ($E_{1/2} = +0.55$ V), or decamethylferrocene ($E_{1/2} = +0.04$ V) as an internal standard. The peak-to-peak separation was less than 100

mV for all reversible couples. Unless otherwise noted, all synthetic reactions were performed in a glovebox under a dry nitrogen atmosphere. Deuterated solvents were used as received. Pyrazole (Pz) protons of the (trispyrazolyl)borate (Tp) ligand were uniquely assigned (e.g., “Pz3B”) using a combination of two-dimensional NMR data and (dimethylamino)pyridine–proton NOE interactions. When unambiguous assignments were not possible, Tp protons were labeled as “Pz3/5 or Pz4”. All J values for Pz protons are 2 (± 0.2) Hz. BH 1H NMR peaks (around 4–5 ppm) are not identified due to their quadrupole broadening; IR data are used to confirm the presence of a BH group (around 2500 cm^{-1}). Compounds **4** and **10-18** are discussed in a subsequent chapter.³³

Synthesis of MoTp(NO)(DMAP)(3,4- η^2 -pyridine-borane) (**1**).

To a 50mL round-bottom flask charged with a stir egg was added MoTp(NO)(DMAP)(η^2 -PhCF₃) (2.04 g, 3.36mmol), followed by pyridine-borane complex (3.10 g, 33.4 mmol) and THF (6.0 mL). This orange mixture was stirred for 3.25 h. The resulting violet solution was added slowly to stirring Et₂O (150 mL). The resulting precipitate was then isolated on a 30 mL fine porosity fritted disc, washed with Et₂O (3 \times 25 mL), and desiccated to yield an orange solid, **1** (1.32 g, 58.9%). CV (DMAc) E_{p,a} = +0.05 V (NHE). IR: $\nu_{\text{NO}} = 1607\text{ cm}^{-1}$. Two coordination diastereomers. **A**:**B** = 4:3 ¹H NMR (d₆-acetone, δ): **A** 8.30 (broad, 1H, H2), 8.06 (d, 1H, PzC5), 8.02 (d, 1H, PzA3), 7.96 (d, 1H, PzA5), 7.90 (d, 1H, PzB5), 7.80 (broad s, 2H, DMAP A), 7.62 (d, 1H, PzC3), 7.02 (d, 1H, PzB3), 6.87 (t, J = 6.3Hz, 1H, H5), 6.77 (d, J = 7.1Hz, 1H, H6), 6.72 (broad s, 2H, DMAP B), 6.40 (t, 1H, PzC4), 6.38 (t, 1H, PzA4), 6.15 (t, 1H, PzB4), 3.63 (dd, J_{H4} = 6.3Hz, J_{H2} = 7.1Hz, 1H, H3), 3.27 (t, J = 6.3, 1H, H4) 3.10 (s, 6H, DMAP Me). **B** 8.54 (broad d, 1H, H2), 8.08 (d, 1H, PzC5), 7.98 (d, 1H, PzA5), 7.91 (d, 1H,

PzB5), 7.83 (d, 1H, PzA3), 7.80 (broad s, 2H, DMAP A), 7.54 (d, 1H, PzC3), 6.94 (d, 1H, PzB3), 6.75 (d, $J = 7.1\text{Hz}$, 1H, H6), 6.72 (broad s, 2H, DMAP B), 6.50 (dd, $J=7.1\text{Hz}$, 6.3Hz , 1H, H5), 6.44 (t, 1H, PzA4), 6.41 (t, 1H, PzC4), 6.15 (t, 1H, PzB4), 3.80 (t, $J = 6.3$, 1H, H4), 3.10 (s, 6H, DMAP Me), 3.06 (dd, $J=6.3\text{Hz}$, 6.0Hz , 1H, H3). ^{13}C NMR (d_6 -acetone, δ): **A** 166.6 (C2), 155.1 (DMAP C), 150.4 (DMAP A), 142.3 (Pz3), 141.6 (Pz3), 141.4 (Pz3), 137.2 (Pz5), 136.7 (Pz5), 135.9 (Pz5), 127.7 (C5), 127.0 (C6), 108.4 (DMAP B), 106.8 (Pz4), 106.5 (Pz4), 106.2 (Pz4), 74.3 (C4), 72.7 (C3), 38.9 (DMAP Me). **B** 167.7 (C2), 155.1 (DMAP C), 150.4 (DMAP A), 144.2 (PzA3), 142.4 (PzB3), 141.0 (PzC3), 137.8 (PzC5), 136.6 (PzA5), 135.2 (PzB5), 127.9 (C5), 127.4 (C6), 108.1 (DMAP B), 106.3 (PzC4), 106.2 (PzA4), 106.1 (PzB4), 77.0 (C4), 70.4 (C3), 38.9 (DMAP Me) Calculated for $\text{C}_{21}\text{H}_{28}\text{B}_2\text{MoN}_{10}\text{O}$: C, 45.52; H, 5.09; N, 25.28. Found: C, 45.17; H, 5.13; N, 24.59.

Synthesis of **MoTp(NO)(DMAP)(3,4- η^2 -2-methoxypyridine) (2)**.

To a 50mL round-bottom flask charged with a stir egg was added $\text{MoTp(NO)(DMAP)(}\eta^2\text{-PhCF}_3\text{)}$ (4.03 g, 6.64 mmol), followed by 2-methoxypyridine (8.30 g, 76.1 mmol) and THF (36.0 mL). This orange mixture was stirred for 4 h. The resulting heterogeneous golden brown mixture was added slowly to stirring Et_2O (300 mL). The resulting precipitate was then isolated on a 60 mL fine porosity fritted disc, washed with Et_2O ($4 \times 30\text{ mL}$), and desiccated to yield a yellow solid, **2** (3.00 g, 79.2%). CV (DMAc) $E_{p,a} = -0.27\text{ V}$ (NHE). IR: $\nu_{\text{NO}} = 1577\text{ cm}^{-1}$. Two coordination diastereomers. **A:B** = 4:3 ^1H NMR (d_6 -acetone, δ): 8.03 (d, 1H, Pz3/5), 8.00 (d, 1H, Pz3/5), 7.92 (d, 1H, Pz3/5), 7.87 (d, 1H, Pz3/5), 7.85 (d, 1H, Pz3/5), 7.75 (bs, 4H, DMAP A **A/B**), 7.51 (d, 1H, Pz3/5), 7.50 (d, 1H, Pz3/5), 6.97 (d, 1H, Pz3/5), 6.95 (d, 1H, Pz3/5),

6.67 (bd, 2H, DMAP B **A/B**), 6.61 (bd, 2H, DMAP B' **A/B**), 6.58 (d, J=6.4Hz, 1H, H6**A**), 6.56 (d, J=6.4Hz, 1H, H6**B**), 6.37 (m, 2H, Pz4), 6.33 (t, 1H, Pz4), 6.26 (t, 1H, Pz4), 6.24 (m, 1H, H5**A**), 6.13 (t, 1H, Pz4), 6.12 (t, 1H, Pz4), 5.85 (m, 1H, H5**B**), 3.79 (s, 3H, H7**B**), 3.65 (dd, J=8.8Hz, 5.5Hz, 1H, H4**B**), 3.62 (s, 3H, H7**A**), 3.28 (d, J=8.8Hz, 1H, H3**A**), 3.23 (dd, J=8.8Hz, 5.5Hz, 1H, H4**A**), 3.08 (s, 6H, DMAP Me **B**), 3.07 (s, 6H, DMAP Me **A**), 2.96 (d, J=8.8Hz, 1H, H3**B**). ¹³C NMR (CDCl₃, δ): 171.4 (C2**B**), 170.7 (C2**A**), 153.9 (DMAP C **B**), 153.8 (DMAP C **A**), 150.7 (broad, DMAP A **A**), 150.1 (DMAP A **B**), 144.0 (Pz3/5), 142.2 (Pz3/5), 142.1 (Pz3/5), 141.9 (Pz3/5), 140.2 (Pz3/5), 139.9 (Pz3/5), 138.7 (Pz3/5), 136.4 (Pz3/5), 136.3 (Pz3/5), 136.0 (Pz3/5), 135.9 (Pz3/5), 134.7 (Pz3/5), 128.4 (C6**A**), 128.0 (C6**B**), 118.2 (C5**A**), 117.3 (C5**B**), 107.4 (DMAP B **B**), 107.4 (DMAP B **A**), 105.9 (Pz4), 105.8 (Pz4), 105.6 (Pz4), 105.5 (Pz4), 105.4 (Pz4), 105.2 (Pz4), 77.2 (C4**B**), 75.4 (C4**A**), 65.0 (C3**A**), 62.4 (C3**B**), 52.4 (C7**A**), 52.1 (C7**B**), 39.3 (DMAP Me). Calculated for C₂₂H₂₇BMoN₁₀O₂: C, 46.33; H, 4.77; N, 24.56. Found: C, 46.23; H, 4.93; N, 24.27.

Synthesis of MoTp(NO)(DMAP)(3,4-η²-2-(dimethylamino)pyridine) (**3**).

To a 4-dram vial charged with a stir pea was added MoTp(NO)(DMAP)(η²-PhCF₃) (2.14 g, 3.52 mmol), followed by 2-(dimethylamino)pyridine (3.10 g, 25.4 mmol) and THF (10.0 mL). This orange mixture was stirred for 16 h. The resulting heterogeneous mixture filtered through a 30 mL fine porosity fritted disc. The isolated solid was washed with Et₂O (4 × 15 mL) and desiccated to yield a yellow solid, **3** (1.58 g, 76.9%). CV (MeCN) E_{p,a} = -0.45 V (NHE). IR: ν_{NO} = 1573 cm⁻¹. Two coordination diastereomers. **A**:**B** = 3:2 ¹H NMR (d₆-acetone, δ, +5 °C): **A** 8.18 (d, 1H, PzC5), 8.15 (d, J= 6.7Hz, 1H, DMAP A), 8.02 (d, 1H, PzA5), 7.92 (d, 1H, PzA3), 7.84 (d, 1H, PzB5), 7.63 (d, 1H, PzC3), 7.09 (d,

J=6.7Hz, 1H, DMAP A'), 6.81 (d, 1H, PzB3), 6.75 (dd, J=6.7Hz, 2.7Hz, 1H, DMAP B), 6.67 (d, J=6.4Hz, 1H, H6), 6.43 (dd, J=6.7Hz, 2.7Hz, 1H, DMAP B'), 6.37 (t, 1H, PzC4), 6.33 (t, 1H, PzA4), 6.09 (t, 1H, PzB4), 5.99 (dd, J=6.4Hz, 5.3Hz, 1H, H5), 3.55 (d, J=9.2Hz, 1H, H3), 3.34 (dd, J=9.2Hz, 5.3Hz, 1H, H4), 3.07 (s, 6H, DMAP Me), 2.61 (broad s, 6H, H7). **B** 8.02 (d, 1H, Pz3/5), 7.93 (d, 1H, Pz3/5), 7.90 (broad s, 2H, DMAP A), 7.82 (d, 1H, Pz3/5), 7.63 (d, 1H, Pz3/5), 7.45 (d, 1H, Pz3/5), 6.87 (d, 1H, Pz3/5), 6.68 (broad s, 2H, DMAP B), 6.66 (d, J=6.4Hz, 1H, H6), 6.38 (t, 1H, Pz4), 6.26 (t, 1H, Pz4), 6.08 (t, 1H, Pz4), 5.63 (dd, J=6.4Hz, 5.3Hz, 1H, H5), 3.67 (dd, J=9.2Hz, 5.3Hz, 1H, H4), 3.08 (s, 6H, DMAP Me), 2.97 (d, J=9.2Hz, 1H, H3), 2.88 (s, 6H, H7). ¹³C NMR (d₂-DCM, δ, 0 °C): **A** 166.5 (C2), 154.3 (DMAP C), 151.6 (DMAP A), 149.9 (DMAP A'), 142.2 (Pz3/5), 142.0 (Pz3/5), 141.0 (Pz3/5), 137.0 (Pz3/5), 136.4 (Pz3/5), 135.1 (Pz3/5), 131.4 (C6), 111.3 (C5), 107.5 (DMAP B'), 106.8 (DMAP B), 106.1 (Pz4), 105.9 (Pz4), 105.8 (Pz4), 75.8 (C4), 62.3 (C3), 39.5 (DMAP Me), 36.8 (broad, C7). **B** 167.2 (C2), 154.3 (DMAP C), 150.0 (broad, DMAP A), 143.0 (Pz3/5), 142.0 (Pz3/5), 140.4 (Pz3/5), 136.7 (Pz3/5), 136.6 (Pz3/5), 135.3 (Pz3/5), 130.1 (C6), 110.2 (C5), 107.7 (DMAP B), 106.4 (Pz4), 106.0 (Pz4), 105.7 (Pz4), 77.8 (C4), 60.7 (C3), 39.5 (DMAP Me), 37.4 (C7). Calculated for C₂₃H₃₀BMoN₁₁O • 1/4 C₄H₁₀O: C, 47.89; H, 5.44; N, 25.60. Found: C, 47.36; H, 5.19; N, 25.24.

Synthesis of MoTp(NO)(DMAP)(3,4-η²-2,6-dimethoxyppyridine) (5).

To a 4-dram vial charged with a stir pea was added MoTp(NO)(DMAP)(η²-PhCF₃) (1.01 g, 1.66 mmol), followed by 2,6-dimethoxyppyridine (2.04 g, 14.66 mmol) and THF (10.0 mL). This heterogeneous mixture was stirred for 3.5 h. The resulting brown heterogeneous mixture was added slowly to stirring Et₂O (100 mL). The resulting

precipitate was isolated on a 30 mL fine porosity fritted disc, washed with Et₂O (4 × 20 mL), and desiccated to yield a yellow solid, **5** (0.784 g, 78.6%). CV (MeCN) E_{p,a} = -0.38 V (NHE). IR: ν_{NO} = 1567 cm⁻¹. Two coordination diastereomers. **A**:**B** = 1:1 ¹H NMR (d₂-DCM, δ, +5 °C): **A** 8.10 (d, 1H, PzA3), 7.83 (d, 1H, PzA5), 7.82 (d, 1H, PzC5), 7.73 (bs, 2H, DMAP A), 7.69 (d, 1H, PzB5), 7.33 (d, 1H, PzC3), 6.95 (d, 1H, PzB3), 6.48 (bs, 2H, DMAP B), 6.32 (t, 1H, PzA4), 6.26 (t, 1H, PzC4), 6.05 (t, 1H, PzB4), 5.46 (d, J=5.8Hz, 1H, H5), 3.75 (s, 3H, H7), 3.74 (s, 3H, H8), 3.42 (dd, J=8.8Hz, 5.8Hz, 1H, H4), 3.16 (d, J=8.8Hz, 1H, H3), 3.01 (s, 6H, DMAP Me). **B** 7.81 (d, 1H, PzC5), 7.80 (d, 1H, PzA3), 7.78 (d, 1H, PzA5), 7.73 (bs, 2H, DMAP A), 7.70 (d, 1H, PzB5), 7.29 (d, 1H, PzC3), 6.95 (d, 1H, PzB3), 6.41 (d, J=5.9Hz, 2H, DMAP B), 6.27 (t, 1H, PzC4), 6.26 (t, 1H, PzA4), 6.05 (t, 1H, PzB4), 5.09 (d, J=5.7Hz, 1H, H5), 3.89 (s, 3H, H7), 3.73 (s, 3H, H8), 3.71 (dd, J=8.8Hz, 5.7Hz, 1H, H4), 3.01 (s, 6H, DMAP Me), 2.93 (d, J=8.8Hz, 1H, H3). ¹³C NMR (d₂-DCM, δ, +5 °C): **A** 172.0 (C2), 154.4 (DMAP C), 154.2 (C6), 150.0 (DMAP A), 142.2 (PzB3), 141.1 (PzA3), 140.8 (PzC3), 136.8 (PzA5), 136.4 (PzC5), 135.2 (PzB5), 107.9 (DMAP B), 106.3 (PzA4), 105.9 (PzC4), 105.8 (PzB4), 89.2 (C5), 77.7 (C4), 62.0 (C3), 54.9 (C7), 52.5 (C8), 39.5 (DMAP Me). **B** 172.4 (C2), 154.7 (DMAP C), 154.0 (C6), 150.8 (DMAP A), 145.5 (PzA3), 142.1 (PzB3), 140.7 (PzC3), 136.8 (PzA5), 136.4 (PzC5), 135.3 (PzB5), 107.1 (DMAP B), 106.3 (PzA4), 105.8 (PzC4), 105.4 (PzB4), 89.0 (C5), 81.0 (C4), 59.2 (C3), 52.9 (C7), 55.0 (C8), 39.5 (DMAP Me). Calculated for C₂₃H₂₉BMoN₁₀O₃: C, 46.02; H, 4.87; N, 23.33. Found: C, 46.28; H, 5.03; N, 23.04.

Synthesis of [MoTp(NO)(DMAP)(3,4-η²-2-methoxypyridinium)]⁺ (OTf) (6**).**

To a 4-dram vial charged with a stir pea was added **2** (508 mg, 0.891 mmol), followed by MeCN (5.0 mL). This mixture was cooled at -30 °C for 15 min. Next, a 1M solution of HOTf/MeCN (1.8 mL, 1.8 mmol) at -30 °C was added to the reaction mixture with stirring, and the resulting yellow mixture was allowed to sit at -30 °C for 15 min. After 15 min, the resulting yellow solution was added slowly to stirring Et₂O (200 mL). The resulting precipitate was isolated on a 30 mL fine porosity fritted disc, washed with Et₂O (4 × 10 mL), and desiccated to yield a yellow solid, **6** (600 mg, 93.5%). CV (MeCN) E_{p,a} = +0.53 V (NHE). IR: ν_{NO} = 1601 cm⁻¹. ¹H NMR (d₆-acetone, δ): 11.10 (bs, 1H, H1), 8.15 (d, 1H, PzC5), 8.10 (d, 1H, PzA5), 7.94 (d, 1H, PzB5), 7.80 (bs, 2H, DMAP A), 7.77 (d, 1H, PzC3), 7.62 (d, 1H, PzA3), 7.03 (d, 1H, PzB3), 6.75 (bs, 2H, DMAP B), 6.50 (t, 1H, PzC4), 6.45 (t, 1H, PzA4), 6.42 (m, 1H, H6), 6.31 (m, 1H, H5), 6.18 (t, 1H, PzB4), 4.17 (dd, J=8.5Hz, 4.5Hz, 1H, H4), 3.80 (s, 3H, H7), 3.14 (s, 6H, DMAP Me), 2.92 (d, J=8.5Hz, 1H, H3). ¹³C NMR (d₆-acetone, δ): 175.9 (C2), 155.6 (DMAP C), 150.4 (DMAP A), 143.8 (PzA3), 143.2 (PzB3), 142.0 (PzC3), 138.6 (PzC5), 138.5 (PzA5), 136.8 (PzB5), 120.8 (C6), 114.2 (C5), 108.9 (DMAP B), 107.8 (PzC4), 107.5 (PzA4), 106.9 (PzB4), 78.2 (C4), 57.9 (C7), 56.1 (C3), 39.2 (DMAP Me). Calculated for C₂₃H₂₈BF₃MoN₁₀O₅S: C, 38.35; H, 3.92; N, 19.44. Found: C, 38.62; H, 4.02; N, 19.52.

Synthesis of [MoTp(NO)(DMAP)(3,4-η²-2-(dimethylamino)pyridinium)]⁺ (OTf) (7**).**

To a 4-dram vial charged with a stir pea was added **3** (500 mg, 0.857 mmol), followed by MeCN (1.2 mL). This mixture was cooled at -30 °C for 15 min. Next, a 1M solution of HOTf/MeCN (1.4 mL, 1.4 mmol) at -30 °C was added to the reaction mixture with stirring, and the resulting yellow mixture was allowed to sit at -30 °C for 5 min. After 5 min, the resulting yellow solution was added dropwise to stirring Et₂O (175 mL). The

resulting precipitate was isolated on a 30 mL fine porosity fritted disc, washed with Et₂O (4 × 20 mL), and desiccated to yield a yellow solid, **7** (577 mg, 91.8%). CV (MeCN) E_{p,a} = +0.44 V (NHE). IR: ν_{NO} = 1591 cm⁻¹. ¹H NMR (d₆-acetone, δ): 9.61 (s, 1H, H1), 8.14 (d, 1H, DMAP A), 8.11 (d, 1H, PzC5), 8.00 (d, 1H, PzA3), 7.98 (d, 1H, PzA5), 7.89 (d, 1H, PzB5), 7.84 (d, 1H, PzC3), 7.16 (d, 1H, DMAP A'), 7.02 (d, 1H, PzB3), 7.01 (dd, 1H, DMAP B), 6.53 (dd, 1H, DMAP B'), 6.45 (t, 1H, PzC4), 6.38 (t, 1H, PzA4), 6.30 (t, 1H, H5), 6.28 (t, 1H, H6), 6.16 (t, 1H, PzB4), 3.40 (d, 1H, H3), 3.30 (s, 3H, H8), 3.23 (dd, 1H, H4), 3.11 (s, 6H, DMAP Me), 2.61 (s, 3H, H7). ¹³C NMR (d₆-acetone, δ): 164.8 (C2), 155.8 (DMAP C), 151.1 (DMAP A), 150.4 (DMAP A'), 143.0 (PzA3), 142.8 (PzB3), 142.2 (PzC3), 138.3 (PzC5), 137.6 (PzA5), 136.3 (PzB5), 115.5 (C5), 115.4 (C6), 109.1 (DMAP B), 108.9 (DMAP B'), 107.5 (PzC4), 106.9 (PzA4), 106.8 (PzB4), 71.8 (C4), 57.2 (C3), 39.3 (DMAP Me), 38.9 (C8), 38.7 (C7). Calculated for C₂₄H₃₁BF₃MoN₁₁O₄S: C, 39.30; H, 4.26; N, 21.01. Found: C, 38.88; H, 4.33; N, 20.59.

Synthesis of [MoTp(NO)(DMAP)(4,5-η²-2-(trifluoromethyl)pyridinium)]⁺ (OTf) (8**).**

To a 4-dram vial charged with a stir pea was added **4A** (500 mg, 0.822 mmol), followed a 0.25M solution of HOTf/MeCN (8.0 mL, 2.0 mmol) at -30 °C. The resulting mixture was stirred briefly and then allowed to sit at -30 °C for 5 min. After 5 min, the resulting solution was added dropwise to stirring Et₂O (175 mL). The resulting precipitate was isolated on a 30 mL fine porosity fritted disc, washed with Et₂O (4 × 20 mL), and desiccated to yield a magenta solid, **8** (540 mg, 86.6%). CV (MeCN) E_{p,a} = +0.83 V (NHE). IR: ν_{NO} = 1623 cm⁻¹. ¹H NMR (d₆-acetone, δ): 8.40 (d, 1H, H6), 8.04 (d, 1H, PzC5), 7.96 (d, 1H, PzA5), 7.86 (d, 1H, PzB5), 7.68 (broad s, 2H, DMAP A), 7.67 (d, 1H, PzA3), 7.54 (d, 1H, PzC3), 7.43 (d, 1H, H3), 7.10 (d, 1H, PzB3), 6.61 (d, 2H, DMAP

B), 6.44 (t, 1H, PzC4), 6.40 (t, 1H, PzA4), 6.16 (t, 1H, PzB4), 3.90 (t, 1H, H5), 3.43 (t, 1H, H4), 3.03 (s, 6H, DMAP Me).

Synthesis of [MoTp(NO)(DMAP)(3,4- η^2 -2,6-dimethoxypyridinium)]⁺ (OTf) (9N and 9C).

To a -30 °C solution of **5** (100 mg, 0.17 mmol) and MeCN (2.0 mL) was added a -30 °C, 1M solution of HOTf/MeCN (0.7 mL, 0.7 mmol). The resulting orange solution was left at -30 °C for 15 min, and subsequently added dropwise to stirring Et₂O (100 mL), yielding a bright orange precipitate. The precipitate was isolated on a 15 mL fine porosity fritted disc, washed with Et₂O (3 x 15 mL), and desiccated to yield **9** (40mg, 32%). CV (DMAc) $E_{p,a} = +0.98$ V (NHE). IR: $\nu_{NO} = 1615$ cm⁻¹. ¹H NMR (d₆-acetone, δ): CV (DMAc) $E_{p,a} = +0.98$ V (NHE). IR: $\nu(\text{C-H sp}^2) = 2954$ cm⁻¹, $\nu(\text{B-H}) = 2511$ cm⁻¹, $\nu(\text{NO}) = 1615$ cm⁻¹. ¹H NMR (d₆-Acetone, δ): 9.93 (1H, bs, N-H **9N**), 8.01 (1H, d, Pz3/5 **9N**), 7.99 (1H, d, Pz3/5 **9N**), 7.98 (1H, d, Pz5A **9C**), 7.93 (1H, d, Pz5C **9C**), 7.82 (1H, d, Pz5B **9C**), 7.74 (1H, d, Pz3C **9C**), 7.73 (2H, buried bs, DMAP-A **9C** and **9N**), 7.58 (1H, d, Pz3/5 **9N**), 7.57 (1H, d, Pz3/5 **9N**), 7.35 (1H, d, Pz3A **9C**), 7.15 (1H, d, Pz3B **9C**), 6.98 (1H, d, Pz3/5 **9N**), 6.83 (2H, m, DMAPB **9N**), 6.66 (2H, bs, DMAP-B **9C**), 6.44 (1H, t, Pz4C **9C**), 6.41 (1H, t, Pz4A **9C**), 6.17 (1H, t, Pz4B **9C**), 6.13 (1H, t, Pz4 **9N**), 5.34 (1H, d, $J = 5.8$, H5 **9N**), 4.22 (3H, s, OMe **9C**), 4.20 (3H, s, OMe **9C**), 4.11 (1H, t, $J = 6.8$, H4 **9N**), 4.04 (1H, dd, $J = 22.5, 8.4$, H5' **9C**), 3.84 (3H, s, OMe **9N**), 3.73 (1H t, $J = 7.9$, H4 **9C**), 3.49 (3H, s, OMe **9N**), 3.47 (1H, dt, $J = 22.5, 1.3$, H5 **9C**), 3.03 (6H, s, NMe **9N**), 3.02 (6H, s, NMe **9C**), 2.94 (1H, dd, $J = 7.9, 1.3$, H3 **9C**) 2.81 (1H, d, $J = 8.3$, H3 **9N**). ¹³C NMR (d₆-Acetone, δ): 191.9 (CO), 186.7 (CO), 155.6 (DMAP-C), 149.9 (2C, DMAP-A), 144.8 (Pz3A), 143.1 (Pz3B), 141.9 (Pz3C), 138.7 (Pz5A/5C), 138.3

(Pz5A/5C), 137.4 (Pz5B), 109.5 (2C, DMAP-B), 107.9 (Pz4A/4C), 107.6 (Pz4A/4C), 107.3 (Pz4B), 71.3 (C4), 58.8 (OMe), 58.4 (OMe), 57.0 (C3), 39.4 (DMAPMe), 33.4 (C5). HRMS: C₂₃H₃₀N₁₀O₃BMo⁺ obsd (%), calcd (%), ppm: 597.1692 (50), 597.1662 (54), 5.0; 599.1664 (55), 599.1659 (49), 0.8; 600.1662 (88), 600.1658 (81), 0.6; 601.1654 (93), 601.1653 (86), 0.2; 602.1664 (87), 602.1666 (75), -0.3; 603.1664 (100), 603.1652 (100), 1.9; 604.1700 (41), 604.1681 (35), 3.2; 605.1690 (41), 605.1672 (39), 3.0.

Synthesis of MoTp(NO)(DMAP)(4,5- η^2 -2-(trifluoromethyl)-6-cyano-N-methyldihydropyridine) (19).

Compound **10** (375 mg, 0.486 mmol) and MeOH (2.0 mL) were combined in a 4 dram vial containing a stir pea. NaCN (83 mg, 1.69 mmol) was added to the resulting solution, and the reaction mixture was stirred for 30 min, during which time solid precipitated. The solid was isolated on a 15 mL fine porosity fritted funnel, and washed with H₂O (3 mL) followed by MeOH (3 x 1.0 mL). The solid was desiccated to yield **19** as a pale orange solid (181 mg, 57%). $E_{p,a} = +0.34$ V (NHE). IR: $\nu_{NO} = 1579$ cm⁻¹. ¹H NMR (d₃-Acetonitrile, δ): 7.88 (d, 1H, PzC5), 7.84 (d, 1H, PzA5), 7.83 (broad s/buried, 2H, DMAP A), 7.83 (d, 1H, PzA3), 7.76 (d, 1H, PzB5), 7.63 (d, 1H, PzC3), 7.15 (d, 1H, PzB3), 6.64 (d, 2H, DMAP B), 6.34 (d, J=6.7Hz, 1H, H3), 6.33 (t, 1H, PzC4), 6.30 (t, 1H, PzA4), 6.14 (t, 1H, PzB4), 4.06 (d, J=1.5Hz, 1H, H6), 3.05 (s, 3H, H7), 3.02 (s, 6H, DMAP Me), 3.01 (dd, J=8.7Hz, 1.5Hz, 1H, H5), 2.41 (dd, J=8.7Hz, 6.7Hz, 1H, H4). ¹³C NMR (d₃-Acetonitrile, δ): 155.4 (DMAP C), 150.6 (DMAP A), 144.5 (PzA3), 142.6 (PzB3), 142.2 (PzC3), 138.0 (PzC5), 137.1 (PzA5), 136.4 (PzB5), 123.7 (q, J=270Hz, CF3), 123.0 (q, J=29.6Hz, C2), 121.7 (CN), 115.0 (q, J=6.6Hz, C3), 109.2 (DMAP B), 107.1 (PzC4),

106.9 (PzA4), 106.9 (PzB4), 76.7 (C5), 56.6 (C6), 54.7 (C4), 39.4 (DMAP Me), 38.4 (C7).

Synthesis of MoTp(NO)(DMAP)(4,5- η^2 -2-(trifluoromethyl)-6-methoxy-N-methyldihydropyridine) (20).

Compound **10** (372 mg, 0.482 mmol) was dissolved in MeOH (0.5 mL) in a 4 dram vial. A 1.0M solution of NEt₄OH in MeOH (0.5 mL) was added to the resulting solution. The reaction mixture was allowed to sit for 30 minutes, resulting in the precipitation of yellow crystals. The crystals were isolated on a 15 mL fine porosity fritted funnel, rinsed with Et₂O (5 mL) and desiccated to yield **20** as a yellow solid (142 mg, 22 %). E_{p,a} = +0.13 V (NHE). IR: $\nu_{\text{NO}} = 1577 \text{ cm}^{-1}$. ¹H NMR (d₃-Acetonitrile, δ): 7.99 (broad s, 2H, DMAP A), 7.87 (d, 1H, PzC5), 7.86 (d, 1H, PzA3), 7.82 (d, 1H, PzA5), 7.76 (d, 1H, PzB5), 7.57 (d, 1H, PzC3), 7.20 (d, 1H, PzB3), 6.64 (d, 2H, DMAP B), 6.32 (t, 1H, PzC4), 6.28 (t, 1H, PzA4), 6.17 (d, J=6.4Hz, 1H, H3), 6.14 (t, 1H, PzB4), 4.46 (d, J=1.5Hz, 1H, H6), 3.26 (s, 3H, H7), 3.17 (s, 3H, H8), 3.01 (s, 6H, DMAP Me), 2.94 (dd, J=9.2Hz, 1.5Hz, 1H, H5), 2.48 (dd, J=9.2Hz, 6.4Hz, 1H, H4). ¹³C NMR (d₃-Acetonitrile, δ): 155.0 (DMAP C), 151.1 (DMAP A), 144.0 (PzA3), 142.3 (PzB3), 141.7 (PzC3), 137.8 (PzC5), 136.9 (PzA5), 136.2 (PzB5), 124.3 (CF₃, J_{CF}=270.1Hz), 123.8 (C2, J_{CF}=28.5Hz), 113.0 (C3, J_{CF}=6.3Hz), 109.0 (DMAP B), 107.1 (PzC4), 106.7 (PzA4), 106.7 (PzB4), 95.6 (C6), 77.1 (C5), 59.3 (C4), 52.7 (C8), 39.6 (C7), 39.4 (DMAP Me).

Synthesis of MoTp(NO)(DMAP)(4,5- η^2 -2-(trifluoromethyl)-6-(piperidin-1-yl)-N-methyldihydropyridine) (21).

Compound **10** (102 mg, 0.132 mmol) and piperidine (110 mg, 1.29mmol) were added to a 4 dram vial. Within minutes, yellow crystals began to precipitate from solution. After

30 minutes, added a 1.0M solution of potassium t-butoxide in 2-propanol (0.14 mL). Isolated the crystals on a 15 mL fine porosity fritted funnel. Desiccated the collected material to yield **21** as a yellow solid (93 mg, 41%). $E_{p,a} = +0.12$ V (NHE). IR: $\nu_{NO} = 1576$ cm^{-1} . ^1H NMR (d_3 -Acetonitrile, δ): 8.03 (broad s, 2H, DMAP A), 7.87 (d, 1H, PzC5), 7.86 (d, 1H, PzA3), 7.81 (d, 1H, PzA5), 7.76 (d, 1H, PzB5), 7.54 (d, 1H, PzC3), 7.20 (d, 1H, PzB3), 6.63 (d, 2H, DMAP B), 6.34 (t, 1H, PzC4), 6.27 (t, 1H, PzA4), 6.13 (t, 1H, PzB4), 5.89 (d, $J=6.4\text{Hz}$, 1H, H3), 4.04 (d, $J=1.0\text{Hz}$, 1H, H6), 3.16 (s, 3H, H7), 3.00 (s, 6H, DMAP Me), 2.76 (broad t, 2H, H8), 2.74 (dd, $J=9.6\text{Hz}$, 1.0Hz , 1H, H5), 2.47 (dd, $J=9.6\text{Hz}$, 6.4Hz , 1H, H4), 2.41 (broad t, 2H, H8'), 1.44 (m, 4H, H9), 1.39 (m, 2H, H10). ^{13}C NMR (d_3 -Acetonitrile, δ): 155.1 (DMAP C), 151.0 (DMAP A), 143.7 (PzA3), 142.4 (PzB3), 141.6 (PzC3), 137.8 (PzC5), 137.0 (PzA5), 136.4 (PzB5), 126.6 (q, $J=29.7\text{Hz}$, C2), 124.2 (q, $J=270\text{Hz}$, CF3), 110.6 (q, $J=6.5\text{Hz}$, C3), 108.9 (DMAP B), 83.8 (C6), 74.1 (C5), 60.3 (C4), 49.6 (C8), 40.4 (C7), 39.4 (DMAP Me), 27.3 (C9), 26.0 (C10).

Synthesis of ring-opened allyl (**22**).

To a 4-dram vial charged with a stir pea, added **11** (114 mg, 0.183 mmol) followed by a 0.25 M solution of HOTf/MeOH (0.90 mL, 0.22 mmol), resulting in an immediate color change from yellow to vibrant orange. The resulting solution was allowed to stir 5 min, and subsequently added dropwise to stirring Et₂O (50 mL). The precipitate was isolated on a 15 mL fine porosity fritted disc, washed with Et₂O (3 × 5 mL), and desiccated to yield a vermilion solid, **22**, as a mixture of isomers (56 mg, 38.3%). Nearly exclusively the 'B' isomer can be isolated by letting the reaction mixture stir for 24 h before precipitation. CV (DMAc) $E_{p,a} = +0.70$ V (NHE). IR: $\nu_{NO} = 1627$ cm^{-1} . ^1H NMR (d_4 -

MeOD, δ): **A** 8.06 (d, 1H, PzC5), 8.02 (d, 1H, PzA5), 8.00 (very broad s, 2H, DMAP A), 7.96 (d, 1H, PzC3), 7.87 (d, 1H, PzB5), 7.47 (d, 1H, PzA3), 7.24 (t, 1H, H4), 7.10 (d, 1H, PzB3), 6.61 (broad s, 2H, DMAP B), 6.51 (t, 1H, PzC4), 6.41 (t, 1H, PzA4), 6.20 (t, 1H, PzB4), 5.28 (d, 1H, H3), 4.35 (ddd, 1H, H5), 3.81 (dd, 1H, H6a), 3.53 (dd, 1H, H6b), 3.05 (broad s, 6H, DMAP Me), 2.83 (s, 3H, H7). **B** 8.10 (d, 1H, PzC3), 8.00 (d, 1H, PzC5), 7.89 (broad s, 2H, DMAP A), 7.86 (d, 1H, PzA5), 7.81 (d, 1H, PzB5), 7.81 (d, 1H, PzA3), 7.53 (d, 1H, PzB3), 7.28 (t, 1H, H4), 6.70 (d, 2H, DMAP B), 6.47 (t, 1H, PzC4), 6.35 (t, 1H, PzA4), 6.19 (t, 1H, PzB4), 5.09 (d, 1H, H3), 4.98 (ddd, 1H, H5), 3.39 (dd, 1H, H6b), 3.07 (s, 6H, DMAP Me), 2.96 (dd, 1H, H6a), 2.59 (s, 3H, H7). ^{13}C NMR (d_4 -MeOD, δ): **A** 162.7 (C4), 155.9 (DMAP C), 150.8 (broad, DMAP A), 149.4 (q, $J=32.0\text{Hz}$, C2), 145.3 (PzA3), 144.0 (PzB3), 142.5 (PzC3), 139.6 (PzC5), 138.6 (PzA5), 137.3 (PzB5), 121.8 (q, $J=270\text{Hz}$, CF3), 109.0 (DMAP A), 108.2 (PzC4), 108.7 (PzA4), 107.3 (PzB4), 101.7 (C3), 95.0 (C5), 75.4 (C6), 39.3 (DMAP Me), 30.8 (C7). **B** 161.0 (C4), 155.5 (DMAP C), 151.0 (broad, DMAP A), 148.7 (q, $J=32.4\text{Hz}$, C2), 144.5 (PzA3), 143.5 (PzB3), 143.5 (PzC3), 138.7 (PzC5), 137.5 (PzA5), 137.2 (PzB5), 121.0 (q, $J=275\text{Hz}$, CF3), 109.1 (DMAP A), 107.8 (PzC4), 107.7 (PzA4), 107.5 (PzB4), 99.1 (C3), 94.8 (C5), 73.4 (C6), 39.3 (DMAP Me), 30.8 (C7).

Synthesis of ring opened compound (23A).

To a 4-dram vial charged with a stir pea, added **11** (114 mg, 0.183 mmol) followed by a 0.25 M solution of HOTf/MeOH (0.90 mL, 0.22 mmol), resulting in an immediate color change from yellow to vibrant orange. The resulting solution was allowed to stir 5 min, and then triethylamine (50.6 mg, 0.50 mmol) was added. The reaction mixture was stirred for 1 min, and subsequently evaporated. The residue was dissolved in minimal DCM and

added dropwise to stirring Et₂O (25 mL). The precipitate was isolated on a 15 mL fine porosity fritted disc, washed with Et₂O (3 × 5 mL), and desiccated to yield an orange solid, **23A**, (35 mg, 31%). $E_{p,a} = +0.42$ V (NHE). ¹H NMR (d₃-Acetonitrile, δ): 7.91 (d, 1H, PzC5), 7.88 (d, 1H, PzA5), 7.81 (d, 1H, PzB5), 7.61 (d, 1H, PzA3), 7.59 (broad s, 2H, DMAP A), 7.58 (d, 1H, PzC3), 7.09 (d, 1H, PzB3), 6.86 (m, 1H, H4), 6.51 (d, 2H, DMAP B), 6.34 (t, 1H, PzC4), 6.27 (t, 1H, PzA4), 6.15 (t, 1H, PzB4), 5.48 (d, 1H, H3), 3.16 (s, 3H, H7), 2.98 (s, 6H, DMAP Me), 2.89 (dd, 1H, H5), 2.69 (dd, 1H, H6a), 2.69 (dd, 1H, H6b). ¹³C NMR (d₃-Acetonitrile, δ): 157.1 (C4), 155.3 (C2, $J_{CF} = 30.1$ Hz), 155.2 (DMAP C), 151.3 (DMAP A), 143.7 (PzA3), 143.1 (PzB3), 141.7 (PzC3), 138.0 (PzA5), 137.8 (PzC5), 136.7 (PzB5), 122.0 (CF₃, $J_{CF} = 278$ Hz) 108.5 (DMAP B), 107.3 (PzC4), 107.1 (PzB4), 106.9 (PzA4), 106.6 (C3), 73.3 (C5), 66.2 (C6), 39.5 (DMAP Me), 38.1 (C7).

Synthesis of [MoTp(NO)(DMAP)(3,4-η²-2-methoxy-N-methylpyridinium)]⁺ (OTf) (24).

To a 4-dram vial was added **2** (1.0 g, 1.7 mmol), CH₃CN (5 mL), and MeOTf (400 mg, 2.44 mmol). This orange mixture was left sitting at room temperature for 10 min, yielding a dark red solution. This solution was added to stirring Et₂O (100 mL) to yield a red precipitate, which was then isolated on a 30 mL fine porosity fritted disc, washed with Et₂O (3x30 mL), and desiccated to yield the dark orange product **24** (1.72 g, 89% yield). CV (DMAc) $E_{p,a} = +0.79$ V (NHE). IR: $\nu(\text{C-H sp}^2) = 3105$ cm⁻¹, $\nu(\text{B-H}) = 2484$ cm⁻¹, $\nu(\text{NO}) = 1596$ cm⁻¹. Product isolated as a 3:1 **A**:**B** ratio. ¹H NMR (d₆-Acetone, δ): 8.27 (1H, d, $J = 7.3$, DMAP-A **B**), 8.16 (1H, d, Pz5C **A**), 8.15 (1H, d, Pz5A **A**), 8.13 (1H, d, Pz3/5 **B**), 8.20 (1H, d, Pz3/5 **B**), 7.96 (1H, d, Pz3/5 **B**), 7.94 (1H, d, Pz3/5 **B**), 7.93

(1H, d, Pz5B **A**), 7.79 (2H, bs, DMAP-B **A**), 7.74 (1H, d, Pz3C **A**), 7.65 (1H, d, Pz3A **A**), 7.28 (1H, d, $J = 7.3$, DMAP **A** **B**), 7.09 (1H, d, Pz3B **B**), 7.02 (1H, bs, DMAP-B **B**), 7.00 (1H, d, Pz3B **A**), 6.75 (2H, bs, DMAP-B **A**), 6.61 (1H, bs, DMAP-B **B**), 6.51 (1H, t, Pz4C **A**), 6.49 (1H, t, Pz4A **A**), 6.48 (1H, t, Pz4 **B**), 6.43 (1H, d, $J = 7.2$, H6 **A**), 6.34 (1H, t, $J = 6.3$, H5 **A**), 6.39 (1H, t, Pz4 **B**), 6.18 (1H, t, Pz4 **B**), 6.17 (1H, t, Pz4B **A**), 4.21 (1H, dd, $J = 8.6, 6.3$, H4 **A**), 3.75 (3H, s, NMe **A**), 3.69 (1H, d, $J = 8.6$, H3 **B**), 3.54 (1H, dd, $J = 8.6, 5.8$, H4 **B**), 3.50 (3H, s, OMe **A**), 3.12 (6H, s, NMe **A**), 3.00 (1H, d, $J = 8.6$, H3 **A**).

^{13}C NMR (d_6 -Acetone, δ) **A**: 175.7 (OMe), 155.89 (DMAP-C), 150.5 (2C, DMAP-A), 143.9 (Pz3A), 143.2(Pz3B), 142.1 (Pz3C), 138.9 (Pz5A/5C), 138.6 (Pz5A/5C), 136.9 (Pz5B), 120.9 (C5/C6), 120.8 (C5/C6), 109.1 (2C, DMAP-B), 108.1 (Pz4A/4C), 107.9 (Pz4A/4C), 106.9 (Pz4B), 78.1 (C4), 58.5 (OMe), 55.9 (C3), 39.3 (DMAP-Me), 37.3 (NMe). **B** (signals are too small for unambiguous assignment): 175.6, 155.9, 150.2, 143.0, 142.5, 138.5, 137.8, 136.5, 121.5, 121.2, 108.9, 107.7, 107.0, 106.9, 76.7, 66.1, 58.3, 56.4, 39.3, 29.8, 15.6. HRMS: $\text{C}_{23}\text{H}_{30}\text{N}_{10}\text{O}_2\text{BMo}^+$ obsd (%), calcd (%), ppm: 581.1728 (49), 581.1713 (54), 2.6; 583.1713 (48), 583.1710 (49), 0.6; 584.1723 (75), 584.1709 (81), 2.4; 585.1716 (85), 585.1704 (86), 2.1; 586.1716 (73), 586.1716 (74), -0.1; 587.1721 (100), 587.1703 (100), 3.0; 588.1724 (32), 588.1731 (34), -1.3; 589.1738 (39), 589.1723 (39), 2.6.

Synthesis of $\text{MoTp}(\text{NO})(\text{DMAP})(3,4\text{-}\eta^2\text{-N-methyldihydropyridine})$ (**25**).

To a solution of **24** (500 mg, 0.679 mmol) and dimethoxyethane (5 mL) was added lithium aluminum hydride (LAH) (75 mg, 1.97 mmol). The resulting dark red solution was then stirred at room temperature for 5 min. This solution was then added to stirring H_2O (30 mL) in a 50 mL round bottom flask, yielding a green precipitate. This mixture

was let stirring at room temperature for 20 h. The resulting yellow precipitate was isolated on a 30 mL medium porosity fritted disc, washed with H₂O (3 x 20 mL) and hexanes (3 x 20 mL) (Note: do not stir the precipitate with washing solvent, just wash through), and dried *in vacuo* 1 h. This precipitate was then triturated in stirring hexanes (20 mL) for 20 h and the resulting precipitate was isolated on a 15 mL fine porosity fritted disc, washed with hexanes (3 x 10 mL), and desiccated to yield **26** (360 mg, 95% mass recovery). CV (DMAc) $E_{p,a} = -0.23$ V (NHE). IR: $\nu(\text{C-H sp}^2) = 2922$ cm^{-1} , $\nu(\text{B-H}) = 2468$ cm^{-1} , $\nu(\text{NO}) = 1566$ cm^{-1} . Product isolated as a 4:1 **A**:**B** ratio. ¹H NMR (d₆-Acetone, δ): 7.95 (1H, d, Pz3A **A**), 7.90 (1H, d, Pz5A/C **A**), 7.88 (2H, buried bs, DMAP-A **A**), 7.85 (1H, d, Pz5A/C **A**), 7.77 (1H, d, Pz5B **A**), 7.49 (1H, d, Pz3C **A**), 7.04 (1H, d, Pz3B **A**), 6.66 (2H, m, DMAP-B **B**), 6.58 (2H, m, DMAP-B **A**), 6.30 (2H, t, Pz4A & C **A**), 6.28 (1H, t, Pz4 **B**), 6.24 (1H, t, Pz4 **B**), 6.12 (1H, t, Pz4 **B**), 6.11 (1H, t, Pz4B **A**), 5.50 (1H, d, $J = 7.4$, H6 **A**), 5.44 (1H, d, $J = 7.4$, H6 **B**), 5.06 (1H, ddd, $J = 7.4, 4.6, \& 0.9$, H5 **B**), 4.75 (1H, ddd, $J = 7.4, 4.6, \& 0.9$, H5 **A**), 3.81 (1H dd, $J = 10.9 \& 2.8$, H2 **A**), 3.61 (1H, dd, $J = 10.9 \& 5.0$, H2' **A**), 3.05 (6H, s, N-Me **A**), 2.62 (3H, s, N-Me **A**), 2.59 (1H, m, H4 **A**), 2.03 (1H, m, H3 **A**). ¹³C NMR (d₆-Acetone, δ): **A** 155.0 (DMAP-C), 151.1 (2C, DMAP-A), 143.5 (Pz3A), 142.0 (Pz3B), 141.3 (Pz3C), 137.1 (Pz5A/C), 136.7 (Pz5A/C), 135.5 (Pz5B), 131.6 (C6), 107.9 (DMAP-B), 106.5 (Pz4A/C), 106.2 (Pz4A/C), 106.1 (Pz4B), 103.6 (C5), 63.5 (C4), 61.7 (C3), 53.9 (C2), 43.2 (NMe), 39.1 (DMAP-Me). HRMS: C₂₂H₂₉N₁₀O₂Mo+H⁺ obsd (%), calcd (%), ppm: 553.1769 (36), 553.1764 (54), 1.0; 555.1762 (65), 555.1760 (49), 0.3; 556.1734 (77), 556.1760 (82), -4.6; 557.1730 (92), 557.1754 (86), -4.3; 558.1783 (80), 558.1767 (74), 2.9; 559.1740 (100),

559.1754 (100), 2.4; 560.1814 (46), 560.1782 (34), 5.7; 561.1866 (44), 561.1773 (39), 16.6.

Synthesis of [MoTp(NO)(DMAP)(3,4- η^2 -N-methyldihydropyridinium)]⁺ (OTf) (26).

Compound **26** (28mg, 0.050 mmol) and a 0.167M solution of HOTf in MeOH (0.6mL) were combined in a 4 dram vial containing a stir pea. The reaction mixture was stirred for 5 min and then added to stirring Et₂O (15 mL). The suspension was stirred for 45 min, and then the suspended solid was isolated on a 15 mL fine porosity fritted funnel. The solid was washed with Et₂O (2 x 3 mL) and desiccated under vacuum to yield **27** as a pale yellow solid (33mg, 93%). CV (MeCN) E_{p,a} = +0.39 V (NHE). IR: $\nu_{\text{NO}} = 1623 \text{ cm}^{-1}$. ¹H NMR (d₆-acetone, δ): 8.97 (bs, 1H, H6), 8.00 (d, 1H, Pz3/5), 7.99 (d, 1H, Pz3/5), 7.97 (d, 1H, Pz3/5), 7.95 (bs, 2H, DMAP A), 7.83 (d, 1H, Pz3/5), 7.72 (d, 1H, Pz3/5), 7.25 (d, 1H, Pz3/5), 6.70 (d, 2H, DMAP B), 6.41 (t, 1H, Pz4), 6.38 (t, 1H, Pz4), 6.16 (t, 1H, Pz4), 4.94 (d, J=17.5Hz, 1H, H2), 4.67 (d, J=17.5Hz, 1H, H2'), 3.97 (s, 3H, H7), 3.92 (bd, J=22.6Hz, 1H, H5), 3.45 (bd, J=22.6Hz, 1H, H5'), 3.06 (s, 3H, H7), 2.55 (dd, J=10.6Hz, 6.1Hz, 1H, H4), 2.14 (dd, J=10.6Hz, 4.9Hz, 1H, H3). ¹³C NMR (d₆-acetone, δ): 178.6 (C6), 155.3 (DMAP C), 150.6 (DMAP A), 143.6 (Pz3), 142.3 (Pz3), 141.6 (Pz3), 138.9 (Pz5), 137.7 (Pz5), 136.3 (Pz5), 109.0 (DMAP B), 107.2 (Pz4), 107.1 (Pz4), 106.5 (Pz4), 55.6 (C3), 55.3 (C2), 54.2 (C4), 39.2 (DMAP Me), 33.6 (C5).

Synthesis of Mo(κ^2 -Tp)(NO)(κ^2 -bipy) (28).

MoTp(NO)(DMAP)(η^2 -PhCF₃) (720 mg, 1.18 mmol) and THF (7.0 mL) were combined in a 4 dram vial with stir pea. 2,2'-bipyridyl (2.0 g, 12.8 mmol) was added to the resulting solution. The reaction mixture was allowed to stir for 3 h, becoming vivid magenta in color. The reaction mixture was added dropwise to stirring pentane (50 mL). The

precipitated solid was collected on a 15 mL fine porosity fritted funnel, washed with Et₂O (4 x 10mL), and desiccated to yield **28** as a magenta solid (709 mg, 89% after accounting for 1/3eq bipy impurity). CV (MeCN) $E_{p,a} = -0.42$ V (NHE). ¹H NMR (d₃-acetonitrile, δ): 8.89 (broad s, 1H), 8.11 (broad, 1H), 7.95 (d, 1H, Pz3/5), 7.91 (m, 1H), 7.79 (d, 1H, Pz3/5), 7.49 (ddd, J=8.5Hz, 6.9Hz, 1.5Hz, 1H), 7.41 (bs, 2H, DMAP A), 7.24 (m, 1H), 7.23 (d, 1H, Pz3/5), 7.02 (d, 1H, Pz3/5), 6.98 (d, 1H, Pz3/5), 6.57 (ddd, J=6.9Hz, 6.0Hz, 1.1Hz, 1H), 6.47 (d, 2H, DMAP B), 6.39 (m, 2H, Pz4 & Pz3/5), 6.31 (t, 1H, Pz4), 6.11 (m, 2H), 5.93 (t, 1H, Pz4), 2.94 (s, 6H, DMAP Me).

Synthesis of TpMo(NO)(DMAP)(3,4- η^2 -N-methylpyridin-2(1H)-one) (**29**).

Compound **24** (1.0 g, 0.0013 mol), DCM (5 mL), and propylamine (1.2 g, 0.020 mol) were added to a 4 dram vial containing a stir pea. This solution was stirred overnight at room temperature (20 h). The resulting green solution was washed with saturated aqueous NaHCO₃ (10 mL), and the aqueous layer was back-extracted with DCM (3 x 5 mL). The organic layers were combined and subsequently dried with MgSO₄. The MgSO₄ was removed on a 15 mL medium porosity fritted disc, washed with DCM (3 x 5 mL), and the resulting filtrate was evaporated *in vacuo* to an oil. This oil was then dissolved in DCM (15 mL), and the resulting solution was added to stirring pentane (200 mL), yielding a pale green precipitate. This precipitate was isolated on a 30 mL fine porosity fritted disc, washed with pentane (3 x 10 mL) and desiccated to yield **29** as a pale green solid (728 mg, 98% yield). CV (DMAc) $E_{p,a} = +0.08$ V (NHE). IR: $\nu(\text{C-H sp}^2) = 2927$ cm⁻¹, $\nu(\text{B-H}) = 2481$ cm⁻¹, $\nu(\text{CO}) = 1615$ cm⁻¹, $\nu(\text{NO}) = 1579$ cm⁻¹. ¹H NMR (d₆-Acetone, δ): \square 8.44 (1H, d, Pz5A A), 8.01 (1H, d, Pz3/5 B), 7.99 (1H, d, Pz3/5 B), 7.98 (1H, d, Pz5C A), 7.91 (1H, d, Pz3/5 B), 7.84 (1H, d, Pz5B A), 7.83 (1H, d, Pz3A A), 7.78 (2H, bs, DMAP-A

A), 7.71 (3H, d, Pz3/5 & DMAP-A **B**), 7.60 (1H, d, Pz3C **A**), 7.51 (1H, d, Pz3/5 **B**), 7.03 (1H, d, Pz3B **A**), 7.00 (1H, d, Pz3/5 **B**), 6.63 (2H, bd, DMAP-B **A**), 6.51 (2H, bd, DMAP-B **B**), 6.37 (1H, t, Pz4 **B**), 6.35 (1H, t, Pz4C **A**), 6.30 (1H, t, Pz4 **B**), 6.21 (1H, t, Pz4A **A**), 6.12 (1H, t, Pz4B **A**), 6.11 (1H, t, Pz4 **B**), 6.08 (1H, d, $J = 7.5$, H6 **B**), 6.07 (1H, d, $J = 7.5$, H6 **A**), 5.73 (1H, t, $J = 7.4$, H5 **B**), 5.33 (1H, dd, $J = 7.5$, 5.4, H5 **A**), 3.48 (1H, dd, $J = 8.6$, 5.4, H4 **A**), 3.29 (3H, s, NMe **A**), 3.28 (3H, s, NMe **B**), 3.07 (6H, s, NMe **A**), 3.05 (6H, s, NMe **A**), 3.00 (1H, m, H3 **B**), 2.69 (1H, d, $J = 8.6$, H3 **A**), 1.69 (1H, m, H4 **B**). ^{13}C NMR (d_6 -Acetone, δ): 173.6 (CO), 155.2 (DMAP-C), 150.5 (DMAP-A), 146.7 (Pz5A), 142.5 (Pz3B), 141.6 (Pz3C), 137.7 (Pz5C), 136.7 (Pz3A/5B), 135.8 (Pz3A/5B), 123.4 (C6), 109.8 (C5), 108.3 (DMAP-B), 106.9 (Pz4C), 106.4 (Pz4B), 105.7 (Pz4A), 75.3 (C4), 62.8 (C3), 39.1 (DMAP-Me), 34.6 (NMe).

Single crystal X-ray diffraction experimental details

Single crystals of **4a**, **28**, **6**, **7**, **17**, **19**, **20**, **21**, **22b**, **25**, and **26** were coated with Paratone oil and mounted on a MiTeGen MicroLoop. The X-ray intensity data were measured on a Bruker Kappa APEXII Duo system. A graphite monochromator and a Mo K_α fine-focus sealed tube ($\lambda = 0.71073 \text{ \AA}$) were used for **4a**, **28**, **6**, **7**, **19**, **20**, **22b**, and **25**. An Incoatec Microfocus I μ S (Cu K_α , $\lambda = 1.54178 \text{ \AA}$) and a multilayer mirror monochromator were used for **17**, **21**, and **26**. The frames were integrated with the Bruker SAINT software package⁴⁰ using a narrow-frame algorithm. Data were corrected for absorption effects using the Multi-Scan method (SADABS or TWINABS).⁴⁰ The structures were solved and refined using the Bruker SHELXTL Software Package⁴¹ within APEX3⁴⁰ and OLEX2.⁴² Non-hydrogen atoms were refined anisotropically. All of the B-H hydrogen atoms except those in **4a** were located in the diffraction map and

refined isotropically, as were the N-H hydrogen atoms in **6**, **7**, **21**, **22b** and the hydrogen atoms on C10, C11, C40 and C41 in **17**. All other hydrogen atoms were placed in geometrically calculated positions with $U_{iso} = 1.2U_{equiv}$ of the parent atom ($U_{iso} = 1.5U_{equiv}$ for methyl).

Compounds **4a** and **17** were each identified a two-component twin using CELL_NOW.⁴⁰ For **4a**, starting with 308 reflections, 284 reflections were fit to the first domain, and 162 to the second domain (24 exclusively), with no unindexed reflections remaining. The twin law was a 179.9° rotation about the reciprocal axis 0.988 1.000 - 0.432, was -0.003 0.991 0.002/ - 1.010 0.004 0.003/ -0.435 -0.434 -1.001. For **17**, starting with 777 reflections, 693 reflections were fit to the first domain, 547 to the second domain (84 exclusively), with no unindexed reflection remaining. The twin domain was oriented at a 179.9° rotation about the real axis real axis -0.001 0.002 1.000. The twin law was -1.000 -0.002 0.001 / 0.002 -0.999 0.651 / -0.003 0.003 0.999. Each structure was refined as a two-component twin on HKLF5 data, with the BASF refining to 0.20144 for **4a**, and 0.39920 for **17**.

In **4a**, one methyl group was disordered over two positions. The relative occupancies were freely refined and a constraint was used on the anisotropic displacement parameters of the disordered atoms. In compound **28**, the methylene carbon of one diethyl ether molecule was disordered by symmetry and the two positions were freely refined with no constraints or restraints. In **6**, the triflate anion, the sulfur atom and two oxygen atoms were found to be disordered over two positions. The relative occupancies of these positions were freely refined, converging at 87/13 for the major and minor positions, respectively. No constraints or restraints were used on the disordered

atoms. In **7**, the occupancy of the carbonyl fragment of the co-crystallized acetone molecule was set to 50% to reflect its location on a center of symmetry. In **17**, one benzyl group was found to be disordered over two positions. The relative occupancies were freely refined, and restraints were used on the bond anisotropic displacement parameters of the disordered atoms. During the refinement of **19**, electron density difference maps revealed that there was disordered solvent that could not be successfully modeled with or without restraints. Thus, the structure factors were modified using the PLATON SQUEEZE⁴³ technique, in order to produce a “solvate-free” structure factor set. PLATON reported a total electron density of 98 e⁻ and total solvent accessible volume of 961 Å³, likely representing two molecules of pentane. In **25**, the symmetry-disordered pentane solvent was modeled with EADP constraints on the carbon atoms and DFIX restraints on the C-C bond lengths.

Table 2.2: Crystal data for **4a**, **6**, **7**, **17**, **19**, and **20**

	4a	6	7	17	19	20
CCDC	1975738	1975739	1975740	1975741	1975742	1975743
Chemical formula	C ₂₂ H ₂₄ BF ₃ MoN ₁₀ O	C ₂₃ H ₂₈ BF ₃ M oN ₁₀ O ₅ S	C ₅₁ H ₆₈ B ₂ F ₆ M o ₂ N ₂₂ O ₉ S ₂	C ₃₀ H ₃₄ BF ₃ MoN ₁₀ O	C ₂₄ H ₂₇ BF ₃ MoN ₁₁ O	C ₂₄ H ₃₀ BF ₃ M oN ₁₀ O ₂
FW (g/mol)	608.26	720.36	1524.89	714.42	649.31	654.33
T (K)	100(2)	150(2)	150(2)	100(2)	150(2)	150(2)
λ (Å)	0.71073	0.71073	0.71073	1.54178	0.71073	0.71073
Crystal size (mm)	0.100 x 0.137 x 0.582	0.110 x 0.142 x 0.394	0.091 x 0.105 x 0.235	0.026 x 0.072 x 0.108	0.155 x 0.184 x 0.265	0.170 x 0.355 x 0.396
Crystal habit	orange rod	yellow block	yellow rod	yellow plate	yellow block	yellow block
Crystal system	triclinic	monoclinic	triclinic	triclinic	monoclinic	monoclinic
Space group	P 1	P 2 ₁ /c	P -1	P -1	P 2 ₁ /c	P 2 ₁ /n
a (Å)	9.151(2)	10.8492(6)	8.0311(12)	11.8504(4)	14.4060(7)	12.2762(11)
b (Å)	9.242(2)	10.2997(6)	11.7308(18)	15.3073(6)	13.6221(6)	13.1760(12)
c (Å)	15.442(4)	26.0371(15)	18.394(3)	19.2976(8)	15.9120(9)	16.7143(15)
α (°)	98.807(8)	90	76.047(2)	69.079(2)	90	90
β (°)	94.156(8)	96.817(2)	87.832(3)	85.331(2)	93.894(2)	93.9670(10)
γ (°)	97.551(8)	90	82.654(2)	83.840(2)	90	90
V (Å³)	1273.7(6)	2888.9(3)	1667.9(4)	3247.4(2)	3115.4(3)	2697.1(4)
Z	2	4	1	4	4	4
ρ_{calc} (g/cm³)	1.586	1.656	1.518	1.461	1.384	1.611
μ (mm⁻¹)	0.574	0.600	0.524	3.805	0.475	0.551
θ range (°)	2.25 to 29.72	1.57 to 29.60	1.80 to 29.62	3.10 to 68.68	1.42 to 29.59	1.97 to 29.59
Index ranges	-12 ≤ h ≤ 12 -12 ≤ k ≤ 12 -21 ≤ l ≤ 21	-14 ≤ h ≤ 15 -14 ≤ k ≤ 13 -36 ≤ l ≤ 36	-11 ≤ h ≤ 11 -16 ≤ k ≤ 16 -25 ≤ l ≤ 25	-14 ≤ h ≤ 14 -16 ≤ k ≤ 18 0 ≤ l ≤ 23	-20 ≤ h ≤ 19 -13 ≤ k ≤ 18 -22 ≤ l ≤ 18	-8 ≤ h ≤ 17 -18 ≤ k ≤ 16 -23 ≤ l ≤ 23
Data / restraints / parameters	11445 / 9 / 695	8124 / 0 / 435	9386 / 0 / 446	11847 / 175 / 918	8740 / 0 / 377	7569 / 0 / 378
Goodness-of-fit on F²	1.185	1.046	1.016	1.031	1.008	1.063
R₁ [I > 2σ(I)]	0.0373	0.0399	0.0476	0.0719	0.0319	0.0235
wR₂ [all data]	0.0863	0.0601	0.0960	0.1950	0.0760	0.0605

Table 2.3: Crystal data for **20**, **21**, **22B**, **25**, **26** and **28**

	21	22B	25	26	28
CCDC	1975744	1975745	1975746	1975747	1975748
Chemical formula	C ₃₃ H ₄₈ BF ₃ Mo N ₁₂ O	C ₂₈ H ₃₇ BF ₆ Mo N ₁₀ O ₅ S	C ₄₉ H ₇₀ B ₂ Mo ₂ N ₂₀ O ₂	C ₂₃ H ₃₀ BF ₃ Mo N ₁₀ O ₄ S	C ₇₄ H ₉₄ B ₂ Mo ₂ N ₂₄ O ₅
FW (g/mol)	792.58	846.48	1184.75	706.38	1613.23
T (K)	150(2)	100(2)	150(2)	150(2)	150(2)
λ (Å)	1.54178	0.71073	0.71073	1.54178	0.71073
Crystal size (mm)	0.031 x 0.037 x 0.218	0.168 x 0.260 x 0.670	0.144 x 0.196 x 0.530	0.051 x 0.088 x 0.171	0.064 x 0.142 x 0.272
Crystal habit	yellow needle	pink rod	yellow rod	yellow rod	violet plate
Crystal system	monoclinic	monoclinic	monoclinic	monoclinic	monoclinic
Space group	P 2 ₁ /n	P 2 ₁ /n	P 2 ₁ /n	C c	P 2 ₁ /c
a (Å)	11.7702(5)	9.7628(3)	7.9732(8)	13.2784(5)	9.4914(7)
b (Å)	24.6128(11)	29.0199(9)	19.1005(19)	29.6134(10)	21.7207(17)
c (Å)	12.7229(5)	12.7666(4)	18.0155(18)	7.6759(3)	18.9828(14)
α (°)	90	90	90	90	90
β (°)	100.590(3)	99.4201(9)	94.263(2)	95.323(3)	100.3530(10)
γ (°)	90	90	90	90	90
V (Å³)	3623.0(3)	3568.20(19)	2736.0(5)	3005.29(19)	3849.8(5)
Z	4	4	2	4	2
ρ_{calc} (g/cm³)	1.453	1.576	1.438	1.561	1.392
μ (mm⁻¹)	3.479	0.510	0.517	4.810	0.393
θ range (°)	3.59 to 68.38	1.40 to 30.54	1.56 to 29.59	2.98 to 68.32	1.44 to 28.33
Index ranges	-14 ≤ h ≤ 14 -26 ≤ k ≤ 29 -15 ≤ l ≤ 15	-13 ≤ h ≤ 13 -38 ≤ k ≤ 41 -18 ≤ l ≤ 18	-11 ≤ h ≤ 11 -26 ≤ k ≤ 26 -25 ≤ l ≤ 22	-16 ≤ h ≤ 16 -35 ≤ k ≤ 35 -9 ≤ l ≤ 9	-12 ≤ h ≤ 11 -28 ≤ k ≤ 28 -21 ≤ l ≤ 25
Data / restraints / parameters	6613 / 0 / 471	10904 / 0 / 480	7676 / 4 / 346	5463 / 2 / 395	9608 / 0 / 503
Goodness-of-fit on F²	1.024	1.053	1.072	1.002	1.010
R₁ [I > 2σ(I)]	0.0426	0.0278	0.0293	0.0427	0.0379
wR₂ [all data]	0.1067	0.0685	0.0709	0.0997	0.0788

References

- (1) Liebov, B. K.; Harman, W. D. *Chemical Reviews* **2017**, *117*, 13721.
- (2) Wilson, K. B.; Smith, J. A.; Nedzbala, H. S.; Pert, E. K.; Dakermanji, S. J.; Dickie, D. A.; Harman, W. D. *The Journal of Organic Chemistry* **2019**, *84*, 6094.
- (3) Ding, F.; Harman, W. D. *Journal of the American Chemical Society* **2004**, *126*, 13752.
- (4) Keane, J. M.; Harman, W. D. *Organomet.* **2005**, *24*, 1786.
- (5) Goti, A.; Semmelhack, M. F. *Journal of Organometallic Chemistry* **1994**, *470*, C4.
- (6) Davies, S. G.; Shipton, M. R. *J. Chem. Soc., Chem. Commun.* **1989**, 995.
- (7) Davies, S. G.; Shipton, M. R. *Journal of the Chemical Society, Perkin Transactions I* **1991**, 501.
- (8) Kleckley, T. S.; Bennett, J. L.; Wolczanski, P. T.; Lobkovsky, E. B. *J. Am. Chem. Soc.* **1997**, *119*, 247.
- (9) Cordone, R.; Taube, H. *J. Am. Chem. Soc.* **1987**, *109*, 8101.
- (10) Cordone, R.; Harman, W. D.; Taube, H. *J. Am. Chem. Soc.* **1989**, *111*, 2896.
- (11) Meiere, S. H.; Brooks, B. C.; Gunnoe, T. B.; Sabat, M.; Harman, W. D. *Organometallics* **2001**, *20*, 1038.
- (12) Bonanno, J. B.; Viege, A. S.; Wolczanski, P. T.; Lobkovsky, E. B. *Inorg. Chim. Acta* **2003**, *345*, 173.
- (13) Covert, K. J.; Neithamer, D. R.; Zonneville, M. C.; LaPointe, R. E.; Schaller, C. P.; Wolczanski, P. T. *Inorg. Chem.* **1991**, *30*, 2493.

- (14) Neithamer, D. R.; Parkanyi, L.; Mitchell, J. F.; Wolczanski, P. T. *J. Am. Chem. Soc.* **1988**, *110*, 4421.
- (15) Welch, K. D.; Harrison, D. P.; Lis, E. C., Jr.; Liu, W.; Salomon, R. J.; Harman, W. D.; Myers, W. H. *Organometallics* **2007**, *26*, 2791.
- (16) Harrison, D. P.; Welch, K. D.; Nichols-Nielander, A. C.; Sabat, M.; Myers, W. H.; Harman, W. D. *J. Am. Chem. Soc.* **2008**, *130*, 16844.
- (17) Kosturko, G. W.; Harrison, D. P.; Sabat, M.; Myers, W. H.; Harman, W. D. *Organometallics* **2009**, *28*, 387.
- (18) Harrison, D. P.; Zottig, V. E.; Kosturko, G. W.; Welch, K. D.; Sabat, M.; Myers, W. H.; Harman, W. D. *Organometallics* **2009**, *28*, 5682.
- (19) Harrison, D. P.; Kosturko, G. W.; Ramdeen, V. M.; Nichols-Nielander, A. C.; Payne, S. J.; Sabat, M.; Myers, W. H.; Harman, W. D. *Organometallics* **2010**, *29*, 1909.
- (20) Harrison, D. P.; Sabat, M.; Myers, W. H.; Harman, W. D. *J. Am. Chem. Soc.* **2010**, *132*, 17282.
- (21) Harrison, D. P.; Iovan, D. A.; Myers, W. H.; Sabat, M.; Wang, S.; Zottig, V. E.; Harman, W. D. *J. Am. Chem. Soc.* **2011**, *133*, 18378.
- (22) Pienkos, J. A.; Zottig, V. E.; Iovan, D. A.; Li, M.; Harrison, D. P.; Sabat, M.; Salomon, R. J.; Strausberg, L.; Teran, V. A.; Myers, W. H.; Harman, W. D. *Organometallics* **2013**, *32*, 691.
- (23) Zhu, G.; Tanski, J. M.; Churchill, D. G.; Janak, K. E.; Parkin, G. *Journal of the American Chemical Society* **2002**, *124*, 13658.

- (24) Veige, A. S.; Kleckley, T. S.; Chamberlin, R. M.; Neithamer, D. R.; Lee, C. E.; Wolczanski, P. T.; Lobkovsky, E. B.; Glassey, W. V. *Journal of Organometallic Chemistry* **1999**, *591*, 194.
- (25) Myers, J. T.; Smith, J. A.; Dakermanji, S. J.; Wilde, J. H.; Wilson, K. B.; Shivokevich, P. J.; Harman, W. D. *J. Am. Chem. Soc.* **2017**, *139*, 11392.
- (26) Spectroscopic evidence for the formation of dihapto-coordinated pyridine-borane was obtained, but this compound could not be cleanly isolated owing to the thermal instability of the complex.
- (27) Delafuente, D. A.; Kosturko, G. W.; Graham, P. M.; Harman, W. H.; Myers, W. H.; Surendranath, Y.; Klet, R. C.; Welch, K. D.; Trindle, C. O.; Sabat, M.; Harman, W. D. *J. Am. Chem. Soc.* **2007**, *129*, 406.
- (28) Myers, J. T.; Shivokevich, P. J.; Pienkos, J. A.; Sabat, M.; Myers, W. H.; Harman, W. D. *Organometallics* **2015**, *34*, 3648.
- (29) Myers, J. T.; Dakermanji, S. J.; Chastanet, T. R.; Shivokevich, P. J.; Strausberg, L. J.; Sabat, M.; Myers, W. H.; Harman, W. D. *Organometallics* **2017**, *36*, 543.
- (30) Brooks, B. C.; Meiere, S. H.; Friedman, L. A.; Carrig, E. H.; Gunnoe, T. B.; Harman, W. D. *Journal of the American Chemical Society* **2001**, *123*, 3541.
- (31) Keane, J. M.; Ding, F.; Sabat, M.; Harman, W. D. *J. Am. Chem. Soc.* **2004**, *126*, 785.
- (32) Wilde, J. H.; Smith, J. A.; Dickie, D. A.; Harman, W. D. *Journal of the American Chemical Society* **2019**.
- (33) Wilde, J. H.; Smith, J. A.; Dickie, D. A.; Harman, W. D. *Journal of the American Chemical Society* **2019**, *141*, 18890.

- (34) Zincke, T. *Ann. Chim.* **1903**, 330, 361.
- (35) König, W. *J. Prakt. Chem.* **1904**, 69, 105.
- (36) Pham, H. V.; Martin, D. B. C.; Vanderwal, C. D.; Houk, K. N. *Chemical Science* **2012**, 3, 1650.
- (37) Cheng, W.-C.; Kurth, M. *Organic Preparations and Procedures International* **2002**, 34, 585.
- (38) Vanderwal, C. D. *The Journal of Organic Chemistry* **2011**, 76, 9555.
- (39) Kleckley, T. S.; Bennett, J. L.; Wolczanski, P. T.; Lobkovsky, E. B. *J. Am. Chem. Soc.* **1997**, 119, 247.
- (40) Bruker, Saint; SADABS; APEX3. Inc., B. A., Ed. Madison, Wisconsin, USA, 2012.
- (41) Sheldrick, G., SHELXT - Integrated space-group and crystal-structure determination. *Acta Crystallographica Section A* **2015**, 71 (1), 3-8.
- (42) Dolomanov, O. V.; Bourhis, L. J.; Gildea, R. J.; Howard, J. A. K.; Puschmann, H., OLEX2: a complete structure solution, refinement and analysis program. *Journal of Applied Crystallography* **2009**, 42 (2), 339-341.
- (43) Spek, A., PLATON SQUEEZE: a tool for the calculation of the disordered solvent contribution to the calculated structure factors. *Acta Crystallographica Section C* **2015**, 71 (1), 9-18.

**Chapter 3: Molybdenum-Promoted Synthesis of Isoquinuclidines with
Bridgehead CF₃ Groups**

Introduction

The coordination of an arene to a transition metal can have a profound effect upon its reactivity, a feature which has often been exploited in organic synthesis. Examples include nucleophilic addition reactions to $\text{Cr}(\text{CO})_3(\eta^6\text{-benzene})$ or $[\text{Mn}(\text{CO})_3(\eta^6\text{-benzene})]^+$, and electrophilic additions to $[\text{Os}(\text{NH}_3)_5(\eta^2\text{-benzene})]^{2+}$, $\text{ReTp}(\text{CO})(\text{MeIm})(\eta^2\text{-naphthalene})$, (MeIm = N-methylimidazole; Tp = tris(pyrazolyl)borate) or $\text{WTp}(\text{NO})(\text{PMe}_3)(\eta^2\text{-benzene})$.¹⁻³ However, transition-metal-promoted dearomatization has been much less explored for aromatic heterocycles, with pyridines often proving to be especially challenging due to the thermodynamic preference for $\kappa\text{-N}$ coordination.⁴ One exception has been the π -basic dearomatization agent $\{\text{WTp}(\text{NO})(\text{PMe}_3)\}$, which has been shown to promote tandem addition and cycloaddition reactions to pyridine, following the dihapto coordination of this heterocycle.^{5,6} The success of this chemistry relies on the blockage of nitrogen, either by substitution at the 2-position or by boronation of the nitrogen prior to coordination. To date, the functionalization of pyridines promoted by dihapto-coordination has only been observed with tungsten. While the molybdenum agent $\{\text{MoTp}(\text{NO})(\text{DMAP})\}$ (DMAP = 4-(dimethylamino)pyridine) can also bind benzene, the substitution half-life (~20 sec at 25 °C) and susceptibility to oxidation of the resulting complex has precluded its use in organic synthesis.⁷ However, the advantages of cost and scale compared to its heavy metal analog, and the paucity of examples of dihapto-coordinated heterocycles with other transition metals compelled a deeper exploration.

Attempts to combine the $\{\text{MoTp}(\text{NO})(\text{DMAP})\}$ synthon $\text{MoTp}(\text{NO})(\text{DMAP})(\eta^2\text{-PhCF}_3)$ with $[\text{pyMe}]\text{OTf}$ resulted in immediate metal oxidation, signaled by formation of

a green paramagnetic material. Efforts to prepare a stable complex with pyridine-borane were more promising, as a cyclic voltammogram (CV) of the reaction solution (100 mV/s) showed an anodic peak at 0.05 V (NHE) (cf. $\text{WTP}(\text{NO})(\text{PMe}_3)(\text{pyBH}_3)$, $E_{\text{p,a}} = +0.47$ V), but isolation of the desired complex could not be accomplished free of impurities due to its thermal instability. Attempts to bind 2-methyl-, 2-ethyl-, and 2-isopropyl- pyridine were also unsuccessful. These reactions resulted in species with $E_{1/2}$ values measured near -0.9 V, consistent with the formation of $\kappa\text{-N}$ complexes. In contrast, 2-phenylpyridine produced a complex which appeared to be dihapto-coordinate by cyclic voltammetry ($E_{\text{p,a}}$ at -0.1 V) and ^1H NMR data, though this complex could not be isolated cleanly, perhaps due to decomposition during isolation.

In earlier work with $\{\text{MoTp}(\text{NO})(\text{DMAP})\}$ arene complexes,⁷ it was shown that while the benzene analog was impractically fragile, the incorporation of a CF_3 arene substituent dramatically enhanced the stability of the corresponding molybdenum complex, enough to enable organic modifications of the aromatic ring.⁷ Thus, we posited that a CF_3 group at the 2-position of pyridine (i.e., 2-(trifluoromethyl)pyridine) would not only block nitrogen coordination, it might stabilize a purported molybdenum η^2 -pyridine complex enough to carry out heterocycle-based organic reactions (Figure 1). Further, given the significant role fluorine plays in modern medicinal chemistry,⁸ the anticipated organic products could serve as novel precursors to pharmacologically relevant compounds. Hence, the aim of this initial phase of our investigation into molybdenum η^2 -pyridine complexes is the metal-moderated stereoselective conversion of an η^2 -(2-trifluoromethyl)pyridine) to novel 1,2-dihydropyridines, which in turn could be elaborated into isoquinuclidines bearing an angular CF_3 group.

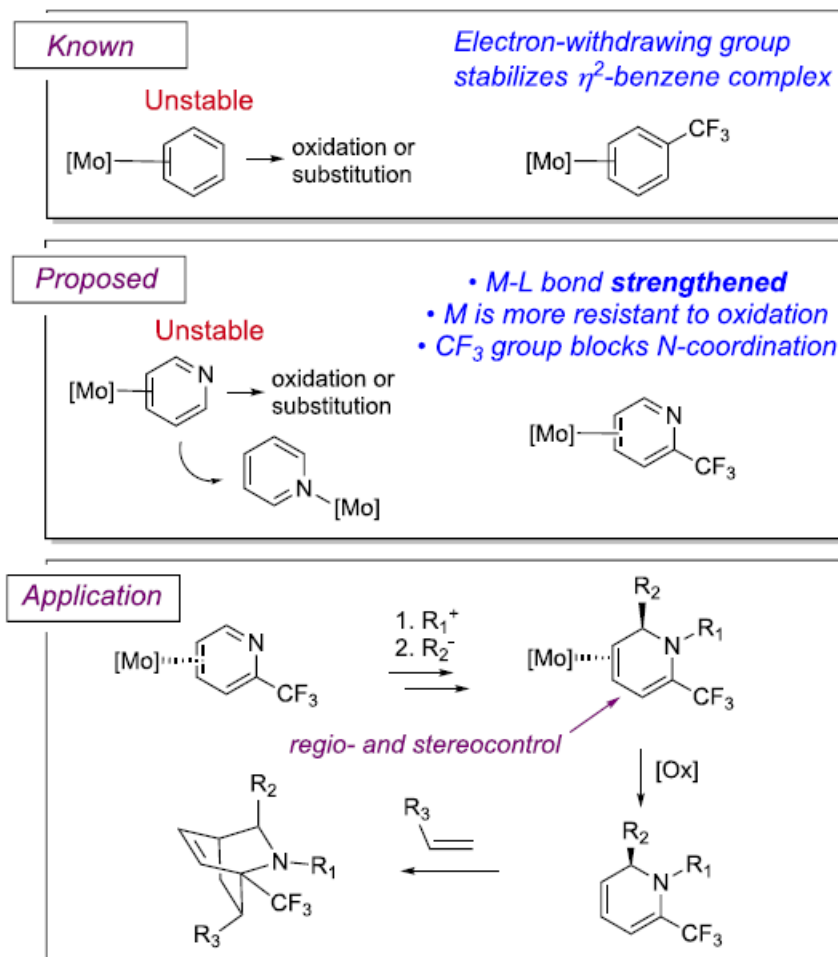


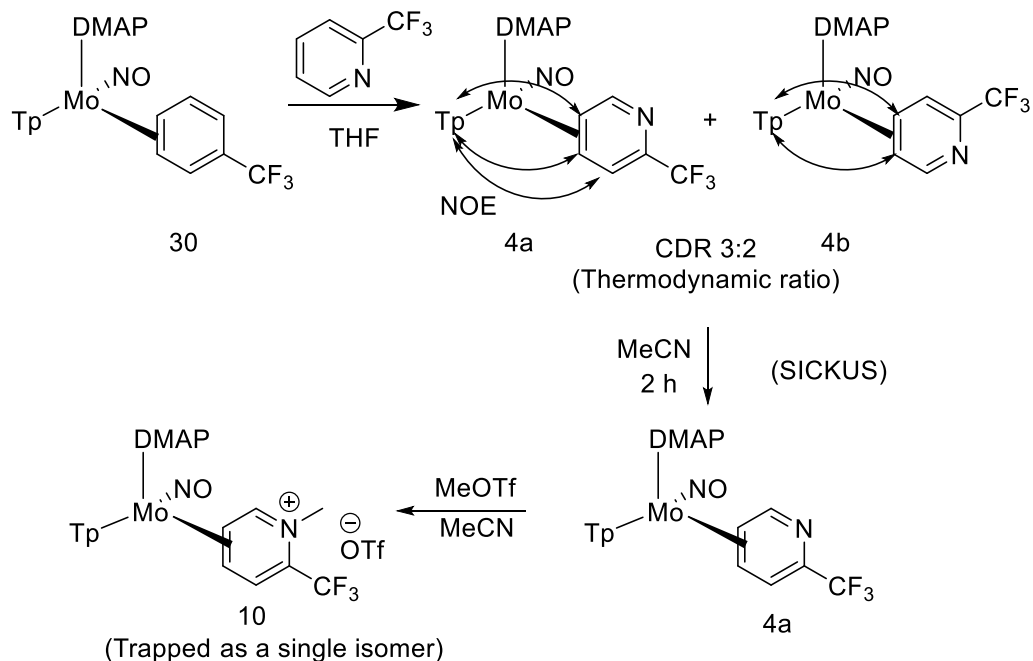
Figure 3.1: The proposed stabilization of a dihapto-coordinated molybdenum-pyridine complex by a CF_3 group and the enabled stereoselective synthesis of novel isoquinuclidines.

Results and Discussion

Stirring the previously reported complex $\text{MoTp}(\text{NO})(\text{DMAP})(\eta^2\text{-PhCF}_3)$ (**30**)⁷ in a THF solution of 2-(trifluoromethyl)pyridine (TFP) generates two new compounds, shown to be coordination diastereomers differentiated by which face of the pyridine ligand is bound by the metal (**4a** and **4b**; coordination diastereomer ratio (cdr) = 3:2 Scheme 1). These diastereomers were characterized by ^1H , ^{13}C , COSY, and NOESY

NMR data, and were identified by NOE correlations of the pyridine ring protons to the Tp ligand (**Scheme 1**).⁹ A cyclic voltammogram of this mix of diastereomers (**4**) in MeCN solution shows an $E_{p,a}$ of -0.08 V (NHE) at 100 mV/s, and an IR absorption spectrum of **4** indicates a $\nu(\text{NO})$ of 1584 cm^{-1} . These features are consistent with an η^2 -aromatic complex of $\{\text{MoTp}(\text{NO})(\text{DMAP})\}$.^{4,7}

The inability to selectively bind a single face of the pyridine ring would limit the ability to control the absolute stereochemistry of organic transformations to the heterocycle. This problem was addressed by taking advantage of differential stability of the two diastereomers (**4a** and **4b**) in the solid state (Solid-State Induced Control of Kinetically Unstable Stereoisomers (SICKUS))¹⁰. Hence when this mixture of coordination diastereomers was stirred as a suspension in MeCN for 2 h, a single coordination diastereomer (**4a**) was recovered as the precipitate in 70% percent yield (7.0 g scale). Although **4a/4b** isomerization occurs within seconds in solution at 20 °C (¹H NMR), the diastereomer present in crystalline form (**4a**) could be selectively reacted by adding the solid to a solution of MeOTf in MeCN. Once “trapped” through methylation, the greatly strengthened back-bonding interaction of the molybdenum with the pyridinium ion dramatically slows the interfacial isomerization, and even heating **10** in MeCN for 24 h at 40 °C fails to produce an observable coordination diastereomer of **10**.

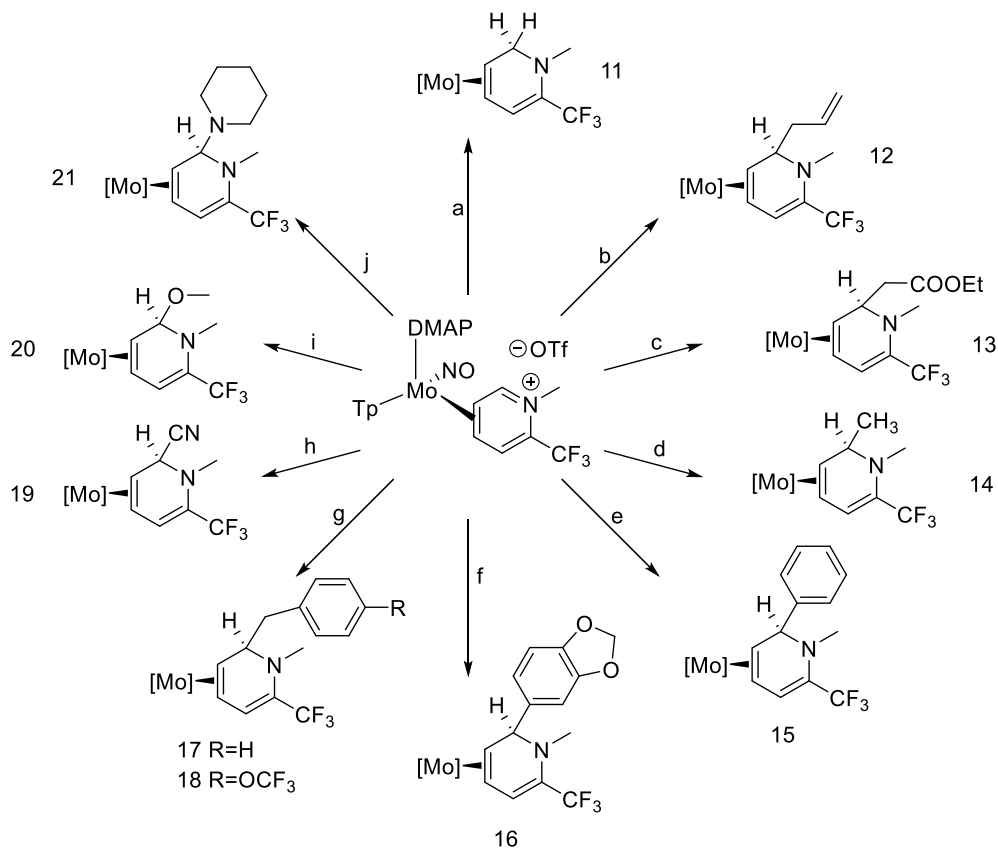


Scheme 3.1: Synthesis of TFP complex **2**, the NOE correlations that differentiate the two diastereomers, **4a** and **4b**, and the selective conversion to a single diastereomer of the methylated pyridinium complex **10**.

Methylation also was expected to increase the reactivity of the complex towards nucleophiles, allowing for further modification of the ligand. While similar pyridinium complexes could be prepared via protonation (triflic acid in MeOH) or Michael addition (MVK) to the nitrogen, these reactions were subsequently found to be reversible in the presence of basic nucleophiles (*vide infra*).

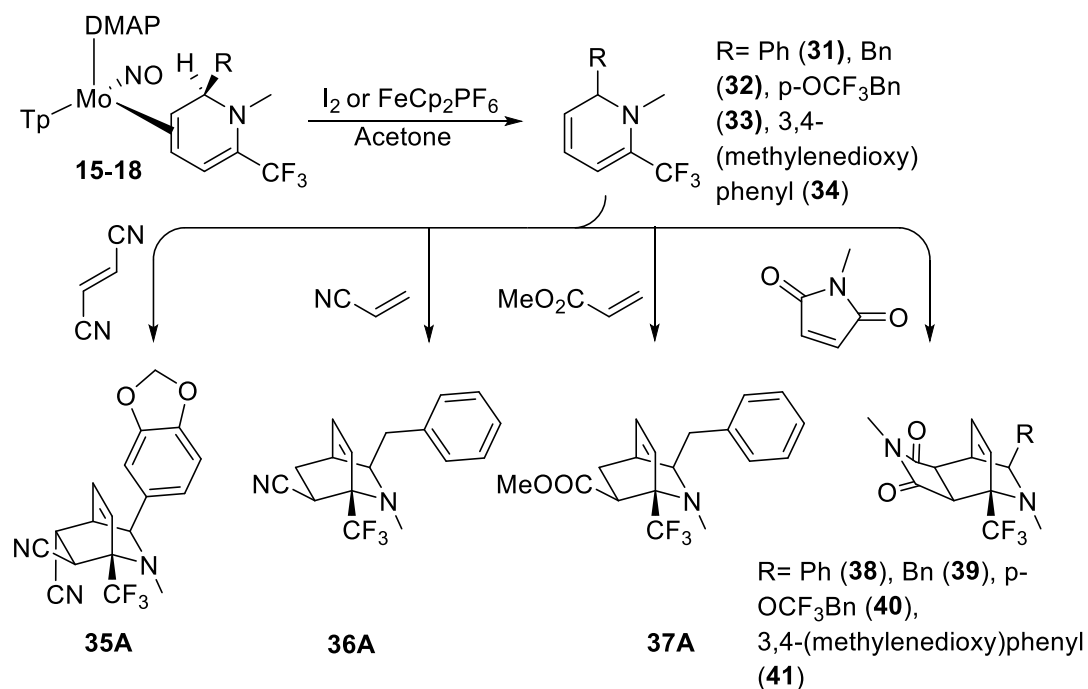
A wide range of Grignard reagents, including those with pharmacologically-relevant functionalities (e.g., benzodioxole, trifluoromethoxy),^{11,12} were found to add to pyridinium complex **10** stereo- and regioselectively, and in good yields (**Scheme 3.2**). As typically seen only for free pyridinium salts reacting with hard nucleophiles,^{13,14} nucleophilic addition was found to occur exclusively at C6, with no addition to C4

observed. The stereochemistry of nucleophilic addition was determined through NOESY data: In every case, addition was found to take place anti to the metal, as indicated by an NOE correlation between proton H2 and the H2/H6 protons of the DMAP ligand. Subsequently, these results were confirmed by single-crystal x-ray diffraction (SC-XRD) experiments (supplementary information). The attempted addition of a Grignard reagent to the neutral TFP complex **4a** resulted in no reaction, and addition of BnMgBr to the *organic* methylated TFP gives mostly C4 addition (vide infra). To our knowledge, there is only one report of TFP (or its pyridinium analog) reacting with an organometallic reagent to form a 1,2-dihydropyridine (DHP); in that disclosure, t-BuLi reacted at C2 to form a quaternary carbon,¹⁵ and this compound rapidly decomposed at ambient temperature. In contrast, halogenated, trifluoromethylated pyridines have been used in coupling reactions to make other pyridines.¹⁶



Scheme 3.2: The addition of various nucleophiles to the methylated pyridine complex **10**.

Although further functionalization of the bound dihydropyridine ligand may be achievable, efforts were directed toward isolation of the free dihydropyridines (DHPs), with the goal of using these compounds as precursors to novel isoquinuclidines.¹⁷ The phenyl and benzyl derivatives **15-18** were chosen as models for further elaboration. It was found that the free organic could be obtained in good yield (70-90%) via oxidative decomplexation by treating complexes **15-18** with $[\text{FeCp}_2]\text{PF}_6$ in acetone (**Scheme 3.3**). Alternatively, I_2 could be used, which afforded the recovery of $\text{MoTp}(\text{NO})(\text{DMAP})(\text{I})$ (79%). In contrast to literature reports,¹⁵ the resulting organic trifluoromethylated DHPs were readily purified by chromatography on silica under ambient conditions, and characterized by ^1H and ^{13}C NMR data.



Scheme 3.3: Decomplexation of DHP and its elaboration to isoquinuclidines.

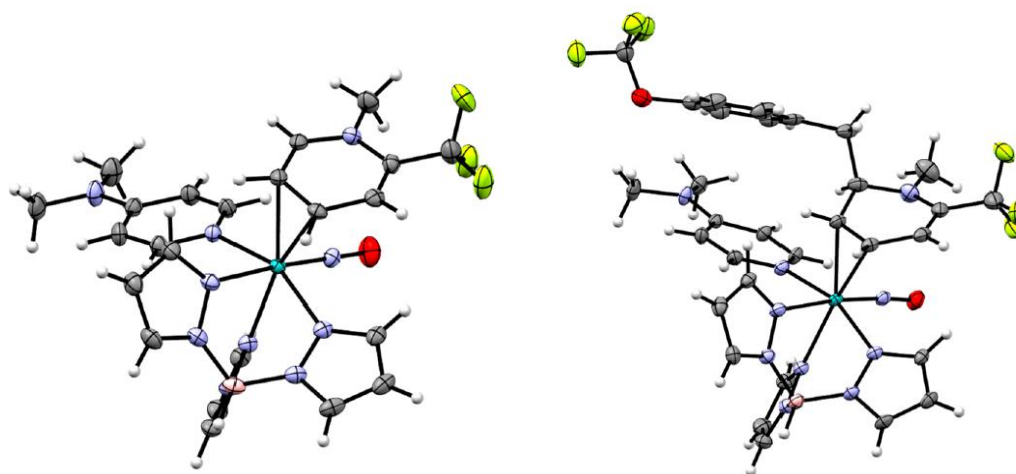


Figure 3.2: ORTEP diagram (50% probability) of a single diastereomer of the methylated TFP complex **10** (left) and its Grignard addition product **18** (right). For both structures, the anion and solvent are omitted for clarity.

To demonstrate the potential utility of these novel fluorinated DHPs in organic synthesis, the released dienes **31-34** were combined with a dienophile: Over the course of 24 h, with mild heating, they reacted with N-methylmaleimide to form endo cycloadducts **38-41**. In addition, when compound **34** was heated in the presence of fumaronitrile, cycloadduct **35** was isolated as a 3:1 ratio of two diastereomers (**35A/B**). A significantly weaker dienophile, acrylonitrile, was also found to undergo a Diels-Alder reaction with **31**, at 77 °C, producing cycloadduct (**36A/B**) in 96% yield (dr = 95:5). These novel isoquinuclidines were characterized by 2D NMR techniques and high-resolution mass spectrometry. Further, the structures of the cycloadducts were confirmed with SC-XRD.

Control experiments. Molybdenum-free reactions were explored to establish whether the same reactivity occurs in the absence of the metal. Hence free 2-(trifluoromethyl)pyridine was methylated in good yield with MeOTf in MeCN. The resulting methylpyridinium salt was then reacted with benzylmagnesium chloride under a range of conditions varying both in temperature (20 °C and -60 °C) and solvent (Et₂O and THF). In each case, the 1,2-dihydropyridine product was produced as a minor species, with the 1,4-dihydropyridine dominating (Figure 3). Ratios of 1,4-DHP to 1,2-DHP ranged from 5:1 in Et₂O at 20 °C to 3:1 in THF at 20 °C. Small amounts (~5%) of two other unidentified minor species were also produced.

To determine if the analogous tungsten system, {TpW(NO)(PMe₃)}, would provide similar reactivity, TpW(NO)(PMe₃)(4,5- η^2 -(2-trifluoromethyl)pyridine) was prepared via exchange from TpW(NO)(PMe₃)(η^2 -benzene).¹⁸ Methylation, Grignard addition, and oxidative decomplexation were carried out, and the same products were

isolated in comparable yield (**Figure 3.3**). However, unlike with molybdenum, oxidative decomplexation required FeCp_2PF_6 , with I_2 resulting in no reaction. The tungsten byproducts were thus not recyclable (*vide infra*).

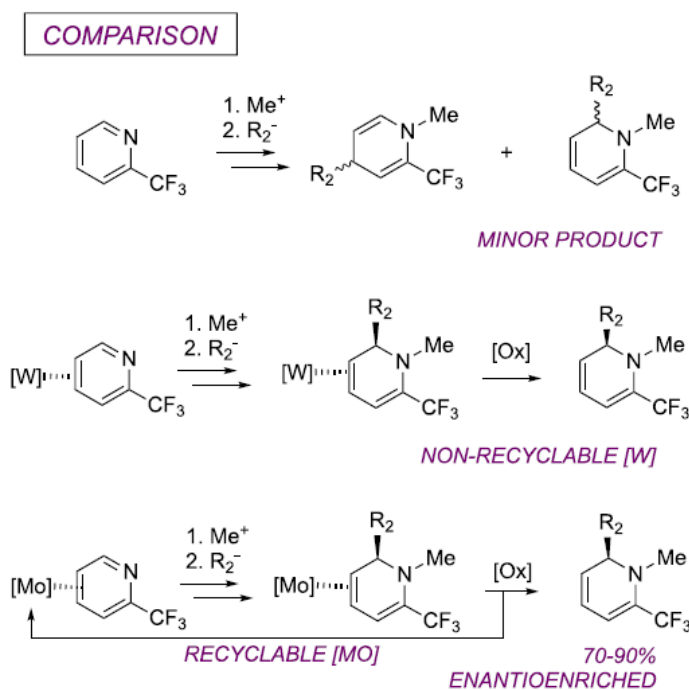
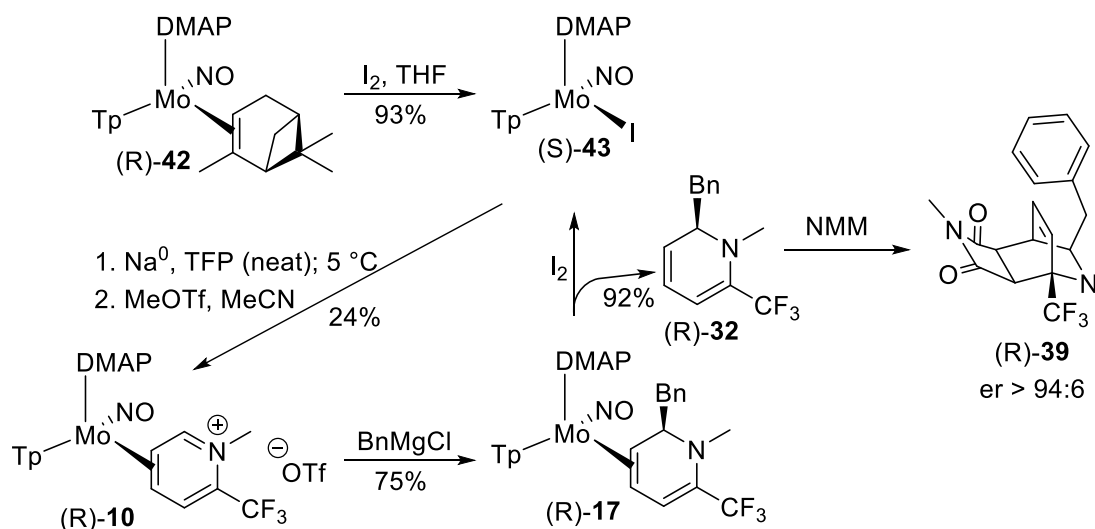


Figure 3.3: A comparison of several methods used to generate 6-(trifluoromethyl)-1,2-dihydropyridines.

Enantioenriched variation. Previous studies have shown the ability of molybdenum to promote enantioselective dearomatization.¹⁹ In this case, the complex must be synthesized by reduction instead of ligand exchange, as the pentacoordinate $\text{Mo}(0)$ intermediate rapidly epimerizes. Although it was feared that the required sodium metal would react with the free pyridine ligand, preventing synthesis of a molybdenum complex via reduction, a dihapto 2-(trifluoromethyl)pyridine complex was successfully produced from the α -pinene complex **42**, via $\text{TpMo}(\text{NO})(\text{DMAP})\text{I}$, (*S*)-**43**, by reduction in neat ligand in usable yield (28 %; **Scheme 3.4**). The pyridine complex was methylated

to generate (*R*)-**10** (24% overall) and this pyridinium salt was reacted with benzylmagnesium chloride. Oxidative decomplexation with I₂ released the enantioenriched DHP (*R*)-**32** with almost quantitative recovery of the molybdenum complex (92%). Meanwhile, (*R*)-**32** was allowed to undergo a Diels-Alder reaction with NMM to form cycloadduct (*R*)-**39**. The final enantiomeric ratio of this product was determined to be 94:6 by ¹H NMR in benzene at +6 °C using 5.0 equivalents of α -methoxy- α -(trifluoromethyl)phenylacetic acid (Mosher's acid).²⁰ The absolute configuration of (*R*)-**39** was confirmed by X-ray crystallography (absolute structure parameter is -0.02(15)). Thus, in principle any of the products characterized herein may be synthesized with high enantioenrichment.



Scheme 3.4: Enantioenriched preparation of isoquinuclidine from α -pinene precursor.

Dihydropyridines may be synthesized by several alternative methods, the simplest of which is nucleophilic addition to acyl or alkyl pyridinium salts.^{21,22} 1,2 addition tends to predominate with harder nucleophiles, such as Grignard reagents, whereas 1,4 addition is generally favored for softer nucleophiles (e.g. organocuprates). However, the products

are usually formed as a mixture of 1,2- and 1,4-isomers, the ratio of which is highly dependent upon the nucleophile, the N-substituent, and any additional functional groups on the pyridine. Additionally, weaker nucleophiles often require acyl activation or the presence of electron-withdrawing substituents on the pyridine in order for addition to be successful. The use of chiral auxiliaries at nitrogen, or more uncommonly at another position of a substituted pyridine, allows for the enantioselective synthesis.²³ An alternative approach utilizes a rhodium-catalyzed C-H alkenylation/electrocyclization to produce 1,2-dihydropyridines from α,β -unsaturated imines and alkynes, and these products have also been employed in the synthesis of isoquinuclidines.^{17,24,25} Furthermore, 1,2-dihydropyridines have also been synthesized by rhodium-catalyzed hydroboration.²⁶

Given the reaction scale and potential diversity of Grignard nucleophiles, the chemistry demonstrated herein presents a practical synthesis of molecules of potential pharmacological interest, including isoquinuclidines with a CF_3 -substituted bridgehead position. Carbobicyclics and heterobicyclics of any kind with CF_3 -substituted bridgehead positions are uncommon, with only a few examples reported as being formed via cycloaddition.²⁷⁻²⁹ Further, although isoquinuclidines constitute the structural nucleus of several classes of biologically active natural products (e.g., iboga alkaloids, dioscorine, cannivonines) and are important in medicinal chemistry,³⁰ this appears to be the first report of an isoquinuclidine with a bridgehead CF_3 group. Roughly one quarter of all drugs contain at least one fluorine,⁸ with notable CF_3 -containing examples including Sustiva, Prozac, and Celebrex. Thus, the ability to prepare isoquinuclidines with a

bridgehead CF₃ group and alkene and carboxyl functional groups for further elaboration creates exciting possibilities for new druggable chemical space.³¹

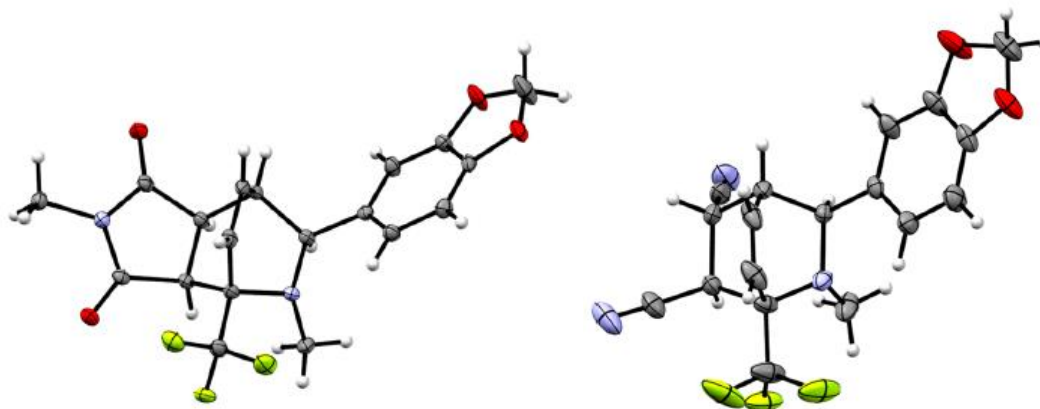


Figure 3.4: ORTEP diagram (50% probability) of isoquinuclidine compounds **41** (left) and **35A** (right). (50% probability)

Conclusion

Previous studies from our group have outlined the potential of tungsten as an η^2 -pyridine dearomatization agent,^{6,32-35} but this is the first report that extends this concept to another metal. The ability to prepare the precursor MoTp(NO)(DMAP)(η^2 -PhCF₃) on a 37 g scale⁷ and recycle the metal³⁶ are key advantages over its heavy metal cousin. We note that the use of stoichiometric molybdenum in the synthesis of pyridine-derived alkaloids was pioneered by the Liebeskind group, who used enantioenriched 3-oxopyridinylmolybdenum scaffolds to access biologically relevant heterocyclic cores.³⁷ The metal-mediated reactions described herein offer a complementary reactivity manifold to explore.

Experimental Section

General Methods. NMR spectra were obtained on a 600 or 800 MHz spectrometer. All chemical shifts are reported in ppm, and proton and carbon shifts are referenced to tetramethylsilane (TMS) utilizing residual ^1H or ^{13}C signals of the deuterated solvents as an internal standard. Coupling constants (J) are reported in hertz (Hz). Infrared spectra (IR) were recorded as a glaze on a spectrometer fitted with a horizontal attenuated total reflectance (HATR) accessory or on a diamond anvil ATR assembly. Electrochemical experiments were performed under a nitrogen atmosphere. Cyclic voltammetry data were taken at ambient temperature ($\sim 25\text{ }^\circ\text{C}$) at 100 mV/s in a standard three-electrode cell with a glassy carbon working electrode, N,N-dimethylacetamide (DMA) or acetonitrile (MeCN) solvent, and tetrabutylammonium hexafluorophosphate (TBAH) electrolyte (approximately 0.5 M). All potentials are reported versus NHE (normal hydrogen electrode) using cobaltocenium hexafluorophosphate ($E_{1/2} = -0.78\text{ V}$), ferrocene ($E_{1/2} = +0.55\text{ V}$), or decamethylferrocene ($E_{1/2} = +0.04\text{ V}$) as an internal standard. The peak-to-peak separation was less than 100 mV for all reversible couples. Unless otherwise noted, all synthetic reactions were performed in a glovebox under a dry nitrogen atmosphere. Deuterated solvents were used as received. Pyrazole (Pz) protons of the (trispyrazolyl)borate (Tp) ligand were uniquely assigned (e.g., “Pz3B”) using a combination of two-dimensional NMR data and (dimethylamino)pyridine–proton NOE interactions. When unambiguous assignments were not possible, Tp protons were labeled as “Pz3/5 or Pz4”. All J values for Pz protons are 2 (± 0.2) Hz. BH ^1H NMR peaks (around 4–5 ppm) are not identified due to their quadrupole broadening; IR data are used to confirm the presence of a BH group (around 2500 cm^{-1}).

TpMo(NO)(DMAP)(3,4- η^2 -2-(trifluoromethyl)pyridine) (4).

Compound **30**, TpMo(NO)(DMAP)(η^2 -PhCF₃) (8.28 g, 13.6 mmol), followed by 2-(trifluoromethyl)pyridine (31.9g, 217 mmol) and THF (85.0 mL) was added to a 250 mL round-bottom flask charged with a stir bar. This orange mixture was stirred for 4 h. The resulting brown heterogeneous mixture was added slowly to stirring pentane (900 mL). The resulting precipitate was isolated on a 150 mL fine porosity fritted disc, washed with Et₂O (3 × 50 mL), and desiccated to yield a tan solid, **4** (7.50 g, 90.4%). CV (MeCN) E_{p,a} = +0.08 V (NHE). IR: $\nu_{\text{NO}} = 1584 \text{ cm}^{-1}$. Two coordination diastereomers. **A:B** = 3:2 ¹H NMR (d₆-acetone, δ): **A** 8.15 (d, J=3.4Hz, 1H, H6), 8.09 (d, 1H, PzC5), 7.99 (d, 1H, PzA5), 7.93 (d, 1H, PzB5), 7.88 (d, 1H, PzA3), 7.79 (broad s, 2H, DMAP A), 7.61 (d, 1H, PzC3), 7.24 (d, J=6.4Hz, 1H, H3), 6.97 (d, 1H, PzB3), 6.74 (d, 2H, DMAP B), 6.41 (t, 1H, PzC4), 6.41 (t, 1H, PzA4), 6.16 (t, 1H, PzB4), 3.68 (dd, 1H, H5), 3.11 (t, 1H, H4), 3.11 (s, 6H, DMAP Me). **B** 8.54 (d, J=3.5Hz, 1H, H6), 8.09 (d, 1H, Pz3/5), 7.98 (d, 1H, Pz3/5), 7.95 (d, 1H, Pz3/5), 7.93 (d, 1H, Pz3/5), 7.79 (broad s, 2H, DMAP A), 7.56 (d, 1H, PzC3), 6.97 (d, 1H, Pz3/5), 6.89 (d, J=6.3Hz, 1H, H3), 6.74 (d, 2H, DMAP B), 6.41 (t, 1H, Pz4), 6.41 (t, 1H, Pz4), 6.16 (t, 1H, Pz4), 3.65 (m, 1H, H5), 3.17 (m, 1H, H4), 3.11 (s, 6H, DMAP Me). ¹³C NMR (d₆-acetone, δ): **A** 165.3 (C6), 155.4 (DMAP C), 150.3 (DMAP A), 142.6 (Tp3/5), 142.3 (Tp3/5), 141.7 (Tp3/5), 137.8 (Tp3/5), 137.1 (Tp3/5), 136.1 (Tp3/5), 130.5 (C2), 127.1 (C3), 123.5 (CF3), 108.5 (DMAP B), 107.1 (Tp4), 106.7 (Tp4), 106.5 (Tp4), 75.0 (C5), 73.5 (C4), 39.1 (DMAP Me). **B** 165.8 (C6), 155.1 (DMAP C), 150.8 (DMAP A), 144.0 (Pz3/5), 142.7 (Pz3/5), 141.7 (Pz3/5), 137.8 (Pz3/5), 137.0 (Pz3/5), 136.1 (Pz3/5), 130.1 (C2), 126.4 (C3), 108.5 (DMAP B), 107.1

(Pz4), 106.7 (Pz4), 106.6 (Pz4), 75.9 (C4), 72.8(C5), 39.1 (DMAP Me). Calculated for $C_{22}H_{24}BF_3MoN_{10}O$: C, 43.44; H, 3.98; N, 23.03. Found: C, 43.15; H, 4.09; N, 22.99.

Preparation of **4a**

4 (7.23 g, 11.9 mmol) and MeCN (70.0 mL) were added to a 100 mL round-bottom flask charged with a stir bar. The resulting suspension was stirred for 2 h at ambient temperature and then filtered through a 60 mL fine porosity fritted funnel. The isolated solid was washed with MeCN (10 mL) followed by Et₂O (2 x 20 mL). The washed solid was desiccated to yield **4a** as a light orange solid (5.06 g, 70.0 %).

Enantioenriched preparation of **4**.

Compound **43**, (S)-TpMo(NO)(DMAP)(I) (2.01 g, 3.42 mmol),¹⁹ followed by 2-(trifluoromethyl)pyridine (25.0 g, 0.170 mol) was added to a 250 mL jacketed round-bottom flask cooled to +5 °C with circulating chilled ethylene glycol and charged with a stir bar. This mixture was stirred for 15 min to cool, and then sodium 35% (w/w) dispersion in toluene, diameter <0.1 mm (10.0 g, 0.152 mol) was added to the reaction mixture. The reaction mixture was stirred vigorously for 16 h and then filtered through a celite plug in a 30 mL medium porosity fritted funnel to remove sodium. The filtrate was loaded onto a column of basic alumina (100 mL) prepared as a slurry with hexanes in a 150 mL medium porosity fritted funnel. The free pyridine was eluted with hexanes (500 mL), then a yellow-orange product was eluted with Et₂O (300 mL). The eluent was evaporated to dryness, and the residue was re-dissolved in DCM (3 mL). EtOAc (6 mL) was added until the complex was nearly saturated, followed by hexanes (100 mL). The suspension was evaporated to half volume under vacuum, and the precipitate was isolated

on a 30 mL fine porosity fritted funnel. The solid was washed with hexanes (3 x 20 mL) and desiccated under vacuum to yield **4** as a pale orange solid (582 mg, 28 %).

[TpMo(NO)(DMAP)(3,4- η^2 -2-(trifluoromethyl)-N-methylpyridinium)]⁺ (OTf) (10**).**

MeOTf (1.72 g, 10.5 mmol) and MeCN (9.0 mL), both of which had been cooled to -30 °C, were added to a 4-dram vial charged with a stir bar. **4a** (4.70 g, 7.73 mmol) was then immediately added to the reaction mixture. The resulting solution was allowed to stir for 15 min, and subsequently added dropwise to a stirring mixture of Et₂O (350 mL) and pentane (150 mL). The resulting precipitate was isolated on a 60 mL fine porosity fritted disc, washed with Et₂O (4 × 25 mL), and desiccated to yield a magenta solid, **10** (5.01 g, 83.9%). CV (DMAc) E_{p,a} = +0.87 V (NHE). IR: $\nu_{\text{NO}} = 1623 \text{ cm}^{-1}$. ¹H NMR (d₆-acetone, δ): 8.42 (d, J=5.2Hz, 1H, H6), 8.03 (d, 1H, PzC5), 7.96 (d, 1H, PzA5), 7.85 (d, 1H, PzB5), 7.72 (broad s, 2H, DMAP A), 7.68 (d, 1H, PzA3), 7.63 (d, J=6.8Hz, 1H, H3), 7.53 (d, 1H, PzC3), 7.17 (d, 1H, PzB3), 6.63 (d, 2H, DMAP B), 6.43 (t, 1H, PzC4), 6.41 (t, 1H, PzA4), 6.17 (t, 1H, PzB4), 4.10 (s, 3H, H7), 3.89 (dd, J=7.0Hz, 5.2Hz, 1H, H5), 3.46 (dd, J=7.0Hz, 6.8Hz, 1H, H4), 3.02 (s, 6H, DMAP Me). ¹³C NMR (d₆-acetone, δ): 172.3 (C6), 155.8 (DMAP C), 151.0 (DMAP A), 143.3 (PzB3), 142.5 (PzC3), 142.2 (PzA3), 138.8 (PzC5), 138.2 (PzA5), 137.0 (PzB5), 136.6 (C3), 109.3 (DMAP B), 108.0 (PzA4), 107.6 (PzC4), 107.2 (PzB4), 74.4 (C4), 73.3 (C5), 43.6 (C7), 39.5 (DMAP Me). Calculated for C₂₄H₂₇BF₆MoN₁₀O₄S: C, 37.32; H, 3.52; N, 18.14. Found: C, 37.61; H, 3.46; N, 18.00.

TpMo(NO)(DMAP)(3,4- η^2 -2-(trifluoromethyl)-N-methyldihydropyridine) (11).

Compound **10** (496 mg, 0.642 mmol) and MeOH (2.0 mL) were added to a 4-dram vial charged with a stir bar. In a separate 4-dram vial, KBH₄ (105mg, 1.95 mmol) was added to MeOH (2.0 mL). The KBH₄ suspension was immediately added to the solution of **10**. The reaction mixture was stirred for 15 min, and subsequently filtered through a 1 cm celite column prepared in a 15 mL fine porosity fritted disc. The filtrate was diluted with DCM (10 mL) and extracted with saturated NaHCO₃ (3 x 20 mL). The organic layer was dried with MgSO₄, filtered, and evaporated *in vacuo*. The resulting residue was dissolved in DCM (2.0 mL) and added dropwise to stirring Et₂O (50 mL). The precipitate was isolated on a 30 mL fine porosity fritted disc, washed with Et₂O (3 x 15 mL), and desiccated to yield a yellow solid, **11** (231 mg, 57.6%). CV (DMAc) E_{p,a} = +0.12 V (NHE). IR: $\nu_{\text{NO}} = 1570 \text{ cm}^{-1}$. ¹H NMR (d₃-MeCN, δ): 7.94 (broad s, 2H, DMAP A), 7.88 (d, 1H, PzA3), 7.86 (d, 1H, PzC5), 7.81 (d, 1H, PzA5), 7.75 (d, 1H, PzB5), 7.56 (d, 1H, PzC3), 7.15 (d, 1H, PzB3), 6.62 (d, 2H, DMAP B), 6.31 (t, 1H, PzC4), 6.29 (t, 1H, PzA4), 6.14 (t, 1H, PzB4), 6.04 (d, J=5.8Hz, 1H, H3), 3.74 (dd, J=11.7Hz, 3.4Hz, 1H, H6b), 3.31 (dd, J=11.7Hz, 2.0Hz, 1H, H6a), 3.00 (s, 6H, DMAP Me), 2.83 (s, 3H, H7), 2.66 (ddd, J=9.5Hz, 3.4Hz, 2.0Hz, 1H, H5), 2.27 (dd, J=9.5Hz, 5.8Hz, 1H, H4). ¹³C NMR (d₃-MeCN, δ): 155.1 (DMAP C), 151.0 (DMAP A), 144.1 (PzA3), 142.3 (PzB3), 141.6 (PzC3), 137.4 (PzC5), 136.5 (PzA5), 135.8 (PzB5), 126.7, (C2, J_{CF}=28.5Hz), 124.2 (CF3, J_{CF}=270.1Hz), 112.3 (C3, J_{CF}=6.7Hz), 108.5 (DMAP B), 106.7 (PzC4), 106.3 (PzA4), 106.2 (PzB4), 72.5 (C5), 56.6 (C6), 56.0 (C4), 39.6 (DMAP Me), 39.1 (C7). Calculated for C₂₃H₂₈BF₃MoN₁₀O: C, 44.25; H, 4.52; N, 22.44. Found: C, 43.83; H, 4.48; N 21.94.

TpMo(NO)(DMAP)(3,4- η^2 -6-allyl-2-(trifluoromethyl)-N-methyldihydropyridine)
(12).

Compound **10** (380 mg, 0.492 mmol), THF (3.0 mL), allyl bromide (100 mg, 0.826 mmol), and zinc dust (250 mg, 3.82 mmol) were added to a 4-dram vial charged with a stir bar. The reaction mixture was stirred for 30 min, and subsequently filtered through a 1 cm celite column prepared in a 15 mL fine porosity fritted disc. The filtrate was diluted with DCM (10 mL) and extracted with saturated NaHCO₃ (3 x 20 mL). The organic layer was dried with MgSO₄, filtered, and evaporated *in vacuo*. The resulting residue was dissolved in DCM (1.0 mL) and added dropwise to stirring pentane (50 mL). The precipitate was isolated on a 15 mL fine porosity fritted disc, washed with pentane (3 x 10 mL), and desiccated to yield a yellow solid, **12** (130 mg, 41.0%). CV (DMAc) E_{p,a} = +0.09 V (NHE). IR: $\nu_{\text{NO}} = 1565 \text{ cm}^{-1}$. ¹H NMR (d₃-MeCN, δ): 7.99 (broad s, 2H, DMAP A), 7.89 (d, 1H, PzA3), 7.86 (d, 1H, PzC5), 7.80 (d, 1H, PzA5), 7.75 (d, 1H, PzB5), 7.53 (d, 1H, PzC3), 7.18 (d, 1H, PzB3), 6.61 (d, 2H, DMAP B), 6.32 (t, 1H, PzC4), 6.27 (t, 1H, PzA4), 6.13 (t, 1H, PzB4), 5.94 (q, J=6.2Hz, 1H, H3), 5.83 (m, 1H, H9), 4.97 (m, 1H, H10), 4.95 (m, 1H, H10'), 3.17 (td, J=6.4Hz, 1.4Hz, 1H, H6), 3.09 (s, 3H, H7), 3.00 (s, 6H, DMAP Me), 2.96 (dd, J=9.6Hz, 1.4Hz, 1H, H5), 2.45 (m, 1H, H8), 2.28 (dd, J=9.6Hz, 6.2Hz, 1H, H4), 2.23 (m, 1H, H8'). ¹³C NMR (d₃-MeCN, δ): 155.1 (DMAP C), 151.0 (DMAP A), 144.0 (PzA3), 142.4 (PzB3), 141.8 (PzC3), 138.2 (C9), 137.8 (PzC5), 136.9 (PzA5), 136.3 (PzB5), 124.4 (C2, J_{CF}=28.5Hz), 124.2 (CF3, J_{CF}=270.1Hz), 116.2 (C10), 110.8 (C3, J_{CF}=6.3Hz), 108.7 (DMAP B), 107.0 (PzC4), 106.7 (PzA4), 106.6 (PzB4), 82.7 (C5), 64.0 (C6), 56.8 (C4), 40.7 (C8), 39.4 (DMAP Me), 39.1 (C7).

Calculated for $C_{26}H_{32}BF_3MoN_{10}O$: C, 47.00; H, 4.86; N, 21.08. Found: C, 46.76; H, 4.95; N 20.96.

TpMo(NO)(DMAP)(3,4- η^2 -ethyl 6-(1-methyl-2-(trifluoromethyl)dihydropyridinyl)acetate) (13).

Compound **10** (380 mg, 0.492 mmol), THF (2.5 mL), ethyl bromoacetate (201 mg, 1.20 mmol), and zinc dust (250 mg, 3.82 mmol) were added to a 4-dram vial charged with a stir bar. The reaction mixture was stirred for 45 min, and subsequently filtered through a 1 cm celite column prepared in a 15 mL fine porosity fritted disc. The filtrate was diluted with DCM (10 mL) and extracted with saturated $NaHCO_3$ (3 x 20 mL). The organic layer was dried with $MgSO_4$, filtered, and evaporated *in vacuo*. The resulting residue was dissolved in DCM (1.0 mL) and added dropwise to stirring Et_2O (50 mL). The precipitate was isolated on a 15 mL fine porosity fritted disc, washed with Et_2O (3 x 10 mL), and desiccated to yield a yellow solid, **13** (140 mg, 40.0%). CV (DMAc) $E_{p,a} = +0.14$ V (NHE). IR: $\nu_{NO} = 1576$ cm^{-1} ; $\nu_{CO} = 1719$ cm^{-1} . 1H NMR (d_3 -MeCN, δ): 7.97 (broad s, 2H, DMAP A), 7.88 (d, 1H, PzA3), 7.86 (d, 1H, PzC5), 7.80 (d, 1H, PzA5), 7.75 (d, 1H, PzB5), 7.48 (d, 1H, PzC3), 7.18 (d, 1H, PzB3), 6.64 (d, 2H, DMAP B), 6.32 (t, 1H, PzC4), 6.28 (t, 1H, PzA4), 6.14 (t, 1H, PzB4), 6.03 (d, $J=6.3$ Hz, 1H, H3), 4.01 (m, 2H, H9), 3.60 (tdd, $J=7.1$ Hz, $J=6.4$ Hz, 1.4Hz, 1H, H6), 3.08 (s, 3H, H7), 3.01 (s, 6H, DMAP Me), 2.93 (dd, $J=9.8$ Hz, 1.4Hz, 1H, H5), 2.68 (dd, $J=13.7$ Hz, $J=7.1$ Hz, 1H, H8), 2.41 (dd, $J=13.7$ Hz, $J=6.4$ Hz, 1H, H8'), 2.28 (dd, $J=9.8$ Hz, 6.3Hz, 1H, H4), 1.14 (t, $J=7.2$ Hz, 3H, H10). ^{13}C NMR (d_3 -MeCN, δ): 173.1 (Ester CO), 155.1 (DMAP C), 151.1 (DMAP A), 144.1 (PzA3), 142.5 (PzB3), 141.8 (PzC3), 137.9 (PzC5), 137.0 (PzA5), 136.4 (PzB5), 124.0 (CF_3 , $J_{CF}=270.1$ Hz), 123.6 (C2, $J_{CF}=28.5$ Hz), 111.7 (C3, $J_{CF}=6.0$ Hz), 108.8

(DMAP B), 107.1 (PzC4), 106.7 (PzA4), 106.7 (PzB4), 83.0 (C5), 61.4 (C6), 60.8 (C9), 56.3 (C4), 40.3 (C8), 39.4 (DMAP Me), 38.9 (C7), 13.5 (C10). Calculated for $C_{27}H_{34}BF_3MoN_{10}O_3$: C, 45.65; H, 4.82; N, 19.72. Found: C, 45.39; H, 4.62; N 19.45.

TpMo(NO)(DMAP)(3,4- η^2 -2-(trifluoromethyl)-6-methyl-N-methyldihydropyridine) (14).

Compound **10** (1.00 g, 1.29 mmol) and THF (16.0 mL), which had previously been cooled to $-40\text{ }^\circ\text{C}$, were added to a 25 mL flame-dried round bottom flask charged with a stir bar. A 1.4 M solution of methylmagnesium bromide in 1:3 THF/toluene (2.10 mL, 2.94 mmol) was added dropwise to the solution of **10**. The reaction mixture changed from vivid magenta to golden yellow over the course of the addition. The reaction mixture was stirred for 5 min, and subsequently filtered through a 1 cm celite column prepared in a 15 mL fine porosity fritted disc. The filtrate was diluted with DCM (30 mL) and extracted with saturated NaHCO_3 (2 x 20 mL). The organic layer was dried with MgSO_4 , filtered, and evaporated *in vacuo*. The resulting residue was dissolved in DCM (4 mL) and added dropwise to stirring Et_2O (100 mL). The precipitate was isolated on a 30 mL fine porosity fritted disc, washed with Et_2O ($3 \times 10\text{ mL}$), and desiccated to yield a yellow solid, **14** (432 mg, 52.5%). CV (DMAc) $E_{p,a} = +0.06\text{ V}$ (NHE). IR: $\nu_{\text{NO}} = 1568\text{ cm}^{-1}$. ^1H NMR (d_3 -MeCN, δ): 7.97 (broad s, 2H, DMAP A), 7.90 (d, 1H, PzA3), 7.86 (d, 1H, PzC5), 7.80 (d, 1H, PzA5), 7.75 (d, 1H, PzB5), 7.59 (d, 1H, PzC3), 7.15 (d, 1H, PzB3), 6.61 (d, 2H, DMAP B), 6.31 (t, 1H, PzC4), 6.27 (t, 1H, PzA4), 6.13 (t, 1H, PzB4), 5.96 (d, $J=6.1\text{ Hz}$, 1H, H3), 3.28 (qd, $J=6.2\text{ Hz}$, 1.7Hz, 1H, H6), 3.00 (s, 6H, DMAP Me), 2.99 (s, 3H, H7), 2.76 (dd, $J=9.6\text{ Hz}$, 1.7Hz, 1H, H5), 2.29 (dd, $J=9.6\text{ Hz}$, 6.1Hz, 1H, H4), 1.13 (d, $J=6.2\text{ Hz}$, 3H, H8). ^{13}C NMR (d_3 -MeCN, δ): 155.0 (DMAP C), 151.1 (DMAP A), 144.0 (PzA3),

142.4 (PzB3), 141.9 (PzC3), 137.8 (PzC5), 137.0 (PzA5), 136.3 (PzB5), 124.5 (C2, $J_{\text{CF}}=28.5\text{Hz}$), 124.2 (CF3, $J_{\text{CF}}=270.1\text{Hz}$), 109.6 (C3, $J_{\text{CF}}=6.3\text{Hz}$), 108.7 (DMAP B), 107.0 (PzC4), 106.7 (PzA4), 106.6 (PzB4), 83.7 (C5), 59.1 (C6), 57.5 (C4), 39.4 (DMAP Me), 37.5 (C7), 19.6 (C8). Calculated for $\text{C}_{24}\text{H}_{30}\text{BF}_3\text{MoN}_{10}\text{O}$: C, 45.16; H, 4.74; N, 21.94. Found: C, 45.18; H, 4.85; N, 21.86.

TpMo(NO)(DMAP)(3,4- η^2 -2-(trifluoromethyl)-6-phenyl-N-methyldihydropyridine) (15).

Compound **10** (1.00 g, 1.29 mmol) and THF (16.0 mL), which had previously been cooled to $-40\text{ }^\circ\text{C}$ were added to a 25 mL flame-dried round bottom flask charged with a stir bar. A 1.0 M solution of phenylmagnesium bromide in THF (3.0 mL, 3.0 mmol) was added dropwise to the solution of **10**. The reaction mixture changed from vivid magenta to golden yellow over the course of the addition. The reaction mixture was stirred for 5 min and subsequently filtered through a 1 cm celite column prepared in a 15 mL fine porosity fritted disc. The filtrate was diluted with DCM (30 mL) and extracted with saturated NaHCO_3 (2 x 20 mL). The organic layer was dried with MgSO_4 , filtered, and evaporated *in vacuo*. The resulting residue was dissolved in DCM (8 mL) and added dropwise to stirring pentane (100 mL). The precipitate was isolated on a 30 mL fine porosity fritted disc, washed with pentane ($3 \times 10\text{ mL}$), and desiccated to yield a yellow solid, **15** (633 mg, 70.0%). CV (MeCN) $E_{\text{p,a}} = +0.13\text{ V}$ (NHE). IR: $\nu_{\text{NO}} = 1576\text{ cm}^{-1}$. ^1H NMR (d_6 -acetone, δ): 8.22 (bs, 2H, DMAP A), 8.01 (d, 1H, PzA3), 7.92 (d, 1H, PzC5), 7.86 (d, 1H, PzA5), 7.80 (d, 1H, PzB5), 7.51 (d, 1H, PzC3), 7.27 (d, 1H, PzB3), 7.23 (m, 2H, H8), 7.21 (m, 2H, H9), 7.13 (m, 1H, H10), 6.79 (d, 2H, DMAP B), 6.30 (t, 2H, PzC4/PzA4), 6.15 (t, 1H, PzB4), 5.96 (d, $J=6.8\text{Hz}$, 1H, H3), 4.34 (s, 1H, H6), 3.11 (s,

3H, DMAP Me), 2.98 (s, 3H, H7), 2.88 (d, J=9.7Hz, 1H, H5), 2.47 (dd, J=9.7Hz, 6.4Hz, 1H, H4). ^{13}C NMR (d_6 -acetone, δ): 155.1 (DMAP C), 151.1 (DMAP A), 148.8 (C8a), 143.9 (PzA3), 142.3 (PzB3), 141.4 (PzC3), 137.4 (PzA5), 136.6 (PzC5), 135.9 (PzB5), 128.9 (C8), 127.4 (C9), 127.0 (C10), 124.4 (q, J=28.6Hz, C2), 124.0 (q, J=270Hz, CF3), 109.4 (q, J=7.0Hz, C3), 108.7 (DMAP B), 106.8 (PzC4), 106.3 (PzA4), 106.2 (PzB4), 82.0 (C5), 67.7 (C6), 56.3 (C4), 39.2 (DMAP Me), 38.1 (C7). Calculated for $\text{C}_{29}\text{H}_{32}\text{BF}_3\text{MoN}_{10}\text{O}$: C, 49.73; H, 4.61; N, 20.00. Found: C, 49.75; H, 4.76; N, 19.82.

TpMo(NO)(DMAP)(3,4- η^2 -2-(trifluoromethyl)-6-(3,4-methylenedioxy)phenyl-N-methyldihydropyridine) (16).

Compound **10** (1.00 g, 1.29 mmol) and THF (16.0 mL), which had previously been cooled to $-40\text{ }^\circ\text{C}$, were added to a 25 mL flame-dried round bottom flask charged with a stir bar. A 1.0 M solution of 3,4-(methylenedioxy)phenylmagnesium bromide in 1:1 toluene/THF (3.0 mL, 3.0 mmol) was added dropwise to the solution of **10**. The reaction mixture changed from vivid magenta to golden yellow over the course of the addition. The reaction mixture was stirred for 5 min, and subsequently filtered through a 1 cm celite column prepared in a 15 mL fine porosity fritted disc. The filtrate was diluted with DCM (30 mL) and extracted with saturated NaHCO_3 (2 x 20 mL). The organic layer was dried with MgSO_4 , filtered, and evaporated *in vacuo*. The resulting residue was dissolved in DCM (8 mL) and added dropwise to stirring Et_2O (100 mL). Half of the solvent was evaporated under vacuum to yield a bright yellow precipitate. The precipitate was isolated on a 30 mL fine porosity fritted disc, washed with Et_2O (3×10 mL), and desiccated to yield a yellow solid, **16** (652 mg, 68%). CV (MeCN) $E_{p,a} = +0.14$ V (NHE). ^1H NMR (d_2 -methylene chloride, δ): 8.14 (bs, 2H, DMAP A), 7.98 (d, 1H, PzA3), 7.76

(d, 1H, PzC5), 7.75 (d, 1H, PzA5), 7.67 (d, 1H, PzB5), 7.40 (d, 1H, PzC3), 7.21 (d, 1H, PzB3), 6.86 (s, 1H, H10), 6.69 (d, J=8.2Hz, 1H, H9), 6.61 (d, J=8.2Hz, 1H, H8), 6.54 (d, 2H, DMAP B), 6.26 (t, 2H, PzA4), 6.22 (t, 2H, PzC4), 6.10 (t, 1H, PzB4), 5.95 (d, J=6.2Hz, 1H, H3), 5.89 (s, 2H, H11), 4.21 (s, 1H, H6), 3.09 (s, 6H, DMAP Me), 2.97 (s, 3H, H7), 2.77 (d, J=9.7Hz, 1H, H5), 2.53 (dd, J=9.7Hz, 6.4Hz, 1H, H4). ¹³C NMR (d₂-methylene chloride, δ): 154.5 (DMAP C), 150.8 (DMAP A), 148.2 (C10a), 146.6 (C9a), 143.8 (PzA3), 142.7 (C8a), 142.0 (PzB3), 140.9 (PzC3), 136.9 (PzA5), 136.2 (PzC5), 135.5 (PzB5), 124.3 (q, J=28.9Hz, C2), 123.7 (q, J=272Hz, CF3), 119.8 (C8), 108.8 (q, J=6.7Hz, C3), 108.2 (DMAP B), 108.0 (C9), 107.8 (C10), 106.2 (PzC4), 106.0 (PzA4), 105.9 (PzB4), 101.4 (C11), 81.7 (C5), 67.0 (C6), 56.4 (C4), 39.5 (DMAP Me), 38.0 (C7). Calculated for C₃₀H₃₂BF₃MoN₁₀O₃ • 1/2 C₄H₁₀O: C, 49.18; H, 4.77; N, 17.92. Found: C, 49.11; H, 4.66; N, 17.97.

TpMo(NO)(DMAP)(3,4-η²-2-(trifluoromethyl)-6-benzyl-N-methyldihydropyridine) (17).

Compound **10** (2.57 g, 3.33 mmol) and THF (45.0 mL), which had previously been cooled to -40 °C, were added to a 100 mL flame-dried round bottom flask charged with a stir bar. A 1.0 M solution of benzylmagnesium chloride in Et₂O (3.50 mL, 3.50 mmol) was added dropwise to the solution of **10**. The reaction mixture changed from vivid magenta to golden yellow over the course of the addition. The reaction mixture was stirred for 5 min and subsequently filtered through a 1 cm celite column prepared in a 30 mL fine porosity fritted disc. The filtrate was diluted with DCM (50 mL) and extracted with saturated NaHCO₃ (2 x 50 mL). The organic layer was dried with MgSO₄, filtered, and evaporated *in vacuo*. The resulting residue was dissolved in minimal DCM and added

dropwise to stirring pentane (250 mL). The precipitate was isolated on a 30 mL fine porosity fritted disc, washed with pentane (3×15 mL), and desiccated to yield a yellow solid, **17** (1.78 g, 75%). CV (MeCN) $E_{p,a} = +0.10$ V (NHE). IR: $\nu_{\text{NO}} = 1567$ cm^{-1} . ^1H NMR (d_6 -acetone, δ): 7.96 (broad s, 2H, DMAP A), 7.95 (d, 1H, PzA3), 7.90 (d, 1H, PzC5), 7.83 (d, 1H, PzA5), 7.78 (d, 1H, PzB5), 7.30 (d, 1H, PzC3), 7.21 (d, 1H, PzB3), 7.19 (m, 2H, H10), 7.13 (m, 1H, H11), 7.05 (m, 2H, H9), 6.64 (d, 2H, DMAP B), 6.30 (t, 1H, PzC4), 6.27 (t, 1H, PzA4), 6.12 (t, 1H, PzB4), 5.96 (d, $J=6.1\text{Hz}$, 1H, H3), 3.42 (dd, $J=7.2\text{Hz}$, 6.4Hz , 1H, H6), 3.11 (s, 3H, DMAP Me), 3.01 (dd, $J=12.7\text{Hz}$, 6.4Hz , H8), 2.96 (s, 3H, H7), 2.87 (d, $J=9.9\text{Hz}$, 1H, H5), 2.75 (dd, $J=12.7\text{Hz}$, 7.2Hz , 1H, H8'), 2.34 (dd, $J=9.9\text{Hz}$, 6.1Hz , 1H, H4). ^{13}C NMR (d_6 -acetone, δ): 155.0 (DMAP C), 150.9 (DMAP A), 143.8 (PzA3), 142.2 (PzB3), 141.7 (H9a), 141.1 (PzC3), 137.4 (PzA5), 136.5 (PzC5), 135.8 (PzB5), 130.2 (H10), 128.8 (H9), 126.2 (H11), 124.1 (q, $J=272\text{Hz}$, CF3), 124.0 (q, $J=28.7\text{Hz}$, C2), 110.3 (q, $J=6.6\text{Hz}$, C3), 108.5 (DMAP B), 106.6 (PzC4), 106.3 (PzA4), 106.1 (PzB4), 81.7 (C5), 66.2 (C6), 56.5 (C4), 42.1 (C8), 39.2 (DMAP Me), 38.0 (C7). Calculated for $\text{C}_{30}\text{H}_{34}\text{BF}_3\text{MoN}_{10}\text{O}$: C, 50.44; H, 4.80; N, 19.61. Found: C, 50.43; H, 4.83; N, 19.46.

TpMo(NO)(DMAP)(3,4- η^2 -2-(trifluoromethyl)-6-(4-trifluoromethoxy)benzyl-N-methyldihydropyridine) (18).

Compound **10** (1.00 g, 1.29 mmol) and THF (16.0 mL), which had previously been cooled to -40 $^\circ\text{C}$, were added to a 25 mL flame-dried round bottom flask charged with a stir bar. A 1.0 M solution of 4-(trifluoromethoxy)benzylmagnesium bromide in Et_2O (3.0 mL, 3.0 mmol) was added dropwise to the solution of **10**. The reaction mixture changed from vivid magenta to golden yellow over the course of the addition. The reaction

mixture was stirred for 5 min and subsequently filtered through a 1 cm celite column prepared in a 15 mL fine porosity fritted disc. The filtrate was diluted with DCM (30 mL) and extracted with saturated NaHCO₃ (2 x 20 mL). The organic layer was dried with MgSO₄, filtered, and evaporated *in vacuo*. The resulting residue was dissolved in minimal DCM and added dropwise to stirring hexanes (100 mL). The precipitate was isolated on a 30 mL fine porosity fritted disc, washed with hexanes (3 x 10 mL), and desiccated to yield a yellow solid, **18** (754 mg, 72%). CV (MeCN) E_{p,a} = +0.13 V (NHE). IR: ν_{NO} = 1568 cm⁻¹. ¹H NMR (d₂-methylene chloride, δ): 7.94 (broad s, 2H, DMAP A), 7.93 (d, 1H, PzA3), 7.74 (d, 1H, PzC5), 7.72 (d, 1H, PzA5), 7.64 (d, 1H, PzB5), 7.17 (d, 1H, PzB3), 7.12 (d, 1H, PzC3), 7.10 (m, 2H, H9), 7.06 (m, 2H, H10), 6.42 (d, 2H, DMAP B), 6.24 (t, 1H, PzA4), 6.23 (t, 1H, PzC4), 6.07 (t, 1H, PzB4), 5.95 (d, J=6.3Hz, 1H, H3), 3.33 (dd, J=7.5Hz, 6.1Hz, 1H, H6), 3.05 (dd, J=12.9Hz, 6.1Hz, H8), 3.03 (s, 6H, DMAP Me), 2.98 (s, 3H, H7), 2.77 (dd, J=12.9Hz, 7.5Hz, 1H, H8'), 2.67 (d, J=9.7Hz, 1H, H5), 2.38 (dd, J=9.7Hz, 6.3Hz, 1H, H4). ¹³C NMR (d₂-methylene chloride, δ): 154.4 (DMAP C), 150.7 (DMAP A), 147.6 (C10a), 143.7 (PzA3), 142.0 (PzB3), 140.7 (C9a), 140.5 (PzC3), 136.9 (PzA5), 136.2 (PzC5), 135.5 (PzB5), 131.2 (C9), 123.9 (q, J=29.3Hz, C2), 123.6 (q, J=272Hz, CF3), 121.3 (q, J=256Hz, OCF3), 121.0 (C10), 109.9 (q, J=6.7Hz, C3), 108.0 (DMAP B), 106.2 (PzC4), 106.0 (PzA4), 105.9 (PzB4), 81.0 (C5), 65.8 (C6), 56.6 (C4), 40.9 (C8), 39.5 (DMAP Me), 38.9 (C7). Calculated for C₃₁H₃₃BF₆MoN₁₀O₂ • 1/3 C₆H₁₄: C, 47.92; H, 4.59; N, 16.93. Found: C, 47.20; H, 4.20; N, 16.98.

1-methyl-2-phenyl-6-(trifluoromethyl)-1,2-dihydropyridine (31).

Compound **15** (250 mg, 0.357 mmol) and acetone (7.5 mL) were combined in a 4 dram vial containing a stir bar. FeCp₂PF₆ (119 mg, 0.359 mmol) was dissolved in acetone (7.5

mL) in a separate 4 dram vial, and then this solution was transferred to the vial containing **15**. The reaction mixture was stirred for 15 min. The reaction mixture was then diluted with DCM (40 mL) and extracted with saturated Na₂CO₃ (2 x 30 mL). The organic layer was dried with Na₂SO₄, and the solids removed by filtration. The filtrate was evaporated onto silica, and purified by Combiflash flash chromatography on a 4 g silica column, using a 100% hexanes mobile phase. The fractions containing the desired product were evaporated *in vacuo* to yield **31** as a colorless oil (65 mg, 76%). ¹H NMR (d₃-Acetonitrile, δ): 7.36 (m, 4H, H8+H9), 7.30 (m, 1H, H10), 6.01 (ddt, J=9.4Hz, 5.9Hz, 1.0Hz, 1H, H4), 5.51 (ddt, J=9.4Hz, 5.8Hz, 1.0Hz, 1H, H5), 5.48 (dt, J=5.8Hz, 1.0Hz, 1H, H3), 5.00 (d, J=5.9Hz, 1H, H6), 2.89 (s, 3H, H7). ¹³C NMR (d₃-Acetonitrile, δ): 143.2 (C8a), 133.8 (q, J=30.2Hz, C2), 129.6 (C8), 128.8 (C10), 127.1 (C9), 122.9 (q, J=273Hz, CF3), 121.5 (C5), 121.4 (C4), 100.1 (q, J=6.9Hz, C3), 65.2 (C6), 38.6 (C7).

2-benzyl-1-methyl-6-(trifluoromethyl)-1,2-dihydropyridine (32).

Compound **17** (179 mg, 0.250 mmol) and acetone (5.0 mL) were combined in a 4 dram vial containing a stir bar. FeCp₂PF₆ (83 mg, 0.251 mmol) was dissolved in acetone (5.0 mL) in a separate 4 dram vial, and then this solution was transferred to the vial containing **17**. The reaction mixture was stirred for 15 min. The reaction mixture was then diluted with DCM (30 mL) and extracted with saturated Na₂CO₃ (2 x 20 mL). The organic layer was dried with Na₂SO₄, and the solids removed by filtration. The filtrate was evaporated onto silica, and purified by Combiflash flash chromatography on a 4 g silica column, using a 100% hexanes mobile phase. The fractions containing the desired product were evaporated *in vacuo* to yield **32** as a colorless oil (51 mg, 80%). ¹H NMR (d-Chloroform, δ): 7.30 (m, 2H, H10), 7.24 (m, 1H, H11), 7.20 (m, 2H, H9), 6.00 (dd, J=9.1Hz, 5.7Hz,

1H, H4), 5.67 (d, J=5.7Hz, 1H, H3), 5.28 (dd, J=9.1Hz, 6.1Hz, 1H, H5), 3.91 (ddd, J=7.9Hz, 6.2Hz, 6.1Hz, 1H, H6), 2.80 (dd, J=13.2Hz, 7.9Hz, 1H, H8), 2.74 (s, 3H, H7), 2.61 (dd, J=13.2Hz, 6.2Hz, 1H, H8'). ¹³C NMR (d-Chloroform, δ): 137.9 (C9a), 132.5 (q, J=31.1Hz, C2), 129.8 (C9), 128.4 (C10), 126.3 (C11), 121.7 (C4), 121.9 (q, J=274Hz, CF3), 118.7 (C5), 101.7 (q, J=6.6Hz, C3), 63.5 (C6), 39.6 (C7), 38.3 (C8).

1-methyl-2-(4-(trifluoromethoxy)benzyl)-6-(trifluoromethyl)-1,2-dihydropyridine (33).

Compound **18** (195 mg, 0.244 mmol) and acetone (5.0 mL) were combined in a 4 dram vial containing a stir bar. FeCp₂PF₆ (81 mg, 0.245 mmol) was dissolved in acetone (5.0 mL) in a separate 4 dram vial, and then this solution was transferred to the vial containing **18**. The reaction mixture was stirred for 15 min. The reaction mixture was then diluted with DCM (30 mL) and extracted with saturated Na₂CO₃ (2 x 20 mL). The organic layer was dried with Na₂SO₄, and the solids removed by filtration. The filtrate was evaporated onto silica, and purified by Combiflash flash chromatography on a 4 g silica column, using a 100% hexanes mobile phase. The fractions containing the desired product were evaporated *in vacuo* to yield **33** as a colorless oil (68 mg, 83%). ¹H NMR (d₃-Acetonitrile, δ): 7.29 (m, 2H, H9), 7.21 (m, 2H, H10), 6.00 (dd, J=9.0Hz, 5.6Hz, 1H, H4), 5.67 (d, J=5.6Hz, 1H, H3), 5.32 (dd, J=9.0Hz, 6.0Hz, 1H, H5), 4.01 (dt, J=7.9Hz, 6.0Hz, 1H, H6), 2.72 (dd, J=13.2Hz, 7.8Hz, 1H, H8), 2.70 (s, 3H, H7), 2.64 (dd, J=13.2Hz, 6.0Hz, 1H, H8'). ¹³C NMR (d₃-Acetonitrile, δ): 148.0 (C10a), 132.5 (q, J=31.6Hz, C2), 136.6 (C9a), 131.0 (C9), 122.0 (C4), 121.9 (q, J=274Hz, CF3), 120.9 (C10), 120.7 (q, J=256Hz, OCF3), 118.3 (C5), 102.1 (q, J=6.3Hz, C3), 63.3 (C6), 39.8 (C7), 37.5 (C8).

2-(benzo[d][1,3]dioxol-5-yl)-1-methyl-6-(trifluoromethyl)-1,2-dihydropyridine (34).

Compound **16** (316 mg, 0.424 mmol) and acetone (4.0 mL) were combined in a 4 dram vial containing a stir bar. FeCp₂PF₆ (140 mg, 0.424 mmol) was dissolved in acetone (7.5 mL) in a separate 4 dram vial, and then this solution was transferred to the vial containing **16**. The reaction mixture was stirred for 15 min. The reaction mixture was then diluted with DCM (30 mL) and extracted with saturated Na₂CO₃ (2 x 20 mL). The organic layer was dried with Na₂SO₄, and the solids removed by filtration. The filtrate was evaporated onto silica, and purified by Combiflash flash chromatography on a 12 g silica column, using a 100% hexanes mobile phase. The fractions containing the desired product were evaporated *in vacuo* to yield **34** as a colorless oil (81 mg, 67%). ¹H NMR (d₁-Chloroform, δ): 6.91 (t, J=0.9Hz, 1H, H10), 6.76 (d, J=0.9Hz, 2H, H8+H9), 5.98 (dd, J=9.4Hz, 5.9Hz, 1H, H4), 5.95 (m, 2H, H11), 5.39 (d, J=5.9Hz, 1H, H3), 5.38 (dd, J=9.4Hz, 5.4Hz, 1H, H5), 4.86 (d, J=5.4Hz, 1H, H6), 2.85 (s, 3H, H7). ¹³C NMR (d₁-Chloroform, δ): 148.3 (C10a), 147.5 (C9a), 136.8 (C8a), 133.5 (q, J=30.4Hz, C2), 123.0 (q, J=273Hz, CF3), 120.8 (C5), 120.2 (C4), 119.5 (C8), 108.2 (C9), 107.3 (C10), 101.2 (C11), 98.1 (C3), 65.5 (C6), 37.9 (C7).

3-(benzo[d][1,3]dioxol-5-yl)-2-methyl-1-(trifluoromethyl)-2-azabicyclo[2.2.2]oct-7-ene-5,6-dicarbonitrile (35A).

Compound **34** (81mg, 0.286mmol) and fumaronitrile (106mg, 1.36mmol) were dissolved in MeCN (1.0 mL) in a small test tube containing a stir bar. The reaction mixture was placed in an oil bath at +80 °C and heated for 72 h. After heating, the reaction solution, containing a 2:1 mixture of diastereomers, was evaporated onto silica and purified by Combiflash flash chromatography on a 12 g silica column using 0-100% EtOAc in

hexanes gradient mobile phase. The fractions containing the desired product were evaporated *in vacuo* to yield a colorless oil, which was crystallized to yield exclusively **35A** by dissolution in minimal Et₂O followed by slow evaporation. (48 mg, 46%). ¹H NMR (d₂-Methylene Chloride, δ): 6.79 (m, 1H, H10), 6.75 (m, 2H, H11/H12), 6.68 (dd, J=8.4Hz, 1.3Hz, 1H, H7), 6.28 (dd, J=8.4Hz, 6.5Hz, 1H, H8), 5.93 (m, 2H, H13), 3.97 (d, J=1.9Hz, 1H, H6), 3.74 (d, J=5.2Hz, 1H, H3), 3.17 (m, 1H, H5), 3.09 (dd, J=5.2Hz, 2.9Hz, 1H, H4), 2.49 (s, 3H, H9). ¹³C NMR (d₂-Methylene Chloride, δ): 148.3 (C10a), 147.8 (C12a), 134.9 (C11a), 132.7 (C8), 131.8 (C7), 125.0 (q, J=283Hz, CF3), 119.5 (C11), 118.3 (CN), 117.3 (CN), 108.5 (C10), 108.0 (C12), 101.9 (C13), 63.7 (C6), 64.2 (q, J=27.5Hz, C2), 40.6 (C5), 36.8 (C9), 33.9 (C4), 28.3 (C3). ESI-MS: obs'd (%), calc'd (%), ppm, (M+H)⁺: 362.1113 (100), 362.1111 (100), 0.6.

3-benzyl-2-methyl-1-(trifluoromethyl)-2-azabicyclo[2.2.2]oct-7-ene-6-carbonitrile (36A).

Compound **32** (158 mg, 0.624 mmol) was dissolved in neat acrylonitrile (850 mg, 16.0 mmol) in a small test tube containing a stir bar. The reaction mixture was heated in an oil bath at +77 °C for 96 hr, and then evaporated onto silica and purified by Combiflash flash chromatography on a 12 g silica column using 0-100% EtOAc in hexanes gradient mobile phase. The fractions containing the desired product were evaporated *in vacuo* to yield **36A** as a colorless oil (118 mg, 62%). To obtain a crystal for X-ray diffraction, the hydrochloride salt of **36A** was prepared with HCl. ¹H NMR (d₃-MeCN, δ): 7.30 (m, 2H, H13), 7.22 (m, 1H, H14), 7.18 (m, 2H, H12), 6.63 (dd, J=8.5Hz, 1.4Hz, 1H, H8), 6.53 (dd, J=8.5Hz, 6.9Hz, 1H, H7), 3.56 (dd, J=9.8Hz, 4.3Hz, 1H, H3), 2.53 (m, 1H, H5), 2.60 (dd, J=13.2Hz, 5.7Hz, 1H, H11), 2.48 (m, 1H, H6), 2.33 (dd, J=13.4Hz, 8.8Hz, 1H,

H11'), 2.28 (s, 3H, H9), 2.10 (ddd, J= 13.2Hz, 9.8Hz, 2.6Hz, 1H, H4), 1.59 (ddd, J= 13.2Hz, 4.3Hz, 3.6Hz, 1H, H4'). ¹³C NMR (d₃-MeCN, δ): 139.7 (C12a), 136.0 (C8), 130.2 (C12), 129.6 (q, J=3.4Hz, C7), 129.3 (C13), 127.2 (C14), 126.6 (q, J=283Hz, CF3), 121.4 (C10), 69.1 (C6), 64.2 (q, J=26.4Hz, C2), 42.6 (C11), 37.9 (C9), 32.8 (C5), 30.9 (C4), 23.2 (C3).

Methyl 3-benzyl-2-methyl-1-(trifluoromethyl)-2-azabicyclo[2.2.2]oct-7-ene-6-carboxylate (37A).

Compound **32** (200 mg, 0.790 mmol) was dissolved in neat methyl acrylate (900mg, 10.4 mmol) in a small test tube containing a stir bar. The reaction mixture was heated in an oil bath at +77 °C for 96 hr, and then evaporated onto silica and purified by Combiflash flash chromatography on a 12 g silica column using 0-100% EtOAc in hexanes gradient mobile phase. The fractions containing the desired product were evaporated *in vacuo* to yield **22** as a colorless oil (188 mg, 70%). To obtain a crystal for X-ray diffraction, the hydrochloride salt of **22** was prepared with HCl (dr = 97:3). ¹H NMR (d₃-MeCN, δ): 7.30 (m, 2H, H13), 7.21 (m, 1H, H14), 7.19 (m, 2H, H12), 6.49 (dd, J=8.5Hz, 6.9Hz, 1H, H8), 6.28 (dd, J=8.5Hz, 1.3Hz, 1H, H7), 3.57 (s, 3H, H10), 3.36 (dd, J=9.4Hz, 5.0Hz, 1H, H3), 2.64 (dd, J=13.1Hz, 5.0Hz, 1H, H11), 2.46 (m, 1H, H5), 2.40 (m, 1H, H6), 2.31 (dd, J=13.1Hz, 9.2Hz, 1H, H11'), 2.35 (s, 3H, H9), 1.77 (ddd, J= 12.7Hz, 9.4Hz, 3.0Hz, 1H, H4), 1.59 (ddd, J= 12.7Hz, 5.0Hz, 3.1Hz, 1H, H4'). ¹³C NMR (d₃-MeCN, δ): 174.2 (Ester CO), 140.1 (C12a), 134.2 (C8), 130.2 (C12), 129.5 (q, J=3.2Hz, C7), 129.3 (C13), 127.1 (C14), 127.1 (q, J=282Hz, CF3), 69.2 (C6), 64.8 (q, J=26.7Hz, C2), 52.4 (C10), 42.7 (C11), 37.2 (C9), 36.9 (C3), 33.0 (C5), 30.2 (C4).

2,9-dimethyl-8-phenyl-4-(trifluoromethyl)-3a,4,7,7a-tetrahydro-1H-4,7-(epiminomethano)isoindole-1,3(2H)-dione (38).

Compound **31** (33.0 mg, 0.138 mmol) and NMM (250 mg, 2.25 mmol) were dissolved in MeCN (1.5 mL) in a 1 dram vial. The reaction mixture was heated at +80 °C in an oil bath for 16 h and then evaporated *in vacuo* onto 1 g silica. The crude product was purified by Combiflash flash chromatography on a 12 g silica column, using a 0-100% EtOAc in hexanes gradient mobile phase. The fractions containing the desired product were evaporated *in vacuo* to yield **38** as a colorless oil, which spontaneously crystallized. (41 mg, 85%). ¹H NMR (d-Chloroform, δ): 7.30 (m, 4H, H11 + H12), 7.24 (m, 1H, H13), 6.45 (dd, J=8.4Hz, 1.3Hz, 1H, H7), 5.96 (dd, J=8.4Hz, 6.5Hz, 1H, H8), 3.73 (d, J=8.2Hz, 1H, H3), 3.55 (d, J=1.4Hz, 1H, H6), 3.43 (m, 1H, H5), 3.30 (dd, J=8.2Hz, 3.5Hz, 1H, H4), 2.92 (s, 3H, H10), 2.46 (s, 3H, H9). ¹³C NMR NMR (d-Chloroform, δ): 176.6 (Imide CO), 174.5 (Imide CO), 141.6 (C11a), 130.6 (C7), 130.5 (C8), 128.3 (C12), 127.6 (C13), 127.1 (C11), 125.2 (q, J=282Hz, CF3), 67.8 (C6), 63.8 (q, J=28.6Hz, C2), 43.3 (C4), 39.5 (C5), 38.9 (C3), 37.3 (C9), 25.2 (C10).). ESI-MS: obs'd (%), calc'd (%), ppm, (M+H)⁺: 351.1318 (100), 351.1315(100), 0.8.

8-benzyl-2,9-dimethyl-4-(trifluoromethyl)-3a,4,7,7a-tetrahydro-1H-4,7-(epiminomethano)isoindole-1,3(2H)-dione (39).

Compound **32** (50.0 mg, 0.197 mmol) and NMM (219 mg, 1.97 mmol) were dissolved in MeCN (1.5 mL) in a 1 dram vial. The reaction mixture was heated at +80 °C in an oil bath for 24 h and then evaporated *in vacuo* onto 1 g silica. The crude product was purified by Combiflash flash chromatography on a 12 g silica column, using a 0-100% EtOAc in hexanes gradient mobile phase. The fractions containing the desired product

were evaporated *in vacuo* to yield **39** as a colorless oil, which was crystallized by dissolution in minimal Et₂O followed by slow evaporation. (67 mg, 91%). ¹H NMR (d₃-Acetonitrile, δ): 7.32 (m, 2H, H13), 7.25 (m, 1H, H14), 7.21 (m, 2H, H12), 6.37 (dd, J=8.4Hz, 1.6Hz, 1H, H7), 6.33 (m, 1H, H8), 3.62 (d, J=8.0Hz, 1H, H3), 3.01 (dd, J=8.0Hz, 3.4Hz, 1H, H4), 2.89 (m, 1H, H5), 2.76 (s, 3H, H10), 2.69 (dd, J=13.4Hz, 5.0Hz, 1H, H11), 2.56 (ddd, J=8.9Hz, 5.7Hz, 1.2Hz, 1H, H6), 2.35 (dd, J=13.4Hz, 8.9Hz, 1H, H11'), 2.33 (s, 3H, H9). ¹³C NMR (d₃-Acetonitrile, δ): 177.8 (Imide CO), 175.9 (Imide CO), 139.6 (C12a), 132.5 (C8), 130.4 (q, J=3.7Hz, C7), 130.3 (C12), 129.4 (C13), 127.3 (C14), 126.5 (q, J=282Hz, CF3), 68.0 (C6), 64.6 (q, J=27.6Hz, C2), 43.0 (C4), 42.2 (C11), 39.6 (C3), 37.8 (C9), 35.6 (C5), 25.1 (C10). ESI-MS: obs'd (%), calc'd (%), ppm, (M+H)⁺: 365.1475 (100), 365.1471 (100), 1.1.

2,9-dimethyl-8-(4-(trifluoromethoxy)benzyl)-4-(trifluoromethyl)-3a,4,7,7a-tetrahydro-1H-4,7-(epiminomethano)isoindole-1,3(2H)-dione (40).

Compound **33** (77.0 mg, 0.228 mmol) and NMM (254 mg, 2.29 mmol) were dissolved in MeCN (2.0 mL) in a 1 dram vial. The reaction mixture was heated at +80 °C in an oil bath for 24 h and then evaporated *in vacuo* onto 1 g silica. The crude product was purified by Combiflash flash chromatography on a 12 g silica column, using a 0-100% EtOAc in hexanes gradient mobile phase. The fractions containing the desired product were evaporated *in vacuo* to yield **40** as a colorless oil, which was crystallized by dissolution in minimal Et₂O followed by slow evaporation. (101 mg, 98%). ¹H NMR (d₆-Acetone, δ): 7.41 (m, 2H, H13), 7.29 (d, J=8.0Hz, 2H, H12), 6.41 (m, 2H, H7+H8), 3.80 (d, J=8.1Hz, 1H, H3), 3.18 (dd, J=8.1Hz, 3.4Hz, 1H, H4), 3.04 (m, 1H, H5), 2.77 (s, 3H, H10), 2.74 (dd, J=12.8Hz, 6.1Hz, 1H, H11), 2.71 (m, 1H, H6), 2.51 (dd, J=12.8Hz,

7.8Hz, 1H, H11'), 2.35 (s, 3H, H9). ^{13}C NMR (d_6 -Acetone, δ): 177.3 (Imide CO), 175.2 (Imide CO), 148.5 (C13a), 139.1 (C12a), 132.4 (C8), 132.0 (C12), 130.3 (q, $J=3.7\text{Hz}$, C7), 126.4 (q, $J=282\text{Hz}$, CF3), 121.9 (C13), 121.5 (q, $J=255\text{Hz}$, OCF3) 68.0 (C6), 64.5 (q, $J=27.6\text{Hz}$, C2), 42.9 (C4), 41.7 (C11), 39.6 (C3), 37.9 (C9), 35.8 (C5), 24.9 (C10). ESI-MS: obs'd (%), calc'd (%), ppm, (M+H) $^+$: 449.1295 (100), 449.1294 (100), 0.2.

8-(benzo[d][1,3]dioxol-5-yl)-2,9-dimethyl-4-(trifluoromethyl)-3a,4,7,7a-tetrahydro-1H-4,7-(epiminomethano)isoindole-1,3(2H)-dione (41).

Compound **34** (56.0 mg, 0.198 mmol) and NMM (219 mg, 1.97 mmol) were dissolved in MeCN (1.5 mL) in a 1 dram vial. The reaction mixture was heated at +80 °C in an oil bath for 24 h and then evaporated *in vacuo* onto 1 g silica. The crude product was purified by Combiflash flash chromatography on a 12 g silica column, using a 0-100% EtOAc in hexanes gradient mobile phase. The fractions containing the desired product were evaporated *in vacuo* to yield **41** as a colorless oil, which was crystallized by dissolution in minimal Et₂O followed by slow evaporation. (68 mg, 87%). ^1H NMR (d_2 -Methylene Chloride, δ): 6.83 (d, $J=1.7\text{Hz}$, 1H, H11), 6.78 (dd, $J=8.0\text{Hz}$, 1.7Hz, 1H, H13), 6.73 (d, $J=8.0\text{Hz}$, 1H, H12), 6.42 (dd, $J=8.4\text{Hz}$, 1.4Hz, 1H, H7), 5.98 (dd, $J=8.4\text{Hz}$, 6.5Hz, 1H, H8), 5.91 (m, 2H, H14), 3.68 (d, $J=8.1\text{Hz}$, 1H, H3), 3.47 (d, $J=1.3\text{Hz}$, 1H, H6), 3.34 (m, 1H, H5), 3.27 (dd, $J=8.1\text{Hz}$, 3.5Hz, 1H, H4), 2.87 (s, 3H, H10), 2.42 (s, 3H, H9). ^{13}C NMR (d_2 -Methylene Chloride, δ): 176.8 (Imide CO), 174.8 (Imide CO), 148.1 (C11a), 147.9 (C12a), 136.6 (C13a), 131.2 (C7), 130.8 (C8), 125.8 (q, $J=282\text{Hz}$, CF3), 120.7 (C13), 108.3 (C11), 108.1 (C12), 101.7 (C14), 67.8 (C6), 64.2 (q, $J=28.4\text{Hz}$, C2), 43.7 (C4), 40.1 (C3), 39.3 (C9), 37.4 (C5), 25.3 (C10). ESI-MS: obs'd (%), calc'd (%), ppm, (M+H) $^+$: 395.1216 (100), 395.1213 (100), 0.8.

Control experiments experimental details

Synthesis of 1-methyl-2-(trifluoromethyl)pyridin-1-ium triflate:

2-(trifluoromethyl)pyridine (2.00 g, 13.6 mmol) was dissolved in Et₂O (50 mL) in a 100 mL round-bottom flask charged with a stir bar. After 1 min, MeOTf (2.21 g, 13.5 mmol) was added dropwise. The reaction mixture was allowed to stir for 3 h, resulting in the formation of a colorless precipitate. The reaction mixture was transferred to a 125 mL filter flask and evaporated to half volume under vacuum. The solid was isolated on a 30 mL medium porosity fritted funnel, washed with cold Et₂O (3 x 15 mL) and desiccated to yield a colorless crystalline solid (3.65 g, 87 %). ¹H NMR (d₃-MeCN, δ): 8.97 (d, J= 6.0Hz, 1H), 8.76 (t, J= 7.9Hz, 1H), 8.48 (d, J= 7.9Hz, 1H), 8.31 (dd, J=7.9Hz, 6.0Hz, 1H), 4.45 (s, 3H).

[TpMo(NO)(DMAP)(3,4-η²-2-(trifluoromethyl)-N-methylpyridinium)]⁺ (OTf) Direct Exchange Synthesis:

Compound **1**, TpMo(NO)(DMAP)(η²-PhCF₃) (100 mg, 0.165 mmol) was added to a 4 dram vial charged with a stir bar, followed by a solution of 1-methyl-2-(trifluoromethyl)pyridin-1-ium triflate (110 mg, 0.353 mmol) in THF (2.0 mL). The reaction mixture immediately changed from orange to deep green. After 15 min, the reaction was checked via CV, indicating an E_{1/2} at -1.3 V, consistent with metal oxidation. A 0.1 mL aliquot was also checked by ¹H NMR in 0.6 mL d₆-acetone, which revealed the absence of starting material or desired product.

Metal-free Grignard additions to 1-methyl-2-(trifluoromethyl)pyridin-1-ium triflate:

1-methyl-2-(trifluoromethyl)pyridin-1-ium triflate (100 mg, 0.321 mmol) was suspended

in either THF (1.0 mL) *or* Et₂O (1.0 mL) in a 4 dram vial charged with a stir pea. The resulting suspension was allowed to stir for 15 min at either ambient temperature *or* at -60 °C in a cold bath, then a 1.0 M solution of benzylmagnesium chloride in Et₂O (0.32 mL, 0.32 mmol) was added dropwise. After addition, the reaction mixture was stirred at ambient temperature for 15 min. A 0.1 mL aliquot was dissolved in 0.5 mL d₈-THF, and analyzed by ¹H NMR. The crude ratios of the two major products are reported in the table below.

Figure 3.5: Dihydropyridine product mixture under Mo-free reaction conditions

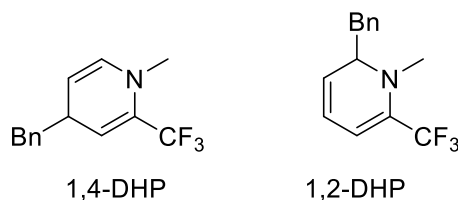


Table 3.1: Dihydropyridine product ratio under various Mo-free reaction conditions

Reaction Conditions	1,4-DHP : 1,2-DHP Product Ratio
THF, -60 °C	2:1
Et ₂ O, -60 °C	3:1
THF, 20 °C	3:1
Et ₂ O, 20 °C	5:1

To isolate the product mixtures, the reaction solutions were passed through a plug of 1 cm basic Al₂O₃ in a 15 mL medium porosity fritted disc, eluted with hexanes (10 mL), and evaporated to dryness. The product ratios did not change. Major Product ¹H NMR (d₂-Methylene Chloride, δ): 7.28 (m, 2H), 7.20 (m, 1H), 7.14 (d, J= 7.7Hz, 2H), 5.74 (d, J= 7.6Hz, 1H), 5.10 (m, 1H), 4.39 (m, 1H), 3.37 (bs, 1H), 2.86 (s, 3H), 2.68 (m, 2H).

Single crystal X-ray diffraction experimental details

A single crystal of **10**, **11**, **12**, **13**, **14**, **16**, **18**, **35A**, **36A·HCl**, or **37A·HCl** was coated with Paratone oil and mounted on a MiTeGen MicroLoop. The X-ray intensity data were measured on a Bruker Kappa APEXII Duo system using an Incoatec Microfocus I μ S source (Cu K α , $\lambda = 1.54178 \text{ \AA}$) and a multi-layer mirror monochromator for **R-39**, **41** and **36A·HCl**, and a graphite monochromator and a fine-focus sealed tube source (Mo K α , $\lambda = 0.71073 \text{ \AA}$) for all others. The frames were integrated with the Bruker SAINT software package³⁸ using a narrow-frame algorithm. Data were corrected for absorption effects using the Multi-Scan method (SADABS).³⁸ Each structure was solved and refined using the Bruker SHELXTL Software Package³⁹ within APEX3³⁸ and OLEX2.⁴⁰ Non-hydrogen atoms were refined anisotropically. The B-H hydrogen atoms in **10-16** were located in the diffraction map and refined isotropically, as were the H10 and H11 atoms in **16**, and the N-H hydrogen atoms in **36A·HCl** and **37A·HCl**. All other hydrogen atoms were placed in geometrically calculated positions with $U_{iso} = 1.2U_{equiv}$ of the parent atom ($U_{iso} = 1.5 U_{equiv}$ for methyl). In **11** and **15**, electron density difference maps revealed that there was disordered solvent that could not be successfully modeled with or without restraints. Thus, the structure factors were modified using the PLATON SQUEEZE⁴¹ technique, in order to produce a “solvate-free” structure factor set. PLATON reported a total electron density of 247 e⁻ and total solvent accessible volume of 959 \AA^3 , likely representing one pentane molecule per asymmetric unit in **15**, and a total electron density of 132 e⁻ and total solvent accessible volume of 535 \AA^3 , likely representing two THF molecules per asymmetric unit in **11**. In **18**, a CH₂Cl₂ solvent molecule was disordered across three different orientations and in **16**, a CH₂Cl₂ solvent molecule was found to be disordered

over two positions. The relative occupancies of the positions were freely refined, and constraints were used on the anisotropic displacement parameters of the disordered atoms, and restraints were used on the disordered bonds.

Table 3.2: Crystal data table for compounds **10**, **15**, **16**, and **18**

	10	15	16	18
CCDC	1935758	1935759	1935761	1935760
Chemical formula	C ₂₇ H ₃₃ BF ₆ Mo N ₁₀ O ₅ S	C ₃₀ H ₃₄ BCl ₂ F ₃ Mo N ₁₀ O	C ₃₂ H ₃₆ BCl ₄ F ₃ Mo N ₁₀ O ₃	C ₆₃ H ₆₈ B ₂ Cl ₂ F ₁₂ Mo ₂ N ₂₀ O ₄
FW (g/mol)	830.44	785.32	914.26	1681.25
T (K)	150(2)	100(2)	100(2)	100(2)
λ (Å)	0.71073	0.71073	0.71073	0.71073
Crystal size (mm)	0.136 x 0.225 x 0.254	0.073 x 0.085 x 0.314	0.075 x 0.170 x 0.320	0.308 x 0.380 x 0.682
Crystal habit	red block	yellow rod	yellow block	yellow block
Crystal system	monoclinic	monoclinic	triclinic	monoclinic
Space group	P2 ₁ /n	C2/c	P-1	P2 ₁ /c
a (Å)	14.228(3)	15.5566(11)	11.3506(8)	13.8205(8)
b (Å)	13.620(3)	25.0893(16)	12.5625(9)	25.6573(19)
c (Å)	18.353(4)	19.727(2)	14.3264(11)	20.2557(14)
α (°)	90	90	84.529(2)	90
β (°)	100.239(4)	102.353(2)	72.615(2)	92.501(3)
γ (°)	90	90	88.843(2)	90
V (Å³)	3499.9(13)	7521.3(10)	1940.6(2)	7175.8(8)
Z	4	8	2	4
ρ_{calc} (g/cm³)	1.576	1.387	1.565	1.556
μ (mm⁻¹)	0.519	0.544	0.676	0.517
θ range (°)	1.67 - 29.61	1.57 - 25.76	1.50 - 30.59	1.28 - 29.61
Index ranges	-19 ≤ h ≤ 18 -18 ≤ k ≤ 16 -23 ≤ l ≤ 25	-18 ≤ h ≤ 19 -27 ≤ k ≤ 30 -24 ≤ l ≤ 21	-15 ≤ h ≤ 16 -17 ≤ k ≤ 17 -20 ≤ l ≤ 20	-19 ≤ h ≤ 19 -35 ≤ k ≤ 35 -28 ≤ l ≤ 27
Reflns coll.	42091	32559	48715	95106
Ind. reflns	9816 [R _{int} = 0.0492]	7173 [R _{int} = 0.0888]	11897 [R _{int} 0.0505]	20173 [R _{int} = 0.0490]
Data / restraints / parameters	9816 / 0 / 469	7173 / 0 / 439	11897 / 4 / 515	20173 / 19 / 991
Goodness-of-fit on F²	1.016	1.028	1.023	1.044
R₁ [I > 2σ(I)]	0.0348	0.0595	0.0363	0.0421
wR₂ [all data]	0.0816	0.1607	0.0852	0.1029

Table 3.3: Crystal data table for compounds **11**, **12**, **13**, **14**

	11	12	13	14
CCDC	1949466	1949464	1949465	1949463
Chemical formula	C ₆₉ H ₈₄ B ₃ F ₉ Mo ₃ N ₃₀ O ₃	C ₂₆ H ₃₂ BF ₃ MoN ₁₀ O	C ₂₇ H ₃₄ BF ₃ MoN ₁₀ O ₃	C ₂₄ H ₃₀ BF ₃ MoN ₁₀ O
FW (g/mol)	1872.91	664.36	710.39	638.33
T (K)	150(2)	150(2)	150(2)	150(2)
λ (Å)	0.71073	0.71073	0.71073	0.71073
Crystal size (mm)	0.201 x 0.229 x 0.381	0.151 x 0.166 x 0.201	0.064 x 0.234 x 0.366	0.081 x 0.116 x 0.182
Crystal habit	yellow plate	yellow block	yellow plate	yellow block
Crystal system	triclinic	monoclinic	triclinic	monoclinic
Space group	P -1	P2 ₁ /c	P -1	P2 ₁ /c
a (Å)	12.4230(10)	13.8170(13)	12.4233(9)	13.7450(6)
b (Å)	18.4355(15)	15.5253(15)	15.1163(11)	15.2669(8)
c (Å)	19.7901(16)	14.0856(13)	19.2382(14)	13.9370(6)
α (°)	98.9410(10)	90	109.4090(10)	90
β (°)	94.1500(10)	104.603(2)	90.2530(10)	105.4320(10)
γ (°)	97.2860(10)	90	109.3240(10)	90
V (Å ³)	4421.5(6)	2923.9(5)	3188.9(4)	2819.1(2)
Z	2	4	4	4
ρ_{calc} (g/cm ³)	1.407	1.509	1.480	1.504
μ (mm ⁻¹)	0.498	0.507	0.475	0.523
θ range (°)	1.66 - 29.61	1.52 - 28.31	1.13 - 29.61	1.54 - 29.62
Index ranges	-17 ≤ h ≤ 17 -25 ≤ k ≤ 25 -27 ≤ l ≤ 27	-18 ≤ h ≤ 11 -20 ≤ k ≤ 20 -18 ≤ l ≤ 18	-17 ≤ h ≤ 16 -20 ≤ k ≤ 21 -26 ≤ l ≤ 26	-18 ≤ h ≤ 19 -19 ≤ k ≤ 21 -19 ≤ l ≤ 19
Reflns coll.	106541	29388	69581	57215
Ind. reflns	24880 [R _{int} = 0.0354]	7276 [R _{int} = 0.0755]	17915 [R _{int} = 0.0682]	7943 [R _{int} = 0.0652]
Data / restraints / parameters	24880 / 0 / 1075	7276 / 0 / 386	17915 / 7 / 827	7943 / 0 / 369
Goodness-of-fit on F ²	1.020	1.050	1.017	1.019
R ₁ [I > 2 σ (I)]	0.0297	0.0461	0.0416	0.0304
wR ₂ [all data]	0.0745	0.0854	0.0916	0.0713

Table 3.4: Crystal data table for compounds **39**, **R-39**, **40**, **41**

	39	R-39	40	41
CCDC	1935762	1957279	1935763	1935764
Chemical formula	C ₁₉ H ₁₉ F ₃ N ₂ O ₂	C ₁₉ H ₁₉ F ₃ N ₂ O ₂	C ₂₀ H ₁₈ F ₆ N ₂ O ₃	C ₁₉ H ₁₇ F ₃ N ₂ O ₄
FW (g/mol)	364.36	364.36	448.36	394.34
T (K)	100(2)	100(2)	100(2)	100(2)
λ (Å)	0.71073	1.54178	0.71073	1.54178
Crystal size (mm)	0.154 x 0.227 x 0.381	0.037 x 0.043 x 0.421	0.228 x 0.390 x 0.613	0.098 x 0.113 x 0.157
Crystal habit	colorless plate	colorless rod	colorless block	colorless block
Crystal system	monoclinic	monoclinic	triclinic	monoclinic
Space group	Cc	P2 ₁	P-1	C2/c
a (Å)	10.8231(12)	10.6487(12)	11.0432(11)	19.0565(11)
b (Å)	20.891(2)	7.4485(8)	11.4785(11)	7.1857(4)
c (Å)	7.2837(8)	10.8541(12)	16.9996(16)	26.1183(14)
α (°)	90	90	101.568(3)	90
β (°)	90.103(3)	102.152(8)	97.159(3)	110.890(3)
γ (°)	90	90	110.427(3)	90
V (Å ³)	1646.9(3)	841.62(16)	1933.4(3)	3341.4(3)
Z	4	2	4	8
ρ_{calc} (g/cm ³)	1.470	1.438	1.540	1.568
μ (mm ⁻¹)	0.119	0.991	0.142	1.143
θ range (°)	1.95 - 29.61	4.17 to 68.44	1.96 - 30.56	3.62 - 68.43
Index ranges	-15 ≤ h ≤ 15 -28 ≤ k ≤ 28 -10 ≤ l ≤ 10	-12 ≤ h ≤ 11 -8 ≤ k ≤ 8 -13 ≤ l ≤ 13	-15 ≤ h ≤ 15 -16 ≤ k ≤ 16 -24 ≤ l ≤ 24	-22 ≤ h ≤ 22 -8 ≤ k ≤ 8 -31 ≤ l ≤ 31
Refins coll.	19226	12088	76270	21883
Ind. reflns	4443 [R _{int} = 0.0266]	3063 [R _{int} = 0.0590]	11852 [R _{int} =0.0282]	3075 [R _{int} = 0.0534]
Data / restraints / parameters	4443 / 2 / 237	3063 / 1 / 237	11852 / 0 / 563	3075 / 0 / 255
Goodness-of-fit on F ²	1.038	1.029	1.053	1.027
R ₁ [I > 2 σ (I)]	0.0290	0.0382	0.0407	0.0341
wR ₂ [all data]	0.0701	0.0953	0.1179	0.0900

Table 3.5: Crystal data table for 35A, 36A·HCl and 37A·HCl

	35A	36A·HCl	37A·HCl
CCDC	1935765	1957280	1957281
Chemical formula	C ₁₈ H ₁₄ F ₃ N ₃ O ₂	C ₁₇ H ₁₈ ClF ₃ N ₂	C ₁₈ H ₂₁ ClF ₃ NO ₂
FW (g/mol)	361.32	342.78	375.81
T (K)	100(2)	100(2)	100(2)
λ (Å)	0.71073	1.54178	0.71073
Crystal size (mm)	0.188 x 0.402 x 0.704	0.061 x 0.078 x 0.119	0.071 x 0.073 x 0.342
Crystal habit	colorless block	colorless block	colorless rod
Crystal system	monoclinic	monoclinic	monoclinic
Space group	I2/a	P2 ₁ /n	C 2/c
a (Å)	19.2180(9)	6.6579(3)	22.224(4)
b (Å)	8.0933(4)	20.4939(9)	12.486(3)
c (Å)	20.8998(16)	12.6239(6)	13.371(3)
α (°)	90	90	90
β (°)	96.456(2)	104.427(3)	92.751(6)
γ (°)	90	90	90
V (Å ³)	3230.1(3)	1668.17(13)	3706.0(12)
Z	8	4	8
ρ _{calc} (g/cm ³)	1.486	1.365	1.347
μ (mm ⁻¹)	0.122	2.307	0.245
θ range (°)	1.96 - 28.32	4.21 to 68.36	1.83 to 25.74
Index ranges	-25 ≤ h ≤ 25 -10 ≤ k ≤ 10 -27 ≤ l ≤ 26	-8 ≤ h ≤ 7 -24 ≤ k ≤ 24 -14 ≤ l ≤ 15	-26 ≤ h ≤ 27 -15 ≤ k ≤ 15 -16 ≤ l ≤ 16
Reflns coll.	18592	13339	18087
Ind. reflns	4022 [R _{int} = 0.0224]	3049 [R _{int} = 0.0573]	3540 [R _{int} = 0.0992]
Data / restraints / parameters	4022 / 0 / 236	3049 / 0 / 213	3540 / 0 / 232
Goodness-of-fit on F ²	1.032	1.039	1.000
R ₁ [I > 2σ(I)]	0.0549	0.0382	0.0479
wR ₂ [all data]	0.1479	0.1037	0.0895

References

- (1) Kundig, E. P. *Transition Metal Arene Complexes in Organic Synthesis and Catalysis*, 2004; Vol. 7.
- (2) Liebov, B. K.; Harman, W. D. *Chemical Reviews* **2017**, *117*, 13721.
- (3) Valahovic, M. T.; Gunnoe, T. B.; Sabat, M.; Harman, W. D. *Journal of the American Chemical Society* **2002**, *124*, 3309.
- (4) Delafuente, D. A.; Kosturko, G. W.; Graham, P. M.; Harman, W. H.; Myers, W. H.; Surendranath, Y.; Klet, R. C.; Welch, K. D.; Trindle, C. O.; Sabat, M.; Harman, W. D. *J. Am. Chem. Soc.* **2007**, *129*, 406.
- (5) Wilson, K. B.; Smith, J. A.; Nedzbala, H. S.; Pert, E. K.; Dakermanji, S. J.; Dickie, D. A.; Harman, W. D. *The Journal of Organic Chemistry* **2019**, *84*, 6094.
- (6) Harrison, D. P.; Zottig, V. E.; Kosturko, G. W.; Welch, K. D.; Sabat, M.; Myers, W. H.; Harman, W. D. *Organometallics* **2009**, *28*, 5682.
- (7) Myers, J. T.; Smith, J. A.; Dakermanji, S. J.; Wilde, J. H.; Wilson, K. B.; Shivokevich, P. J.; Harman, W. D. *J. Am. Chem. Soc.* **2017**, *139*, 11392.
- (8) Müller, K.; Faeh, C.; Diederich, F. *Science* **2007**, *317*, 1881.
- (9) Welch, K. D.; Harrison, D. P.; Lis, E. C., Jr.; Liu, W.; Salomon, R. J.; Harman, W. D.; Myers, W. H. *Organometallics* **2007**, *26*, 2791.
- (10) Keane, J. M.; Ding, F.; Sabat, M.; Harman, W. D. *J. Am. Chem. Soc.* **2004**, *126*, 785.
- (11) Orr, S. T. M.; Ripp, S. L.; Ballard, T. E.; Henderson, J. L.; Scott, D. O.; Obach, R. S.; Sun, H.; Kalgutkar, A. S. *Journal of Medicinal Chemistry* **2012**, *55*, 4896.
- (12) Leroux, F. R.; Manteau, B.; Vors, J.-P.; Pazenok, S. *Beilstein journal of organic chemistry* **2008**, *4*, 13.

- (13) Poddubnyi, I. S. *Chemistry of Heterocyclic Compounds* **1995**, *31*, 682.
- (14) Sowmiah, S.; Esperança, J. M. S. S.; Rebelo, L. P. N.; Afonso, C. A. M. *Organic Chemistry Frontiers* **2018**, *5*, 453.
- (15) Porwisiak, J.; Dmowski, W. *Tetrahedron* **1994**, *50*, 12259.
- (16) Gillman, K. W.; Parker, M. F.; Silva, M.; Degnan, A. P.; Tora, G. O.; Lodge, N. J.; Li, Y.-W.; Lelas, S.; Taber, M.; Krause, R. G.; Bertekap, R. L.; Newton, A. E.; Pieschl, R. L.; Lengyel, K. D.; Johnson, K. A.; Taylor, S. J.; Bronson, J. J.; Macor, J. E. *Bioorganic & Medicinal Chemistry Letters* **2013**, *23*, 407.
- (17) Martin, R. M.; Bergman, R. G.; Ellman, J. A. *Organic Letters* **2013**, *15*, 444.
- (18) Wilson, K. B.; Myers, J. T.; Nedzbala, H. S.; Combee, L. A.; Sabat, M.; Harman, W. D. *Journal of the American Chemical Society* **2017**, *139*, 11401.
- (19) Shivokevich, P. J.; Myers, J. T.; Smith, J. A.; Pienkos, J. A.; Dakermanji, S. J.; Pert, E. K.; Welch, K. D.; Trindle, C. O.; Harman, W. D. *Organometallics* **2018**.
- (20) Villani, F. J.; Costanzo, M. J.; Inners, R. R.; Mutter, M. S.; McClure, D. E. *The Journal of Organic Chemistry* **1986**, *51*, 3715.
- (21) Fowler, F. W. *The Journal of Organic Chemistry* **1972**, *37*, 1321.
- (22) Sundberg, R. J.; Bloom, J. D. *The Journal of Organic Chemistry* **1981**, *46*, 4836.
- (23) Bull, J. A.; Mousseau, J. J.; Pelletier, G.; Charette, A. B. *Chemical Reviews* **2012**, *112*, 2642.
- (24) Colby, D. A.; Bergman, R. G.; Ellman, J. A. *Journal of the American Chemical Society* **2008**, *130*, 3645.
- (25) Duttwyler, S.; Lu, C.; Rheingold, A. L.; Bergman, R. G.; Ellman, J. A. *Journal of the American Chemical Society* **2012**, *134*, 4064.

- (26) Oshima, K.; Ohmura, T.; Suginome, M. *Journal of the American Chemical Society* **2012**, *134*, 3699.
- (27) Pittol, C. A.; Pryce, R. J.; Roberts, S. M.; Ryback, G.; Sik, V.; Williams, J. O. *Journal of the Chemical Society, Perkin Transactions 1* **1989**, 1160.
- (28) Szilagyi, S.; Ross, J. A.; Lemal, D. M. *Journal of the American Chemical Society* **1975**, *97*, 5586.
- (29) Baker, F. W.; Stock, L. M. *The Journal of Organic Chemistry* **1967**, *32*, 3344.
- (30) Faisal, M.; Shahzad, D.; Saeed, A.; Lal, B.; Saeed, S.; Larik, F. A.; Channar, P. A.; Mahesar, P. A.; Mahar, J. *Tetrahedron: Asymmetry* **2017**, *28*, 1445.
- (31) Lovering, F.; Bikker, J.; Humblet, C. *Journal of Medicinal Chemistry* **2009**, *52*, 6752.
- (32) Harrison, D. P.; Welch, K. D.; Nichols-Nielander, A. C.; Sabat, M.; Myers, W. H.; Harman, W. D. *J. Am. Chem. Soc.* **2008**, *130*, 16844.
- (33) Harrison, D. P.; Iovan, D. A.; Myers, W. H.; Sabat, M.; Wang, S.; Zottig, V. E.; Harman, W. D. *J. Am. Chem. Soc.* **2011**, *133*, 18378.
- (34) Harrison, D. P.; Sabat, M.; Myers, W. H.; Harman, W. D. *J. Am. Chem. Soc.* **2010**, *132*, 17282.
- (35) Kosturko, G. W.; Harrison, D. P.; Sabat, M.; Myers, W. H.; Harman, W. D. *Organometallics* **2009**, *28*, 387.
- (36) Myers, J. T.; Shivokevich, P. J.; Pienkos, J. A.; Sabat, M.; Myers, W. H.; Harman, W. D. *Organometallics* **2015**, *34*, 3648.
- (37) Garnier, E. C.; Liebeskind, L. S. *Journal of the American Chemical Society* **2008**, *130*, 7449.

- (38) Bruker, Saint; SADABS; APEX3. Inc., B. A., Ed. Madison, Wisconsin, USA, 2012.
- (39) Sheldrick, G., SHELXT - Integrated space-group and crystal-structure determination. *Acta Crystallographica Section A* 2015, 71 (1), 3-8.
- (40) Dolomanov, O. V.; Bourhis, L. J.; Gildea, R. J.; Howard, J. A. K.; Puschmann, H., OLEX2: a complete structure solution, refinement and analysis program. *Journal of Applied Crystallography* 2009, 42 (2), 339-341.
- (41) Spek, A., PLATON SQUEEZE: a tool for the calculation of the disordered solvent contribution to the calculated structure factors. *Acta Crystallographica Section C* 2015, 71 (1), 9-18.

Chapter 4: Tungsten-Promoted Synthesis of Aminotetrahydropyridines

Introduction

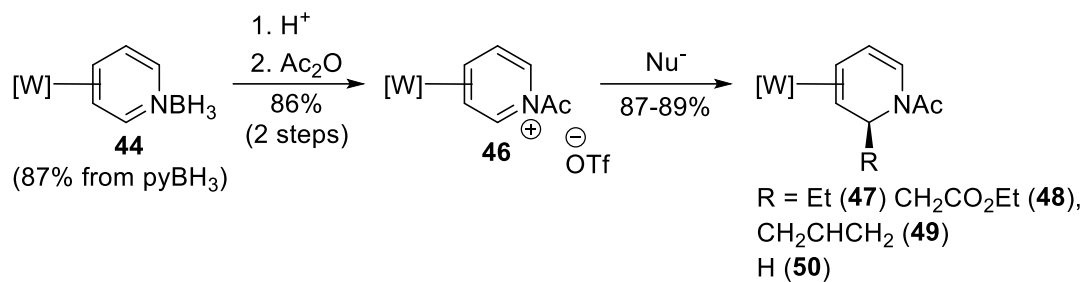
Nitrogen heterocycles are abundant in natural products and FDA-approved small molecule drugs.^{1,2} Many of these molecules also feature exocyclic nitrogen functional groups. However, this functionality can be difficult to incorporate, especially stereoselectively.

Previously, we have investigated tandem electrophilic-nucleophilic additions to dihapto-coordinate $\{\text{WTP}(\text{NO})(\text{PMe}_3)\}$ complexes of arenes and heteroarenes, including pyridine.³⁻⁵ In these examples, carbon nucleophiles were used almost exclusively. More recently, heteroatom nucleophiles, including methylamine, were successfully added to coordinated benzene and α,α,α -trifluorotoluene.^{6,7} Due to the medicinal relevance of amines and their derivatives, a more extensive survey of amine nucleophiles was undertaken using the complex $\text{WTP}(\text{NO})(\text{PMe}_3)(3,4\text{-}\eta^2\text{-1-acetylpyridinium})\text{OTf}$. The resulting 3-aminopiperidine products contain a structural motif found in drugs such as troxipide, tasocitinib, and alogliptin.^{8,9}

Results and Discussion

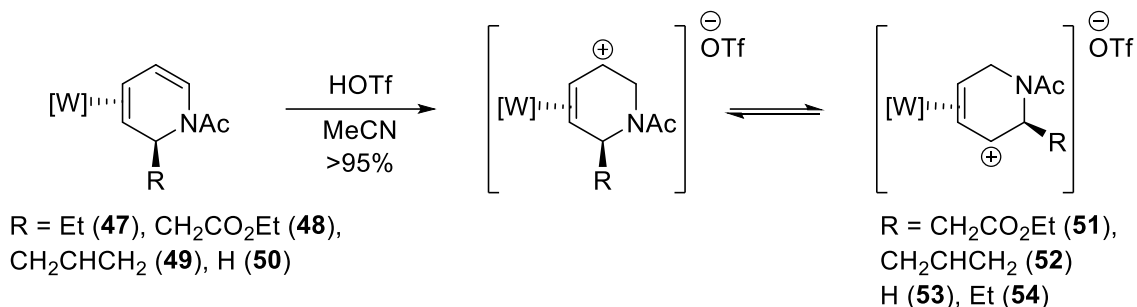
Due to preferential κN -coordination, pyridine must be bound to the $\{\text{WTP}(\text{NO})(\text{PMe}_3)\}$ fragment as pyridine-borane. Established procedures allow for deprotection of the nitrogen to yield the protonated pyridinium complex **45** and subsequent acetylation to yield $\text{WTP}(\text{NO})(\text{PMe}_3)(3,4\text{-}\eta^2\text{-N-acetylpyridinium})\text{OTf}$ (**46**).³ Amine addition to this complex would yield an aldoinal, which is expected to be unstable. Therefore, carbon or hydride nucleophiles were instead employed for this first nucleophilic addition. Treatment of $[\text{WTP}(\text{NO})(\text{PMe}_3)(3,4\text{-}\eta^2\text{-N-acetylpyridinium})]^+$ with

diethylzinc, zinc dust and ethyl bromoacetate, or zinc dust and allyl bromide yields the nucleophilic addition products **47** - **49**,⁴ respectively (**Scheme 4.1**). Similarly, this acetylpyridinium complex reacts with NaBH₄ to yield the dihydropyridine complex **50** according to literature procedures.⁵



Scheme 4.1: Synthesis of dihydropyridine complexes [W] = WTp(NO)(PMe₃)

Compounds **47-50** all undergo facile protonation to yield η^2 -allyl complexes **51** - **54** (**Scheme 4.2**).⁵ These allyl complexes may be isolated prior to treatment with a nucleophile, or the protonation may be conducted *in situ* to yield tetrahydropyridine complexes directly. These allyl complexes exist as two conformational isomers (**Scheme 4.2**) in which the metal forms strong bonds with two adjacent carbons and weakly coordinates a third carbon that chemically resembles a carbocation (denoted with a positive charge).¹⁰

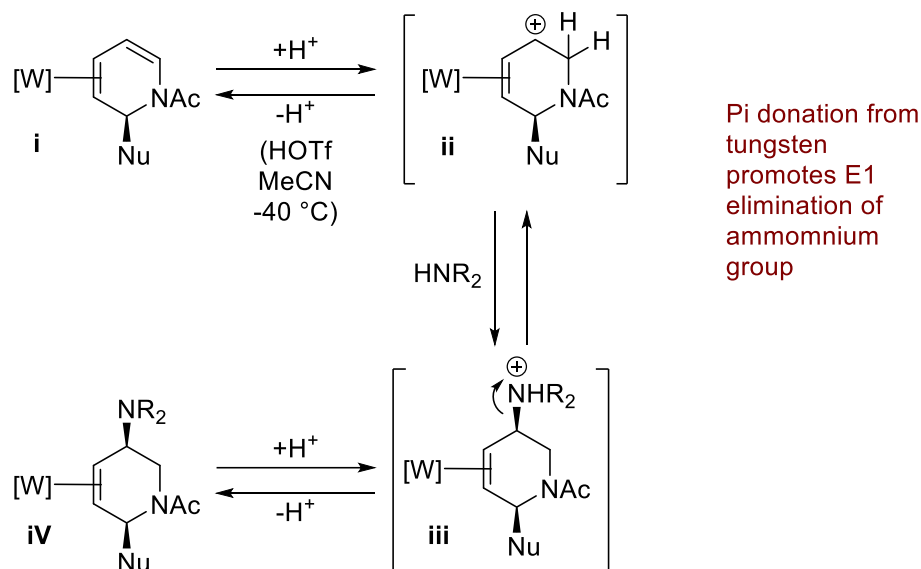


Scheme 4.2: Synthesis of allyl complex via protonation. [W] = WTp(NO)(PMe₃)

Although limited further chemistry has been demonstrated previously with compounds **53** and **54**, the addition reaction at C5 was restricted to a small number of carbon nucleophiles, such as lithium dimethylmalonate.⁵ Additionally, the substituent on C2 was found to have a considerable impact on the reactivity of the piperidine-based η^2 -allyl complexes. For example, reaction of the parent allyl **7** with ZnEt₂/CuCN at 0 °C gave exclusively the tetrahydropyridine addition product; in contrast, the analogous 2-ethyl substituted η^2 -allyl complex **54** gave a 1.9:1 mixture of addition to elimination products (i.e., , even at -30 °C.⁵ The C2-functionalized allyl complexes (R ≠ H) **51**, **52**, and **54** were thus anticipated to be significantly more prone to elimination than the parent allyl **53**. The nature of the nucleophile and reaction conditions thus had to be carefully selected to avoid deprotonation, which would regenerate the starting dihydropyridine complex.⁵ These factors made successful amine addition highly uncertain, particularly for the more complex substituted allyls **51**, **52**, and **54**.

Consistent with our concerns for elimination, treating **51-54** with methylamine in THF at 0 °C resulted only in formation of the precursor dihydropyridine complexes. Repeating this experiment at -30 °C likewise yielded only dihydropyridine products. However, when the reaction of **51** was conducted at -40 °C, frozen in liquid nitrogen, and

immediately analyzed by ^1H NMR, a new complex **55** was evident which lacked the characteristic alkene proton resonances of the dihydropyridine complex. However, after only a few minutes of warming, all of this new product had converted back to the dihydropyridine complex (**48**). It thus became evident that the amine products were highly sensitive to an E1-type elimination mechanism. The acid generated in the course of the reaction (in the form of an ammonium salt) can protonate the amino group of the product and result in a rapid elimination reaction, despite the large excess of free amine present in the reaction (**Scheme 4.3**).



Scheme 4.3: Reversible addition of an amine to a tungsten allyl complex and irreversible elimination upon warming

With the strong π -donor tungsten complex coordinated, the η^2 -dihydropyridine elimination product (i.e., **Scheme 4.3, i**) is thermodynamically preferred over the 5-aminotetrahydropyridine complex (**Scheme 4.3, iv**). It is only by the kinetic preference for addition over deprotonation that the desired tetrahydropyridine addition product (**iv**)

can be isolated. As the amine addition is reversible, unlike addition of the previously-employed carbon nucleophiles, stringent control of the reaction conditions is required to mitigate conversion to the thermodynamic product (i.e. the dihydropyridine complex **i**). Fortunately, it was found that quenching the reaction mixture with a strong base (*tert*-butoxide) before warming could almost completely prevent elimination. A relatively small amount of dihydropyridine product (**i**; 10-20%) was still observed in the quenched crude reaction mixtures, presumably caused by direct deprotonation of the allyl complex (**ii**) by the free amine.

Attempts to precipitate the addition complexes in water failed due to the E1 elimination described above, but the products were fairly stable to basic aqueous solution. The reaction mixtures were thus purified by extraction with saturated aqueous Na₂CO₃ followed by precipitation into Et₂O or hexanes. While extraction under neutral conditions yielded only elimination product, the initial ratio of addition to elimination products (5:1) was not significantly altered by extraction under basic conditions.

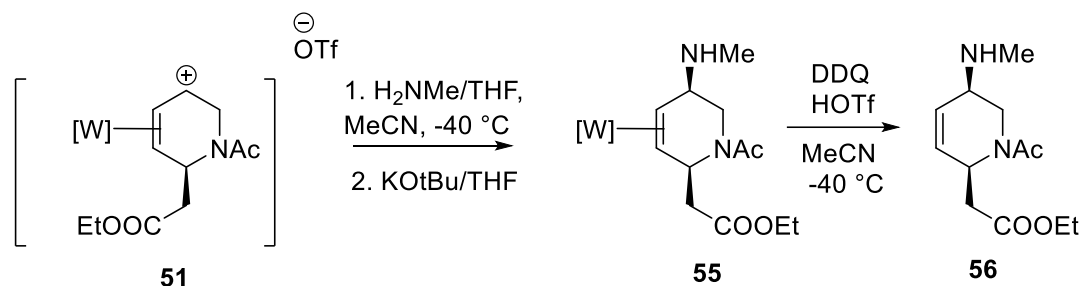
The metal complex **55** was characterized by ¹H, ¹³C, NOESY, COSY, HMBC, and HSQC NMR. It was determined that addition had occurred exclusively at C5, a regioselectivity seen previously in the addition of carbon nucleophiles to substituted piperidine allyl complexes. We note that this pattern is in contrast to the lack of selectivity sometimes seen for additions to substituted cyclohexadiene-derived allyl complexes of tungsten.^{5,7} As seen previously for both η²-pyridine and other systems, the nucleophilic addition takes place exclusively *anti* to the metal center, as determined by NOESY experiments. An NOE interaction was observed between H5 and a proton on the Tp ligand. Exchange peaks in the NOESY spectrum also revealed the presence of an

amide rotamer (4:1 rotamer ratio in CD₃CN). Such rotational isomers have been observed previously for other tetrahydropyridine complexes.⁵

Given that the amine addition complex (**55**) slowly eliminates in MeCN or DCM solution, it was decided to attempt to oxidize the tungsten complex without further purification. A wide variety of oxidants were screened, including NOPF₆, FeCp₂PF₆, DDQ, CAN, and O₂/silica. CAN oxidation resulted in complete destruction of the desired organic product, while FeCp₂PF₆ and O₂/silica resulted in incomplete oxidation. Both NOPF₆ and DDQ gave satisfactory recovery of the desired free amine (**56**) in similar yields. Once the metal was no longer coordinated, the allyl amine is expected to be much more resistant to elimination. However, due to the potential for acidic impurities which could promote such a reaction while still bound to the metal, particularly in NOPF₆, the complex was first dissolved in MeCN and the solution cooled to -40 °C before a cold solution of oxidant in MeCN was added. It was imperative that the complex was completely dissolved, as the oxidant appeared to oxidize the free amine if the metal complex was not immediately available for oxidation. The stoichiometry was also crucial, with the best results being obtained with 1 molar equivalent of oxidant. Oxidation was also attempted on the crude reaction mixtures (prior to precipitation), but this approach did not yield any appreciable amount of liberated organic product.

Following decomplexation, the allylic amine **56** (**Scheme 4.4**) was characterized by ¹H, ¹³C, NOESY, COSY, HMBC, and HMQC NMR, as well as HRMS. **56** was found to exist as a 5:2 mixture of rotamers in CD₃CN at 25 °C, with chemical exchange evident by NOESY. Unlike complex **55**, compound **56** found to be stable to elimination, even under acidic aqueous conditions. The relative stability of the decomplexed product

supports the notion that the tungsten facilitates E1 elimination of the protonated amine in the complex (**55**), via stabilization of the resulting allyl cation.



Scheme 4.4: Synthesis of aminotetrahydropyridine products

With the reaction and work-up conditions optimized for the addition of methylamine to yield **56**, the reaction was repeated under identical conditions with allyl complex **52** in place of **51**. An analogous addition complex (**57**) was isolated, which was also successfully oxidized with DDQ to yield compound **58**. Next, a range of primary and secondary amines were tested for comparable activity to examine the scope of the amine. Complexes resulting from amine addition were successfully formed from morpholine (**59** and **60**), propargylamine (**61**), benzylamines (**62** and **63**), an azetidine (**71**) as well as the nitrogen heterocycle imidazole (**64**). Preliminary success was also achieved with 2-(aminomethyl)pyridine, indicating that the reaction likely tolerates aromatic nitrogen heterocycles. These complexes were all isolated with between 5-20% of elimination product impurity. Complexes **59-64** were oxidized by DDQ/HOTf without further purification, yielding organic compounds **65-70**, as shown in **Figure 4.1**.

Due to the variety of metal byproducts formed during oxidation, purification of the free amines proved to be somewhat challenging. Nonetheless, Combiflash flash

chromatography followed by preparative reverse-phase HPLC was effective for providing pure samples, as determined by NMR and LC-MS.

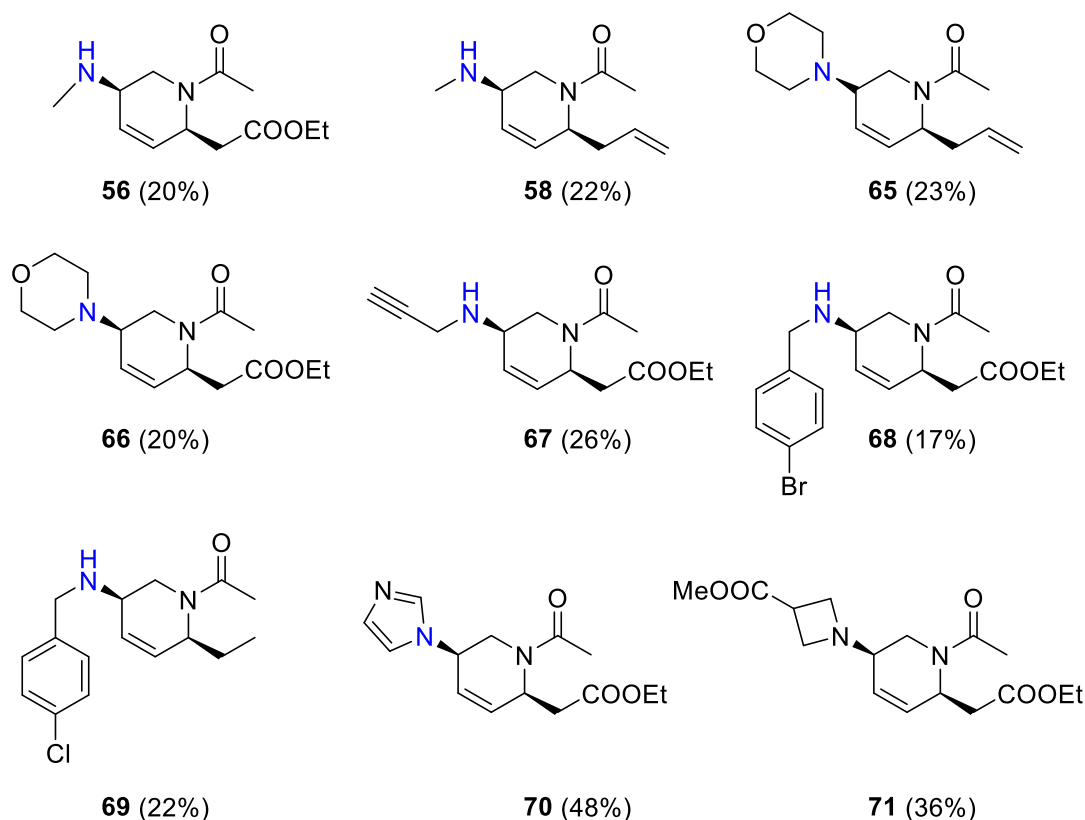
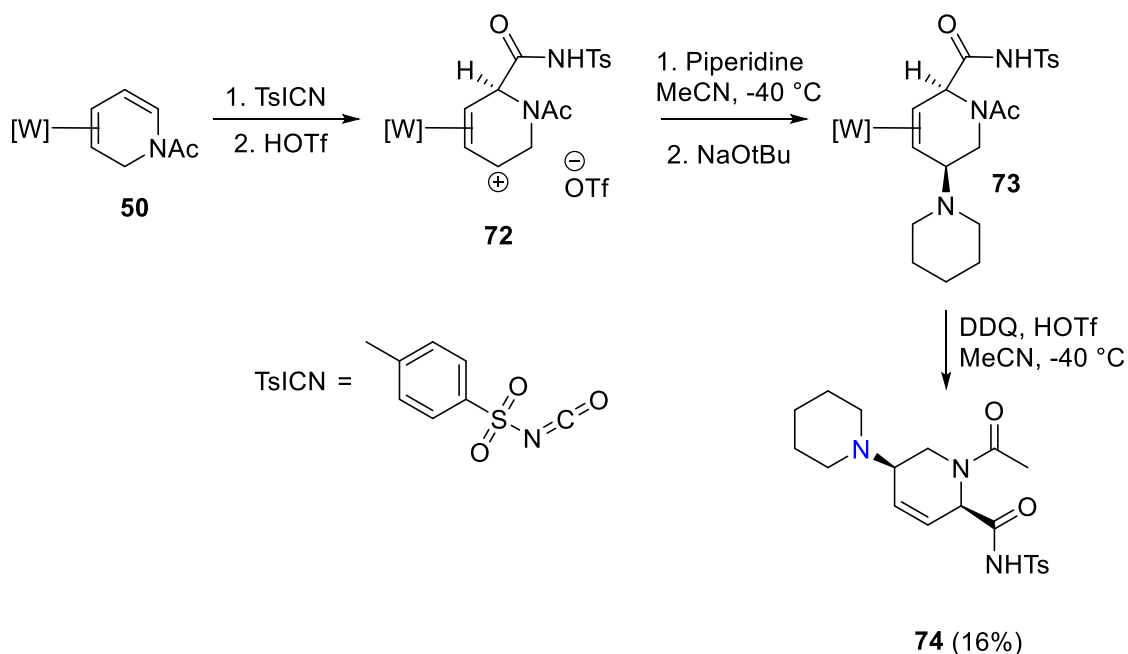


Figure 4.1: The range of amine organics produced by tungsten-mediated amination of pyridine (yield over 2 steps)

In order to further explore the range of organic products accessible by this methodology, the hydride addition complex **50** was treated with tosyl isocyanate followed by triflic acid to yield the allyl complex **72** (Scheme 4.5).¹¹ Unlike in previous examples, the substituent on the piperidine ring in **72** is derived from an electrophilic rather than a nucleophilic source, and acts as an electron-withdrawing group. The acylsulfonamide moiety is also acidic and can be deprotonated during an attempted amine addition, or even after the addition via an intramolecular nucleophilic addition.¹¹ Despite

these concerns, reaction of **72** with piperidine at $-40\text{ }^{\circ}\text{C}$ in MeCN yielded the addition product **73**. Complex **73** was substantially more prone to elimination than any of the other amine addition complexes, and could not be purified by any type of aqueous work-up due to elimination issues. Instead, the reaction mixture was quenched, evaporated to near-dryness *in vacuo*, dissolved in minimal DCM, and precipitated into Et₂O. The precipitation was successful due to the substantially lower solubility of **73** in Et₂O compared to the similar products **65** and **66**. The isolated solid **73** was oxidized with DDQ and HOTf in MeCN to yield the free organic **74**.



Scheme 4.5: Variation of second electrophile to produce an acylsulfonamide

Disubstituted piperidines have been investigated for their biological activity.^{12,13} In particular, the 3-aminopiperidine moiety is found in a number of drugs, including linagliptin, nemonoxacin, and tofacitinib. This motif is often produced by Buchwald–Hartwig amination of a 3-halopyridine, followed by hydrogenation.¹⁴ Alternatively, the

piperidine ring may be formed by cyclization,¹⁵ and the amino group may be incorporated by reductive amination of a 3-piperidone.^{16,17} These methods are somewhat limited in scope, particularly if a particular stereoisomer of the compound is sought. Producing the compounds prepared in this paper by these traditional organic methods would entail a lengthy synthesis. Examples of 3-aminopiperidines prepared from the direct addition of an amine to a pyridine ring are virtually unknown.

This metal-mediated divergent synthesis enables rapid generation of diverse aminotetrahydropyridines, and is ideal for the creation of drugs or drug fragments with this motif. The acetylpyridine complex can be prepared on large scale (10 g), the range of nucleophiles that can be selectively added to C2 include Grignard reagents, organozincs, enolates, indoles and pyrroles. The amine addition can be carried out without the need of precious metals or halides with complete control of the ring stereocenter, and a site of unsaturation remains for further elaboration.

Conclusion

The chemistry demonstrated in this paper allows for the synthesis of a wide variety of amine-substituted piperidines from pyridine borane in *overall yields* ranging from 9-16% over 7 steps (71-77% per step). All additions are regio- and stereoselective (dr of isolated products > 15:1), and single enantiomers are theoretically accessible due to the previously demonstrated enantioenrichment of a tungsten exchange precursor.¹⁸ The first nucleophile, second electrophile, and second amine nucleophile may all be varied, presenting the opportunity for a convenient divergent synthesis. Given the abundance of piperidines in biologically-active small molecules, this methodology is useful for the development of compound libraries of medicinal interest.

Experimental Section

General Methods: NMR spectra were obtained on a 600 or 800 MHz spectrometer. All chemical shifts are reported in ppm, and proton and carbon shifts are referenced to tetramethylsilane (TMS) utilizing residual ^1H or ^{13}C signals of the deuterated solvents as an internal standard. Coupling constants (J) are reported in hertz (Hz). Infrared spectra (IR) were recorded as a glaze on a spectrometer fitted with a horizontal attenuated total reflectance (HATR) accessory or on a diamond anvil ATR assembly. Electrochemical experiments were performed under a nitrogen atmosphere. Cyclic voltammetry data were taken at ambient temperature ($\sim 25\text{ }^\circ\text{C}$) at 100 mV/s in a standard three-electrode cell with a glassy carbon working electrode, N,N-dimethylacetamide (DMA) or acetonitrile (MeCN) solvent, and tetrabutylammonium hexafluorophosphate (TBAH) electrolyte (approximately 0.5 M). All potentials are reported versus NHE (normal hydrogen electrode) using cobaltocenium hexafluorophosphate ($E_{1/2} = -0.78\text{ V}$), ferrocene ($E_{1/2} = +0.55\text{ V}$), or decamethylferrocene ($E_{1/2} = +0.04\text{ V}$) as an internal standard. The peak-to-peak separation was less than 100 mV for all reversible couples. Unless otherwise noted, all synthetic reactions were performed in a glovebox under a dry nitrogen atmosphere. Deuterated solvents were used as received. Pyrazole (Pz) protons of the (trispyrazolyl)borate (Tp) ligand were uniquely assigned (e.g., “Pz3B”) using a combination of two-dimensional NMR data and PMe_3 -proton NOE interactions. When unambiguous assignments were not possible, Tp protons were labeled as “Pz3/5 or Pz4”. All J values for Pz protons are 2 (± 0.2) Hz. BH ^1H NMR peaks (around 4–5 ppm) are not identified due to their quadrupole broadening; IR data are used to confirm the presence of

a BH group (around 2500 cm^{-1}). Compounds **47** – **54** or analogs were previously reported.^{4,19,20}

All organic compounds were synthesized according to the general method presented for compound **56**, except where noted. The synthesis of **71** details a procedure utilizing an amine salt rather than the free base.

Synthesis of WTp(NO)(PMe₃)(3,4-η²-ethyl 2-(1-acetyl-5-(methylamino)-1,2,5,6-tetrahydropyridin-2-yl)acetate) (55)

Compound **51** (376 mg, 0.436 mmol) and MeCN (4.0 mL) were combined in a test tube containing a stir pea. The solution was cooled in a cold bath at $-40\text{ }^{\circ}\text{C}$ for 15 min, and then a $-30\text{ }^{\circ}\text{C}$ solution of 2 M methylamine in THF (2.2 mL, 4.4 mmol) was added. The reaction mixture was stirred at $-40\text{ }^{\circ}\text{C}$ for 16 h, and then 1 M potassium t-butoxide solution in t-butanol was added (1.8 mL, 1.8 mmol). The reaction mixture was diluted with DCM (75 mL) and extracted with saturated aqueous sodium carbonate (100 mL). The organic layer was dried with sodium sulfate, filtered, and evaporated to dryness under vacuum. The residue was redissolved in DCM (4 mL) and added to stirring hexanes (100 mL). The precipitate was isolated on a 15 mL fine porosity fritted funnel, washed with hexanes (3 x 10 mL) and desiccated under vacuum to yield a tan solid (174 mg, 54% by mass). Two rotamers **A**:**B** = 4:1. Only **A** assigned due to extensive overlap. ¹H NMR (*d*₃-MeCN, δ): 8.41 (d, 1H, Tp3/5), 7.98 (d, 1H, Tp3/5), 7.74 (d, 1H, Tp3/5), 7.73 (d, 1H, Tp3/5), 7.65 (d, 1H, Tp3/5), 7.26 (d, 1H, Tp3/5), 6.30 (d, 1H, Tp4), 6.26 (d, 1H, Tp4), 6.21 (d, 1H, Tp4), 5.87 (dd, *J*=7.5, 6.8Hz, 1H, H2), 3.91 (m, 1H, H9), 3.82 (m, 1H, H9'), 3.82 (dd, *J*=12.9, 5.8, 1H, H6), 3.68 (dd, *J*=6.1, 5.8Hz, 1H, H5), 3.05 (dd, *J*=12.9, 6.1Hz, 1H, H6'), 2.97 (dd, *J*=13.8, 6.8Hz, 1H, H8), 2.83 (dd, *J*=13.8, 7.5Hz, 1H,

H8'), 2.58 (d, $J=6.4\text{Hz}$, 1H, H11), 2.43 (ddd, $J=11.5, 11.2, 2.2\text{Hz}$, 1H, H4), 2.02 (s, 3H, H7), 1.22 (d, $J=8.4\text{Hz}$, 9H, PMe_3), 0.96 (d, $J=11.2\text{Hz}$, 1H, H3), 0.91 (t, $J=7.1\text{Hz}$, 1H, H10). ^{13}C NMR ($\text{d}_3\text{-MeCN}$, δ): 172.2 (Ester CO), 170.3 (Amide CO), 143.8 (Tp3/5), 142.9 (Tp3/5), 139.9 (Tp3/5), 136.4 (Tp3/5), 136.0 (Tp3/5), 135.8 (Tp3/5), 106.2 (Tp4), 106.0 (Tp4), 105.8 (Tp4), 59.8 (C9), 58.1 (C5), 54.6 (C3), 51.6 (C4), 47.3 (C2), 46.3 (C6), 44.6 (C8), 34.3 (C11), 22.8 (C7), 13.6 (C10) 13.3 (PMe_3). ^{31}P NMR ($\text{d}_3\text{-MeCN}$, δ): -11.83, $J_{\text{WP}} = 275\text{ Hz}$.

Synthesis of ethyl 2-(1-acetyl-5-(methylamino)-1,2,5,6-tetrahydropyridin-2-yl)acetate (56)

Step 1: Compound **51** (188 mg, 0.218 mmol) and MeCN (4.0 mL) were combined in a test tube containing a stir pea. The solution was cooled in a cold bath at $-40\text{ }^\circ\text{C}$ for 15 min, and then a $-30\text{ }^\circ\text{C}$ solution of 2 M methylamine in THF (1.1 mL, 2.2 mmol) was added. The reaction mixture was stirred at $-40\text{ }^\circ\text{C}$ for 16 h, and then 1 M potassium t-butoxide solution in t-butanol was added (0.9 mL, 0.9 mmol). The reaction mixture was diluted with DCM (40 mL) and extracted with saturated aqueous sodium carbonate (100 mL). The organic layer was dried with sodium sulfate, filtered, and evaporated to dryness under vacuum. The residue was redissolved in DCM (2 mL) and added to stirring hexanes (50 mL). The precipitate was isolated on a 15 mL fine porosity fritted funnel, washed with hexanes (3 x 10 mL) and desiccated under vacuum to yield a tan solid, **55** (96 mg).

Step 2: This solid (**55**) was dissolved in MeCN (2.0 mL) in a small test tube, and cooled at $-40\text{ }^\circ\text{C}$ in a cold bath for 15 minutes. Separately, NOPF_6 (42mg, 0.242 mmol) was dissolved in MeCN (2.0 mL). The NOPF_6 solution was added to the solution of the metal

complex, and the reaction mixture was allowed to stir for 5 min. The reaction mixture was then removed from the glovebox, diluted with DCM (40 mL), and extracted with saturated sodium carbonate (15 mL). The organic layer was back extracted with DCM (20 mL). The combined organic layers were dried with sodium sulfate, filtered, and evaporated to dryness onto basic alumina. The product was purified by Combiflash flash chromatography on an 8g basic alumina column using a gradient elution of 0-100% EtOAc in hexanes. The fractions containing the product (~100% EtOAc) were evaporated to yield **56** as a colorless oil (10.5 mg, 20% over two steps). Two rotamers **A**:**B** = 5:2. ¹H NMR (d₃-MeCN, δ): **A** 5.81 (dd, J=10.3Hz, 1.5Hz, 1H, H4), 5.74 (ddd, J=10.3Hz, 3.8Hz, 2.3Hz, 1H, H3), 5.02 (m, 1H, H2), 4.07 (m, 2H, H9), 3.89 (dd, J=13.3Hz, 5.4Hz, 1H, H6), 3.13 (m, 1H, H5), 2.75 (dd, J=13.3Hz, 10.4Hz, 1H, H6'), 2.49 (dd, J=14.2Hz, 6.4Hz, 1H, H8), 2.43 (dd, J=14.2Hz, 8.1Hz, 1H, H8'), 2.39 (s, 3H, H11), 2.04 (s, 3H, H7), 1.21 (t, J=6.7Hz, 3H, H10). **B** 5.81 (dd, J=10.3Hz, 1.5Hz, 1H, H4), 5.74 (m, 1H, H3), 4.64 (dd, J=12.6Hz, 5.6Hz, 1H, H6), 4.59 (m, 1H, H2), 4.10 (m, 2H, H9), 2.99 (m, 1H, H5), 2.62 (m, 2H, H8), 2.38 (s, 3H, H11), 2.29 (dd, J=12.6Hz, 10.2Hz, 1H, H6'), 2.05 (s, 3H, H7), 1.22 (t, J=6.2Hz, H10). ¹³C NMR (d₃-MeCN, δ): **A** 171.7 (Amide CO), 169.7 (Ester CO), 131.5 (C4), 128.4 (C3), 61.3 (C9), 54.9 (C5), 48.2 (C2), 46.3 (C6), 38.5 (C8), 33.6 (C11), 22.0 (C7), 14.5 (C10). **B** 171.6 (Amide CO), 169.7 (Ester CO), 132.2 (C4), 128.2 (C3), 61.5 (C9), 54.1 (C5), 52.4 (C2), 40.6 (C6), 39.5 (C8), 33.7 (C11), 21.6 (C7), 14.5 (C10). ESI-MS: obs'd (%), calc'd (%), ppm, (M+H)⁺: 241.1548 (100), 241.1547 (100), 0.4.

Synthesis of 1-(6-allyl-3-(methylamino)-3,6-dihydropyridin-1(2H)-yl)ethan-1-one (58)

Yield: 76 mg (22% over two steps), as a colorless oil. Two rotamers **A**:**B** = 3:2. ¹H NMR (d₃-MeCN, δ): **A** 5.82 (m, 1H, H9), 5.79 (m, 1H, H4), 5.74 (ddd, J=10.3Hz, 4.5Hz, 2.0Hz, 1H, H3), 5.04 (m, 2H, H10), 4.90 (m, 1H, H2), 3.88 (dd, J=13.2Hz, 5.5Hz, 1H, H6), 3.16 (m, 1H, H5), 2.85 (dd, J=13.2Hz, 10.5Hz, 1H, H6'), 2.51 (s, 3H, H11), 2.35 (m, 2H, H8), 2.12 (s, 3H, H7). **B** 5.82 (m, 1H, H9), 5.79 (m, 1H, H4), 5.73 (ddd, J=10.3Hz, 4.0Hz, 2.5Hz, 1H, H3), 5.12 (m, 2H, H10), 4.88 (dd, J=13.2Hz, 5.8Hz, 1H, H6), 4.14 (m, 1H, H2), 3.16 (m, 1H, H5), 2.50 (s, 3H, H11), 2.36 (buried, 1H, H6'), 2.35 (m, 2H, H8), 2.10 (s, 3H, H7). ¹³C NMR (d-chloroform, δ): **A** 169.0 (Amide CO), 134.6 (C9), 129.6 (C4), 128.6 (C3), 117.6 (C10), 54.1 (C5), 50.1 (C2), 46.0 (C6), 37.8 (C8), 33.5 (C11), 22.1 (C7). **B** 169.3 (Amide CO), 133.6 (C9), 130.5 (C4), 128.1 (C3), 118.8 (C10), 54.8 (C2), 53.3 (C5), 40.1 (C6), 38.8 (C8), 33.6 (C11), 21.8 (C7). ESI-MS: obs'd (%), calc'd (%), ppm, (M+H)⁺: 195.1491 (100), 195.1492 (100), 0.5.

Synthesis of WTp(NO)(PMe₃)(3,4-η²- ethyl 2-(1-acetyl-5-(1H-imidazol-1-yl)-1,2,5,6-tetrahydropyridin-2-yl)acetate (64)

Compound **51** (360 mg, 0.436 mmol) and MeCN (7.0 g) were combined in a test tube containing a stir pea. The solution was cooled in a cold bath at -40 °C for 15 min, and then imidazole (400 mg, 5.88 mmol) was added. The reaction mixture was stirred at -40 °C for 16 h, and then 2 M sodium t-butoxide solution in THF was added (0.9 mL, 1.8 mmol). The reaction mixture was diluted with DCM (60 mL) and extracted with saturated aqueous sodium carbonate (3 x 75 mL). The aqueous layer was back-extracted with DCM (15 mL). The combined organic layers were dried with sodium sulfate, filtered, and

evaporated to ~1 mL volume under vacuum. The concentrate was diluted with EtOAc (4 mL) and added to stirring hexanes (125 mL). The precipitate was isolated on a 15 mL fine porosity fritted funnel, washed with hexanes (3 x 10 mL) and desiccated under vacuum to yield a pale tan solid (250 mg, 73% by mass). Two rotamers **A**:**B** = 6:1. Only **A** assigned due to extensive overlap. ¹H NMR (d₃-MeCN, δ): 8.60 (d, 1H, Tp3/5), 7.99 (d, 1H, Tp3/5), 7.97 (t, J=1.5Hz, 1H H13), 7.84 (d, 1H, Tp3/5), 7.83 (d, 1H, Tp3/5), 7.78 (d, 1H, Tp3/5), 7.55 (t, J=1.5Hz, 1H, H12), 7.31 (d, 1H, Tp3/5), 7.08 (t, J=1.5Hz, 1H, H11), 6.35 (d, 1H, Tp4), 6.32 (d, 1H, Tp4), 6.26 (d, 1H, Tp4), 6.04 (dd, J=7.8, 6.8Hz, 1H, H2), 5.53 (dd, J=9.9, 6.4Hz, 1H, H5), 3.83 (m, 2H, H9), 3.83 (buried, 1H, H6), 3.25 (dd, J=13.7, 9.9Hz, 1H, H6'), 2.89 (ddd, J=13.7, 11.2, 2.7Hz, 1H, H4), 2.81 (dd, J=13.6, 6.8Hz, 1H, H8), 2.59 (dd, J=13.8, 7.8Hz, 1H, H8'), 2.02 (s, 3H, H7), 0.91 (buried, 1H, H3), 0.90 (d, J=8.4Hz, 9H, PMe₃), 0.86 (t, J=7.1Hz, 1H, H10). ¹³C NMR (d₃-MeCN, δ): 172.2 (Ester CO), 170.3 (Amide CO), 144.8 (Tp3/5), 144.0 (Tp3/5), 141.4 (Tp3/5), 137.8 (C13), 137.7 (Tp3/5), 137.6 (Tp3/5), 137.6 (Tp3/5), 130.1 (C11), 119.2 (C12), 107.6 (Tp4), 107.3 (Tp4), 107.0 (Tp4), 60.7 (C9), 55.8 (C3), 55.6 (C5), 48.3 (C6), 48.1 (C4), 47.6 (C2), 44.8 (C8), 23.4 (C7), 14.2 (C10) 13.3 (PMe₃). ³¹P NMR (d₃-MeCN, δ): -11.35, J_{WP} = 275 Hz.

Synthesis of 1-(6-allyl-3-morpholino-3,6-dihydropyridin-1(2H)-yl)ethan-1-one (**65**)

Yield: 17 mg (23% over two steps), as a colorless oil. Two rotamers **A**:**B** = 5:4. ¹H NMR (d-chloroform, δ): **A** 5.86 (m, 2H, H3 + H4), 5.81 (m, 1H, H9), 5.05 (m, 2H, H10), 4.91 (m, 1H, H2), 3.73 (dd, J=12.8Hz, 5.0Hz, 1H, H6), 3.71 (m, 4H, H11), 3.20 (m, 1H, H5), 3.16 (m, 1H, H6'), 2.65 (m, 4H, H12), 2.35 (m, 2H, H8), 2.10 (s, 3H, H7). **B** 5.86 (m, 2H, H3 + H4), 5.81 (m, 1H, H9), 5.13 (m, 2H, H10), 4.75 (dd, J=12.5Hz, 5.5Hz, 1H, H6),

4.12 (m, 1H, H2), 3.71 (m, 4H, H11), 3.20 (m, 1H, H5), 2.65 (m, 4H, H12), 2.64 (buried, 1H, H6'), 2.35 (m, 2H, H8), 2.10 (s, 3H, H7). ^{13}C NMR (d-chloroform, δ): **A** 169.2 (Amide CO), 134.5 (C9), 130.9 (C3/C4), 126.9 (C3/C4), 117.6 (C10), 67.5 (C11), 59.0 (C5), 49.9 (C2), 49.3 (C12), 41.1 (C6), 37.9 (C8), 22.1 (C7). **B** 169.5 (Amide CO), 133.6 (C9), 129.7 (C3/C4), 129.4 (C3/C4), 118.9 (C10), 67.5 (C11), 58.0 (C5), 54.7 (C2), 49.3 (C12), 38.8 (C8), 34.8 (C6), 21.8 (C7). ESI-MS: obs'd (%), calc'd (%), ppm, (M+H)⁺: 251.1755 (100), 251.1754, 0.4.

Synthesis of ethyl 2-(1-acetyl-5-morpholino-1,2,5,6-tetrahydropyridin-2-yl)acetate (66)

Yield: 13.1 mg (20% over two steps), as a colorless oil. Two rotamers **A**:**B** = 2:1. ^1H NMR ($\text{d}_3\text{-MeCN}$, δ): **A** 5.88 (m, 1H, H4), 5.84 (m, 1H, H3), 5.03 (m, 1H, H2), 4.07 (m, 2H, H9), 3.76 (dd, $J=13.6\text{Hz}$, 5.6Hz , 1H, H6), 3.60 (m, 4H, H11), 3.27 (m, 1H, H5), 3.10 (dd, $J=13.6\text{Hz}$, 10.8Hz , 1H, H6'), 2.61 (m, 4H, H12), 2.47 (m, 2H, H8), 2.04 (s, 3H, H7), 1.21 (t, $J=6.7\text{Hz}$, 3H, H10). **B** 5.88 (m, 1H, H4), 5.84 (m, 1H, H3), 4.60 (m, 1H, H2), 4.52 (dd, $J=12.5\text{Hz}$, 5.6Hz , 1H, H6), 4.09 (m, 2H, H9), 3.60 (m, 4H, H11), 3.11 (m, 1H, H5), 2.61 (buried, 1H, H6'), 2.61 (m, 4H, H12), 2.61 (buried, 2H, H8), 2.06 (s, 3H, H7), 1.21 (t, $J=6.7\text{Hz}$, 3H, H10). ^{13}C NMR ($\text{d}_3\text{-MeCN}$, δ): **A** 171.6 (Amide CO), 169.9 (Ester CO), 130.2 (C4), 129.7 (C3), 68.0 (C11), 61.3 (C9), 59.4 (C5), 49.9 (C12), 48.1 (C2), 41.4 (C6), 38.5 (C8), 22.0 (C7), 14.5 (C10). **B** 171.6 (Amide CO), 169.9 (Ester CO), 130.6 (C4), 130.1 (C3), 68.0 (C11), 61.6 (C9), 58.6 (C5), 52.4 (C2), 49.9 (C12), 39.3 (C8), 35.6 (C6), 21.6 (C7), 14.5 (C10). ESI-MS: obs'd (%), calc'd (%), ppm, (M+H)⁺: 297.1808 (100), 297.1809 (100), 0.3.

Synthesis of ethyl 2-(1-acetyl-5-(prop-2-yn-1-ylamino)-1,2,5,6-tetrahydropyridin-2-yl)acetate (67)

Yield: 15 mg (26% over two steps), as a colorless oil. Two rotamers **A**:**B** = 7:3. ¹H NMR (d₃-MeCN, δ): **A** 5.80 (m, 1H, H4), 5.76 (m, 1H, H3), 5.01 (m, 1H, H2), 4.07 (m, 2H, H9), 3.95 (dd, J=13.6Hz, 5.5Hz, 1H, H6), 3.48 (s, 2H, H11), 3.40 (m, 1H, H5), 2.77 (dd, J=13.6Hz, 10.4Hz, 1H, H6'), 2.49 (dd, J=14.2Hz, 6.1Hz, 1H, H8), 2.46 (t, J=2.4Hz, 1H, H12), 2.44 (dd, J=14.2Hz, 8.1Hz, 1H, H8'), 2.04 (s, 3H, H7), 1.21 (t, J=7.2Hz, 3H, H10). **B** 5.80 (m, 1H, H4), 5.76 (m, 1H, H3), 4.67 (dd, J=12.7Hz, 5.6Hz, 1H, H6), 4.59 (m, 1H, H2), 4.11 (m, 2H, H9), 3.45 (m, 2H, H11), 3.26 (m, 1H, H5), 2.62 (m, 2H, H8), 2.43 (t, J=2.6Hz, 1H, H12), 2.32 (dd, J=12.7Hz, 10.4Hz, 1H, H6'), 2.06 (s, 3H, H7), 1.22 (t, J=7.1Hz, 3H, H10). ¹³C NMR (d₃-MeCN, δ): **A** 171.6 (Amide CO), 169.7 (Ester CO), 131.3 (C4), 128.7 (C3), 83.4 (C11a), 72.6 (C12), 61.3 (C9), 52.5 (C5), 48.1 (C2), 46.4 (C6), 38.4 (C8), 22.0 (C7), 14.5 (C10). **B** 171.6 (Amide CO), 169.7 (Ester CO), 131.7 (C4), 128.6 (C3), 83.4 (C11a), 72.4 (C12), 61.6 (C9), 52.2 (C5), 51.5 (C2), 40.7 (C6), 39.4 (C8), 21.6 (C7), 14.5 (C10). ESI-MS: obs'd (%), calc'd (%), ppm, (M+H)⁺: 265.1548 (100), 265.1547 (100), 0.4.

Synthesis of ethyl 2-(1-acetyl-5-((4-bromobenzyl)amino)-1,2,5,6-tetrahydropyridin-2-yl)acetate (68)

Yield: 14 mg (17% over two steps), as a near-colorless oil. Two rotamers **A**:**B** = 7:3. ¹H NMR (d₃-MeCN, δ): **A** 7.48 (m, 2H, H13), 7.29 (m, 2H, H12), 5.83 (m, 1H, H4), 5.75 (m, 1H, H3), 5.00 (m, 1H, H2), 4.07 (m, 2H, H9), 3.86 (dd, J=13.5Hz, 5.5Hz, 1H, H6), 3.84 (d, J=13.7Hz, 1H, H11), 3.80 (d, J=13.7Hz, 1H, H11'), 3.25 (m, 1H, H5), 2.79 (dd, J=13.5Hz, 10.4Hz, 1H, H6'), 2.49 (dd, J=14.3Hz, 6.4Hz, 1H, H8), 2.43 (dd, J=14.3Hz,

8.1Hz, 1H, H8'), 1.99 (s, 3H, H7), 1.20 (t, J=7.2Hz, 3H, H10). **B** 7.48 (m, 2H, H13), 7.29 (m, 2H, H12), 5.85 (m, 1H, H4), 5.76 (m, 1H, H3), 4.65 (dd, J=12.5Hz, 5.7Hz, 1H, H6), 4.59 (m, 1H, H2), 4.09 (m, 2H, H9), 3.80 (s, 2H, H11), 3.11 (m, 1H, H5), 2.62 (m, 2H, H8), 2.35 (dd, J=12.5Hz, 10.4Hz, 1H, H6'), 2.04 (s, 3H, H7), 1.21 (t, J=7.3Hz, 3H, H10). ¹³C NMR (d₃-MeCN, δ): **A** 171.6 (Amide CO), 169.8 (Ester CO), 141.6 (C12a), 132.2 (C13), 131.7 (C4), 131.1 (C12), 128.6 (C3), 120.9 (C13a), 61.3 (C9), 53.0 (C5), 50.6 (C11), 48.2 (C2), 46.6 (C6), 38.4 (C8), 22.0 (C7), 14.5 (C10). **B** 171.6 (Amide CO), 169.7 (Ester CO), 141.5 (C12a), 132.2 (C4), 132.1 (C13), 131.1 (C12), 128.5 (C3), 120.9 (C13a), 61.6 (C9), 52.3 (C5), 52.0 (C2), 50.4 (C11), 40.9 (C6), 39.4 (C8), 21.5 (C7), 14.5 (C10). ESI-MS: obs'd (%), calc'd (%), ppm, (M+H)⁺: 395.0967 (100), 395.0965 (100), 0.5.

Synthesis of 1-(3-((4-chlorobenzyl)amino)-6-ethyl-3,6-dihydropyridin-1(2H)-yl)ethan-1-one (69)

Yield: 32 mg (22% over two steps), as a colorless oil. Two rotamers **A**:**B** = 5:4. ¹H NMR (d-chloroform, δ): **A** 7.48 (m, 4H, H11+H12), 5.79 (m, 1H, H3), 5.76 (m, 1H, H4), 4.75 (m, 1H, H2), 3.87 (m, 2H, H10), 3.81 (dd, J=13.3Hz, 5.4Hz, 1H, H6), 3.26 (m, 1H, H5), 2.84 (dd, J= 13.3Hz, 10.5Hz, 1H, H6'), 2.06 (s, 3H, H7), 1.59 (m, 2H, H8), 0.94 (t, J=7.5Hz, 3H, H9). **B** 7.48 (m, 4H, H11+H12), 5.79 (m, 1H, H3), 5.76 (m, 1H, H4), 4.88 (dd, J=12.4Hz, 5.5Hz, 1H, H6), 3.98 (m, 1H, H2), 3.85 (m, 2H, H10), 3.26 (m, 1H, H5), 2.38 (dd, J=12.4Hz, 10.5Hz, 1H, H6'), 2.09 (s, 3H, H7), 1.66 (m, 2H, H8), 0.98 (t, J=7.5Hz, 3H, H9). ¹³C NMR (d-chloroform, δ): **A** 170.0 (Amide CO), 138.8 (C12a), 133.2 (C11a), 130.3 (C4), 129.6 (C11), 128.9 (C12), 128.6 (C3), 52.4 (C5), 51.6 (C2), 50.5 (C10), 46.4 (C6), 27.4 (C8), 22.0 (C7), 10.8 (C9). **B** 169.3 (Amide CO), 138.8

(C12a), 133.0 (C11a), 130.5 (C4), 129.7 (C11), 128.8 (C12), 128.6 (C3), 56.1 (C2), 51.5 (C5), 50.4 (C10), 40.6 (C6), 26.3 (C8), 21.6 (C7), 11.0 (C9). ESI-MS: obs'd (%), calc'd (%), ppm, (M+H)⁺: 293.1415 (100), 293.1415 (100), 0.0; 295.1386 (32) 295.1386 (32), 0.0.

Synthesis of ethyl 2-(1-acetyl-5-(1H-imidazol-1-yl)-1,2,5,6-tetrahydropyridin-2-yl)acetate (70)

Yield: 57 mg (48% over two steps), as a near colorless oil. Two rotamers **A**:**B** = 1:1. ¹H NMR (d-chloroform, δ): **A** 7.76 (s, 1H, H13), 7.01 (s, 1H, H11), 6.96 (s, 1H, H12), 6.11 (ddd, J=10.2, 4.0, 2.6Hz, 1H, H3), 5.86 (d, J=10.2Hz, 1H, H3), 5.21 (m, 1H, H2), 4.86 (m, 1H, H5), 4.13 (m, 2H, H9), 4.04 (dd, J=13.2Hz, 5.7Hz, 1H, H6), 2.31 (dd, J=13.2Hz, 10.7Hz, 1H, H6'), 2.62 (m, 2H, H8), 2.14 (s, 3H, H7), 1.25 (t, J=7.2Hz, 3H, H10). **B** 7.61 (s, 1H, H13), 7.01 (s, 1H, H11), 6.93 (s, 1H, H12), 6.06 (ddd, J=10.2, 4.0, 2.6Hz, 1H, H3), 5.93 (d, J=10.2Hz, 1H, H3), 4.91 (dd, J=12.9Hz, 5.8Hz, 1H, H6), 4.77 (m, 1H, H5), 4.72 (m, 1H, H2), 4.13 (m, 2H, H9), 2.69 (buried, 1H, H6'), 2.69 (m, 2H, H8), 2.18 (s, 3H, H7), 1.25 (t, J=7.2Hz, 3H, H10). ¹³C NMR (d-chloroform, δ): **A** 170.4 (Ester CO), 169.0 (Amide CO), 136.1 (C13), 131.8 (C3), 129.2 (C11), 125.8 (C4), 117.2 (C12), 60.9 (C9), 51.8 (C5), 46.9 (C2), 46.9 (C6), 37.1 (C8), 21.8 (C7), 14.2 (C10). **B** 170.0 (Ester CO), 169.7 (Amide CO), 135.9 (C13), 131.1 (C3), 129.3 (C11), 127.6 (C4), 117.4 (C12), 61.3 (C9), 51.0 (C2), 50.8 (C5), 41.2 (C6), 38.4 (C8), 21.2 (C7), 14.1 (C10). ESI-MS: obs'd (%), calc'd (%), ppm, (M+H)⁺: 278.1500 (100), 278.1499 (100), 0.4.

Synthesis of methyl 1-(1-acetyl-6-(2-ethoxy-2-oxoethyl)-1,2,3,6-tetrahydropyridin-3-yl)azetidine-3-carboxylate (71)

Step 1: Compound **51** (370 mg, 0.429 mmol) and MeCN (4.0 mL) were combined in a test tube containing a stir pea. In a separate test tube, 3-(methoxycarbonyl)azetidinium chloride (325 mg, 2.15 mmol) was dissolved in MeCN (2.0 mL). Both solutions were cooled in a cold bath at -40 °C for 10 min, then a 2M solution of LDA in THF (1.0 mL, 2.0 mmol) was added dropwise to the 3-(methoxycarbonyl)azetidinium chloride solution. After a few seconds, white solid (LiCl) precipitated. After 5 minutes of stirring at -40 °C, the basified amine solution was added to the solution of compound **51**. The reaction mixture was stirred at -40 °C for 12 h, and then 2 M sodium t-butoxide THF solution was added (0.9 mL, 1.8 mmol). The reaction mixture was diluted with DCM (50 mL) and extracted with saturated aqueous sodium carbonate (2 x 100 mL). The aqueous layer was back-extracted with DCM (15 mL). The combined organic layers were dried with sodium sulfate, filtered, and evaporated to dryness under vacuum. The residue was redissolved in EtOAc (4 mL) and added to stirring hexanes (150 mL). The precipitate was isolated on a 15 mL fine porosity fritted funnel, washed with hexanes (3 x 10 mL) and desiccated under vacuum to yield a tan solid (274 mg, 77% by mass with 5% elimination product).

Step 2: The solid from step 1 (265 mg, 0.320 mmol) was dissolved in a mixture of MeCN (6.0 mL) and DCM (4.0 mL) in a small test tube, and cooled at -40 °C in a cold bath for 15 minutes. Separately, DDQ (72 mg, 0.317 mmol) was dissolved in MeCN (2.0 mL). HOTf (161 mg, 1.07 mmol) was added to the DDQ solution, and the resulting mixture was cooled to -40 °C for 10 minutes. The DDQ solution was then added to the solution of

the metal complex, and the reaction mixture was allowed to stir for 1 min. The reaction mixture was then removed from the glovebox, diluted with DCM (50 mL), and extracted with saturated sodium carbonate (60 mL). The organic layer was back extracted with DCM (20 mL). The combined organic layers were dried with sodium sulfate, filtered, and evaporated to dryness onto basic alumina. The product was purified by Combiflash flash chromatography on an 8g basic alumina column using a gradient elution of 0-100% EtOAc in hexanes. The fractions containing the product (~80% EtOAc) were evaporated to yield 71. Yield: 49 mg (36% over two steps), as a near colorless oil. Two rotamers **A**:**B** = 5:3. ¹H NMR (d₂-methylene chloride, δ): **A** 5.84 (ddd, J=10.3, 3.8, 2.1Hz, 1H, H3), 5.72 (m, 1H, H3), 5.07 (m, 1H, H2), 4.09 (m, 2H, H9), 3.69 (s, 3H, H13), 3.66 (dd, J=13.3Hz, 5.5Hz, 1H, H6), 3.56 (m, 2H, H11), 3.42 (m, 2H, H11'), 3.31 (m, 1H, H12), 2.93 (m, 1H, H5), 2.76 (dd, J=13.3Hz, 10.4Hz, 1H, H6'), 2.52 (dd, J=14.6Hz, 6.2Hz, 1H, H8), 2.43 (dd, J=14.2Hz, 8.2Hz, 1H, H8'), 2.06 (s, 3H, H7), 1.23 (t, J=7.2Hz, 3H, H10). **B** 5.79 (ddd, J=10.3, 3.9, 2.0Hz, 1H, H3), 5.72 (m, 1H, H3), 4.58 (m, 1H, H2), 4.57 (dd, J=12.7Hz, 5.5Hz, 1H, H6), 4.13 (m, 2H, H9), 3.69 (s, 3H, H13), 3.56 (m, 1H, H11), 3.50 (m, 1H, H11), 3.44 (m, 1H, H11'), 3.40 (m, 1H, H11'), 3.29 (m, 1H, H12), 2.87 (m, 1H, H5), 2.60 (m, 2H, H8), 2.28 (dd, J=12.7Hz, 10.3Hz, 1H, H6'), 2.09 (s, 3H, H7), 1.24 (t, J=7.2Hz, 3H, H10). ¹³C NMR (d₂-methylene chloride, δ): **A** 173.7 (Ester CO), 171.1 (Ester CO), 169.2 (Amide CO), 129.4 (C3), 125.8 (C4), 61.4 (C9), 60.9 (C5), 55.1 (C11), 54.9 (C11'), 52.4 (C13), 47.8 (C2), 43.9 (C6), 39.3 (C8), 34.6 (C12), 21.7 (C7), 14.5 (C10). **B** 173.7 (Ester CO), 171.0 (Ester CO), 169.5 (Amide CO), 128.4 (C3), 127.3 (C4), 61.4 (C9), 60.3 (C5), 55.4 (C11), 55.0 (C11'), 52.4 (C13), 51.8 (C2), 39.3 (C8), 38.1 (C6), 34.6 (C12), 21.7 (C7), 14.5 (C10). (M+H)⁺: 325.1758 (100), 325.1758 (100), 0.0.

Synthesis of 1-acetyl-5-(piperidin-1-yl)-N-tosyl-1,2,5,6-tetrahydropyridine-2-carboxamide (74)

Yield: 8 mg (16% over two steps), as a near colorless solid. Two rotamers **A**:**B** = 7:1. ¹H NMR (d₃-MeCN/TFA, δ): **A** 7.84 (m, 2H, H8), 7.40 (m, 2H, H9), 6.24 (dd, J=10.1Hz, 4.6Hz, 1H, H3), 6.16 (ddd, J=10.1Hz, 4.5Hz, 1.6Hz, 1H, H4), 4.88 (dt, J=4.6Hz, 1.6Hz, 1H, H2), 3.94 (m, 1H, H5), 3.82 (dd, J=14.0Hz, 6.0Hz, 1H, H6), 3.72 (dd, J=14.0Hz, 3.7Hz, 1H, H6'), 3.46 (d, J=12.1Hz, 1H, H11), 3.09 (d, J=12.1Hz, 1H, H11), 2.95 (m, 1H, H11), 2.86 (m, 1H, H11), 2.42 (s, 3H, H10), 2.11 (s, 3H, H7), 1.93 (d, J=14.9Hz, 1H, H12), 1.82 (d, J=14.9Hz, 1H, H12), 1.72 (m, 2H, H12), 1.54 (m, 1H, H13), 1.41 (m, 1H, H13). **B** extensively buried; not characterized. ¹³C NMR (d₃-MeCN/TFA, δ): **A** 172.4 (Acetyl CO), 169.8 (Amide CO), 146.6 (C9a), 136.1 (C8a), 130.4 (C9), 129.5 (C3), 128.8 (C8), 125.1 (C4), 58.9 (C5), 56.9 (C2), 51.9 (C11), 51.8 (C11'), 42.1 (C6), 24.1 (C12), 24.0 (C12'), 21.8 (C10), 21.7 (C13), 21.4 (C7).

References

- (1) Walsh, C. T. *Tetrahedron Letters* **2015**, 56, 3075.
- (2) Vitaku, E.; Smith, D. T.; Njardarson, J. T. *Journal of Medicinal Chemistry* **2014**, 57, 10257.
- (3) Harrison, D. P.; Welch, K. D.; Nichols-Nieler, A. C.; Sabat, M.; Myers, W. H.; Harman, W. D. *J. Am. Chem. Soc.* **2008**, 130, 16844.
- (4) Harrison, D. P.; Zottig, V. E.; Kosturko, G. W.; Welch, K. D.; Sabat, M.; Myers, W. H.; Harman, W. D. *Organometallics* **2009**, 28, 5682.
- (5) Harrison, D. P.; Sabat, M.; Myers, W. H.; Harman, W. D. *J. Am. Chem. Soc.* **2010**, 132, 17282.
- (6) Wilson, K. B.; Myers, J. T.; Nedzbala, H. S.; Combee, L. A.; Sabat, M.; Harman, W. D. *Journal of the American Chemical Society* **2017**, 139, 11401.
- (7) Wilson, K. B.; Smith, J. A.; Nedzbala, H. S.; Pert, E. K.; Dakermanji, S. J.; Dickie, D. A.; Harman, W. D. *The Journal of Organic Chemistry* **2019**, 84, 6094.
- (8) Feng, J.; Zhang, Z.; Wallace, M. B.; Stafford, J. A.; Kaldor, S. W.; Kassel, D. B.; Navre, M.; Shi, L.; Skene, R. J.; Asakawa, T.; Takeuchi, K.; Xu, R.; Webb, D. R.; Gwaltney, S. L. *Journal of Medicinal Chemistry* **2007**, 50, 2297.
- (9) Jiang, J.-k.; Ghoreschi, K.; Deflorian, F.; Chen, Z.; Perreira, M.; Pesu, M.; Smith, J.; Nguyen, D.-T.; Liu, E. H.; Leister, W.; Costanzi, S.; O'Shea, J. J.; Thomas, C. J. *Journal of Medicinal Chemistry* **2008**, 51, 8012.

- (10) Harrison, D. P.; Nichols-Nielander, A. C.; Zottig, V. E.; Strausberg, L.; Salomon, R. J.; Trindle, C. O.; Sabat, M.; Gunnoe, T. B.; Iovan, D. A.; Myers, W. H.; Harman, W. D. *Organometallics* **2011**, *30*, 2587.
- (11) Harrison, D. P.; Iovan, D. A.; Myers, W. H.; Sabat, M.; Wang, S.; Zottig, V. E.; Harman, W. D. *J. Am. Chem. Soc.* **2011**, *133*, 18378.
- (12) Jiang, R.; Song, X.; Bali, P.; Smith, A.; Bayona, C. R.; Lin, L.; Cameron, M. D.; McDonald, P. H.; Kenny, P. J.; Kamenecka, T. M. *Bioorganic & Medicinal Chemistry Letters* **2012**, *22*, 3890.
- (13) Skudlarek, J. W.; DiMarco, C. N.; Babaoglu, K.; Roecker, A. J.; Bruno, J. G.; Pausch, M. A.; O'Brien, J. A.; Cabalu, T. D.; Stevens, J.; Brunner, J.; Tannenbaum, P. L.; Wuelfing, W. P.; Garson, S. L.; Fox, S. V.; Savitz, A. T.; Harrell, C. M.; Gotter, A. L.; Winrow, C. J.; Renger, J. J.; Kuduk, S. D.; Coleman, P. J. *Bioorganic & Medicinal Chemistry Letters* **2017**, *27*, 1364.
- (14) Nienburg, H. *Berichte der deutschen chemischen Gesellschaft (A and B Series)* **1937**, *70*, 635.
- (15) Freed, M. E.; Day, A. R. *The Journal of Organic Chemistry* **1960**, *25*, 2105.
- (16) Atobe, M.; Yamazaki, N.; Kibayashi, C. *The Journal of Organic Chemistry* **2004**, *69*, 5595.
- (17) Macchia, B.; Macchia, M.; Martinelli, A.; Martinotti, E.; Orlandini, E.; Romagnoli, F.; Scatizzi, R. *European Journal of Medicinal Chemistry* **1997**, *32*, 231.

- (18) Lankenau, A. W.; Iovan, D. A.; Pienkos, J. A.; Salomon, R. J.; Wang, S.; Harrison, D. P.; Myers, W. H.; Harman, W. D. *Journal of the American Chemical Society* **2015**, *137*, 3649.
- (19) Harrison, D. P.; Sabat, M.; Myers, W. H.; Harman, W. D. *Journal of the American Chemical Society* **2010**, *132*, 17282.
- (20) Harrison, D. P.; Welch, K. D.; Nichols-Nielander, A. C.; Sabat, M.; Myers, W. H.; Harman, W. D. *Journal of the American Chemical Society* **2008**, *130*, 16844.

Chapter 5: Synthesis of Methylphenidate Analogs via Tungsten Dearomatization

Introduction

Nitrogen heterocycles are ubiquitous in natural products and biologically-active substances. In fact, N-heterocycles are found in more than half of FDA-approved small molecule drugs, with piperidine being the most common.¹ Piperidine is thus one of the most medicinally-relevant structural motifs and a valuable target for synthetic chemists. One such piperidine-based drug is methylphenidate, the methyl ester of phenyl(piperidin-2-yl)acetic acid. Methylphenidate is a central nervous stimulant commonly prescribed for the treatment of Attention Deficient Hyperactivity Disorder.² This stimulant activity results from inhibition of dopamine and norepinephrine reuptake, via blocking of the monoamine transporters DAT and NET, respectively.³

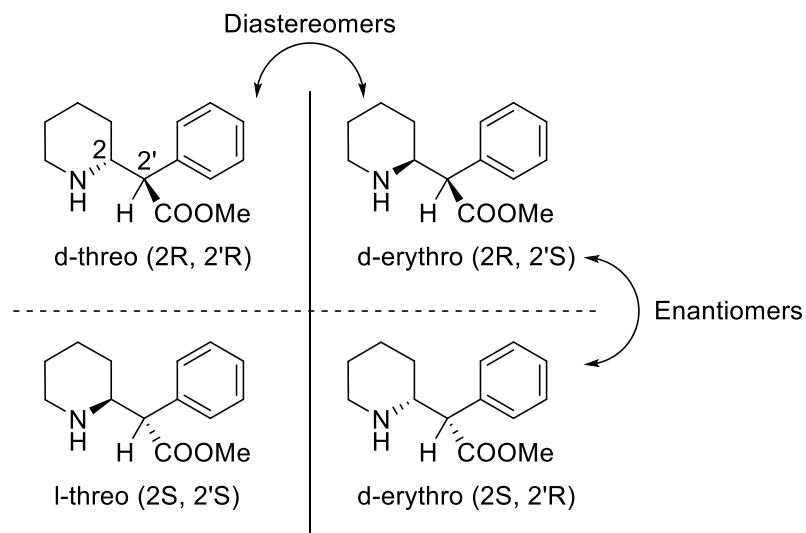


Figure 5.1: Enantiomers and diastereomers of methylphenidate

While numerous analogs of methylphenidate are known, most are derived from modifications of the phenyl or ester groups.³⁻⁵ Modification of the piperidine moiety has generally been limited to alkylation or acylation at nitrogen.⁶ Derivatization of the other positions in the piperidine ring is more challenging, particularly with respect to the

number of stereoisomers that may result. Given the past success of tungsten-mediated dearomatization in the synthesis of tetrahydropyridines,^{7,8} it was hoped that this chemistry could be extended to generate methylphenidate analogs. Such a synthetic approach would allow rapid generation of an analog chemical library that would otherwise be time-consuming to access.

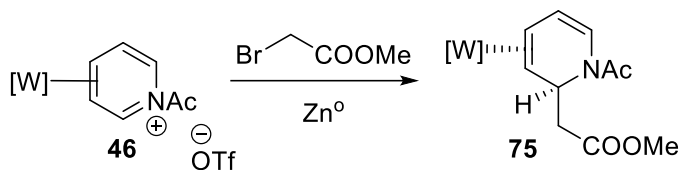
Results and Discussion

Previous work in our lab has demonstrated the synthesis of an N-functionalized pyridinium complex, WTp(NO)(PMe₃)(3,4- η^2 -N-acetylpyridinium)OTf (**46**).⁹ This complex readily undergoes regioselective nucleophilic additions exclusively at the C2 position.¹⁰ Due to the steric bulk of the metal and associated ligands, one face of the arene is blocked. Thus, addition of nucleophiles occurs stereoselectively *anti* to metal coordination.¹⁰ The resulting dihydropyridine can be further derivatized with an additional electrophilic, nucleophilic tandem addition sequence to generate highly-substituted tetrahydropyridines (THPs).⁷ The functionalized THP may be liberated by oxidation, which disrupts metal back-bonding and weakens the η^2 bond.

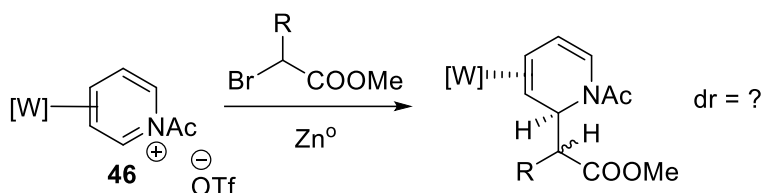
This methodology is particularly suitable for a divergent synthesis due to the numerous sites of chemical elaboration and the stepwise sequence of reactions. Thus, we questioned if analogs of a known drug, such as methylphenidate, could quickly be generated by this strategy. Reformatsky-like reaction had shown to be effective at introducing a zinc enolate derived from methyl bromoacetate to yield **75**, and it was hoped that the reaction would also be successful with a secondary α -bromo ester to yield **76**.¹⁰ In this way, the carbon framework of methylphenidate could be generated in one

step from the acetylpyridinium precursor (**46**). Typically, methylphenidate is prepared by hydrogenation of the corresponding pyridine, making analog synthesis less efficient.¹¹

Previous work:



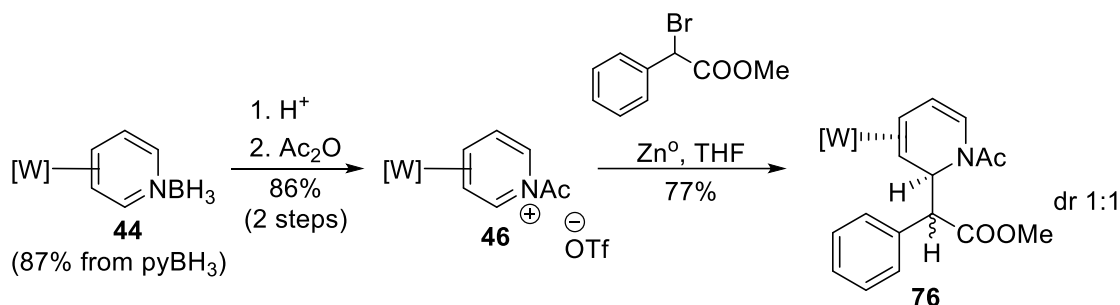
Proposed Reaction:



Scheme 5.1: Previous work and proposed Reformatsky-like reaction

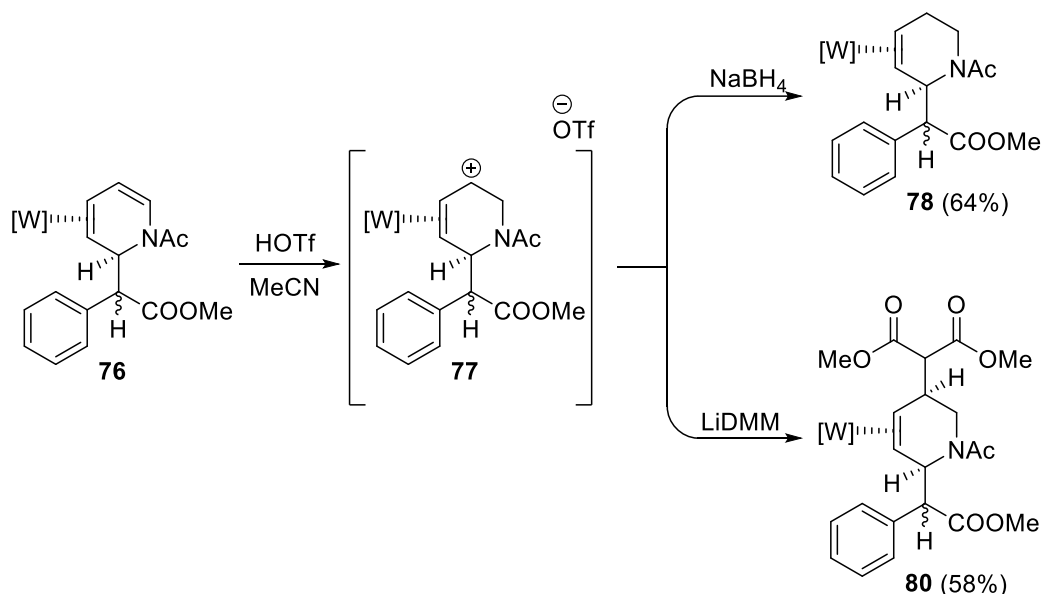
When the commercially-available compound methyl α -bromophenylacetate was combined with $\text{WTP}(\text{NO})(\text{PMe}_3)(3,4\text{-}\eta^2\text{-N-acetylpyridinium})\text{OTf}$ (**46**) and zinc dust in d_8 -THF, a successful nucleophilic addition (**Scheme 5.2**) was observed by ^1H NMR, as evidenced by the disappearance of the characteristic acyliminium-like proton (H2) signal at 9.0 ppm. In both the crude reaction mixture and the purified material, the product (**76**) had a 1:1 diastereomeric ratio (dr). The resulting complexes were analyzed by ^1H NMR, ^{13}C NMR, and 2D NMR techniques (COSY, NOESY, HSQC, and HMBC). Although the C2 stereocenter had been set relative to the metal, there was no control over the stereocenter created on the prochiral enolate nucleophile. Attempts to epimerize the complex with NaOMe in d_4 -MeOD resulted in complete deuteration of the ester α -position, but no change in the dr, suggesting 1:1 was the equilibrium ratio in solution. However, this stereocenter is known to be epimerizable in methylphenidate itself, and

indeed such a reaction is employed in the pharmaceutical synthesis of this compound.¹² Thus, the mixture of diastereomers of **76** was carried forward without separation of the diastereomers.

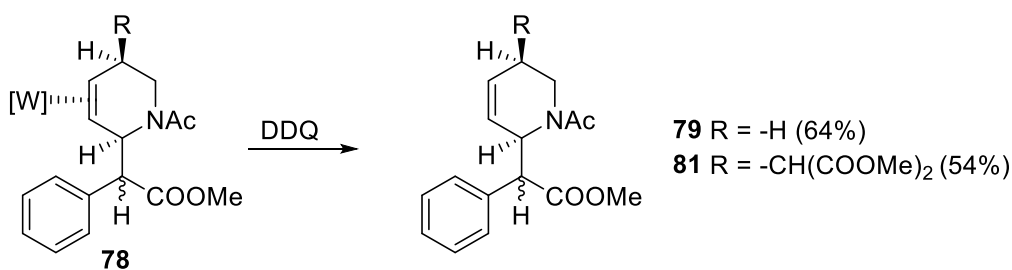


Scheme 5.2: Metal-mediated synthesis of methylphenidate core

Treatment of **76** with HOTf in MeCN appears to yield the allyl complex **77**. Frustratingly, this complex displays two amide rotamers for each diastereomer, making characterization by NMR very challenging.⁷ The allyl complex need not be isolated, however, as *in situ* protonation followed by nucleophilic addition has previously proven to give comparable reactivity to the isolated allyl complex.⁷ Thus, when an MeCN solution of **76** at -40 °C was treated with 1.1 molar equivalents of HOTf followed by NaBH₄, hydride addition occurred to yield complex **78** (**Scheme 5.3**). While the presence of four similar yet distinct species (two diastereomers with two rotamers each) once again made full characterization difficult, the absence of alkene signals was a characteristic sign of successful addition. Thus, **78** was oxidized with DDQ to liberate the tetrahydropyridine product **79** as a 1:1 mixture of diastereomers.



Scheme 5.3: Protonation and nucleophilic additions to a methylphenidate dihydropyridine derivative



Scheme 5.4: Oxidative decomplexation of functionalized methylphenidate organics

This organic product was purified via extraction and flash chromatography to yield the final product in 64% yield (dr 1:1). Attempted isomerization with NaOH in d_4 -MeOD did not prove successful at improving the dr. However, slow evaporation from an Et₂O solution yielded crystals which were analyzed by SC-XRD (**Figure 5.2**). The analyzed crystal proved to be the 3*S*,8*R* isomer (*erythro*) and its enantiomer (**79A**). Powder diffraction on the remainder of the crystals suggested the bulk solid material

consisted solely of one diastereomer, while the other diastereomer appeared to remain as an oil. Though this crystallization provides a way to separate the diastereomers, bulk separation was not pursued due to the small scale (<10 mg).

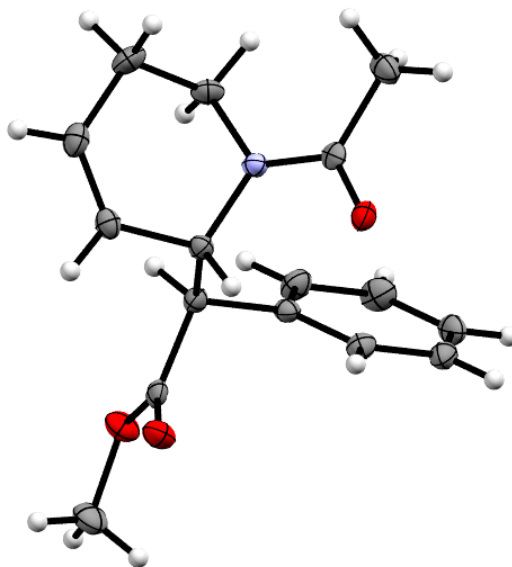


Figure 5.2: ORTEP diagram (50% ellipsoids) of the solid-state structure of compound **79A**, revealing the *erythro* stereochemistry

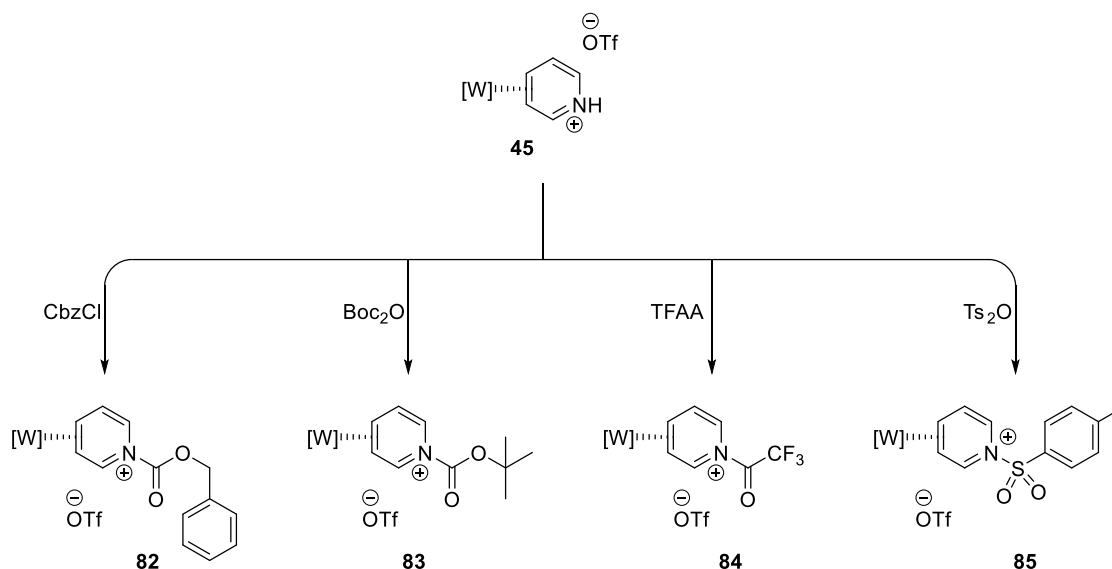
To test the scope of the reaction, **76** was reacted with HOTf followed by LiDMM, producing complex **80** in 58% yield. Complex **80** was oxidized with DDQ, yielding 54% of tetrahydropyridine **81** (dr 1:1) (**Scheme 5.4**). Compound **81** proved amenable to separation by Combiflash chromatography, and one diastereomer (**81A**) was isolated with a dr > 98:2. Though this compound appears to be an oil at room temperature and never crystallized, it is tentatively assigned as the R/R and S/S (*threo*) enantiomer pair, by analogy with **79**. In the crystallized *erythro* isomer of compound **79**, the H2-H8 coupling constant was 10.4 Hz for the major rotamer and 9.4 Hz for the minor rotamer. The *threo* isomer was determined to have H2-H8 coupling constants of 10.2 Hz for the

major rotamer and 7.8 Hz for the minor rotamer. The latter *threo* coupling constants are in good agreement with those in the single diastereomer of **81**: 10.4 Hz for the major rotamer and 7.7 Hz for the minor rotamer. In methylphenidate itself and many of its analogs, stereochemistry of a given isomer has a profound impact on its biological effects, with the *threo* isomer possessing orders of magnitude higher activity.^{13,14} Control over stereochemistry is therefore important, though for initial screening purposes, access to either diastereomer is preferred.

To date, all organic compounds derived from tungsten dearomatization of pyridine-borane have featured an acetyl protected nitrogen.^{7,8,15,16} While other protecting groups were screened (methyl, benzoyl, triflyl), none of these were suitable for subsequent nucleophilic additions.¹⁰ In attempt to further explore one potential point of diversity, a number of common nitrogen protecting groups were evaluated. It was also hoped that the issue of amide rotamers, which often greatly complicates NMR assignments, could be mitigated.

Initially, carbamates were explored, as these groups would allow facile deprotection of the organic product following decomplexation. The carboxybenzyl (Cbz) was investigated first due to the potential for deprotection via hydrogenolysis. Benzyl chloroformate was introduced to a solution of $\text{WTP}(\text{NO})(\text{PMe}_3)(3,4\text{-}\eta^2\text{-pyridinium})\text{OTf}$ (**45**) and DTBP. The reaction was still incomplete after 24 h, and thus the acylation was attempted again using 2,6-lutidine. With this less hindered base, the reaction appeared complete by ³¹P NMR within 20 min, giving product **82** (**Scheme 5.5**). By ¹H NMR, **82** was strikingly similar to the acetyl analog except for the presence of phenyl protons. The coordination diastereomer ratio (CDR) of the isolated product was 3:1. Upon standing in

solution for several days or heating in solution at +40 °C for 4 h, the CDR could be improved to 9:1, which appeared to be the equilibrium ratio, as no further improvement was noted. However, this isomerization was accompanied by about 10% decomposition by either method. When **82** was reacted with NaBH₄ or NaCN, a mixture of numerous products resulted. It appeared the Cbz group was susceptible to attack by nucleophiles, and a more robust protecting group was required for further functionalization



Scheme 5.5: Synthesis of various N-protected pyridinium complexes. Only major coordination diastereomer is shown.

The greater steric hinderance of Boc suggested that the Boc pyridinium complex would be more resistant to deprotection. Thus, WTp(NO)(PMe₃)(3,4-η²-pyridinium)OTf (**45**) was reacted with di-*tert*-butyl dicarbonate (Boc₂O) in the presence of 2,6-lutidine, forming product **83** with a 3:1 CDR. Cyclic voltammetry revealed an E_{p,a} of +1.08 V, and by ¹H NMR the *tert*-butyl singlet integrating for 12 protons (9 for each coordination diastereomer) was evident at 1.60 ppm. Attempts to improve the diastereomer ratio by

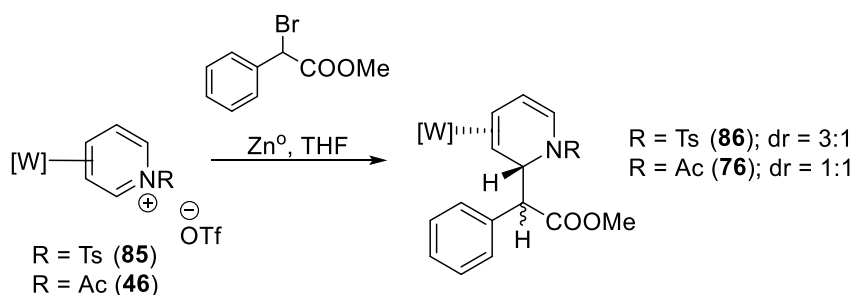
heating resulted in a CDR of 7:1 and about 10% deprotection, reforming **45**. This result was similar to compound **82**, though the rate of isomerization was slower and the equilibrium CDR appeared to be lower. As with **82**, attempted nucleophilic additions with NaCN or NaBH₄ also resulted in a mixture of product that was not synthetically useful.

Trifluoroacetyl was also investigated as a protecting group, with the expectation that this more electron-withdrawing functionality would enable weaker nucleophiles, such as activated arenes, to add to the pyridinium complex. When DTBP was added to an MeCN solution of **45** and trifluoroacetic anhydride (TFAA), an immediate reaction resulted to form complex **84** with a cdr of 3:1. Upon heating or prolonged standing in solution, **84** appeared to decompose rather than isomerize, and ³¹P signals were consistent with an oxidized product.

As more labile protecting groups proved to have fatal shortcomings, the tosyl protecting group was tried next. Compound **45** was reacted with tosyl anhydride in the presence of 2,6-lutidine to yield complex **85**. Again, the product was initially formed with a 3:1 CDR. However, heating **85** at +50 °C for 5 h improved the CDR to >10:1 with less than 5% decomposition, as determined by ³¹P NMR. The tosyl group proved resistant to deprotection by nucleophiles, and NMR-scale tests combining **85** with ethyl bromoacetate/zinc or NaBH₄ produced products consistent with N-tosyl dihydropyridines. The scope of these nucleophilic additions is being explored as part of an independent project.

With these encouraging results, an attempt was made to synthesize the tosyl analog of dihydropyridine complex **76**. Compound **85** was combined with with α -

bromophenylacetate and zinc dust, resulting in formation of complex **86** (Scheme 5.6). Surprisingly, **86** was formed with a dr of 3:1, in contrast to the 1:1 dr observed for the acetyl analog, **76**. It should be noted that in both of these experiments, a single *coordination* diastereomer (CDR >10:1) of the starting pyridinium complex was employed. The CDR did not change during the reaction, and the dr referenced here arises due to the stereocenter that is formed indiscriminately on the incoming prochiral nucleophile. Reaction monitoring by ^{31}P NMR revealed this 3:1 dr to be the initial kinetic product ratio. If the reaction is allowed to run longer, epimerization slowly results, lowering the dr.



Scheme 5.6: Comparison of methyl α -bromophenylacetate addition to tosyl- and acetyl-pyridinium complexes

With dihydropyridine **86** in hand, the question arose whether the tosyl group would influence the outcome of subsequent protonation and nucleophilic addition. Compound **86** was thus reacted with HOTf/MeCN followed by $\text{NaBH}_4/\text{MeOH}$, yielding compound **87**, the tosyl analog of tetrahydropyridine **78**. Complex **87** was analyzed by ^1H NMR, ^{13}C NMR, and 2D NMR techniques (COSY, NOESY, HSQC, and HMBC), and found to be the desired hydride addition product with the tosyl group intact. The absence of rotamers in **87** made full assignment possible. It was also discovered that the minor

diastereomer (**87B**) was significantly more soluble in MeCN and easily separated. Additionally, the insoluble diastereomer (**87A**) readily crystallized. The resulting crystal was analyzed by SC-XRD, allowing assignment of the stereochemistry (**Figure 5.3**). It was found that the complexed diastereomer in **87A** was the same as the crystallized decomplexed organic, **79A** (*erythro*).

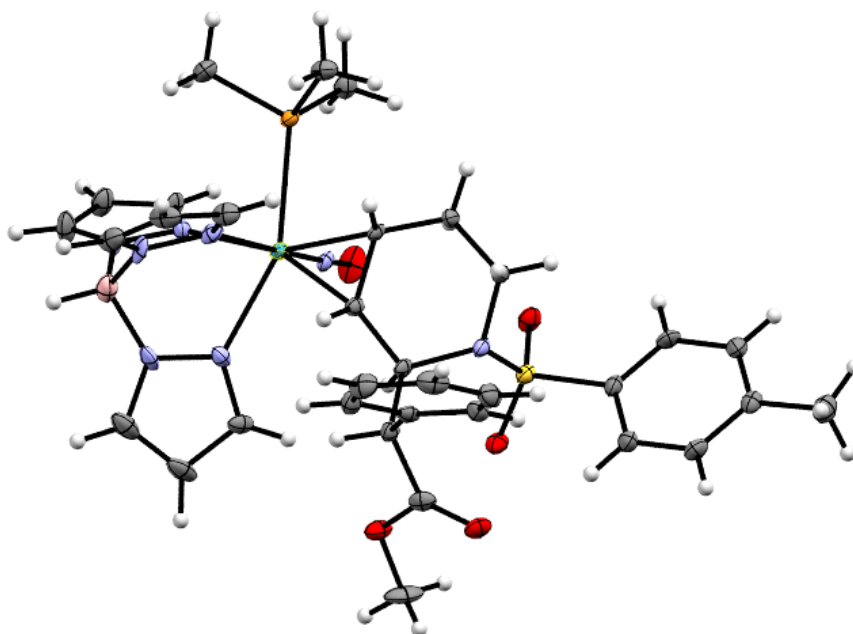
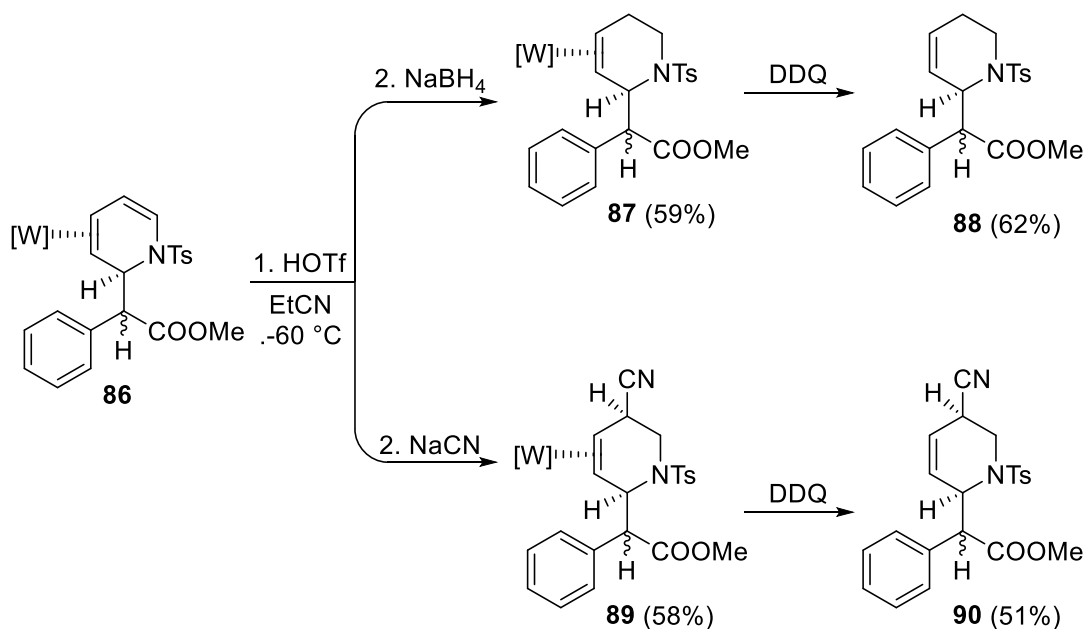


Figure 5.3: ORTEP diagram (50% ellipsoids) of the solid-state structure of compound **87A**, elucidating the stereochemistry

As isotopologues have been attracting increasing interest among medicinal chemists,¹⁷ a selectively deuterated compound was sought to illustrate the potential synthetic utility of this chemistry. Compound **⁵d₁-87** was synthesized by substituting NaBD₄ and d₄-MeOH in the synthesis of **87**. ¹H NMR analysis revealed an isotopic purity of > 93%. Furthermore, the H5 proton (2.62 ppm) *anti* to the metal was selectively

deuterated; no deuterium incorporation was observed at any other position, including H8 α to the ester.

The tetrahydropyridine ligand of **87A** was liberated with DDQ to furnish **88** (Scheme 5.7). The ester α position is seemingly sensitive to epimerization under these reaction conditions, as **88** was formed with a dr of 1:1, despite the dr of **87A** being in excess of 11:1. Alternative oxidants will be screened to mitigate this undesirable isomerization. After extraction and flash chromatography, purified **88** was isolated in 62% yield, almost exactly the same as acetyl analog **79**. Therefore, the substitution of tosyl appears to have little influence on the oxidative decomplexation.



Scheme 5.7: Functionalization of a tosylmethylphenidate complex, followed by oxidative decomplexation of the resulting tetrahydropyridine

To explore the scope of this reaction beyond hydride nucleophiles, **86** was reacted with HOTf/MeCN, followed by NaCN/MeOH at -60 °C. ¹H NMR analysis of a crude

aliquot taken 5 h later revealed a new addition product, **89**. As there was also 20% starting material, suggesting an incomplete reaction, the reaction was allowed to continue at -60 °C 15 h longer. However, the product ratio did not change, and it appears **86** was reformed by deprotonation of the allyl formed *in situ*. Compound **89** was carried on to oxidation without further purification. Oxidation of **89** with DDQ yielded tetrahydropyridine **90** in 51% yield after extraction and flash chromatography. This nitrile-functionalized organic serves as proof-of-concept for a range of functionalized N-tosylmethylphenidate analogs.

Conclusion

The metal-promoted dearomatization described herein presents a novel way of synthesizing medicinally-relevant chemical libraries. This synthesis of functionalized methylphenidate analogs illustrates the ability to selectively modify specific positions in a stereo- and regioselective manner. Additionally, the tetrahydropyridines produced by this chemistry contain a remaining double bond, permitting further derivatization. Previous work has demonstrated the ability to enantioenrich a tungsten exchange precursor, $\text{TpW}(\text{NO})(\text{PMe}_3)(\eta^2\text{-1,3-dimethoxybenzene})$, which can undergo ligand exchange without epimerization of the metal stereocenter.¹⁸ Consequently, all of the organics produced by this chemistry should be available as single enantiomers. Metal-promoted dearomatization thus allows access to organic molecules that are challenging to produce by traditional organic chemistry.

Experimental Section

General Methods. NMR spectra were obtained on a 600 or 800 MHz spectrometer (22–25 °C). All chemical shifts are reported in ppm, and proton and carbon shifts are referenced to tetramethylsilane (TMS) utilizing residual ^1H or ^{13}C signals of the deuterated solvents as an internal standard. Coupling constants (J) are reported in hertz (Hz). Infrared spectra (IR) were recorded as a glaze on a spectrometer fitted with a horizontal attenuated total reflectance (HATR) accessory or on a diamond anvil ATR assembly. Electrochemical experiments were performed under a nitrogen atmosphere. Cyclic voltammetry data were taken at ambient temperature (22–25 °C) at 100 mV/s in a standard three-electrode cell with a glassy carbon working electrode, N,N-dimethylacetamide (DMA) or acetonitrile (MeCN) solvent, and tetrabutylammonium hexafluorophosphate (TBAH) electrolyte (approximately 0.5 M). All potentials are reported versus NHE (normal hydrogen electrode) using cobaltocenium hexafluorophosphate ($E_{1/2} = -0.78$ V), ferrocene ($E_{1/2} = +0.55$ V), or decamethylferrocene ($E_{1/2} = +0.04$ V) as an internal standard. The peak-to-peak separation was less than 100 mV for all reversible couples. Unless otherwise noted, all synthetic reactions were performed in a glovebox under a dry nitrogen atmosphere. Deuterated solvents were used as received. Pyrazole (Pz) protons of the (trispyrazolyl)borate (Tp) ligand were uniquely assigned (e.g., “Pz3B”) using a combination of two-dimensional NMR data and PMe_3 -proton NOE interactions. When unambiguous assignments were not possible, Tp protons were labeled as “Pz3/5 or Pz4”. All J values for Pz protons are 2 (± 0.2) Hz. BH ^1H NMR peaks (around 4–5 ppm) are not identified due to their quadrupole broadening; IR data are used to confirm the presence of a BH group (around 2500 cm^{-1}).

Synthesis of methyl 2-(1-acetyl-1,2,5,6-tetrahydropyridin-2-yl)-2-phenylacetate (79)

Erythro isomer: A mixture of two rotamers **A**:**B** = 4:3. ¹H NMR (d-chloroform, δ): **A** 7.45-7.25 (m, 5H, H9-H11), 6.00 (m, 1H, H4), 5.88 (m, 1H, H3), 4.72 (dd, J=13.1Hz, 6.2Hz, 1H, H6), 4.60 (m, 1H, H2), 3.87 (d, J=10.4Hz, 1H, H8), 3.76 (s, 3H, H12), 2.83 (m, 1H, H6'), 2.27 (m, 1H, H5), 2.04 (dt, J=18.1Hz, 5.0Hz, 1H, H5'), 1.44 (s, 3H, H7). **B** 7.45-7.25 (m, 5H, H9-H11), 5.88 (m, 1H, H4), 5.85 (m, 1H, H3), 5.60 (m, 1H, H2), 3.89 (d, J=9.4Hz, 1H, H8), 3.64 (dd, J=13.9Hz, 5.9Hz, 1H, H6), 3.72 (s, 3H, H12), 3.22 (ddd, J=13.9Hz, 12.9Hz, 4.2Hz, 1H, H6'), 2.27 (m, 1H, H5), 1.96 (dt, J=18.3Hz, 5.0Hz, 1H, H5'), 1.90 (s, 3H, H7). ¹³C NMR (d-chloroform, δ): **A** 172.0 (Ester CO), 170.0 (Amide CO), 135.3 (C9a), 129.1 (C9), 128.5 (C10), 127.8 (C11), 129.2 (C4), 126.2 (C3), 57.2 (C2), 55.3 (C8), 52.4 (C12), 34.8 (C6), 24.9 (C5), 20.9 (C7). **B** 172.4 (Ester CO), 169.1 (Amide CO), 134.8 (C9a), 128.8 (C9), 128.4 (C10), 127.8 (C11), 126.6 (C3), 126.2 (C4), 55.3 (C8), 52.4 (C12), 51.6 (C2), 40.3 (C6), 24.5 (C5), 21.6 (C7).

Threo isomer: A mixture of two rotamers **A**:**B** = 1:1. ¹H NMR (d-chloroform, δ): **A** 7.45-7.25 (m, 5H, H9-H11), 5.85 (m, 1H, H4), 5.27 (m, 1H, H3), 4.79 (m, 1H, H2), 4.66 (dd, J=13.5Hz, 6.4Hz, 1H, H6), 3.94 (d, J=10.2Hz, 1H, H8), 3.69 (s, 3H, H12), 2.82 (m, 1H, H6'), 2.32 (s, 3H, H7), 2.22 (m, 1H, H5), 2.08 (dt, J=17.2Hz, 4.4Hz, 1H, H5'). **B** 7.45-7.25 (m, 5H, H9-H11), 5.85 (m, 1H, H4), 5.69 (m, 1H, H3), 5.54 (m, 1H, H2), 4.07 (d, J=7.8Hz, 1H, H8), 3.67 (s, 3H, H12), 3.54 (dd, J=13.8Hz, 5.8Hz, 1H, H6), 2.63 (ddd, J=14.1Hz, 12.7Hz, 3.9Hz, 1H, H6'), 2.13 (s, 3H, H7), 2.13 (m, 1H, H5), 1.90 (buried, 1H, H5'). ¹³C NMR (d-chloroform, δ): **A** 172.3 (Ester CO), 170.6 (Amide CO), 135.3 (C9a), 129.0 (C9), 128.6 (C4), 128.4 (C10), 128.3 (C11), 125.6 (C3), 57.3 (C2), 54.5 (C8), 52.3 (C12), 35.1 (C6), 24.6 (C5), 21.7 (C7). **B** 172.5 (Ester CO), 169.4 (Amide

CO), 135.3 (C9a), 129.9 (C9), 128.8 (C10), 128.4 (C11), 127.3 (C4), 126.2 (C3), 56.5 (C8), 52.3 (C2), 52.2 (C12), 40.5 (C6), 25.3 (C5), 22.1 (C7).

ESI-MS: obs'd (%), calc'd (%), ppm, (M+H)⁺: 274.1439 (100), 274.1438 (100), 0.4.

Synthesis of WTP(NO)(PMe₃)(3,4-η²-1-((benzyloxy)carbonyl)pyridinium)OTf (**82**)

WTP(NO)(PMe₃)(3,4-η²-pyridinium)OTf (**45**) (300 mg, 0.410 mmol) was suspended in MeCN (700 mg) in a 4 dram vial containing an egg-shaped stir bar. Benzyl chloroformate (1.20 g, 7.03 mmol) was added to the reaction mixture. After stirring for 5 min, a solution of 2,6-lutidine (93 mg, 0.868 mmol) in MeCN (300 mL) was added to the reaction, which quickly became homogenous. After 20 min of stirring at room temperature, the reaction was placed in an oil bath at +40 °C and heated for 3 h. Checking the reaction by ³¹P NMR revealed a >9:1 CDR after this time. The reaction mixture was removed from the oil bath and allowed to cool for 10 min, then the solution was added dropwise to a stirring solution of Et₂O (60 mL). The precipitate was isolated on a 15 mL fine porosity fritted funnel, washed with Et₂O (3 x 10 mL) and desiccated to yield compound **82** as a vivid orange powder (211 mg, 59%). CV (MeCN) E_{p,a} = +1.09 V. A mixture of two coordination diastereomers **A**:**B** > 9:1. ¹H NMR (d₃-acetonitrile, δ): **A** 8.9 (d, J=5.8Hz, 1H, H2), 8.03 (Pz3/5), 8.00 (Pz3/5), 7.99 (Pz3/5), 7.88 (Pz3/5), 7.85 (Pz3/5), 7.65 (Pz3/5), 7.48-7.42 (m, 5H, H8+H9+H10), 6.52 (dd, J=7.3, 1.2Hz, 1H, H6), 6.46 (ddd, J=7.3, 5.5, 1.6Hz, 1H, H5), 6.45 (Pz4), 6.43 (Pz4), 6.41 (Pz4), 4.22 (m, 1H, H4), 3.33 (ddd, J=7.3, 5.9, 1.8Hz, 1H, H3), 1.21 (d, J=9.5Hz, 9H, PMe₃).

Synthesis of WTP(NO)(PMe₃)(3,4-η²-1-(tert-butoxycarbonyl)pyridinium)OTf (**83**)

WTP(NO)(PMe₃)(3,4-η²-pyridinium)OTf (**45**) (258 mg, 0.352 mmol) was suspended in MeCN (550 mg) in a 4 dram vial containing an egg-shaped stir bar. Boc₂O (1.07 g, 4.90 mmol) was added to the reaction mixture. After stirring for 1 min, a solution of 2,6-lutidine (117 mg, 1.09 mmol) in MeCN (100 mg) was added to the reaction. The heterogenous reaction mixture was stirred for 1 h, over which time it became homogenous. The reaction was placed in an oil bath at +40 °C and heated for 6 h. Checking the reaction by ³¹P NMR revealed a >6:1 CDR after this time. The reaction mixture was removed from the oil bath and allowed to cool for 10 min, then the solution was added dropwise to a stirring solution of Et₂O (75 mL). The precipitate was isolated on a 15 mL fine porosity fritted funnel, washed with Et₂O (3 x 10 mL) and desiccated to yield compound **83** as a vivid orange powder (180 mg, 61%). CV (MeCN) E_{p,a} = +1.07 V. A mixture of two coordination diastereomers **A**:**B** = 6.5:1. ¹H NMR (d₃-acetonitrile, δ): **A** 8.96 (d, J=5.6Hz, 1H, H2), 8.06 (Pz3/5), 8.04 (Pz3/5), 7.99 (Pz3/5), 7.98 (Pz3/5), 7.85 (Pz3/5), 7.75 (Pz3/5), 6.50 (d, J=7.3Hz, 1H, H6), 6.49 (Pz4), 6.47 (m, 1H, H5), 6.44 (Pz4), 6.41 (Pz4), 4.20 (m, 1H, H4), 3.26 (m, 1H, H3), 1.60 (s, 9H, H7), 1.22 (d, J=9.4Hz, 9H, PMe₃). **B** 9.07 (d, J=4.9Hz, 1H, H2), 8.04 (Pz3/5), 8.02 (Pz3/5), 8.02 (Pz3/5), 7.89 (Pz3/5), 7.88 (Pz3/5), 7.62 (Pz3/5), 6.70 (dd, J=7.3, 4.9Hz, 1H, H5), 6.47 (d, J=7.3Hz, 1H, H6), 6.45 (Pz4), 6.44 (Pz4), 6.35 (Pz4), 4.09 (m, 1H, H3), 2.88 (m, 1H, H4), 1.60 (s, 9H, H7), 1.27 (d, J=9.0Hz, PMe₃).

Synthesis of WTP(NO)(PMe₃)(3,4-η²-1-tosylpyridinium)OTf (**85**)

WTP(NO)(PMe₃)(3,4-η²-pyridinium)OTf (**45**) (3.40 g, 4.64 mmol) was suspended in MeCN (20 mL) in a large test tube containing an egg-shaped stir bar. Tosyl anhydride

(2.62 g, 9.29 mmol) was added to the reaction mixture. After stirring for 5 min, a solution of 2,6-lutidine (498 mg, 4.64 mmol) in MeCN (2.0 mL) was added to the reaction, which almost immediately became homogenous, aside from some crystals of triflic anhydride. After 25 min of stirring at room temperature, the reaction was placed in an oil bath at +50 °C and heated for 2 h. Checking the reaction by ^{31}P NMR revealed a >10:1 CDR after this time. The reaction was diluted with DCM (100 mL) and extracted with saturated aqueous ammonium chloride (3 x 100 mL). The combined aqueous layers were back-extracted with DCM (50 mL). The combined organic layers were dried with Na_2SO_4 , filtered, and evaporated to dryness under vacuum. The residue was redissolved in DCM (20 mL) and added to stirring Et_2O (1.2 L). After 1 minute, stirring was stopped and the suspended precipitate was allowed to settle. The supernatant was decanted and the solids were isolated on a 60 mL medium porosity fritted funnel. The solids were washed with Et_2O (4 x 40 mL) and desiccated to yield compound **85** as a vivid orange solid (3.10 g, 75%, cdr >10:1). Note that the material is initially isolated as a mixed triflate/tosylate salt (approximately in a 3:1 ratio). The tosylate counterion may be removed by dissolving the solid in MeCN, adding 1 molar equivalent of triflic acid in minimal MeCN, and re-precipitating the solid as described above. CV (MeCN) $E_{p,a} = +1.31$ V (NHE). ^1H NMR (d_3 -acetonitrile, δ): 9.22 (d, $J=6.3\text{Hz}$, 1H, H2), 8.05 (d, $J=8.5\text{Hz}$, 1H, H7), 8.03 (PzC5), 8.00 (PzB5), 7.99 (PzB3), 7.88 (PzA3), 7.85 (PzA5), 7.65 (PzC3), 7.53 (d, $J=8.5\text{Hz}$, 1H, H8), 6.61 (ddd, $J=7.7, 5.5, 1.9\text{Hz}$, 1H, H5), 6.46 (dd, $J=7.7, 1.5\text{Hz}$, 1H, H6), 6.45 (PzC4), 6.43 (PzB4), 6.41 (PzA4), 4.06 (m, 1H, H4), 2.97 (td, $J=6.3, 2.0\text{Hz}$, 1H, H3), 2.46 (s, 3H, H9), 1.18 (d, $J=9.4\text{Hz}$, 9H, PMe_3). ^{13}C NMR (d_3 -acetonitrile, δ): 168.7 (C2), 149.0 (C7a), 147.2 (PzA3), 146.7 (PzB3), 142.8 (PzC3), 139.4 (PzC5), 139.3 (PzB5), 138.5 (PzA5),

133.7 (C8a), 131.9 (C8), 129.5 (C7), 124.9 (C5), 115.1 (C6), 108.8 (PzB4), 108.4 (PzC4), 108.3 (PzA4), 67.8 (C4), 67.2 (C3), 21.9 (C9), 12.9 (d, J=31.6Hz, PMe₃). ESI-MS: obs'd (%), calc'd (%), ppm, M⁺: 737.1576 (100), 737.1580 (100), 0.5.

Synthesis of WTp(NO)(PMe₃)(3,4-η²-methyl 2-phenyl-2-(1-tosyl-1,2-dihydropyridin-2-yl)acetate) (86)

Compound **85** (2.50 g, 2.82 mmol) and methyl α-bromophenylacetate (1.30 g, 5.68 mmol) were added to THF (25.0 mL) in a 50 mL round-bottom flask containing an egg-shaped stir bar. The reaction mixture was stirred for 3 minutes, then zinc dust (1.20 g, 18.4 mmol) was added. The reaction mixture was rapidly stirred for 1 h, becoming homogenous. The reaction mixture was filtered through Celite (1 cm) in a 15 mL medium porosity fritted funnel. The Celite was washed with THF (5 mL). The filtrate was diluted with DCM (75 mL) and extracted with saturated aqueous sodium bicarbonate (3 x 50 mL). The combined aqueous layers were back-extracted with DCM (20 mL). The combined organic layers were dried with Na₂SO₄, filtered, and evaporated to dryness under vacuum. The residue was redissolved in DCM (1.0 mL) and added dropwise to stirring hexanes (150 mL). The precipitate was isolated on a 30 mL fine porosity fritted funnel, washed with hexanes (3 x 20 mL), and desiccated to yield compound **86** as a beige solid (1.89 g, 76%, dr = 3:1). Note that longer reaction times will yield a product with a lower dr. ¹H NMR (d₃-acetonitrile, δ): Diastereomer **A** 7.99 (d, J=8.2Hz, 2H, H7), 7.97 (Pz3/5), 7.83 (Pz3/5), 7.80 (Pz3/5), 7.71 (Pz3/5), 7.49 (Pz3/5), 7.42 (d, J=8.2Hz, 2H, H8), 7.21 (Pz3/5), 7.15-7.00 (m, 5H, H11+H12+H13), 6.34 (Pz4), 6.24 (Pz4), 6.19 (Pz4), 5.74 (d, J=7.9Hz, 1H, H6), 5.38 (d, J=4.0Hz, 1H, H2), 5.14 (buried, 1H, H5), 4.30 (d, J=4.0Hz, 1H, H10), 3.26 (s, 3H, H14), 2.46 (m, 1H, H4), 2.42 (s, 3H, H9), 1.21 (d,

J=10.6Hz, 1H, H3), 1.06 (d, J=8.6Hz, 9H, PMe₃). Diastereomer **B** 8.01 (Pz3/5), 7.85 (Pz3/5), 7.83 (Pz3/5), 7.80 (Pz3/5), 7.70 (d, J=8.3Hz, 2H, H7), 7.68 (Pz3/5), 7.36 (Pz3/5), 7.25 (d, J=8.3Hz, 2H, H8), 7.15-7.00 (m, 5H, H11+H12+H13), 6.35 (Pz4), 6.26 (Pz4), 6.15 (Pz4), 5.99 (d, J=7.9Hz, 1H, H6), 5.75 (buried, 1H, H5), 5.12 (buried, 1H, H2), 4.07 (d, J=4.6Hz, 1H, H10), 3.48 (s, 3H, H14), 2.82 (m, 1H, H4), 2.36 (s, 3H, H9), 1.52 (d, J=10.6Hz, 1H, H3), 1.17 (d, J=8.6Hz, 9H, PMe₃). ¹³C NMR (d₃-acetonitrile, δ): Diastereomer **A** 173.6 (Ester CO), 144.9 (C7a), 144.1 (Pz3/5), 141.4 (Pz3/5), 141.1 (Pz3/5), 138.9 (C8a), 137.8 (Pz3/5), 137.3 (Pz3/5), 137.2 (C11a), 137.0 (Pz3/5), 131.9 (C11), 130.6 (C8), 129.6 (C12), 129.6 (C7), 128.0 (C13), 116.3 (C6), 113.2 (C5), 107.5 (Pz4), 107.2 (Pz4), 106.5 (Pz4), 58.6 (C10), 58.2 (C3), 57.6 (C2), 52.1 (C14), 46.1 (C4), 21.6 (C9), 13.1 (d, J=28.4Hz, PMe₃). Diastereomer **B** 173.4 (Ester CO), 144.2 (C7a), 144.1 (Pz3/5), 144.1 (Pz3/5), 141.1 (Pz3/5), 139.6 (C8a), 138.3 (C11a), 137.8 (Pz3/5), 137.8 (Pz3/5), 137.0 (Pz3/5), 130.4 (C8), 129.6 (C11), 128.9 (C7), 128.6 (C12), 127.7 (C13), 116.9 (C6), 114.5 (C5), 107.5 (Pz4), 107.2 (Pz4), 106.7 (Pz4), 60.2 (C2), 59.2 (C3), 57.8 (C10), 52.1 (C14), 44.9 (C4), 21.5 (C9), 13.3 (d, J=28.4Hz, PMe₃).

Synthesis of WTP(NO)(PMe₃)(3,4-η²-methyl 2-phenyl-2-(1-tosyl-1,2,5,6-tetrahydropyridin-2-yl)acetate) (87)

Compound **86** (250 mg, 0.282 mmol) and EtCN (4.5 mL) were combined in a large test tube containing a stir pea. This solution was placed in a cold bath at -60 °C and cooled for 10 min. Separately, HOTf (48 mg, 0.322 mmol) was dissolved in EtCN (1.0 mL) in a 4 dram vial. The HOTf solution was added to the cold solution of compound **86**, and the reaction mixture was stirred at -60 °C for 10 min. Meanwhile, NaBH₄ (90 mg, 2.38 mmol) and MeOH (2.57g) were added to *separate* small test tubes and cooled for 5 min

at -60 °C. After 5 min, the MeOH was added to the NaBH₄. The mixture was mixed with a pipette to suspend the solid, then the suspension was poured into the large test tube containing the reaction mixture. The reaction was stirred at -60 °C for 3 hr. The reaction mixture was then removed from the cold bath and allowed to warm up to room temperature over 15 min, over which time gas was evolved. After 15 min, Et₂O (20 mL) was added to the reaction mixture, causing further gas evolution. When the gas evolution had nearly ceased, the solution was loaded onto a column of basic alumina (30 mL)/Et₂O slurry in a 60 mL coarse fritted funnel. A pale golden band was eluted with Et₂O (125 mL), and the eluent was evaporated under vacuum. The residue was redissolved in EtOAc (3 mL) and added dropwise to cold stirring hexanes (75 mL). The precipitate was isolated on a 15 mL fine porosity fritted funnel, washed with hexanes (2 x 5 mL), and desiccated under vacuum to yield **87** a tan solid (134 mg, 53%, dr = 3:1). To enrich the major diastereomer (**87A**), the solid product (134 mg, 0.151 mmol) was stirred with MeCN (1.5 mL) for 3 hr. The suspended solid was isolated on a 15 mL fine porosity fritted funnel and desiccated to yield **87A** as a tan solid with a d.r. of 11:1 (80 mg, 80 %).

¹H NMR (d₂-methylene chloride, δ): 8.04 (Pz3/5), 7.93 (Pz3/5), 7.74 (Pz3/5), 7.72 (Pz3/5), 7.62 (Pz3/5), 7.44 (d, J=8.3Hz, 2H, H7), 7.21 (Pz3/5), 7.10 (d, J=8.3Hz, 2H, H8), 7.04 (m, 3H, H11+H13), 6.96 (m, 2H, H12), 6.31 (Pz4), 6.24 (Pz4), 6.17 (Pz4), 5.47 (dd, J=6.1, 1.8Hz, 1H, H2), 4.18 (d, J=6.1Hz, 1H, H10), 3.56 (m, 1H, H6), 3.20 (s, 3H, H14), 3.14 (m, 1H, H6'), 2.84 (m, 1H, H4), 2.73 (m, 1H, H5), 2.62 (m, 1H, H5'), 2.35 (s, 3H, H9), 1.23 (d, J=8.2Hz, 9H, PMe₃), 0.87 (d, J=12.2Hz, 1H, H3). ¹³C NMR (d₂-methylene chloride, δ): 173.0 (Ester CO), 143.9 (Pz3/5), 143.3 (Pz3/5), 142.5 (C7a), 140.1 (Pz3/5), 139.5 (C8a), 137.6 (C11a), 136.6 (Pz3/5), 136.5 (Pz3/5), 136.0 (Pz3/5),

129.7 (C8), 129.7 (C11), 128.4 (C12), 127.7 (C7), 127.3 (C13), 106.6 (Pz4), 106.4 (Pz4), 106.4 (Pz4), 61.8 (C10), 59.6 (C2), 53.4 (C3), 51.6 (C14), 46.2 (d, J=12.4Hz, C4), 42.1 (C6), 28.7 (C5), 21.6 (C9), 13.9 (d, J=27.8Hz, PMe₃).

Synthesis of methyl 2-phenyl-2-(1-tosyl-1,2,5,6-tetrahydropyridin-2-yl)acetate (**88**)

Compound **87** (70 mg, 0.0788 mmol) was dissolved in MeCN (3.0 mL) in a 4 dram vial containing a stir pea. Separately, DDQ (40 mg, 0.176 mmol) was dissolved in MeCN (1.0 mL). The DDQ solution was added to the solution of **87**, and the resulting mixture was stirred for 5 min. The reaction mixture was then diluted with DCM (50 mL) and extracted with saturated aqueous NaHCO₃ (50 mL). The aqueous layer was back-extracted with DCM (15 mL), and the combined organic layers were dried with Na₂SO₄. The solids were filtered off on a 30 mL medium fritted funnel, and rinsed with DCM (10 mL). The filtrate was evaporated on a rotary evaporator. The residue was dissolved in DCM (2 mL) and added to stirring Et₂O (100 mL). The precipitate was filtered off on a 30 mL medium porosity fritted funnel and rinsed with Et₂O (10 mL). The filtrate was evaporated onto silica on a rotary evaporator. The desired product was purified by Combiflash flash chromatography using a 0-100% EtOAc in hexanes gradient 30 mL/min elution on a 12g silica column. The desired product eluted at ~48% EtOAc. The fractions containing the product were combined and evaporated on a rotary evaporator. The residue was desiccated under high vacuum for 30 min to yield compound **88** as a colorless oil which spontaneously crystallized (19 mg, 62% over two steps).

Two diastereomers **A**:**B**. ¹H NMR (d-chloroform, δ): **A** 7.72 (d, J=8.3Hz, 2H, H9), 7.36-7.28 (m, 5H, H12+H13+H14), 7.25 (d, J=8.3Hz, 2H, H10), 5.63 (m, 1H, H4), 5.54 (m, 1H, H3), 5.03 (m, 1H, H2), 4.00 (d, J=8.2Hz, 1H, H8), 3.68 (dd, J=14.8, 6.4Hz, 1H, H6),

3.66 (s, 3H, H15), 2.69 (dd, J=14.8, 4.6Hz, 1H, H6'), 2.40 (s, 3H, H11), 1.71 (m, 1H, H5), 1.58 (ddd, J=18.0, 6.4, 4.6Hz, 1H, H5'). **B** 7.36-7.28 (m, 5H, H12+H13+H14), 7.23 (d, J=8.3Hz, 2H, H9), 7.07 (d, J=8.3Hz, 2H, H10), 6.84 (m, 1H, H3), 5.79 (m, 1H, H4), 5.03 (m, 1H, H2), 3.80 (d, J=9.8Hz, 1H, H8), 3.69 (s, 3H, H15), 3.54 (dd, J=14.8, 6.4Hz, 1H, H6), 3.07 (ddd, J=14.8, 12.0Hz, 4.6Hz, 1H, H6'), 2.35 (s, 3H, H11), 2.06 (m, 1H, H5), 1.80 (ddd, J=18.0, 6.4, 4.6Hz, 1H, H5'). ¹³C NMR (d-chloroform, δ): **A** 171.9 (Ester CO), 143.4 (C9a), 138.3 (C10a), 134.8 (C12a), 129.7 (C10), 129.7 (C12), 128.6 (C13), 128.0 (C14), 127.2 (C9), 127.1 (C3), 125.0 (C4), 57.5 (C8), 55.3 (C2), 52.3 (C15), 38.8 (C6), 22.7 (C5), 21.6 (C11). **B** 172.2 (Ester CO), 143.1 (C9a), 137.4 (C10a), 135.6 (C12a), 129.4 (C10), 129.0 (C12), 128.8 (C13), 128.0 (C14), 127.5 (C9), 127.3 (C4), 126.1 (C3), 56.7 (C8), 54.9 (C2), 52.4 (C15), 38.4 (C6), 22.9 (C5), 21.6 (C11). ESI-MS: obs'd (%), calc'd (%), ppm, (M+H)⁺: 386.1420 (100), 386.1421 (100), 0.2. (M+Na)⁺: 408.1242(100), 408.1240 (100), 0.5.

Synthesis of methyl 2-(5-cyano-1-tosyl-1,2,5,6-tetrahydropyridin-2-yl)-2-phenylacetate (**90**)

Step 1: Compound **86** (460 mg, 0.519 mmol) and EtCN (4.5 mL) were combined in a large test tube containing a stir pea. This solution was placed in a cold bath at -60 °C and cooled for 10 min. Separately, HOTf (90 mg, 0.600 mmol) was dissolved in EtCN (1.0 mL) in a 4 dram vial. The HOTf solution was added to the cold solution of compound **86**, and the reaction mixture was stirred at -60 °C for 15 min. Meanwhile, NaCN (127 mg, 2.60 mmol) and MeOH (2.5 mL) were added to a small test tube containing a stir pea. The mixture was vigorously stirred for 5 min at ambient temperature to dissolve the NaCN, and then was cooled in a cold bath at -60 °C for 10 min. The cold solution of

NaCN was then added to the large test tube containing the reaction mixture. The reaction was stirred at $-60\text{ }^{\circ}\text{C}$ for 5 hr. The reaction mixture was then removed from the cold bath and allowed to warm up to room temperature over 15 min. The reaction mixture was then diluted with DCM (60 mL) and extracted with saturated aqueous NaHCO_3 (3 x 60 mL). The combined aqueous layers were back-extracted with DCM (20 mL). The combined organic layers were dried with Na_2SO_4 , filtered, and evaporated to dryness. The residue was redissolved in EtOAc (3 mL) and added dropwise to cold stirring hexanes (100 mL). The precipitate was isolated on a 15 mL fine porosity fritted funnel, washed with hexanes (2 x 5 mL), and desiccated under vacuum to yield **89** a tan solid (336 mg), which was found to contain 20% starting material (due to deprotonation of the intermediate allyl). After accounting for this impurity, the yield was calculated to be 58%.

Step 2: Compound **89** (320 mg, 0.350 mmol) was dissolved in MeCN (2.0 mL) in a 4 dram vial containing a stir pea. Separately, DDQ (88 mg, 0.385 mmol) was dissolved in MeCN (2.0 mL). The DDQ solution was added to the solution of **89**, and the resulting mixture was stirred for 5 min. The reaction mixture was then diluted with DCM (50 mL) and extracted with saturated aqueous NaHCO_3 (50 mL). The aqueous layer was back-extracted with DCM (15 mL), and the combined organic layers were dried with Na_2SO_4 . The solids were filtered off on a 30 mL medium fritted funnel, and rinsed with DCM (10 mL). The filtrate was evaporated on a rotary evaporator. The residue was dissolved in DCM (2 mL) and added to stirring Et_2O (100 mL). The precipitate was filtered off on a 30 mL medium porosity fritted funnel and rinsed with Et_2O (10 mL). The filtrate was evaporated onto silica on a rotary evaporator. The desired product was purified by Combiflash flash chromatography using a 0-100% EtOAc in hexanes gradient 30 mL/min

elution on a 12g silica column. The desired product eluted at ~60% EtOAc. The fractions containing the product were combined and evaporated on a rotary evaporator. The residue was desiccated under high vacuum for 30 min to yield compound **90** as a colorless oil which spontaneously crystallized (74 mg, 35% over two steps). Two diastereomers **A**:**B**. ^1H NMR (d-chloroform, δ): **A** 7.32-7.39 (m, 5H, H12+H13+H14), 7.06 (d, $J=8.2\text{Hz}$, 2H, H10), 7.00 (d, $J=8.2\text{Hz}$, 2H, H9), 6.14 (ddd, $J=10.4, 3.9, 3.1\text{Hz}$, 1H, H3), 5.82 (dd, $J=10.4, 1.2\text{Hz}$, 1H, H4), 5.16 (m, 1H, H2), 3.75 (d, $J=10.3\text{Hz}$, 1H, H8), 3.69 (s, 3H, H15), 3.68 (dd, $J=14.5, 5.6\text{Hz}$, 1H, H6), 3.56 (m, 1H, H5), 3.16 (dd, $J=14.5, 11.0\text{Hz}$, 1H, H6'), 2.39 (s, 3H, H11). **B** 7.72 (d, $J=8.2\text{Hz}$, 2H, H9), 7.32-7.39 (m, 5H, H12+H13+H14), 7.32 (buried, 2H, H10), 5.85 (ddd, $J=10.4, 3.6, 3.0\text{Hz}$, 1H, H3), 5.64 (dd, $J=10.4, 1.1\text{Hz}$, 1H, H4), 5.12 (m, 1H, H2), 3.93 (d, $J=8.7\text{Hz}$, 1H, H8), 3.90 (dd, $J=14.6, 11.0\text{Hz}$, 1H, H6), 3.61 (s, 3H, H15), 3.11 (m, 1H, H5), 2.75 (dd, $J=14.6, 5.7\text{Hz}$, 1H, H6'), 2.44 (s, 3H, H11). ^{13}C NMR (d-chloroform, δ): **A** 171.6 (Ester CO), 144.2 (C9a), 135.4 (C10a), 135.1 (C12a), 129.9 (C3), 129.7 (C10), 129.1 (C12), 128.8 (C13), 128.2 (C14), 127.7 (C9), 122.0 (C4), 118.2 (CN), 55.5 (C8), 53.7 (C2), 52.6 (C15), 40.5 (C6), 25.0 (C5), 21.6 (C11). **B** 171.4 (Ester CO), 144.5 (C9a), 136.9 (C10a), 133.7 (C12a), 130.0 (C10), 129.3 (C12), 129.0 (C13), 128.9 (C3), 128.6 (C14), 127.3 (C9), 121.9 (C4), 117.9 (CN), 56.5 (C8), 54.4 (C2), 52.4 (C15), 40.7 (C6), 24.9 (C5), 21.7 (C11). ESI-MS: obs'd (%), calc'd (%), ppm, $(\text{M}+\text{H})^+$: 411.1375 (100), 411.1373 (100), 0.5.

Single crystal X-ray diffraction experimental details

A single crystal of **79A** or **87A** was coated with Paratone oil and mounted on a MiTeGen MicroLoop. The X-ray intensity data were measured on a Bruker Kappa APEXII CCD

system equipped with a Incoatec Microfocus I μ S (Cu K α , $\lambda = 1.54178 \text{ \AA}$) and a multi-layer mirror monochromator.

The frames were integrated with the Bruker SAINT software package¹⁹ using a narrow-frame algorithm. Data were corrected for absorption effects using the Multi-Scan method (SADABS).¹⁹ The structure was solved and refined using the Bruker SHELXTL Software Package²⁰ within APEX3¹⁹ and OLEX2.²¹ Non-hydrogen atoms were refined anisotropically. The B-H hydrogen atom was located in the diffraction map and refined isotropically, as were H10 and H11. All other hydrogen atoms were placed in geometrically calculated positions with $U_{iso} = 1.2U_{equiv}$ of the parent atom ($U_{iso} = 1.5U_{equiv}$ for methyl).

Table 5.1: Crystal Data for **79A** and **87A**

	79A	87A
Chemical formula	C ₁₆ H ₁₉ NO ₃	C ₃₃ H ₄₂ BN ₈ O ₅ PSW
FW (g/mol)	273.32	888.43
T (K)	100(2)	100(2)
λ (Å)	1.54178	1.54178
Crystal size (mm)	0.076 x 0.081 x 0.422	0.036 x 0.037 x 0.066
Crystal habit	colorless rod	colorless plate
Crystal system	monoclinic	monoclinic
Space group	C 2/c	P 2 ₁ /n
a (Å)	22.6503(8)	10.2965(3)
b (Å)	5.8701(2)	11.9839(4)
c (Å)	21.6027(8)	29.0679(10)
α (°)	90	90
β (°)	96.692(3)	92.732(2)
γ (°)	90	90
V (Å³)	2852.72(18)	3582.7(2)
Z	8	4
ρ_{calc} (g/cm³)	1.273	1.647
μ (mm⁻¹)	0.711	7.379
θ range (°)	3.93 to 68.30	3.04 to 68.30
Index ranges	-27 ≤ h ≤ 27 -7 ≤ k ≤ 7 -23 ≤ l ≤ 26	-12 ≤ h ≤ 12 -14 ≤ k ≤ 14 -34 ≤ l ≤ 34
Reflns coll.	11322	28057
Ind. reflns	2596 [R _{int} = 0.0569]	6568 [R _{int} = 0.0580]
Data / restraints / parameters	2596 / 0 / 183	6568 / 0 / 468
Goodness-of-fit on F²	1.047	1.021
R₁ [I > 2σ(I)]	0.0382	0.0322
wR₂ [all data]	0.1003	0.0801

References

- (1) Vitaku, E.; Smith, D. T.; Njardarson, J. T. *Journal of Medicinal Chemistry* **2014**, *57*, 10257.
- (2) Swanson, J. M.; McBurnett, K.; Christian, D. L.; Wigal, T. In *Advances in Clinical Child Psychology*; Ollendick, T. H., Prinz, R. J., Eds.; Springer US: Boston, MA, 1995, p 265.
- (3) Froimowitz, M.; Gu, Y.; Dakin, L. A.; Nagafuji, P. M.; Kelley, C. J.; Parrish, D.; Deschamps, J. R.; Janowsky, A. *Journal of Medicinal Chemistry* **2007**, *50*, 219.
- (4) Deutsch, H. M.; Shi, Q.; Gruszecka-Kowalik, E.; Schweri, M. M. *Journal of Medicinal Chemistry* **1996**, *39*, 1201.
- (5) Misra, M.; Shi, Q.; Ye, X.; Gruszecka-Kowalik, E.; Bu, W.; Liu, Z.; Schweri, M. M.; Deutsch, H. M.; Venanzi, C. A. *Bioorganic & Medicinal Chemistry* **2010**, *18*, 7221.
- (6) Ojo, B. *Synthetic Communications* **2012**, *42*, 1731.
- (7) Harrison, D. P.; Sabat, M.; Myers, W. H.; Harman, W. D. *Journal of the American Chemical Society* **2010**, *132*, 17282.
- (8) Harrison, D. P.; Iovan, D. A.; Myers, W. H.; Sabat, M.; Wang, S.; Zottig, V. E.; Harman, W. D. *Journal of the American Chemical Society* **2011**, *133*, 18378.
- (9) Harrison, D. P.; Welch, K. D.; Nichols-Nielander, A. C.; Sabat, M.; Myers, W. H.; Harman, W. D. *Journal of the American Chemical Society* **2008**, *130*, 16844.
- (10) Harrison, D. P.; Zottig, V. E.; Kosturko, G. W.; Welch, K. D.; Sabat, M.; Myers, W. H.; Harman, W. D. *Organometallics* **2009**, *28*, 5682.
- (11) Hartmann M., Panizzon L. US patent 2507631, **1950**.
- (12) Rometsch, R. US Patent 2,858,519, **1958**.

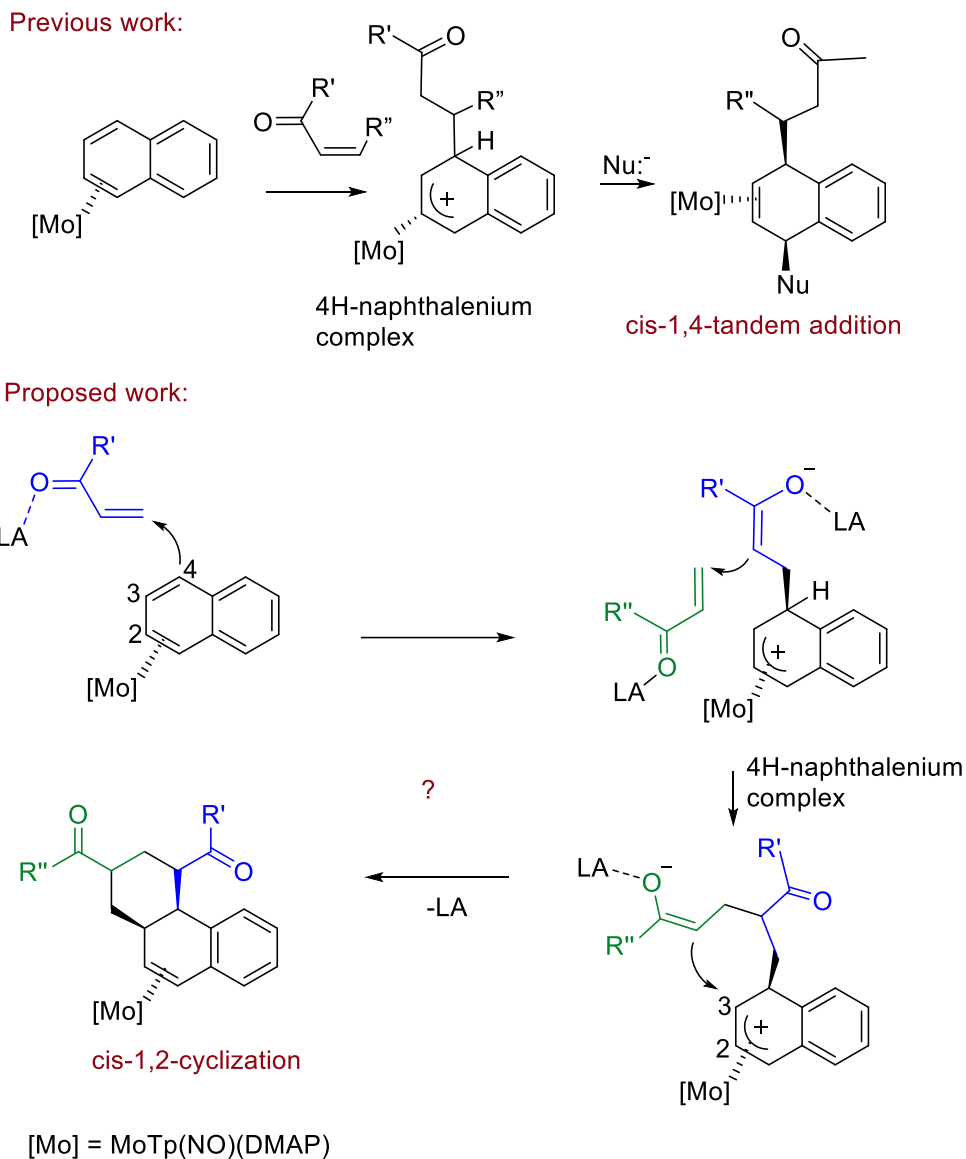
- (13) FERRIS, R. M.; TANG, F. L. M.; MAXWELL, R. A. *Journal of Pharmacology and Experimental Therapeutics* **1972**, *181*, 407.
- (14) Szporony, L.; Görög, P. *Biochemical Pharmacology* **1961**, *8*, 263.
- (15) Harrison, D. P.; Kosturko, G. W.; Ramdeen, V. M.; Nichols-Nielander, A. C.; Payne, S. J.; Sabat, M.; Myers, W. H.; Harman, W. D. *Organometallics* **2010**, *29*, 1909.
- (16) Kosturko, G. W.; Harrison, D. P.; Sabat, M.; Myers, W. H.; Harman, W. D. *Organometallics* **2009**, *28*, 387.
- (17) Atzrodt, J.; Derdau, V.; Kerr, W. J.; Reid, M. *Angewandte Chemie International Edition* **2018**, *57*, 1758.
- (18) Lankenau, A. W.; Iovan, D. A.; Pienkos, J. A.; Salomon, R. J.; Wang, S.; Harrison, D. P.; Myers, W. H.; Harman, W. D. *Journal of the American Chemical Society* **2015**, *137*, 3649.
- (19) Bruker, Saint; SADABS; APEX3. Inc., B. A., Ed. Madison, Wisconsin, USA, 2012.
- (20) Sheldrick, G., SHELXT - Integrated space-group and crystal-structure determination. *Acta Crystallographica Section A* 2015, *71* (1), 3-8.
- (21) Dolomanov, O. V.; Bourhis, L. J.; Gildea, R. J.; Howard, J. A. K.; Puschmann, H., OLEX2: a complete structure solution, refinement and analysis program. *Journal of Applied Crystallography* 2009, *42* (2), 339-341.

**Chapter 6: Michael-Michael-Ring-Closure Reactions for a Dihapto-Coordinated
Naphthalene Complex of Molybdenum**

Introduction

The Michael reaction, which involves enolate addition to an α,β -unsaturated carbonyl, is one of the most useful and well-recognized C-C bond forming reactions in organic synthesis.¹⁻³ Pioneering studies by Posner and others have explored a variant of this reaction where the enolate resulting from the conjugate addition undergoes a second Michael addition, and that resulting enolate terminates in a new six-membered ring.⁴ These so called Michael-Michael-Ring Closure (MIMIRC) reactions⁵⁻¹¹ are normally enolate-driven, but we questioned whether it would be possible to promote such a reaction sequence with an organometallic arene complex. We have a long-standing interest in promoting novel organic reactions of aromatic molecules through their dihapto-coordination,¹²⁻¹⁵ and have recently investigated the ability of the complex {MoTp(NO)(DMAP)} (DMAP = 4-(dimethylamino)pyridine; Tp = tris(pyrazolyl)borate) to dearomatize naphthalene via a 1,4-tandem addition reaction sequence (**Scheme 6.1**).¹⁶

¹⁷ We questioned whether this highly pi-basic metal complex was sufficiently electron-donating to promote a MIMIRC sequence, using this common aromatic hydrocarbon as the initial nucleophile (**Scheme 6.1**). Herein we describe our attempts to effect such reactions, both where the Michael acceptors are the same ($R' = R''$), and when they are different ($R' \neq R''$), using a Lewis acid to initiate the process.



Scheme 6.1. The proposed acid-promoted Michael-Michael-Ring-Closure (MIMIRC) sequence with an η^2 -coordinated naphthalene

Results

In order for the desired sequence to be successful, the molybdenum complex would have to sufficiently activate the naphthalene for the initial conjugate addition reaction at C4 (**Scheme 6.1**), and stabilize the 4H-naphthalenium product long enough for

the second enolate to close at C3. The complex MoTp(NO)(DMAP)(η^2 -naphthalene) (**91**) was prepared on a 10 g scale according to literature methods as a 3:1 mixture of coordination diastereomers by reducing MoTp(NO)(DMAP)(I) with magnesium or sodium in the presence of naphthalene.^{16, 17}

In an initial attempt to induce a MIMIRC reaction under neutral conditions, a 0.05 M solution of the naphthalene complex **91** and an excess of ethyl vinyl ketone (EVK) was stirred at 25 °C. Monitoring this reaction with cyclic voltammetry showed no change over several days. We next attempted to induce reactivity using various Lewis acids to activate the α,β -unsaturated carbonyl. The addition of either LiOTf or $\text{BF}_3 \cdot \text{OEt}_2$ yielded only free naphthalene after treatment with an oxidant (I_2 or air). However, treating a propionitrile solution of **91** and EVK (-60 °C) with TMSOTf generated a vivid red solution, indicative of a π -allyl complex of {MoTp(NO)(DMAP)}.¹⁷ After stirring for an additional hour, the solution was loaded onto an alumina column and compound **92** was isolated as a yellow solid (45%). In agreement with the 1,2-dihydronaphthalene complex of {MoTp(NO)(DMAP)},^{16, 17} a solution of compound **92** showed a chemically irreversible anodic wave with $E_{p,a} = +0.16$ V (100 mV/s; vs NHE), and IR absorbance data for this material included an peak corresponding to the Mo^0 -NO stretch at 1567 cm^{-1} . 2D NMR data for **92** (COSY, NOESY, HSQC, HMBC) were fully consistent with the proposed MIMIRC product, present as an 8:1 mixture of diastereomers.

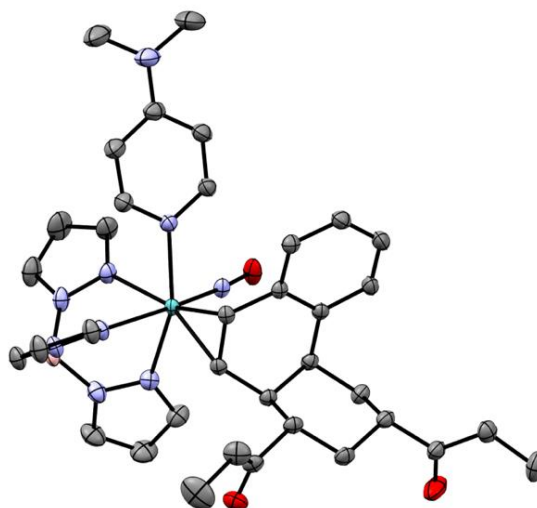
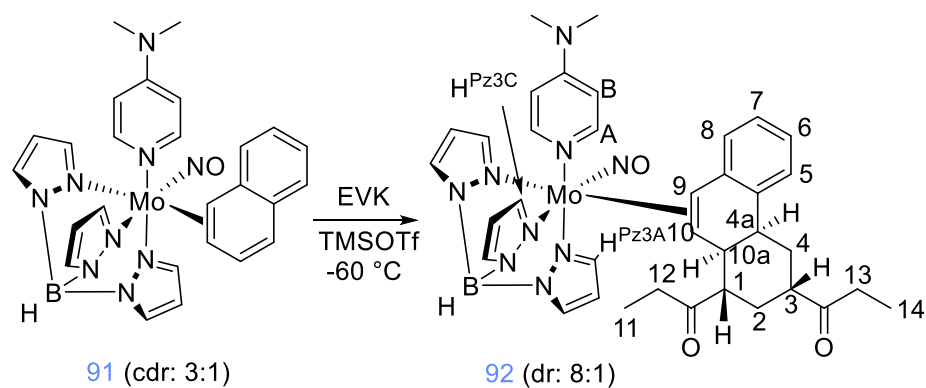
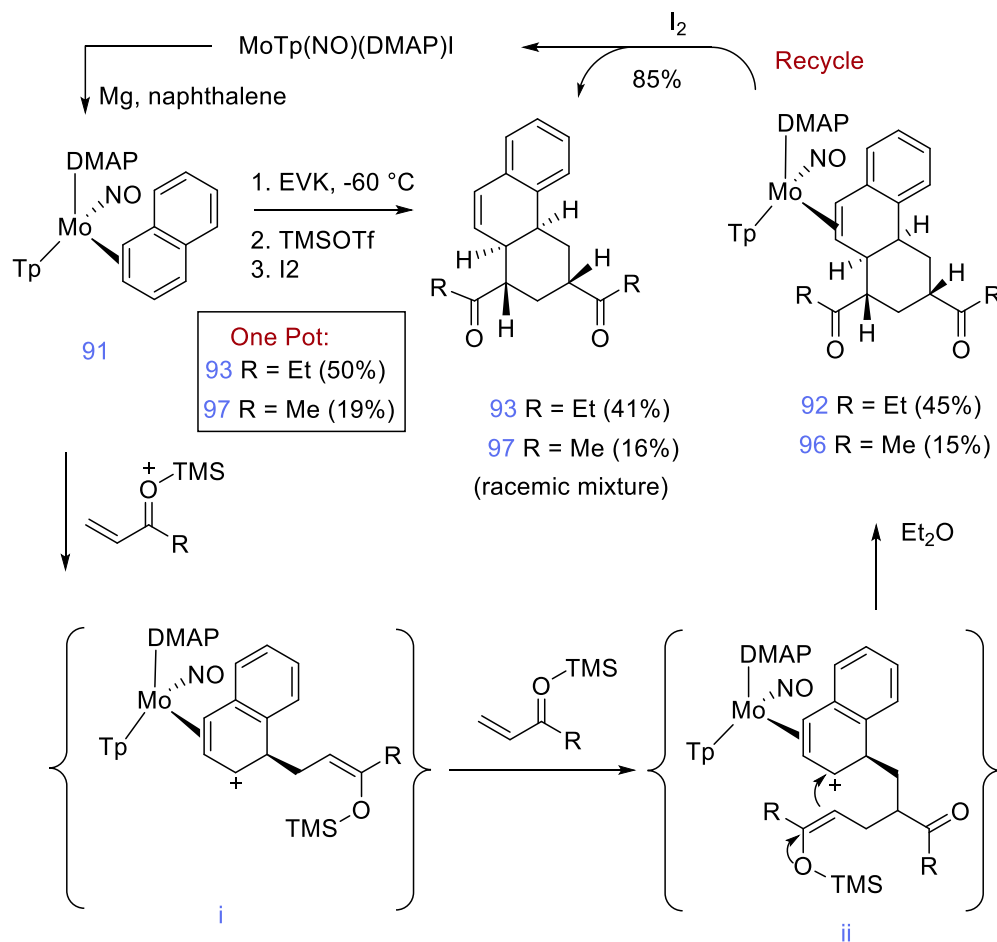


Figure 6.1: Synthesis, numbering scheme (major isomer; dr = 8:1), and ORTEP diagram of compound **92** (50% ellipsoidal probability)

We anticipated that the metal complex would control the stereochemistry of the additions to the naphthalene framework (C4a and C10a), with both electrophilic addition and nucleophilic addition occurring *anti* to metal coordination. However, two additional stereocenters alpha to the carbonyl groups (C1, C3) are also formed selectively. We speculate that the latter preference is a result of an acid-catalyzed epimerization of these carbons, occurring *after* the initial C-C bond-forming event. This epimerization, via enol intermediates, would allow the carbonyl groups to adopt equatorial positions, as shown in

Figure 6.1. This geometry was ultimately confirmed from XRD data. A detailed analysis of both XRD and NMR data for **92** is presented in the SI.

The MIMIRC sequence that rendered compound **92** is believed to take place by the mechanism shown in **Scheme 6.2**, wherein the α,β -unsaturated ketone is first activated via silylation of the carbonyl, followed by conjugate addition of the nucleophilic η^2 -naphthalene ligand of **91** to yield **i**. The resulting silylated enolate can then undergo a second conjugate addition with TMS-activated EVK (R = Et) to yield intermediate **ii**. In both intermediates **i** and **ii**, the η^2 -naphthalenium fragment is stabilized by molybdenum, forming a highly asymmetric π -allyl complex,¹⁷ which can serve as the electrophile in the final step of the annulation process (**Scheme 6.2**).



Scheme 6.2: Proposed mechanism of a Michael-Michael-Ring-Closure with EVK

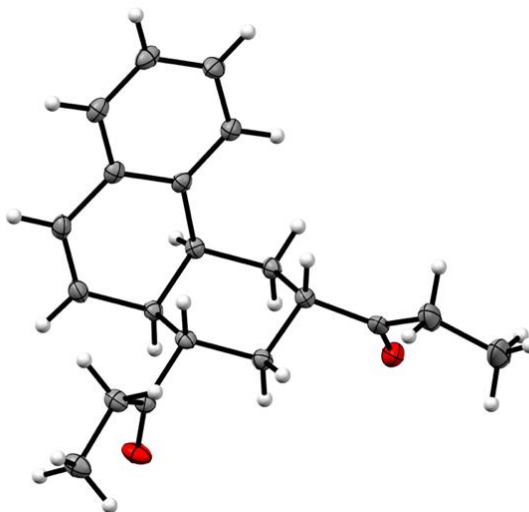


Figure 6.2: ORTEP diagram of compound **93** (50% ellipsoidal probability; H₂O omitted).

The optimization of the synthesis of **92** was carried out by running the reaction under various conditions (time, temperature, addition order, and concentration), then quenching any acidic species with an excess of TEA. The reaction mixture was then oxidized with iodine to liberate the desired product **93**. The inorganic material was removed via its precipitation from Et₂O, and the filtrate was condensed and analyzed by ¹H NMR. This analysis revealed that two substitution products (**94** and **95**, **Figure 6.3**)¹⁸ were often formed during the course of the reaction, in addition to free naphthalene and the desired product **93** (*vide infra*).

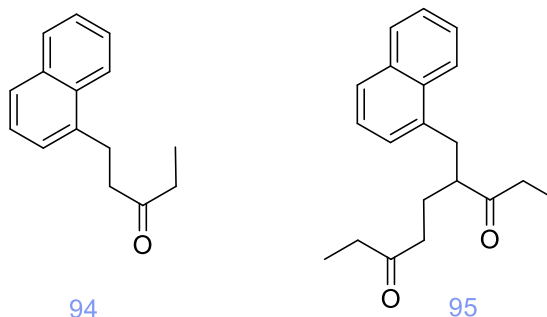


Figure 6.3: Side-products from the MIMIRC reaction

To confirm that the substituted naphthalene complexes **94**¹⁸ and **95**¹⁹ were formed during the initial reaction period and not formed from decomposition of the tricyclic **93**, or its molybdenum precursor **92**, an isolated sample of **93** was stirred under similar reaction conditions and monitored via ¹H NMR. The absence of **94** or **95** in this experiment indicates that these compounds are formed as a result of the silyl enolate intermediates **i** or **ii** reacting with an acidic impurity such as HOTf. With the reaction stalled, subsequent treatment with base effects the deprotonation of the purported allyl species to form naphthalenes **94** and **95**. To help mitigate adventitious proton sources, 2,6-di-*tert*-butylpyridine (DTBP) was added to the reaction mixture. With this addition, the formation of **94** and **95** was minimized and the isolated overall yield of **92** rose to 45% (77% per C-C bond formed).

With an optimized procedure developed, a variety of other ketone Michael acceptors (2-cyclopenten-1-one, 2-cyclohexen-1-one, 3-penten-2-one, 4-hexen-3-one, 3-methyl-3-buten-2-one) were screened to determine their compatibility with this procedure. Unfortunately, this MIMIRC sequence was found to be incompatible with further α -vinyl substitution or substitution at the β -position of the Michael acceptor. The additional bulk of even these sterically undemanding substituents apparently slows the

conjugate addition step significantly, with the result being that the metal is oxidized before the more robust allyl species can form. The reaction also fails with α,β -unsaturated esters (methyl acrylate, α -methylene- γ -butyrolactone). In these reactions, only the starting complex was recovered, indicating that the molybdenum backbonding into the naphthalene π^* orbital is not sufficient to make it a competent nucleophile for these less electrophilic α,β -unsaturated esters. However, replacement of EVK with methyl vinyl ketone (MVK) did yield the desired tricyclic **96**, albeit in low overall yield (15%). Suspecting that metal oxidation was primarily responsible for the low yield, the MVK and EVK addition reactions were attempted with a metal system established to be more resistant to oxidation, {Wtp(NO)(PMe₃)}.²⁰ Unfortunately, the tendency of this complex to protonate at C4 led only to the formation of the parent *4H*-naphthalenium species.²¹

With the isolation of the complexes **92** and **96**, the liberation of their hexahydrophenanthrene organic ligands was pursued. The oxidative decomplexation of the organic products directly from **92** and **96** was accomplished using iodine, yielding **93** and **97** in modest yields (**93**: 41% **97**: 16%), but with good recovery of the Mo(I) precursor, MoTp(NO)(DMAP)(I) (85% average yield). Ultimately SC-XRD data confirmed the identity of **3** (**Figure 6.2**). For this compound, a substantially higher *overall* yield (50% overall from **91** for 4 steps; average 84% per step; 200 mg final product) can be achieved via an iodine oxidation of the evaporated reaction mixture, thereby bypassing the isolation of **92**. These observations indicate that a significant amount of product remains in solution during precipitation of the MIMIRC product complex (**2**). A similar approach with **96** provided a one-pot yield of 19% for the MVK-derived compound **7** (19% for 4 steps; average 66% per step).

To further explore the promise of this method, A+B MIMIRC reactions from **91** were also investigated. Our approach was to stop the reaction at enolate **i** (**Scheme 6.2**) and then introduce the second Michael acceptor to complete the ring closure. This was attempted by limiting the initial Michael acceptor (e.g., EVK) to one molar equivalent to prevent a second addition from occurring. To a -60 °C propionitrile solution of **91**, either MVK or EVK was added (1.0 equivalent), along with DTBP and TMSOTf; after stirring at -60 °C for 1 minute, a solution of either MVK, cyclopentenone, or cyclohexenone was added, then the reaction mixture was left at -60 °C for 18 h.

The cleanest, highest yielding product of these A+B MIMIRC reactions was obtained when EVK was followed by MVK. This led to the isolation of the metal complex **98** in 30% yield. A solid-state structure of **98** was determined via single crystal x-ray diffraction (**Figure 6.4**). As expected, the structure of **98** again shows a 1,3-diequatorial geometry of the acyl groups. Also observed is the *cis* ring fusion consistent with the C-C bond forming reactions to naphthalene occurring *anti* to the metal center. Although the metal complex **98** can be isolated and oxidized, a higher mass recovery of the organic tricyclic **99** was accomplished by direct treatment of the reaction mixture with iodine. Compound **99** can be isolated from **91** in an *overall* yield of 15% (4 steps; 62%/step average). The remaining mass is assumed to be made up from substituted naphthalenes analogous to **94** and **95** (**Figure 6.3**), but these byproducts were not pursued.

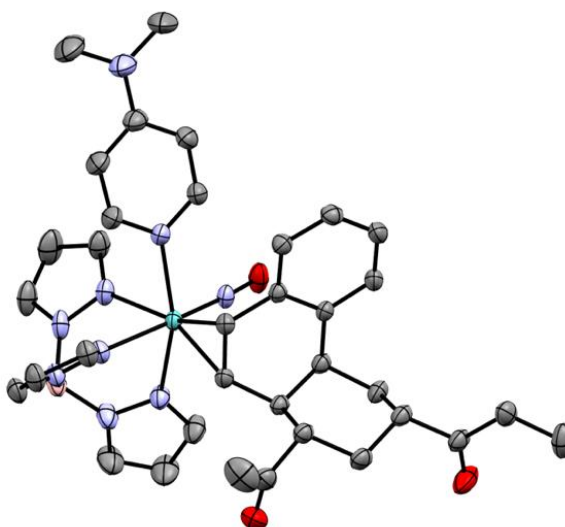
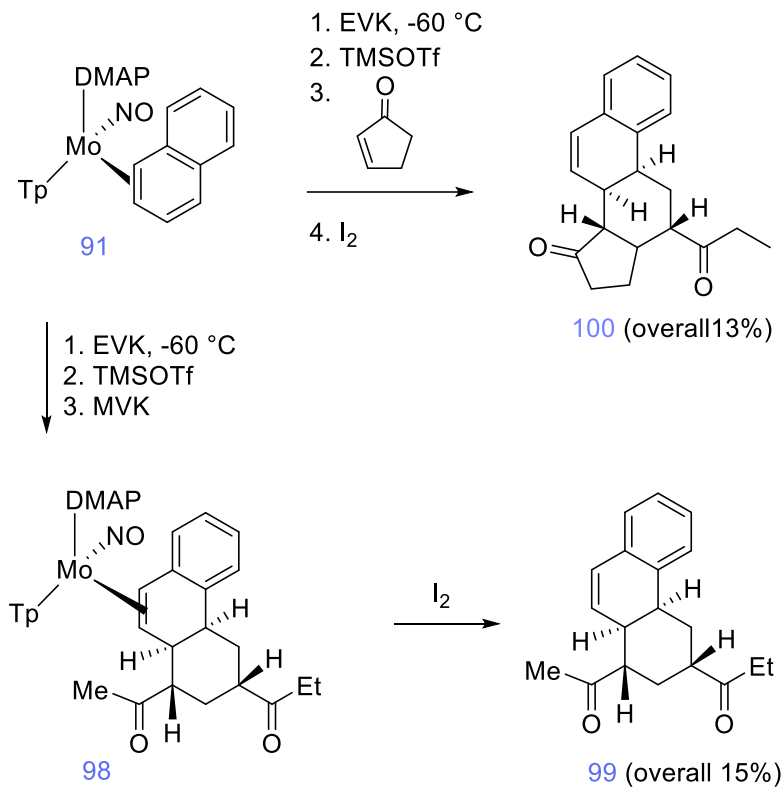


Figure 6.4: ORTEP diagram of **98** (50% ellipsoidal probability, co-crystallized THF molecule omitted for clarity)

The reaction sequence was then repeated using EVK as the first Michael acceptor and cyclopent-2-en-1-one as the second (**Scheme 6.3**). Flash chromatography resulted in isolation of compound **100** in 13% *overall* yield as a single isomer, along with ~6% impurity of **95**. While this yield is low, we note that it still represents an average yield per step (4) of 60%.



Scheme 6.3: [A+B] Michael-Michael ring closure reactions (products are formed as racemic mixtures)

A solid-state structure was determined from SC-XRD data (**Figure 6.5**). This structure confirms the presence of *cis*-BC and *cis*-CD ring fusions predicted by HNMR data (SI), the *trans* relationship between H8 and H14, and the equatorial orientations of both acyl groups.

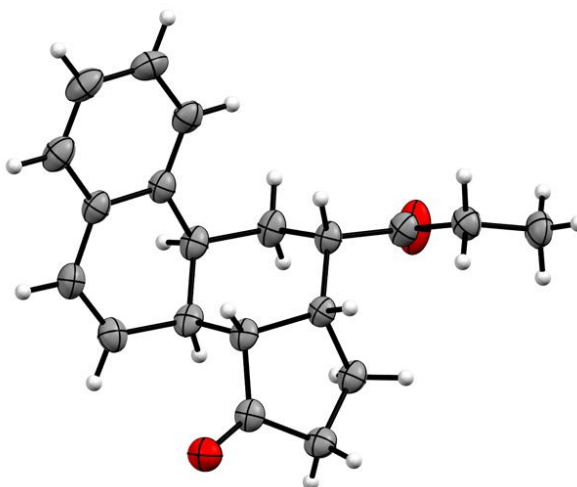


Figure 6.5: ORTEP diagram of **100** (50% ellipsoidal probability).

Discussion

We have on rare occasion observed unintentional [A+A] MIMIRC reactions with other π -basic metal complexes of aromatic molecules. These were cases in which the aromatic ligand possessed a π -donor substituent which enhanced its nucleophilicity. For example, $[\text{Os}(\text{NH}_3)_5(\eta^2\text{-dimethylaniline})]^{2+}$ undergoes a TBSOTf-promoted MIMIRC reaction with α -methylene- γ -butyrolactone to give a tetracyclic structure.²² Similarly, $\{\text{Os}(\text{NH}_3)_5(\eta^2\text{-2-methylfuran})\}^{2+}$ was shown to undergo MIMIRC reaction with furan and MVK, activated by boron trifluoride diethyl etherate ($\text{BF}_3 \cdot \text{OEt}_2$).²³ The resulting benzofuran skeleton was formed as a mixture of stereoisomers. Alternatively, $\text{ReTp}(\text{CO})(\text{MeIm})(\eta^2\text{-2-methoxynaphthalene})$ was found to undergo cyclization with methyl acrylate.²⁴ In this case the stereocenters set by the metal were lost once the organic was liberated due to an elimination of the methoxy group. In none of these cases was a systematic study performed, nor was an A+B MIMIRC cyclization achieved.

To our knowledge, only one other example of the synthesis of a steroidal core from naphthalene has been reported. Berndt *et al.*²⁵ closed a pendant cyclopentanone ring using samarium diiodide. The isolation of **100** demonstrates the potential of the MIMIRC method with dihapto-coordinated aromatics. While the overall yield is moderate, *five new stereocenters and three C-C bonds are selectively formed from naphthalene* and simple enones in a one-pot procedure with average yield per step of 60-84% (4 steps). Although a majority of naturally occurring steroidal cores have *trans*-BC and *trans*-CD ring fusions, steroidal cores with *cis*-fused BC rings have also attracted interest (I and II; **Figure 6.6**).²⁶⁻²⁹ Investigations have shown that I and II have an affinity for estrogen receptors while also providing osteoprotective action, a significant benefit for their use in hormone replacement therapy. Particularly noteworthy, a 2017 study found that compounds III and IV, which possess the same *cisB/C-anti-cisC/D* configuration as **100** were shown to be promising therapeutics for treatment of malaria.³⁰ Although this steroid configuration has not yet been widely studied, access to a library of such *cis-anti-cis* steroidal cores could provide insight into their potential as therapeutic agents. Furthermore, the compounds **93**, **97**, and **99** contain the same hexahydrophenanthrene core as compounds that have been studied for their efficacy as selective estrogen receptor-beta agonists.³¹ These hexahydrophenanthrenes also share a similar core with aromatic abietane diterpenoids (i.e., carnosic acid, ferruginol, and abietic acid), which have been studied for their antimicrobial and antibacterial properties.^{32,33}

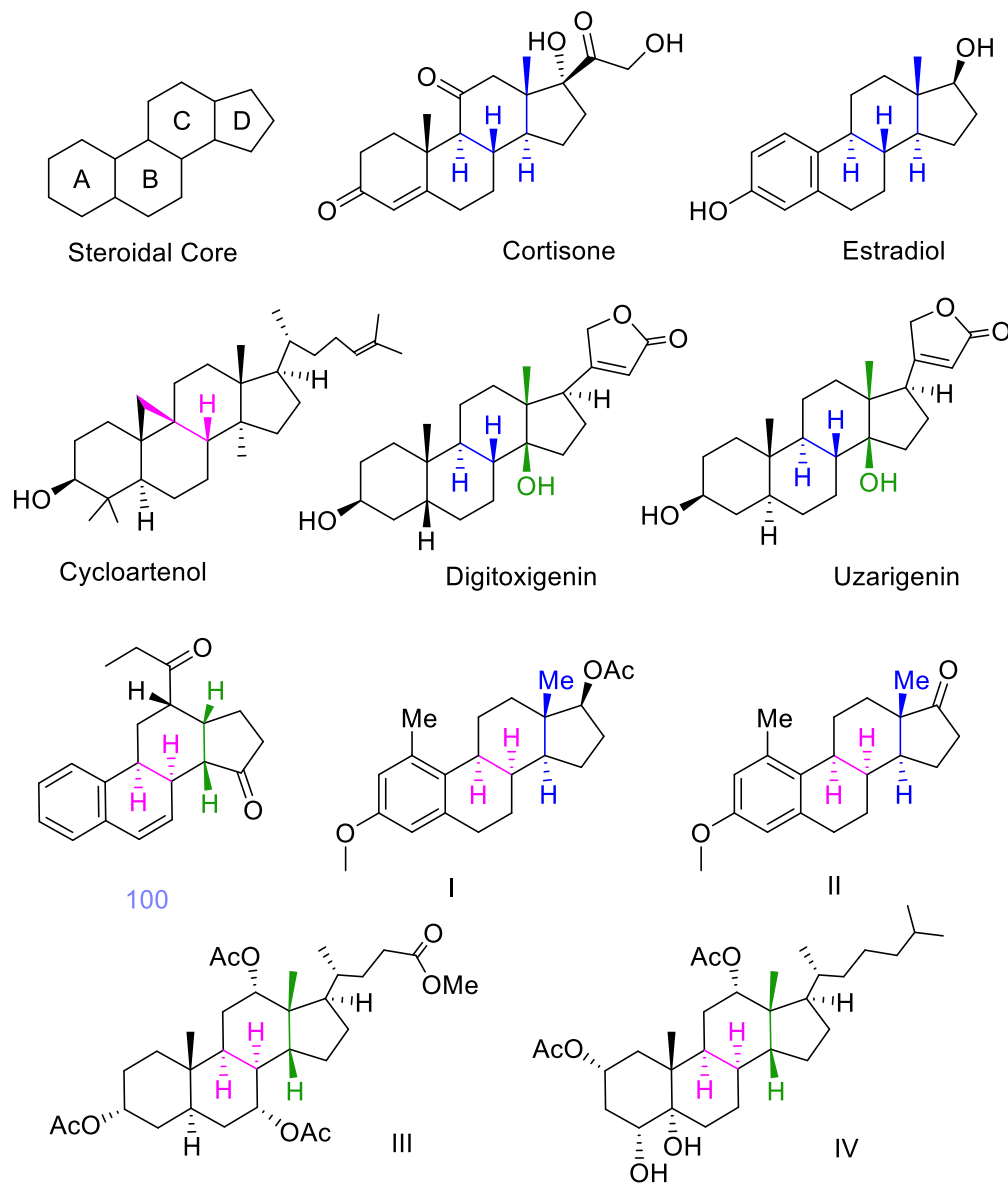


Figure 6.6: Examples of natural and unnatural steroid cores. Blue: *trans*-B/C and *trans*-C/D ring fusions (common); pink: *cis*-B/C ring fusion; green: *cis*-C/D ring fusion.

Finally, we note that because the molybdenum of **91** constitutes a stereogenic center, the potential exists to prepare enantioenriched variants of **93**, **97**, **99**, and **100**, as has been previously shown for molybdenum complexes of α,α,α -trifluorotoluene and 2-(trifluoromethyl)pyridine.^{34,35} Unfortunately, initial attempts to form an enantioenriched form of **1** through reduction of (*S*)-MoTp(NO)(DMAP)(I) in the presence of naphthalene

were unsuccessful, owing to the inability to achieve high enough concentrations of naphthalene to prevent racemization during the iodide/naphthalene exchange.^{34, 35}

Conclusion

Starting from the fully aromatic core of naphthalene, organic products with at least four new stereocenters and three new carbon-carbon bonds have been prepared and characterized. Tricyclic systems resulting from both [A+A] and [A+B] MIMIRC reactions has been carried out in a one-pot procedure with average yields ranging from 60-84% per step. The oxidative decomplexation step regenerates a molybdenum(I) species that is the immediate precursor to the naphthalene complex (**91**). While naphthylboronic acid has been shown to undergo conjugate addition with MVK,¹⁸ and **91** has previously been shown to react with enones,¹⁷ this report appears to describe the first examples of naphthalene participating in a MIMIRC reaction sequence for any metal.

Experimental Section

General Methods. NMR spectra were obtained on a 600 or 800 MHz spectrometer (22-25 °C). All chemical shifts are reported in ppm, and proton and carbon shifts are referenced to tetramethylsilane (TMS) utilizing residual ¹H or ¹³C signals of the deuterated solvents as an internal standard. Coupling constants (J) are reported in hertz (Hz). Infrared spectra (IR) were recorded as a glaze on a spectrometer fitted with a horizontal attenuated total reflectance (HATR) accessory or on a diamond anvil ATR assembly. Electrochemical experiments were performed under a nitrogen atmosphere. Cyclic voltammetry data were taken at ambient temperature (22-25 °C) at 100 mV/s in a standard three-electrode cell with a glassy carbon working electrode, N,N-

dimethylacetamide (DMA) or acetonitrile (MeCN) solvent, and tetrabutylammonium hexafluorophosphate (TBAH) electrolyte (approximately 0.5 M). All potentials are reported versus NHE (normal hydrogen electrode) using cobaltocenium hexafluorophosphate ($E_{1/2} = -0.78$ V), ferrocene ($E_{1/2} = +0.55$ V), or decamethylferrocene ($E_{1/2} = +0.04$ V) as an internal standard. The peak-to-peak separation was less than 100 mV for all reversible couples. Unless otherwise noted, all synthetic reactions were performed in a glovebox under a dry nitrogen atmosphere. Deuterated solvents were used as received. Pyrazole (Pz) protons of the (trispyrazolyl)borate (Tp) ligand were uniquely assigned (e.g., “Pz3B”) using a combination of two-dimensional NMR data and (dimethylamino)pyridine–proton NOE interactions. When unambiguous assignments were not possible, Tp protons were labeled as “Pz3/5 or Pz4”. All J values for Pz protons are 2 (± 0.2) Hz. BH ^1H NMR peaks (around 4–5 ppm) are not identified due to their quadrupole broadening; IR data are used to confirm the presence of a BH group (around 2500 cm^{-1}).

Synthesis of TpMo(NO)(DMAP)(η^2 -1,1'-((1S,3S,4aS,10aS)-1,2,3,4,4a,10a-hexahydrophenanthrene-1,3-diyl)bis(propan-1-one)) (92)

Compound **91** (400 mg, 0.679 mmol), $\text{CH}_3\text{CH}_2\text{CN}$ (15 mL), EVK (212 mg, 2.53 mmol), and DTBP (135 mg, 0.706 mmol) were added to a test tube. The reaction mixture was then cooled at $-60\text{ }^\circ\text{C}$ for 15 min. TMSOTf (275 mg, 1.24 mmol) was added to the reaction mixture, and the resulting red solution was left stirring at $-60\text{ }^\circ\text{C}$ for 1 h. The reaction mixture was loaded onto 30 mL of dry basic alumina in a 60 mL coarse porosity fritted disc. The product was eluted with 1:1 $\text{Et}_2\text{O}:\text{THF}$ (100 mL) as a yellow band, collected as a yellow solution, and evaporated *in vacuo*. The resulting oil was dissolved

in DCM (2 mL) and the product was precipitated in stirring pentane (100 mL). The precipitate was collected on a 15 mL fine porosity fritted disc, washed with pentane (3 x 10 mL), and dried for 1 h yielding the yellow solid **92** (230 mg, 45%). CV (DMAc) $E_{p,a} = +0.16$ V (NHE). IR: $\nu(\text{B-H}) = 2480$ cm^{-1} , $\nu(\text{CO}) = 1703$ and 1620 cm^{-1} , $\nu(\text{NO}) = 1562$ cm^{-1} . ^1H NMR (d^6 -Acetone, δ): 7.93 (1H, d, Pz5A), 7.87 (1H, d, Pz3A), 7.79 (1H, d, Pz5B), 7.69 (1H, d, Pz3C), 7.41 (2H, bs, DMAP-A), 7.35 (1H, d, $J = 7.9$, H5), 6.98 (1H, d, Pz3B), 6.93 (1H, t, $J = 7.5$, H6), 6.86 (1H, t, $J = 7.5$, H7), 6.51 (2H, m, DMAP-B), 6.37 (1H, t, Pz4A), 6.35 (1H, t, Pz4C), 6.21 (1H, d, $J = 7.2$, H8), 6.09 (1H, t, Pz4B), 3.73 (1H, m, H4a), 3.31 (1H, d, $J = 9.0$, H9), 3.06 (6H, s, NMe), 2.84 (1H, m, H4), 2.77 (1H, m, H10a), 2.65 (3H, m, H3, H1, & H13/12), 2.55 (1H, m, H13/H12), 2.40 (1H, m, H13/H12), 2.30 (1H, m, H13/12), 2.07 (1H, dd, $J = 9.0$ & 2.6 , H10), 1.87 (1H, m, H4), 1.70 (1H, m, H2), 1.52 (1H, q, $J = 12.4$, H2), 1.00 (3H, t, $J = 7.3$, H11/H14), 0.68 (3H, t, $J = 7.2$, H11/14). ^{13}C NMR (d^6 -Acetone, δ): 215.1 (CO), 213.8 (CO), 155.1 (DMAP-C), 150.7 (DMAP-A), 144.7 (Pz5), 143.6 (Pz3A), 142.1 (Pz3B), 141.2 (Pz3C), 137.6 (Pz5), 136.9 (Pz5), 135.8, 134.1, 128.1 (C8), 125.6 (C5), 125.1 (C7), 123.9 (C6), 108.3 (2C, DMAP-B), 106.9 (Pz4A/C), 106.8 (Pz4A/C), 106.5 (Pz4B), 70.9 (C10), 68.1 (C9), 55.0, 45.3, 43.1 (C10a), 39.3, 37.5, 35.9 (C4a), 34.3, 32.6 (C2), 31.0 (C4), 8.2 (C11/14), 7.8 (C11/14).

Synthesis of 1,1'-((1S,3S,4aS,10aS)-1,2,3,4,4a,10a-hexahydrophenanthrene-1,3-diyl)bis(propan-1-one) (93)

Compound **91** (400 mg, 0.679 mmol), $\text{CH}_3\text{CH}_2\text{CN}$ (15 mL), EVK (212 mg, 2.53 mmol), and DTBP (135 mg, 0.706 mmol) were added to a test tube. The reaction mixture was then cooled at -60 $^\circ\text{C}$ for 15 min. TMSOTf (275 mg, 1.24 mmol) was added to the

reaction mixture, and the resulting red solution was left stirring at $-60\text{ }^{\circ}\text{C}$ for 1 h. The reaction mixture was loaded onto 30 mL of dry basic alumina in a 60mL coarse porosity fritted disc. The product was eluted with 1:1 Et₂O:THF (100 mL) as a yellow band, collected as a yellow solution, and evaporated to dryness *in vacuo*. The residue was dissolved in DCM (15 mL), and to this solution was added a solution of I₂ (173 mg, 0.682 mmol) in Et₂O (5 mL). The vivid green solution was evaporated *in vacuo*. The residue was dissolved in DCM (3 mL) and added to stirring hexanes (100 mL). The green precipitate was filtered off on a 30 mL fine porosity fritted disc, and the filtrate was removed from the glovebox and evaporated onto SiO₂ *in vacuo*. The product was purified using Combiflash flash chromatography on 12 g SiO₂ column using EtOAc in hexanes. The product eluted at 15% EtOAc. The fractions containing the product were evaporated and desiccated to yield **93** as a colorless oil (200 mg, 50 %). IR: $\nu(\text{CO}) = 1702\text{ cm}^{-1}$. ¹H NMR (CDCl₃, δ): 7.28 (1H, d, $J = 7.3$, H5), 7.26 (1H, t, $J = 7.0$, H6/7), 7.21 (1H, t, $J = 7.0$, H6/7), 7.10 (1H, d, $J = 7.3$, H8), 6.45 (1H, d, $J = 9.6$, H9), 6.01 (1H, dd, $J = 9.6$ & 6.20, H10), 3.34 (1H, bs, H4a), 2.70 (2H, m, H3 & H4), 2.57 (1H, m, H10a), 2.55 (2H, m, H13), 2.42 (2H, m, H1 & H12), 2.27 (1H, dq, $J = 18.0$ & 7.3, H12), 1.85 (1H, m, H2), 1.80 (1H, m, H4), 1.43 (1H, m, H2), 1.09 (3H, t, $J = 7.4$, H14), 0.98 (3H, t, $J = 7.2$, H11). ¹³C NMR (CDCl₃, δ): 213.4 (CO), 213.2 (CO), 135.4 (C8a/4b), 134.2 (C8a/4b), 131.2 (C10), 128.2 (C9), 127.9 (C6/7), 127.1 (C8), 126.7 (C6/7), 124.8 (C4), 49.3 (C1), 44.4 (C3), 37.2 (C10a), 36.5 (C12), 35.9 (C4a), 34.0 (C13), 30.9 (C2), 27.8 (C4), 7.9 (C11/14), 7.6 (C11/14). EA: Calculated for C₂₀H₂₄O₂ • 0.25 CH₂Cl₂: C, 76.57; H, 7.77. Found: C, 76.50; H, 7.88.

Synthesis of TpMo(NO)(DMAP)(η^2 -1,1'-((1S,3S,4aS,10aS)-1,2,3,4,4a,10a-hexahydrophenanthrene-1,3-diyl)bis(ethan-1-one)) (96)

Compound **91** (400 mg, 0.679 mmol), CH₃CH₂CN (15 mL), MVK (177 mg, 2.53 mmol), and DTBP (135 mg, 0.706 mmol) were added to a test tube. The reaction mixture was then cooled at -60 °C for 15 min. TMSOTf (275 mg, 1.24 mmol) was added to the reaction mixture, and the resulting red solution was left stirring at -60 °C for 1 h. The reaction mixture was loaded onto 30 mL of dry basic alumina in a 60mL coarse porosity fritted disc. The product was eluted with 1:1 Et₂O:THF (100 mL) as a yellow band, collected as a yellow solution, and evaporated *in vacuo*. The resulting oil was dissolved in DCM (2 mL) and the product was precipitated in stirring pentane (100 mL). The precipitate was collected on a 15 mL fine porosity fritted disc, washed with pentane (3 x 10 mL), and dried for 1 h yielding the yellow solid **96** (74 mg, 15%). CV (DMAc) $E_{p,a} = +0.17$ V (NHE). IR: $\nu(\text{B-H}) = 2478$ cm⁻¹, $\nu(\text{CO}) = 1698$ and 1619 cm⁻¹, $\nu(\text{NO}) = 1562$ cm⁻¹. ¹H NMR (d⁶-Acetone, δ): 7.94 (1H, d, Pz5A/C), 7.91 (1H, d, Pz3A), 7.88 (1H, d, Pz5A/C), 7.78 (1H, d, Pz5B), 7.72 (1H, d Pz3C), 7.37 (2H, bs, DMAP-A), 7.34 (1H, d, $J = 7.5$, H5), 6.98 (1H, d, Pz3B), 6.94 (1H, td, $J = 7.5$ & 1.5, H6), 6.86 (1H, t, $J = 7.4$, H7), 6.50 (2H, m, DMAP-B), 6.36 (2H, m, Pz4A&C), 6.24 (1H, dd, $J = 7.6$ & 1.0, H8), 6.09 (1H, t, Pz4B), 3.79 (1H, m, H4a), 3.32 (1H, d, $J = 9.5$, H9), 3.05 (6H, s, NMe), 2.87 (1H, m, H4), 2.79 (1H, m, H10a), 2.59 (2H, m, H3 & H1), 2.19 (3H, s, H13), 2.14 (1H, dd, $J = 9.5$ & 2.5, H10), 1.89 (3H, s, H12), 1.86 (1H, m, H4), 1.77 (1H, m, H2), 1.52 (1H, q, $J = 12.6$, H2). ¹³C NMR (d⁶-Acetone, δ): 212.5 (CO), 211.0 (CO), 154.9 (DMAP-C), 151.1 (2C, DMAP-A), 144.6 (C4b/9a), 143.5 (Pz3A), 141.9 (Pz3B), 141.3 (Pz3C), 137.5 (Pz5A/C), 136.8 (Pz5A/C), 135.7 (Pz5B), 133.8 (C4b/9a), 128.0 (C8), 125.4 (C5), 124.9

(C7), 123.8 (C6), 108.1 (2C, DMAP-B), 106.9 (Pz4A/C), 106.6 (Pz4A/C), 106.3 (Pz4B), 70.4 (C10), 68.0 (C9), 55.9 (C1/3), 45.9 (C1/3), 42.7 (C10a), 39.1 (2C, DMAP-Me), 35.5 (C4a), 32.2 (C2), 30.7 (C4), 30.2 (C11), 28.1 (C12).

Synthesis of 1,1'-((1S,3S,4aS,10aS)-1,2,3,4,4a,10a-hexahydrophenanthrene-1,3-diyl)bis(ethan-1-one) (97)

Compound **91** (430 mg, 0.730 mmol), CH₃CH₂CN (24 mL), MVK (177 mg, 2.53 mmol), and DTBP (135 mg, 0.706 mmol) were added to a test tube. The reaction mixture was then cooled at -60 °C for 15 min. TMSOTf (275 mg, 1.24 mmol) was added to the reaction mixture, and the resulting red solution was left stirring at -60 °C for 1 h. The reaction mixture was loaded onto 30 mL of dry basic alumina in a 60mL coarse porosity fritted disc. The product was eluted with 1:1 Et₂O: THF (100 mL) as a yellow band, collected as a yellow solution, and evaporated to dryness *in vacuo*. The residue was dissolved in MeCN (15 mL), and to this solution was added a solution of I₂ (79 mg, 0.156 mmol) in Et₂O (5 mL). The yellow-green solution was evaporated *in vacuo*. The residue was dissolved in DCM (3 mL) and added to stirring hexanes (100 mL). The green precipitate was filtered off on a 30 mL fine porosity fritted disc, and the filtrate was removed from the glovebox and evaporated onto SiO₂ *in vacuo*. The product was purified using Combiflash flash chromatography on 12 g SiO₂ column using EtOAc in hexanes. The product eluted at 20% EtOAc. The fractions containing the product were evaporated *in vacuo* and desiccated to yield the colorless oil **97** (37 mg, 19% yield). IR: $\nu(\text{CO}) = 1701 \text{ cm}^{-1}$. ¹H NMR (CDCl₃, δ): 7.28 (1H, d, $J = 7.3$, H5), 7.27 (1H, m, H6/7), 7.22 (1H, m, H6/7), 7.10 (1H, d, $J = 7.3$, H8), 6.46 (1H, d, $J = 9.6$, H9), 1H, dd, $J = 9.6$ & 6.08, H10), 3.35 (1H, m, H4a), 2.73 (1H, m, H4), 2.70 (1H, m, H3), 2.54 (1H, m, H10a), 2.45

(1H, td, $J = 12.2$ & 3.5 , H1), 2.23 (3H, s, H13), 2.07 (3H, s, H12), 1.95 (1H, m, H2), 1.77 (1H, m, H4), 1.42 (1H, q, $J = 12.3$, H2). ^{13}C NMR (CDCl_3 , δ): 210.8 (CO), 210.6 (CO), 135.3 (C9a/4b), 134.2 (C9a/4b), 131.2 (C10), 128.2 (C9), 128.0 (C6/7), 127.1 (C8), 126.8 (C6/7), 124.8 (C5), 50.2 (C1), 45.3 (C3), 37.0 (C10a), 35.9 (C4a), 30.5 (C2), 30.2 (C11), 28.2 (C12), 27.7 (C4).

Synthesis of TpMo(NO)(DMAP)(η^2 -1-(((1S,3S,4aS,10aS)-1-acetyl-1,2,3,4,4a,10a-hexahydrophenanthren-3-yl)propan-1-one)) (98)

Compound **91** (200 mg, 0.34 mmol), $\text{CH}_3\text{CH}_2\text{CN}$ (6 mL), EVK (33 mg, 0.4 mmol), and DTBP (54 mg, 0.3 mmol) were added to a test tube. The reaction mixture was then cooled at -60 °C for 15 min. TMSOTf (0.1 mL, 0.5 mmol) was added to the reaction mixture, and the resulting red solution was stirred at -60 °C for 1 minute. MVK (50 mg, 0.7 mmol) was added to the reaction mixture, which was then stirred at -60 °C for 18 h. The reaction mixture was loaded onto 30 mL of dry silica in a 60mL coarse porosity fritted disc. The product was eluted with Et_2O (50 mL) as a yellow band, collected as a yellow solution, and evaporated to dryness *in vacuo*. The resulting oil was dissolved in DCM (1 mL) and the product was precipitated in stirring pentane (50 mL). The precipitate was collected on a 15 mL fine porosity fritted disc, washed with pentane (3 x 10 mL), and dried for 1 h yielding the yellow solid **98** (77 mg, 30%). CV (DMAc) $E_{p,a} = +0.16$ V (NHE). IR: $\nu(\text{B-H } sp^2) = 2474$ cm^{-1} , $\nu(\text{CO}) = 1702$ & 1618 cm^{-1} , $\nu(\text{NO}) = 1561$ cm^{-1} . ^1H NMR (d^6 -Acetone, δ): 7.94 (1H, d, Pz5A/C), 7.91 (1H, d, Pz3A), 7.88 (1H, d, Pz5A/C), 7.78 (1H, d, Pz5B), 7.72 (1H, d, Pz3C), 7.37 (2H, bs, DMAP-A), 7.35 (1H, d, $J = 7.4$, H5), 7.00 (1H, d, Pz3B), 6.94 (1H, t, $J = 7.4$, H6), 6.86 (1H, t, $J = 7.5$, H7), 6.51 (2H, m, DMAP-B), 6.37 (1H, t, Pz4A/C), 6.36 (1H, t, Pz4A/C), 6.21 (1H, d, $J = 7.5$, H8),

6.09 (1H, t, Pz4B), 3.78 (1H, m, H4a), 3.31 (1H, d, $J = 9.5$, H9), 3.05 (6H, s, N-Me), 2.83 (1H, m, H4), 2.79 (1H, ddd, $J = 10.6, 5.1, 2.4$, H10a), 2.63 (2H, m, H3 & H12), 2.56 (2H, m, H1 & H12), 2.14 (1H, dd, $J = 9.5, 2.5$, H10), 1.88 (3H, s, H11), 1.74 (1H, d, $J = 12.7$, H2), 1.55 (1H, q, $J = 12.7$, H2), 1.01 (3H, t, $J = 7.3$, H13). ^{13}C NMR (d^6 -Acetone, δ): 213.7 (CO), 212.5 (CO), 155.11 (DMAP-C), 150.7 (2C, DMAP-A), 144.7 (C4b/9a), 143.6 (Pz3A), 142.1 (Pz3B), 141.4 (Pz3C), 137.6 (Pz5A/C), 137.0 (Pz5A/C), 135.8 (Pz5B), 133.9 (C4b/9a), 128.2 (C8), 125.6 (C5), 125.1 (C7), 123.9 (C6), 108.3 (2C, DMAP-B), 107.0 (Pz4A/C), 106.7 (Pz4A/C), 106.5 (Pz4B), 70.6 (C10), 68.2 (C9), 56.2 (C1), 45.2 (C3), 42.9 (C10a), 39.3 (2C, DMAP-Me), 35.7 (C4a), 34.4 (C12), 32.4 (C2), 31.0 (C4), 8.24 (C13).

Synthesis of 1-((1S,3S,4aS,10aS)-1-acetyl-1,2,3,4,4a,10a-hexahydrophenanthren-3-yl)propan-1-one (99)

Compound **91** (430 mg, 0.730 mmol), $\text{CH}_3\text{CH}_2\text{CN}$ (24 mL), EVK (66 mg, 0.784 mmol), and DTBP (135 mg, 0.706 mmol) were added to a test tube. The reaction mixture was then cooled at $-60\text{ }^\circ\text{C}$ for 15 min. TMSOTf (275 mg, 1.24 mmol) was added to the reaction mixture, and the resulting red solution was stirred at $-60\text{ }^\circ\text{C}$ for 1 minute. MVK (255 mg, 3.64 mmol) was added to the reaction mixture, which was then stirred at $-60\text{ }^\circ\text{C}$ for 1 h. The reaction mixture was loaded onto 30 mL of dry basic alumina in a 60mL coarse porosity fritted disc. The product was eluted with MeCN (40 mL) as a yellow band, collected as a yellow solution, and evaporated to dryness *in vacuo*. The residue was dissolved in MeCN (15 mL), and to this solution was added a solution of I_2 (79 mg, 0.156 mmol) in Et_2O (5 mL). The solution was evaporated *in vacuo*. The residue was dissolved in DCM (3 mL) and added to stirring hexanes (100 mL). The brown precipitate

was filtered off on a 30 mL fine porosity fritted disc, and the filtrate was removed from the glovebox and evaporated onto SiO₂ *in vacuo*. The product was purified using Combiflash flash chromatography on 12 g SiO₂ column using EtOAc in hexanes. The product eluted at 18% EtOAc. The fractions containing the product were evaporated *in vacuo* and desiccated to yield the colorless oil **99** (27 mg, 13% yield). IR: $\nu(\text{CO}) = 1702 \text{ cm}^{-1}$. ¹H NMR (CDCl₃, δ): 7.28 (1H, d, $J = 7.3$, H5), 7.26 (1H, t, $J = 7.3$, H6), 7.21 (1H, t, $J = 7.1$, H7), 7.09 (1H, d, $J = 7.2$, H8), 6.44 (1H, d, $J = 9.6$, H10), 6.08 (1H, dd, $J = 9.6$ & 5.9, H9), 3.34 (1H, bs, H4a), 2.70 (2H, m, H3 & H4), 2.58 (1H, m, H10a), 2.53 (2H, q, H12), 2.42 (1H, m, H1), 2.06 (3H, s, H11), 1.92 (1H, m, H2), 1.78 (1H, m, H4), 1.43 (1H, m, H2), 1.09 (3H, t, $J = 7.3$, H13). ¹³C NMR (CDCl₃, δ): 213.2 (CO), 210.8 (CO), 135.4 (C4b/9a), 134.2 (C4b/9a), 131.2 (C9), 128.1 (C10), 127.9 (C6/7), 127.1 (C8), 126.1 (C6/7), 124.8 (C5), 50.3 (C1), 44.4 (C3), 36.9 (C10a), 35.9 (C4a), 34.1 (C12), 30.6 (C2), 30.1 (C11), 27.9 (C4), 7.9 (C13).

Synthesis of (8*S*,9*S*,12*S*,13*S*,14*S*)-12-propionyl-8,9,11,12,13,14,16,17-octahydro-15*H*-cyclopenta[*a*]phenanthren-15-one (100)

Compound **91** (398 mg, 0.676 mmol), CH₃CH₂CN (22 mL), EVK (55 mg, 0.654 mmol), and DTBP (110 mg, 0.575 mmol) were added to a test tube. The reaction mixture was then cooled at -60 °C for 15 min. TMSOTf (275 mg, 1.24 mmol) was added to the reaction mixture, and the resulting red solution was stirred at -60 °C for 1 minute. 2-cyclopenten-1-one (294 mg, 3.58 mmol) was added to the reaction mixture, which was then stirred at -60 °C for 18 h. The reaction mixture was loaded onto 30 mL of dry basic alumina in a 60mL coarse porosity fritted disc. The product was eluted with MeCN (50 mL) as a yellow band, collected as a yellow solution, and evaporated to dryness *in vacuo*.

The residue was dissolved in MeCN (15 mL), and to this solution was added a solution of I₂ (79 mg, 0.156 mmol) in Et₂O (5 mL). The solution was evaporated *in vacuo*. The residue was dissolved in DCM (3 mL) and added to stirring hexanes (100 mL). The brown precipitate was filtered off on a 30 mL fine porosity fritted disc, and the filtrate was removed from the glovebox and evaporated onto SiO₂ *in vacuo*. The product was purified using Combiflash flash chromatography on 12 g SiO₂ column using EtOAc in hexanes. The product eluted at 25% EtOAc. The fractions containing the product were evaporated *in vacuo* and desiccated to yield the colorless oil **100** (27 mg, 13% yield). IR: $\nu(\text{C-H sp}^2) = 2932 \text{ cm}^{-1}$, $\nu(\text{CO}) = 1731 \text{ and } 1703 \text{ cm}^{-1}$. ¹H NMR (CDCl₃, δ): 7.22 (3H, m, H1, H2, & H3), 7.11 (1H, d, $J = 7.3$, H4), 6.58 (1H, d, $J = 9.6$, H6), 6.15 (1H, dd, $J = 9.6$ & 6.2, H7), 3.27 (1H, m, H9), 3.11 (1H, dt, $J = 13.0$ & 4.4, H12), 2.58 (2H, m, H13 & H18), 2.47 (3H, m, H11, H16, H18), 2.25 (1H, m, H8), 2.17 (2H, m, H11 & H16), 2.06 (1H, dd, $J = 12.2$ & 6.7, H14), 1.97 (1H, m, H17), 1.69 (1H, m, H17), 1.10 (3H, t, $J = 7.2$, H19). ¹³C NMR (CDCl₃, δ): 218.5 (CO), 212.5 (CO), 134.6 (C5/10), 134.3 (C5/10), 130.6 (C7), 128.7 (C6), 127.9 (C2/3), 127.2 (C4), 126.8 (C2/3), 124.9 (C1), 51.1 (C14), 43.8 (C12), 37.9 (C13), 37.1 (C16), 35.2 (C9), 34.5 (C18), 30.8 (C8), 21.2 (C11), 21.0 (C17), 7.9 (C19). EA: Calculated for C₂₀H₂₂O₂ • 0.25 EtOAc: C, 79.14; H, 7.68. Found: C, 78.96; H, 7.51.

Table 6.1: Coupling constants for **100** where H13 is *cis* to H14 and H12

H13 <i>cis</i> to H14 and H12			
Protons Considered	Dihedral Angle (°)	Dihedral Angle (rad)	Coupling Constant (Hz)
H14 H8	160	2.72	11.66
H14 H13	34	0.578	7.02
H13 H12	46	0.782	5.03
H12 H11 _{syn}	62	1.054	2.44
H12 H11 _{anti}	177	3.009	13.76

Table 6.2: Coupling constants for **10** where H13 is *trans* to H14 and H12

H13 <i>trans</i> to H14 and H12			
Protons Considered	Dihedral Angle (°)	Dihedral Angle (rad)	Coupling Constant (Hz)
H14 H8	179	3.043	13.86
H14 H13	171	2.907	13.24
H13 H12	176	2.992	13.69
H12 H11 _{syn}	61	1.037	2.59
H12 H11 _{anti}	176	2.992	13.69

Table 6.3: Comparison of predicted and measured dihedral angles for **100**

H13 <i>cis</i> to H14 and H12		
Protons Considered	Predicted Dihedral Angle (°)	Observed Dihedral Angle (°)
H14 H8	160	165
H14 H13	34	37
H13 H12	46	44.5
H12 H11 _{syn}	62	54
H12 H11 _{anti}	177	171

Single crystal X-ray diffraction experimental details

Single crystals of **92**, **93**, **98** and **100** were coated with Paratone oil and mounted on a MiTeGen MicroLoop. The X-ray intensity data were measured on a Bruker Kappa APEXII Duo system. A graphite monochromator and a Mo K α fine-focus sealed tube ($\lambda = 0.71073 \text{ \AA}$) were used for **92**, **93** and **98**. An Incoatec Microfocus I μ S (Cu K α , $\lambda = 1.54178 \text{ \AA}$) and a multilayer mirror monochromator were used for **100**. The frames were integrated with the Bruker SAINT software package³⁶ using a narrow-frame algorithm. Data were corrected for absorption effects using the Multi-Scan method (SADABS).³⁶ The structures were solved and refined using the Bruker SHELXTL Software Package³⁷ within APEX3³⁶ and OLEX2.³⁸ Non-hydrogen atoms were refined anisotropically. The B-H hydrogen atoms in **92** and **98** and the O-H hydrogen atoms in **93** were located in the diffraction map and refined isotropically. All other hydrogen atoms were placed in geometrically calculated positions with $U_{iso} = 1.2U_{equiv}$ of the parent atom ($U_{iso} = 1.5U_{equiv}$ for methyl). One THF molecule in **92** was found to be severely disordered and could not be adequately modeled with or without restraints. Thus, the structure factors were modified using the PLATON SQUEEZE³⁹ technique, in order to produce a “solvate-free” structure factor set. PLATON reported a total electron density of 166 e⁻ and total solvent accessible volume of 717 Å³. In **93**, the occupancy of the partially-occupied water site was freely refined with no constraints or restraints on the disordered

atoms. In **98**, the relatively occupancy of the two positions of the disordered THF molecule was freely refined, with restraints on the bond lengths and anisotropic displacement parameters of the disordered atoms.

Table 6.4: Crystal Data for the X-ray diffraction structures **92**, **93**, **98** and **100**

	92	93	98	100
CCDC	1976642	1976643	1976644	1976645
Chemical formula	C ₄₀ H ₅₂ BMoN ₉ O ₄	C ₄₀ H _{48.64} O _{4.32}	C ₄₃ H ₅₈ BMoN ₉ O ₅	C ₂₀ H ₂₂ O ₂
FW (g/mol)	829.65	598.54	887.73	294.37
T (K)	153(2)	100(2)	153(2)	100(2)
λ (Å)	0.71073	0.71073	0.71073	1.54178
Crystal size (mm)	0.36 x 0.38 x 0.44	0.075 x 0.284 x 0.370	0.22 x 0.23 x 0.35	0.074 x 0.075 x 0.586
Crystal habit	yellow block	colorless rod	yellow needle	colorless needle
Crystal system	monoclinic	monoclinic	monoclinic	monoclinic
Space group	P 2 ₁ /n	C 2/c	P 2 ₁ /c	P 2 ₁ /n
a (Å)	10.0056(11)	35.692(5)	9.7891(17)	9.8451(7)
b (Å)	19.620(2)	6.2580(10)	19.700(4)	8.2499(7)
c (Å)	23.515(3)	15.140(2)	23.471(4)	19.2811(15)
α (°)	90	90	90	90
β (°)	101.948(2)	100.451(4)	99.409(3)	93.492(5)
γ (°)	90	90	90	90
V (Å³)	4516.2(9)	3325.6(9)	4465.4(14)	1563.1(2)
Z	4	4	4	4
ρ_{calc} (g/cm³)	1.220	1.195	1.320	1.251
μ (mm⁻¹)	0.337	0.076	0.3474	0.619
θ range (°)	3.19 to 29.57	1.16 to 27.52	4.08 to 31.51	4.93 to 68.50
Index ranges	-13 ≤ h ≤ 13 -27 ≤ k ≤ 27 -32 ≤ l ≤ 32	-46 ≤ h ≤ 46 -8 ≤ k ≤ 8 -19 ≤ l ≤ 19	-14 ≤ h ≤ 14 -28 ≤ k ≤ 28 -34 ≤ l ≤ 34	-11 ≤ h ≤ 8 -9 ≤ k ≤ 9 -20 ≤ l ≤ 23
Reflns coll.	80528	29048	90723	13540
Ind. reflns	12641 [R(int) = 0.0237]	3830 [R(int) = 0.0452]	14818 [R(int) = 0.0318]	2865 [R(int) = 0.1634]
Data / restraints / parameters	12641 / 0 / 504	3830 / 0 / 211	14818 / 89 / 571	2865 / 0 / 200
Goodness-of-fit on F²	1.185	1.028	1.055	1.056
R₁ [I > 2σ(I)]	0.0371	0.0404	0.0486	0.0790
wR₂ [all data]	0.0885	0.1008	0.1345	0.2275

References

- (1) Boehm, M.; Lorthiois, E.; Meyyappan, M.; Vasella, A. *Helvetica Chimica Acta* **2003**, *86*, 3787-3817.
- (2) Cheng, W.; Wu, D.; Liu, Y. *Biomacromolecules* **2016**, *17*, 3115-3126.
- (3) Zhang, Y.; Wang, W. *Catalysis Science & Technology* **2012**, *2*, 42-53.
- (4) Little, R. D.; Masjedizadeh, M. R.; Wallquist, O.; McLoughlin, J. I. *Organic Reactions* **2004**, 315-552.
- (5) Genna, D. T.; Maio, W. A. *Tetrahedron* **2016**, *72*, 5956-5967.
- (6) Posner, G. H. *Chem. Rev.* **1986**, *86*, 831.
- (7) Posner, G. H.; Asirvatham, E. *Tetrahedron Letters* **1986**, *27*, 663-666.
- (8) Posner, G. H.; Lu, S.-B.; Asirvatham, E. *Tetrahedron Letters* **1986**, *27*, 659-662.
- (9) Posner, G. H.; Lu, S. B.; Asirvatham, E.; Silversmith, E. F.; Shulman, E. M. *J. Am. Chem. Soc.* **1986**, *108*, 511-512.
- (10) Posner, G. H.; Mallamo, J. P.; Black, A. Y. *Tetrahedron* **1981**, *37*, 3921-3926.
- (11) Posner, G. H.; Switzer, C. *J. Am. Chem. Soc.* **1986**, *108*, 1239-1244.
- (12) Liebov, B. K.; Harman, W. D. *Chemical Reviews* **2017**, *117*, 13721-13755.
- (13) Harman, W. D. *Chem. Rev.* **1997**, *97*, 1953-1978.
- (14) Keane, J. M.; Harman, W. D. *Organomet.* **2005**, *24*, 1786-1798.
- (15) Smith, P. L.; Chordia, M. D.; Harman, W. D. *Tetrahedron* **2001**, 8203-8225.

- (16) Myers, J. T.; Shivokevich, P. J.; Pienkos, J. A.; Sabat, M.; Myers, W. H.; Harman, W. D. *Organometallics* **2015**, *34*, 3648-3657.
- (17) Myers, J. T.; Dakermanji, S. J.; Chastanet, T. R.; Shivokevich, P. J.; Strausberg, L. J.; Sabat, M.; Myers, W. H.; Harman, W. D. *Organometallics* **2017**, *36*, 543-555.
- (18) Zhang, L.; Xie, X.; Fu, L.; Zhang, Z. *J. Org. Chem.* **2013**, *78*, 3434-3437.
- (19) Compounds **4** and **5** co-eluted. The structural identity of **5** is postulated based on the similarity of its HNMR resonances to those of the previously reported compound **4**. In addition to those signals characteristic of a 1-substituted naphthalene, **5** shows two triplets at 1.05 and 0.85 ppm.
- (20) Welch, K. D.; Harrison, D. P.; Lis, E. C.; Liu, W.; Salomon, R. J.; Harman, W. D.; Myers, W. H. *Organometallics* **2007**, *26*, 2791-2794.
- (21) Pienkos, J. A.; Zottig, V. E.; Iovan, D. A.; Li, M.; Harrison, D. P.; Sabat, M.; Salomon, R. J.; Strausberg, L.; Teran, V. A.; Myers, W. H.; Harman, W. D. *Organometallics* **2013**, *32*, 691-703.
- (22) Gonzalez, J.; Sabat, M.; Harman, W. D. *J. Am. Chem. Soc.* **1993**, *115*, 8857-8858.
- (23) Chen, H.; Liu, R.; Myers, W. H.; Harman, W. D. *J. Am. Chem. Soc.* **1998**, *120*, 509-520.
- (24) Ding, F.; Valahovic, M. T.; Keane, J. M.; Anstey, M. R.; Sabat, M.; Trindle, C. O.; Harman, W. D. *J. Org. Chem.* **2004**, *69*, 2257-2267.

- (25) Aulenta, F.; Berndt, M.; Brüdgam, I.; Hartl, H.; Sörgel, S.; Reißig, H.-U. *Chemistry – A European Journal* **2007**, *13*, 6047-6062.
- (26) Dauben, W. G.; Fullerton, D. S. *J. Org. Chem.* **1971**, *36*, 3277-3282.
- (27) Egorov, M. S.; Grinenko, E. V.; Zorina, A. D.; Balykina, L. V.; Selivanov, S. I.; Shavva, A. G. *Russian Journal of Organic Chemistry* **2001**, *37*, 802-810.
- (28) Morozkina, S. N.; Abusalimov, S. N.; Selivanov, S. I.; Shavva, A. G. *Russian Journal of Organic Chemistry* **2013**, *49*, 603-609.
- (29) Morozkina, S. N.; Abusalimov, S. N.; Starova, G. L.; Selivanov, S. I.; Shavva, A. G. *Russian Journal of General Chemistry* **2010**, *80*, 1324-1330.
- (30) Pavadai, E.; Kaur, G.; Wittlin, S.; Chibale, K. *MedChemComm* **2017**, *8*, 1152-1157.
- (31) Koehler, K. F.; Helguero, L. A.; Haldosén, L.-A.; Warner, M.; Gustafsson, J.-A. k. *Endocrine Reviews* **2005**, *26*, 465-478.
- (32) Gonzalez, M. A. *Natural Product Reports* **2015**, *32*, 684-704.
- (33) González, M. A. *European Journal of Medicinal Chemistry* **2014**, *87*, 834-842.
- (34) Shivokevich, P. J.; Myers, J. T.; Smith, J. A.; Pienkos, J. A.; Dakermanji, S. J.; Pert, E. K.; Welch, K. D.; Trindle, C. O.; Harman, W. D. *Organometallics* **2018**, *37*, 4446-4456.
- (35) Wilde, J. H.; Smith, J. A.; Dickie, D. A.; Harman, W. D. *J. Am. Chem. Soc.* **2019**, *141*, 18890-18899.

- (36) Bruker; Inc., B. A., Ed. Madison, Wisconsin, USA, 2012.
- (37) Sheldrick, G. *Acta Crystallographica Section A* **2015**, *71*, 3.
- (38) Dolomanov, O. V.; Bourhis, L. J.; Gildea, R. J.; Howard, J. A. K.; Puschmann, H. *Journal of Applied Crystallography* **2009**, *42*, 339.
- (39) Spek, A. *Acta Crystallographica Section C* **2015**, *71*, 9.

Chapter 7: Concluding Remarks

The initial goal of this research was to explore pyridine dearomatization with a second-row metal system, {MoTp(NO)(DMAP)}.¹⁻³ The $\eta^2/\kappa\text{N}$ equilibrium was of particular interest, as the similarity of a molybdenum complex to the established heavy metal analogs was uncertain in this regard.⁴ While the tungsten complex {Wtp(NO)(PMe₃)} has demonstrated organic chemistry with pyridine,⁵⁻⁹ it was unknown if molybdenum analogs would be amenable to isolation and subsequent synthetic manipulations. Due to weaker backbonding, dihapto coordinated ligands dissociate more readily from molybdenum than tungsten.¹⁰ A dihapto-coordinate molybdenum pyridine-borane complex was synthesized, however its sensitivity to oxidation made organic reactions impractical. A similar challenge was evident for pyridines bearing electron-donating groups.

Nevertheless, 2-(trifluoromethyl)pyridine, with its strong inductively-withdrawing substituent, proved very suitable for organic transformations. Methylation followed by nucleophilic addition yielded dihydropyridines. The second electrophilic, nucleophilic tandem addition was stymied by an unexpected, though not unprecedented,^{11,12} ring-opening reaction. Nevertheless, the dihydropyridines were useful in their own right. Following facile oxidative decomplexation, the dihydropyridines were shown to participate in Diels-Alder reactions, generating bridgehead CF₃-substituted isoquinuclidines. The isoquinuclidine core, which appears in a number of natural products and medicinally-useful substances,^{13,14} prompted us to begin exploring the more practical applications of this dearomatization chemistry.

The primary advantage of the molybdenum system was found to be its large scale, as the exchange precursor MoTp(NO)(DMAP)(η^2 -PhCF₃) is accessible on a 37 g scale

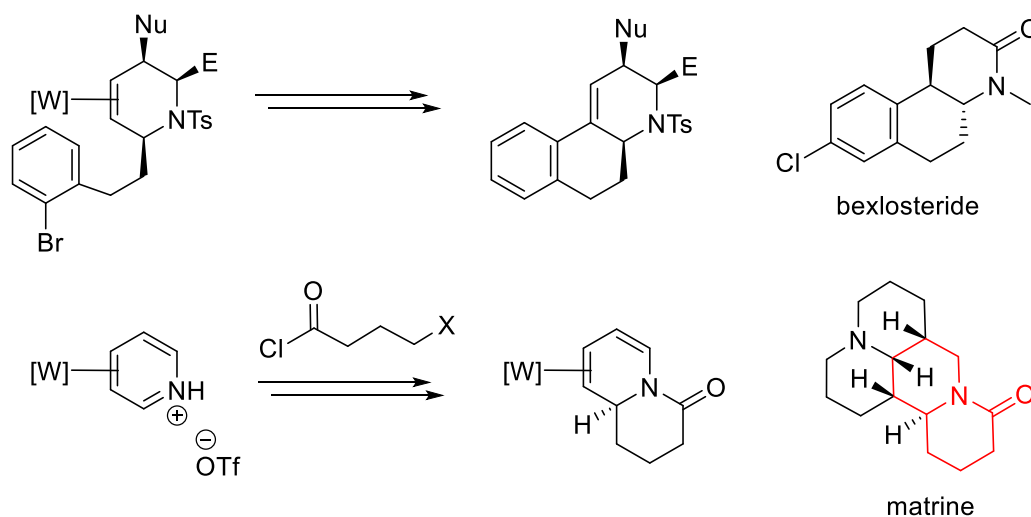
without chromatography.¹⁰ Furthermore, the greater ease of oxidation allows the use of milder oxidants for oxidative decomplexation. These milder conditions did not cause rearomatization of the dihydropyridines, which had been an issue with the tungsten system.⁵ The functional group tolerance of the oxidative decomplexation step is also theoretically significantly greater. Unfortunately, this ease of oxidation is also the biggest barrier to organic chemistry with molybdenum, as many complexes are easily oxidized prematurely by acids and other electrophilic reagents. Therefore, the second phase of the project, which was focused on medicinal chemistry applications, was conducted with the tungsten analog.

WTP(NO)(PMe₃)(3,4-η²-pyridine borane) has shown to be a versatile starting material for a range of tetrahydropyridine complexes.⁵⁻⁹ Nevertheless, a great deal of this complex's chemistry had remained unexplored. Heteroatom nucleophiles had not been investigated, and all functionalized organics were derived from the WTP(NO)(PMe₃)(3,4-η²-N-acetylpyridinium)OTf derivative. Due to the prevalence of amines in biologically-active substances, this class of nucleophiles was investigated in detail. Despite significant challenges, the amine addition was found to have a wide scope, allowing the synthesis of nearly a dozen tetrahydropyridine derivatives. Several derivatives of a known drug, methylphenidate, were also produced. Furthermore, functionalized tetrahydropyridine organics were synthesized with a tosyl substituent on nitrogen, eliminating the characterization issues that are caused by acetyl rotamers.⁸

With these advances, the future of dihapto-coordinate pyridine chemistry appears promising. Since enantioenrichment of a tungsten exchange precursor has been demonstrated, it should be straightforward to synthesize a single enantiomer of the

tungsten pyridine-borane complex.¹⁵ From this enantioenriched complex, single enantiomers of all of the tetrahydropyridines reported herein are accessible. Such enantioselective synthesis is crucial if dihapto-coordination dearomatization is to be utilized for medicinal chemistry applications. It also appears the metal stereocenter can control stereocenter formation on an incoming prochiral nucleophile. This aspect of the chemistry should be explored further in order to form single isomers of stereochemically complex molecules.

The synthesis of more elaborate ring systems could also be explored. Using a bifunctional electrophile or nucleophile, it may be possible to form bi- or polycyclic scaffolds. For example, nucleophilic addition of a substituted β -phenethylmagnesium bromide, followed by an intramolecular Heck reaction post-decomplexation, could be used to form a benzo[f]quinoline core (as found in bexlosteride).¹⁶



Scheme 7.1: Proposed synthesis of nitrogenous bi- and tricyclic ring systems

Alternatively, if a bifunctional protecting group (e.g. a halogenated acyl chloride) can be added to nitrogen, then systems such as quinolizidines can be produced. These

cyclization reactions will provide access to a greater range of products than ever before, increasing the appeal of this chemistry to the broader synthetic community.

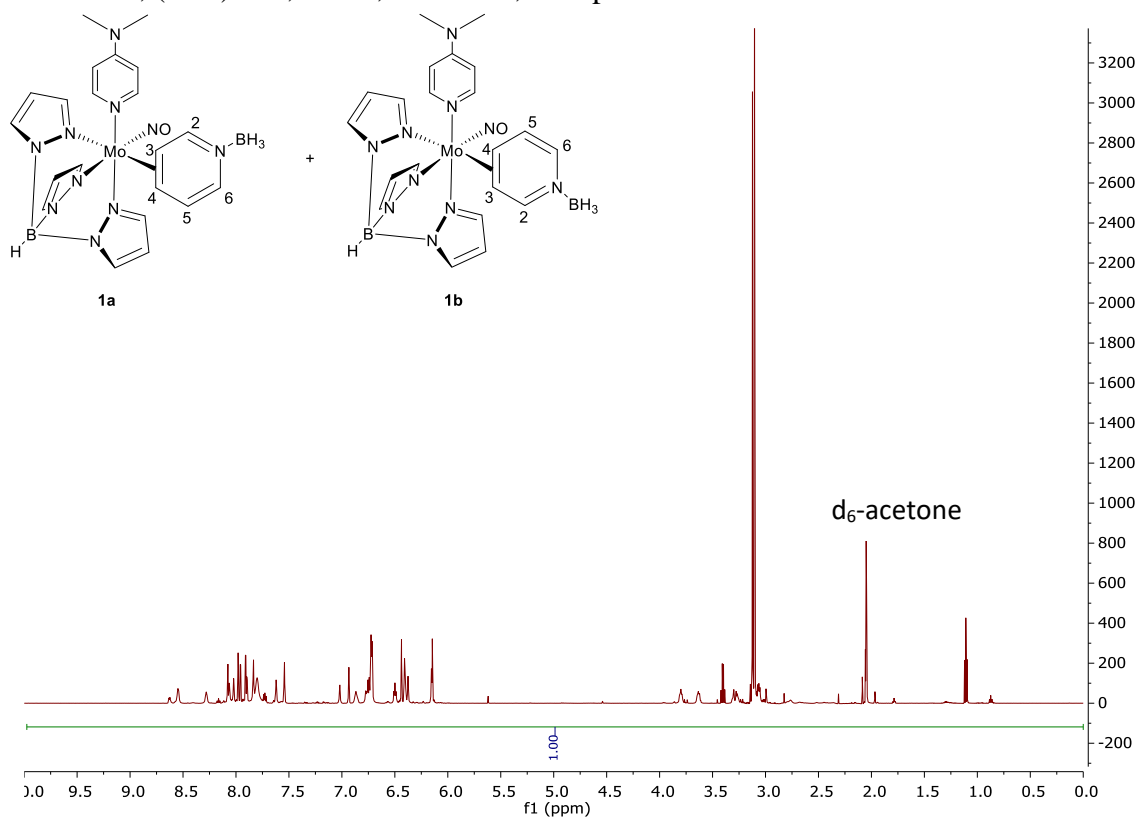
References

- (1) Meiere, S. H.; Keane, J. M.; Gunnoe, T. B.; Sabat, M.; Harman, W. D. *Journal of the American Chemical Society* **2003**, *125*, 2024.
- (2) Mocella, C. J.; Delafuente, D. A.; Keane, J. M.; Warner, G. R.; Friedman, L. A.; Sabat, M.; Harman, W. D. *Organometallics* **2004**, *23*, 3772.
- (3) Myers, J. T.; Dakermanji, S. J.; Chastanet, T. R.; Shivokevich, P. J.; Strausberg, L. J.; Sabat, M.; Myers, W. H.; Harman, W. D. *Organometallics* **2017**, *36*, 543.
- (4) Delafuente, D. A.; Kosturko, G. W.; Graham, P. M.; Harman, W. H.; Myers, W. H.; Surendranath, Y.; Klet, R. C.; Welch, K. D.; Trindle, C. O.; Sabat, M.; Harman, W. D. *J. Am. Chem. Soc.* **2007**, *129*, 406.
- (5) Harrison, D. P.; Welch, K. D.; Nichols-Nielander, A. C.; Sabat, M.; Myers, W. H.; Harman, W. D. *J. Am. Chem. Soc.* **2008**, *130*, 16844.
- (6) Kosturko, G. W.; Harrison, D. P.; Sabat, M.; Myers, W. H.; Harman, W. D. *Organometallics* **2009**, *28*, 387.
- (7) Harrison, D. P.; Zottig, V. E.; Kosturko, G. W.; Welch, K. D.; Sabat, M.; Myers, W. H.; Harman, W. D. *Organometallics* **2009**, *28*, 5682.
- (8) Harrison, D. P.; Sabat, M.; Myers, W. H.; Harman, W. D. *J. Am. Chem. Soc.* **2010**, *132*, 17282.

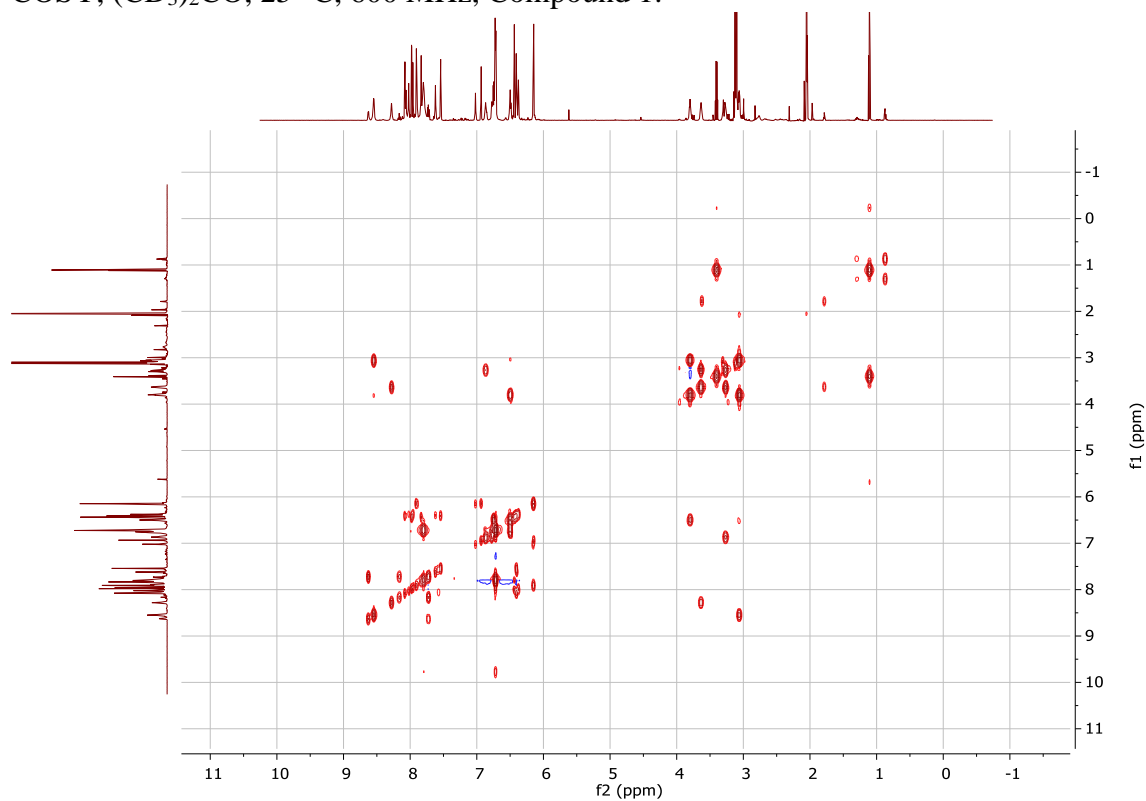
- (9) Harrison, D. P.; Iovan, D. A.; Myers, W. H.; Sabat, M.; Wang, S.; Zottig, V. E.; Harman, W. D. *J. Am. Chem. Soc.* **2011**, *133*, 18378.
- (10) Myers, J. T.; Smith, J. A.; Dakermanji, S. J.; Wilde, J. H.; Wilson, K. B.; Shivokevich, P. J.; Harman, W. D. *J. Am. Chem. Soc.* **2017**, *139*, 11392.
- (11) Harrison, D. P.; Kosturko, G. W.; Ramdeen, V. M.; Nichols-Nielander, A. C.; Payne, S. J.; Sabat, M.; Myers, W. H.; Harman, W. D. *Organometallics* **2010**, *29*, 1909.
- (12) Zincke, T. *Ann. Chim.* **1903**, *330*, 361.
- (13) Faisal, M.; Shahzad, D.; Saeed, A.; Lal, B.; Saeed, S.; Larik, F. A.; Channar, P. A.; Mahesar, P. A.; Mahar, J. *Tetrahedron: Asymmetry* **2017**, *28*, 1445.
- (14) Banerjee, T. S.; Paul, S.; Sinha, S.; Das, S. *Bioorganic & Medicinal Chemistry* **2014**, *22*, 6062.
- (15) Lankenau, A. W.; Iovan, D. A.; Pienkos, J. A.; Salomon, R. J.; Wang, S.; Harrison, D. P.; Myers, W. H.; Harman, W. D. *Journal of the American Chemical Society* **2015**, *137*, 3649.
- (16) Salvador, J. A. R.; Pinto, R. M. A.; Silvestre, S. M. *The Journal of Steroid Biochemistry and Molecular Biology* **2013**, *137*, 199.

Appendix

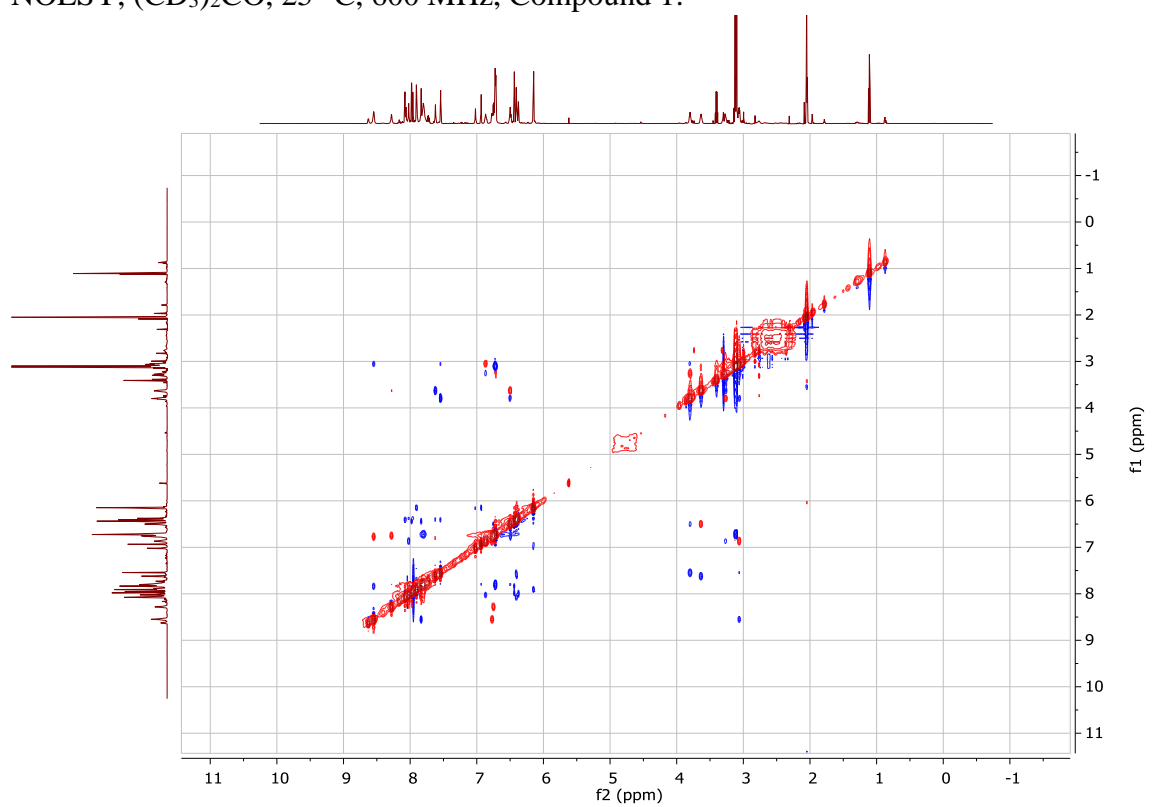
^1H NMR, $(\text{CD}_3)_2\text{CO}$, 25 °C, 600 MHz, Compound 1:



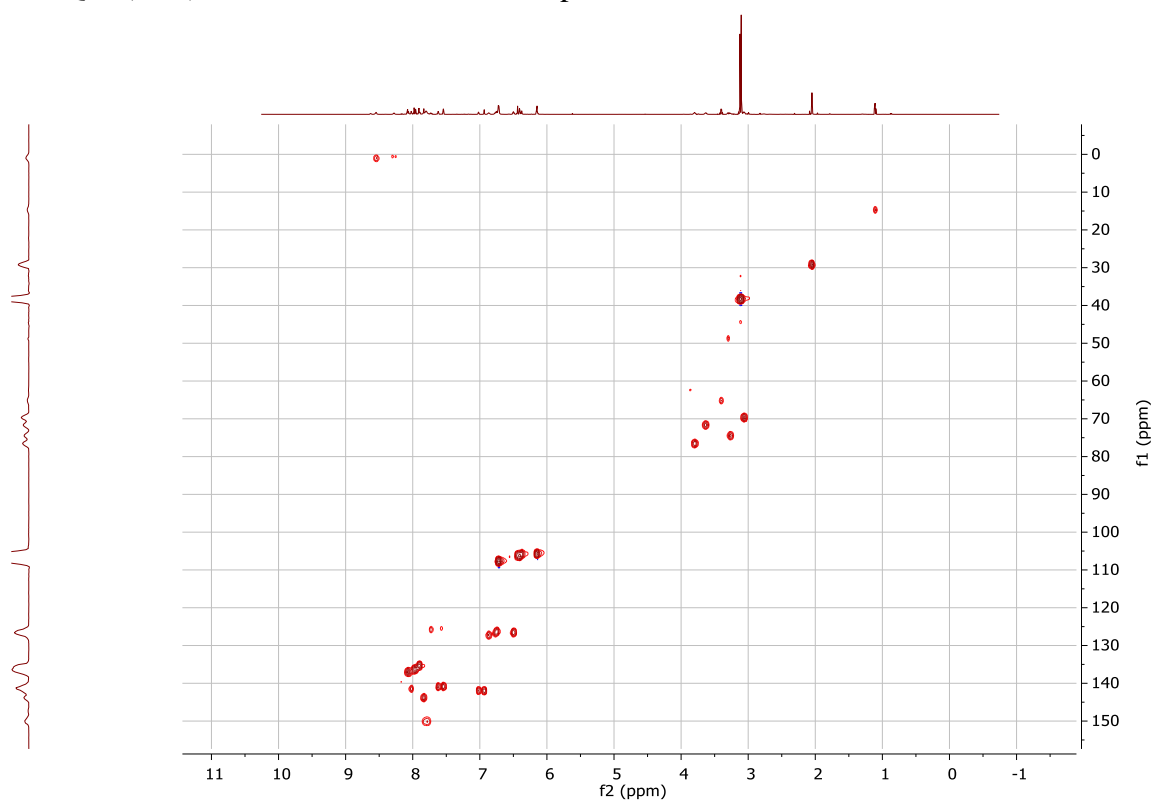
COSY, $(\text{CD}_3)_2\text{CO}$, 25 °C, 600 MHz, Compound 1:



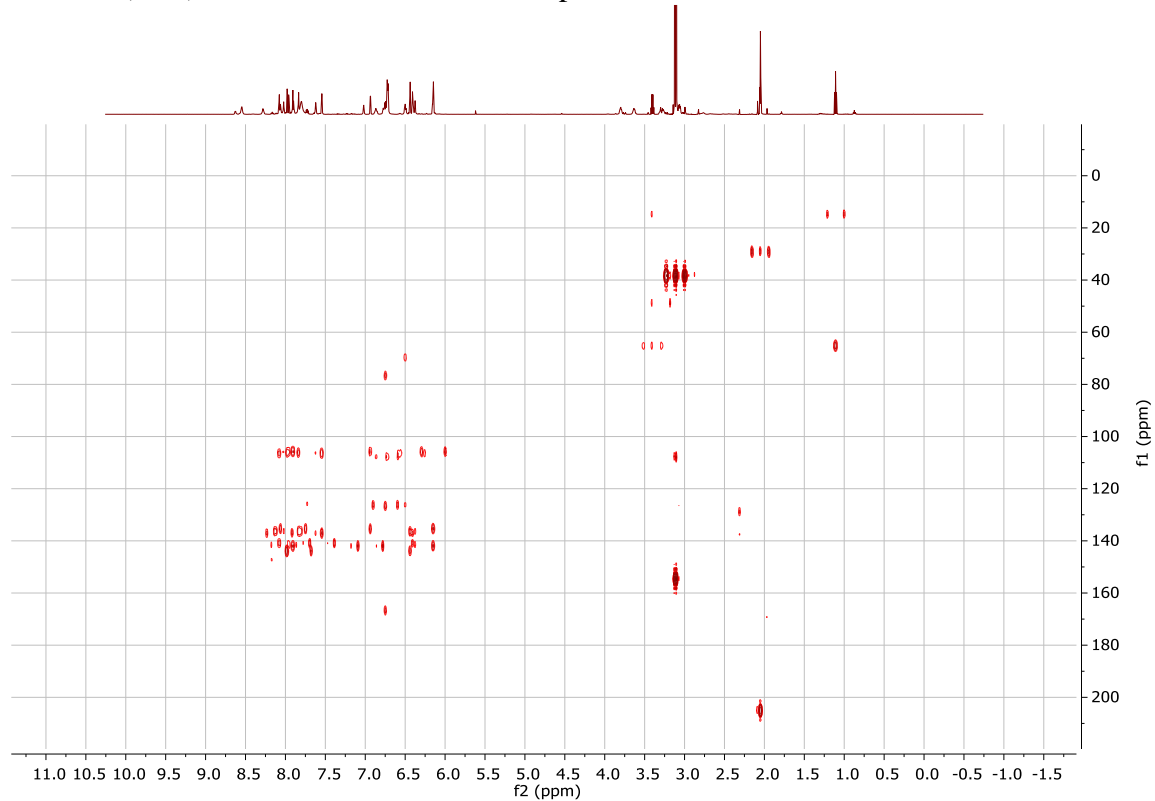
NOESY, (CD₃)₂CO, 25 °C, 600 MHz, Compound 1:



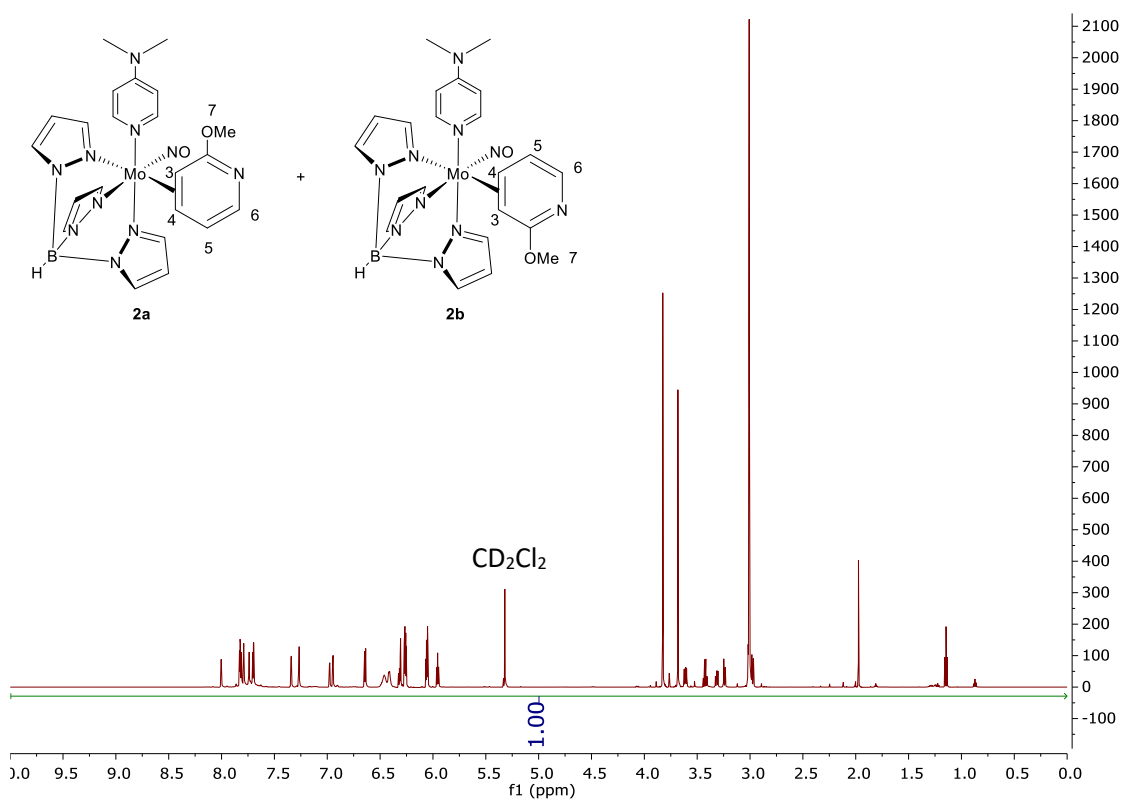
HMQC, (CD₃)₂CO, 25 °C, 600 MHz, Compound 1:



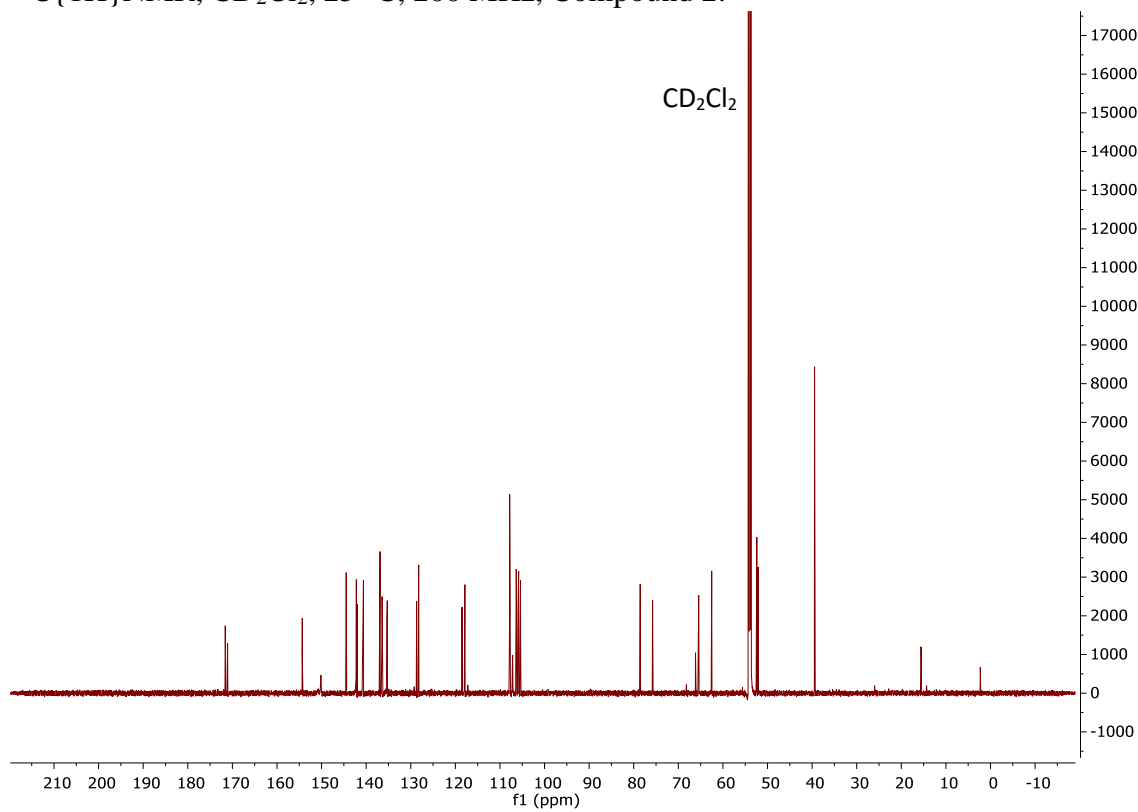
HMBC, (CD₃)₂CO, 25 °C, 600 MHz, Compound 1:



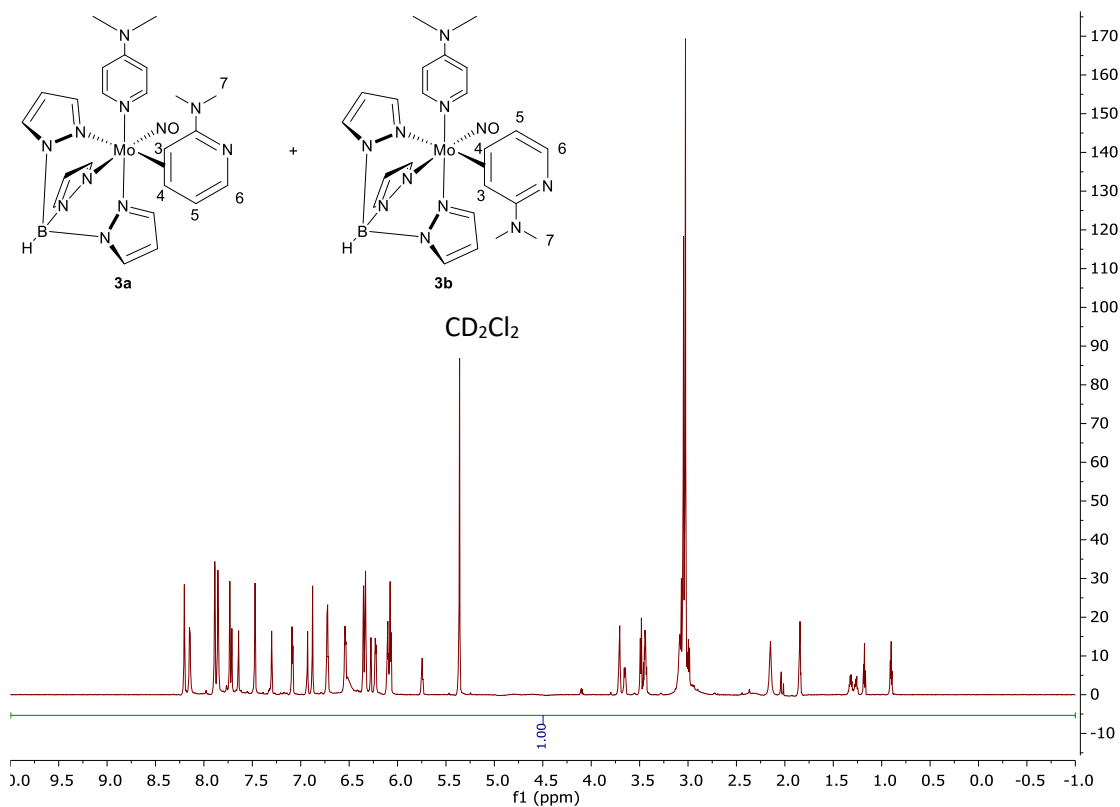
^1H NMR, CD_2Cl_2 , 25 °C, 600 MHz, Compound 2:



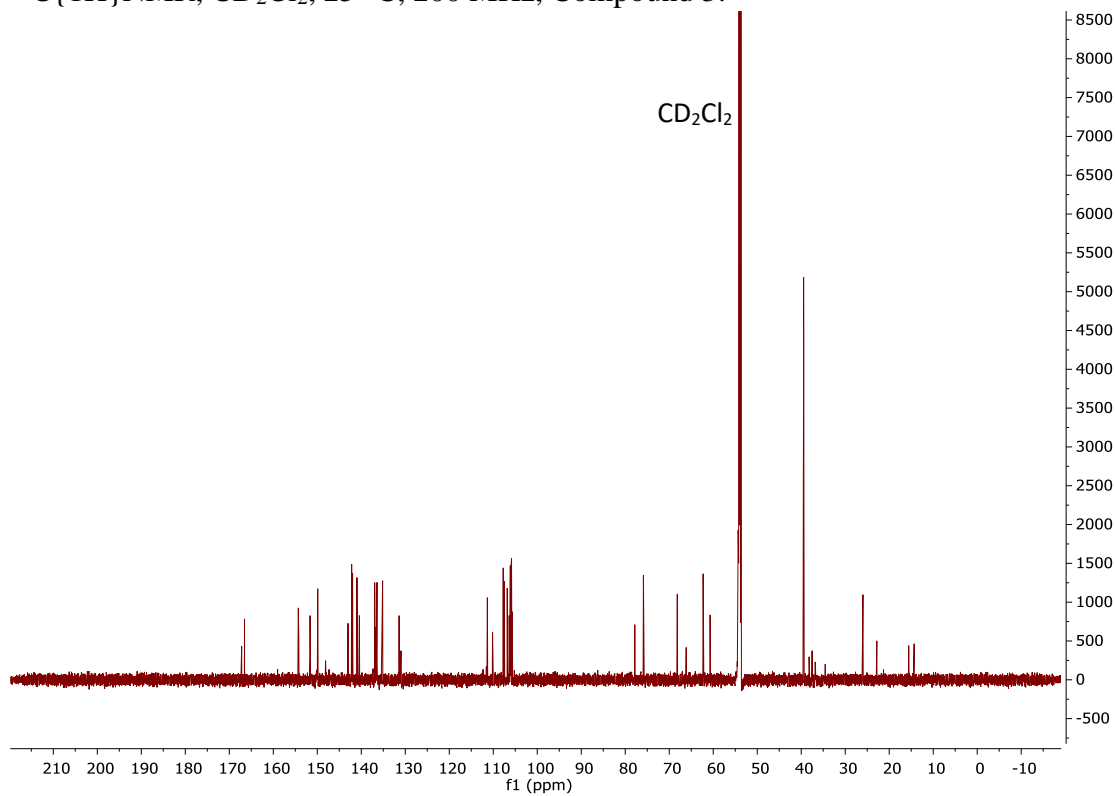
$^{13}\text{C}\{^1\text{H}\}$ NMR, CD_2Cl_2 , 25 °C, 200 MHz, Compound 2:

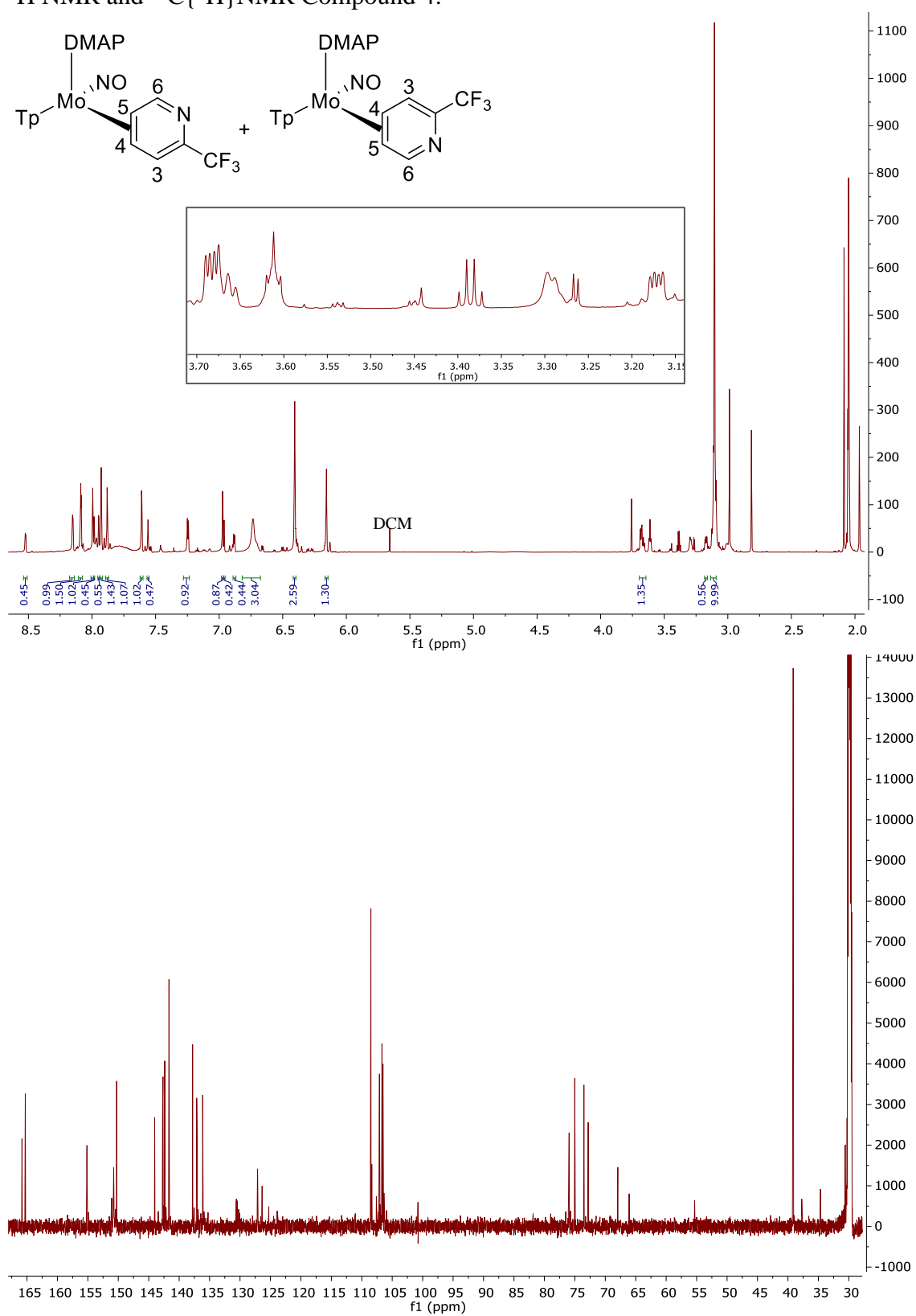


^1H NMR, CD_2Cl_2 , 25 °C, 600 MHz, Compound 3:

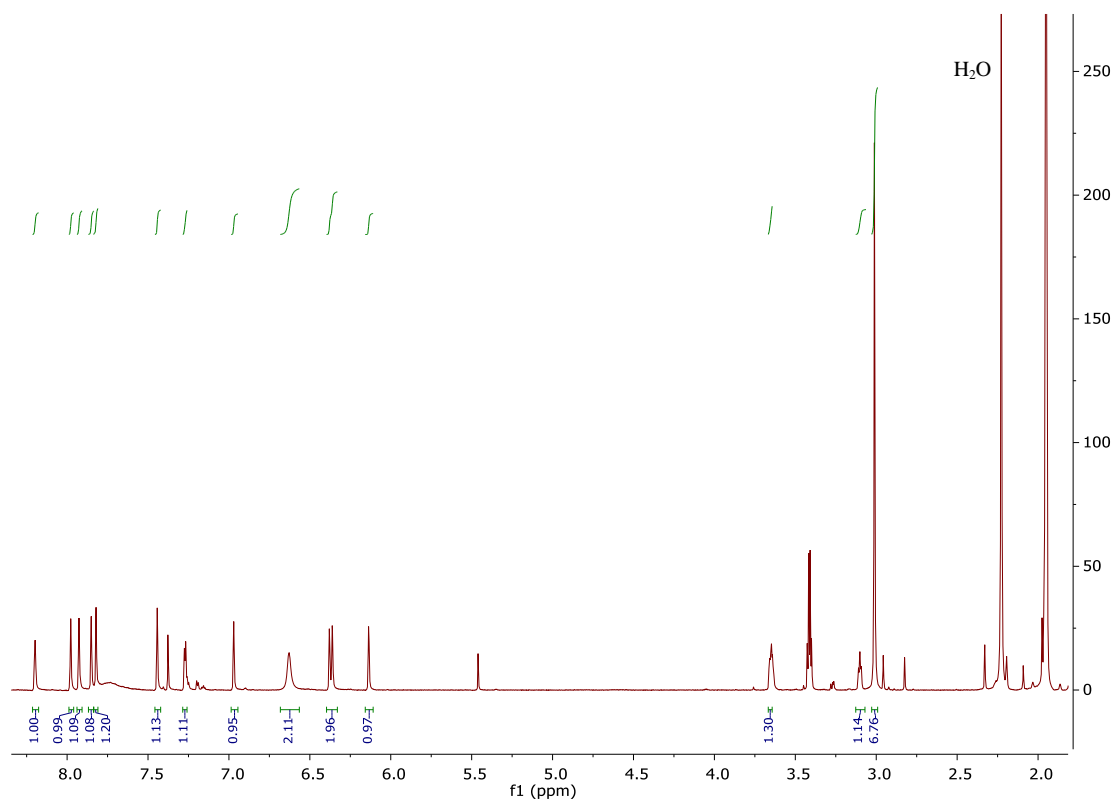
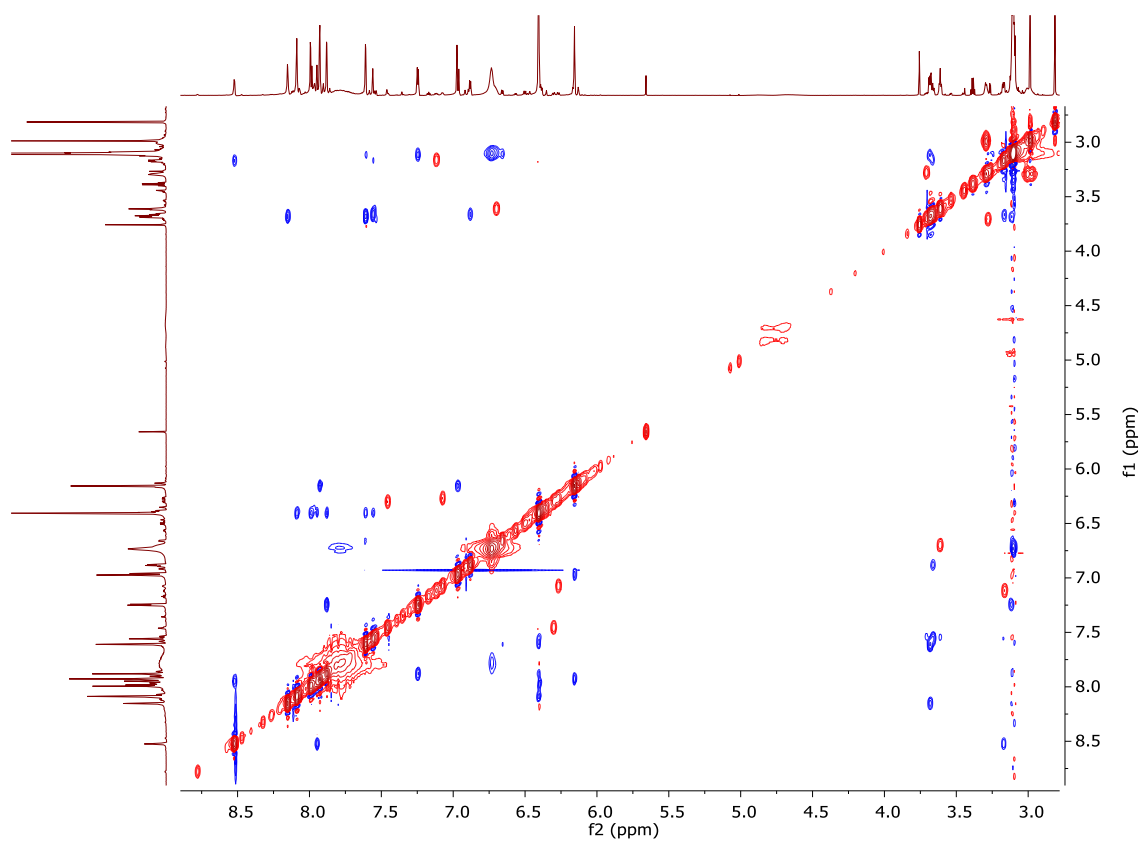


$^{13}\text{C}\{^1\text{H}\}$ NMR, CD_2Cl_2 , 25 °C, 200 MHz, Compound 3:

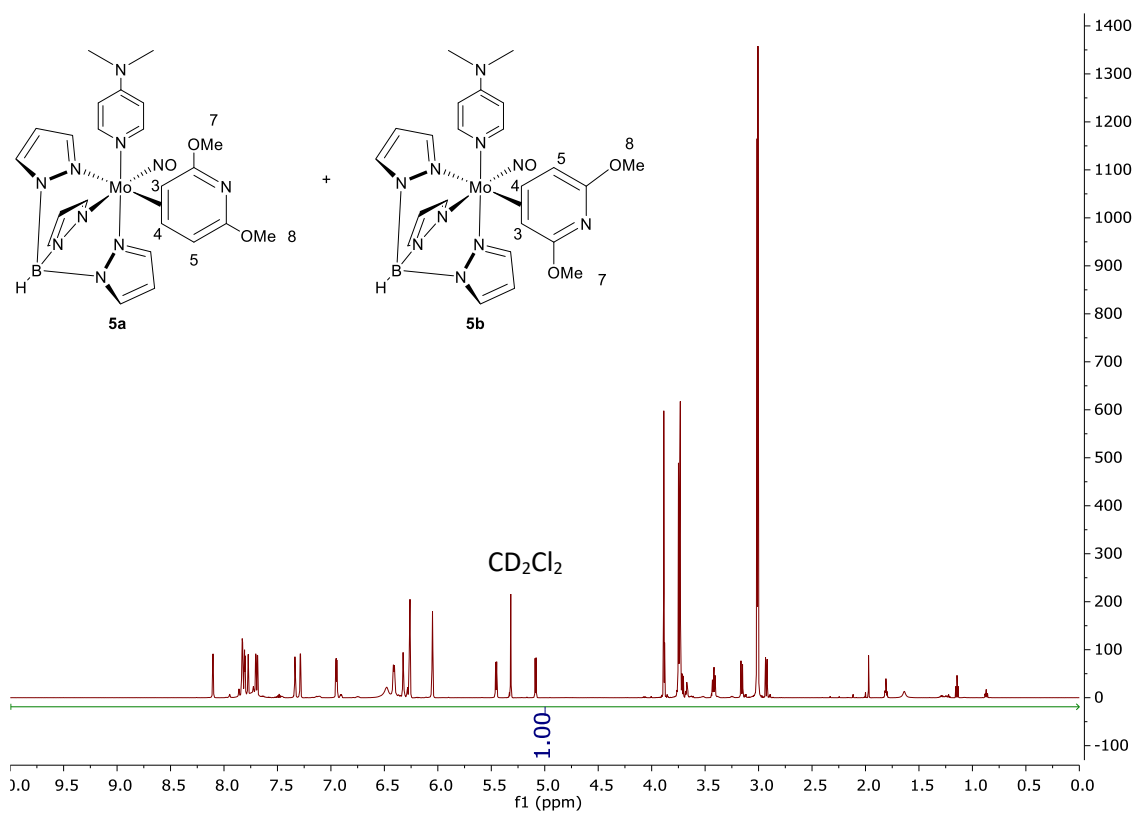


^1H NMR and $^{13}\text{C}\{^1\text{H}\}$ NMR Compound 4:

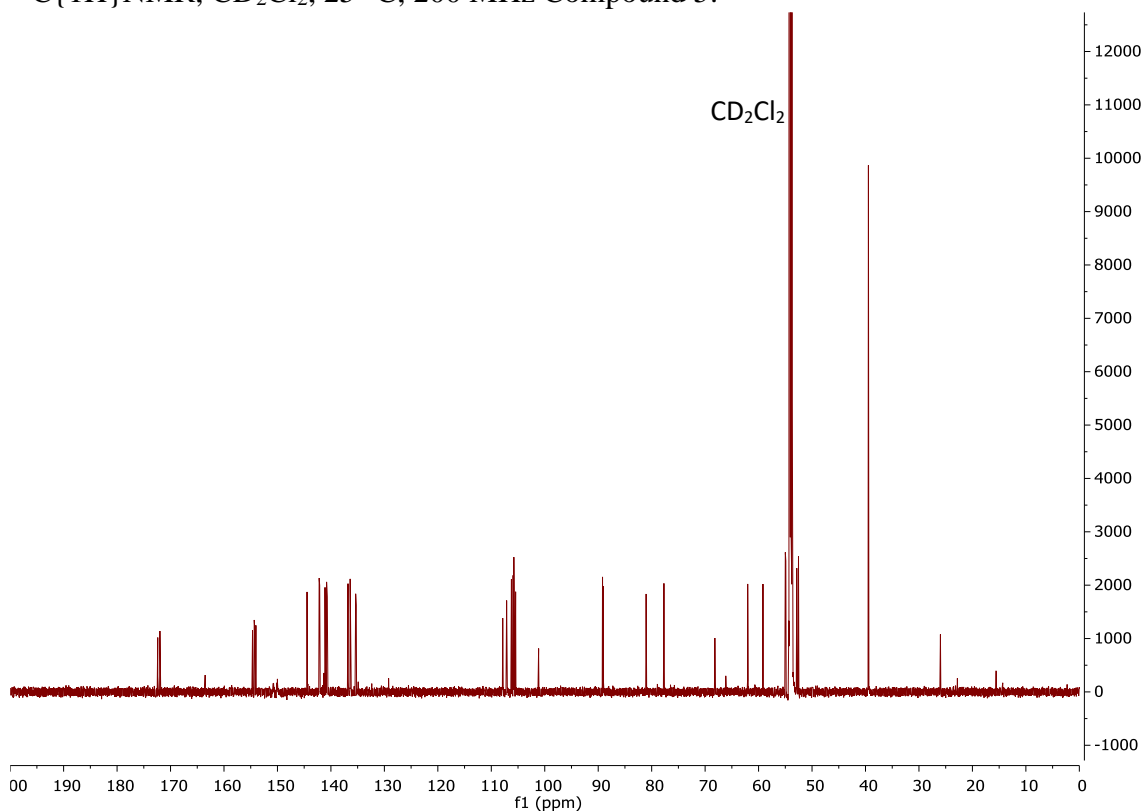
NOESY NMR of Compound 2, ^1H NMR of Compound 4a (0 °C):



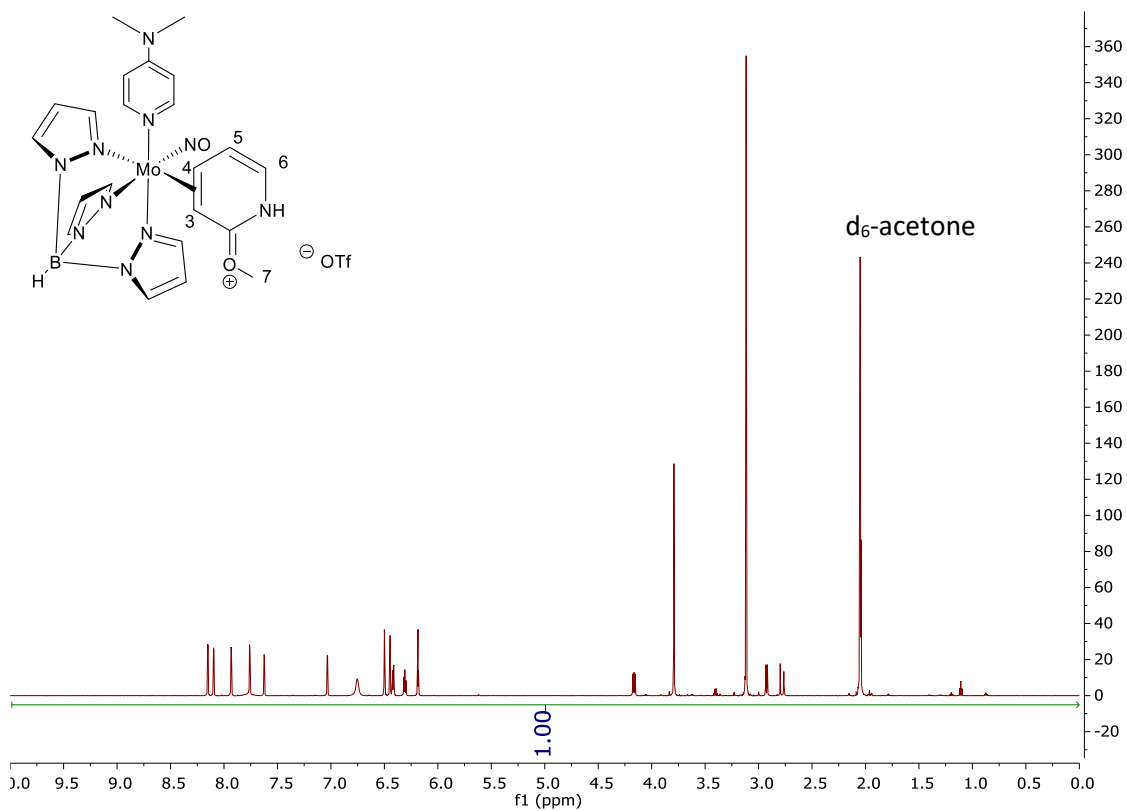
^1H NMR, CD_2Cl_2 , 25 °C, 600 MHz, Compound 5:



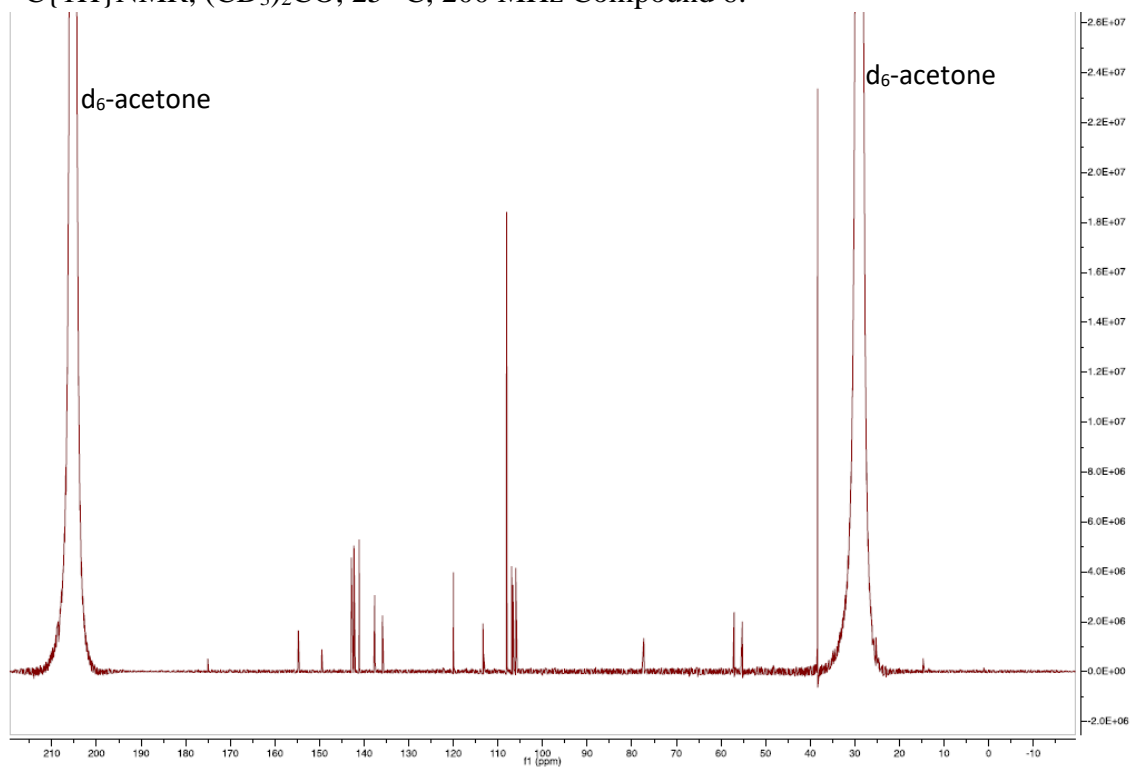
$^{13}\text{C}\{^1\text{H}\}$ NMR, CD_2Cl_2 , 25 °C, 200 MHz Compound 5:



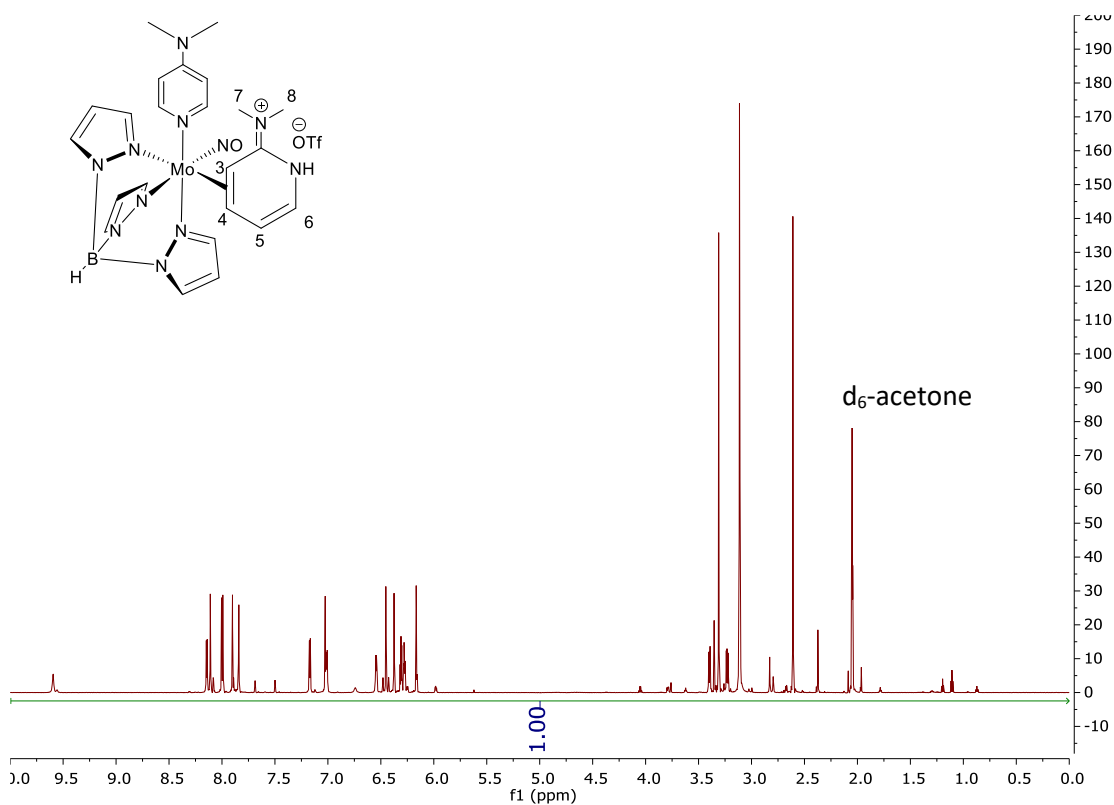
^1H NMR, $(\text{CD}_3)_2\text{CO}$, 25 °C, 600 MHz, Compound 6:



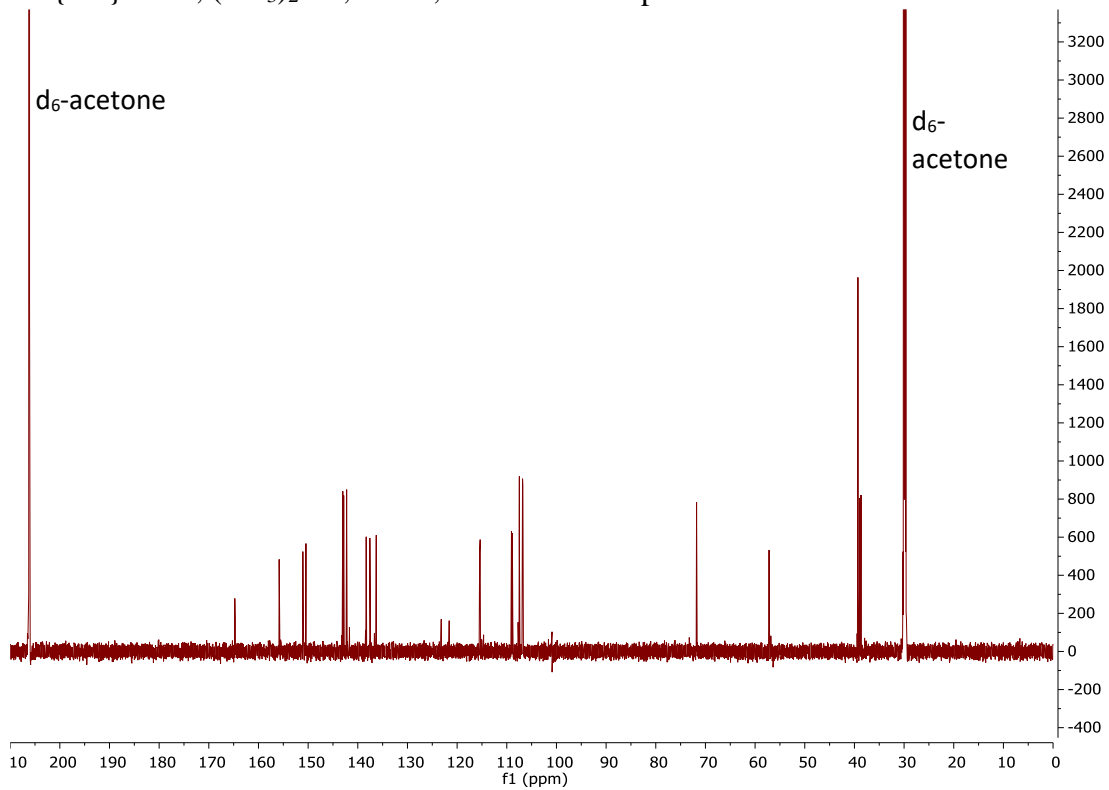
$^{13}\text{C}\{^1\text{H}\}$ NMR, $(\text{CD}_3)_2\text{CO}$, 25 °C, 200 MHz Compound 6:



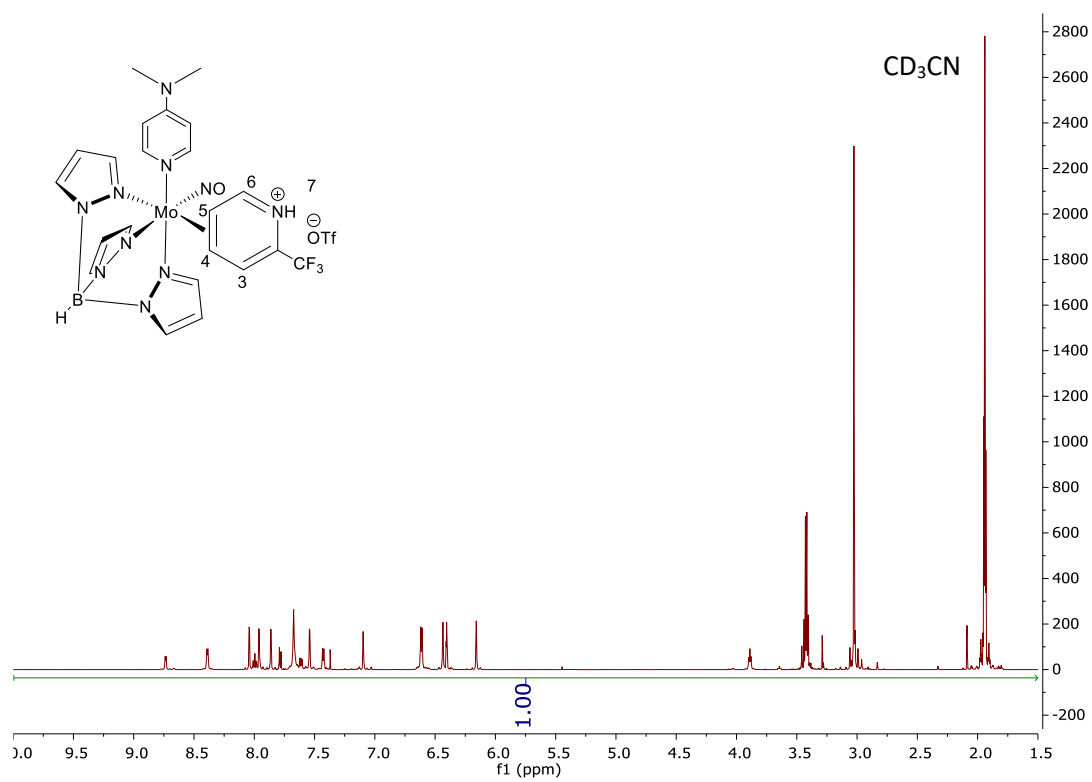
^1H NMR, $(\text{CD}_3)_2\text{CO}$, 25 °C, 600 MHz, Compound 7:



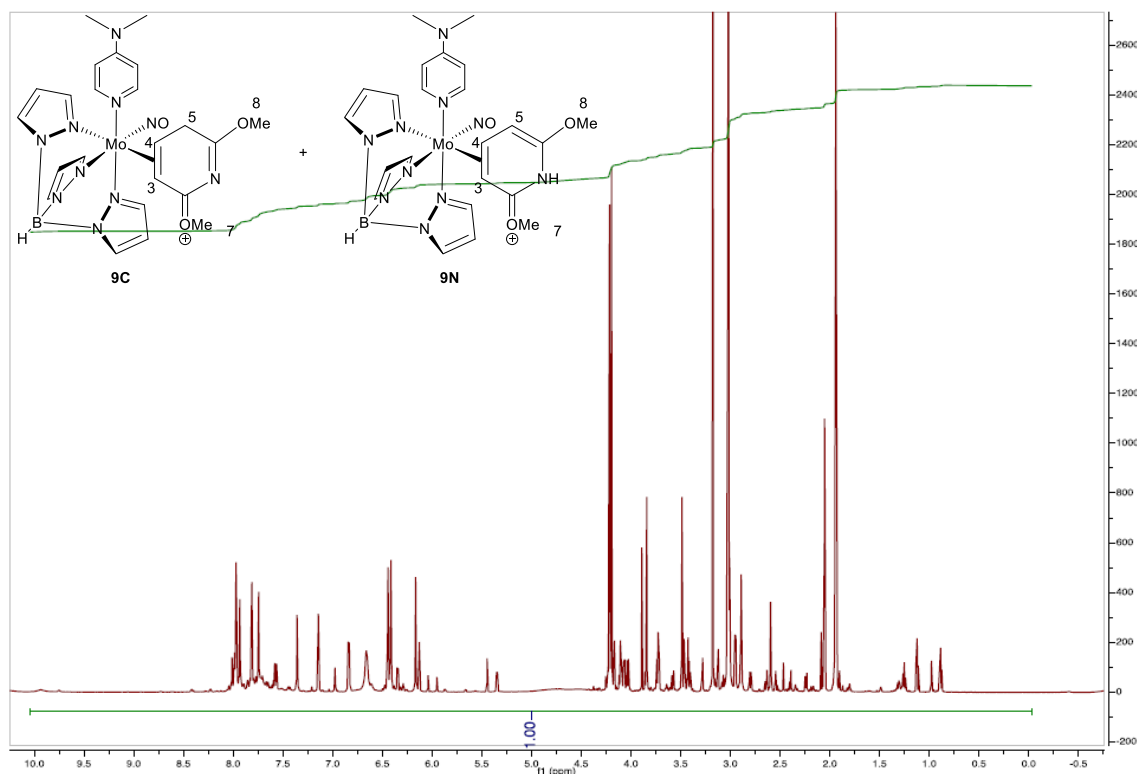
$^{13}\text{C}\{^1\text{H}\}$ NMR, $(\text{CD}_3)_2\text{CO}$, 25 °C, 200 MHz Compound 7:



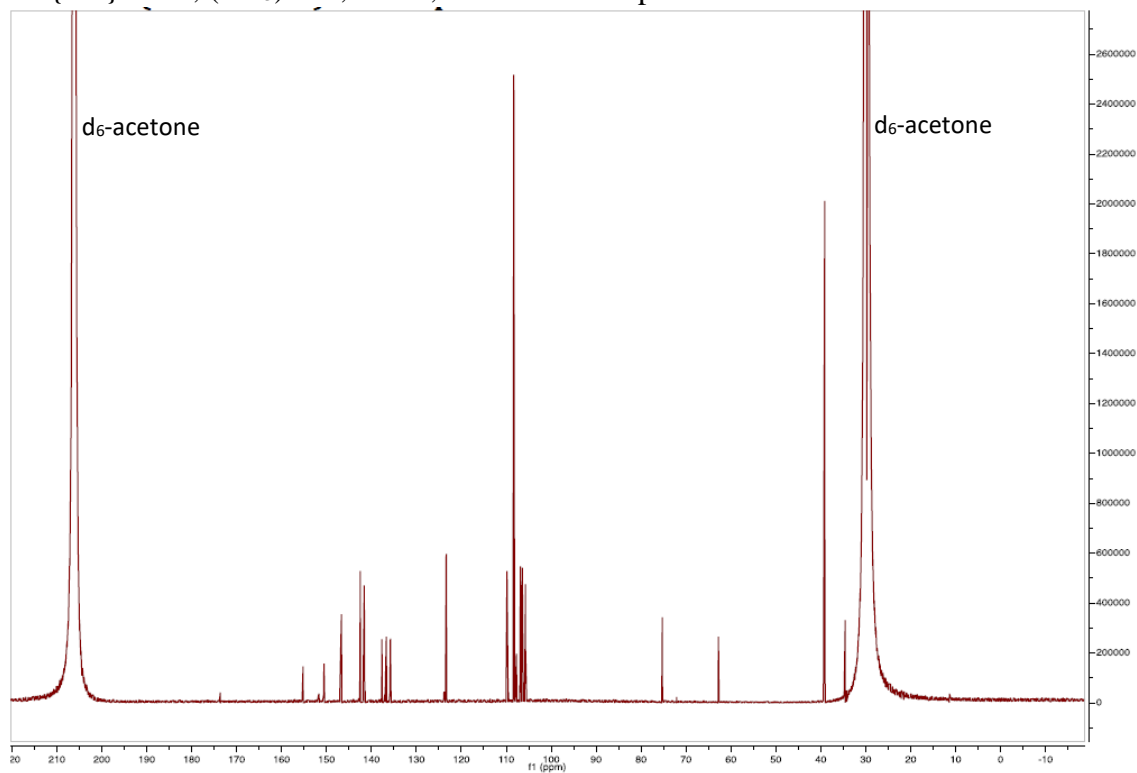
^1H NMR, CD_3CN , $25\text{ }^\circ\text{C}$, 600 MHz, Compound 8:

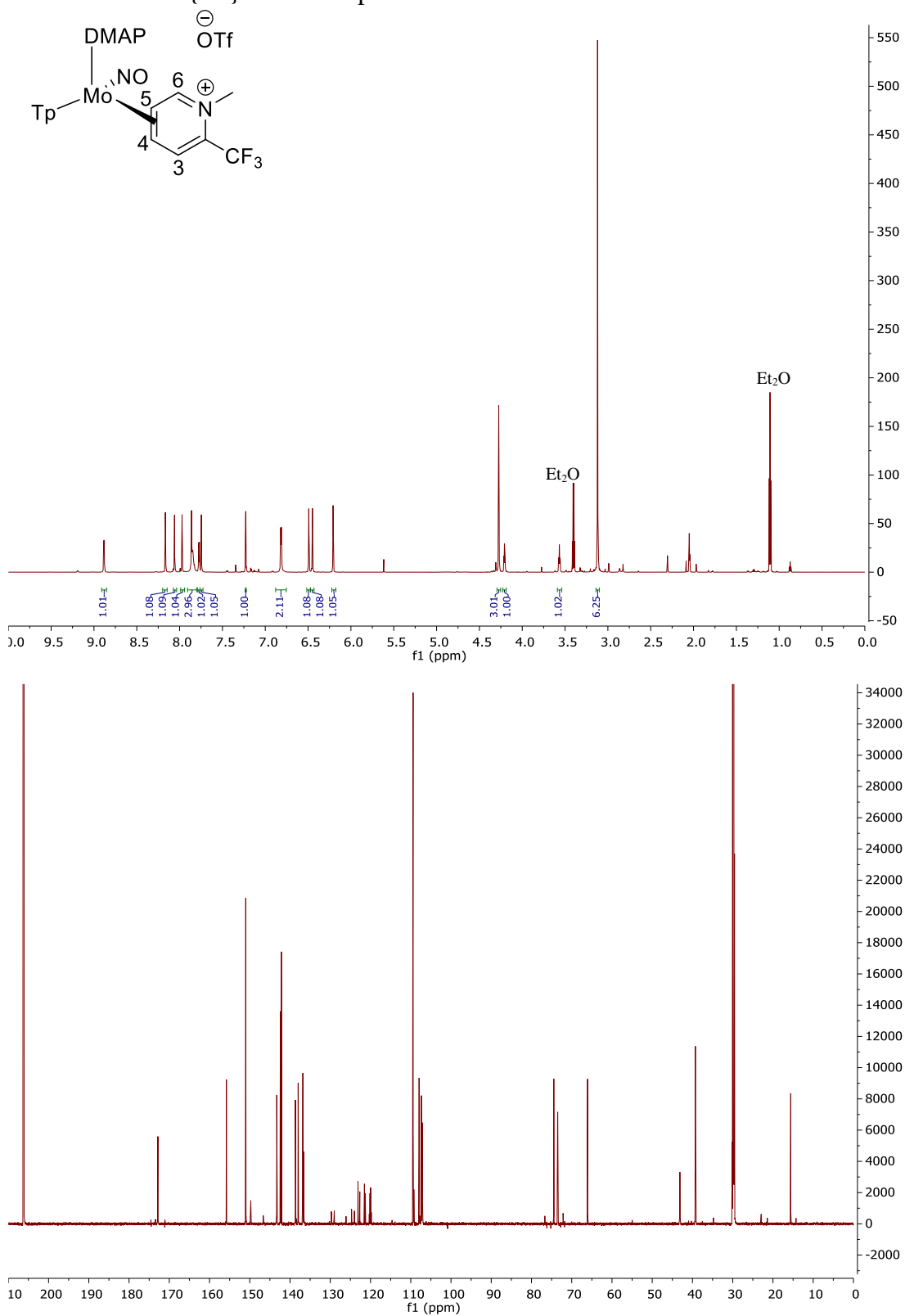


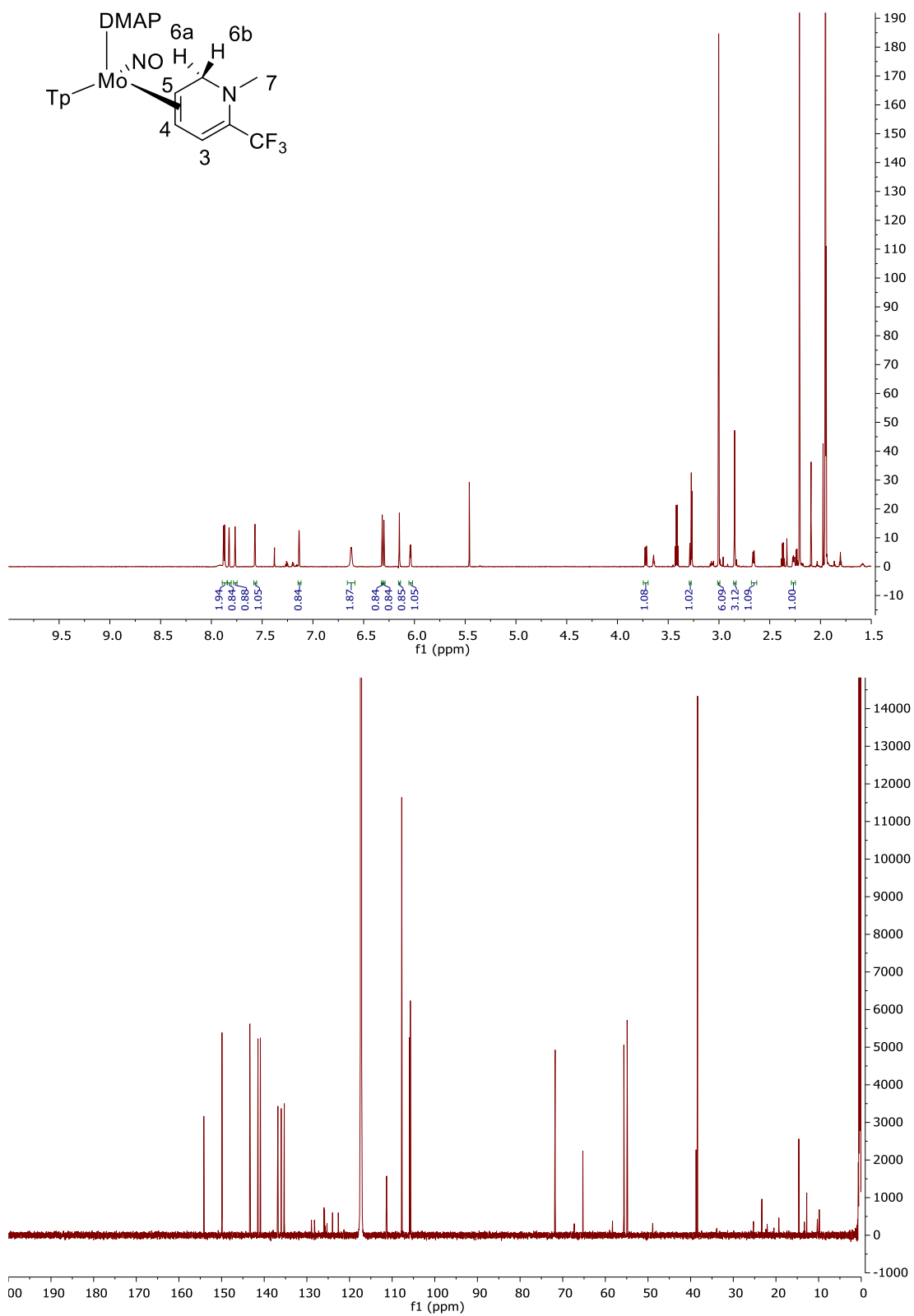
^1H NMR, $(\text{CD}_3)_2\text{CO}$, 25 °C, 600 MHz, Compound 9:

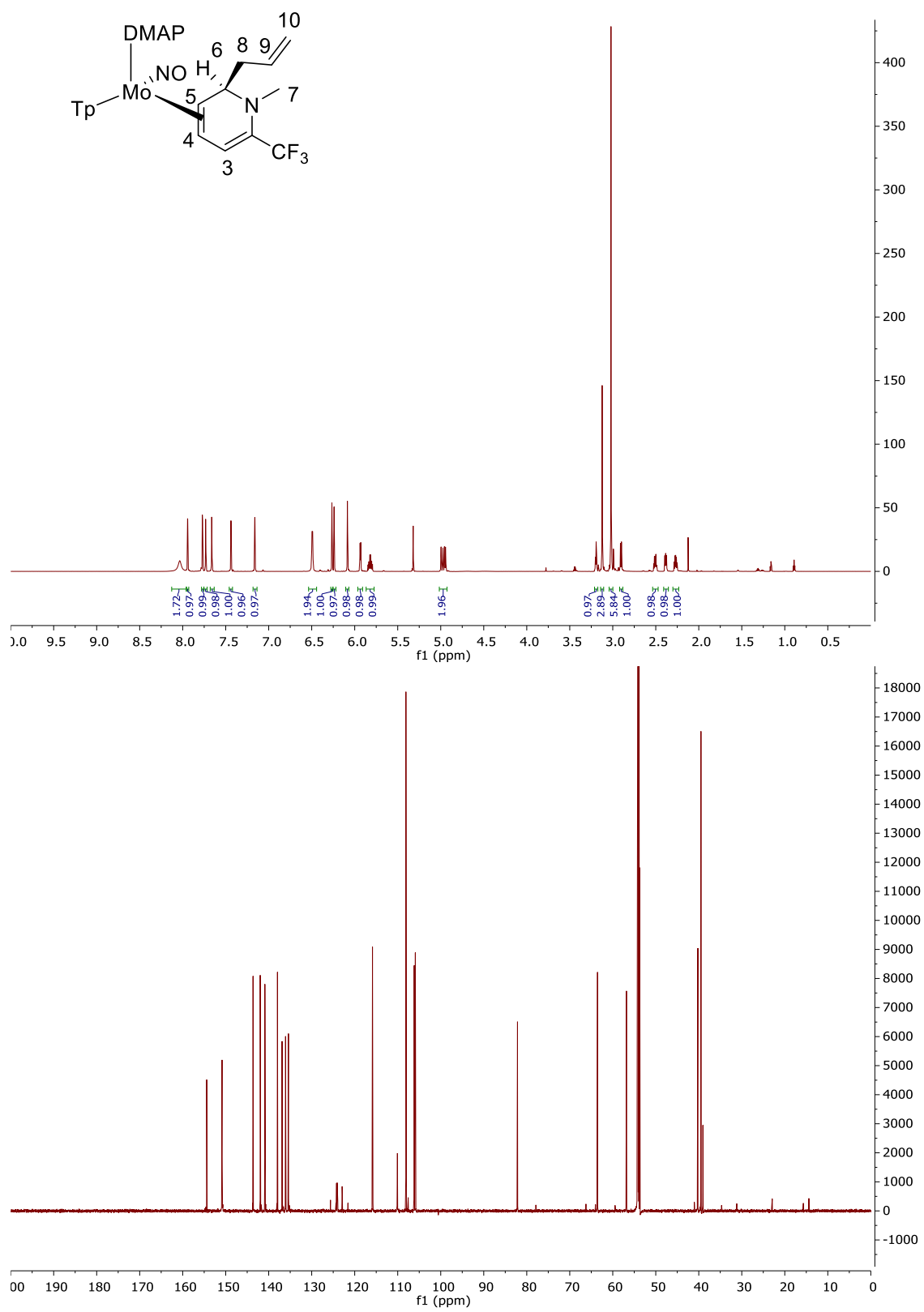


$^{13}\text{C}\{^1\text{H}\}$ NMR, $(\text{CD}_3)_2\text{CO}$, 25 °C, 200 MHz Compound 9:

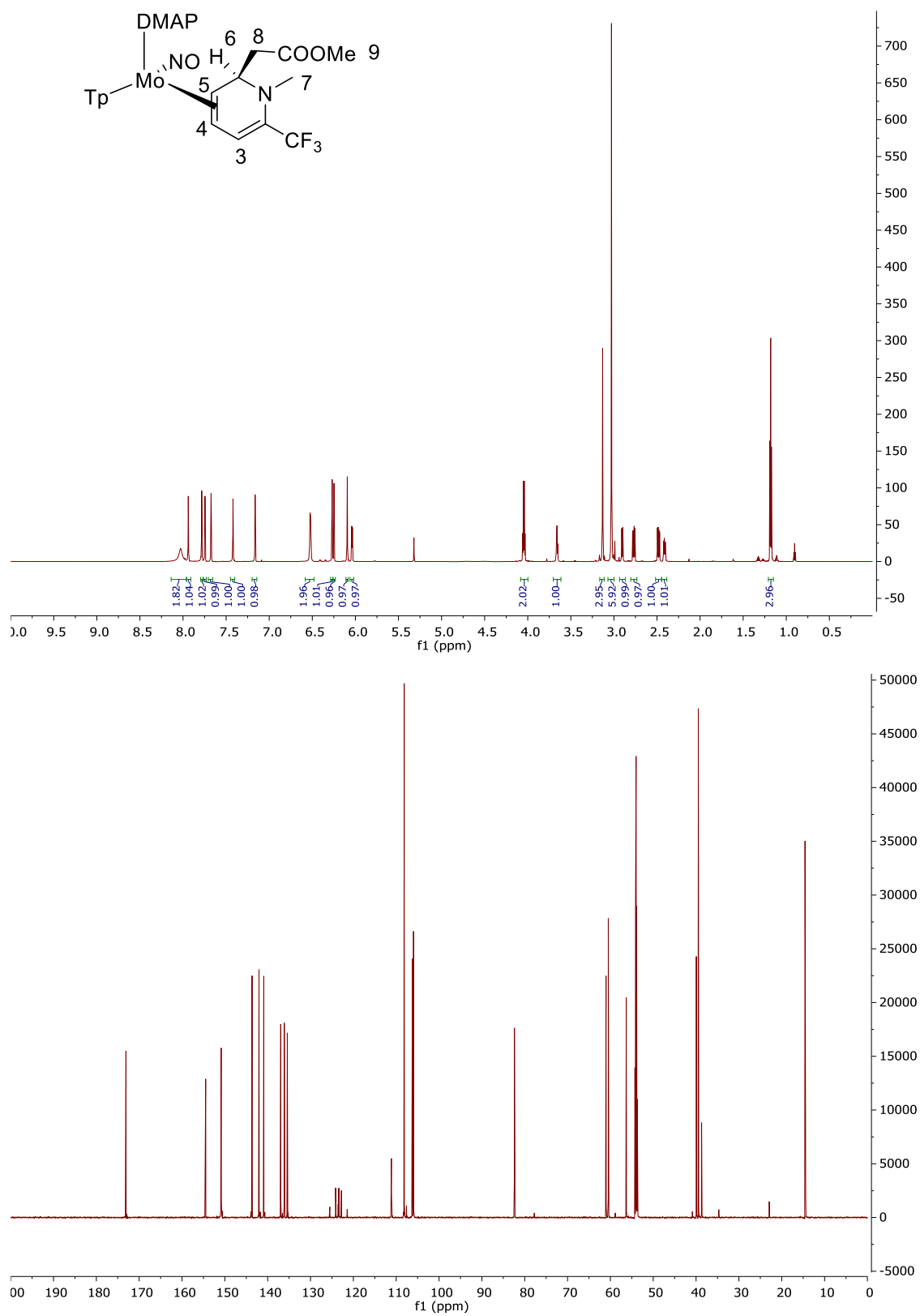


^1H NMR and $^{13}\text{C}\{^1\text{H}\}$ NMR Compound 10:

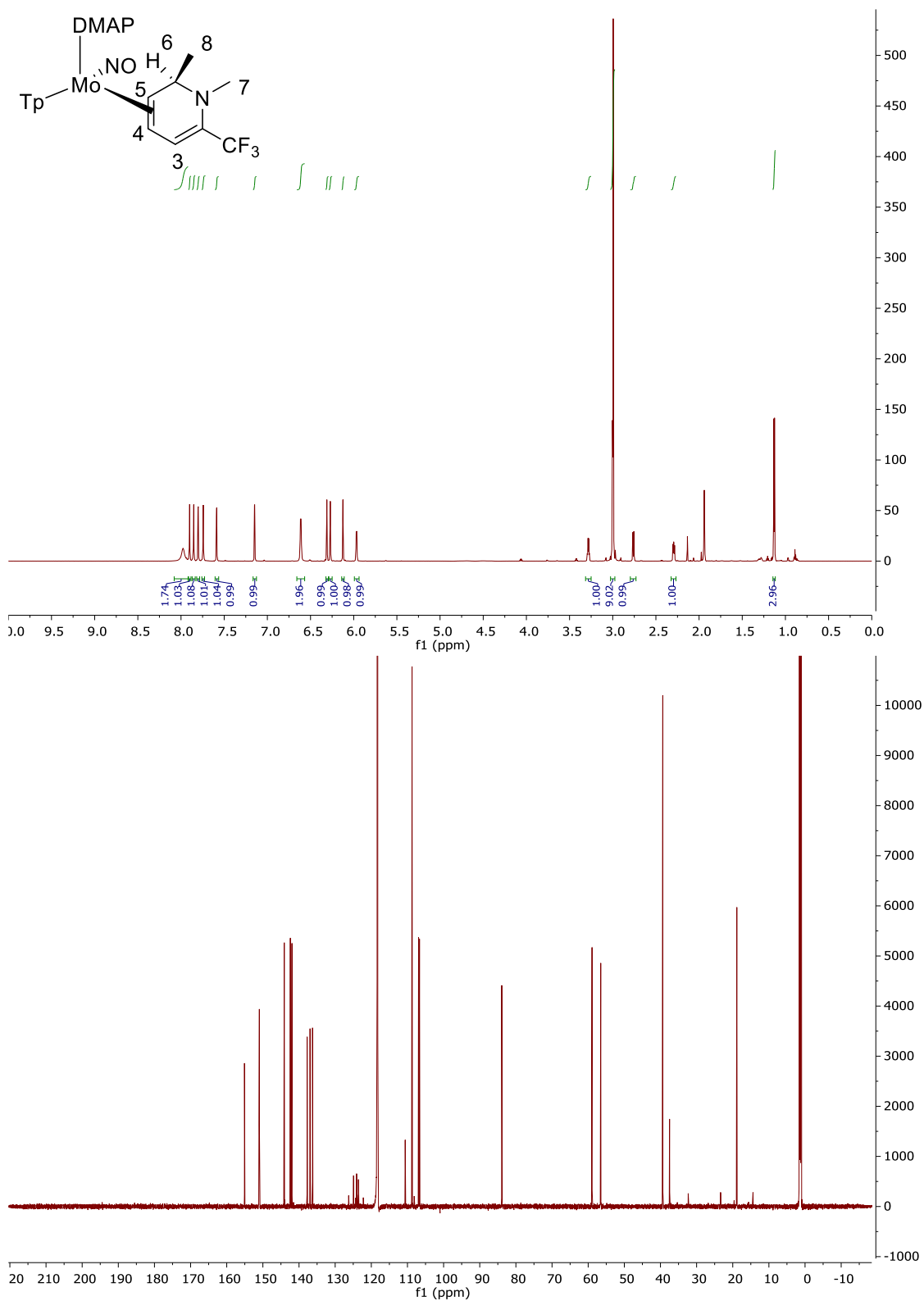
^1H NMR and $^{13}\text{C}\{^1\text{H}\}$ NMR Compound 11:

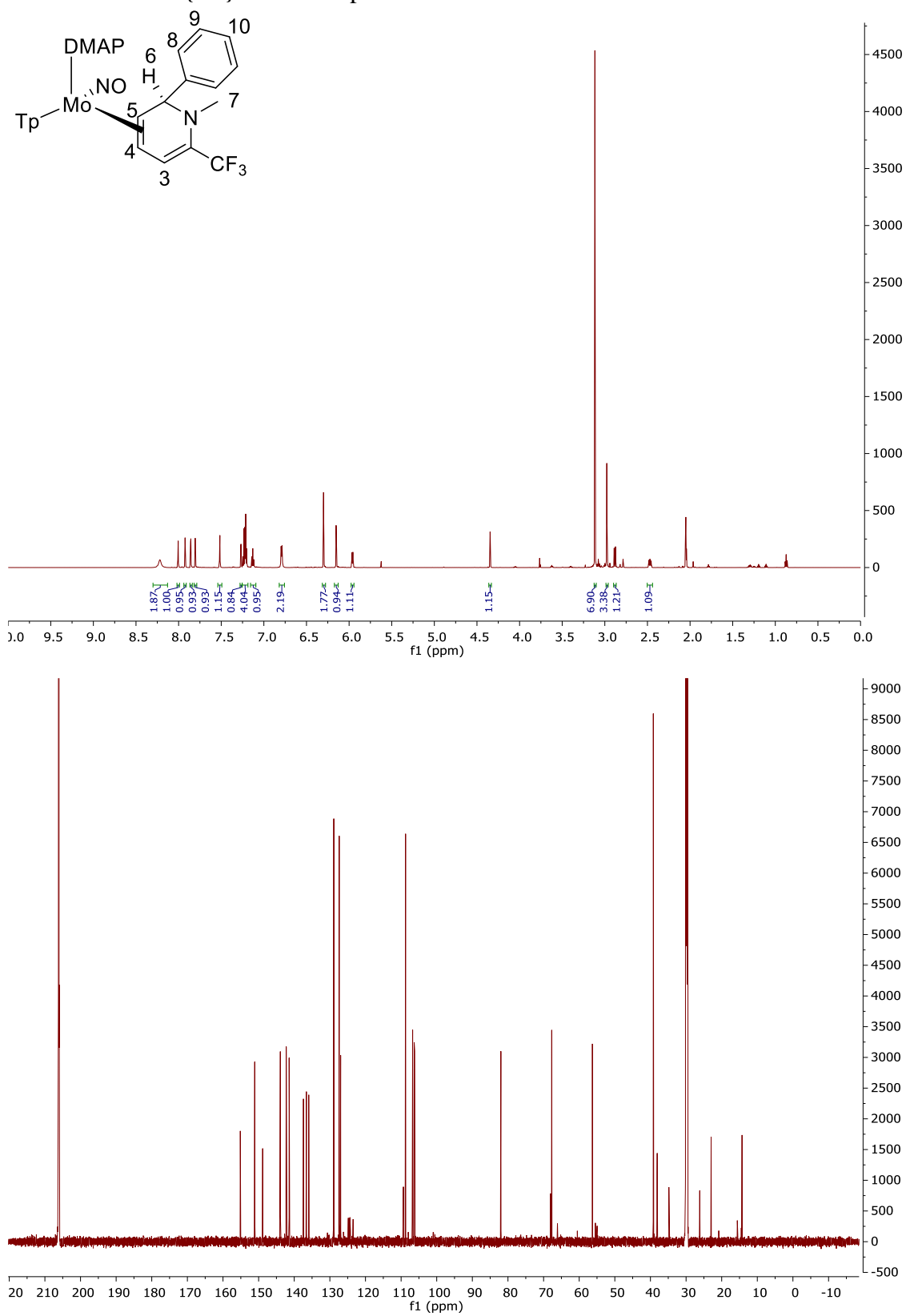
^1H NMR and $^{13}\text{C}\{^1\text{H}\}$ NMR Compound 12:

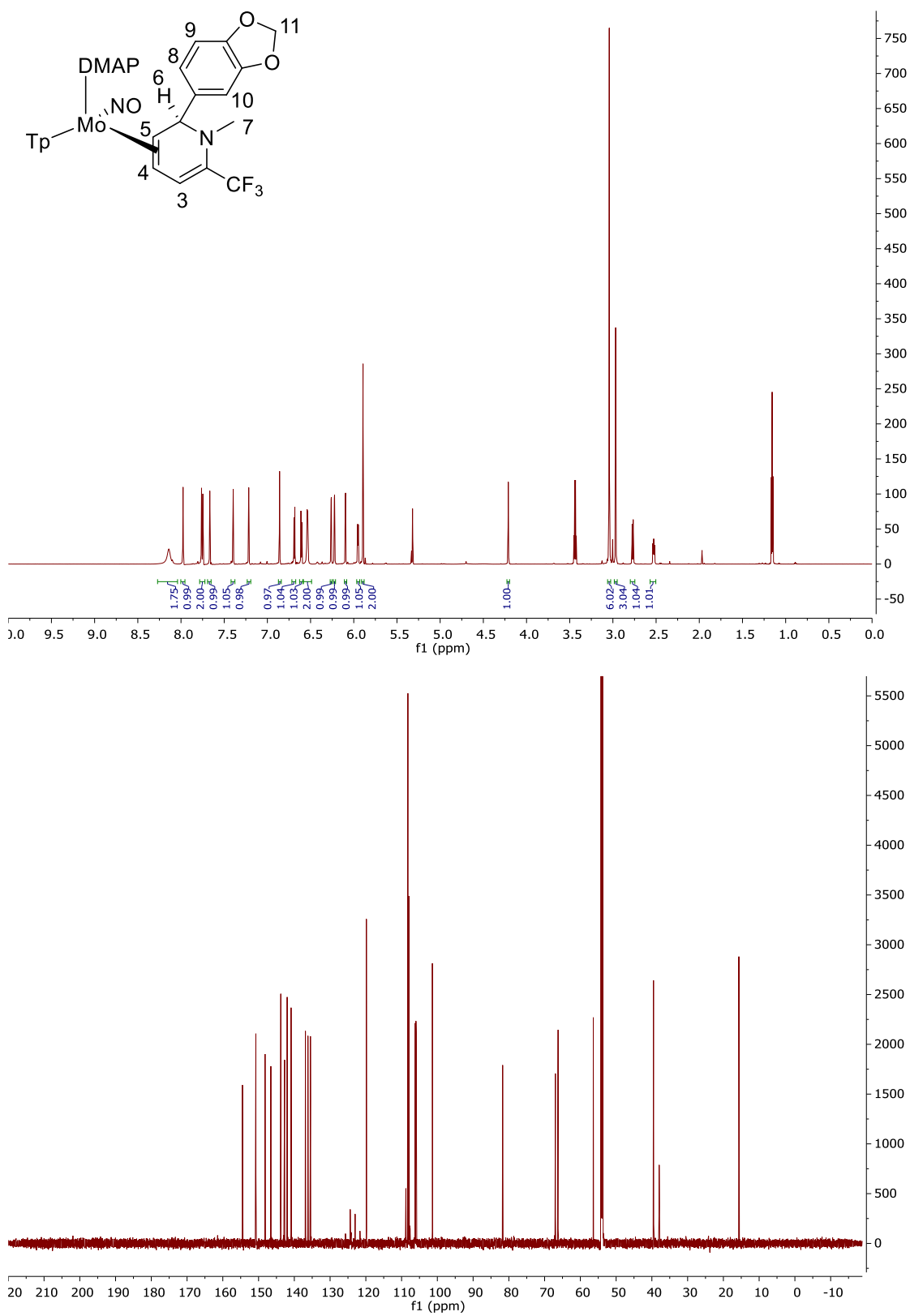
^1H NMR and $^{13}\text{C}\{^1\text{H}\}$ NMR Compound 13:

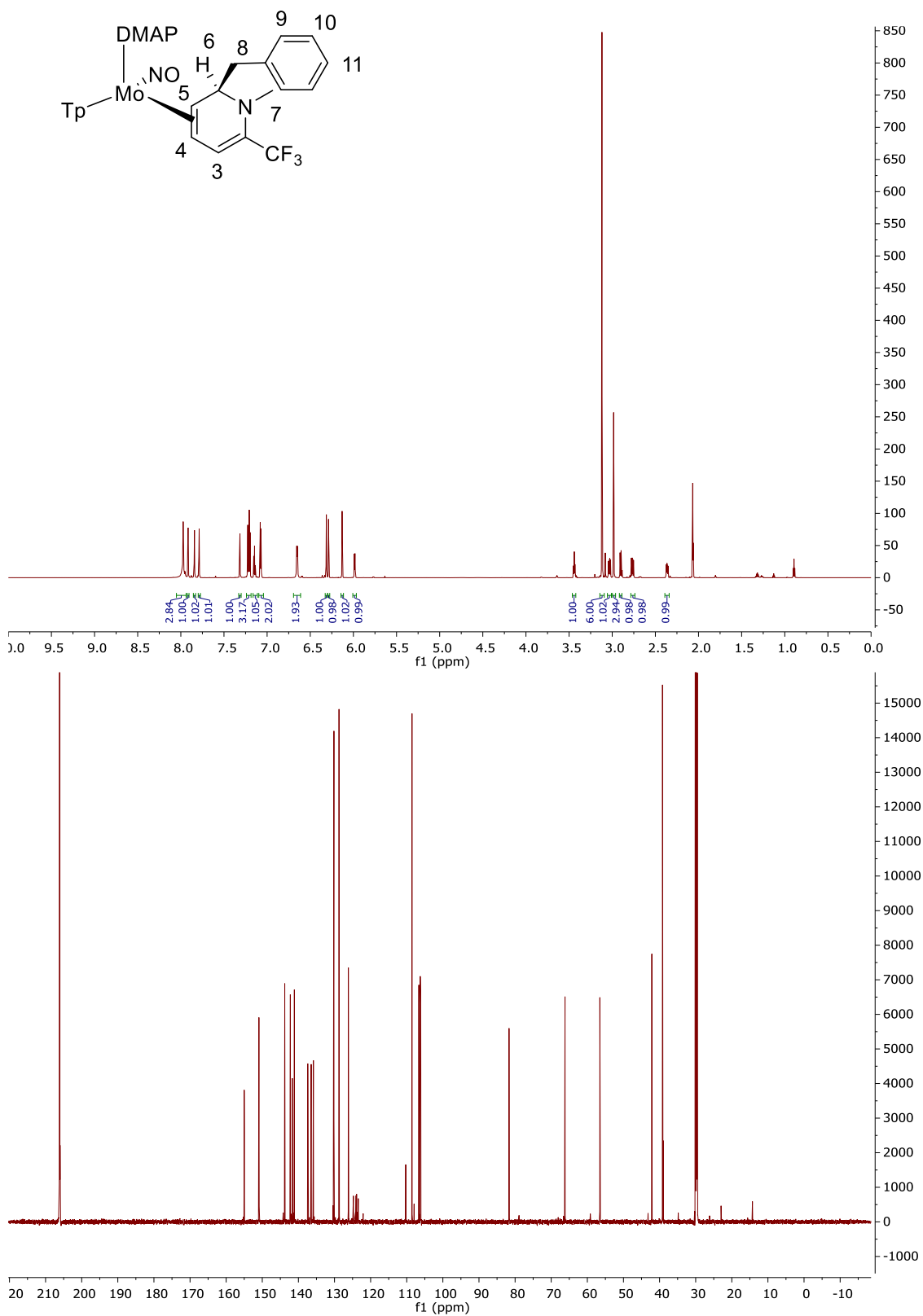


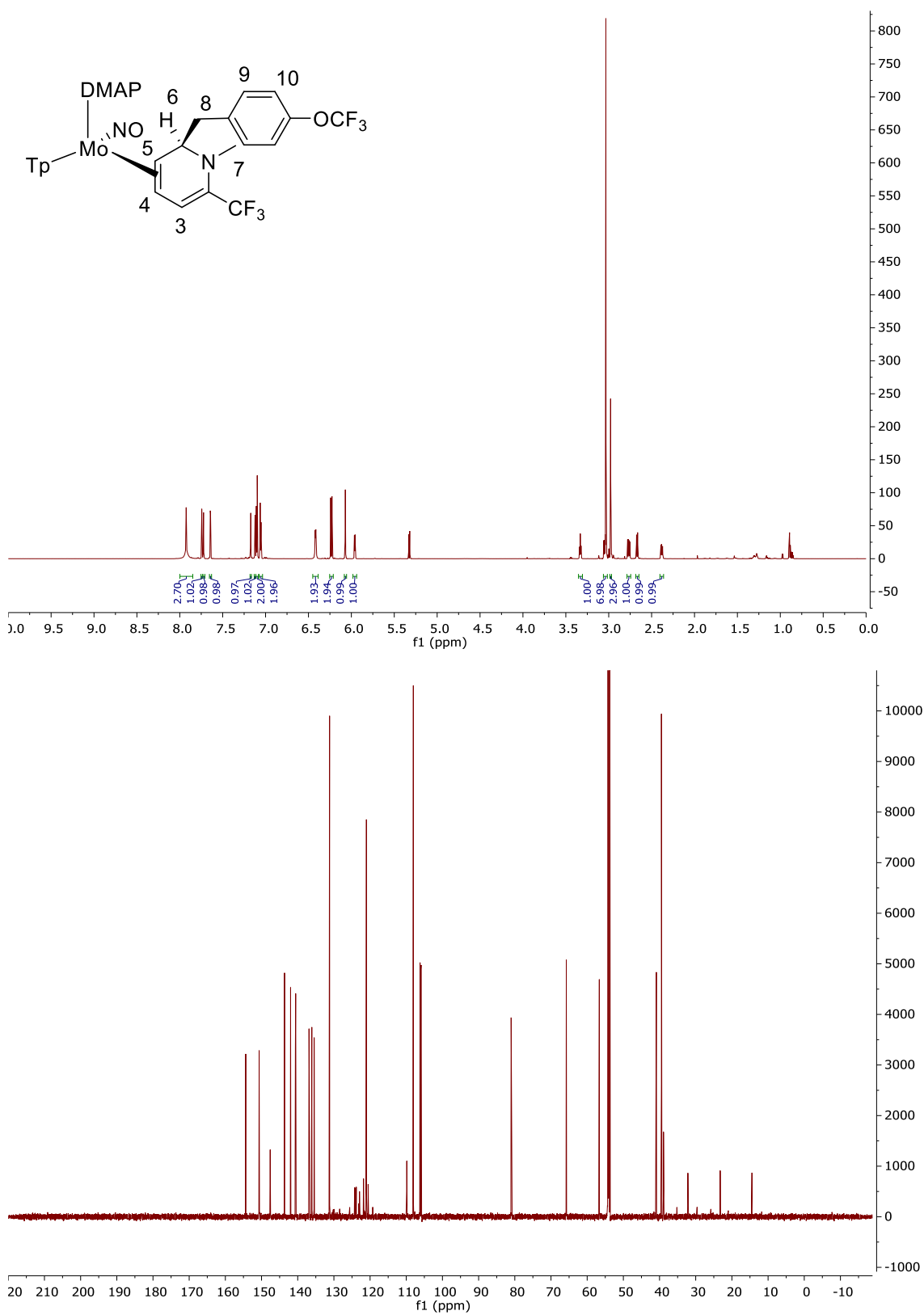
^1H NMR and $^{13}\text{C}\{^1\text{H}\}$ NMR Compound 14:



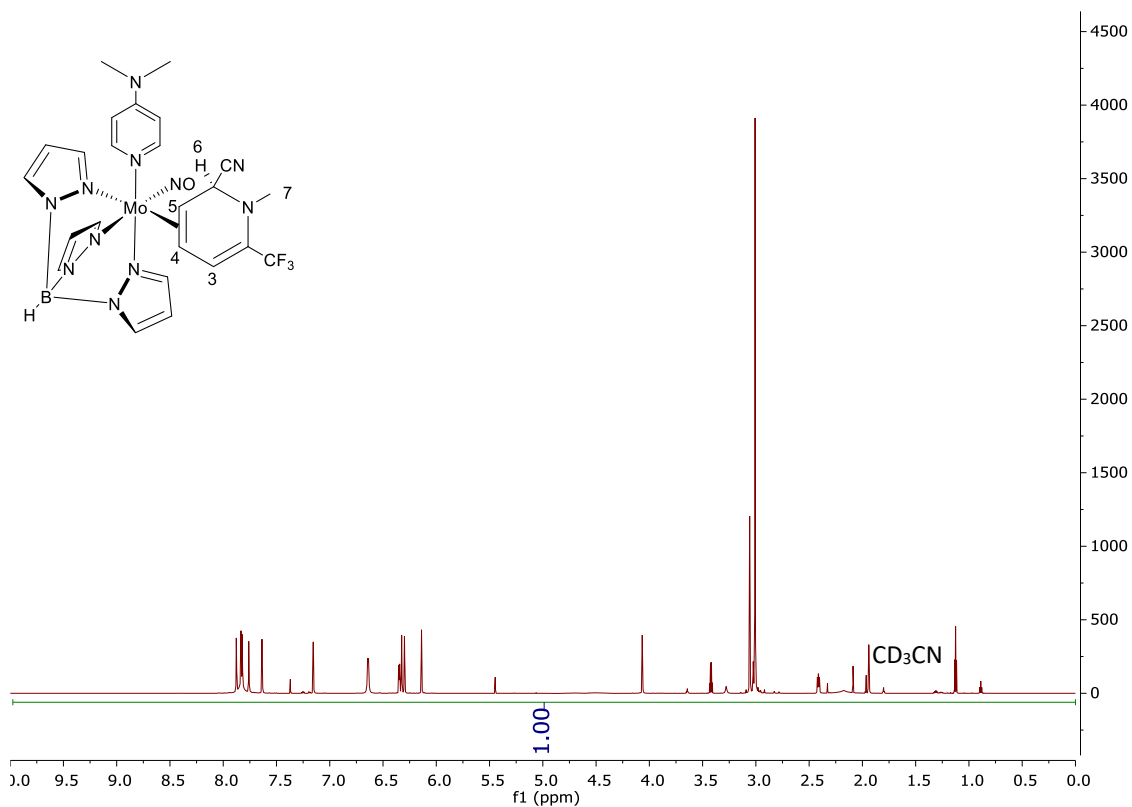
^1H NMR and $^{13}\text{C}\{^1\text{H}\}$ NMR Compound 15:

^1H NMR and $^{13}\text{C}\{^1\text{H}\}$ NMR Compound 16:

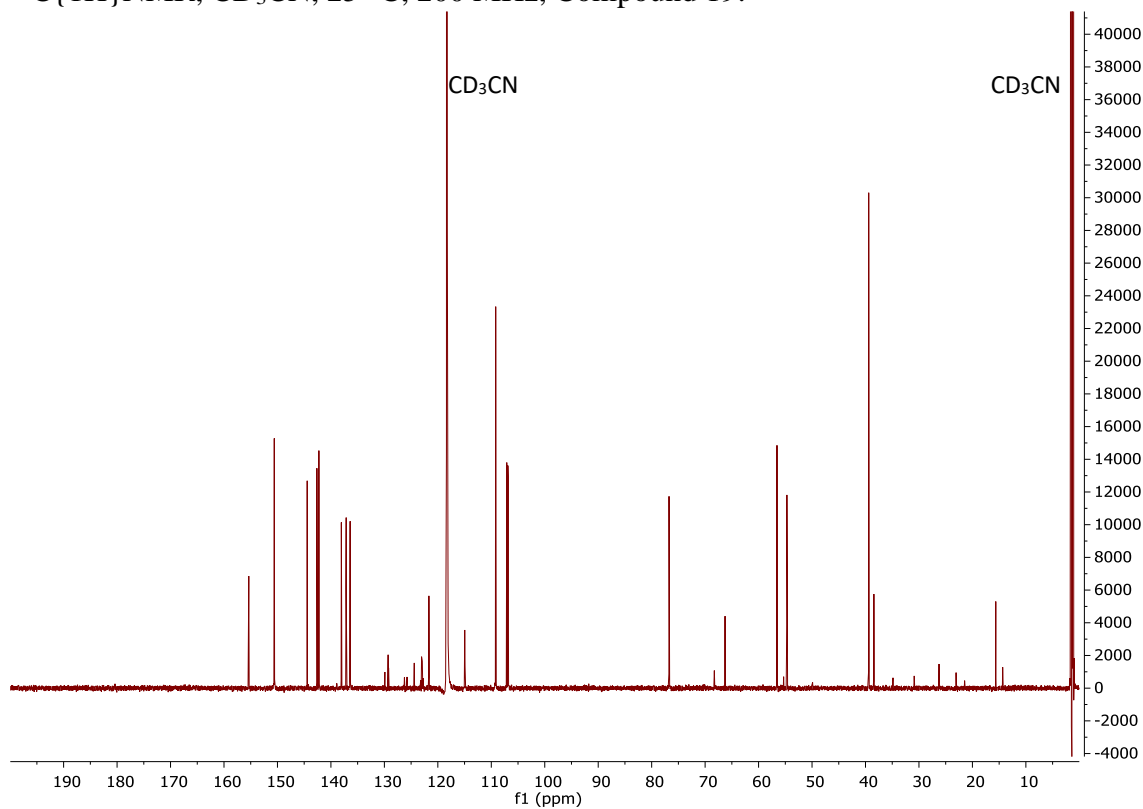
^1H NMR and $^{13}\text{C}\{^1\text{H}\}$ NMR Compound 17:

^1H NMR and $^{13}\text{C}\{^1\text{H}\}$ NMR Compound 18:

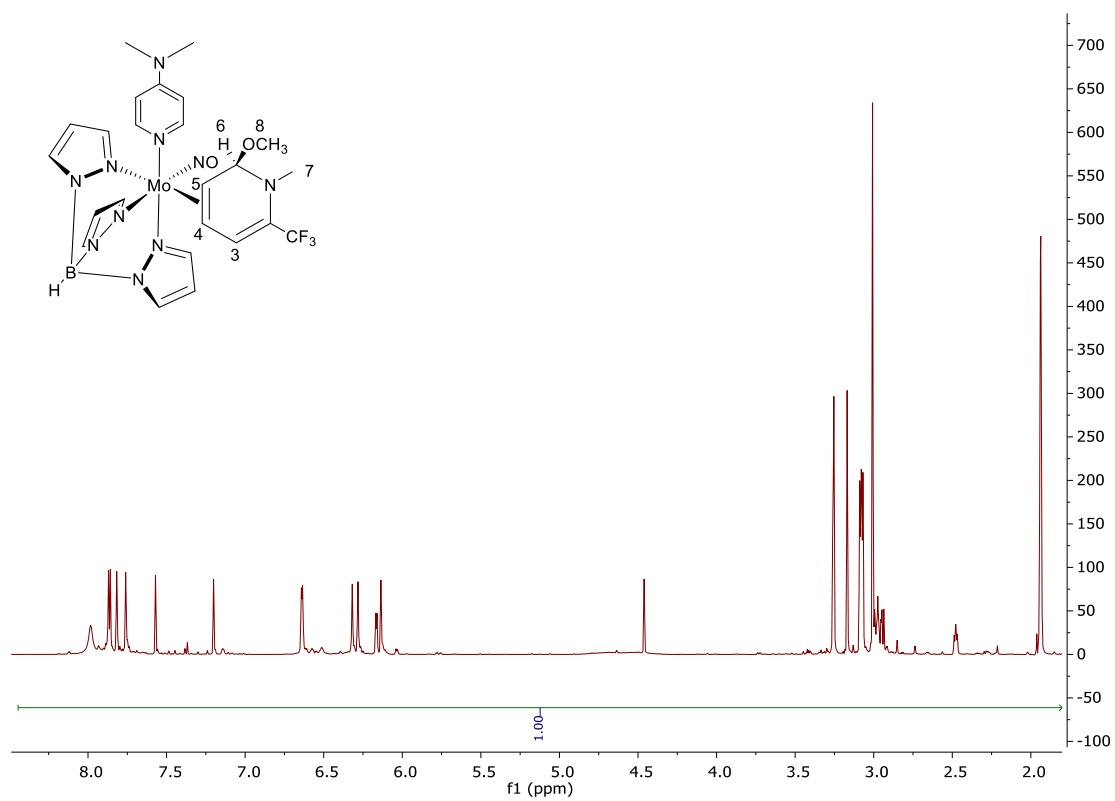
^1H NMR, CD_3CN , 25 °C, 800 MHz, Compound 19:



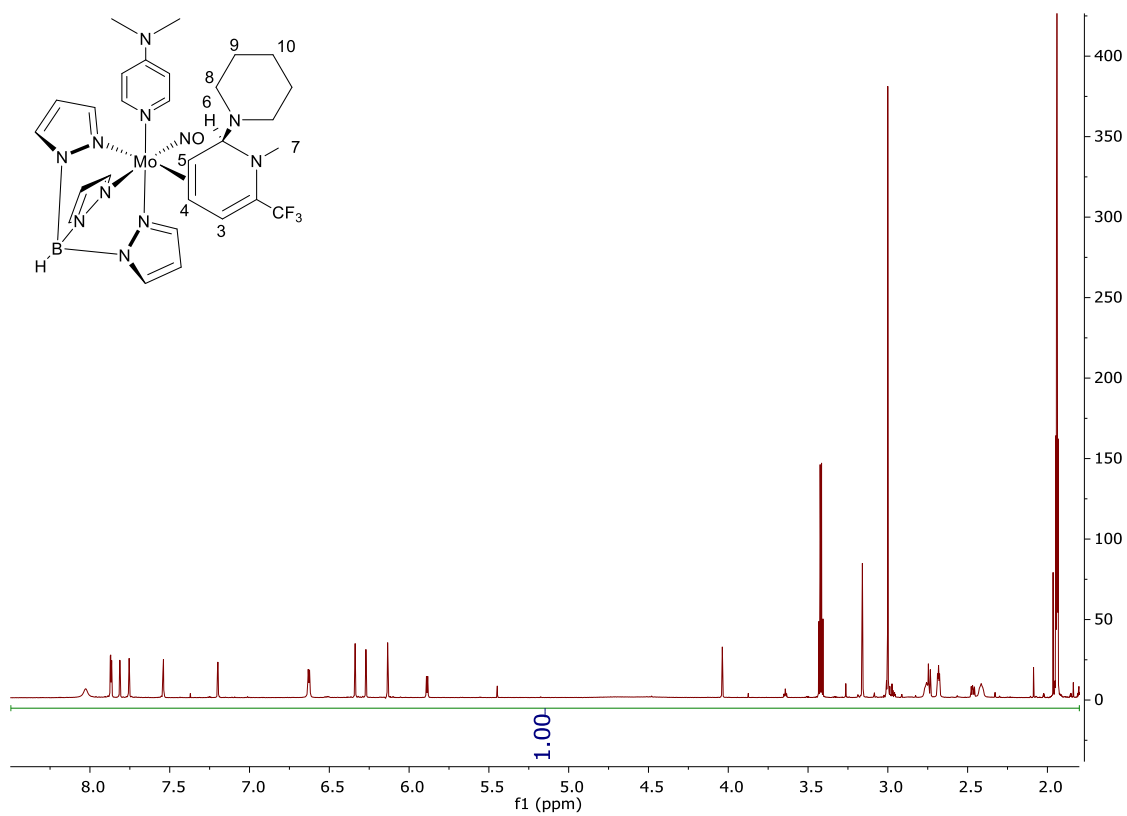
$^{13}\text{C}\{^1\text{H}\}$ NMR, CD_3CN , 25 °C, 200 MHz, Compound 19:



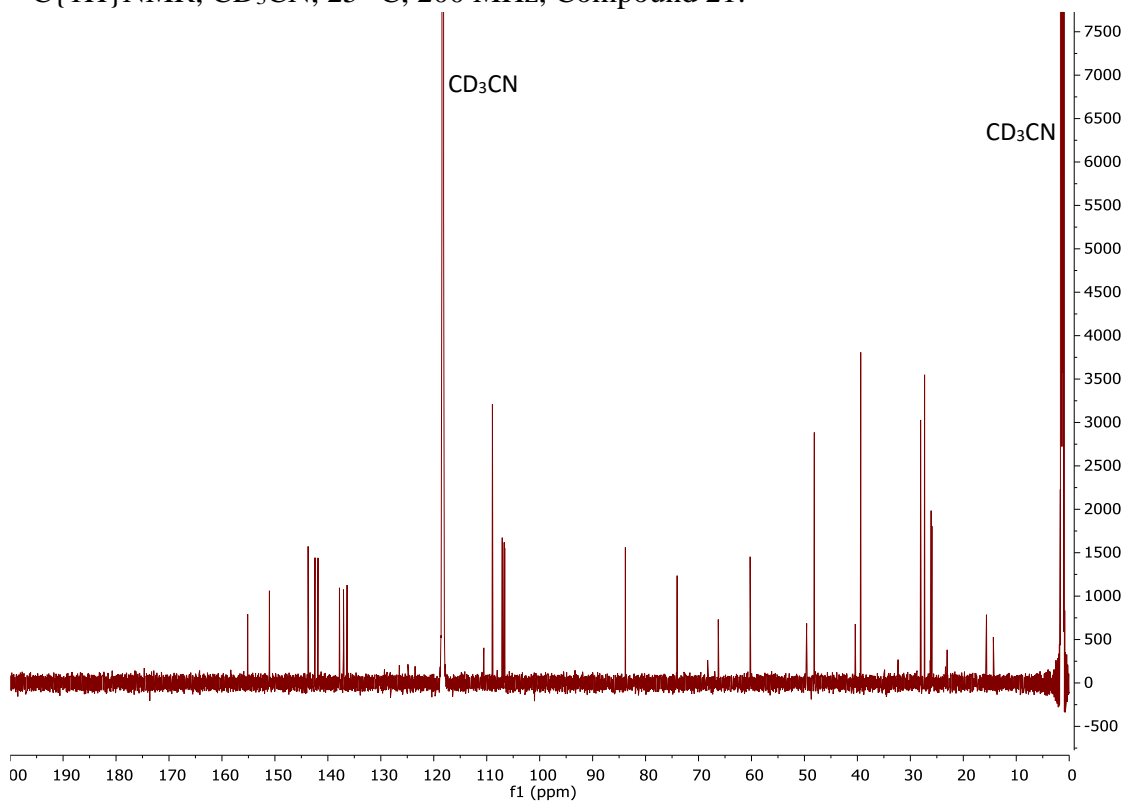
^1H NMR, CD_3CN , 25 °C, 800 MHz, Compound 20:



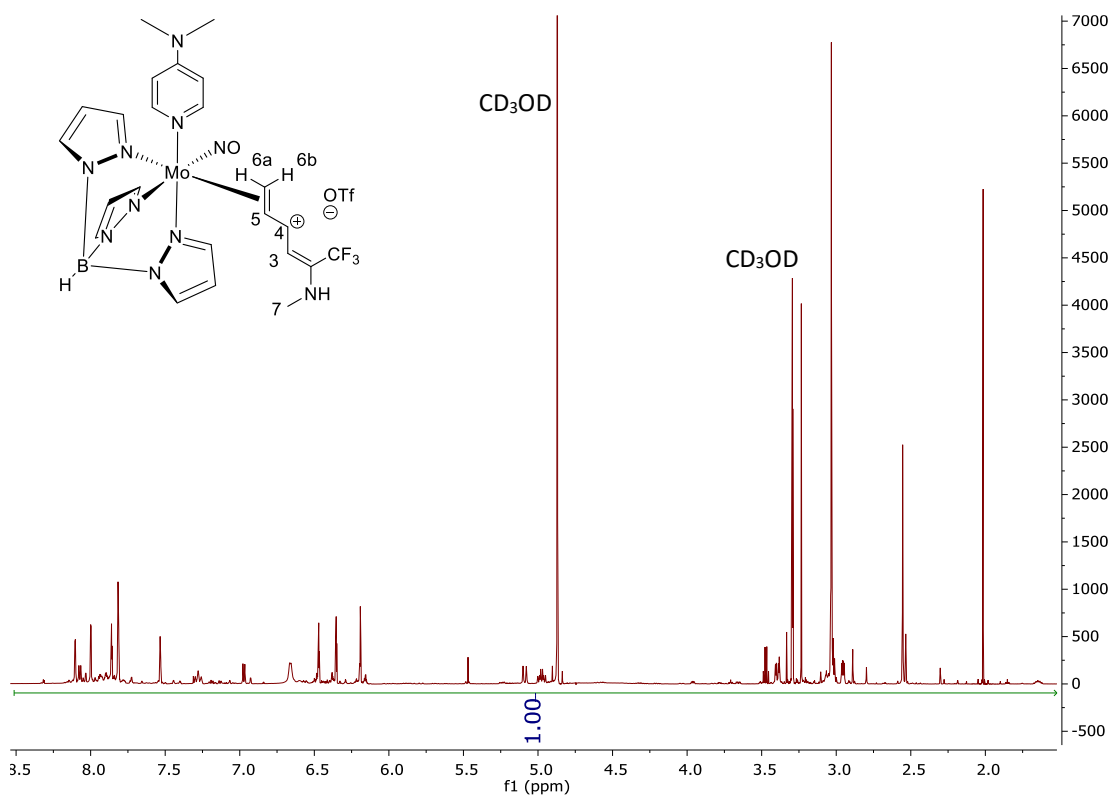
^1H NMR, CD_3CN , 25 °C, 800 MHz, Compound 21:



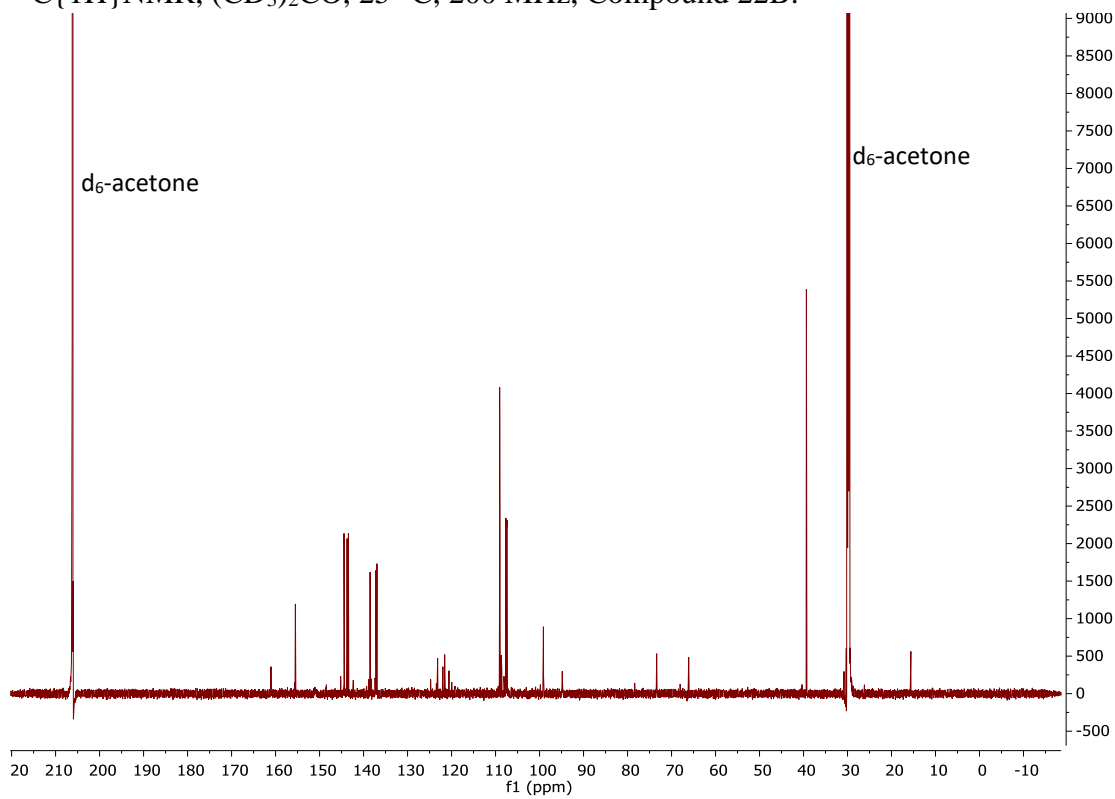
$^{13}\text{C}\{^1\text{H}\}$ NMR, CD_3CN , 25 °C, 200 MHz, Compound 21:



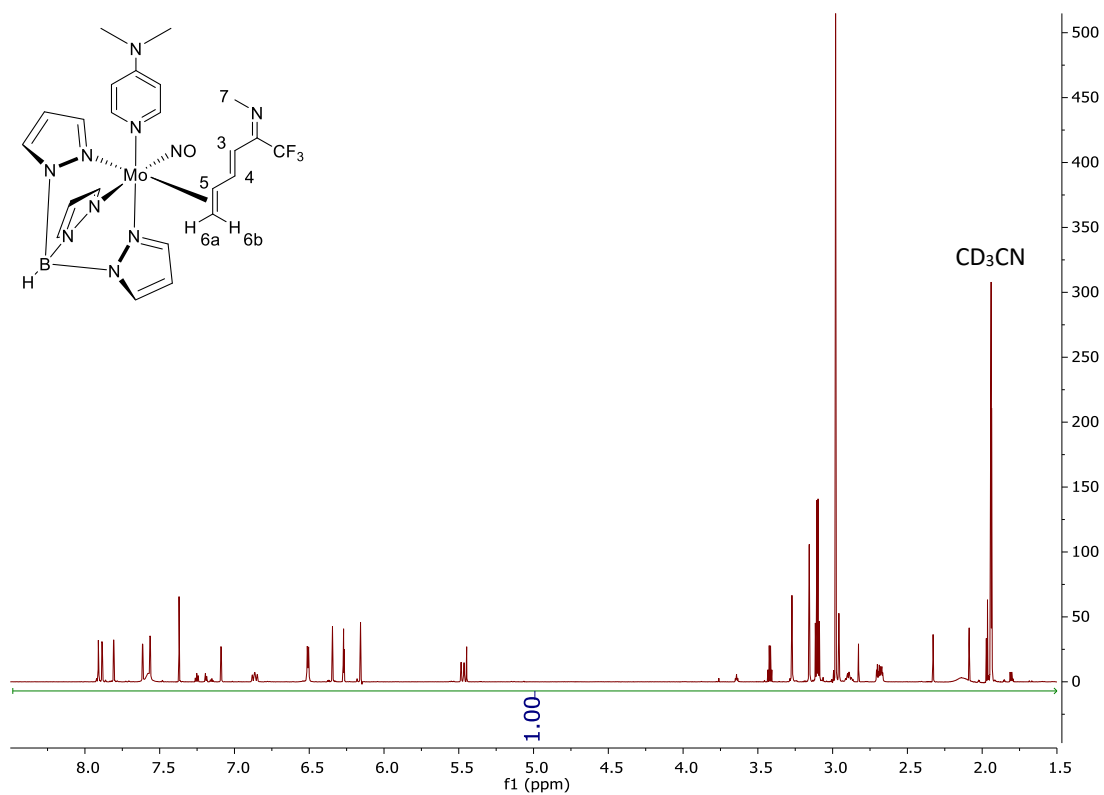
^1H NMR, CD_3OD , 25°C , 600 MHz, Compound 22B:



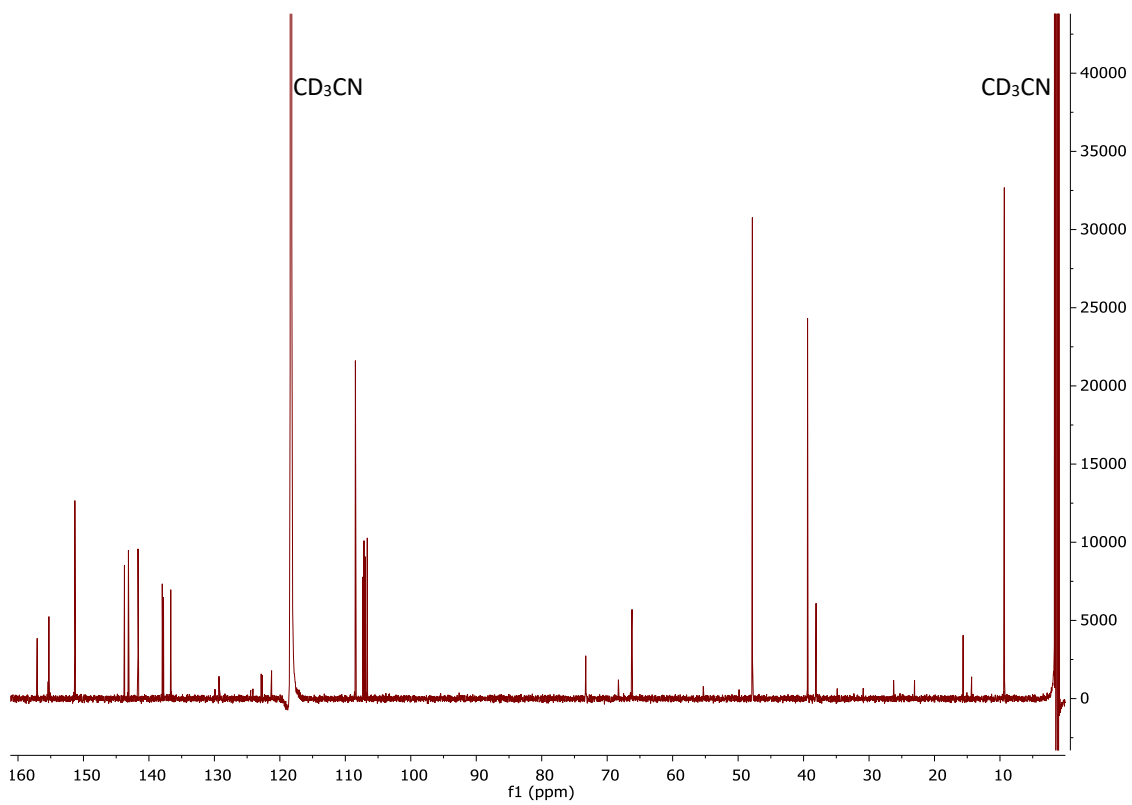
$^{13}\text{C}\{^1\text{H}\}$ NMR, $(\text{CD}_3)_2\text{CO}$, 25°C , 200 MHz, Compound 22B:



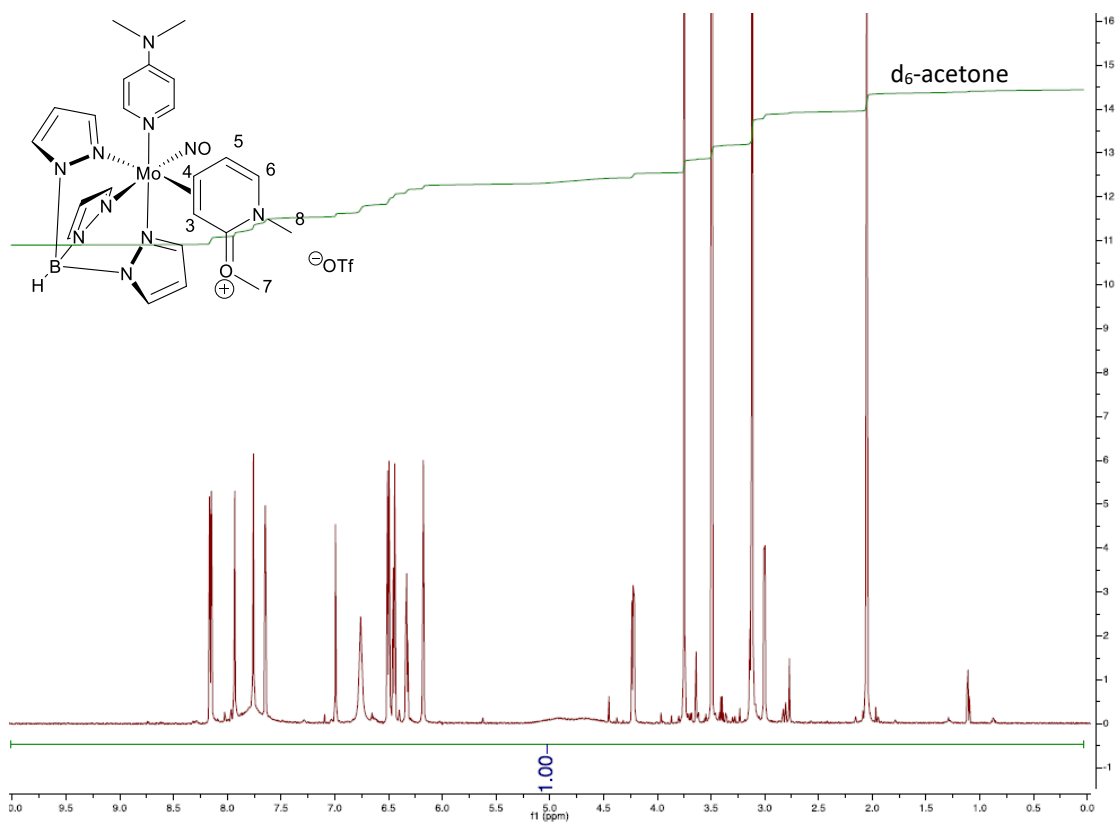
^1H NMR, CD_3CN , $25\text{ }^\circ\text{C}$, 800 MHz, Compound 23A:



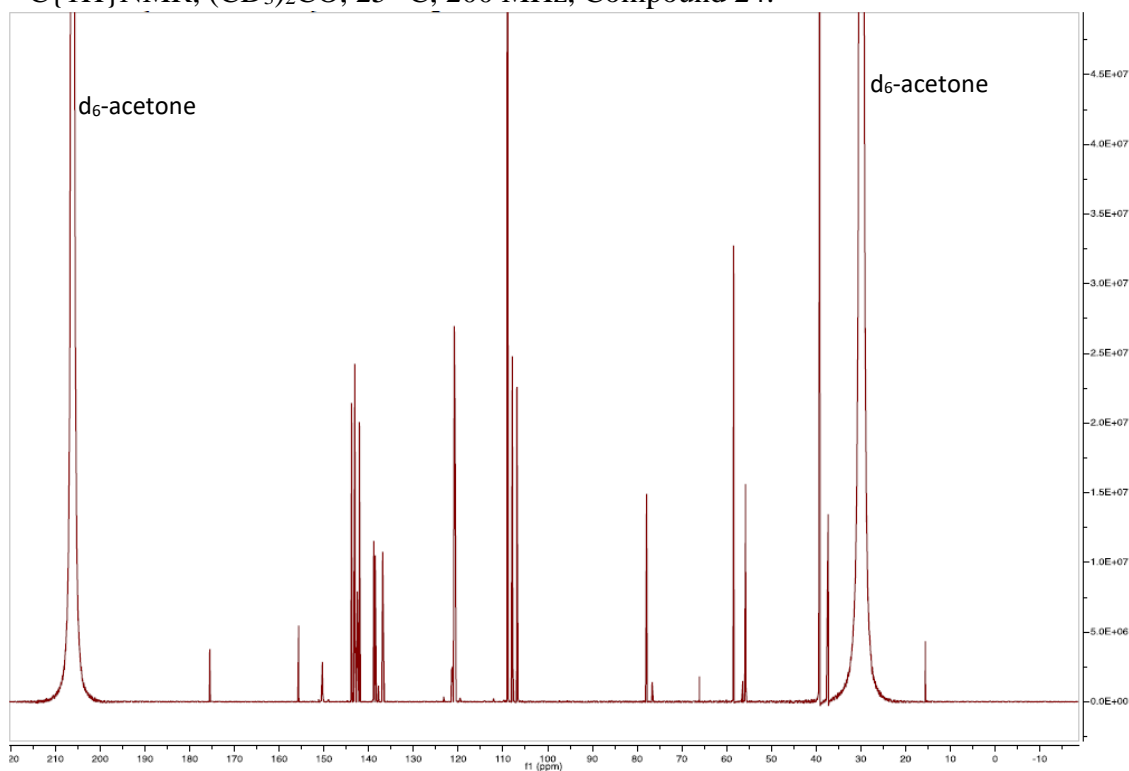
$^{13}\text{C}\{^1\text{H}\}$ NMR, CD_3CN , $25\text{ }^\circ\text{C}$, 200 MHz, Compound 23A:



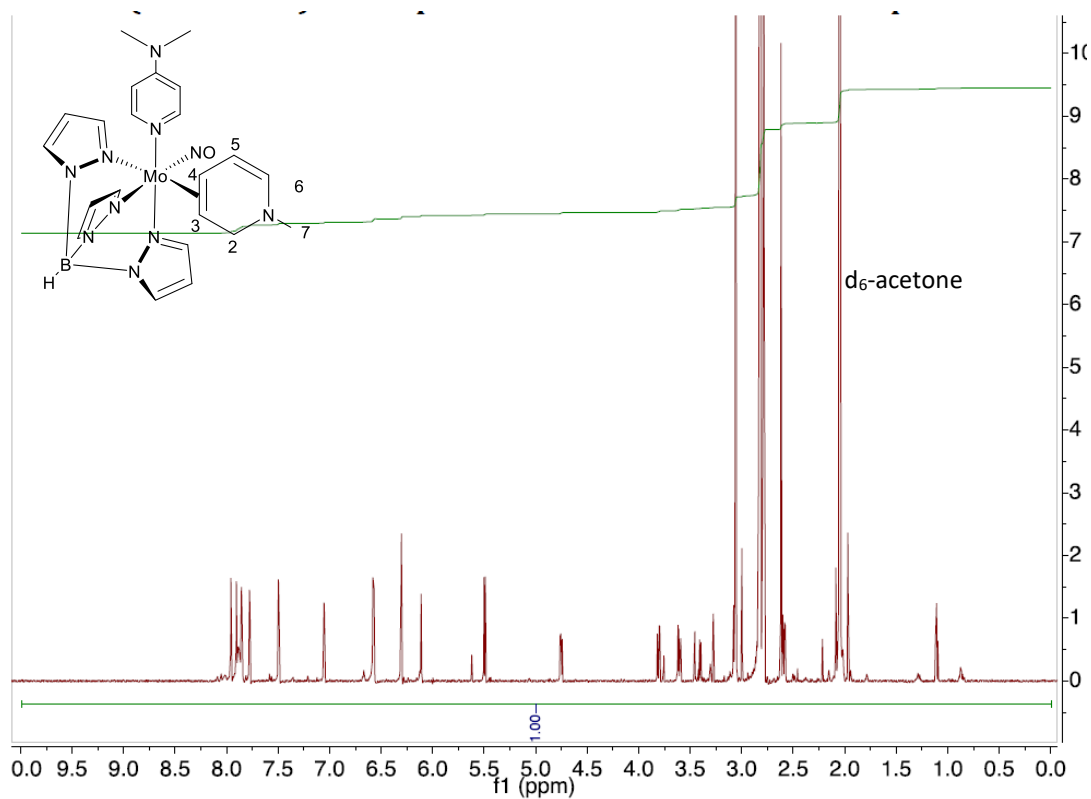
^1H NMR, $(\text{CD}_3)_2\text{CO}$, 25 °C, 600 MHz, Compound 24:



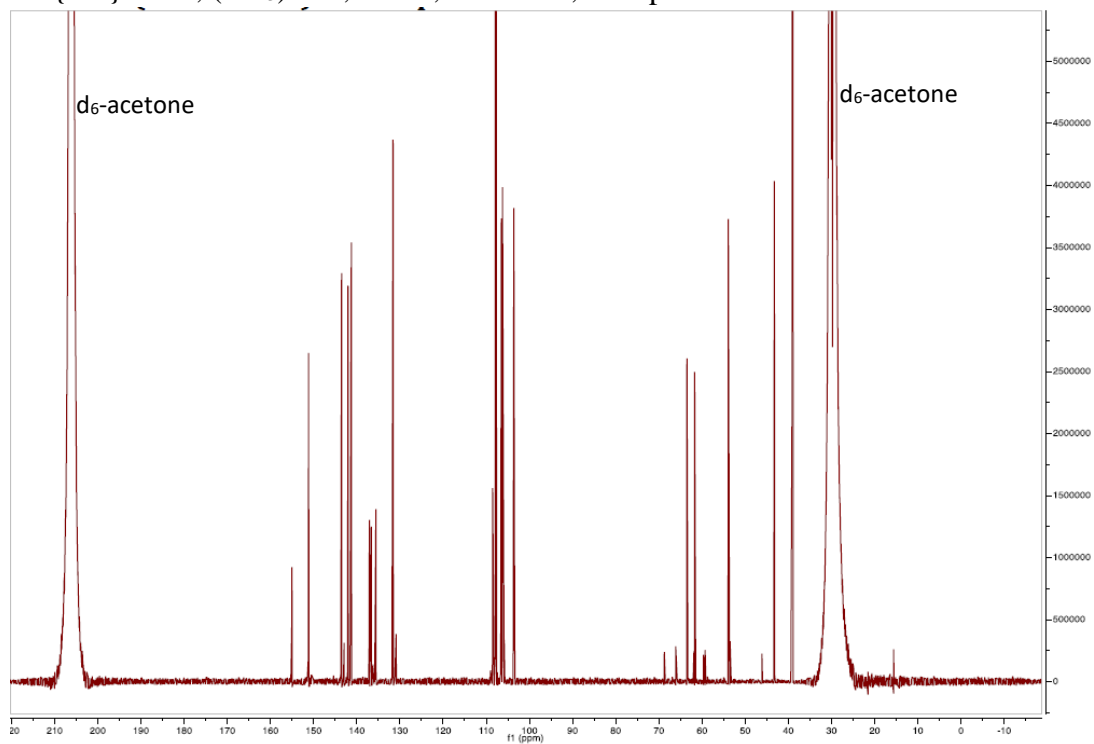
$^{13}\text{C}\{^1\text{H}\}$ NMR, $(\text{CD}_3)_2\text{CO}$, 25 °C, 200 MHz, Compound 24:



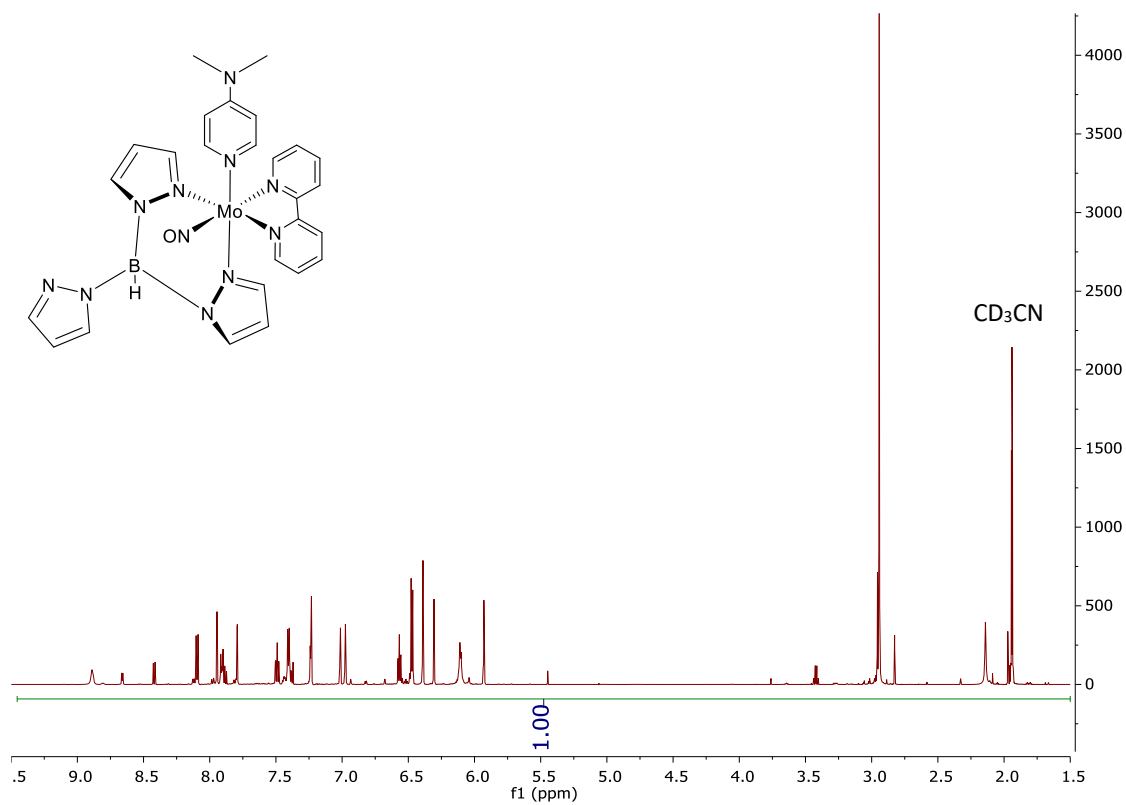
^1H NMR, $(\text{CD}_3)_2\text{CO}$, 25 °C, 600 MHz, Compound 25:



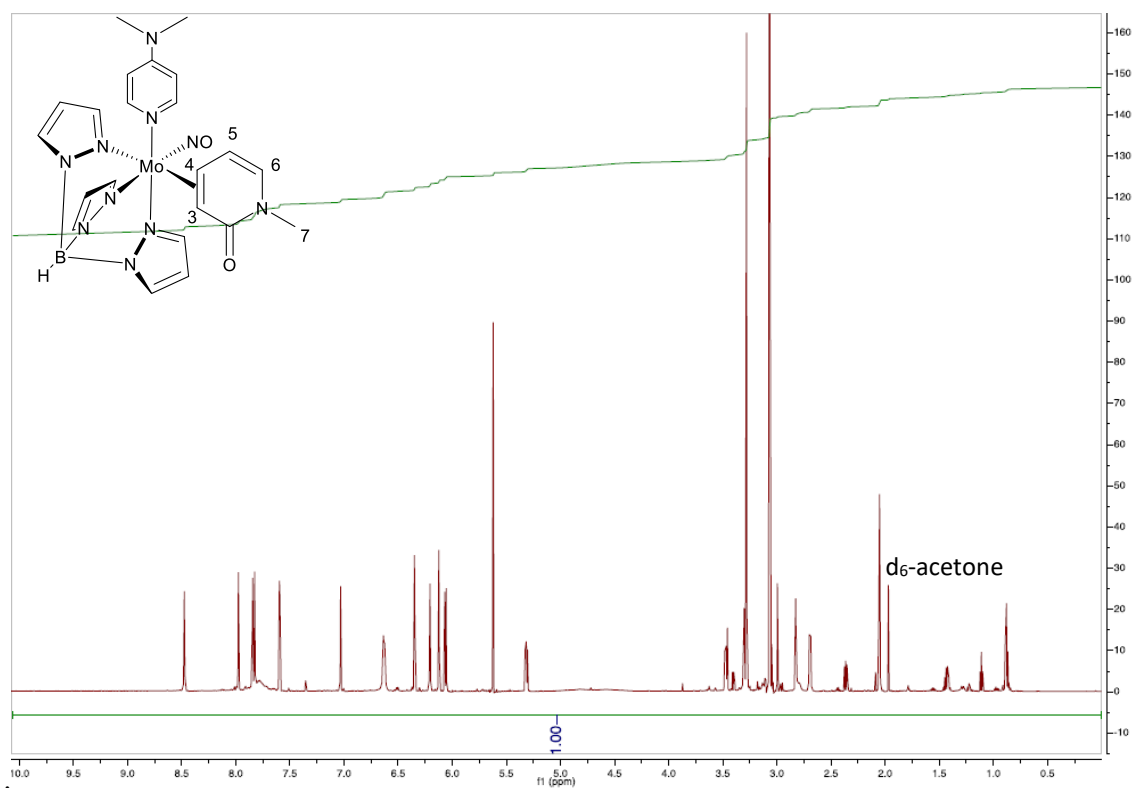
$^{13}\text{C}\{^1\text{H}\}$ NMR, $(\text{CD}_3)_2\text{CO}$, 25 °C, 200 MHz, Compound 25:



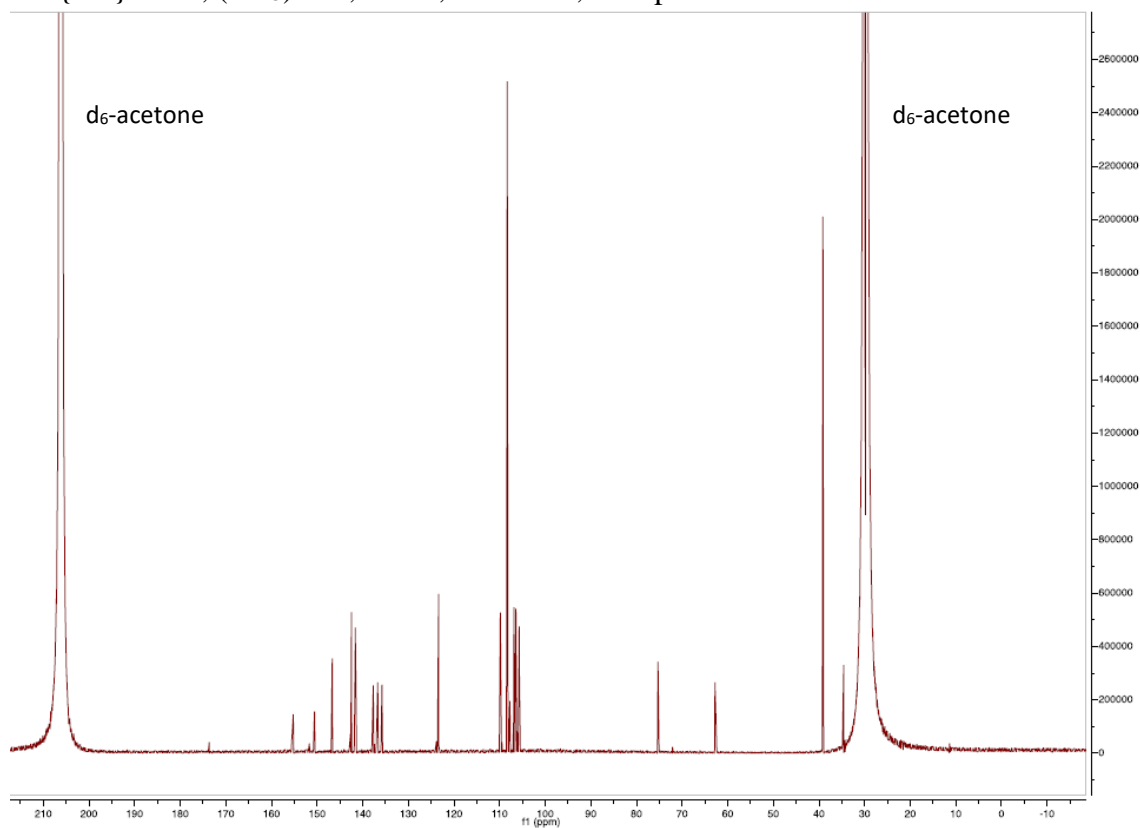
^1H NMR, CD_3CN , 25 °C, 600 MHz, Compound 28:

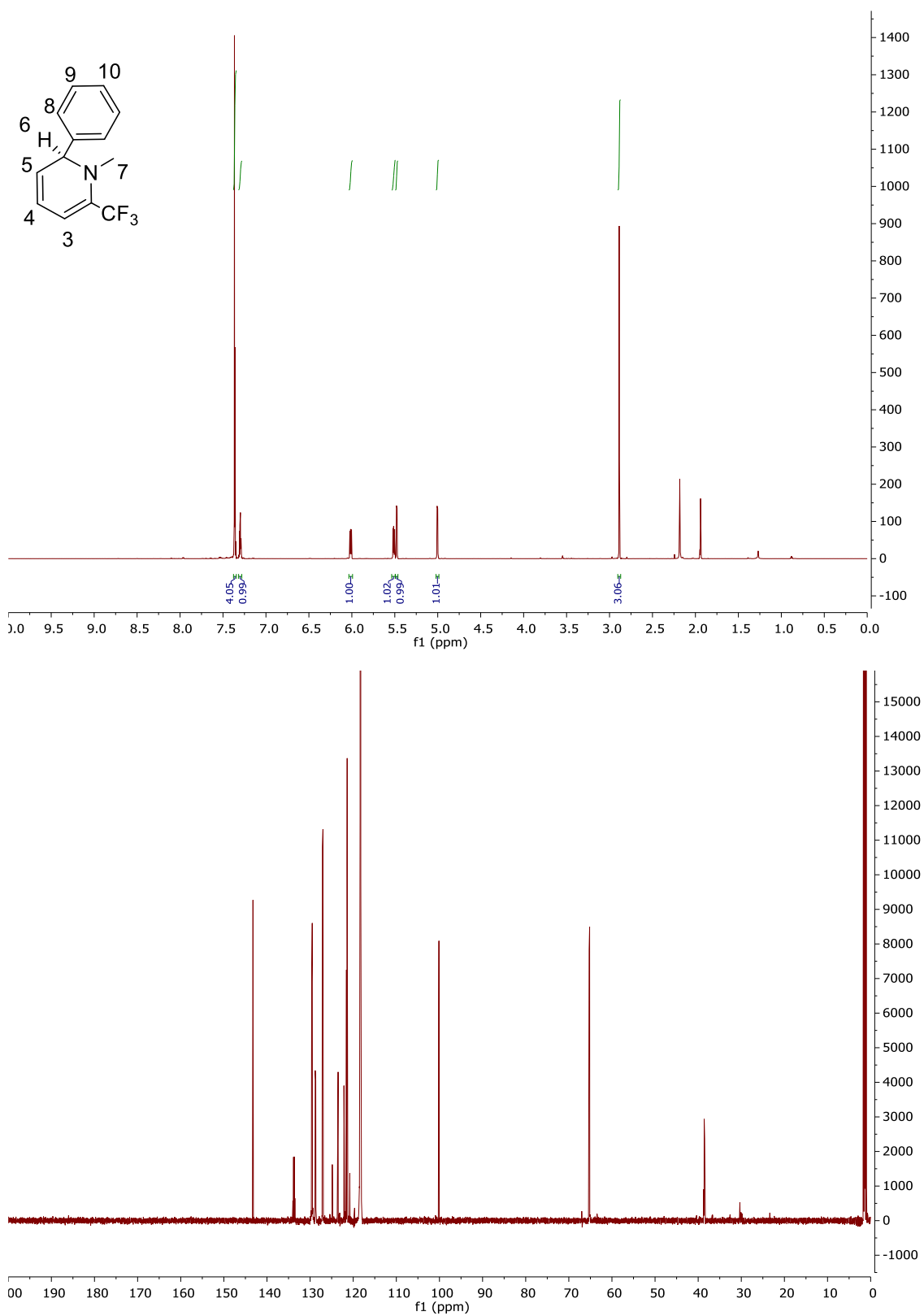


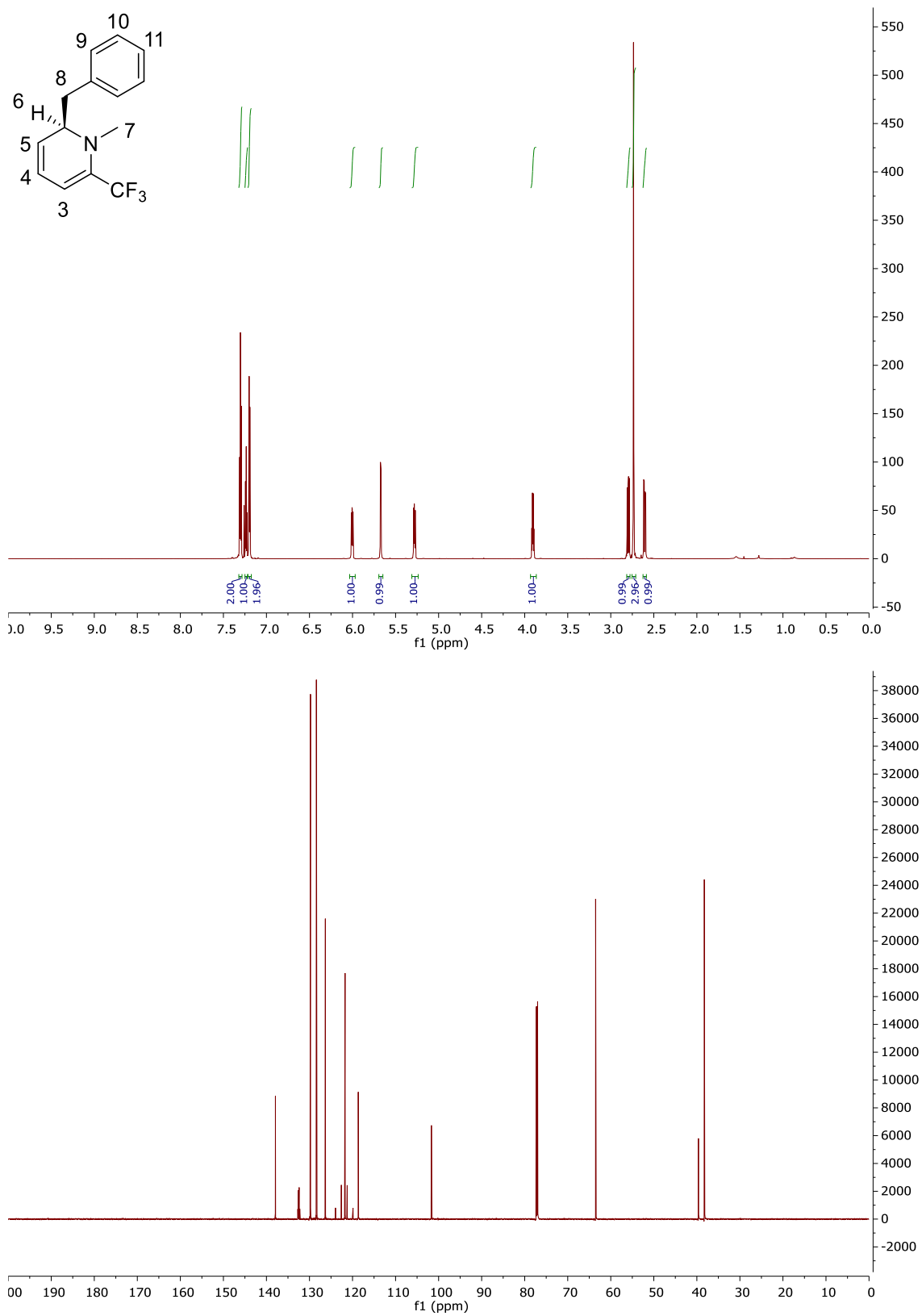
^1H NMR, $(\text{CD}_3)_2\text{CO}$, 25 °C, 600 MHz, Compound 29:

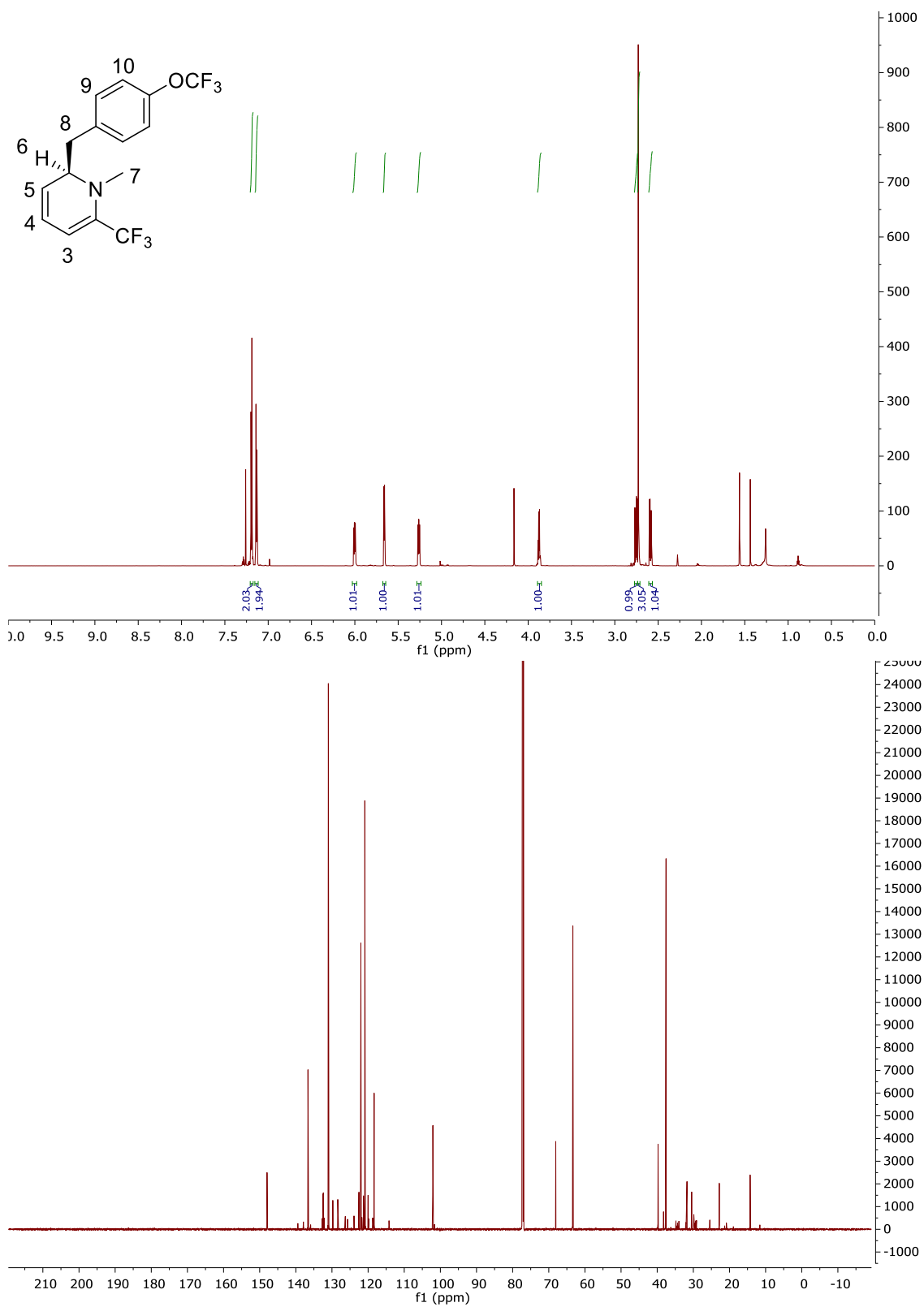


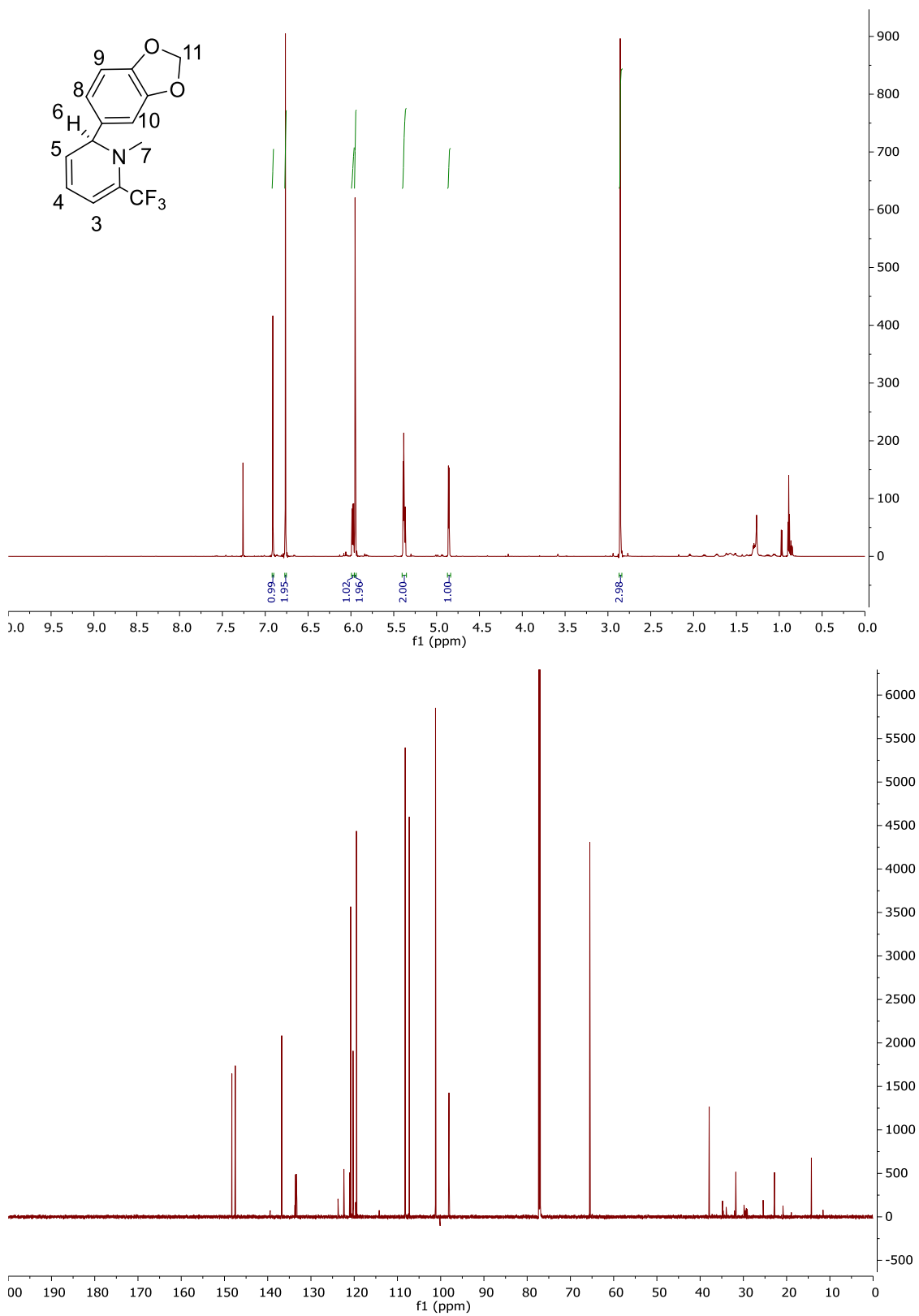
$^{13}\text{C}\{^1\text{H}\}$ NMR, $(\text{CD}_3)_2\text{CO}$, 25 °C, 200 MHz, Compound 29:

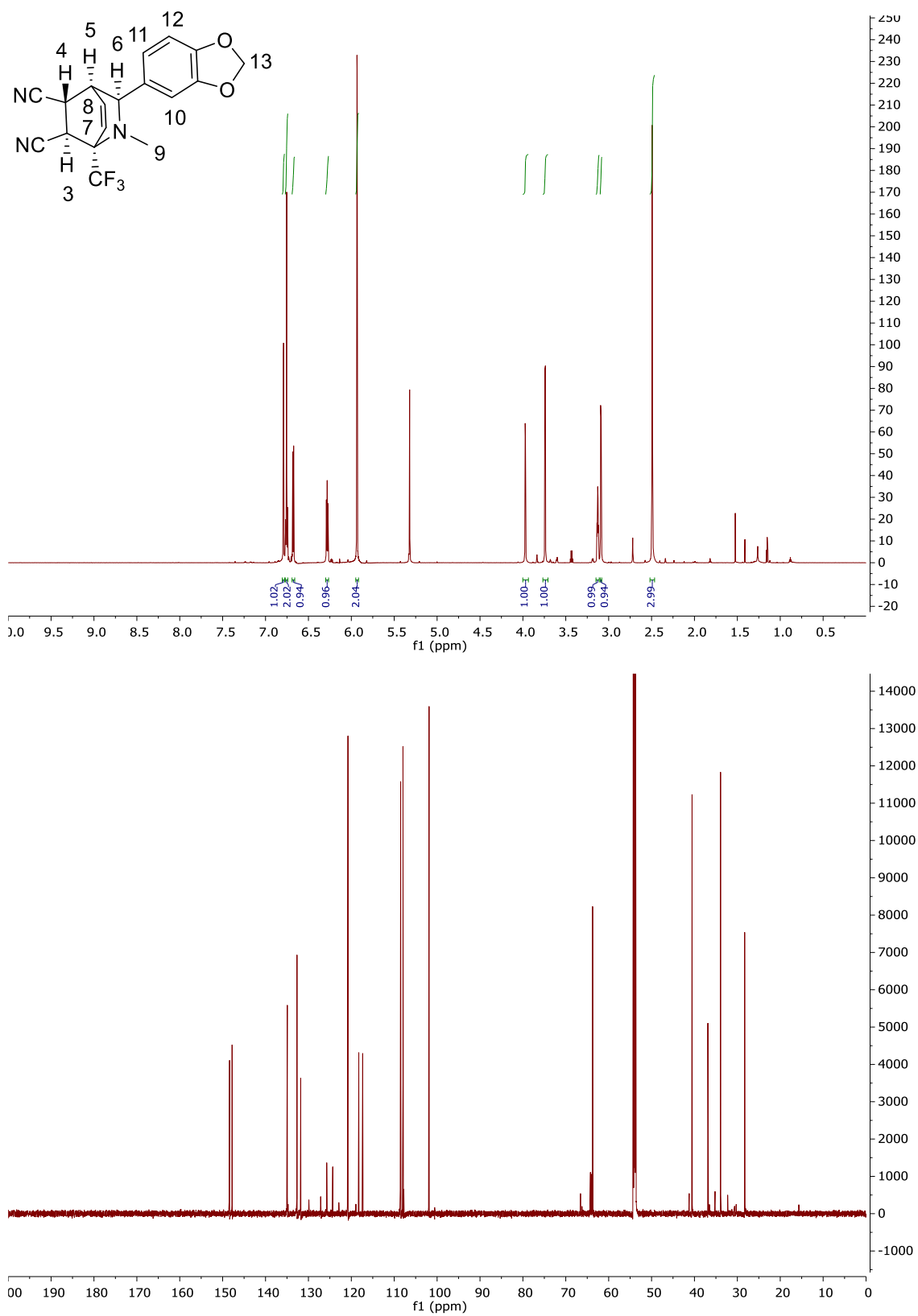


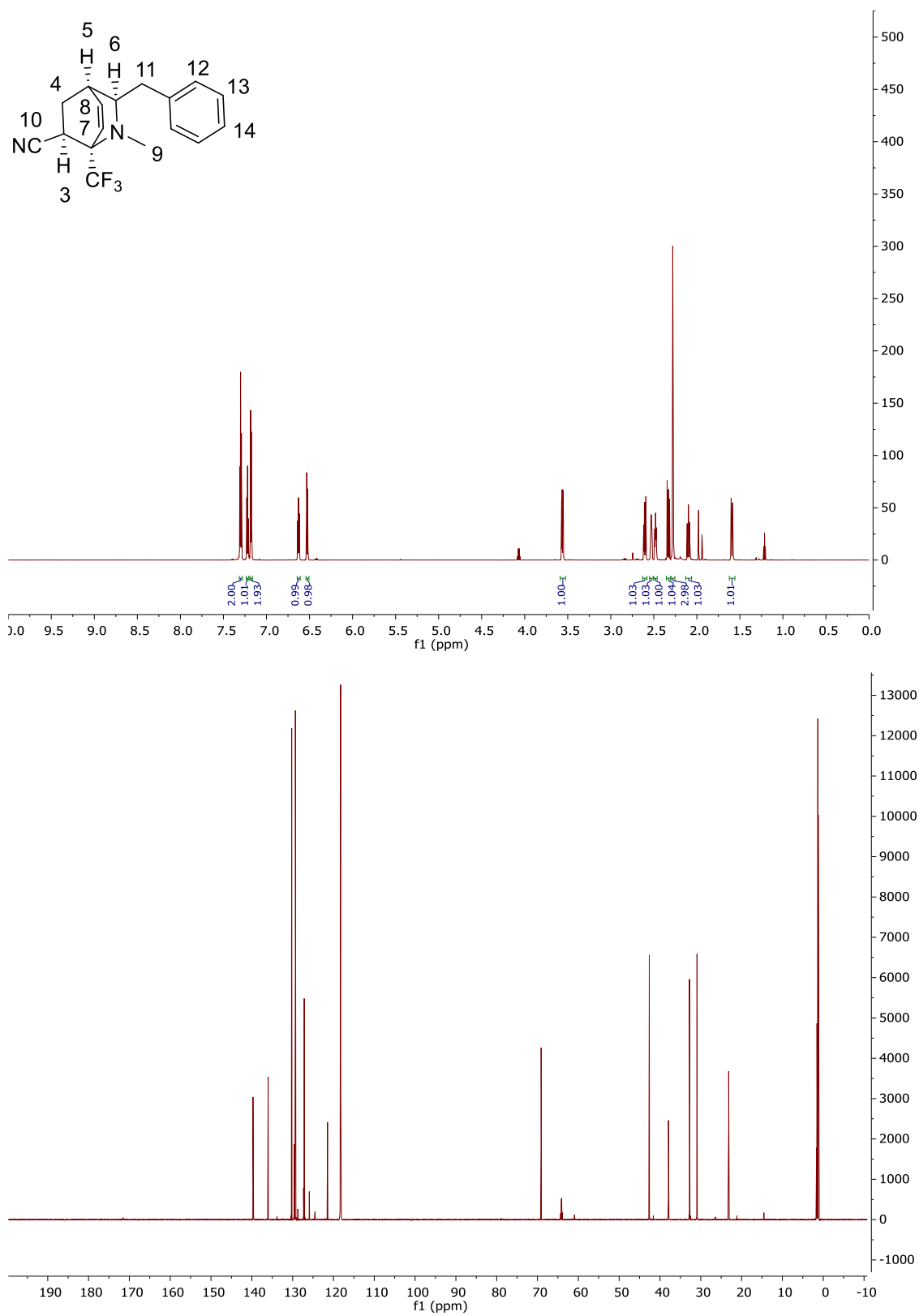
^1H NMR and $^{13}\text{C}\{^1\text{H}\}$ NMR Compound 31:

^1H NMR and $^{13}\text{C}\{^1\text{H}\}$ NMR Compound 32:

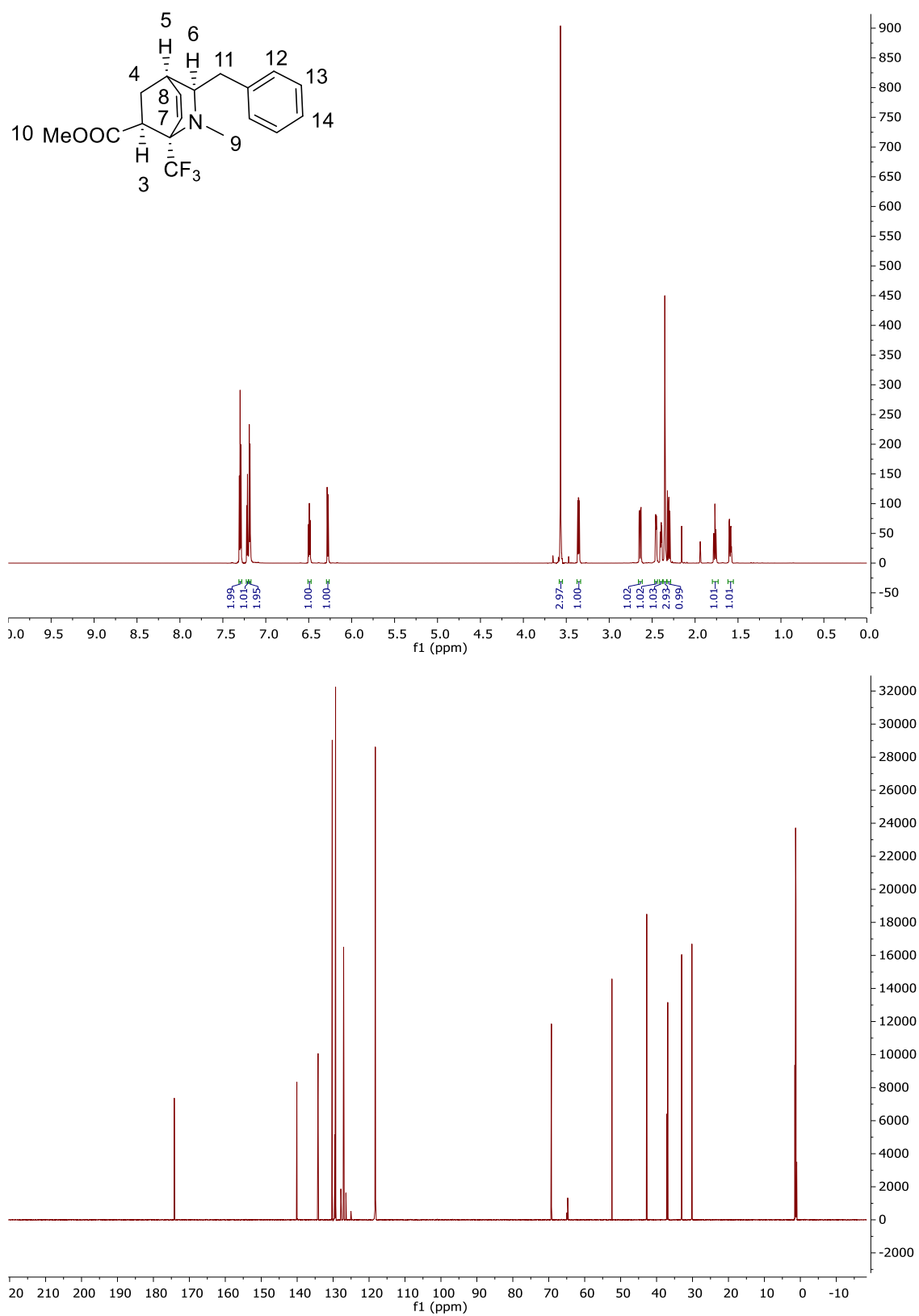
^1H NMR and $^{13}\text{C}\{^1\text{H}\}$ NMR Compound 33:

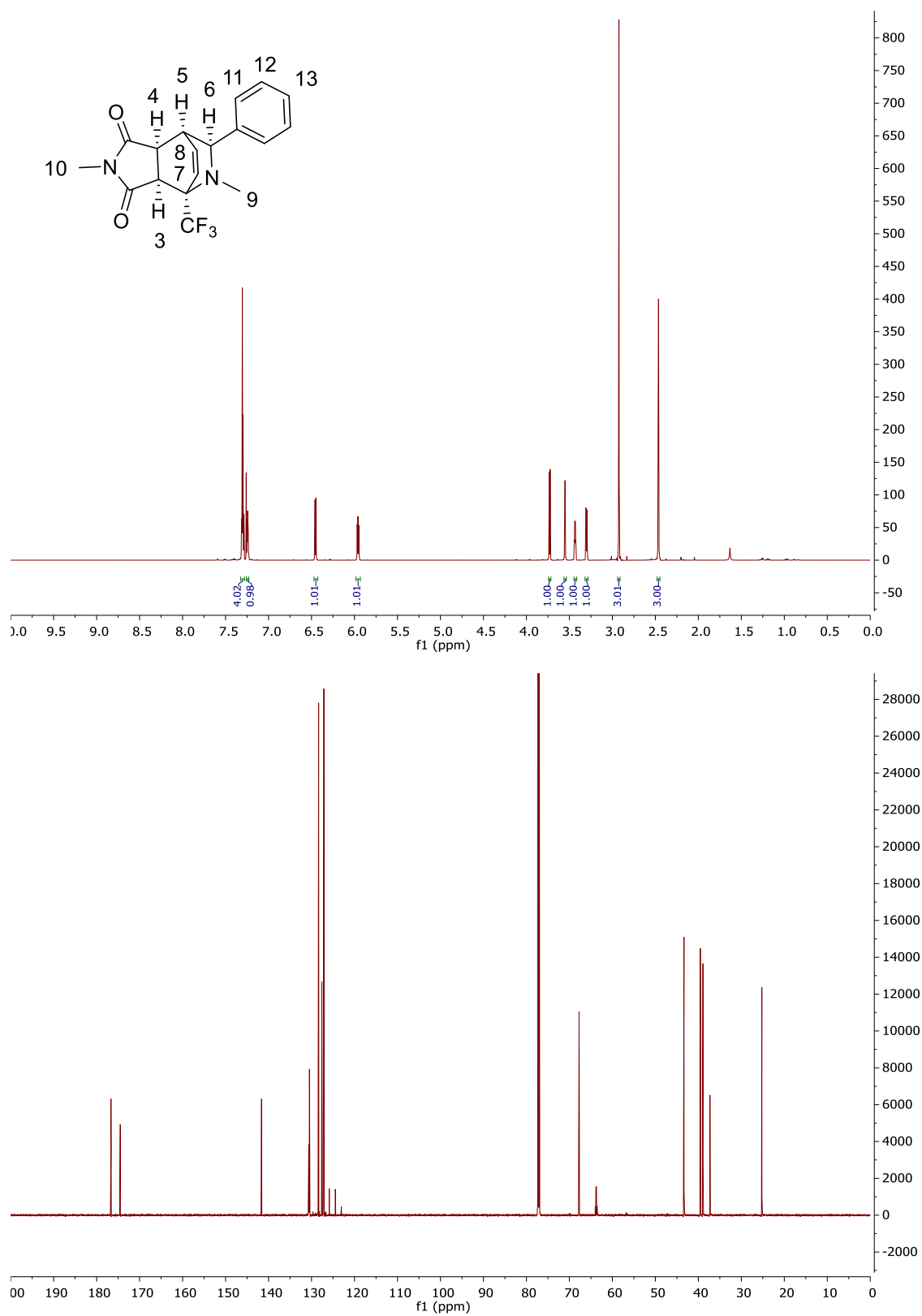
^1H NMR and $^{13}\text{C}\{^1\text{H}\}$ NMR Compound 34:

^1H NMR and $^{13}\text{C}\{^1\text{H}\}$ NMR Compound 35A:

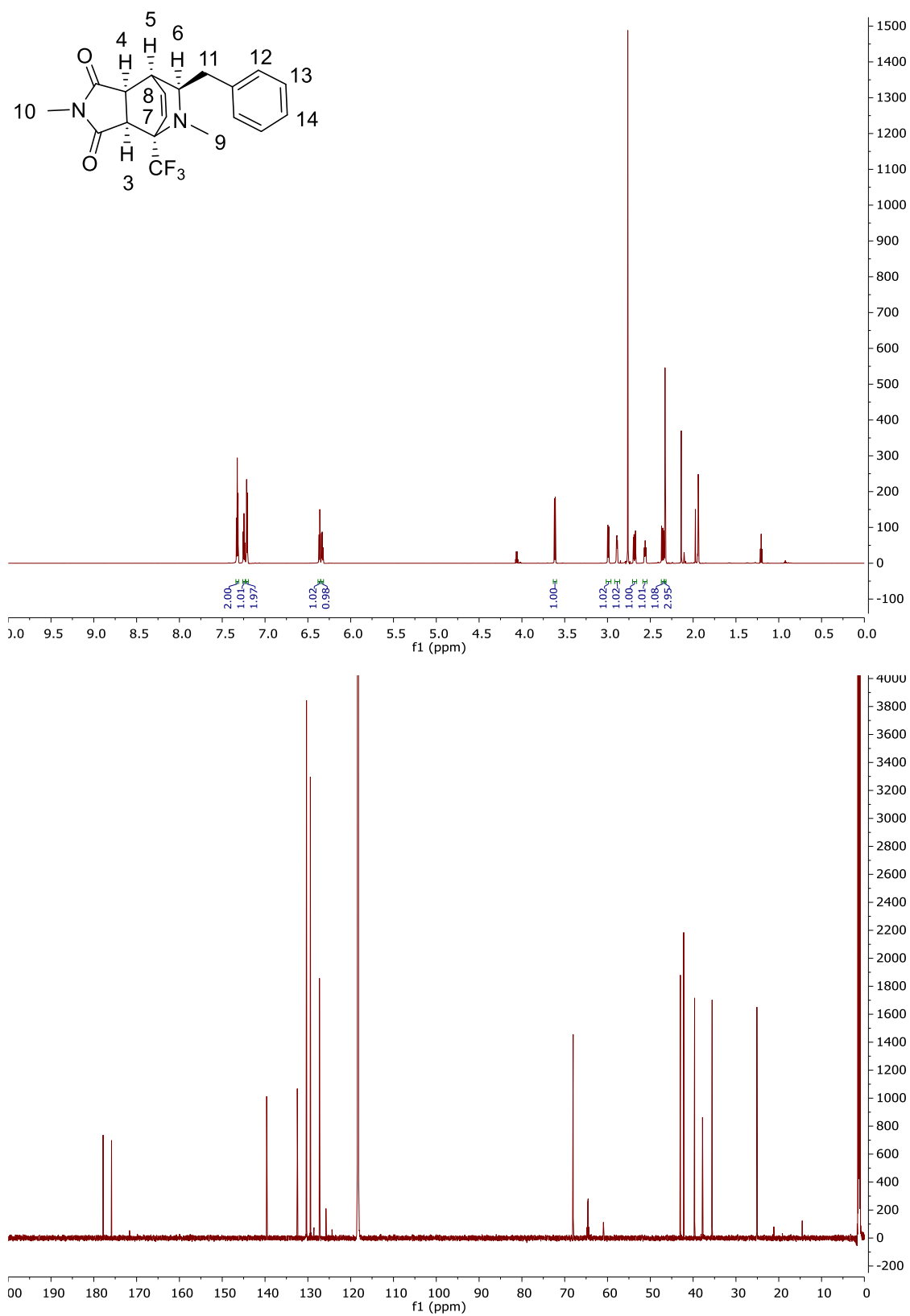
^1H NMR and $^{13}\text{C}\{^1\text{H}\}$ NMR Compound 36A:

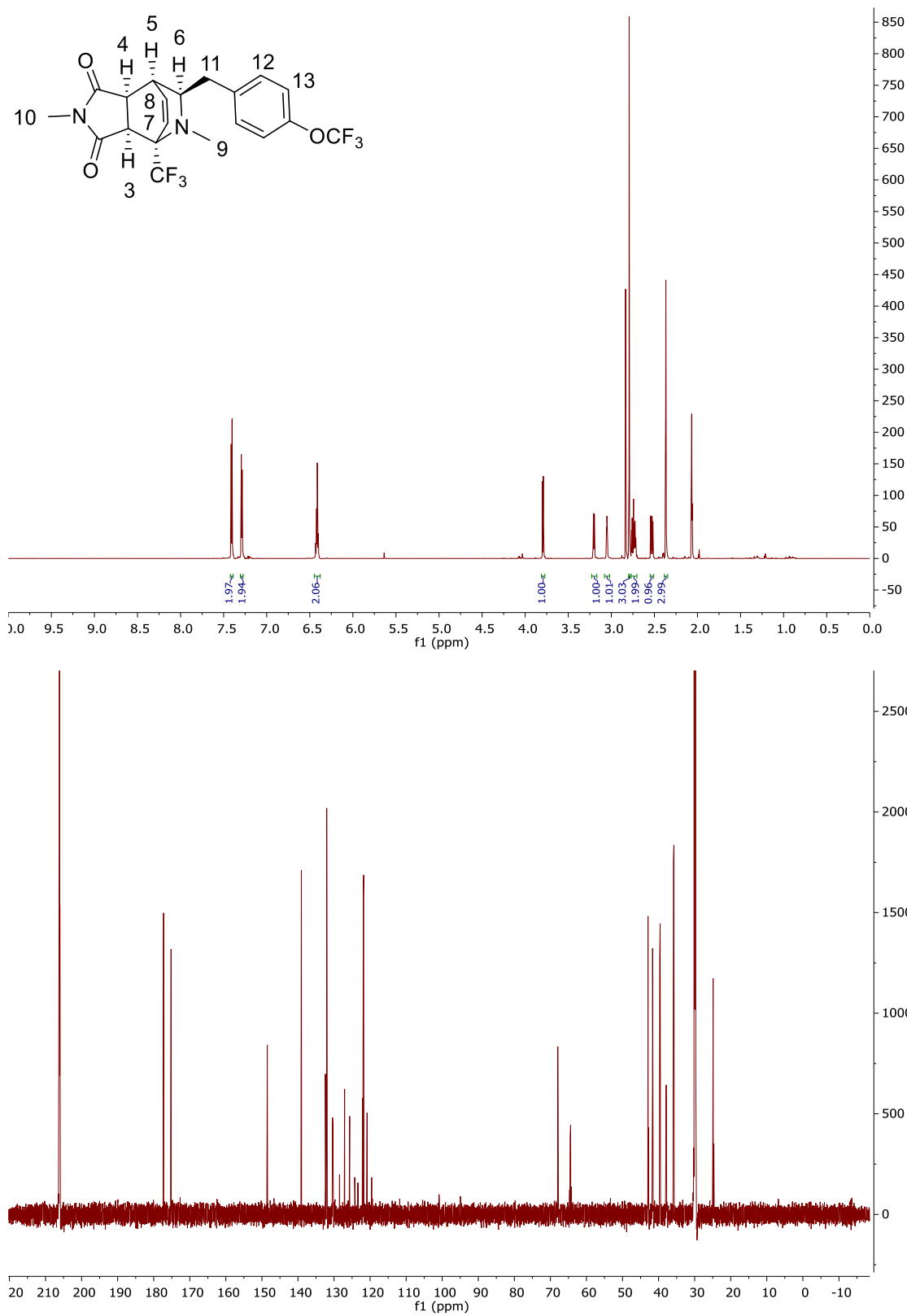
^1H NMR and $^{13}\text{C}\{^1\text{H}\}$ NMR Compound 37A:

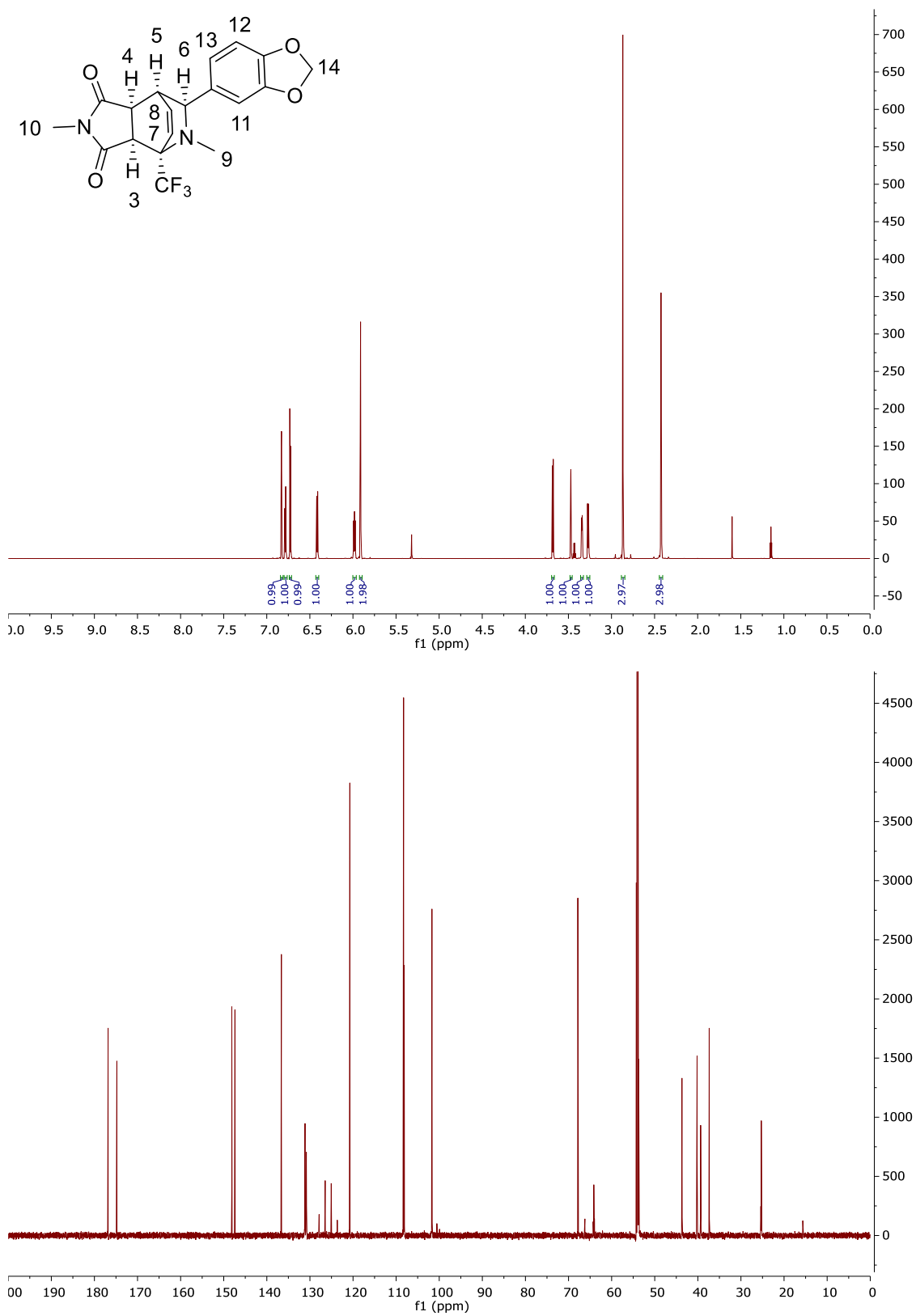


^1H NMR and $^{13}\text{C}\{^1\text{H}\}$ NMR Compound 38:

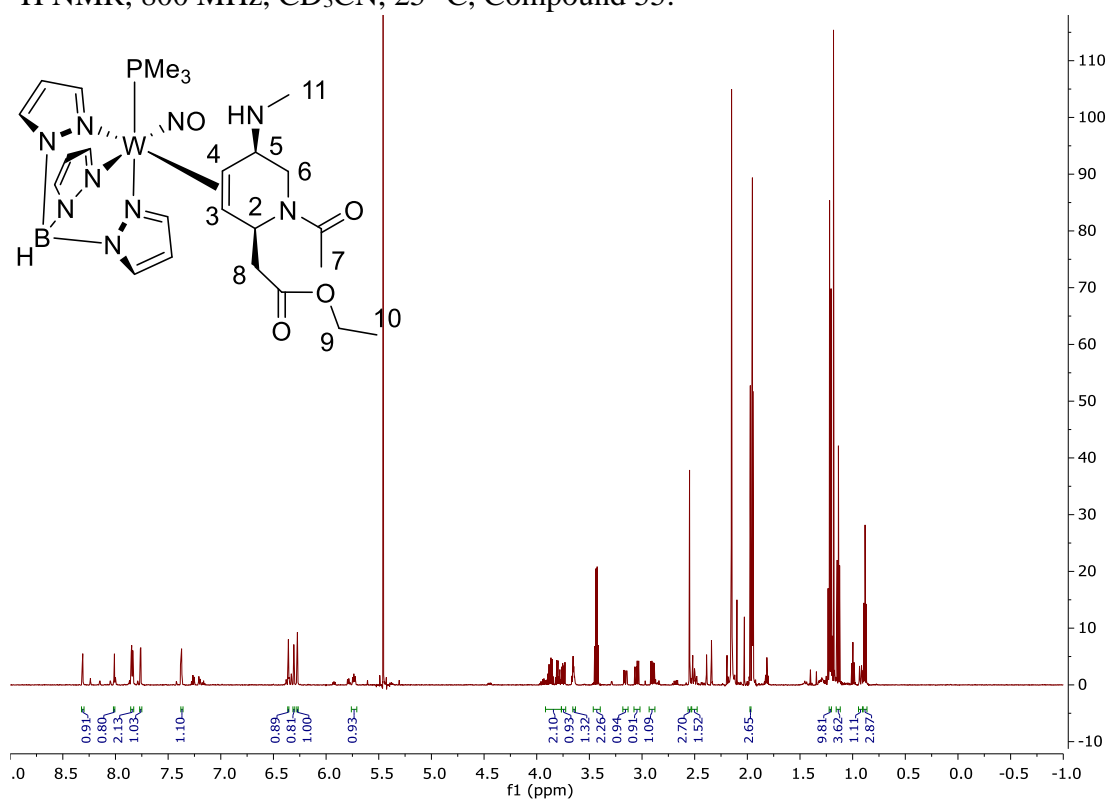
^1H NMR and $^{13}\text{C}\{^1\text{H}\}$ NMR Compound 39:



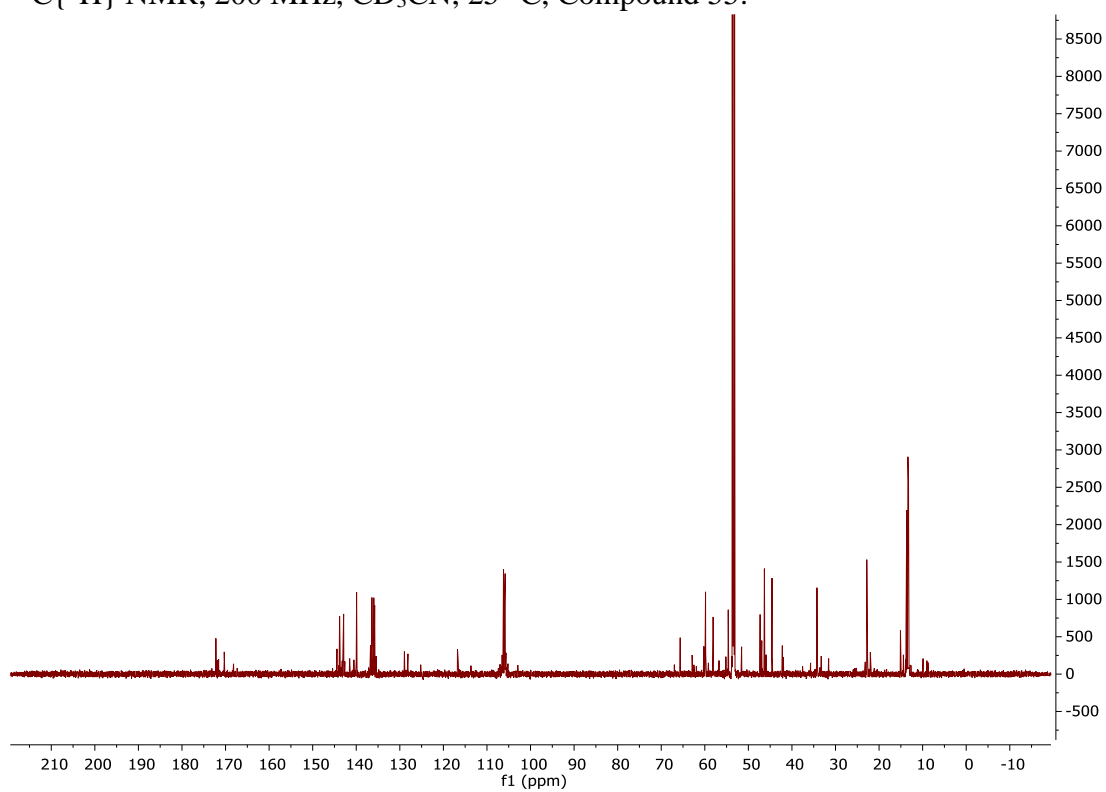
^1H NMR and $^{13}\text{C}\{^1\text{H}\}$ NMR Compound 40:

^1H NMR and $^{13}\text{C}\{^1\text{H}\}$ NMR Compound 41:

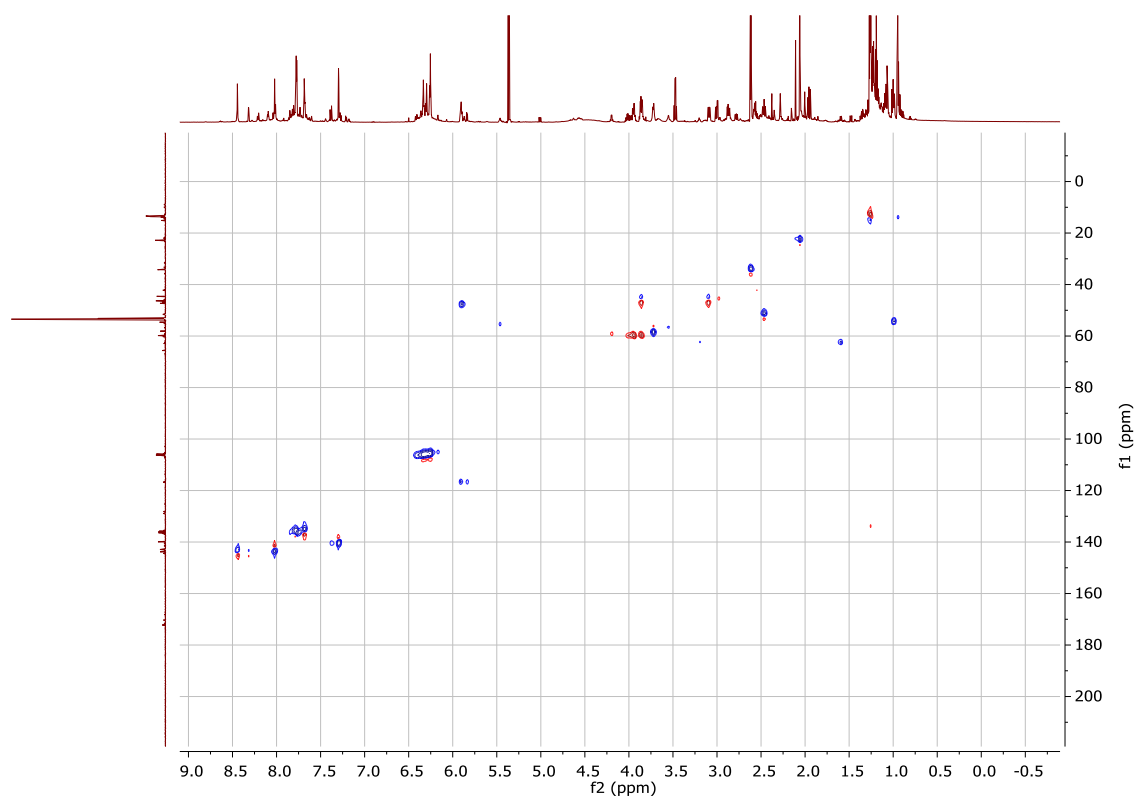
^1H NMR, 800 MHz, CD_3CN , 25 °C, Compound 55:



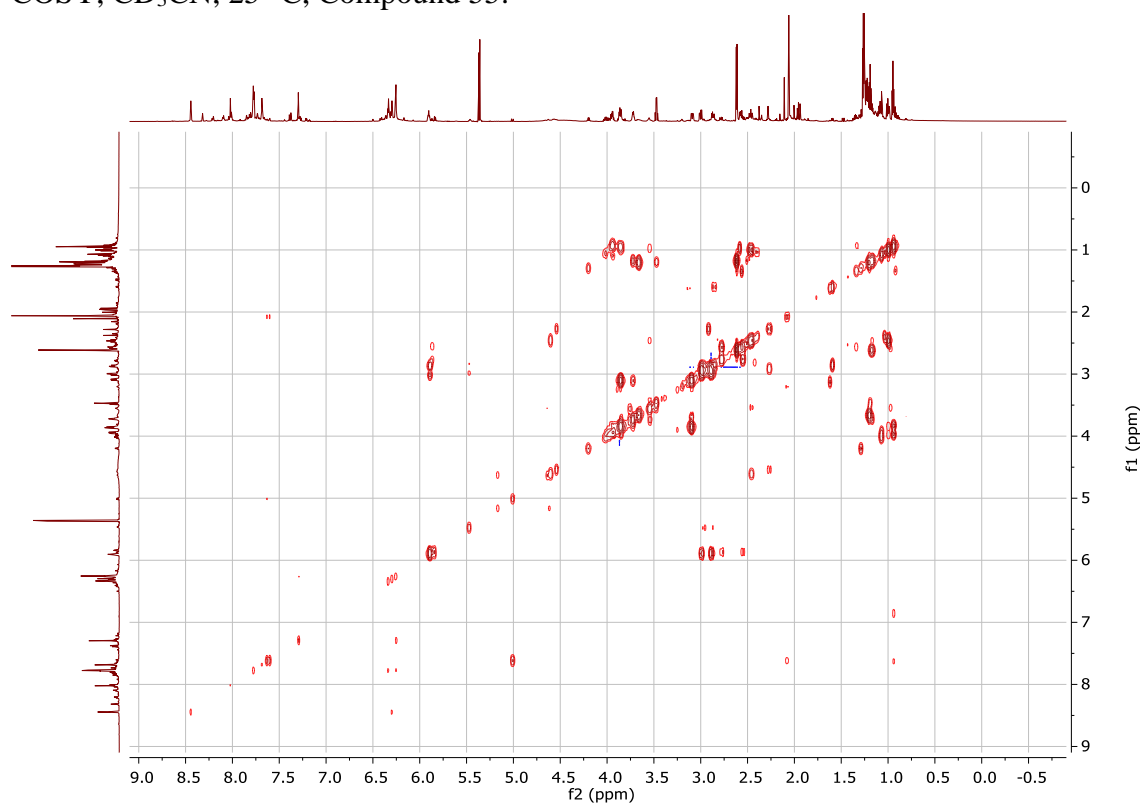
$^{13}\text{C}\{^1\text{H}\}$ NMR, 200 MHz, CD_3CN , 25 °C, Compound 55:



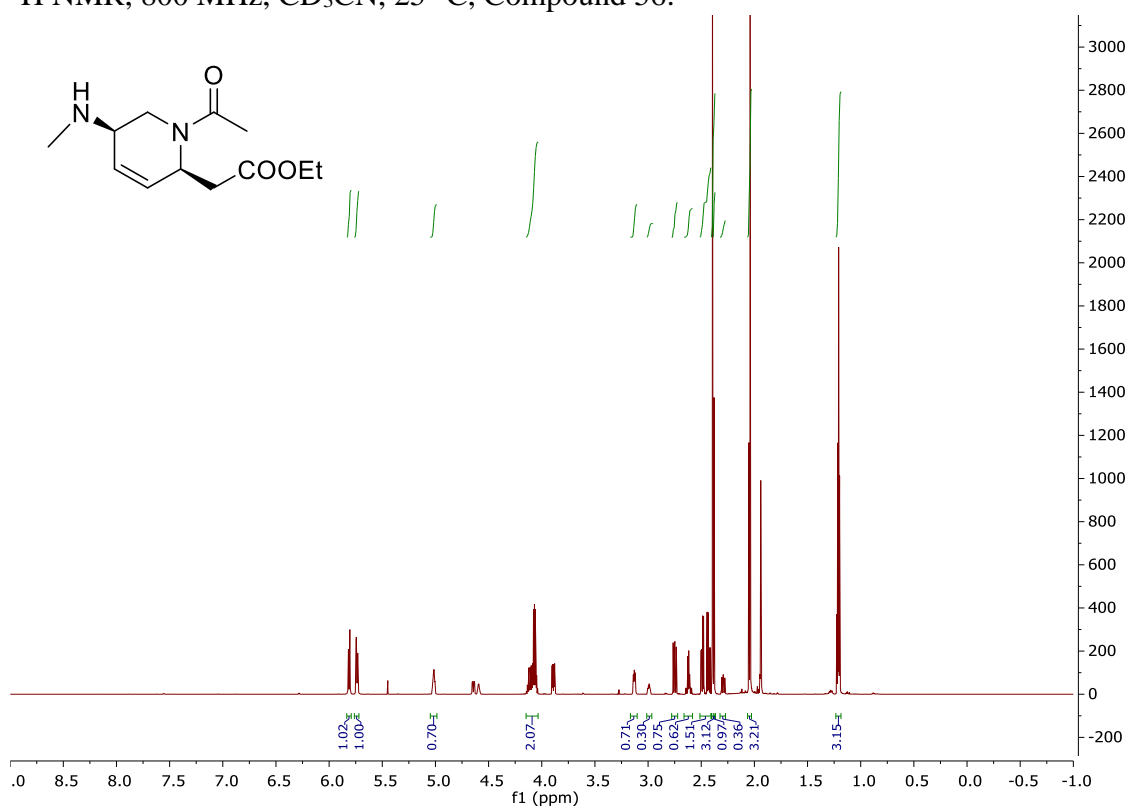
HSQC, CD₃CN, 25 °C, Compound 55:



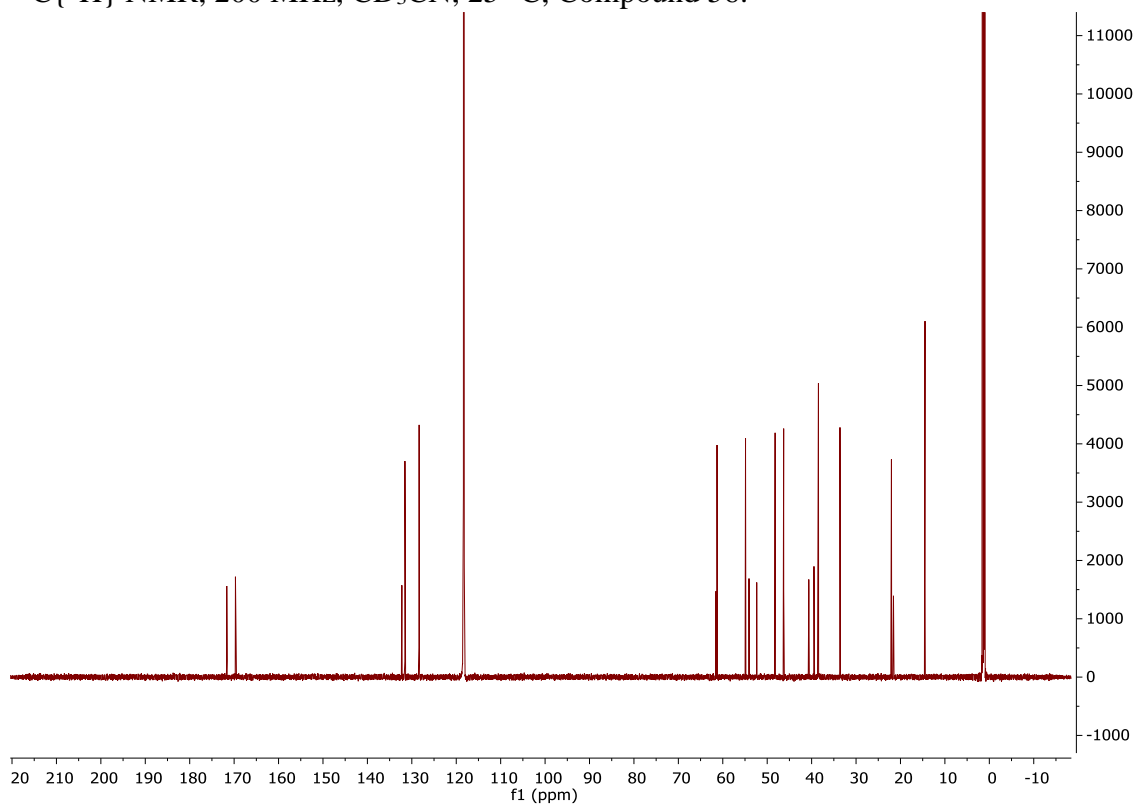
COSY, CD₃CN, 25 °C, Compound 55:



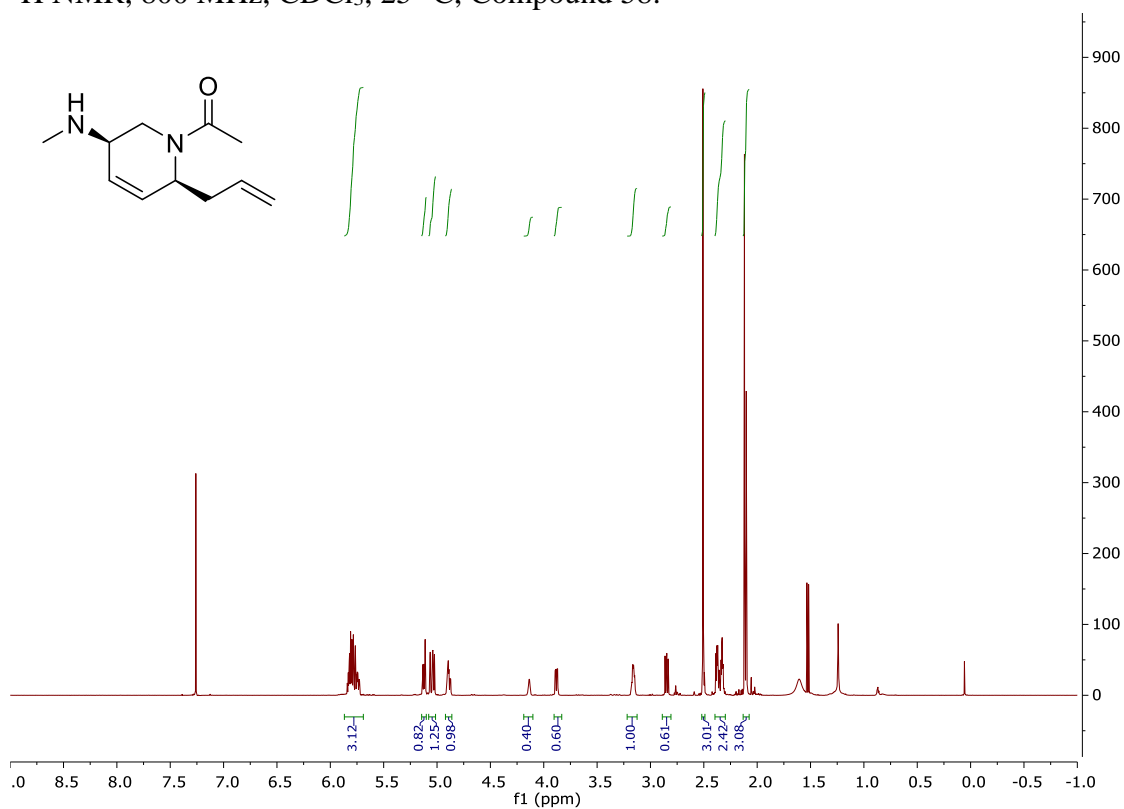
^1H NMR, 800 MHz, CD_3CN , 25 °C, Compound 56:



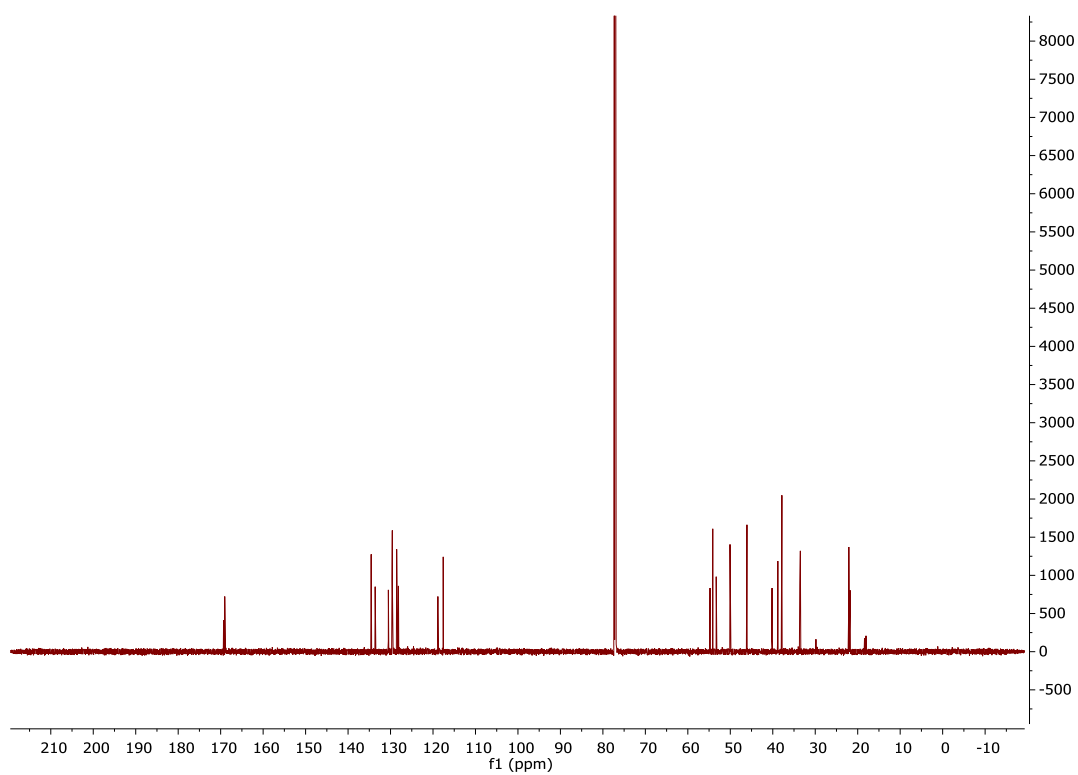
$^{13}\text{C}\{^1\text{H}\}$ NMR, 200 MHz, CD_3CN , 25 °C, Compound 56:



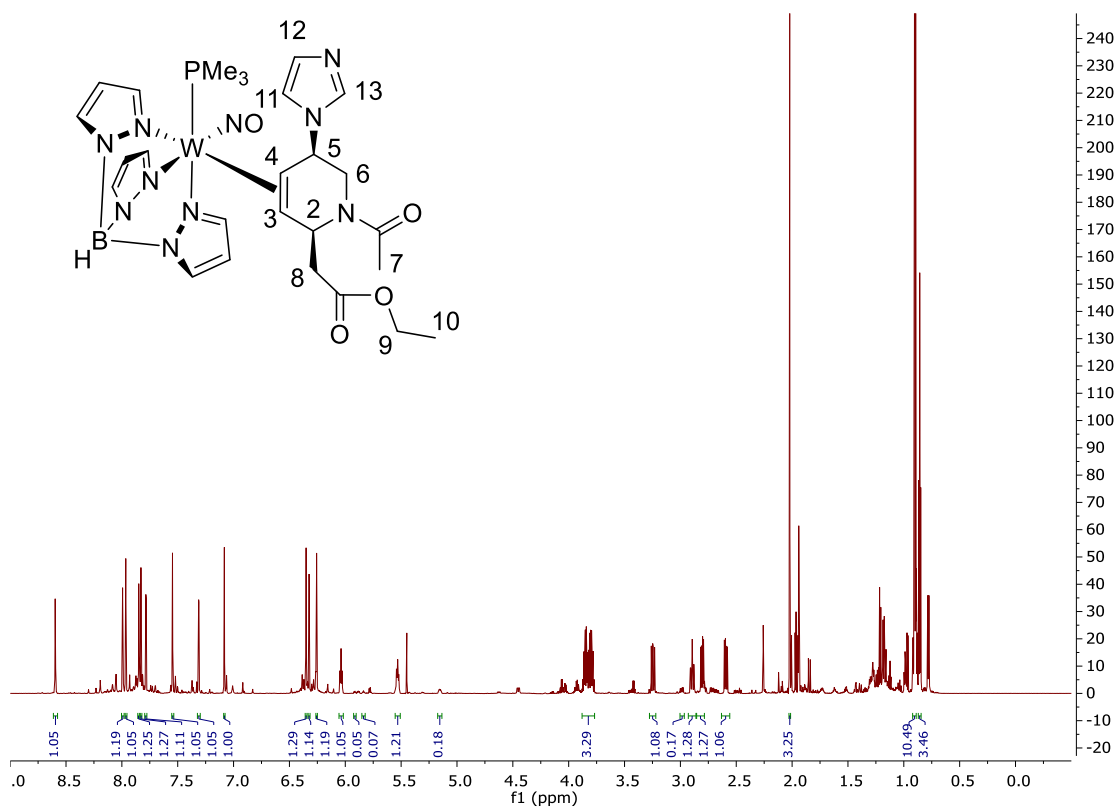
^1H NMR, 800 MHz, CDCl_3 , 25 °C, Compound 58:



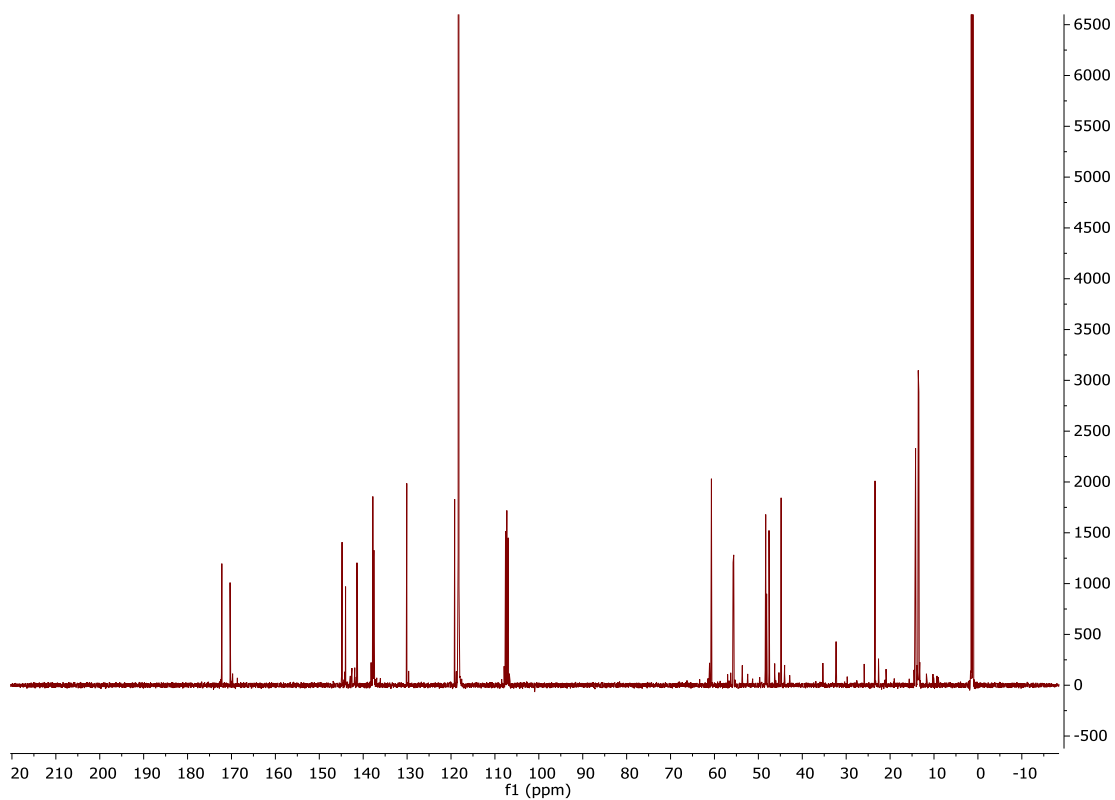
$^{13}\text{C}\{^1\text{H}\}$ NMR, 200 MHz, CDCl_3 , 25 °C, Compound 58:



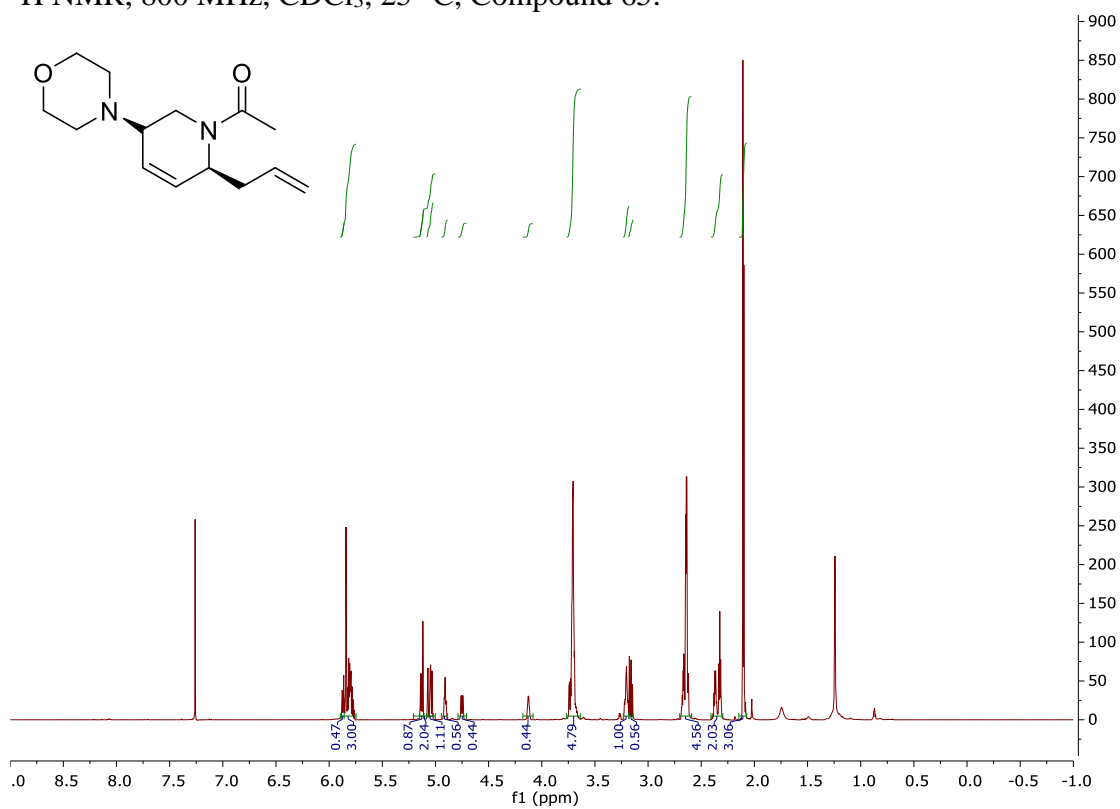
^1H NMR, 800 MHz, CD_3CN , 25 °C, Compound 64:



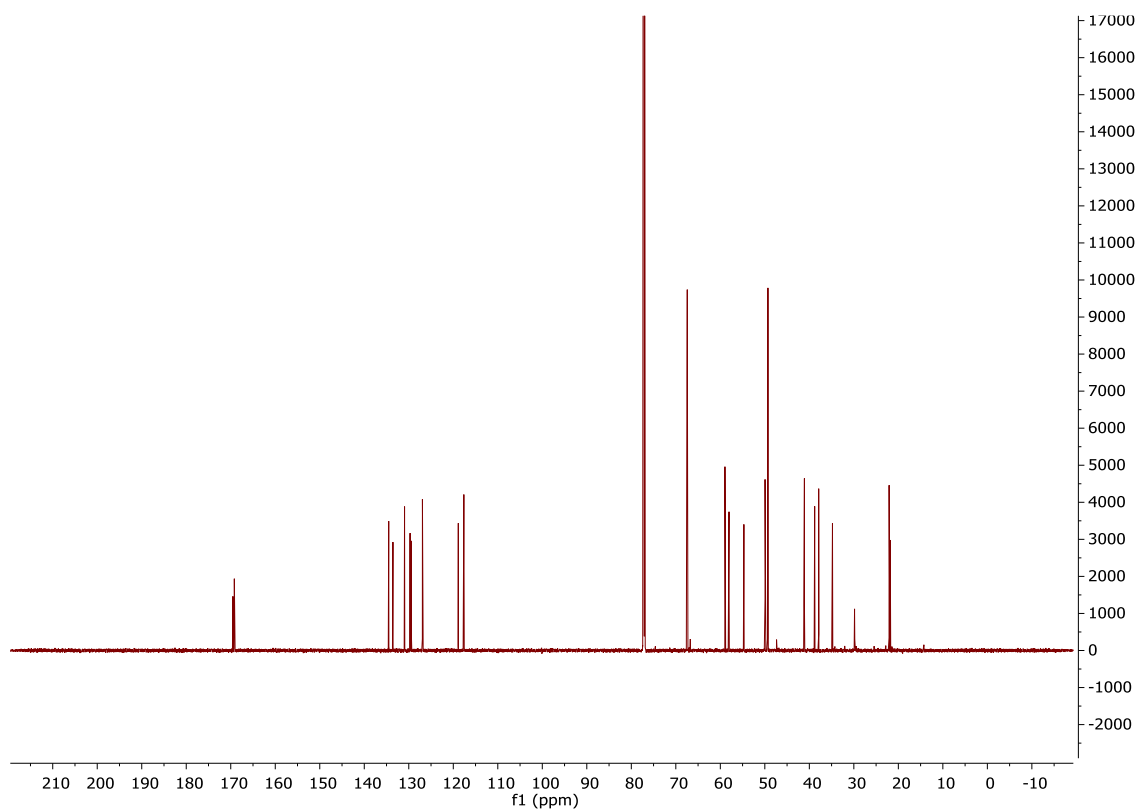
$^{13}\text{C}\{^1\text{H}\}$ NMR, 200 MHz, CD_3CN , 25 °C, Compound 64:



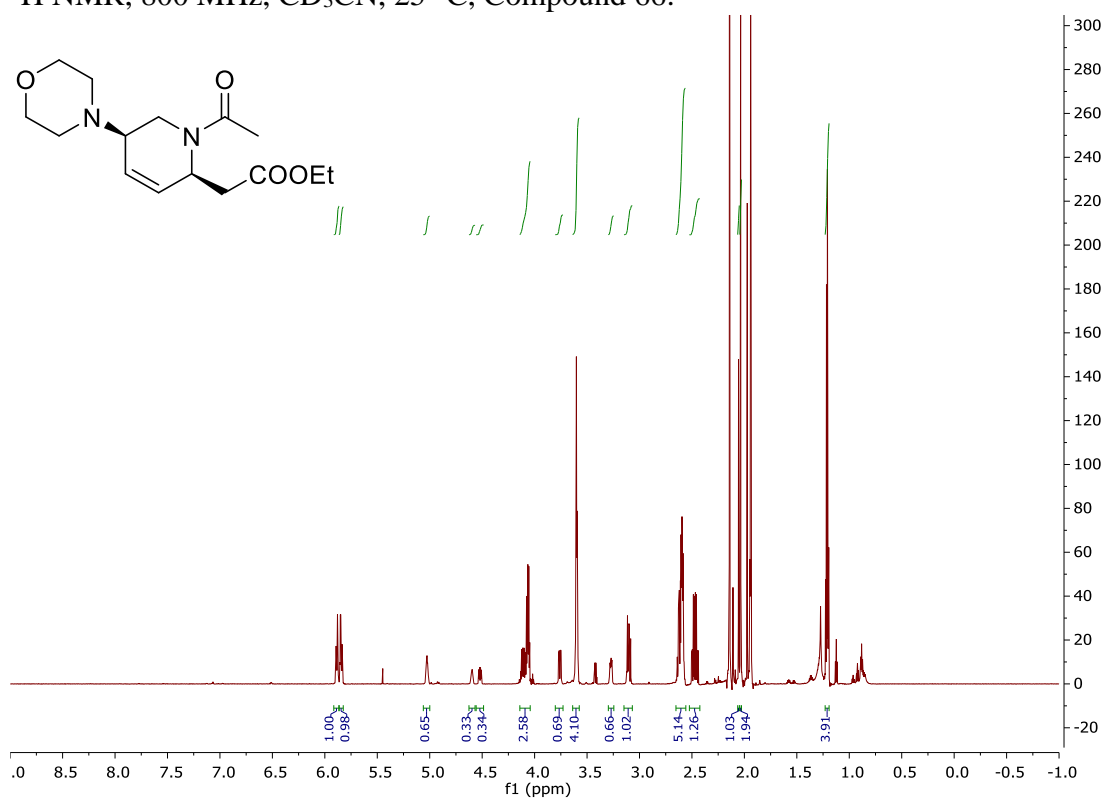
^1H NMR, 800 MHz, CDCl_3 , 25 °C, Compound 65:



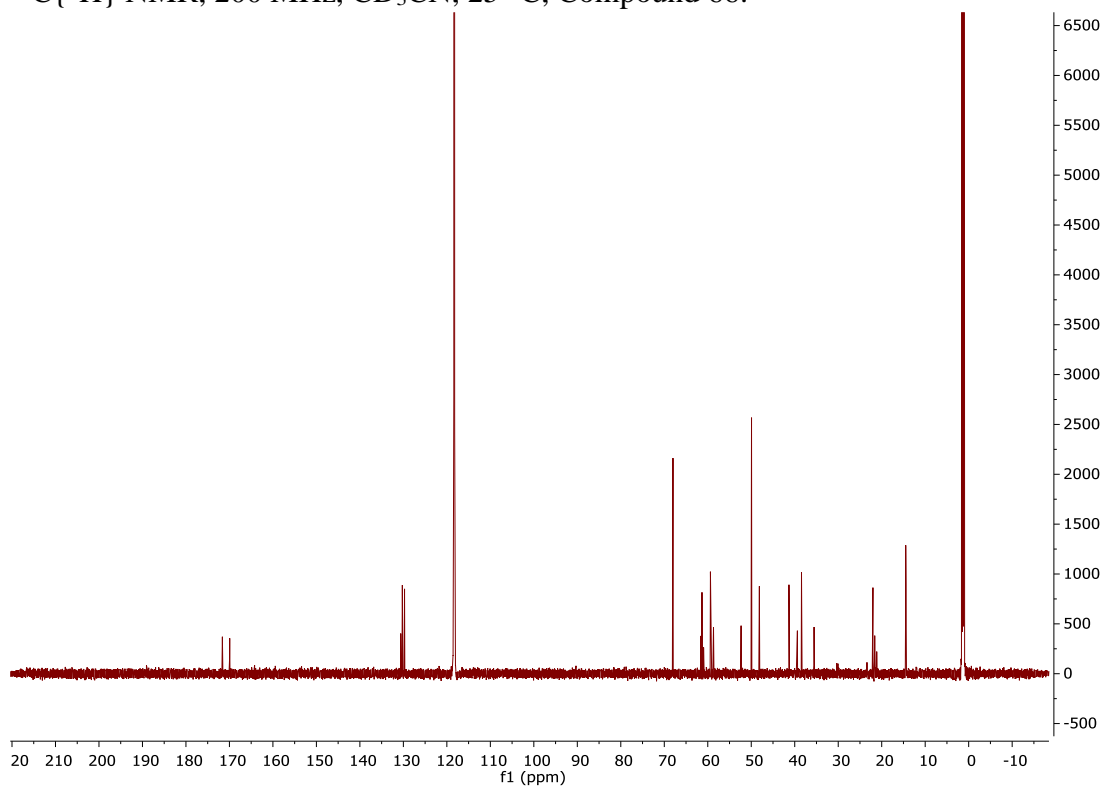
$^{13}\text{C}\{^1\text{H}\}$ NMR, 200 MHz, CDCl_3 , 25 °C, Compound 65:



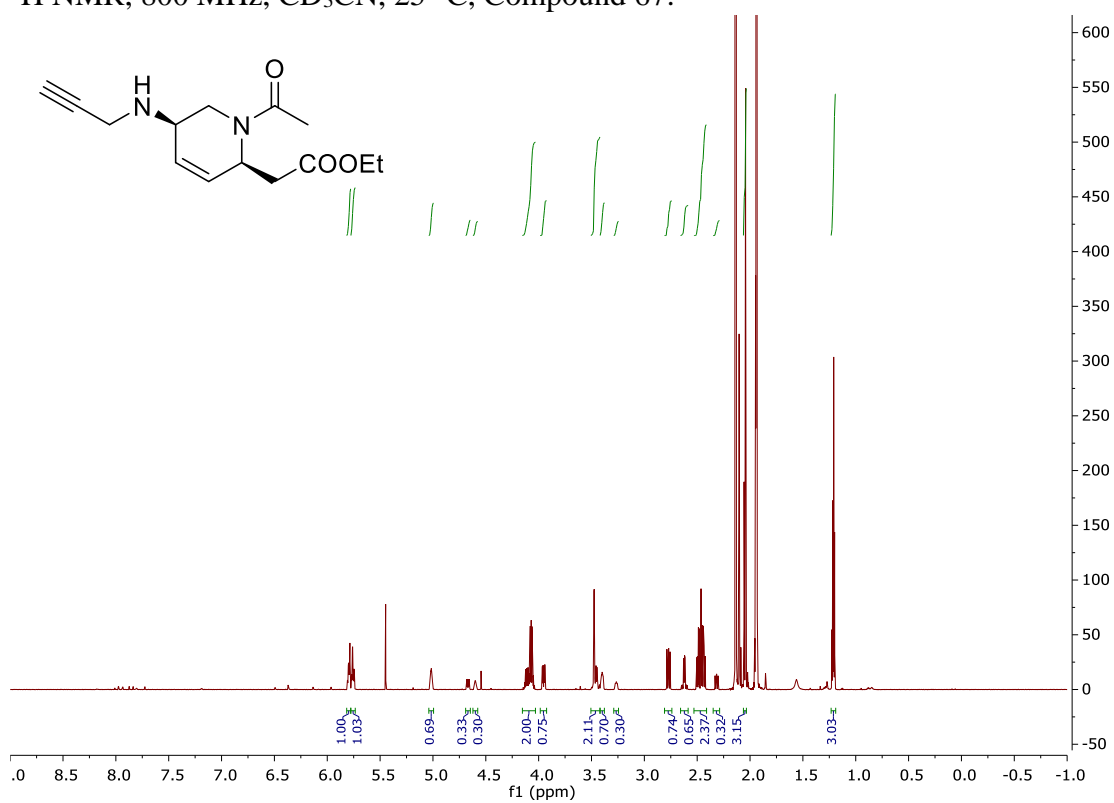
^1H NMR, 800 MHz, CD_3CN , 25 °C, Compound 66:



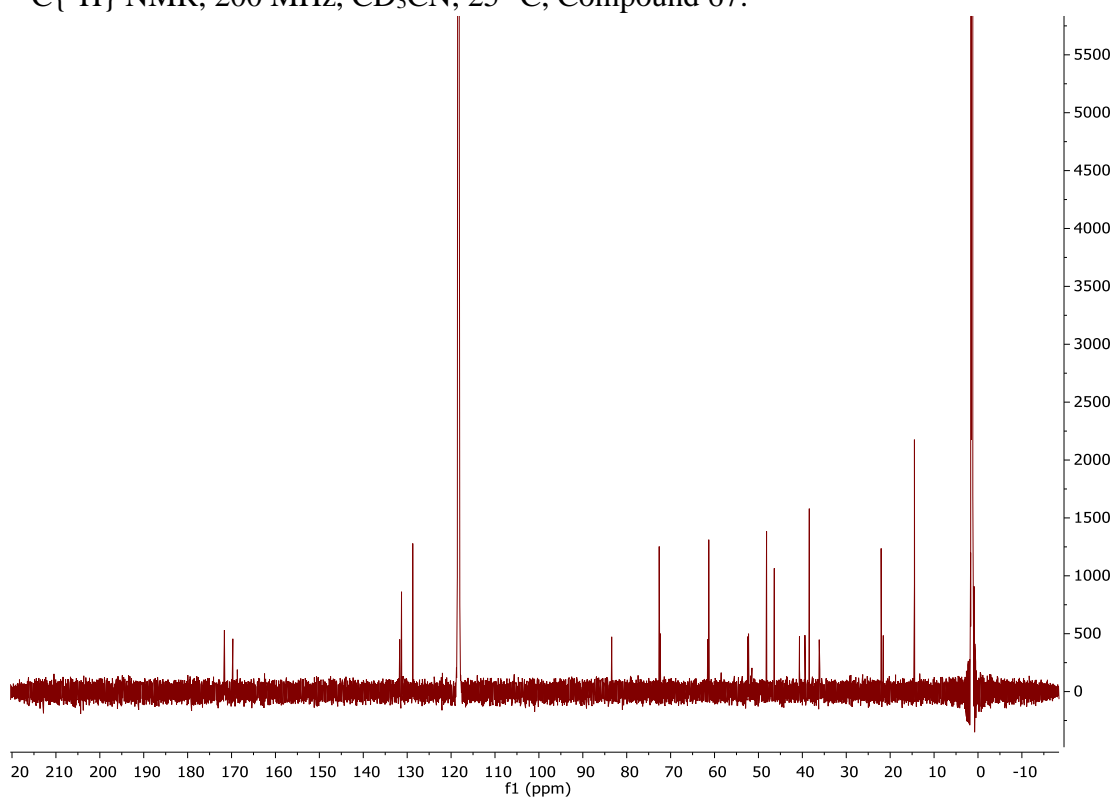
$^{13}\text{C}\{^1\text{H}\}$ NMR, 200 MHz, CD_3CN , 25 °C, Compound 66:



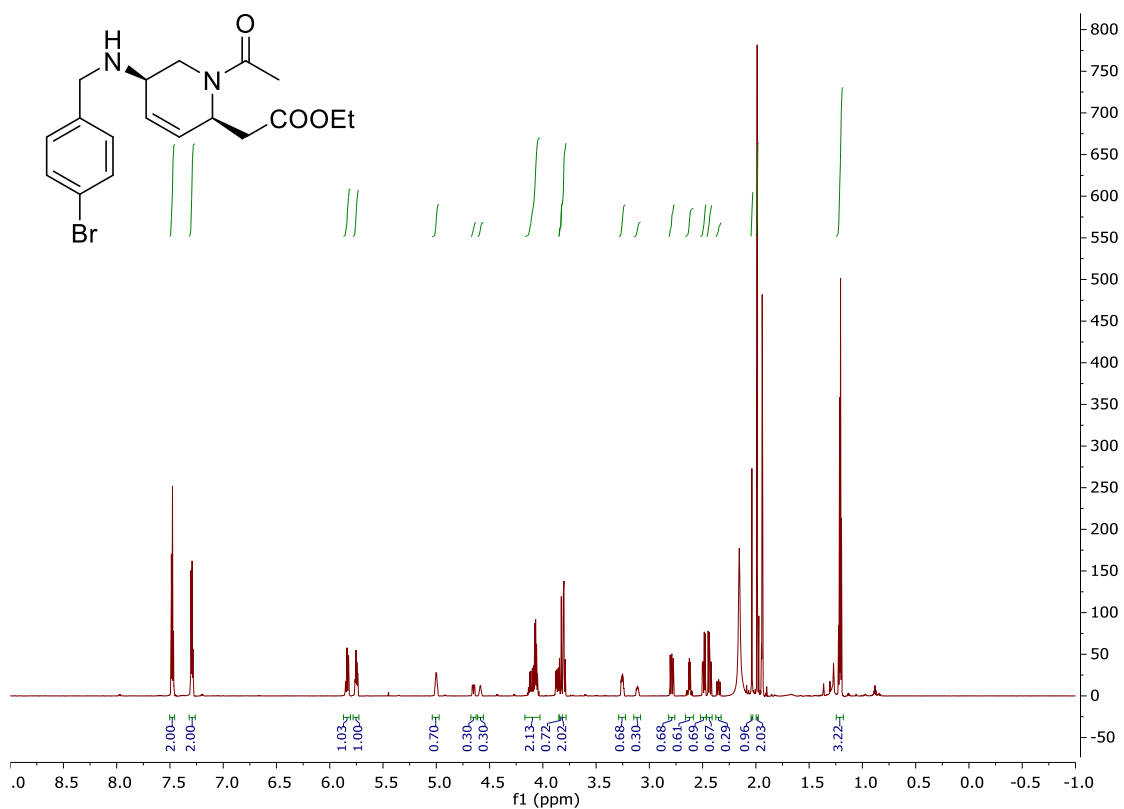
^1H NMR, 800 MHz, CD_3CN , 25 °C, Compound 67:



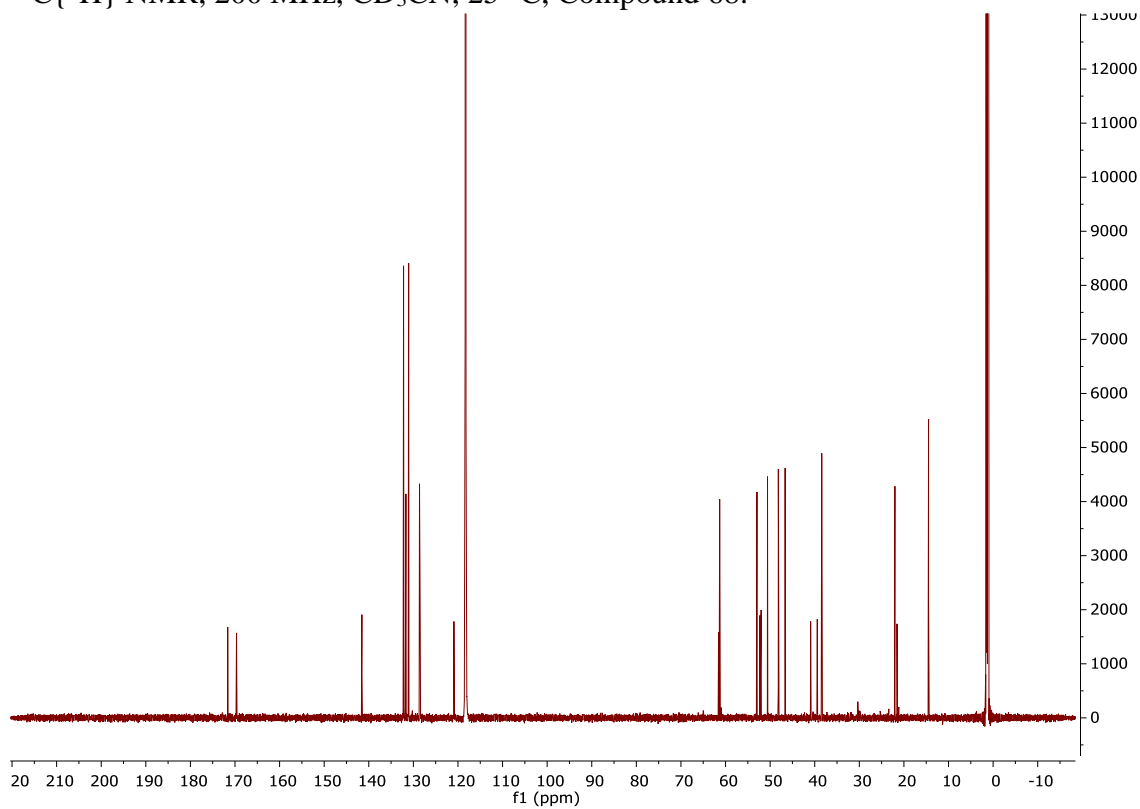
$^{13}\text{C}\{^1\text{H}\}$ NMR, 200 MHz, CD_3CN , 25 °C, Compound 67:



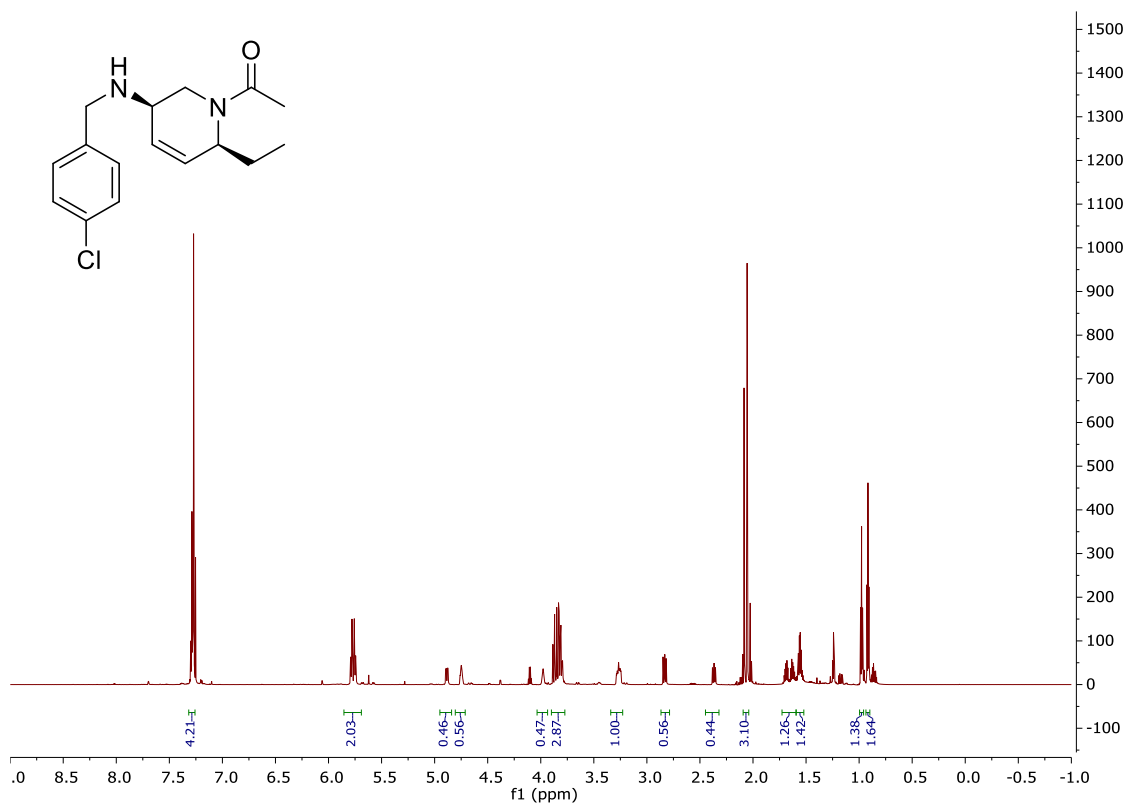
^1H NMR, 800 MHz, CD_3CN , 25 °C, Compound 68:



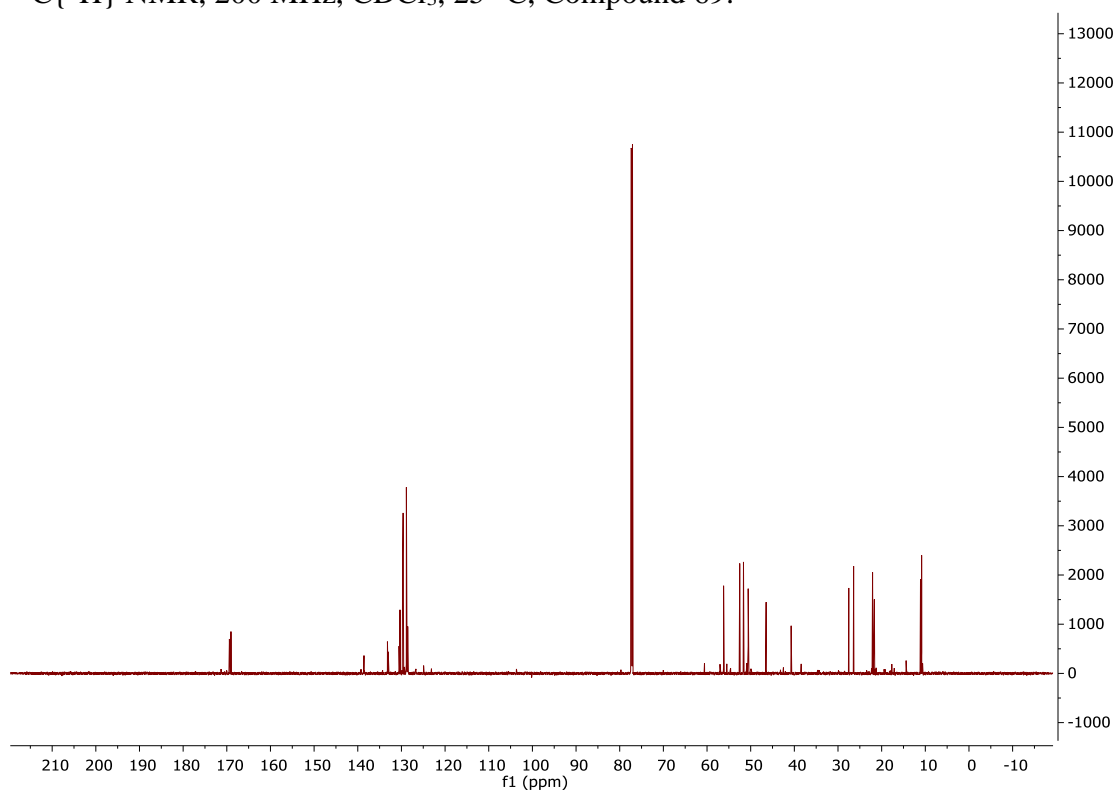
$^{13}\text{C}\{^1\text{H}\}$ NMR, 200 MHz, CD_3CN , 25 °C, Compound 68:



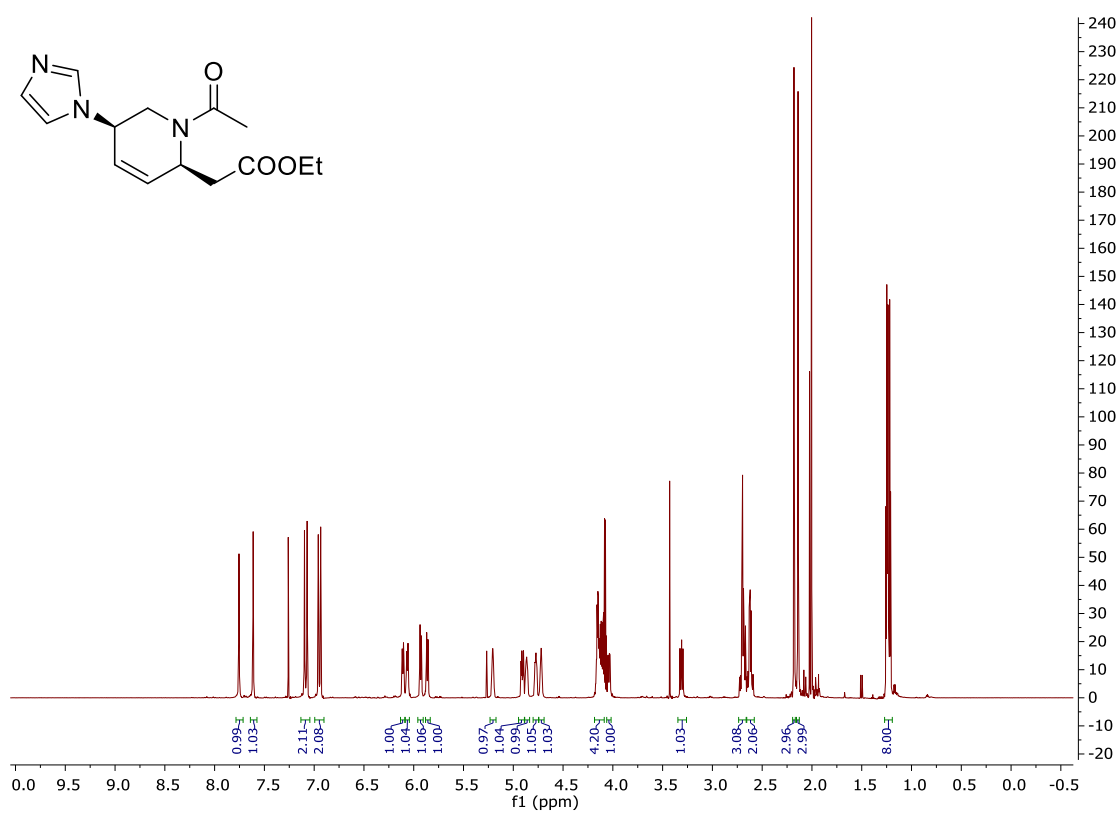
^1H NMR, 800 MHz, CDCl_3 , 25 °C, Compound 69:



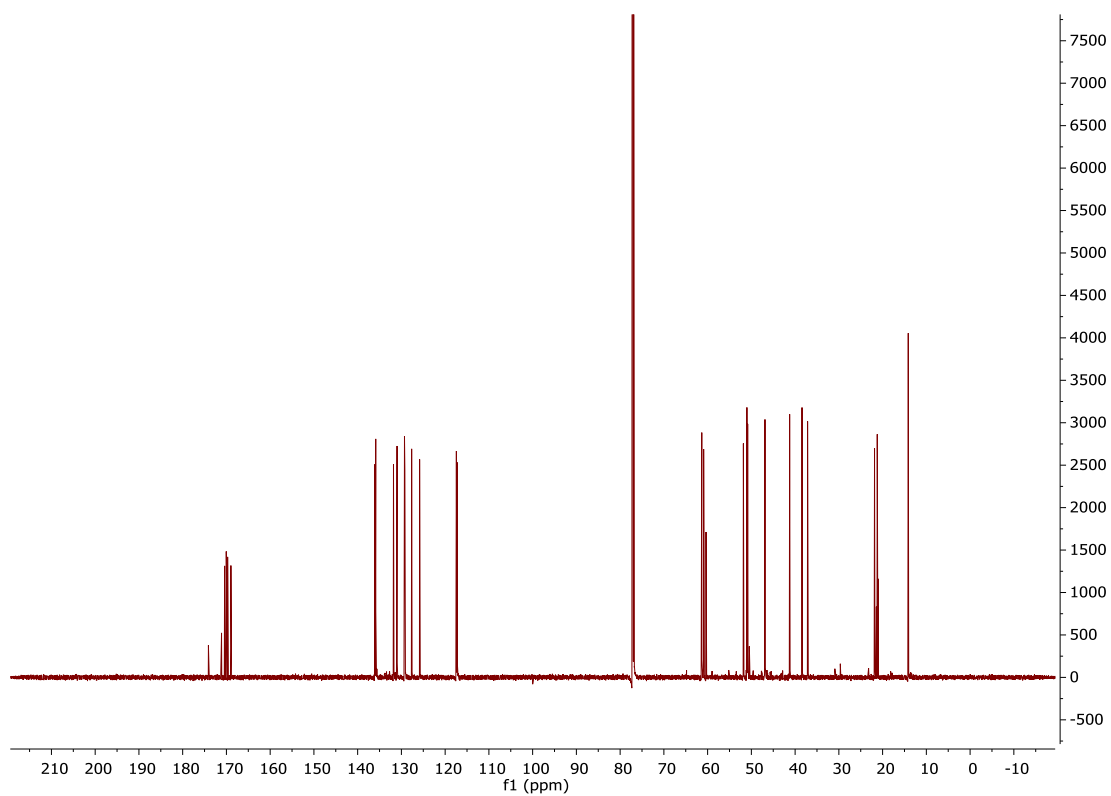
$^{13}\text{C}\{^1\text{H}\}$ NMR, 200 MHz, CDCl_3 , 25 °C, Compound 69:

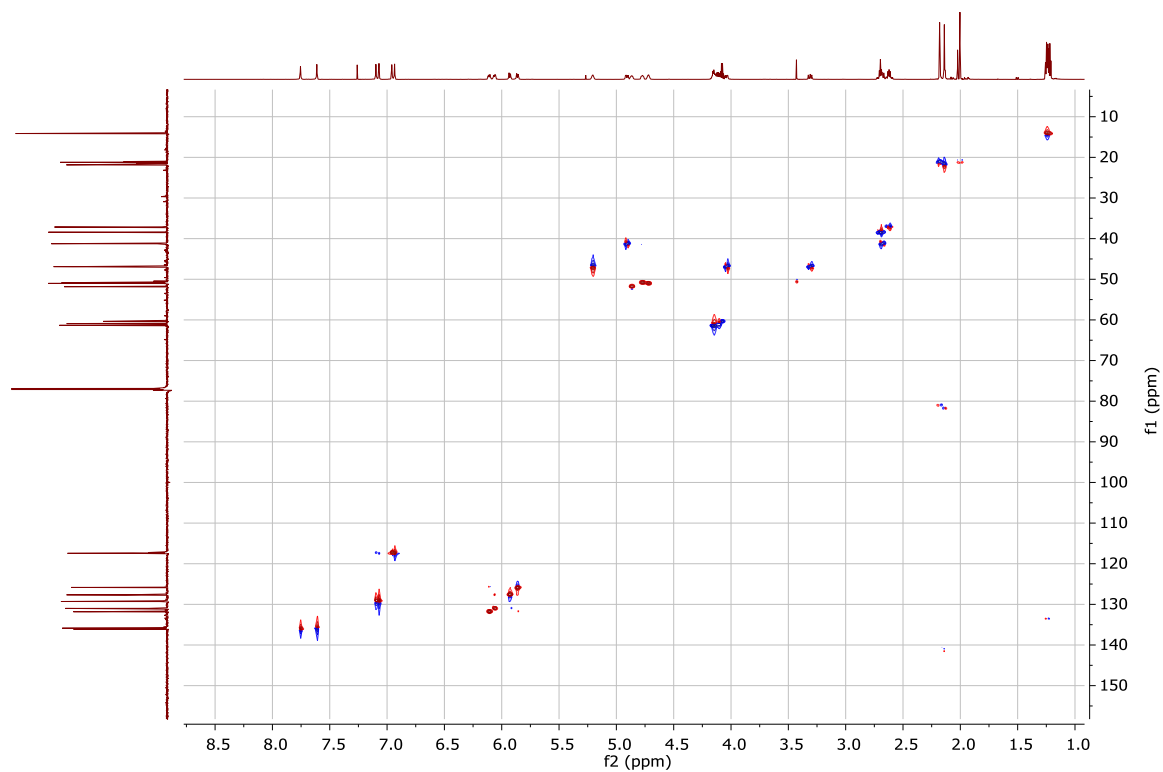
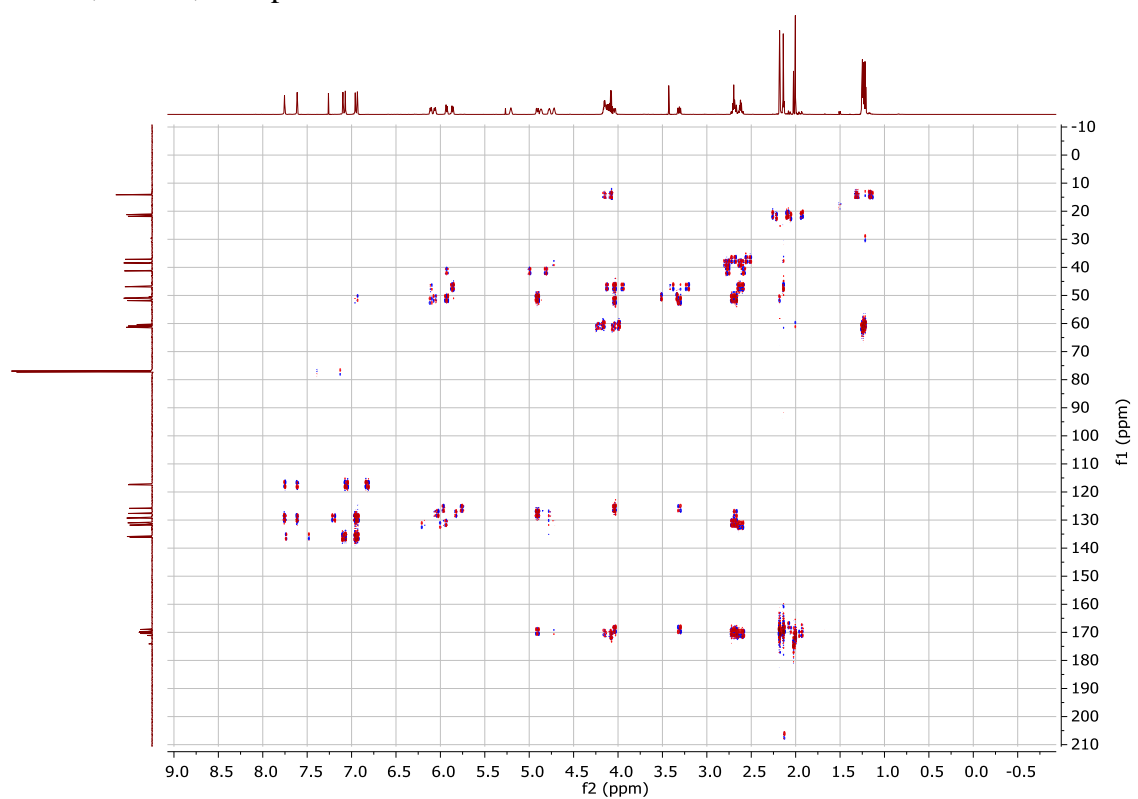


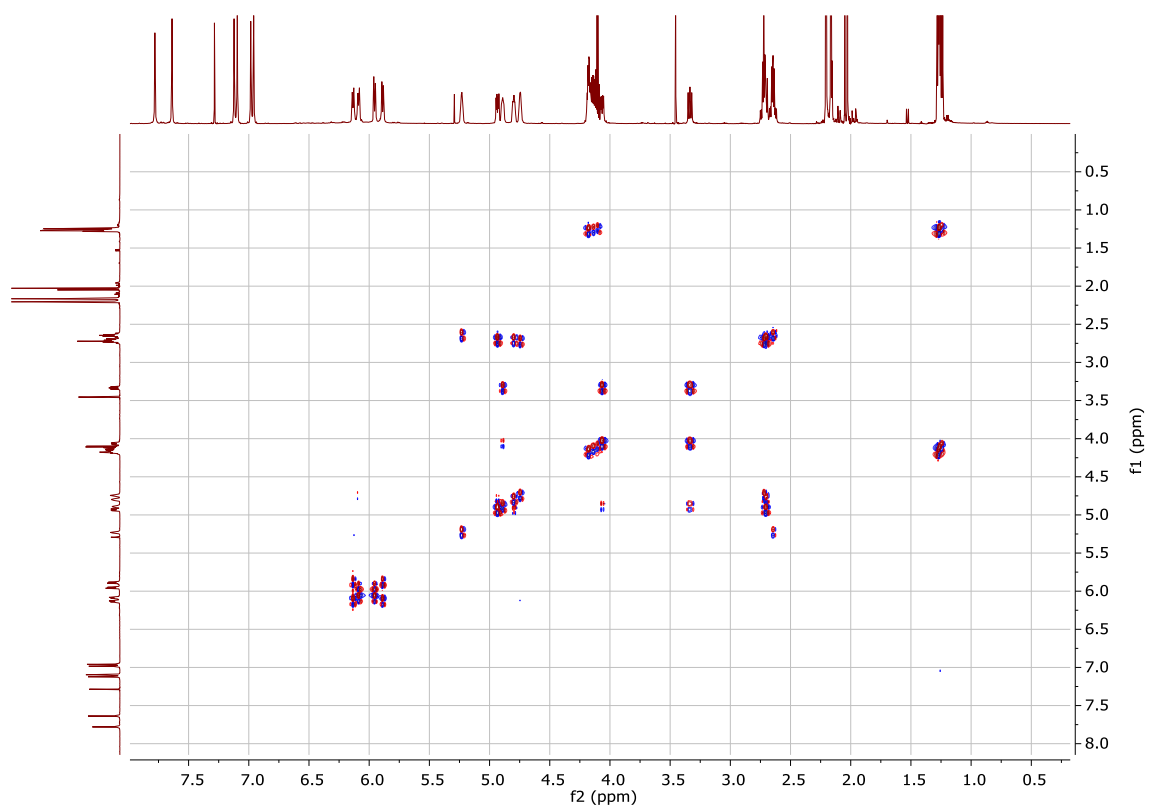
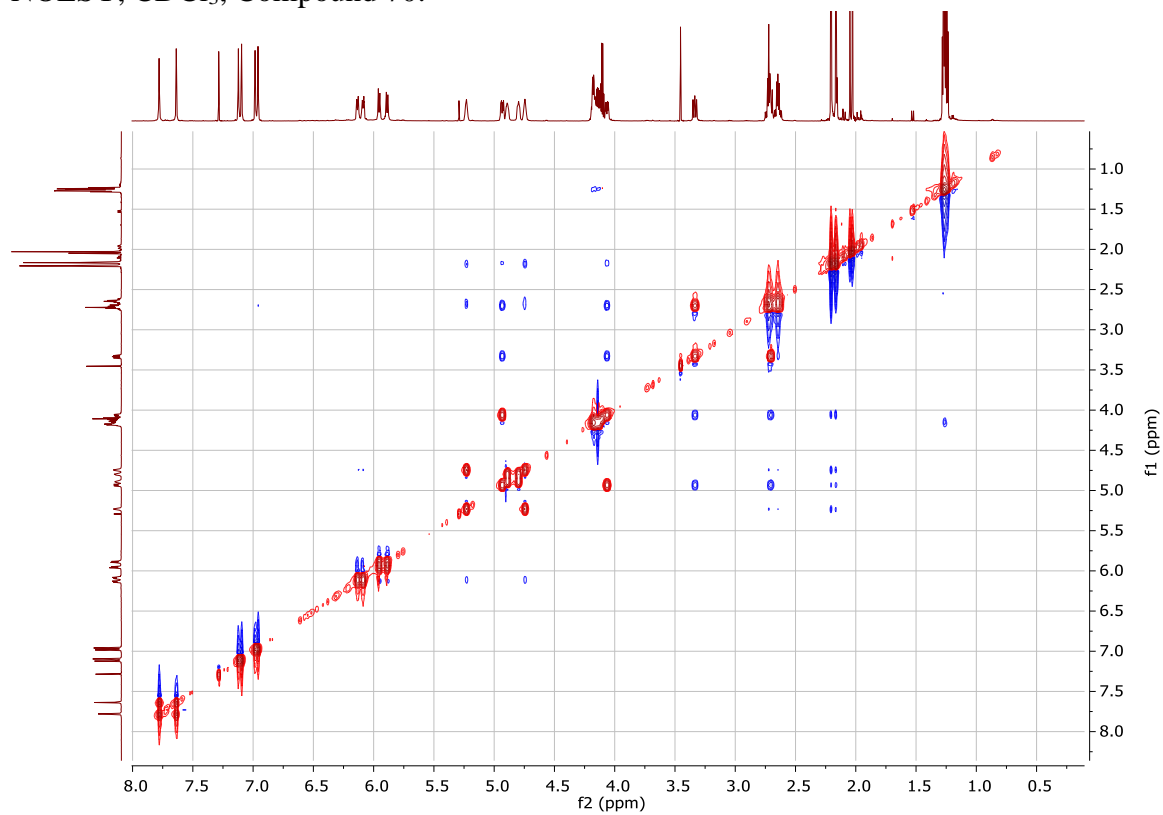
^1H NMR, 800 MHz, CDCl_3 , 25 °C, Compound 70:



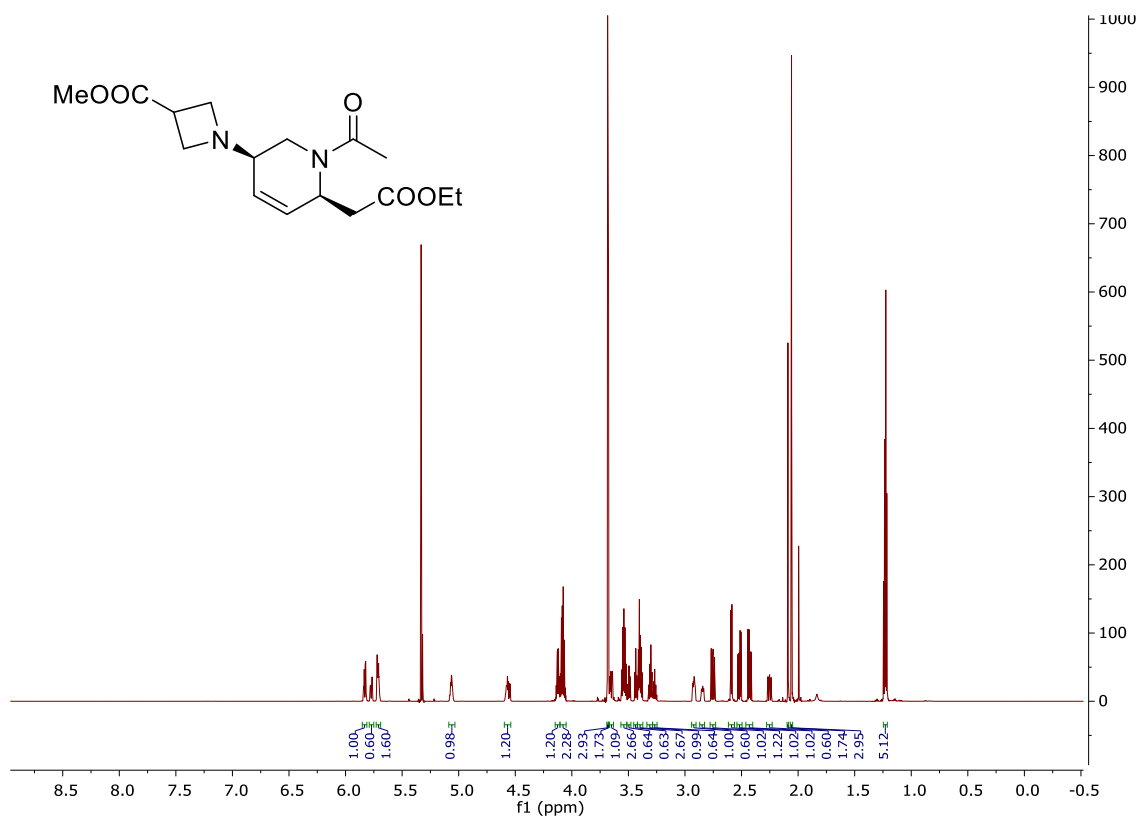
^{13}C NMR, 200 MHz, CDCl_3 , 25 °C, Compound 70:



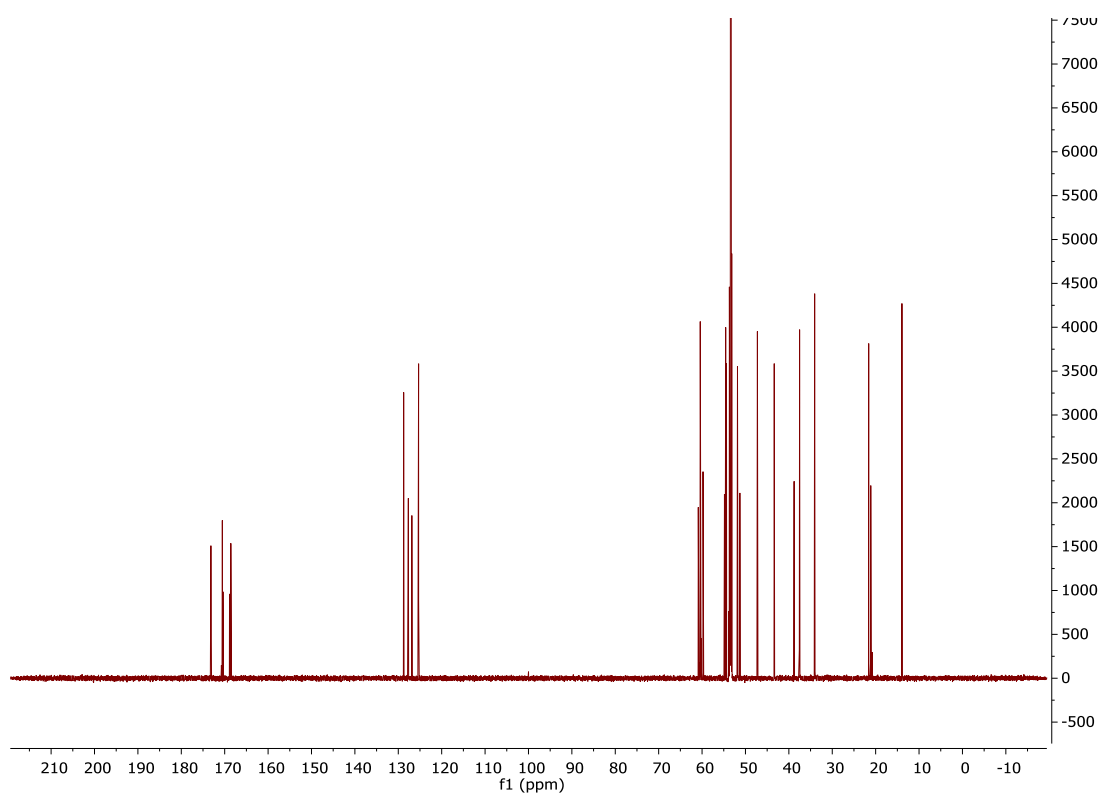
HSQC, CDCl₃, Compound 70:HMBC, CDCl₃, Compound 70:

COSY, CDCl₃, Compound 70:NOESY, CDCl₃, Compound 70:

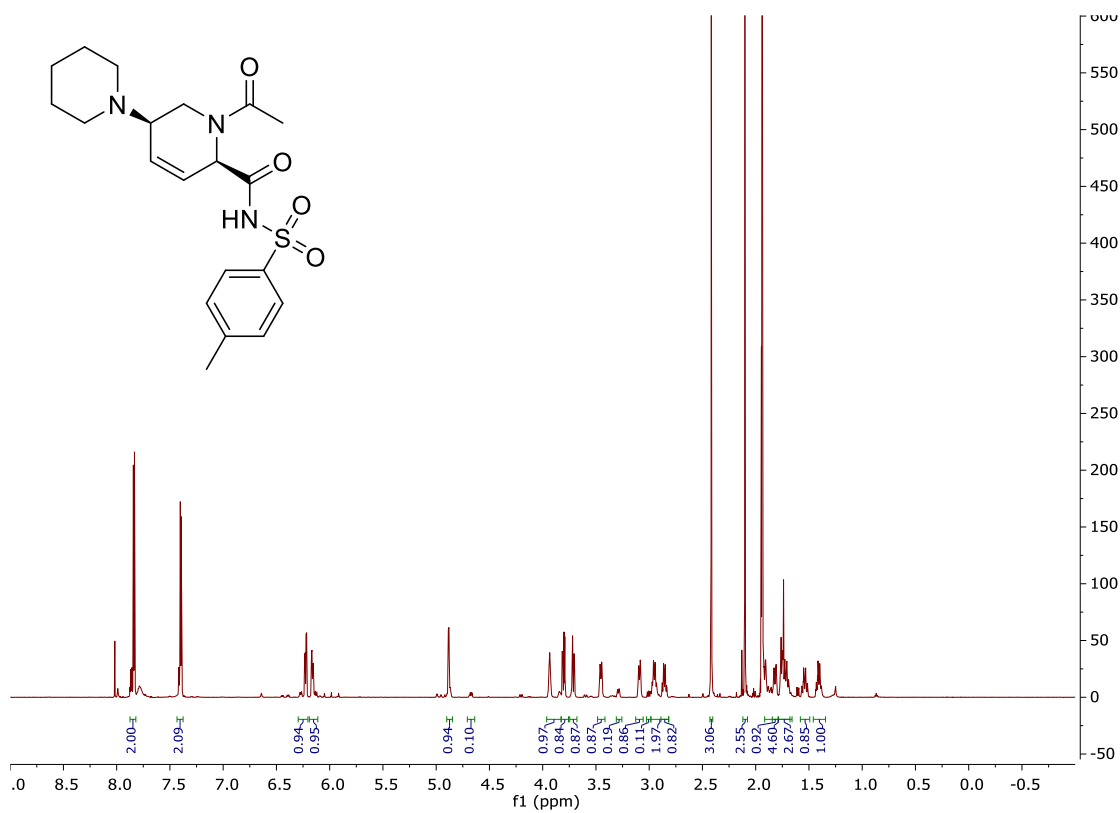
^1H NMR, 800 MHz, CD_2Cl_2 , 25 °C, Compound 71:



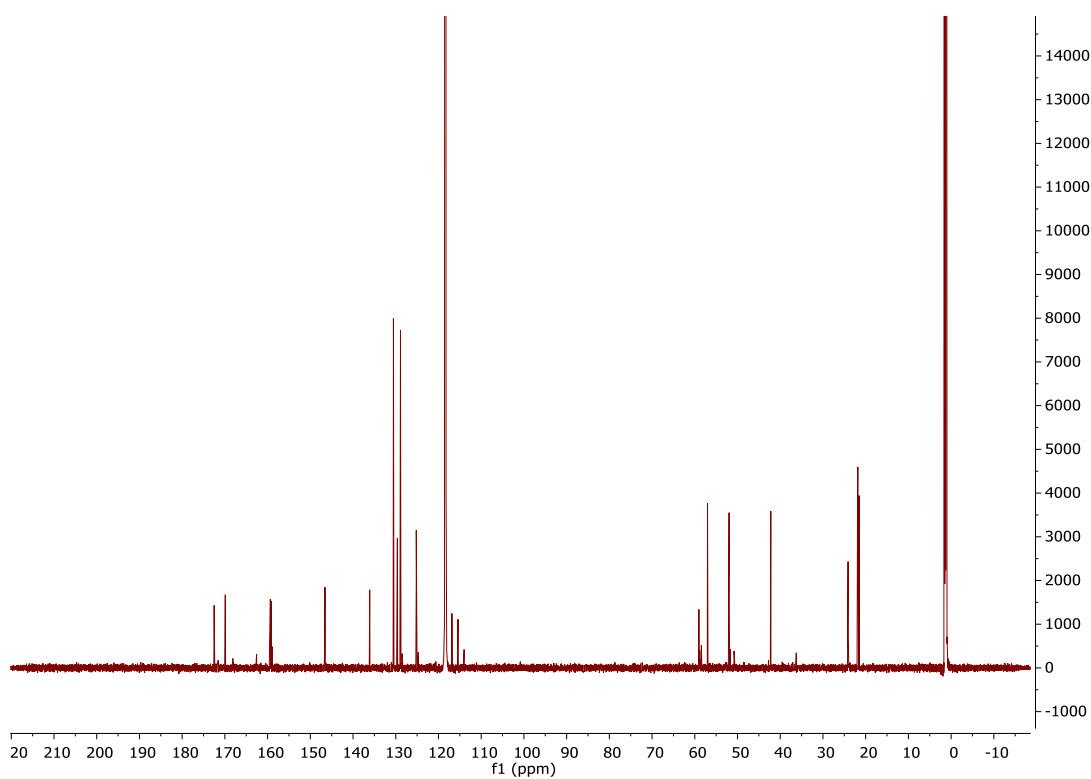
^{13}C NMR, 200 MHz, CD_2Cl_2 , 25 °C, Compound 71:



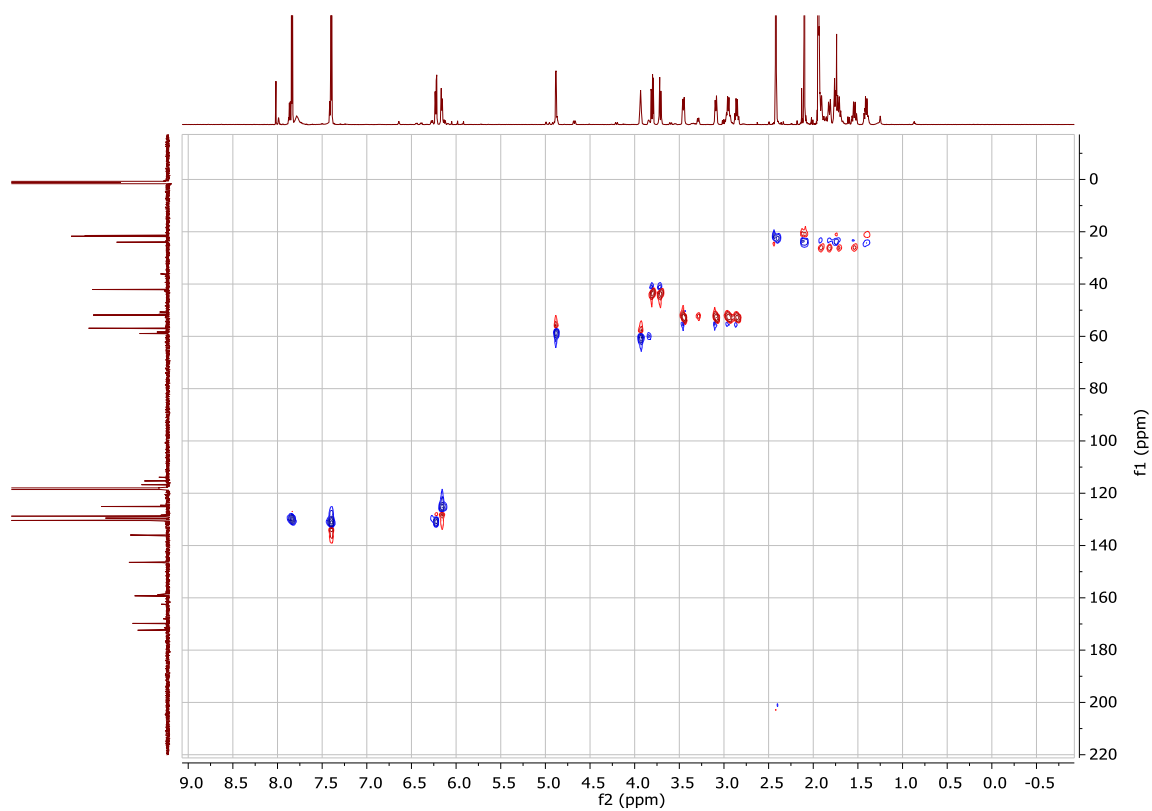
^1H NMR, 800 MHz, $\text{CD}_3\text{CN}/10\%$ TFA, 0°C , Compound 74:



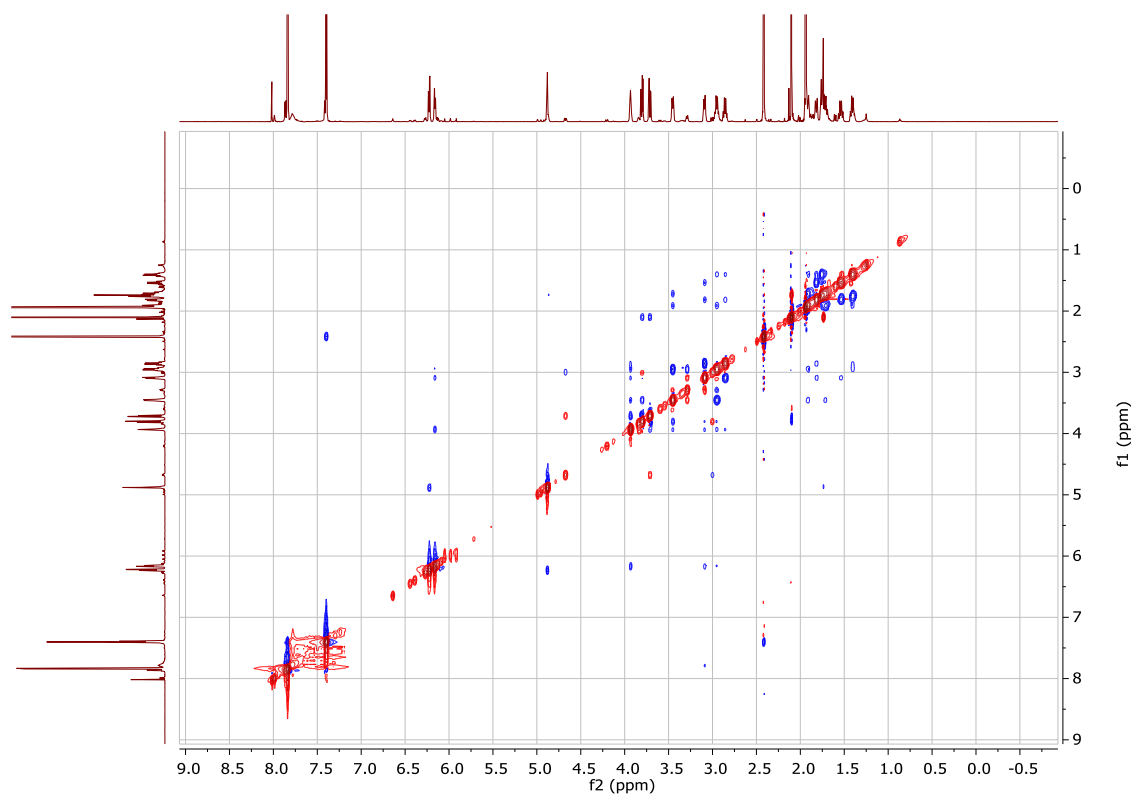
$^{13}\text{C}\{^1\text{H}\}$ NMR, 200 MHz, $\text{CD}_3\text{CN}/10\%$ TFA, 0°C , Compound 74:



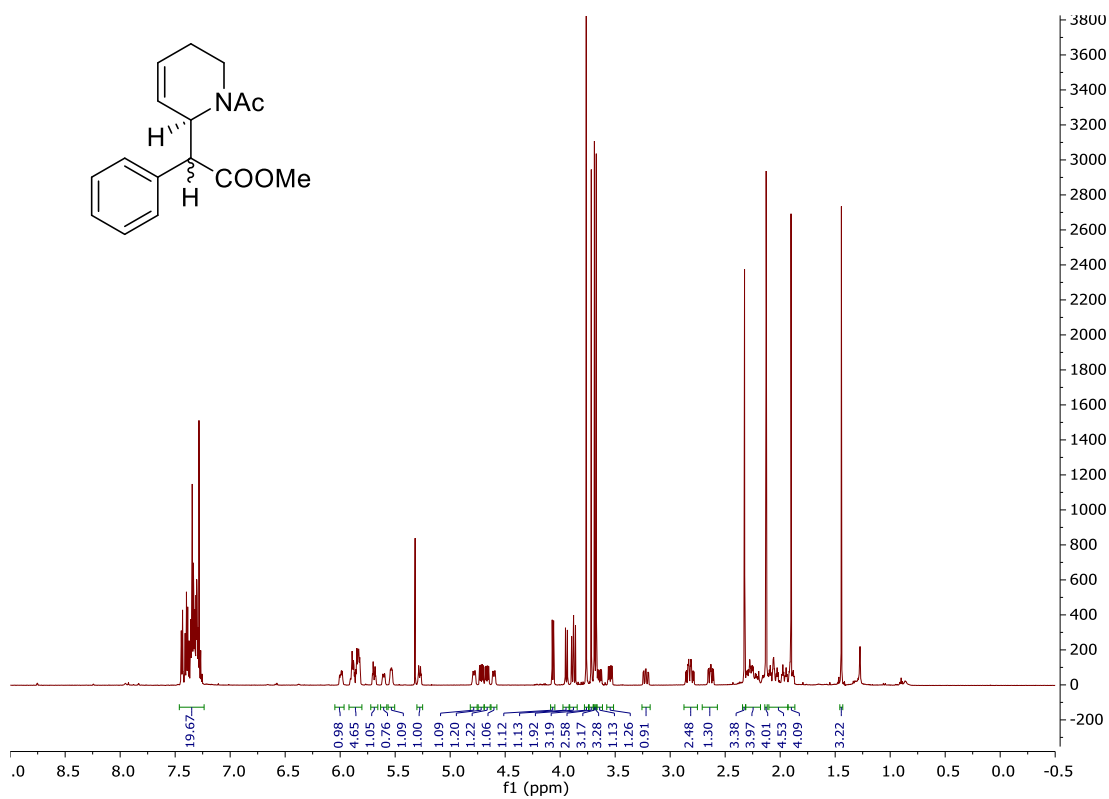
HSQC, CD₃CN, 0 °C, Compound 74:



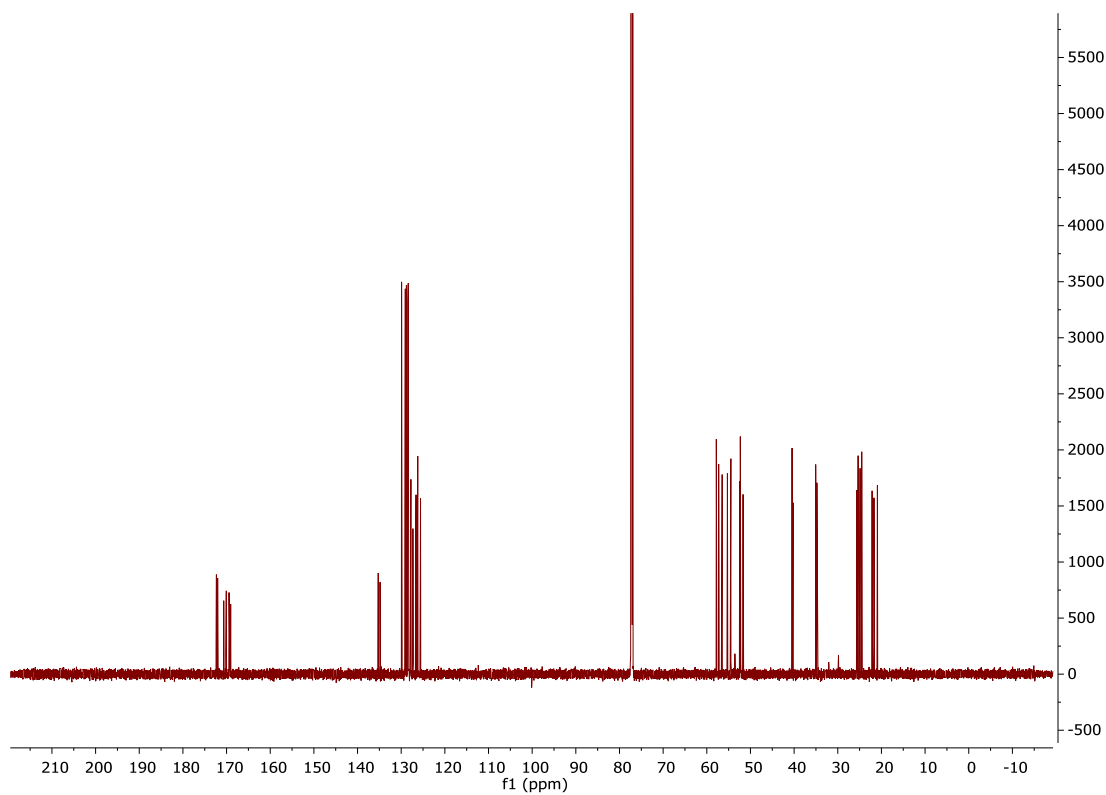
NOESY, CD₃CN, 0 °C, Compound 74:

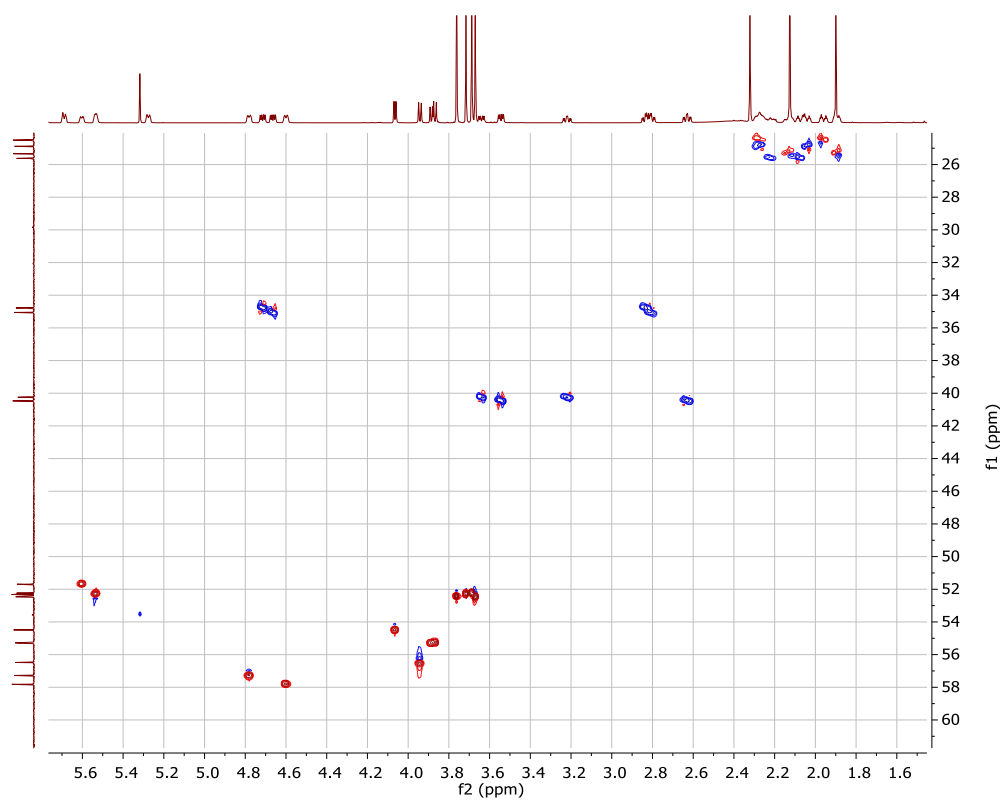
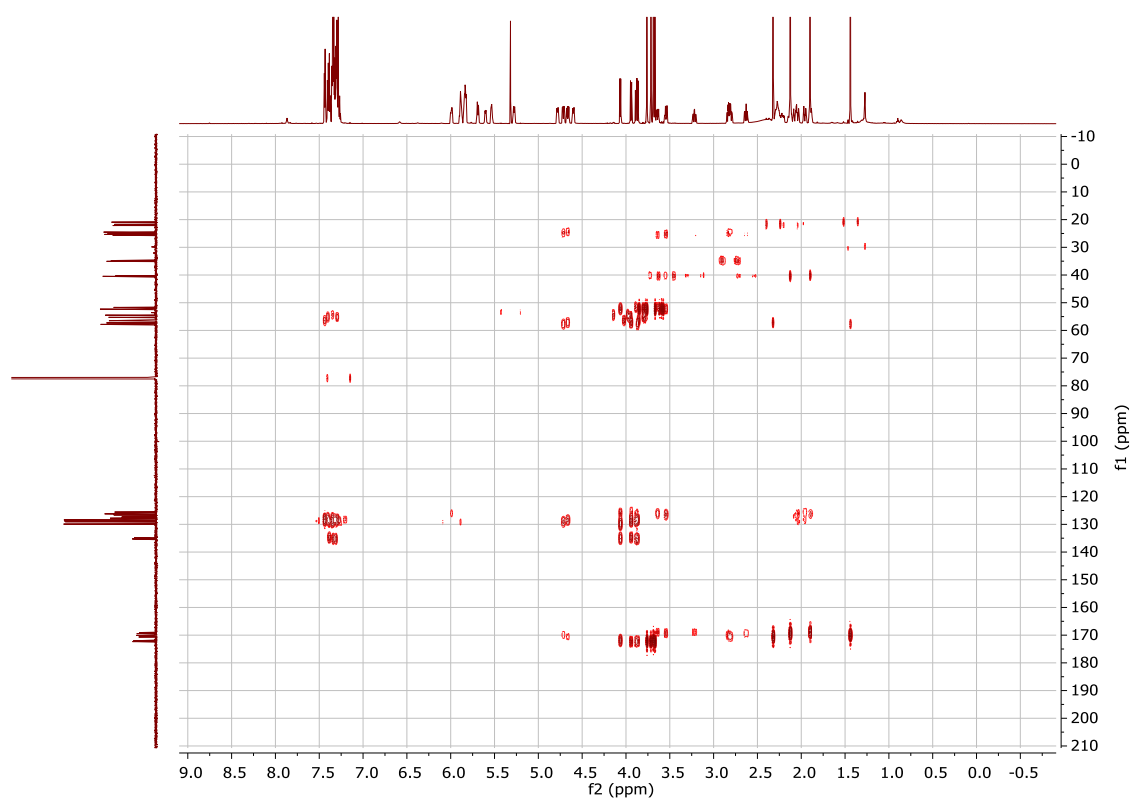


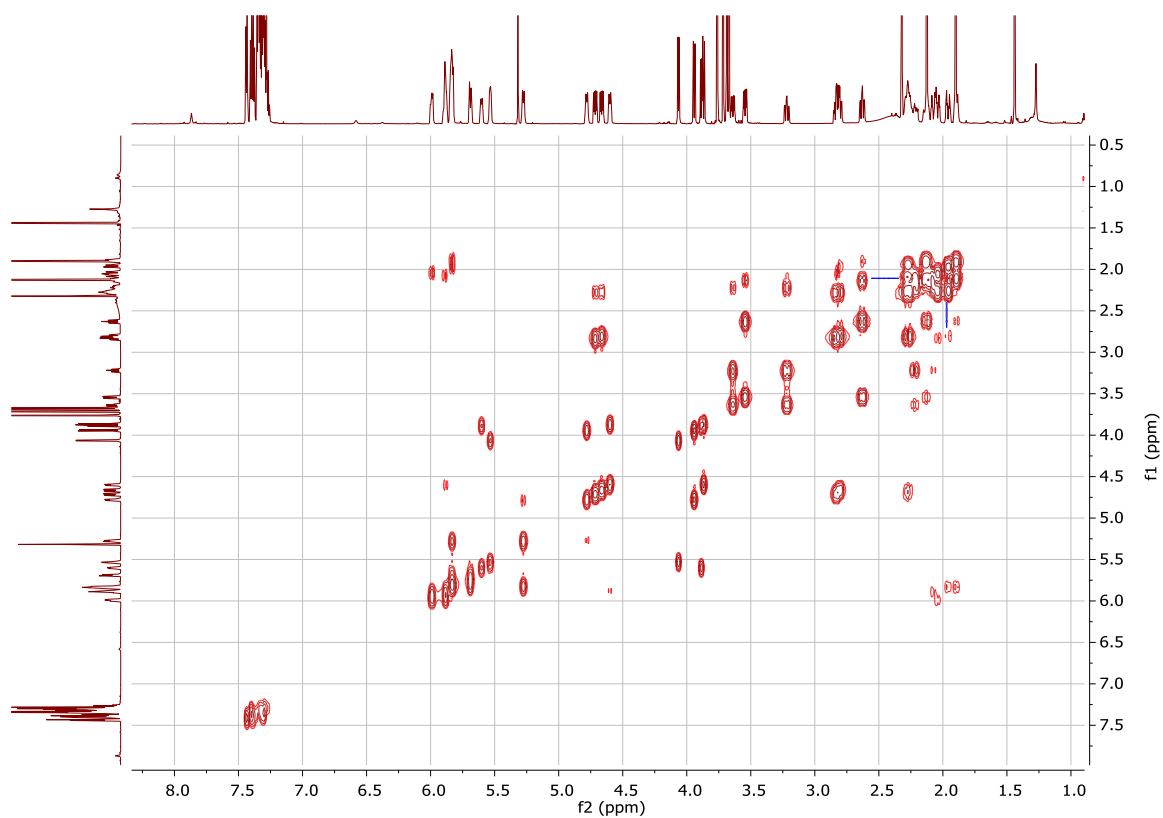
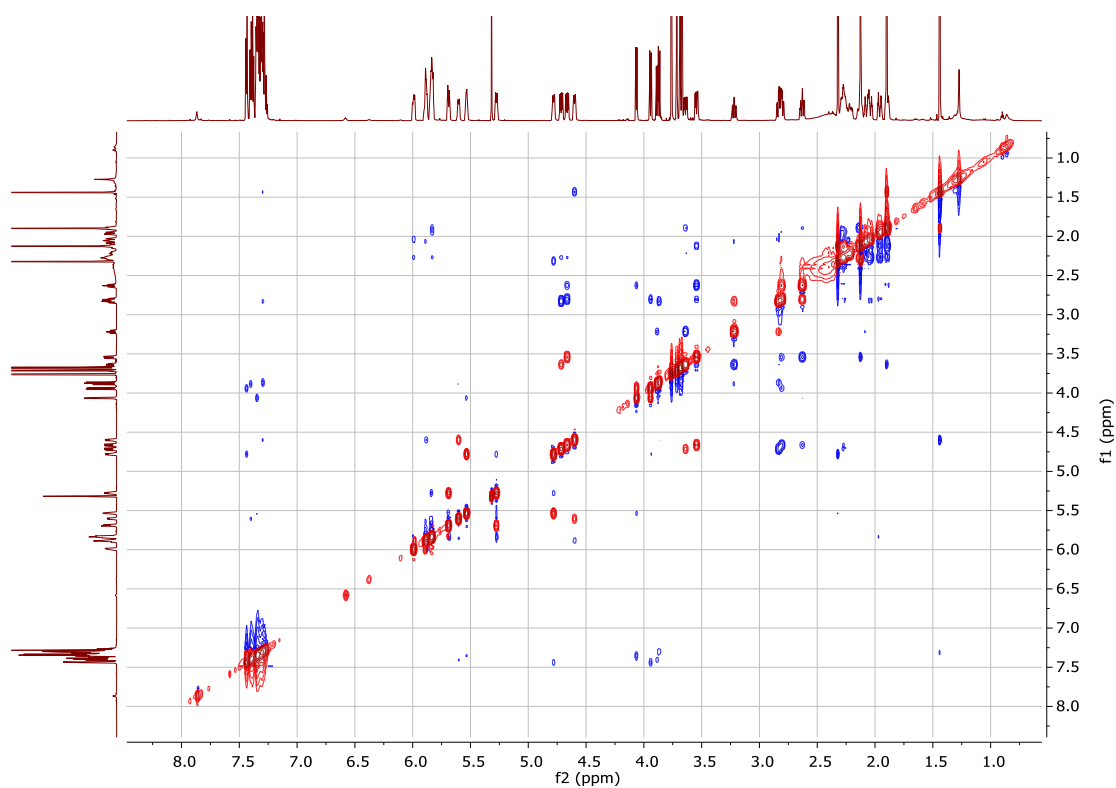
^1H NMR (CDCl_3), 600 MHz of Compound 79:



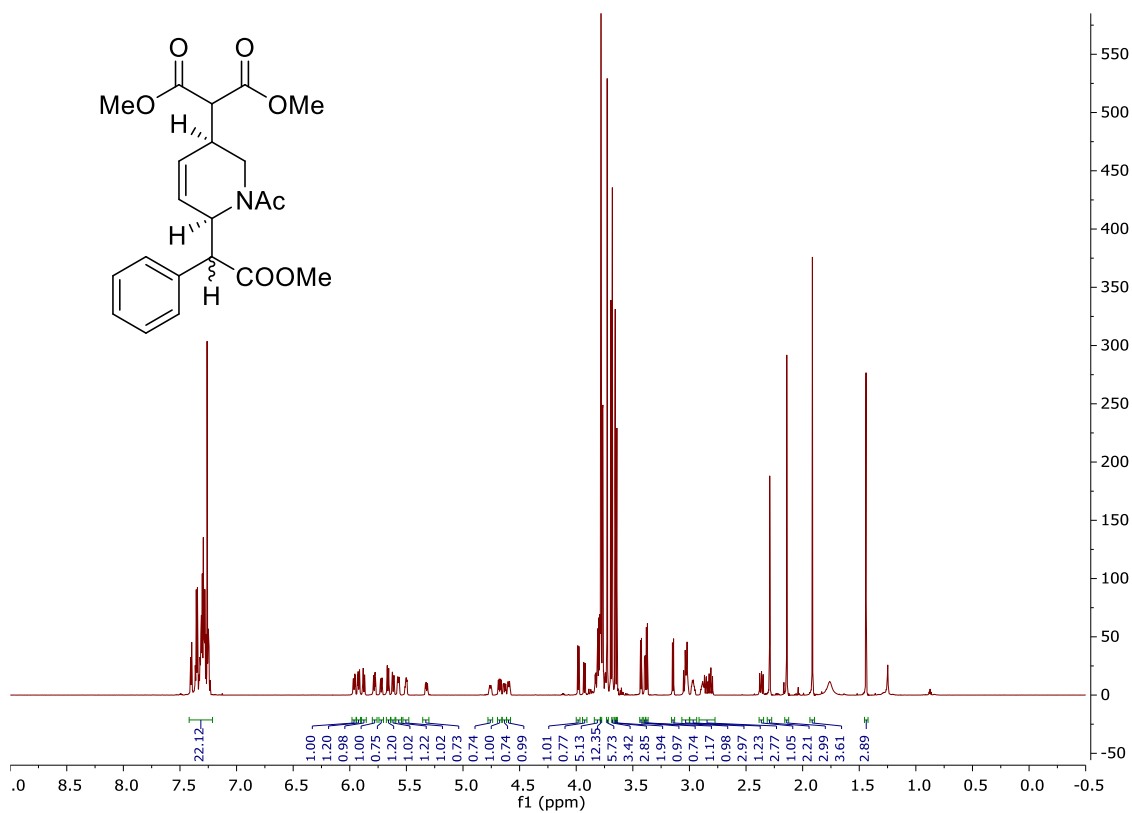
$^{13}\text{C}\{^1\text{H}\}$ NMR (CDCl_3), 200 MHz of Compound 79:



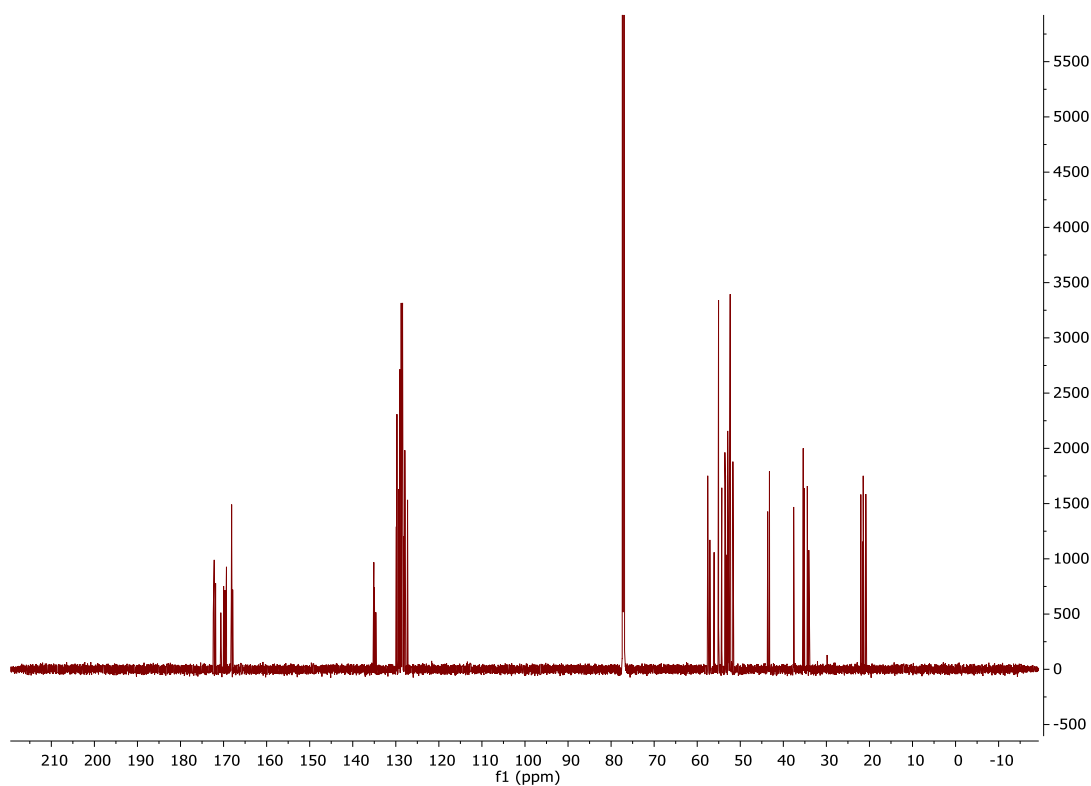
HSQC (CDCl₃), 200 MHz of Compound 79:HMBC (CDCl₃) of Compound 79:

COSY (CDCl₃) of Compound 79:NOESY (CDCl₃) of Compound 79:

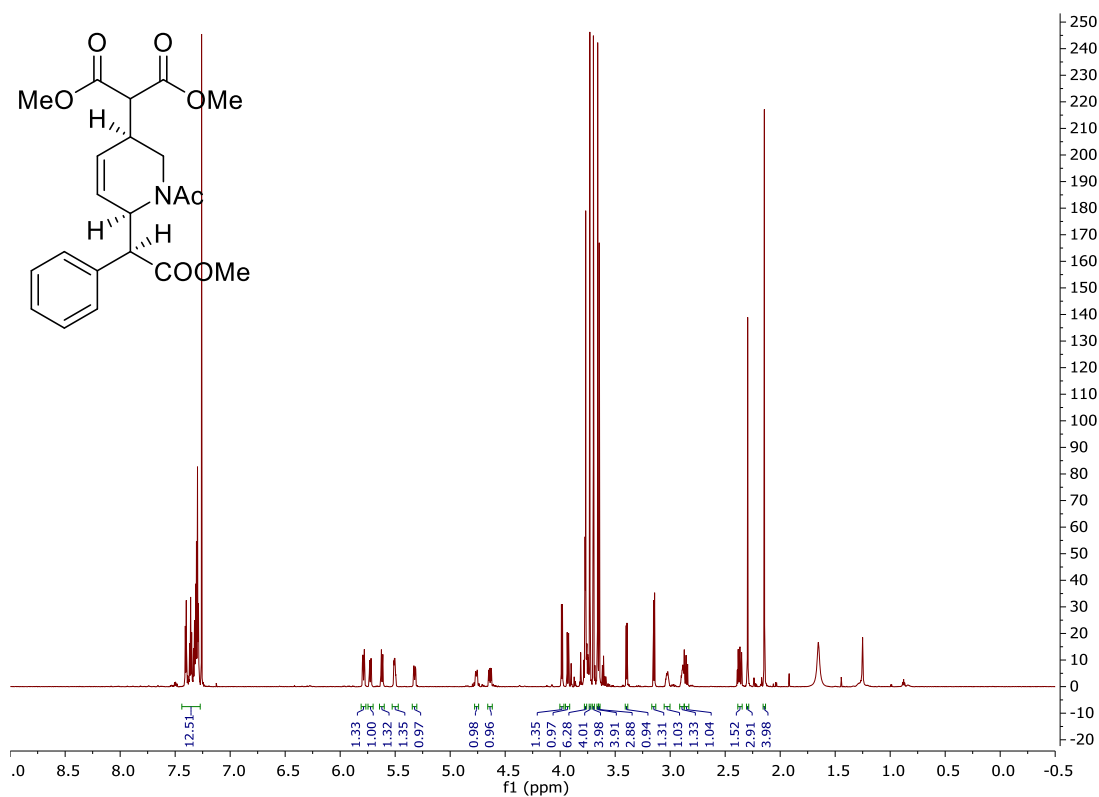
^1H NMR (CDCl_3), 600 MHz of Compound 81:



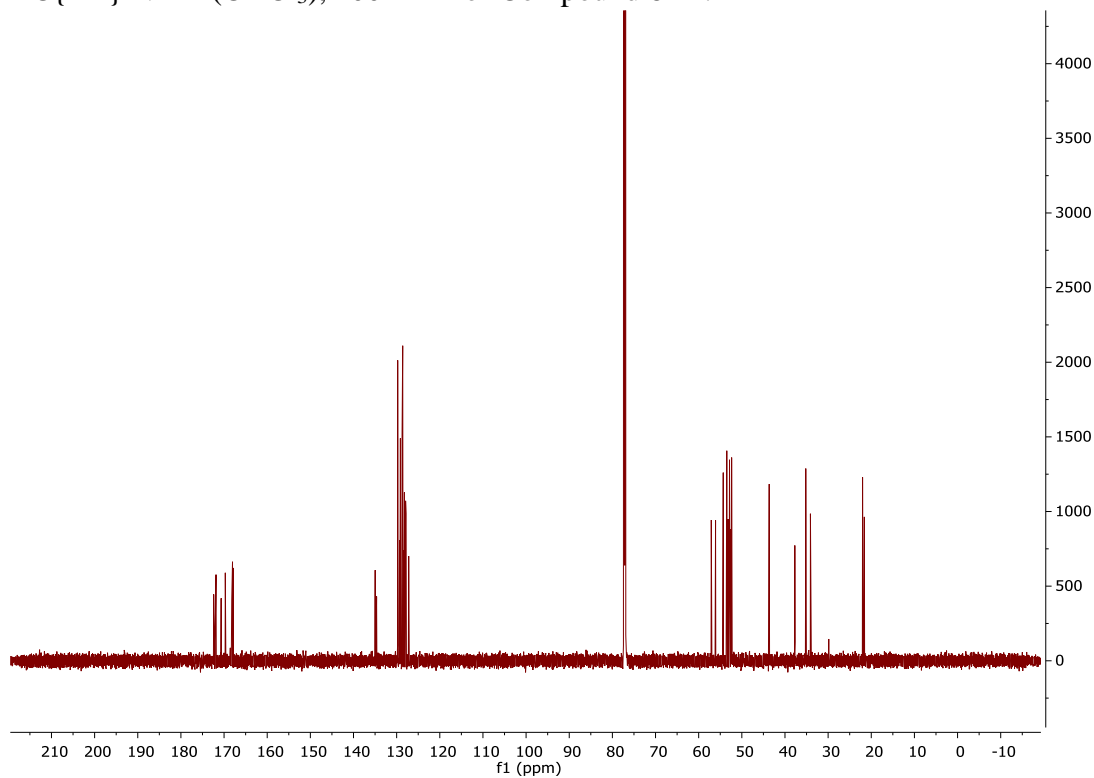
$^{13}\text{C}\{^1\text{H}\}$ NMR (CDCl_3), 200 MHz of Compound 81:



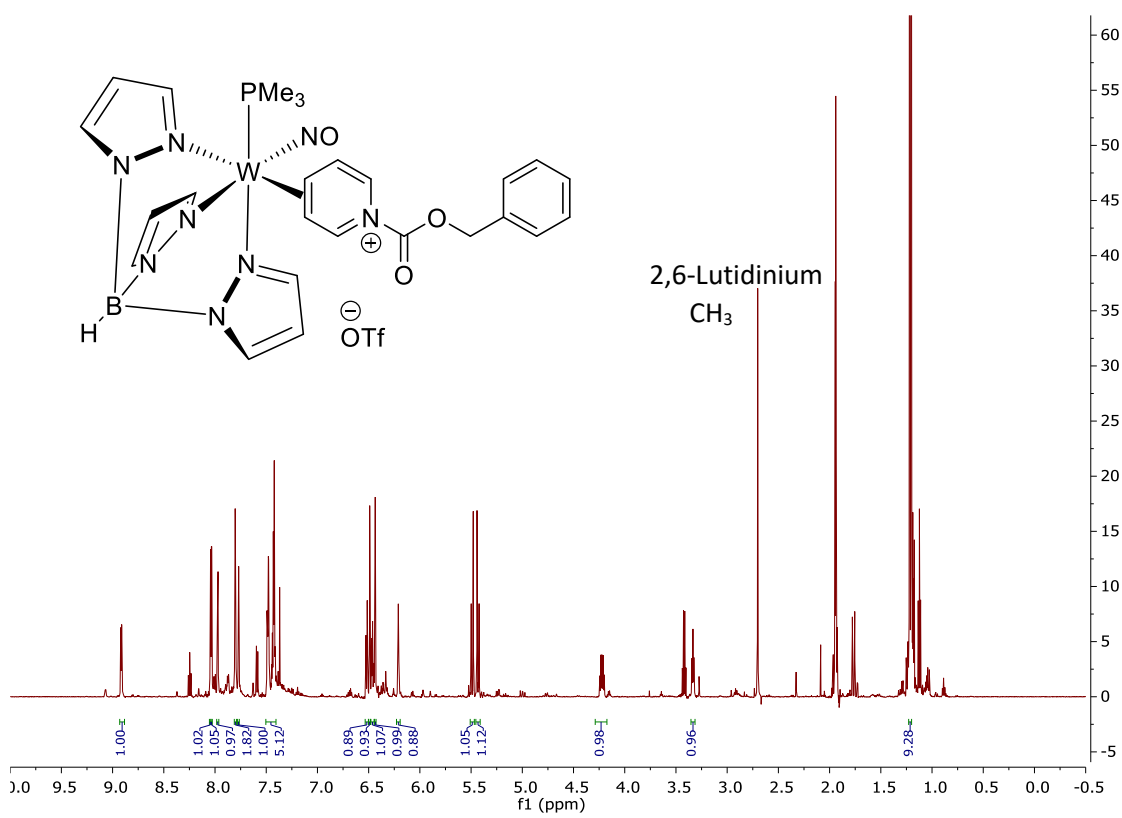
^1H NMR (CDCl_3), 600 MHz of Compound 81A:



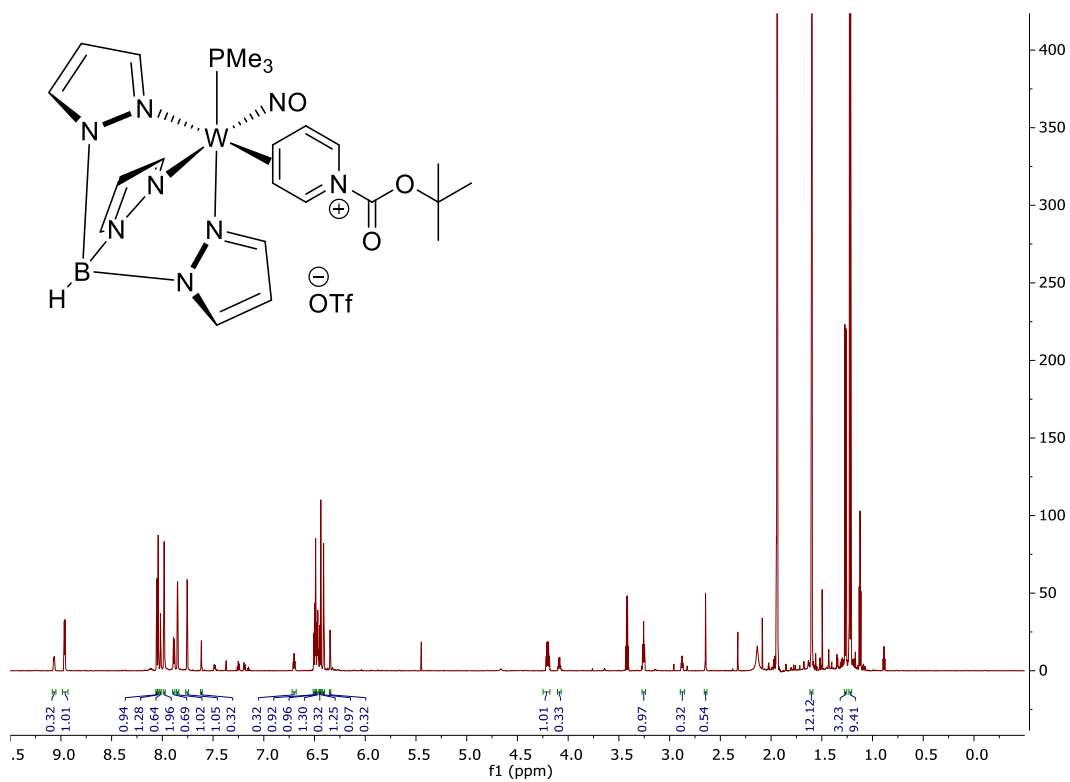
$^{13}\text{C}\{^1\text{H}\}$ NMR (CDCl_3), 200 MHz of Compound 81A:



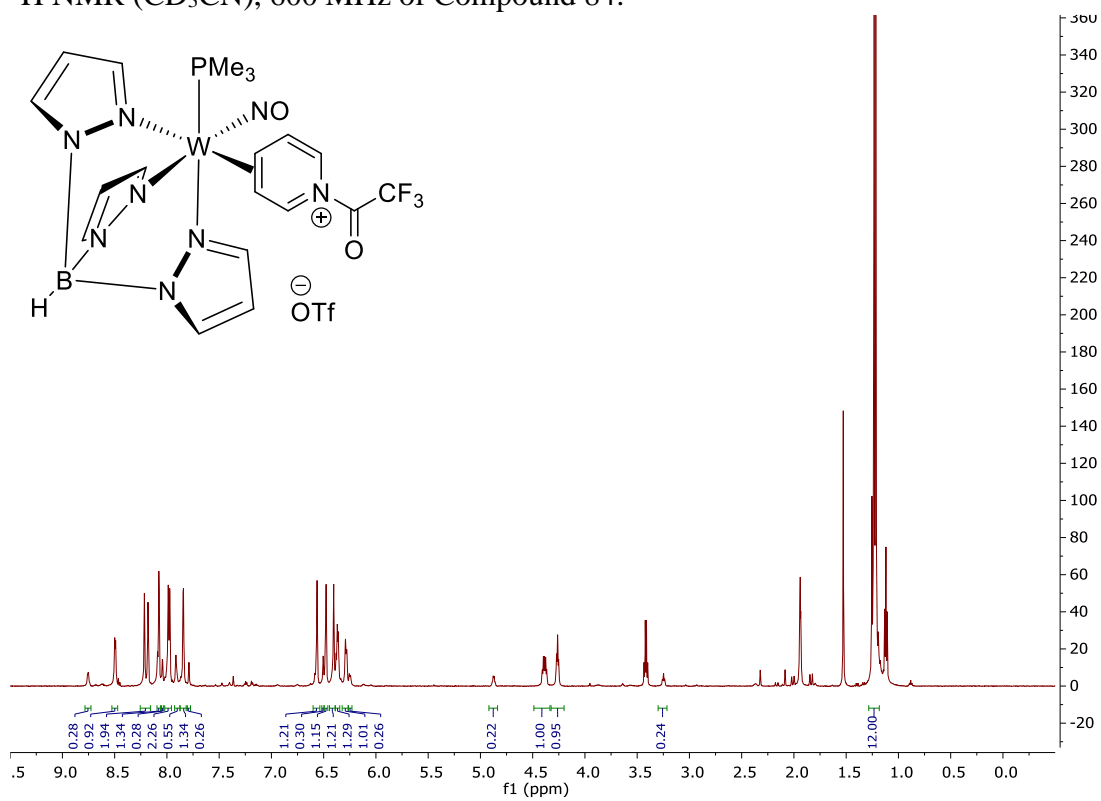
^1H NMR (CD_3CN), 600 MHz of Compound 82:



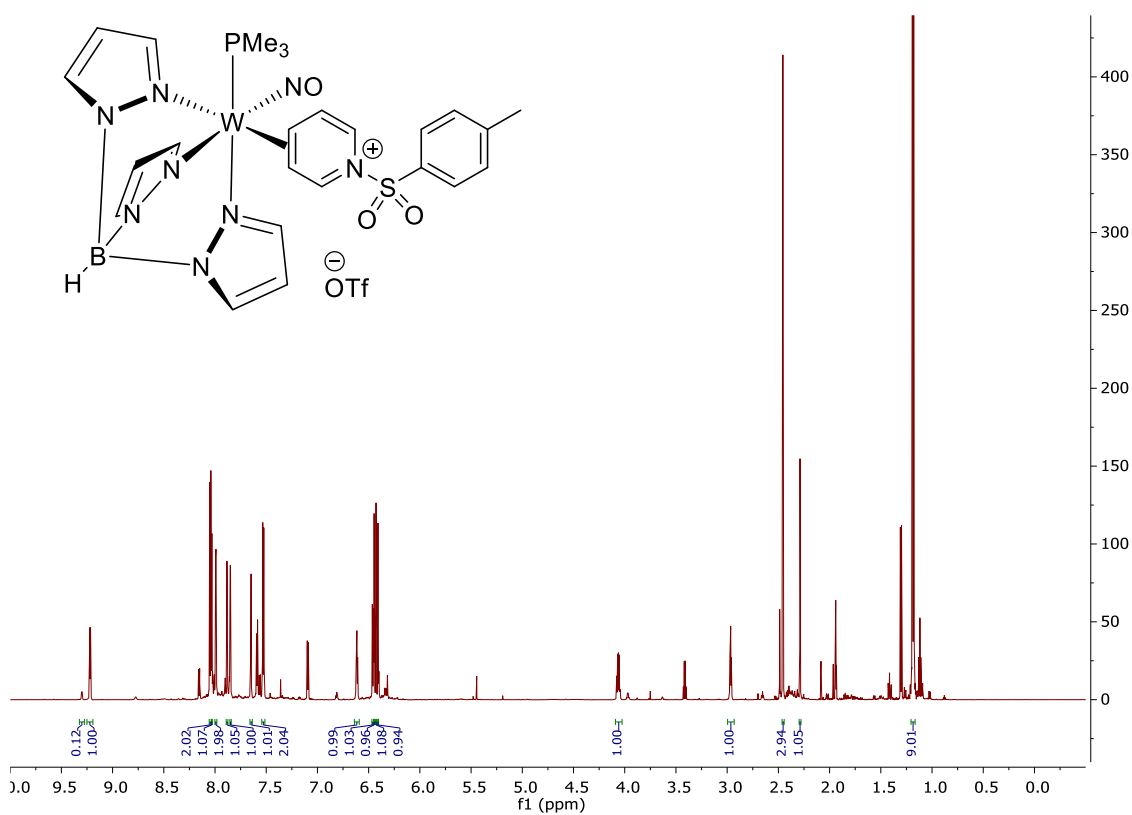
^1H NMR (CD_3CN), 600 MHz of Compound 83:



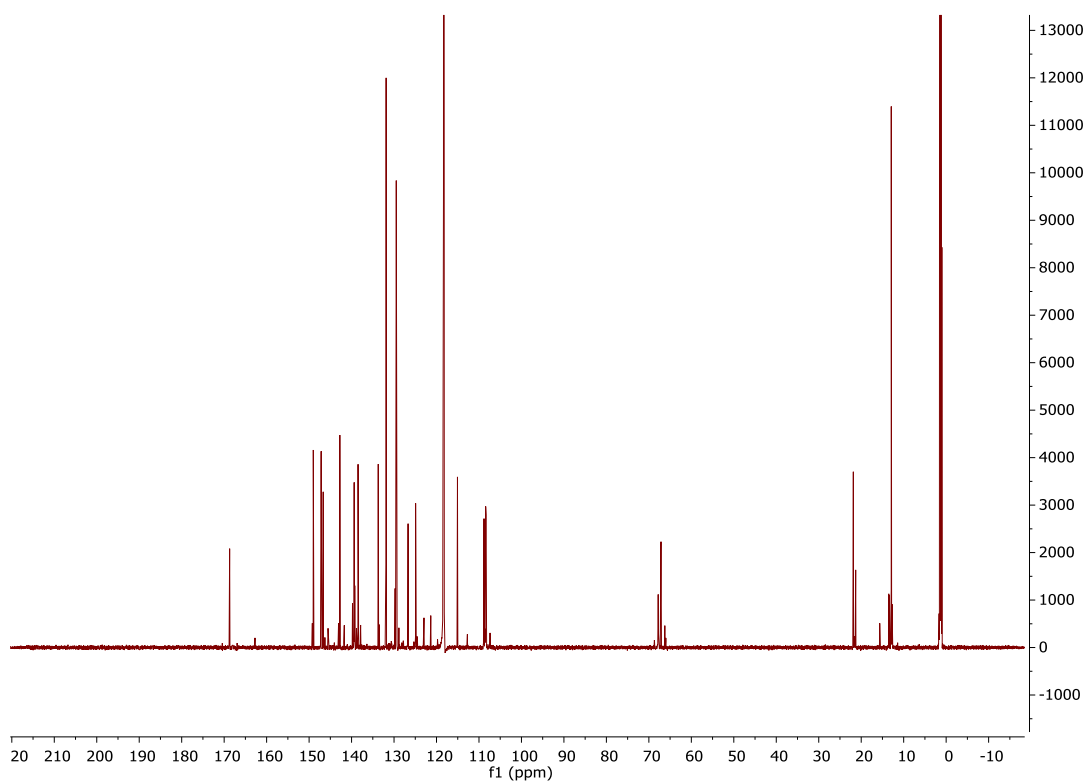
^1H NMR (CD_3CN), 600 MHz of Compound 84:



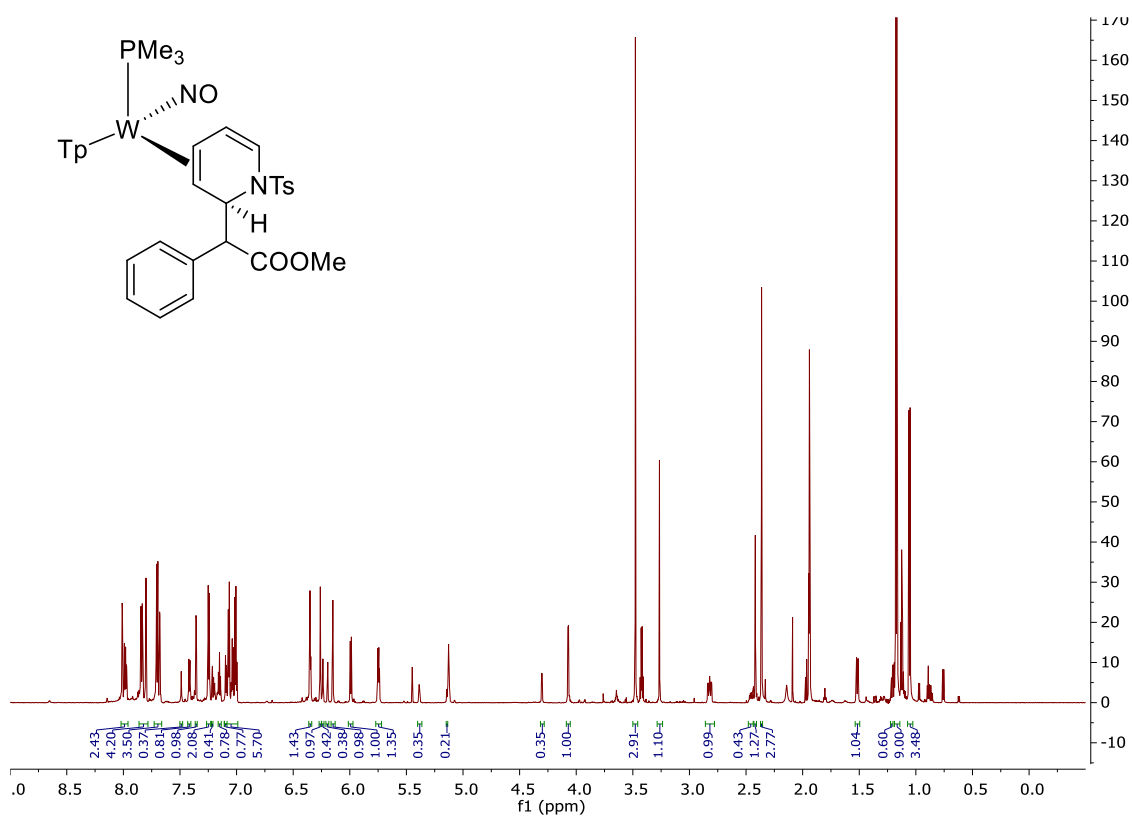
^1H NMR (CD_3CN), 600 MHz of Compound 85:



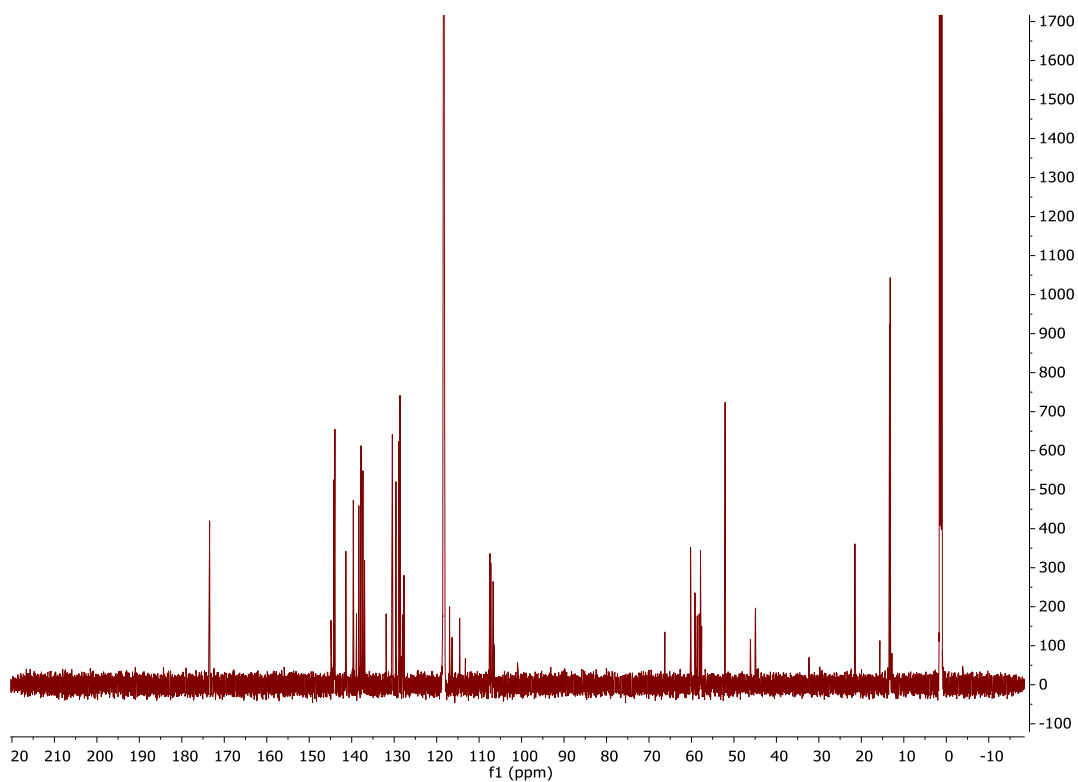
^{13}C NMR (CD_3CN), 200 MHz of Compound 85:



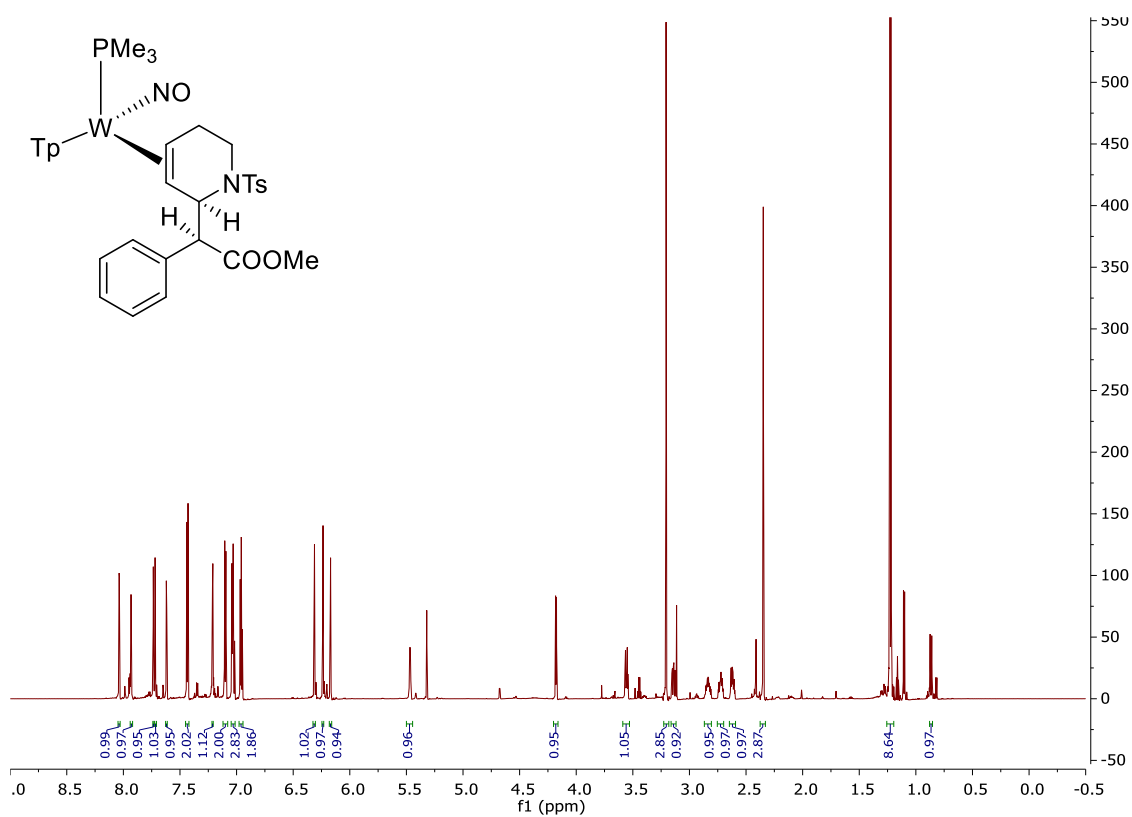
^1H NMR (CD_3CN), 600 MHz of Compound 86:



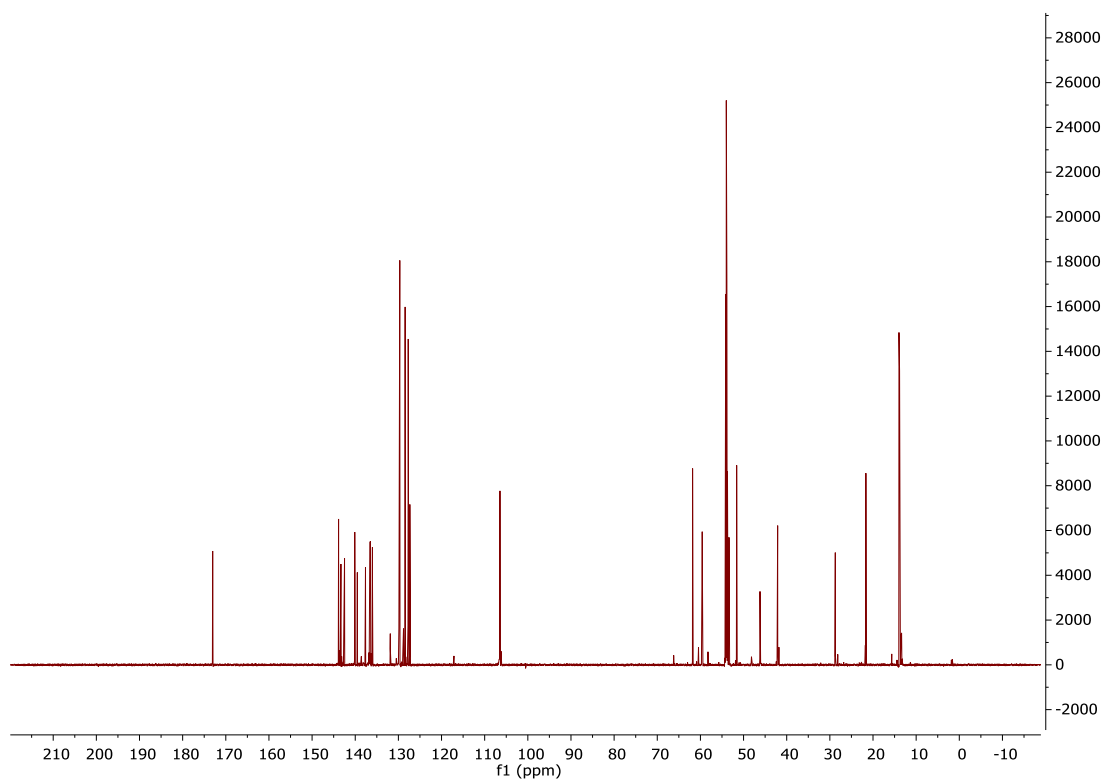
^{13}C NMR (CD_3CN), 600 MHz of Compound 86:



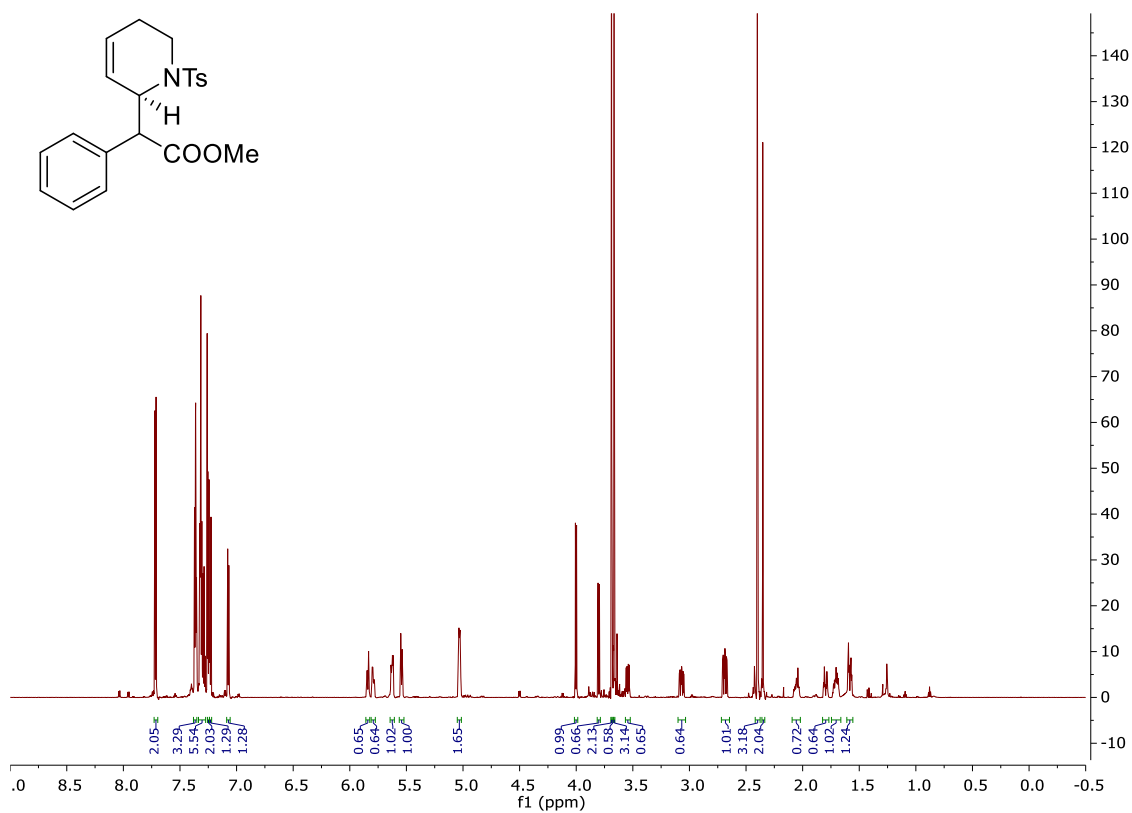
^1H NMR (CD_2Cl_2), 600 MHz of Compound 87A:



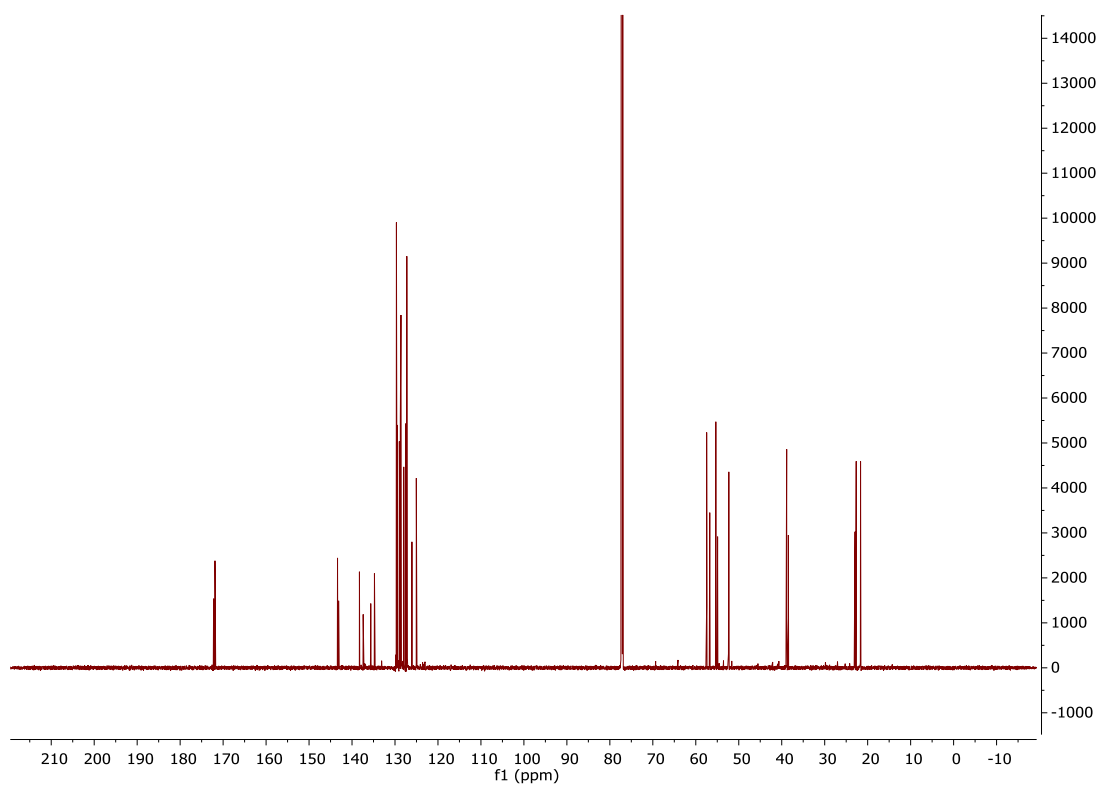
^{13}C NMR (CD_2Cl_2), 200 MHz of Compound 87A:

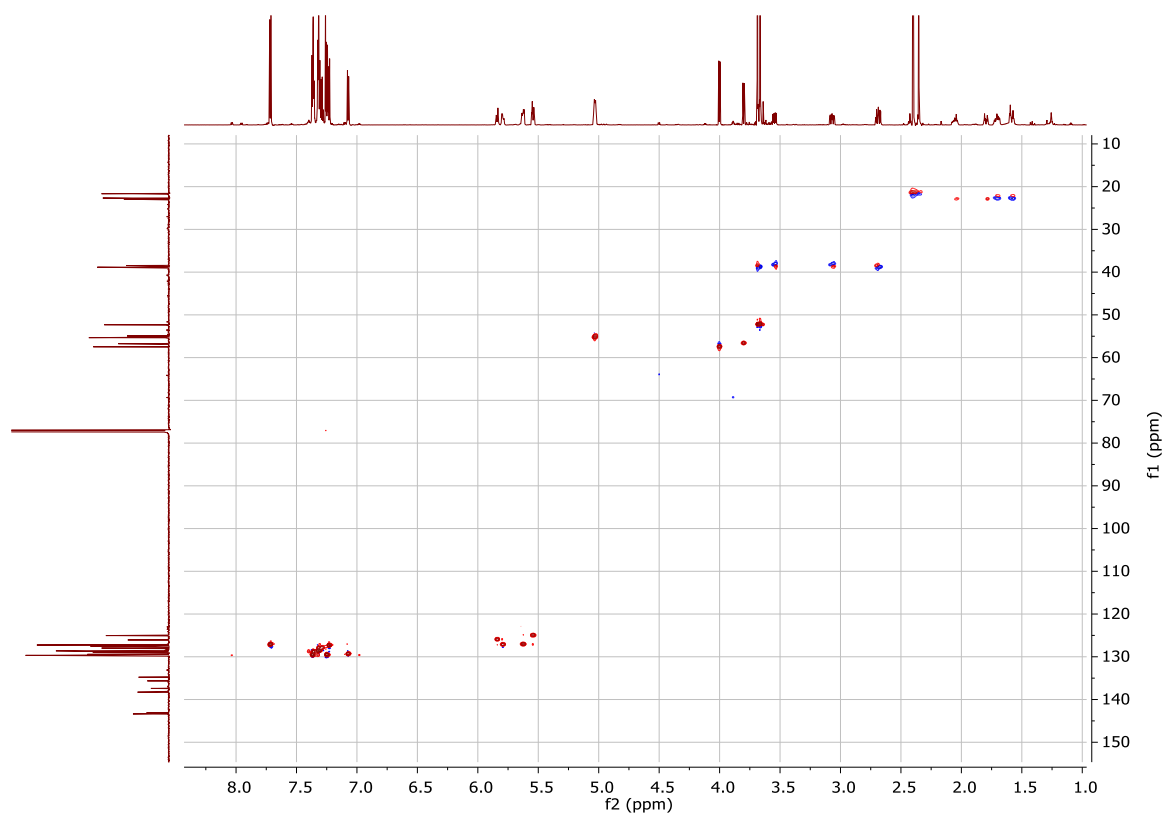
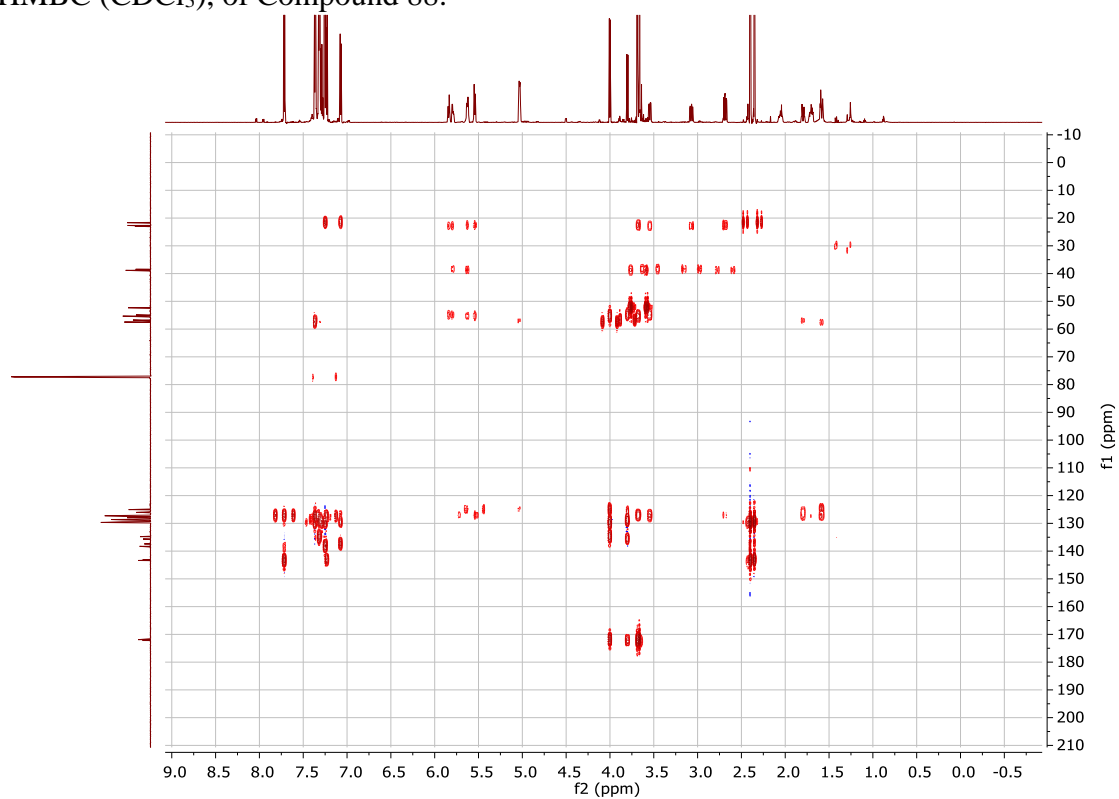


^1H NMR (CDCl_3), 600 MHz of Compound 88:

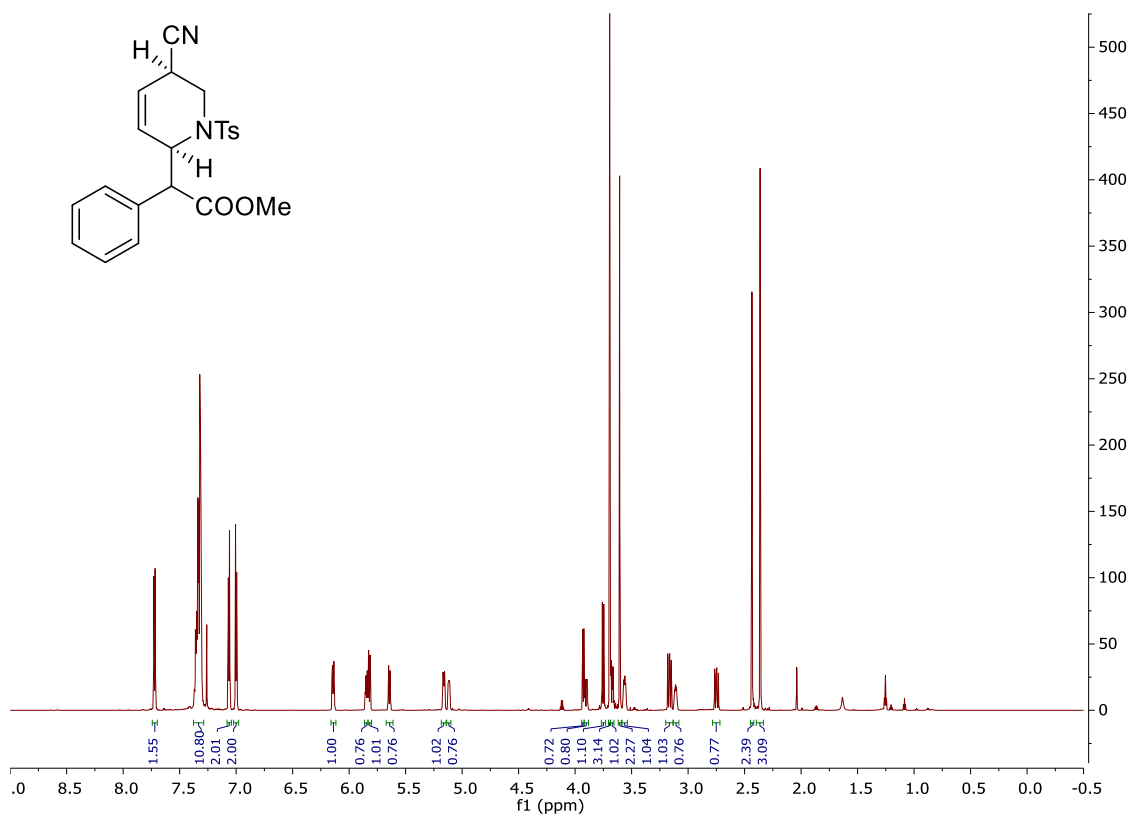


^{13}C NMR (CDCl_3), 200 MHz of Compound 88:

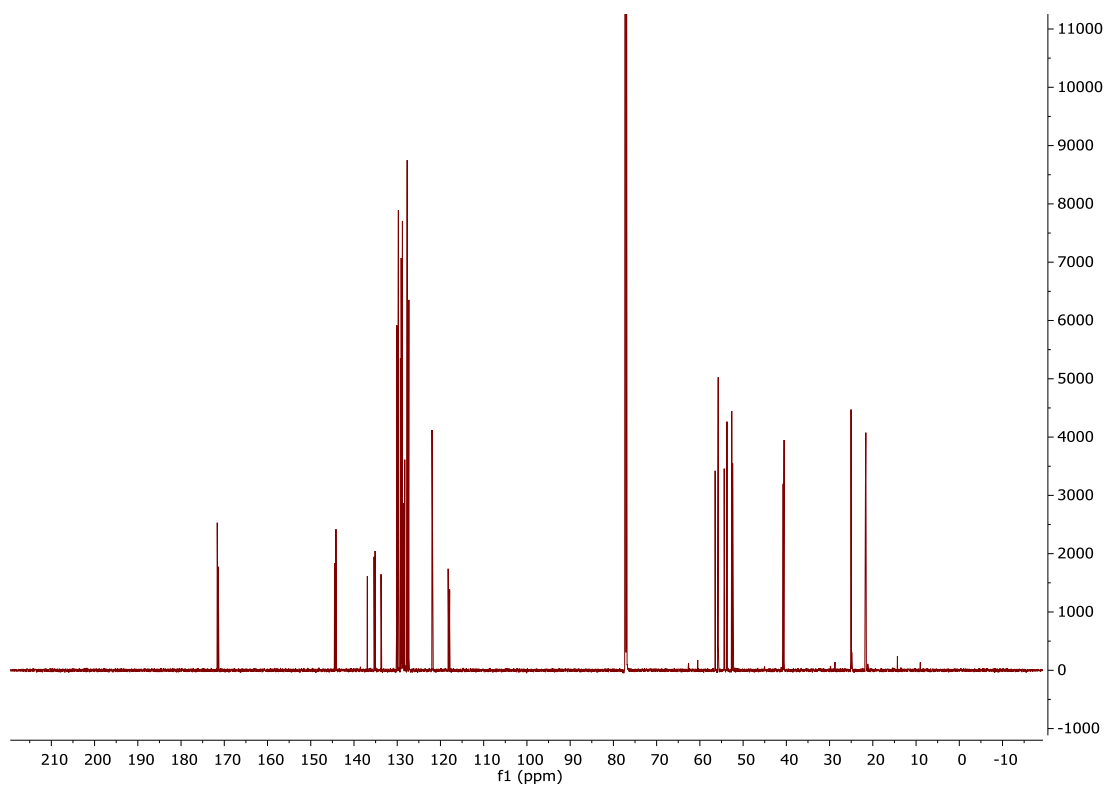


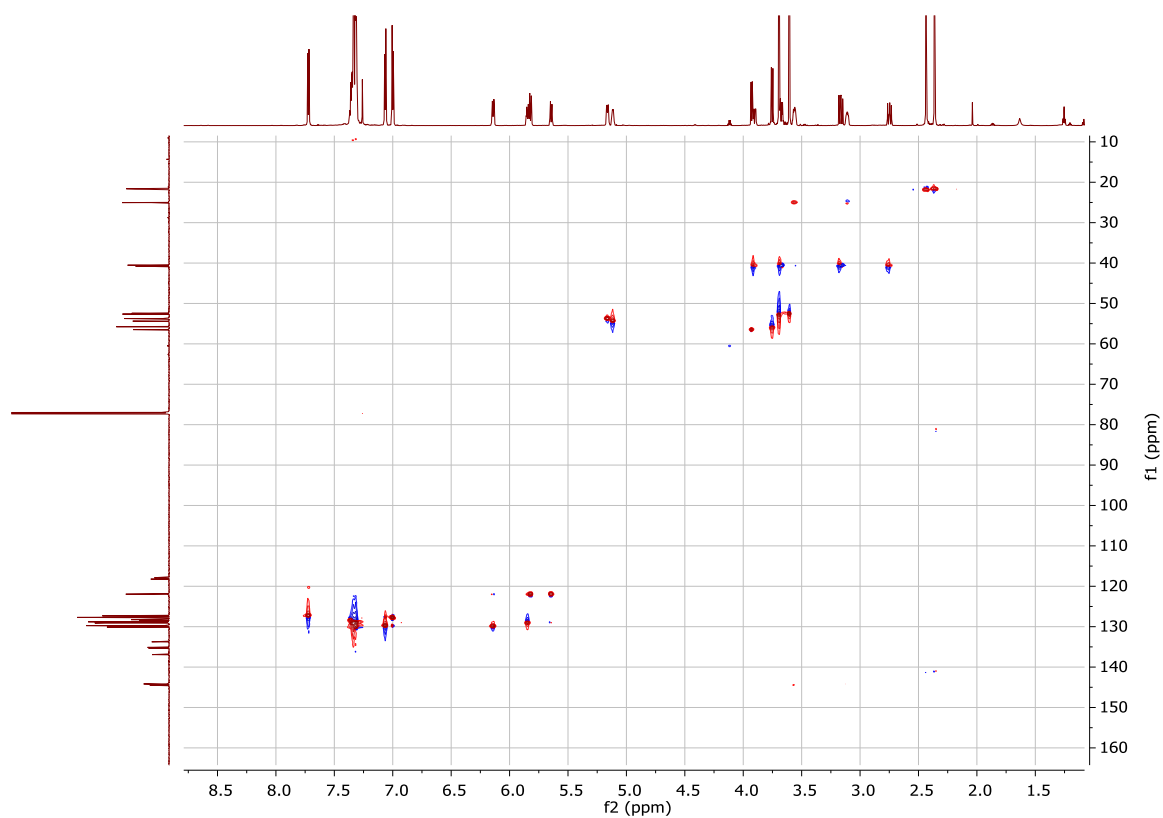
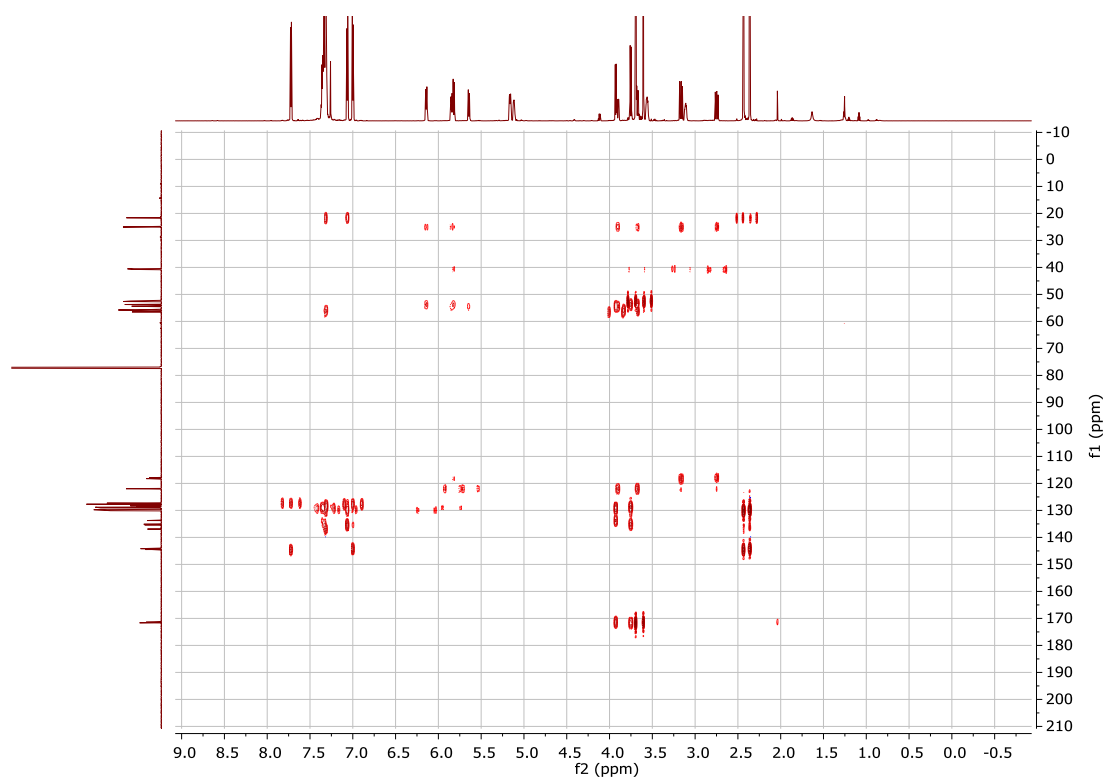
HSQC (CDCl₃), of Compound 88:HMBC (CDCl₃), of Compound 88:

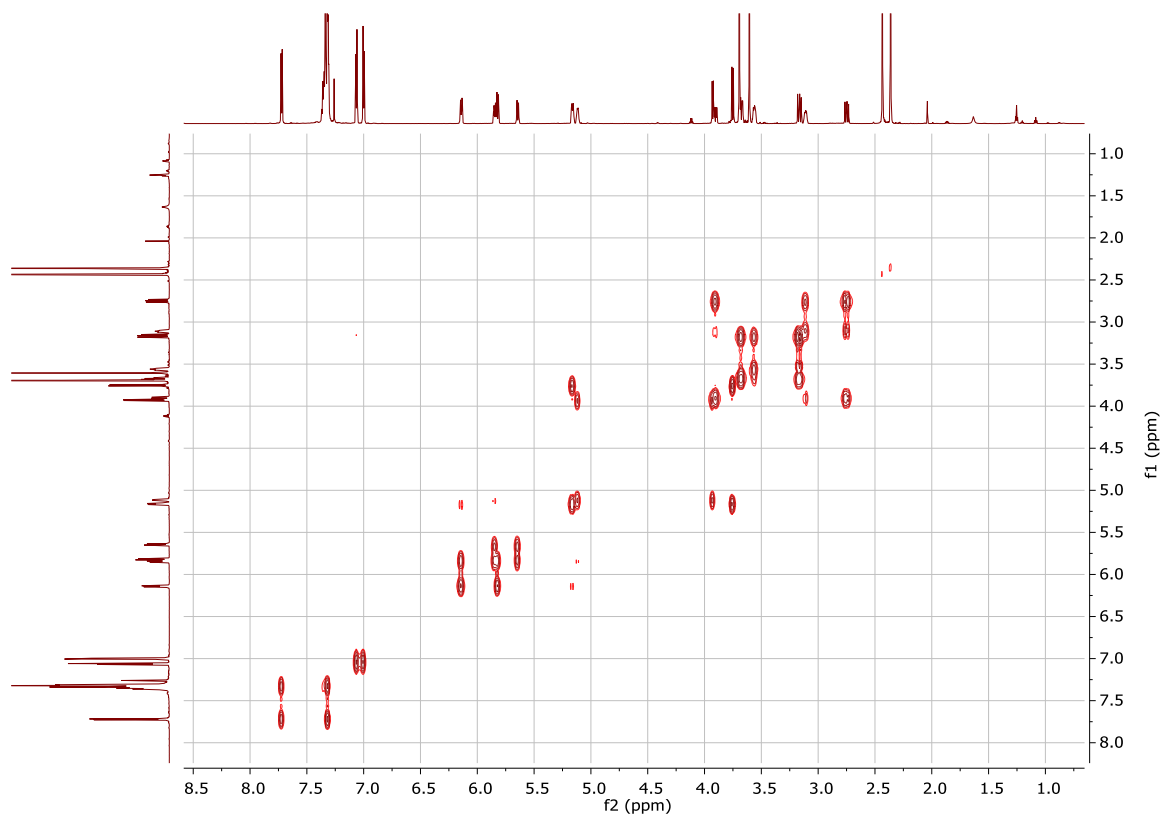
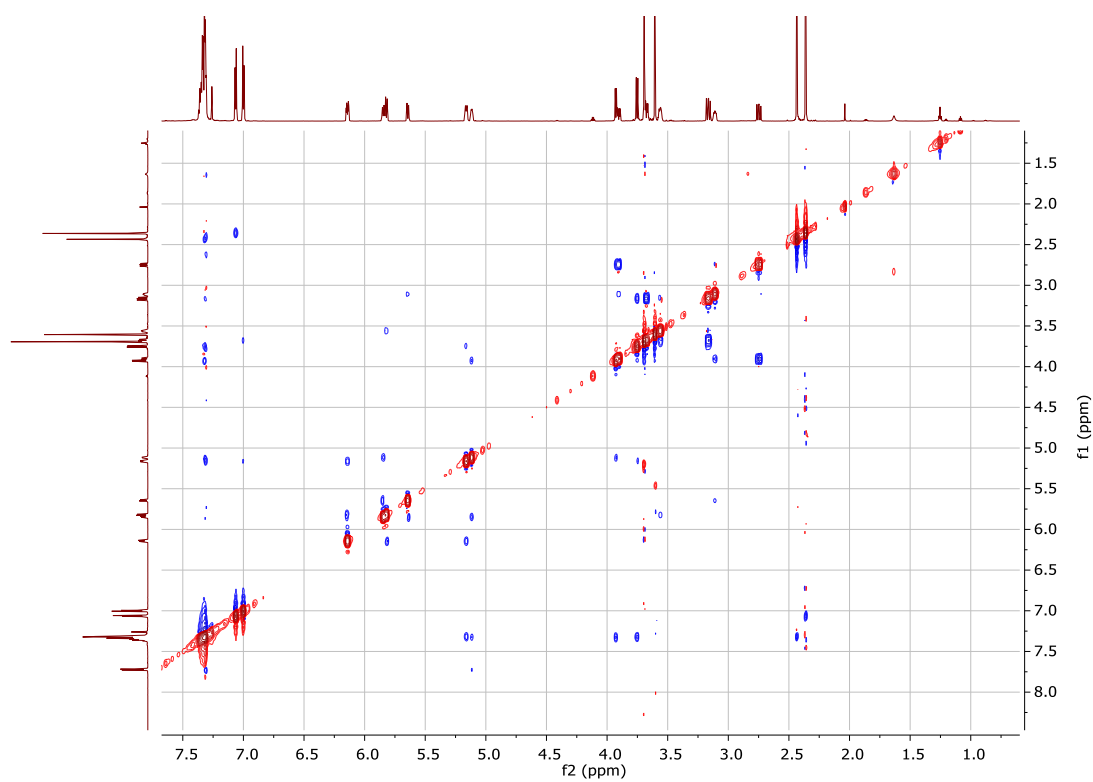
^1H NMR (CDCl_3), 600 MHz of Compound 90:



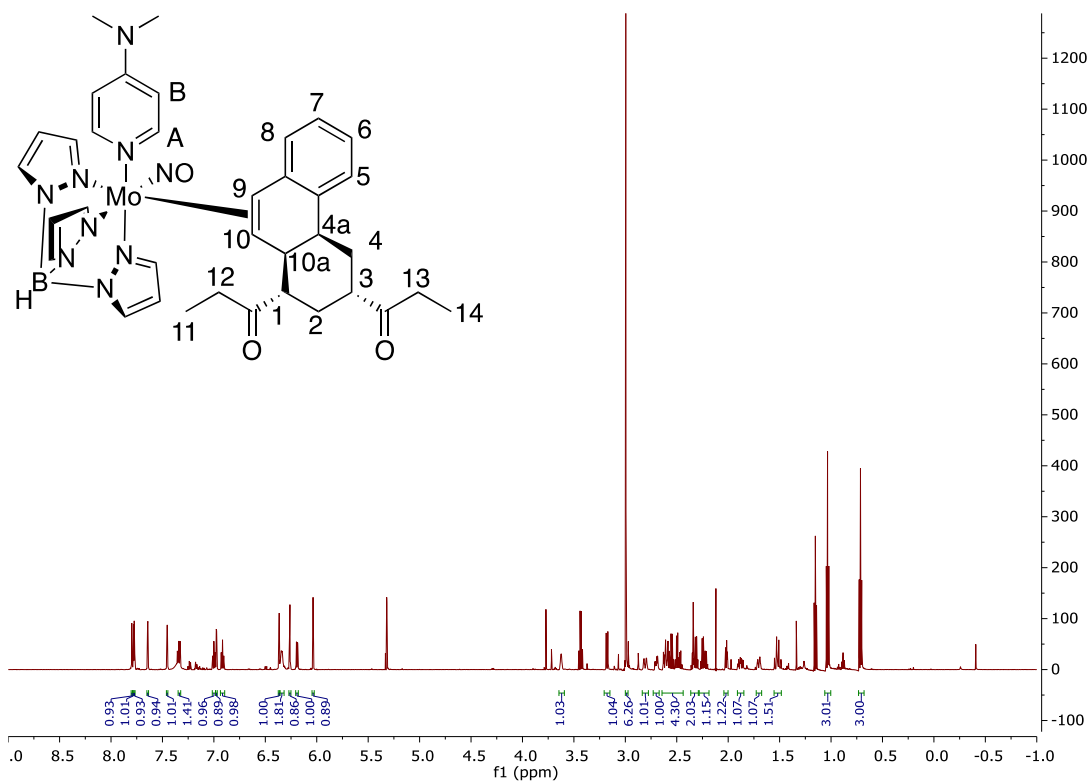
^{13}C NMR (CDCl_3), 200 MHz of Compound 90:



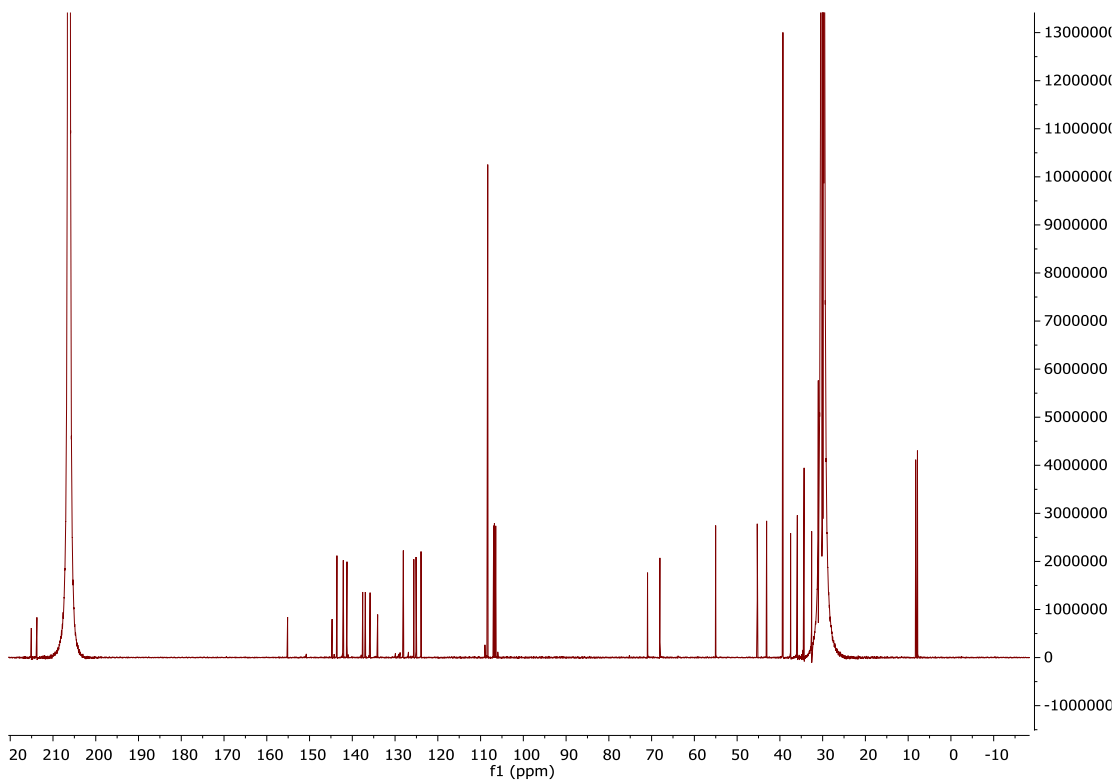
HSQC (CDCl₃), of Compound 90:HMBC (CDCl₃), of Compound 90:

COSY (CDCl₃), of Compound 90:NOESY (CDCl₃), of Compound 90:

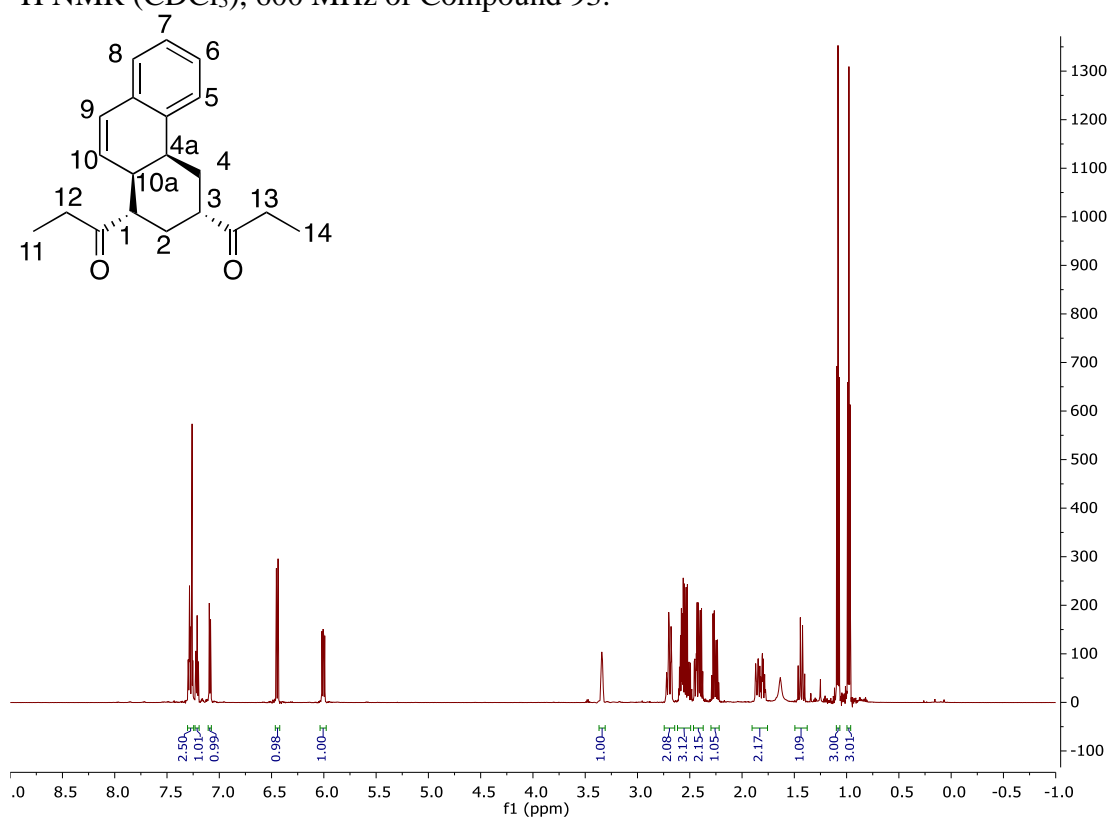
^1H NMR (CD_2Cl_2), 600 MHz of Compound 92:



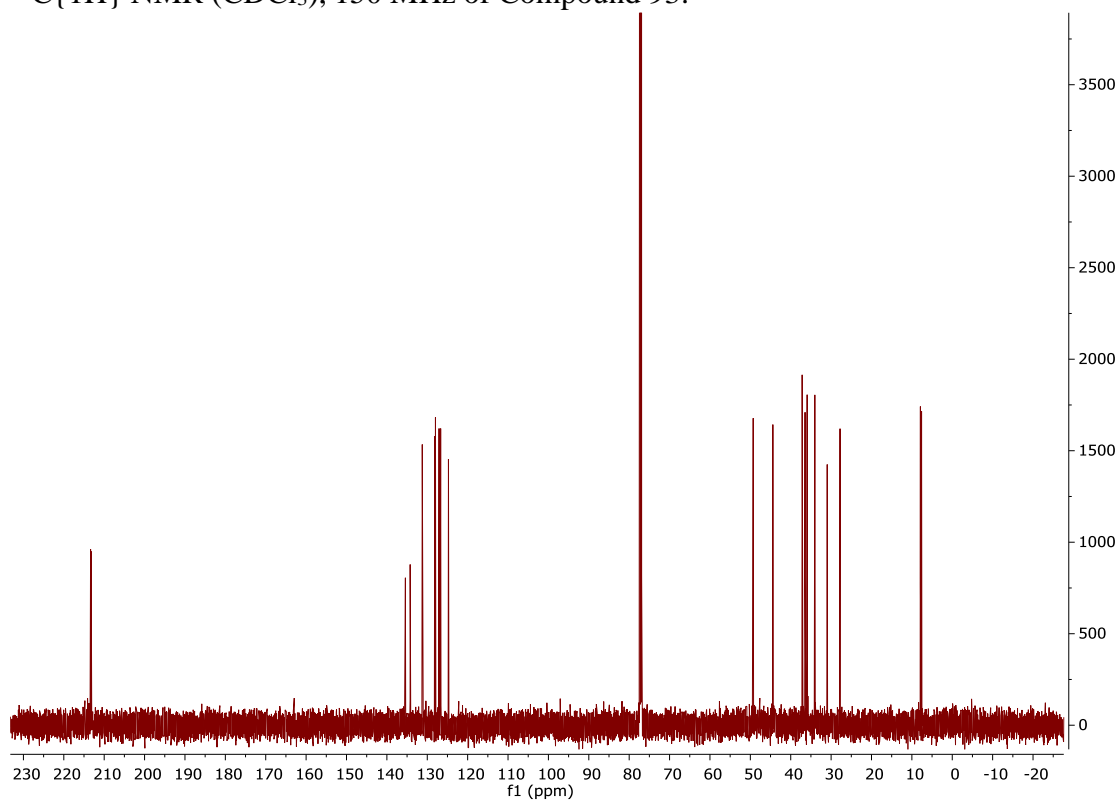
$^{13}\text{C}\{^1\text{H}\}$ NMR (d^6 -Acetone), 200 MHz of Compound 92:

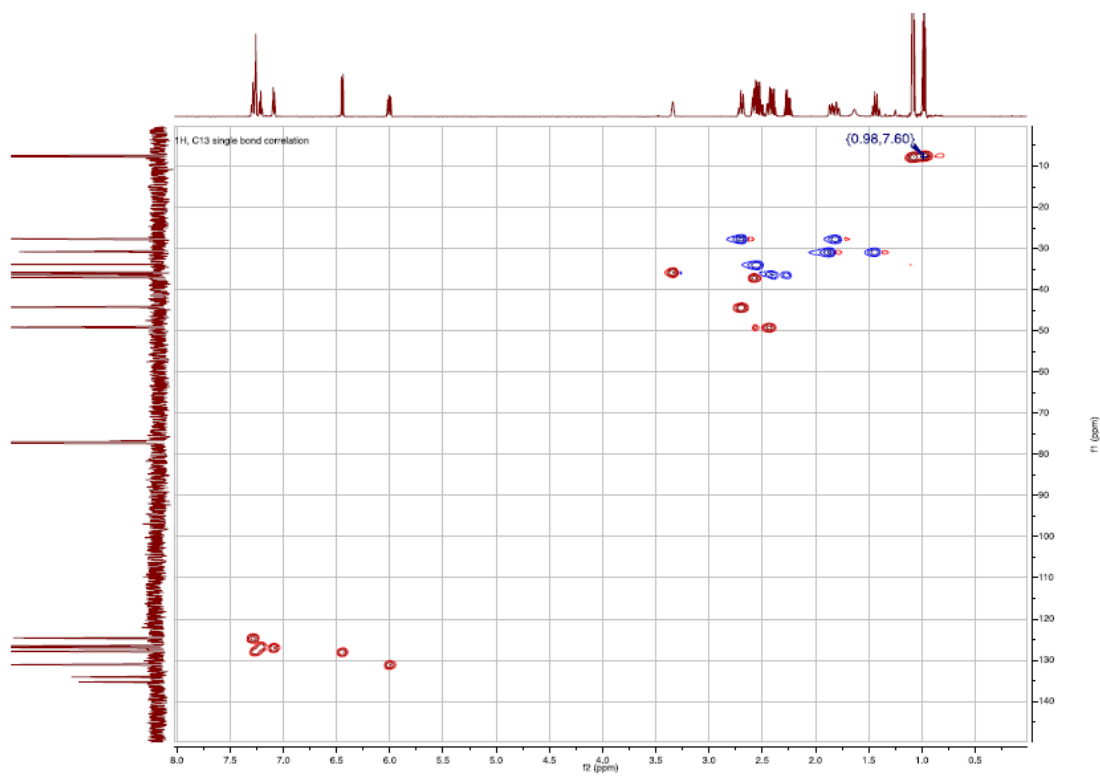
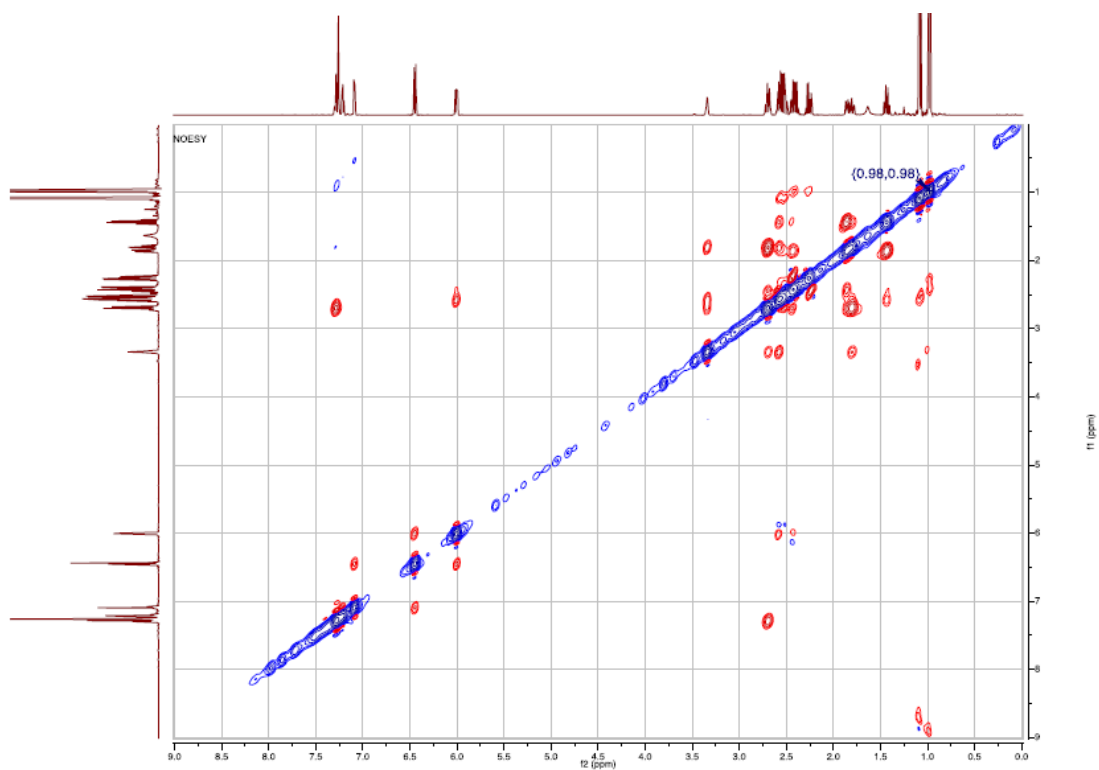


^1H NMR (CDCl_3), 600 MHz of Compound 93:

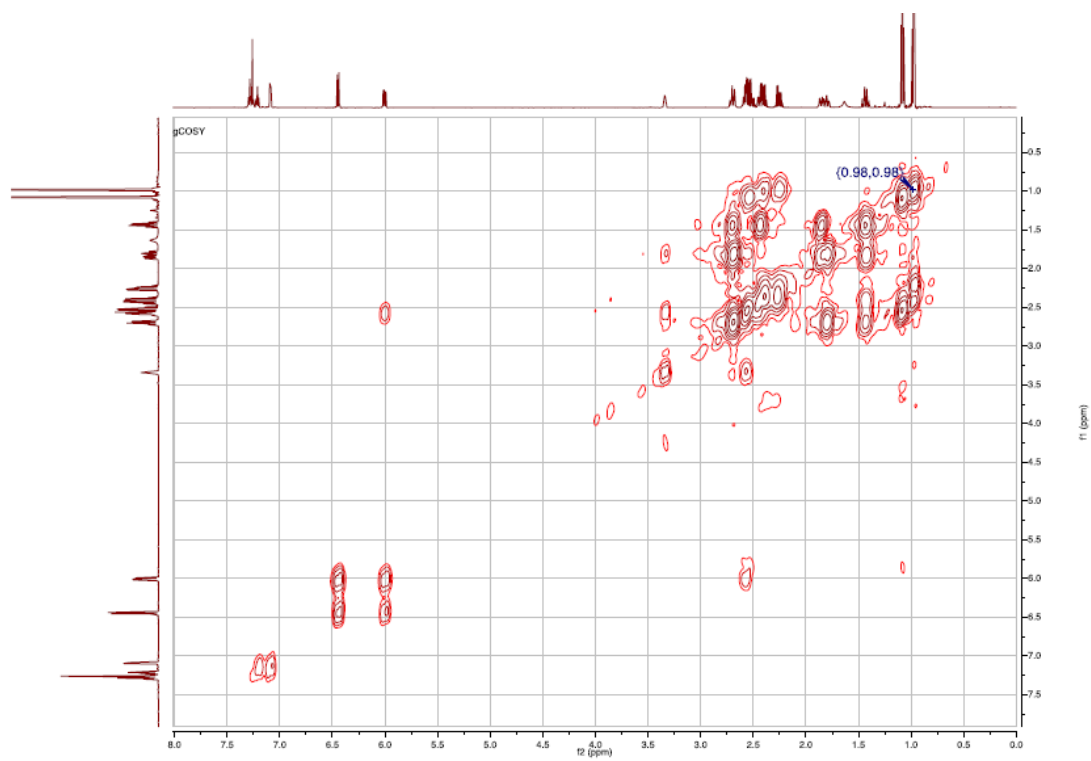


$^{13}\text{C}\{^1\text{H}\}$ NMR (CDCl_3), 150 MHz of Compound 93:

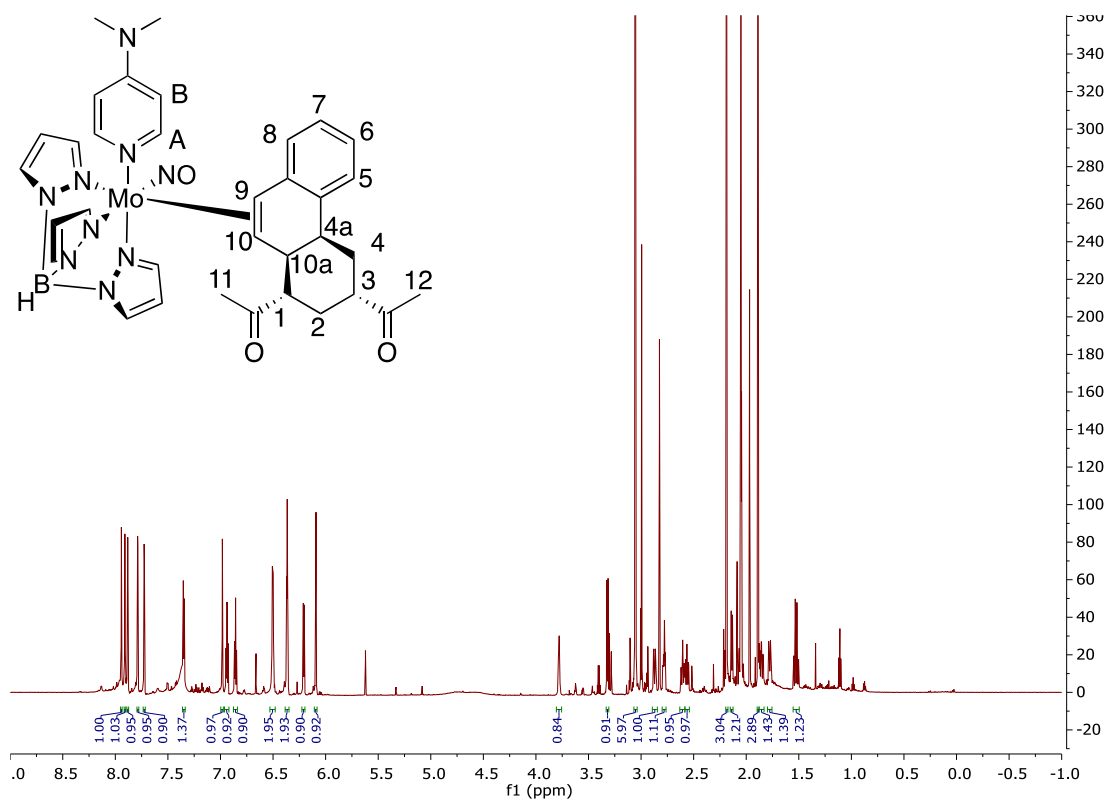


HSQC (CDCl₃) of Compound 93:NOESY (CDCl₃) of Compound 93:

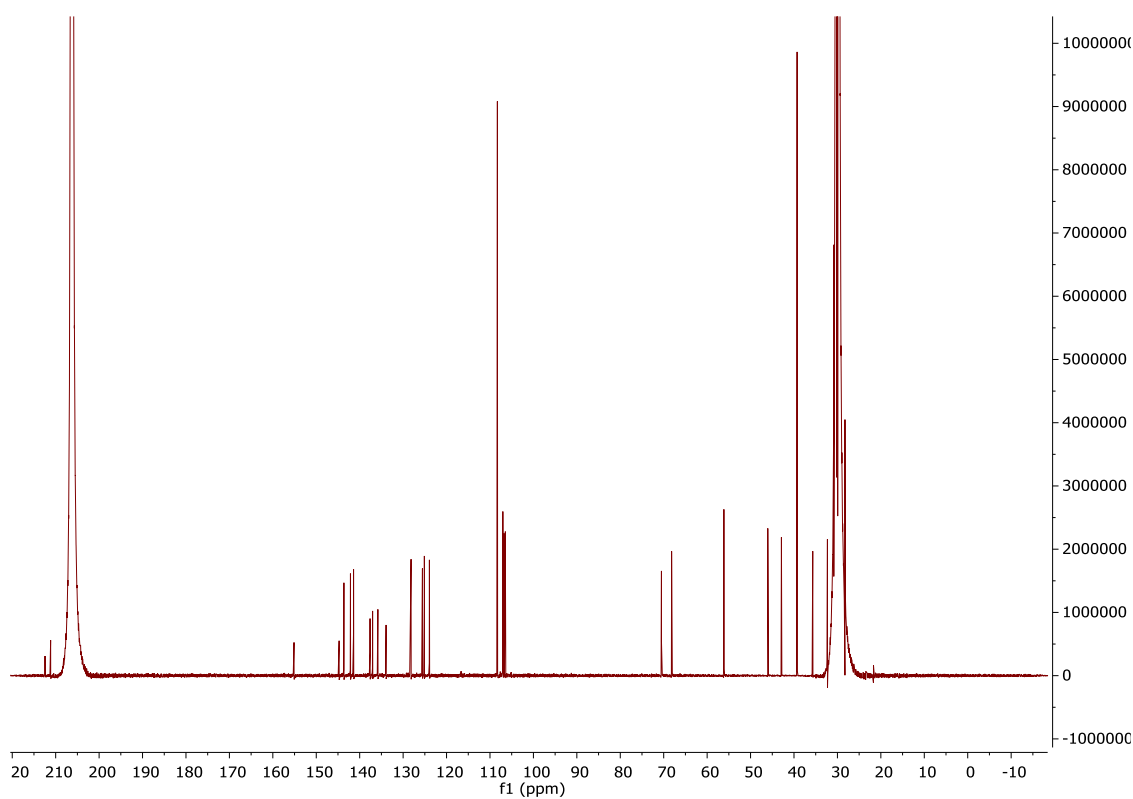
COSY (CDCl₃) of Compound 93:



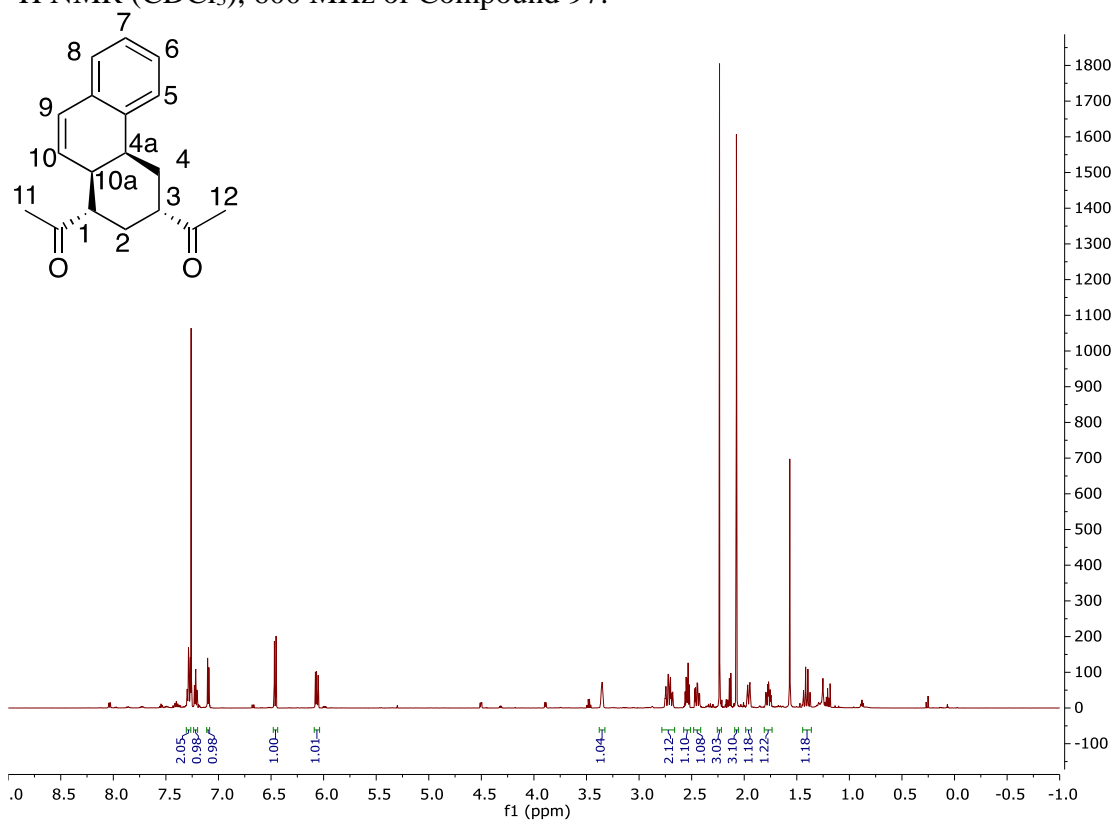
^1H NMR (d^6 -Acetone), 600 MHz of Compound 96:



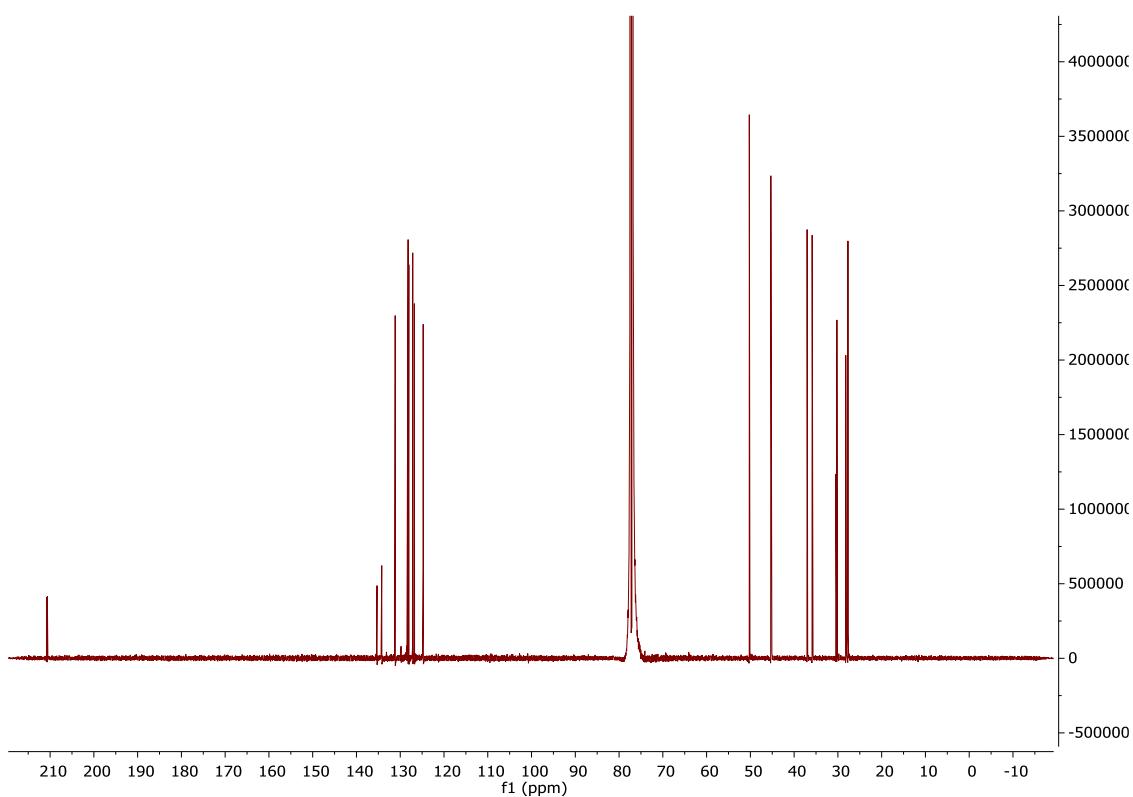
^{13}C NMR { ^1H } (d^6 -Acetone), 200 MHz of Compound 96:



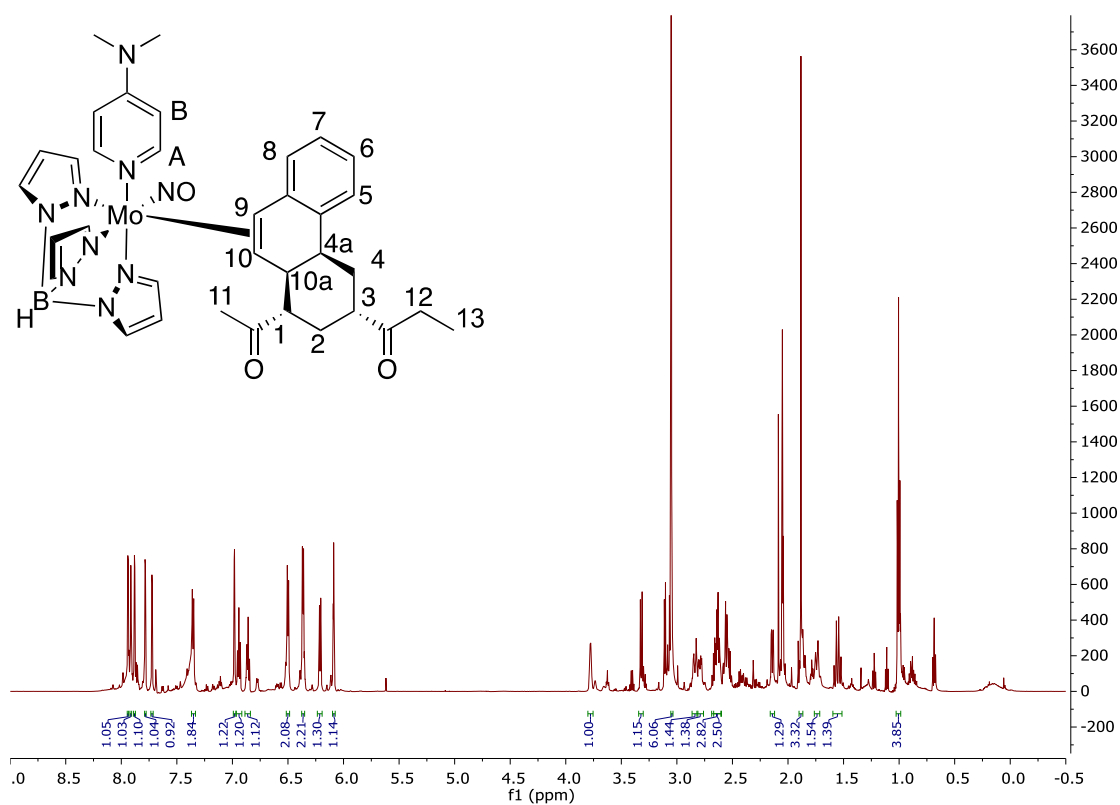
^1H NMR (CDCl_3), 600 MHz of Compound 97:



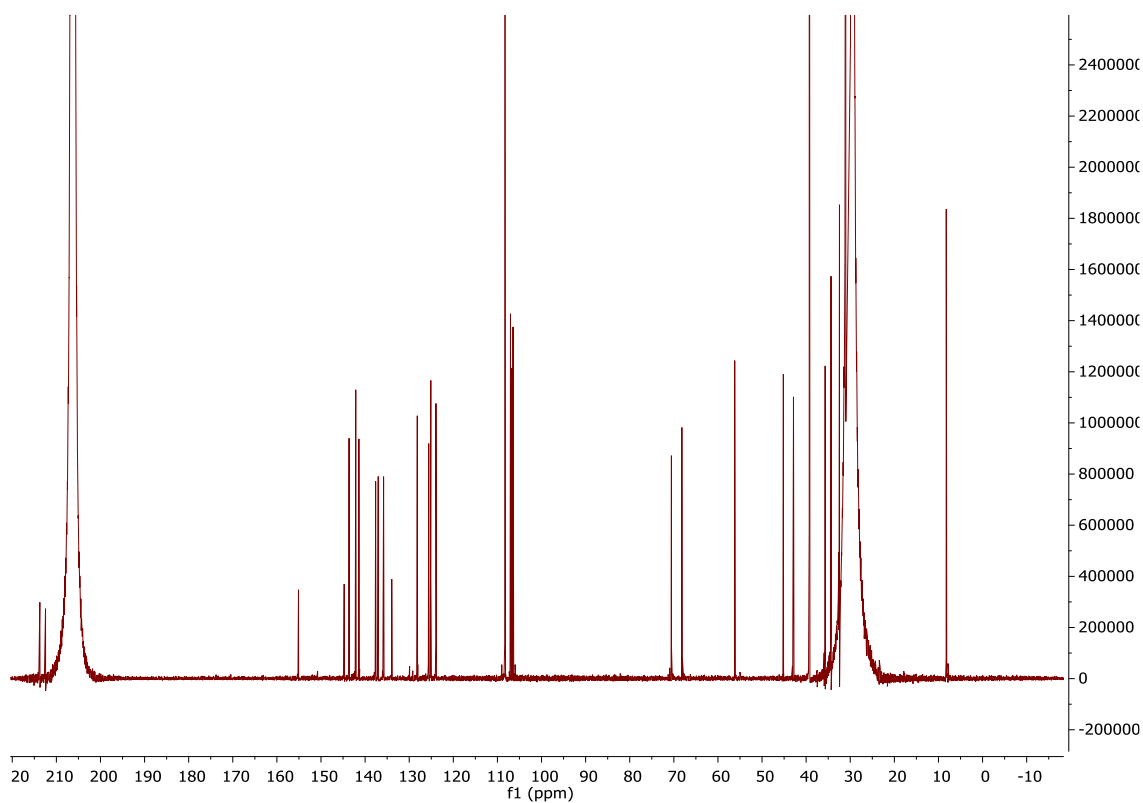
$^{13}\text{C}\{^1\text{H}\}$ NMR (CDCl_3), 200 MHz of Compound 97:



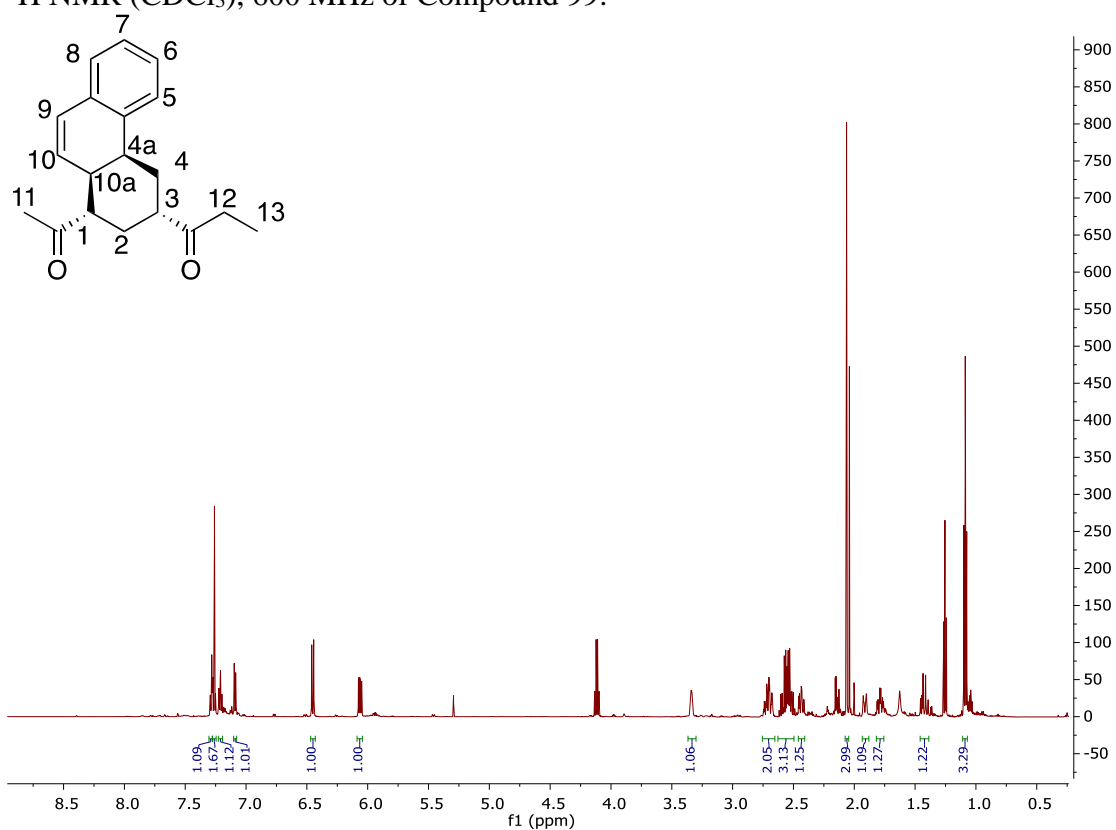
^1H NMR (d^6 -Acetone), 600 MHz of Compound 98:



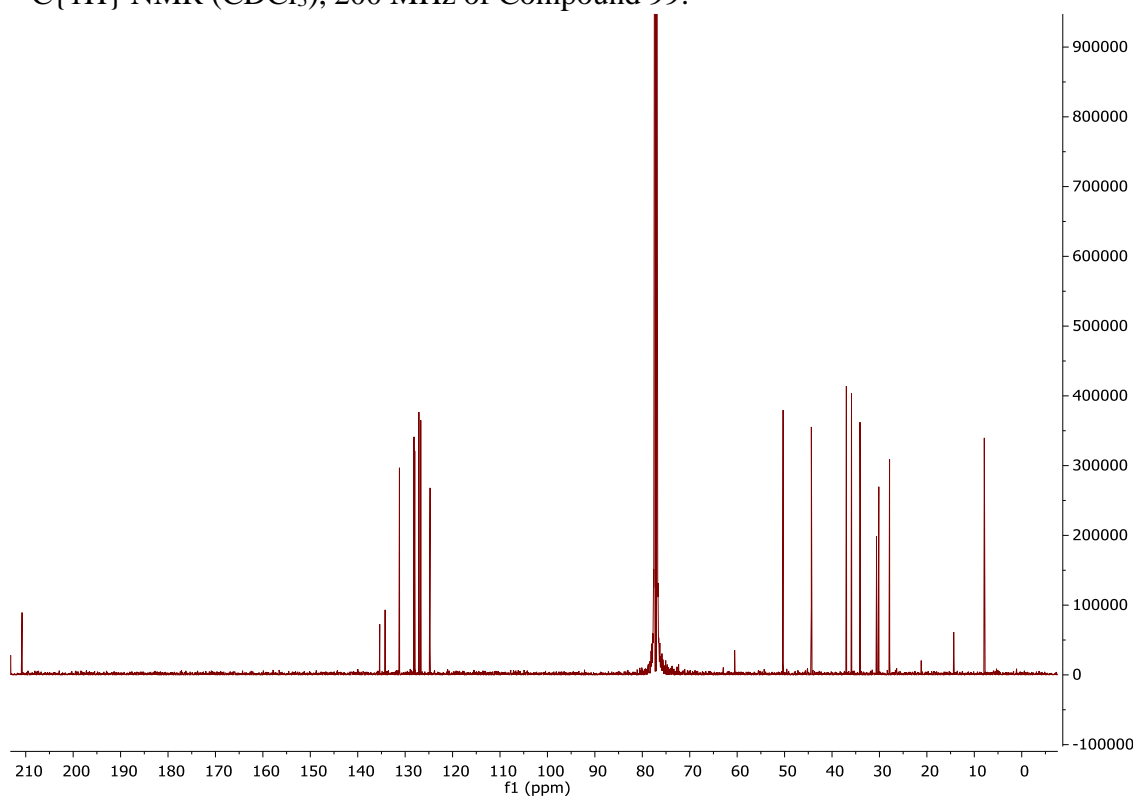
$^{13}\text{C}\{^1\text{H}\}$ NMR (d^6 -Acetone), 200 MHz of Compound 98:



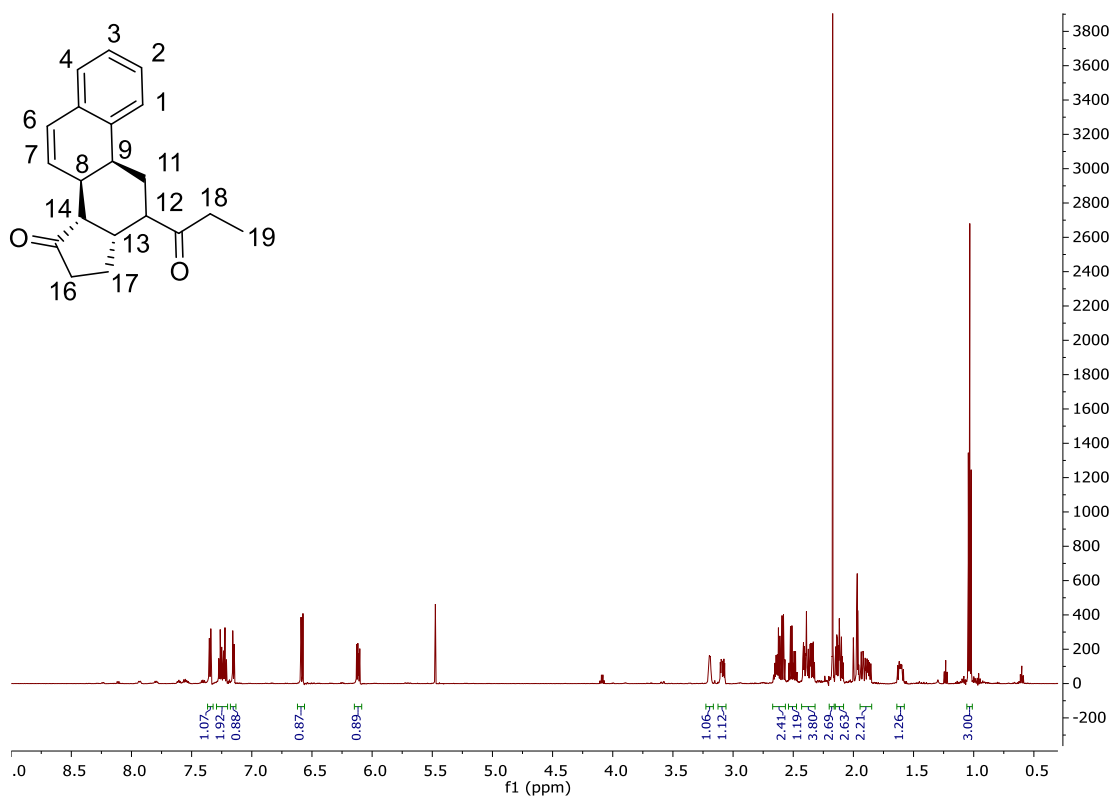
^1H NMR (CDCl_3), 600 MHz of Compound 99:



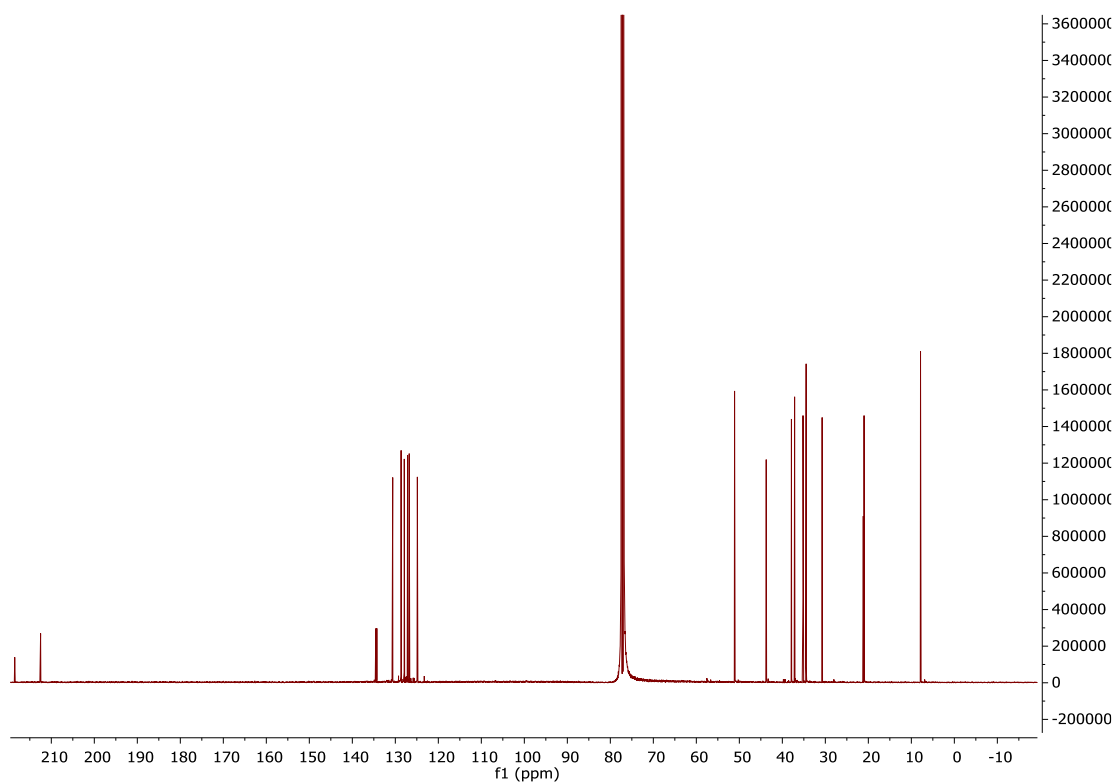
$^{13}\text{C}\{^1\text{H}\}$ NMR (CDCl_3), 200 MHz of Compound 99:

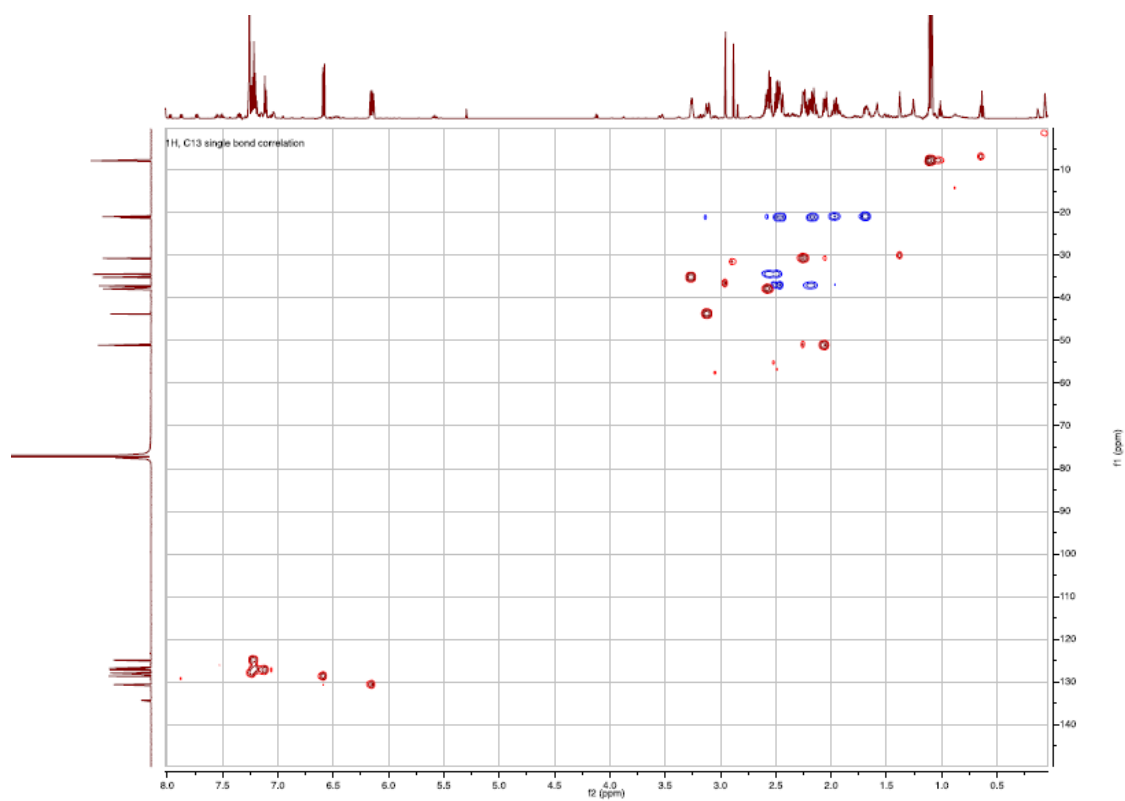
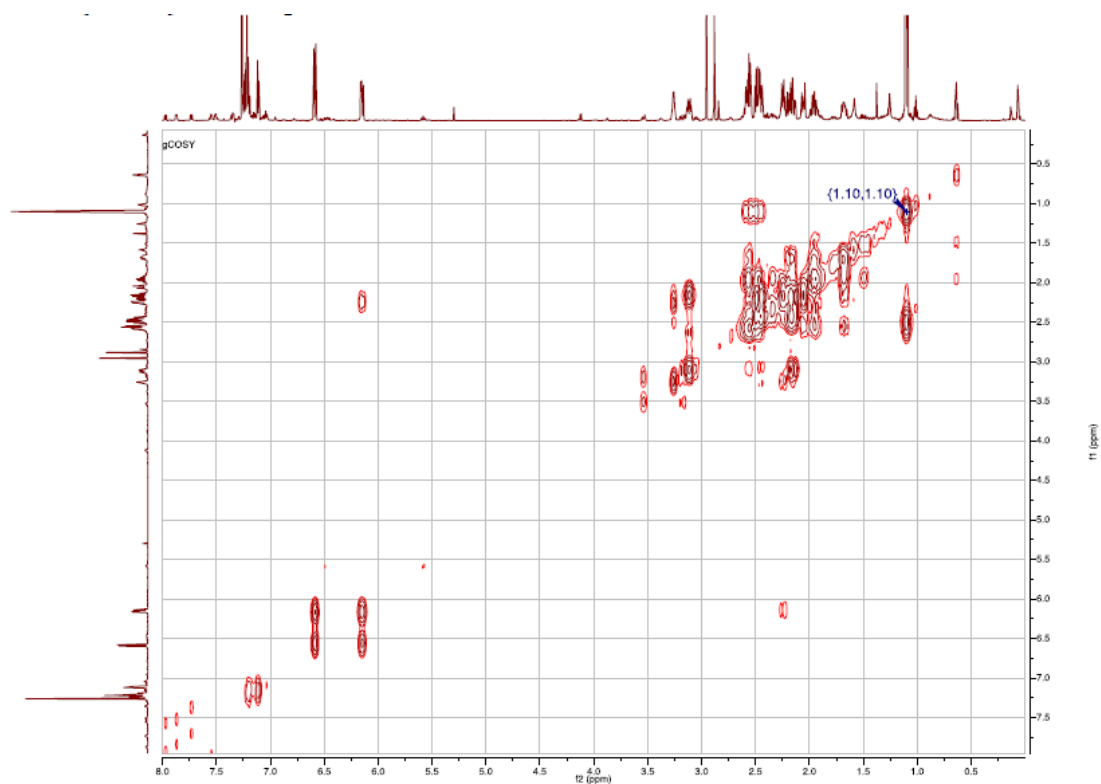


^1H NMR (d^6 -Acetone), 600 MHz of Compound 100:



$^{13}\text{C}\{^1\text{H}\}$ NMR (CDCl_3), 200 MHz of Compound 100:



HSQC (CDCl₃) of Compound 100:COSY (CDCl₃) of Compound 100:

NOESY (CDCl₃) of Compound 100:

